# Investigating how widely used biocides alter the physiology of *Staphylococcus aureus*

---

Thesis submitted to The University of Nottingham for the degree of Doctor of Philosophy

Dean Walsh, BSc (Hons), MSc

January 2021

# Declaration

Unless otherwise acknowledged, the work presented in this thesis is entirely my own. No part has been submitted for another degree in The University of Nottingham or any other institute of learning.

Dean Walsh

January 2021

# Abstract

The biocide triclosan is used extensively in both household and hospital settings, resulting in chronic exposure to the biocide in individuals that use triclosan-containing products. The ubiquitous use of triclosan has therefore facilitated low levels of this biocide to accumulate within the human body. These low levels of triclosan are thought to induce antibiotic tolerance and alter biofilm formation, although the causative mechanisms of these changes are yet to be elucidated. The potential for physiologically relevant levels of triclosan to alter bacterial physiology is concerning, particularly in the case of *Staphylococcus aureus*, a pathogen that triclosan is frequently used against to achieve MRSA decolonisation. If triclosan exposure can alter the antibiotic tolerance and biofilm formation of *S. aureus,* this could contribute to antibiotic treatment failures, and therefore requires investigation.

To determine how triclosan induces antibiotic tolerance, *S. aureus* was pretreated with physiologically relevant concentrations of triclosan prior to treatment with ciprofloxacin, rifampicin, and vancomycin. Planktonic *S. aureus* cultures pretreated with triclosan had 1,000 fold higher viable counts compared to non triclosan pretreated cultures and exhibited inhibited growth. Live/dead staining revealed that triclosan pretreatment protected *S. aureus* biofilms from treatment with otherwise lethal doses of antibiotics. Biofilms of mutant strains with a defective stringent response were not protected from antibiotic treatment, even in the presence of triclosan. Biocide induced antibiotic tolerance was not only limited to triclosan as subinhibitory concentrations of the biocides benzalkonium chloride and chlorhexidine digluconate were also able to induce tolerance against ciprofloxacin. Interestingly, this antibiotic tolerance also occurred in the stringent response mutant strain, indicating that tolerance induced by benzalkonium chloride and chlorhexidine digluconate was independent of the stringent response.

Confocal laser scanning microscopy revealed that incubation of *S. aureus* with triclosan during biofilm formation altered biofilm structure, resulting in increased proportions of polysaccharide intercellular adhesin

(PIA) in the biofilm matrix that could potentially mediate protection against antibiotics and the immune response. It was found that the stringent response played no role in triclosan-induced changes to biofilm matrix composition. A repressor of PIA biosynthesis genes, the transcriptional repressor CodY was also investigated, due to the activity of this repressor being closely linked to the stringent response. Although CodY deletion mutants did produce more PIA in *S. aureus* biofilms, this augmented triclosan-induced PIA production, rather than causing it. Therefore, it was concluded that CodY had minimal involvement in triclosan-induced PIA production. Exposure to subinhibitory concentrations of the biocides benzalkonium chloride and chlorhexidine digluconate throughout biofilm formation had no effect on biofilm architecture.

Both triclosan-induced antibiotic tolerance and triclosan-induced changes to biofilm architecture could be alleviated by supplementation with oleic acid, illustrating that these responses were induced by fatty acid starvation caused by triclosan exposure. In light of previous protection against antibiotics provided by triclosan exposure, the ability of triclosan exposure to protect *S. aureus* against killing by *Pseudomonas aeruginosa* in polymicrobial biofilms was investigated. Triclosan exposed *S. aureus* was far less able to survive in polymicrobial biofilms compared to untreated *S. aureus*.

Further interrogation of the mechanisms underlying triclosan-induced changes was carried out via RNA-sequencing. Untreated and triclosan-induced *S. aureus* was examined in both planktonic (1 hour after triclosan exposure) and biofilm (12 hours after triclosan exposure) culture. From this, it was confirmed that there was an upregulation of the stringent response gene *rsh* in triclosan treated planktonic cultures. Transcriptomics data also suggests that stringent response induced tolerance may be supplemented by efflux pumps, as significant upregulations in efflux genes were detected following triclosan exposure. RNA-sequencing was also used to investigate the expression of *ica* genes, which encode PIA biosynthesis machinery. Transcriptome data showed that triclosan exposure could lead to both upregulations of the

*ica* operon and downregulation of the *icaR*, the repressor of this operon. This change in *ica* gene expression could be mediated by the alternative sigma factor SigB, known to both repress of *icaR* and upregulate the *ica* operon. Evidence supporting this hypothesis was observed via significant upregulation of *sigB* in both triclosan treated biofilms and planktonic cultures. The implication of SigB, a regulator known to alter not only biofilm formation, but also antibiotic tolerance and virulence, suggests triclosan could alter the physiology of *S. aureus* beyong what has currently been observed. Potentially, this could allow *S. aureus* to endure many stresses of antibiotic, environmental, and host origin. Although more data is needed to validate the proposed mechanism, it is suggestive of triclosan triggering multiple global regulatory systems in *S. aureus*. These systems subsequently induce tolerance to multiple antibiotic classes and alter biofilm structure.

# Acknowledgements

Firstly, I would like to thank Kim Hardie and Jon Aylott for providing me with the opportunity to work on this project and for all the guidance and support provided over the past 4 years. I have thoroughly enjoyed my PhD project, particularly discussing my work at conferences and taking part in outreach events.

I would also like to thank the postdocs Elena Jordana-Lluch, James Brown and Veeren Chauhan for all of their invaluable help in the lab throughout my PhD. To my fellow members of team nanosensors, Birte Hollmann and Mark Perkins, thank you for welcoming me so warmly to the lab and being great friends over these past few years. I would also like to thank everyone past and present in C51/C69/C75/C81, particularly Clair, Claire, Maria, Marina and Izzy, who had to put up with the stressed out 'RNA Dean'. Thank you all so much for the long boffins lunches, pints after work at the Johnson Arms, crazy Christmas parties and all the other adventures shared in and out of the lab that I will never forget.

I cannot forget to mention my housemates Tom, Jamie and honorary housemate Hannah. Thank you for everything from the wild nights in Cav Cres to just listening to me moan after a long day of failed experiments, my time in Nottingham would have been a lot less fun without you. I am also incredibly grateful to Hristo for his endless support throughout the turbulent but memorable year 2020. Putting up with me during both coronavirus and thesis writing could not have been easy, but there is no one else I would rather be in lockdown with. Lastly, I am thankful for the support of my family, who have always believed in me despite having no clue what I am rambling on about. Please don't show me anything I don't want to see though, I won't be that kind of doctor. Just listening to me rant on about bacteria means a lot, and I am quite proud that some of you now know what a biofilm is (sort of).

# Abbreviations

| | |
|---|---|
| ±SEM | Plus/minus standard error of the mean |
| % | Percent |
| ≤ | Less than or equal to |
| µg | Microgram |
| µg/mL | Microgram per millilitre |
| µl | Microlitre |
| µm | Micrometre |
| µM | Micromolar |
| $^{o}C$ | Degrees Celsius |
| Agr | Accessory gene regulator |
| AIP | Autoinducing peptide |
| AMP | Antimicrobial peptide |
| AOT | Dioctylsulfosuccinate sodium |
| APMA | N-(3-Aminopropyl) methacrylamide hydrochloride |
| APS | Ammonium persulfate |
| Arl | Autolysin regulated locus |
| ATP | Adenosine triphosphate |
| BAC | Benzalkonium chloride |
| BCAA | Branched chain amino acid |
| BHI | Brain heart infusion media |
| $dH_2O$ | Distilled water |

| | |
|---|---|
| CAMP test | Christie–Atkins–Munch-Peterson test |
| CA-MRSA | Community acquired MRSA |
| cDNA | Complementary DNA |
| CF | Cystic fibrosis |
| CFU | Colony forming units |
| CFU/mL | Colony forming units per mL |
| CHG | Chlorhexidine digluconate |
| CHIPS | Chemotaxis inhibitory proteins of *S. aureus* |
| CLSM | Confocal laser scanning microscopy |
| $Cm^R$ | Chlorampenicol resistance |
| CV | Crystal violet |
| DAPI | 4',6-diamidino-2-phenylindole |
| DEG | Differentially expressed genes |
| DNA | Deoxyribonucleic acid |
| eDNA | Extracellular DNA |
| EDTA | Ethylenediaminetetraacetic acid |
| EtOH | Ethanol |
| Ex/Em | Excitation/Emission |
| FAM | 5-(and-6)-carboxyfluorescein |
| FASII | Fatty acid synthesis |
| FDR | False discovery rate |
| FPKM | Fragments Per Kilobase |

| | |
|---|---|
| g | Gram(s) |
| GDP | Guanosine diphosphate |
| GFP | Green fluorescent protein |
| GTP | Guanosine-5’-triphosphate |
| $H_2O_2$ | Hydrogen peroxide |
| HQNO | 2-*n*-heptyl-4-hydroxyquinoline *N*-oxide |
| Hrs | Hours |
| IFN | Interferon |
| IL | Interleukin |
| KEGG | Kyoto encyclopaedia of genes and genomes |
| kHz | KiloHertz |
| L | Litre |
| LB | Luria Bertani media |
| MBC | Minimum bactericidal concentration |
| MBEC | Minimum biofilm eradication concentration |
| MDK | Minimum duration of killing |
| mg | Milligram |
| MIC | Minimum inhibitory concentration |
| min | Minute |
| mL | Millilitre |
| mM | Millimolar |
| mRNA | Messenger RNA |

| | |
|---|---|
| MRSA | Methicillin-resistance *S. aureus* |
| $NAD^+$ | nicotinamide adenine dinucleotide |
| NADH | nicotinamide adenine dinucleotide hydride |
| ncRNA | Non-coding RNA |
| NCTC | National collection of type cultures |
| NET | Neutrophil extracellular trap |
| ng | Nanograms |
| ng/mL | Nanograms per millilitre |
| nm | Nanometres |
| NO | Reactive nitrogen |
| MSA | Mannitol salt agar |
| MSCRAMM | Microbial surface components recognising adhesive matrix molecules |
| OD | Optical density |
| $OD_{600}$ | Optical density at 600 nanometres |
| OG | Oregon Green® 488 carboxylic acid |
| P*adj* | Adjusted *P* value |
| PBP | Penicillin binding protein |
| PBS | Phosphate buffered saline |
| PCR | Polymerase chain reaction |

| | |
|---|---|
| pH | Potenz (power) of hydrogen |
| PIA | Polysaccharide intercellular adhesin |
| PNAG | Poly-N-Acetylglucosamine |
| ppGpp | Guanosine tetraphosphate |
| pppGpp | Guanosine pentaphosphate |
| (p)ppGpp | ppGpp and pppGpp |
| PQS | *Pseudomonas* quinolone signal |
| PSM | Phenol soluble modulin |
| PVL | Pantone-Valentine leukocidin |
| QAC | Quaternary ammonium compound |
| QS | Quorum sensing |
| RNA | Ribonucleic acid |
| RNA-Seq | RNA sequencing |
| ROI | Region of interest |
| ROS | Reactive oxygen species |
| rpm | Revolutions per minute |
| RPMI-1640 | Roswell Park Memorial Institute 1640 medium |
| rRNA | Ribosomal RNA |
| RSH | RelA/SpoT homolog |
| Sae | *S. aureus* exoprotein expression |
| Sar | Staphylococcal accessory regulator |

| | |
|---|---|
| SCV | Small colony variant |
| SD | Standard deviation |
| SEM | Scanning electron microscopy |
| sRNA | Small RNA |
| TAMRA | 5-(and-6)-carboxytetramethylrhodamine |
| $Tc^R$ | Tetracycline resistance |
| TCT | Triclosan containing toothpaste |
| TE | Tris-HCl-EDTA buffer |
| Tet | Tectracycline |
| Tris | Tris hydroxymethyl aminomethane |
| Tris-HCl | Tris hydrochloride |
| tRNA | Transfer RNA |
| TSST | Toxic shock syndrome toxin |
| UTR | Untranslated region |
| UV | Ultraviolet |
| v/v | Volume to volume ratio |
| VISA | Vancomycin intermediate *S. aureus* |
| VRSA | Vancomycin resistant *S. aureus* |
| WGA | Wheat germ agglutinin |
| WT | Wild type |
| x | Times |

| | |
|---|---|
| x *g* | Times gravitational force |

# Table of Contents

Declaration ..... I
Abstract ..... II
Acknowledgements ..... V
Abbreviations ..... VI
1. Introduction ..... 1
1.1 *Staphylococcus aureus* ..... 1
1.2 Biofilm formation of *Staphylococci* ..... 2
1.3 Virulence coordination in *S. aureus* by *agr* and SarA ..... 5
1.4 Antibiotic treatment failure ..... 8
1.5 Widely used biocides ..... 17
1.6 Previous work and research aims ..... 20
2. Materials and Methods ..... 23
2.1 Bacterial growth and culture media ..... 23
2.2 Bacterial strains ..... 23
2.3 Antibiotic susceptibility testing ..... 24
2.3.1 Antibiotics tested ..... 24
2.3.2 Minimum inhibitory concentration (MIC) determination ..... 24
2.3.3 Minimum bactericidal concentration (MBC) determination ..... 25
2.3.4 Minimum biofilm eradication concentration (MBEC) ..... 25
2.4 Nanosensor synthesis ..... 25
2.4.1 Nanosensor materials ..... 25
2.4.2 Conjugation of the OG, FAM and TAMRA fluorophores to APMA ..... 26
2.4.3 Synthesis of polyacrylamide pH-sensitive fluorescent nanosensors ..... 26
2.5 Planktonic pH measurements of *S. aureus* ..... 27
2.6 Scanning electron microscopy (SEM) ..... 28
2.7 Time-kill curve assays ..... 28
2.8 Confocal laser scanning microscopy (CLSM) of biofilms ..... 29
2.8.1 Growth of *S. aureus* biofilms with pH-sensitive fluorescent nanosensors ..... 29
2.8.2 Live/dead staining of biofilms ..... 30
2.8.3 Staining of biofilm matrix components ..... 30
2.8.4 Imaging polymicrobial biofilms ..... 31
2.8.5 Image analysis using Comstat software ..... 31

2.9 Single cell imaging to determine changes in cell size ..... 32
2.10 Quantification of total saccharide using phenol-sulfuric acid method ..... 32
2.11 Crystal violet staining of biofilms ..... 32
2.12 Polymicrobial endpoint CFU experiments ..... 33
2.13 Statistical analysis ..... 33
2.14 RNA-Sequencing ..... 34
2.14.1 Preparation of samples and RNA extraction ..... 34
2.14.2 Library preparation and transcriptome sequencing ..... 35
2.15 Data analysis of RNA-Seq data carried out by Novogene (UK) Co., Ltd ..... 36
2.15.1 Quality control ..... 36
2.15.2 Reads mapping to *S. aureus* NCTC8325 reference genome ..... 36
2.15.3 Novel gene and gene structure analysing ..... 36
2.15.4 Quantification of gene expression level ..... 37
2.15.5 Differential expression analysis of biological replicates ..... 37
2.15.6 KEGG enrichment analysis of differentially expressed genes ..... 37
3. Biocides can induce antibiotic tolerance in *Staphylococcus aureus* via multiple regulatory mechanisms ..... 38
3.1 Introduction ..... 38
3.1.1 Antibiotic tolerance ..... 38
3.1.2 Mechanisms underlying antibiotic tolerance in *S. aureus* ..... 40
3.2 Chapter aims ..... 44
3.3 Results ..... 45
3.3.1 Susceptibility profiles among *S. aureus* strains across different antibiotics and biocides ..... 45
3.3.2 Sub-MIC and physiologically relevant levels of triclosan inhibit growth and metabolism of *S. aureus* ..... 46
3.3.3. Inhibition in *S. aureus* cell division by physiological levels of triclosan can be observed at a single cell level ..... 47
3.3.4 Pretreatment with physiologically relevant levels of triclosan induce antibiotic tolerance to ciprofloxacin in planktonic *S. aureus* 49
3.3.5 Exposure to subinhibitory concentrations throughout biofilm development can protect *S. aureus* biofilms from eradication by ciprofloxacin treatment ..... 50

3.3.6 Planktonic *S. aureus* can utilise exogenous fatty acids to prevent triclosan-induced antibiotic tolerance ..... 52
3.3.7 Oleic acid supplementation also restores susceptibility to ciprofloxacin in triclosan-exposed biofilms ..... 54
3.3.8 The *agr* quorum sensing system plays a role in triclosan-induced antibiotic tolerance in planktonic *S. aureus* ..... 57
3.3.8 Triclosan-induced antibiotic tolerance in biofilms is unaffected by the *agr* quorum sensing system ..... 58
3.3.9 The global repressor CodY shows no involvement in biocide induced tolerance in planktonic culture ..... 61
3.3.10 The stringent response is essential for triclosan-induced antibiotic tolerance against multiple, mechanistically different antibiotics in planktonic culture ..... 62
3.3.11 The stringent response is essential for triclosan-induced antibiotic tolerance in biofilms, whilst the CodY repressor is not ... 64
3.3.12 The stringent response facilitates triclosan-induced protection against differing classes of antibiotics in *S. aureus* biofilms ..... 68
3.3.13 Triclosan-induced antibiotic tolerance can be visualised at a single-cell level ..... 72
3.3.14 Triclosan is able to induce antibiotic tolerance against multiple antibiotics in MRSA ..... 74
3.3.15 The widely used biocides chlorhexidine digluconate and benzalkonium chloride can induce antibiotic tolerance in planktonic *S. aureus*, independent of the stringent response ..... 77
3.3.16 Exposure to sub-MIC doses of chlorhexidine digluconate or benzalkonium chloride are unable to induce antibiotic tolerance in *S. aureus* biofilms ..... 78
3.4 Discussion ..... 84
4. Triclosan exposure alters *Staphylococcus aureus* biofilm formation and composition ..... 92
4.1 Introduction ..... 92
4.1.1 Stress-induced changes to biofilm formation ..... 92
4.1.2 Polymicrobial biofilms ..... 94
4.2 Chapter aims ..... 96
4.3 Results ..... 97
4.3.1 Triclosan does not greatly alter biofilm pH microenvironments, but does change biofilm structure in a concentration dependent manner ..... 97

4.3.2 Triclosan-induced changes to biofilm structure are caused by excess polysaccharide production ..... 99
4.3.3 Polysaccharide accumulation begins rapidly and continues for at least 48 hours after triclosan exposure ..... 101
4.3.4 Triclosan exposure does not alter the proportion of eDNA or protein in the biofilm matrix ..... 104
4.3.5 Triclosan-induced polysaccharide production is prevented in the presence of oleic acid ..... 106
4.3.6 Despite a significant role in triclosan-induced antibiotic tolerance, the stringent response is not involved in triclosan-induced changes in biofilm structure ..... 109
4.3.7 The CodY repressor contributes to the regulation of polysaccharide production in *S. aureus* biofilms. However, this is in addition to, rather than the cause of triclosan-induced biofilm alterations ..... 112
4.3.8 Biofilms of strains with deficient *agr* quorum sensing systems produce excess polysaccharide in the presence of triclosan ..... 115
4.3.9 Triclosan can alter the biofilm formation of the clinically relevant CA-MRSA strain USA300 ..... 118
4.3.10 The phenol-sulfuric acid method confirms that triclosan exposure induces excess polysaccharide production ..... 121
4.3.11 Even though triclosan exposure increases matrix polysaccharide, overall biomass is reduced in triclosan treated biofilms ..... 123
4.3.12 Neither chlorhexidine digluconate nor benzalkonium chloride significantly alter the concentration of biofilm matrix components 125
4.3.13 Untreated *S. aureus* produces more polysaccharide in the presence of *P. aeruginosa*. However, triclosan-exposed *S. aureus* is less able to survive in a polymicrobial biofilm ..... 127
4.3.14 Triclosan exposure reduces *S. aureus* survival in polymicrobial biofilms, but *P. aeruginosa* is unaffected ..... 130
4.3.15 Triclosan exposed *S. aureus* is more susceptible to killing by *P. aeruginosa*, even when mutations in quorum sensing have reduced virulence ..... 131
4.4 Discussion ..... 134
5. RNA-Sequencing reveals widespread transcriptomic changes in response to triclosan exposure in both planktonic and biofilm culture. ..... 144
5.1 Introduction ..... 144
5.1.1 Gene expression changes associated with survival ..... 144
5.1.2 RNA-Sequencing in *S. aureus* ..... 145

5.2 Chapter Aims ..... 148
5.3 Results ..... 150
5.3.1 The transcriptome of *S. aureus* is extensively altered by both triclosan treatment and the transition from a planktonic to biofilm lifestyle ..... 150
5.3.2 KEGG enrichment shows significant upregulation and downregulation in response to triclosan exposure and changes in bacterial lifestyle ..... 153
5.3.3 Differential expression of stringent response associated genes provides evidence for triclosan mediated stringent response induction ..... 157
5.3.4 Triclosan exposure leads to significant upregulation of efflux pump genes, potentially further facilitating antibiotic tolerance ..... 158
5.3.5 Triclosan exposed biofilms display significant downregulation of *icaR*, a repressor of PIA biosynthesis ..... 160
5.3.6 SigB, an alternate sigma factor implicated in both antibiotic tolerance and altered biofilm formation, may be responsible for numerous triclosan induced changes ..... 161
5.4 Discussion ..... 163
6. Discussion ..... 173
7. References ..... 185
8. Appendix ..... 210
8.1 Supplementary data ..... 210
8.2 Supplementary references ..... 244
8.3 Profession Internship for PhD students ..... 247

# List of figures

Figure 1.1. Schematic of *S. aureus* biofilm formation. ..... 5
Figure 1.2. Schematic of interactions between virulence regulators in *S. aureus*. ..... 8
Figure 1.3. Differentiating antibiotic resistance, tolerance, and persistence. ..... 15
Figure 1.4. The FASII pathway and the structure of FabI inhibition by triclosan in *S. aureus*. ..... 19
Figure 3.1. Growth inhibition by triclosan corresponds with reduced environmental acidification. ..... 46
Figure 3.2. Sub-MIC levels of triclosan impair cell division of *S. aureus*. ..... 48

Figure 3.3. Pretreatment with triclosan protects *S. aureus* from ciprofloxacin treatment. ..... 49

Figure 3.4. Triclosan exposure increases biofilm tolerance to ciprofloxacin. ..... 52

Figure 3.5. Supplementation with exogenous fatty acids restores susceptibility to ciprofloxacin in triclosan exposed *S. aureus*. ..... 53

Figure 3.6. Triclosan exposure increases biofilm tolerance to ciprofloxacin, but susceptibility can be restored with oleic acid supplementation. ..... 56

Figure 3.7. Agr quorum sensing deficient mutants are not protected against ciprofloxacin by triclosan-induced tolerance..... 57

Figure 3.8. The *agr* quorum sensing system does not prevent triclosan-induced ciprofloxacin tolerance in *S. aureus* biofilms. ..... 60

Figure 3.9. The CodY repressor has no effect on triclosan-induced antibiotic tolerance in planktonic culture. ..... 61

Figure 3.10. The stringent response plays a role in triclosan-induced antibiotic tolerance against multiple antibiotics. ..... 63

Figure 3.11. The stringent response plays a role in triclosan-induced ciprofloxacin tolerance in *S. aureus* biofilms. However, the CodY repressor does not..... 67

Figure 3.12. The stringent response is also responsible for triclosan-induced antibiotic tolerance against vancomycin and rifampicin in *S. aureus* biofilms. ..... 71

Figure 3.13. Triclosan-induced antibiotic tolerance, and the influence of the stringent response on this phenotype, can be visualised at a single cell level. ..... 73

Figure 3.14. Exposure to physiologically relevant levels of triclosan protects MRSA biofilms against multiple, mechanistically distinct antibiotics. ..... 76

Figure 3.15. Both chlorhexidine digluconate and benzalkonium chloride are capable of inducing antibiotic tolerance in planktonic *S. aureus*. .. 77

Figure 3.16. Neither chlorhexidine digluconate nor benzalkonium chloride were able to induce antibiotic tolerance in *S. aureus* biofilms. 82

Figure 3.17. Schematic diagram of potential mechanisms underlying triclosan-induced antibiotic tolerance..... 88

Figure 4.1. Triclosan alters biofilm thickness in a concentration dependent manner, as revealed by fluorescent nanoparticles. ..... 98

Figure 4.2. Single dye fluorescent nanoparticles reveal that triclosan exposure increases the presence of biofilm polysaccharide. ..... 100

Figure 4.3. Polysaccharide biomass increases over time. ..... 103

Figure 4.4. Triclosan exposure does not significantly alter the proportion of eDNA and protein biofilm components in the SH1000 biofilm matrix. ..... 105

Figure 4.5. Oleic acid supplementation significantly decreases polysaccharide biomass in triclosan exposed biofilms. ..... 108

Figure 4.6. The stringent response has no effect on triclosan-induced polysaccharide production. ..... 111

Figure 4.7. Deletion of codY increases polysaccharide production. .. 114

Figure 4.8. Deletion of *agr* has no effect on triclosan-induced polysaccharide production. ..... 117

Figure 4.9. Physiologically relevant levels of triclosan also alter the biofilm formation of MRSA ..... 120

Figure 4.10. Although triclosan exposed biofilms produce more polysaccharide, they consist of significantly fewer cells ..... 122

Figure 4.11. Triclosan exposure significantly decreases biofilm biomass ..... 124

Figure 4.12. Neither CHG or BAC exposure induced changes in biofilm structure ..... 126

Figure 4.13. Triclosan-induced polysaccharide production can be detected in polymicrobial biofilms even though *S. aureus* has been eradicated or rendered nonviable ..... 129

Figure 4.14. Triclosan exposure makes *S. aureus* more susceptible to killing by *P. aeruginosa* ..... 130

Figure 4.15. Triclosan exposed *S. aureus* is more susceptible to killing by *P. aeruginosa* quorum sensing mutants, but the survival of *P. aeruginosa* remains unaffected ..... 132

Figure 4.16. Summary of triclosan-induced alterations to biofilm structure. ..... 141

Figure 5.1. The vast majority of *S. aureus* transcripts are co-expressed across multiple conditions. ..... 151

Figure 5.2. Both triclosan exposure and bacterial lifestyle cause drastic changes in the transcriptome profile of *S. aureus* ..... 152

Figure 5.3. KEGG enrichment analysis shows upregulation in diverse pathways in response to triclosan treatment and changes in bacterial lifestyle ..... 154

Figure 5.4. KEGG enrichment analysis shows downregulation in diverse pathways in response to triclosan treatment and changes in bacterial lifestyle. ..... 156

Figure 5.5. Triclosan exposure induces patterns of gene expression indicative of stringent response induction ..... 158

Figure 5.6. Triclosan treatment prompts significant upregulation of genes encoding efflux pumps ..... 159

Figure 5.7. Triclosan exposure in planktonic *S. aureus* increases expression of the PIA export genes *icaB* and *icaC*, whilst triclosan exposed biofilms downregulate the *icaR* repressor of PIA synthesis. 160

Figure 5.8. Triclosan exposure results in increased *sigB* expression, upregulation of genes positively regulated by SigB, and downregulation of genes negatively controlled by SigB. ..... 161

Figure 5.9. Schematic of gene expression changes and proposed interactions following triclosan exposure ..... 171

Figure 6.1. Summary of the proposed mechanisms and responses to triclosan exposure. ..... 183

# List of tables

Table 1.1. Antibiotic resistance mechanisms used by *S. aureus*. ..... 9

Table 2.1. Table of strains used in this study. ..... 23

Table 3.1. Average minimum inhibitory concentration, minimum bactericidal concentration and minimum biofilm eradication concentration of *S. aureus* strains against a panel of antibiotics and biocides. ..... 45

Supplementary table 1. Fold changes and hypothesised roles of additional selected genes from RNA-Seq data of triclosan treated *S. aureus*, ns = not significant. ..... 210

Supplementary table 2. All significant fold changes of genes in PT vs PU. Genes with non-significant fold changes were not included. Padj is the adjusted P value (significance threshold P<0.05). Genes ordered by significance. ..... 214

Supplementary table 3. All significant fold changes of genes in BFT vs BFU. Genes with non-significant fold changes were not included. Padj is the adjusted P value (significance threshold P<0.05). Genes ordered by significance. ..... 227

# 1. Introduction

## 1.1 *Staphylococcus aureus*

*Staphylococcus aureus* can reside within the human host as either commensal or pathogen (Wertheim et al., 2005; Etter et al., 2020). *S. aureus* benignly colonises the human anterior nares, throat, and skin. Approximately 20-30% of the population permanently carry the bacterium asymptomatically (Sakr et al., 2018), with an additional 20-60% being intermittent carriers (Kluytmans et al., 1997; Wertheim et al., 2005). Colonisation by *S. aureus* can take place from the first few days of life after mother to child transmission (Maayan-Metzger et al., 2017). Following birth, hands typically transmit *S. aureus* to the nares of the host (Wertheim et al., 2005). Once colonised, the nose of the host acts as a reservoir to spread the pathogen and disseminate *S. aureus* across the carrier (Nouwen et al., 2006). Using a vast array of virulence factors (discussed in detail in chapter 5), this versatile pathogen can cause lethal, invasive infections throughout the host. *S. aureus* infections have been observed in almost any host tissue, including skin, muscle, bones, joints, lungs, kidneys, heart, eyes, and brain (Freidlin et al., 2007; Tong et al., 2015; Kuehl et al., 2020). The versatility of *S. aureus* can result in infections ranging from mild skin and soft tissue infections, to serious infective endocarditis, osteomyelitis, bacteraemia, and fatal pneumonia (Lowy, 1998; Humphreys, 2012; Tong et al., 2015; Guo et al., 2020). Furthermore, *S. aureus* can complicate patient treatment by also colonising indwelling devices such as orthopaedic implants, prosthetic heart valves, and catheters, which often need to be removed via surgery as a result (Ascione et al., 2015; Kuehl et al., 2020). *S. aureus* is highly resilient to antibiotic treatment, so much so that *S. aureus* can still be found within the blood of patients three days after receiving appropriate antibiotic therapy (Fowler et al., 2003; Welsh et al., 2011; Chong et al., 2013). The mortality associated with this bacteraemia is approximately 2-10/100,000 population (van Hal et., 2012). In 2015, *S. aureus* was associated with 434 food-borne outbreaks in the EU and in 2017 caused

over 100,000 cases of bacteraemia in the USA (Tong et al., 2015; Kourtis et al., 2019). The global public health concern of *S. aureus* is ever increasing, as a potential post-antibiotic era looms closer (Vestergaard, Frees and Ingmer, 2019).

## 1.2 Biofilm formation of *Staphylococci*

An estimated 60% of nosocomial infections are derived from biofilms (O'Toole, Kaplan and Kolter, 2000). Staphylococcal biofilms make up a large proportion of this percentage, illustrating the clinical significance of these species (Lister and Horswill, 2014). Previous studies have suggested that Staphylococcal biofilm formation follows the three classical steps of (i) attachment, (ii) maturation, (iii) dispersal (O'Toole, Kaplan and Kolter, 2000; Lister and Horswill, 2014). However, recent studies using microfluidic technologies suggest that Staphylococci may shift away from the established paradigm of biofilm formation. Real-time evaluation of Staphylococcal biofilm formation is summarised in Fig 1.1 and described as a five-step process: (i) attachment, (ii) multiplication, (iii) exodus, (iv) maturation, (v) dispersal (Moormeier and Bayles, 2017).

Attachment of *S. aureus* to biotic surfaces is largely protein-mediated. Microbial surface components recognizing adhesive matrix molecules (MSCRAMMs) are a group of proteins that vary in binding specificity, allowing for adhesion to a broad spectrum of host surfaces (Marraffini et al., 2006). Examples of MSCRAMMs include fibronectin-binding proteins, collagen adhesion, and bone sialoprotein, which respectively bind to fibronectin and fibrinogen (Piroth et al., 2008), collagen (Speziale et al., 2009), and bone (Vazquez et al., 2011). In the absence of a biological surface, Staphylococci utilise electrostatic and hydrophobic interactions to adhere to abiotic surfaces (Kennedy and O'Gara, 2004). This is exemplified by negatively charged teichoic acids mediating adhesion to glass and polystyrene (Gross et al., 2001).

Following attachment, cells with adequate nutrition begin to accumulate due to multiplication. Due to the lack of an established extracellular matrix during this early stage, newly divided cells are susceptible to dispersal by flow and other physical forces (Moormeier and Bayles, 2017). Many MSCRAMM proteins are recruited to maintain the integrity of fledgling biofilms (Speziale et al., 2009). At this stage polysaccharide intercellular adhesin (PIA) produced following expression of the *ica* operon begins to form a biofilm matrix (O'Gara, 2007). However, it has been shown that the production of PIA is highly strain dependent, with strains favouring either a PIA-dependent or PIA-independent method of biofilm formation (Boles et al., 2010; Brooks and Jefferson, 2014; Salzer et al., 2020). In addition to polysaccharide, the lysis of subpopulations of cells within the immature biofilm leads to release of extracellular DNA (eDNA) and cytoplasmic proteins, encasing neighbouring cells (Moormeier et al., 2014; Moormeier and Bayles, 2017). The exodus stage of biofilm formation occurs after multiplication and is characterised as an early dispersal event. This event is not typically witnessed in studies examining static biofilms due to the absence of flow to mediate dispersal (Moormeier and Bayles, 2017). Unlike the final dispersal step of biofilm formation, the dispersal during the exodus phase is *agr*-independent. Exodus events are triggered by degradation of matrix eDNA by the secretion of the *nuc* nuclease (Moormeier et al., 2014). The importance of polysaccharide during exodus is yet to be studied. The composition of the remaining biofilm matrix is drastically altered following biofilm exodus, no longer exclusively reliant on proteins but dependent on multiple matrix components (Moormeier et al., 2014). Whilst the purpose of exodus during *S. aureus* biofilm formation is still largely unknown, this dynamic restructuring of the biofilm matrix does dispel the notion that biofilm formation is exclusively focused around a particular matrix component (Moormeier and Bayles, 2017).

Biofilms then advance to the maturation stage after exodus. As with many other species, this stage of biofilm formation is characterised by microcolony formation – allowing waste removal and nutrient exchange

(Hall-Stoodley et al., 2004). Lastly, *S. aureus* biofilms undergo dispersal, which has been shown to be under the control of the *agr* quorum sensing system. Despite this, the effector systems under *agr* control that mediate dispersal are yet to be fully elucidated. Boles and Horswill (2008) suggested that dispersal was facilitated by increased protease activity, degrading proteins in the biofilm matrix. However, the *agr* system is not the only system that controls protease expression in *S. aureus* biofilms, with SarA, SigB and SaeRS also contributing. Alternatively, it has been suggested that *agr* controlled phenol soluble modulin (PSM) peptides contribute to dispersal. Evidence for PSM involvement includes the induction of both *agr* and *psm* promoters during dispersal events (Yarwood et al., 2004; Periasamy et al., 2012). The mechanism of PSM mediated dispersal appears to be through PSMs acting as a surfactant. PSMs are also implicated in the earlier maturation of biofilms by dispersing certain regions of biomass to facilitate channel formation within microcolonies (Periasamy et al., 2012).

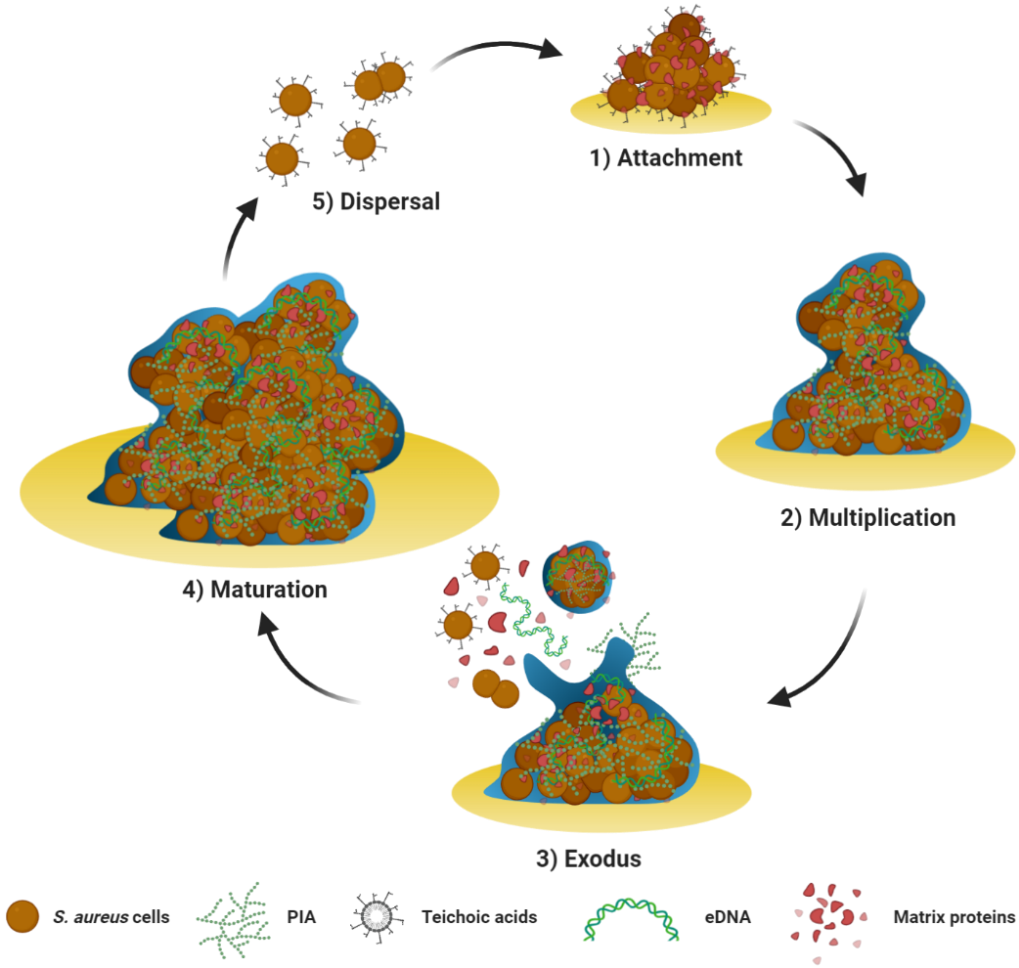



**Figure 1.1. Schematic of *S. aureus* biofilm formation. 1)** Attachment: proteins such as MSCRAMMs mediate attachment to biotic surfaces whilst teichoic acids facilitate attachment to abiotic surfaces. **2)** Multiplication: once attached, *S. aureus* cells multiply and coat themselves with a matrix consisting of PIA, eDNA, and proteins. **3)** Exodus: degradation of eDNA induces an early dispersal event. This occurs when *S. aureus* biofilms are under flow conditions and in an *agr*-independent manner. **4)** Maturation: microcolonies form; the channels within facilitate transport of nutrients and waste. **5)** Dispersal: *agr*-mediated dispersal occurs due to degradation of matrix proteins.

## 1.3 Virulence coordination in *S. aureus* by *agr* and SarA

*S. aureus* maintains multiple, divergent mechanisms to regulate virulence factor production, allowing the pathogen to adapt and thrive in dynamic environments. Genes encoding virulence factors and their regulators are known as accessory genes, as they are not essential for growth (Jenul and Horswill, 2019). Instead, these genes facilitate host cell adherence,

immune evasion, and destruction of host tissue for the purpose of nutrient acquisition (Jenul and Horswill, 2019). The accessory gene regulator (*agr*) quorum sensing system uses an autoinducing peptide (AIP) as a means of signal detection. Once AIP reaches a critical concentration in extracellular surroundings, the *agr* system is triggered and changes to gene expression facilitate environmental adaption and virulence regulation (Thoendel et al., 2011). RNAII and RNAIII are the transcripts of the *agr* system, with promoters P2 and P3 respectively controlling their expression (Peng et al., 1988). RNAII consists of the *agrBDCA* operon, which encodes proteins AgrB, AgrD, AgrC and AgrA (Fig 5.1). The membrane bound peptidase AgrB cleaves AgrD, the AIP precursor peptide (Thoendel and Horswill, 2010). AgrC then detects AIP once it is extracellular, with AgrC acting as a membrane-bound histidine sensor kinase that is autophosphorylated in response to AIP detection. The aspartate receiver of response regulator AgrA transmits this signal, with a phosphorylated AgrA subsequently binding to promoters P2 and P3 to enable expression of both RNAII and RNAIII (Novick et al., 1995). Further expression of RNAII, and by extension the *agrBDCA* operon, creates a positive feedback loop that is characteristic of quorum-sensing systems. In *S. aureus* this permits the acceleration of toxin production despite a deceleration of cell growth (Novick et al., 1995).

The RNAIII transcript, the effector of the *agr* system, regulates the expression of *agr*-dependent genes, as well as encoding delta-haemolysis on the *hld* gene (Novick et al., 1993). Virulence factors upregulated by RNAIII include alpha-toxin (encoded on *hla*), a key virulence determinate in multiple infection types, serine proteases (SspA), cysteine proteases (SspB), and leukocidins including LukGH (Cheung et al., 2011). Contrary to this, RNAIII also downregulates virulence factors including protein A (encoded by *spa*) (Dunman et al., 2001), a surface protein heavily associated with pneumonia (Wardenburg, Patel and Schneewind, 2007), sepsis (Date et al., 2014), and septic arthritis (Palmqvist et al., 2002) caused by *S. aureus*. In

addition to expression of RNAIII, AgrA also facilitates positive regulation of PSM cytolysin genes (Wang et al., 2007).

SarA is the original and archetypal protein of the SarA protein family (Jenul and Horswill, 2019). SarA can upregulate its own expression through binding to one of its three promoters (Cheung, Nishina and Manna, 2008). Downregulation of SarA can occur via SarR, another member of the SarA protein family, that accomplishes regulation by binding to all three *sarA* promoters (Manna, Bayer and Cheung, 1998) (Fig 5.1). SarA indirectly promotes toxin gene expression through binding to *agr* promoter P2 and subsequent upregulation of the *agr* system (Fig 1.2). SarR can override this, displacing SarA due to an increased binding affinity when negative regulation of *agr* and SarA is required (Reyes et al., 2011). Contrastingly, SarA post-translationally downregulates expression of the Protein A encoding gene *spa* through altering of mRNA turnover (Reyes et al., 2011). To complement *agr* mediated production of toxins, SarA is a strong repressor of extracellular proteases therefore protecting extracellular virulence factors from degradation (Zelinska et al., 2011). SarA is also associated with direct upregulation of TSST-1 (Andrey at al., 2010) and direct downregulation of exfoliative toxin A (encoded on *eta*) and B (*etb*), the causative toxins of scaled-skin syndrome (Kato et al., 2011). However, the role of SarA on the direct regulation of these toxins has been found to be highly strain dependent (Andrey et al., 2015). The alternative sigma factor SigB can act upon both the *agr* system and *sarA*. Through repression of *agr* function, SigB prevents toxin production and facilitates the maintainance of an avirulent 'stealth' phenotype. This avoids detection by the immune response and facilitates long-term survival within the host (Tuchscherr et al., 2015; Tuchscherr, Loffler and Proctor, 2020).

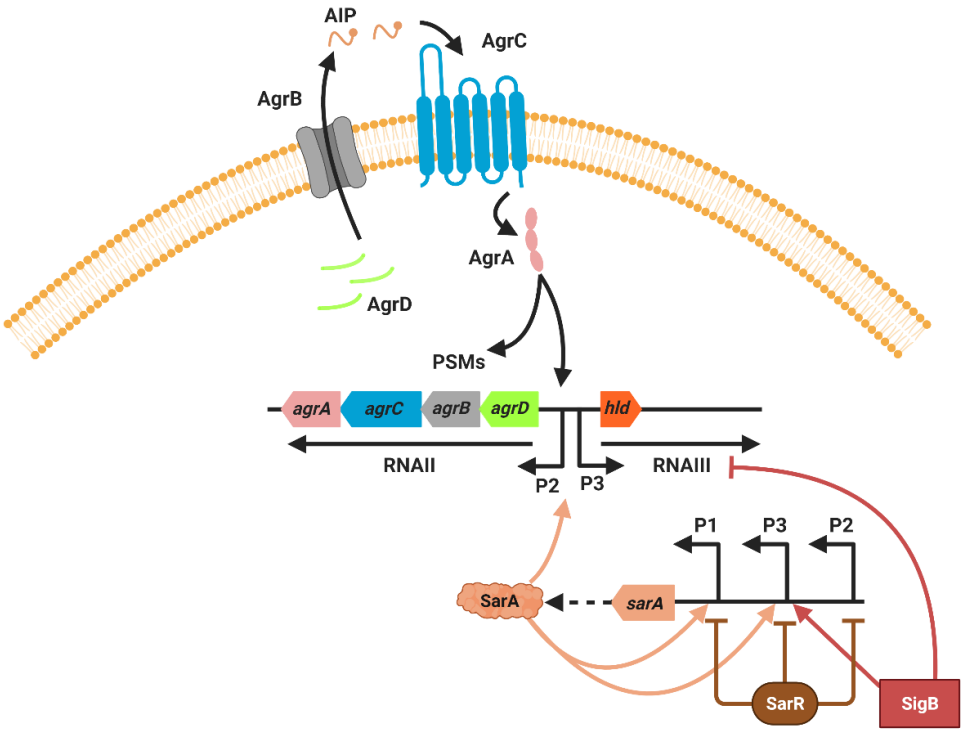



**Figure 1.2. Schematic of interactions between virulence regulators in *S. aureus*.** This interaction network gives a summary of how the *agr* quorum sensing system, SigB, and SarA-like proteins (SarA and SarR) regulate eachother. The molecular organisation of the *agr* system and the promoter region of *sarA* are also depicted.

## 1.4 Antibiotic treatment failure

Antibiotic treatment failure can occur via multiple different paths; the most widely described being antibiotic resistance (Vestergaard, Frees and Ingmer, 2018). Broadly, *S. aureus* is treated by antimicrobials that inhibit either cell envelope synthesis, protein synthesis, DNA replication, translation or metabolism (Boyle-Vavra and Daum, 2016; Vestergaard, Frees and Ingmer, 2018). As in other species, *S. aureus* has a repertoire of resistance mechanisms to thwart killing by these treatments (Table 1.2). The spread of antibiotic resistance is enabled by the usage of mobile genetic elements such as resistance gene cassettes and plasmids (Haaber, Penades and Ingmer, 2017).

**Table 1.1. Antibiotic resistance mechanisms used by *S. aureus*.**

| Antibiotic | Target | Resistance mechanism | Reference |
|---|---|---|---|
| **β-lactams** | Penicillin-binding proteins | Alteration of antibiotic target, enzymatic inactivation of antimicrobials | Tenover et al., 2006; Rolo et al., 2017 |
| **Glycopeptides** | MurNac pentapeptide | Alteration of antibiotic target, impeded drug accessibility | Cui et al., 2003; McGuiness, Malachowa and DeLeo, 2017 |
| **Lipopeptides** | Cell membrane | Impeded drug accessibility | Peleg et al., 2012; Bayer et al., 2015 |
| **Macrolides** | 50S ribosomal subunit | Alteration of antibiotic target, efflux pumps, enzymatic inactivation of antimicrobials | Roberts, 2008; Costa et al., 2013 |
| **Lincosamides** | 50S ribosomal subunit | Alteration of antibiotic target, efflux pumps | Roberts, 2008; Costa et al., 2013 |
| **Streptogramins** | 50S ribosomal subunit | Alteration of antibiotic target, efflux pumps | Roberts, 2008; Costa et al., 2013 |
| **Chloramphenicol** | 50S ribosomal subunit | Alteration of antibiotic target, efflux pumps, enzymatic inactivation of antimicrobials | Schwarz et al., 2004; Kehrenberg et al., 2005; Costa et al., 2013 |
| **Tetracycline** | 30S ribosomal subunit | Alteration of antibiotic target, efflux pumps | Costa et al., 2013; Larsen et al., 2016 |
| **Aminoglycosides** | 30S ribosomal subunit | Alteration of antibiotic target, enzymatic | Garneau-Tsodikova and Labby, 2016 |

| | | | |
|---|---|---|---|
| | | inactivation of antimicrobials | |
| **Mupirocin** | Isoleucyl-tRNA synthase | Alteration of antibiotic target | Thomas et al., 2010 |
| **Fusidic acid** | Elongation factor G | Alteration of antibiotic target | Farrell, Castanheira and Chopra, 2011 |
| **Fluoroquinolones** | DNA gyrase, topoisomerase IV | Alteration of antibiotic target, efflux pumps | Ito et al., 1994; Costa et al., 2013 |
| **Rifampicin** | RNA polymerase | Alteration of antibiotic target | Wichelhaus et al., 2002 |
| **Trimethoprim-sulfamethoxazole** | Dihydrofolate reductase (trimethoprim), dihydrofolate synthetase (sulfamethoxazole) | Alteration of antibiotic target | Hampele et al., 1997 |
| **Fosfomycin** | Enoylpyruvate transferase (MurA) | Alteration of antibiotic target, enzymatic inactivation of antimicrobials | Roberts et al., 2013; Fu et al., 2016 |

Drug resistance among *S. aureus* isolates was identified almost immediately after the introduction of the antibiotic penicillin into the clinic (Kirby, 1944). An early determinate in drug resistance in *S. aureus* was the *blaZ* encoded β-lactamase capable of hydrolysing the essential β-lactam ring structure of penicillin (Tenover et al., 2006). As well as being integrated into the chromosome, *blaZ* could also be part of large conjugative plasmids that harboured additional antibiotic resistance genes (Berg et al., 1998). As a result, as many as 99% of *S. aureus* clinical strains are now penicillin resistant (Boyle-Vavra and Daum, 2016).

Perhaps the most infamous of drug resistant *S. aureus* strains is methicillin-resistant *S. aureus* (MRSA). Acquisition of a single genetic element, the staphylococcal cassette chromosome *mec* (SCC*mec*)

facilitates resistance to the β-lactam subclasses of penicillin, cephalosporin, monobactam and carbapenem antibiotics (Vestergaard, Frees and Ingmer, 2018). The SCC*mec* consists of *mecA*, its regulators *mecR1* and *mecI*, and lastly the *ccr* complex. The *ccr* complex mediates chromosomal integration of the SCC*mec* element whilst *mecA* encodes an alternative penicillin binding protein (PBP) called PBP2a. This alternative PBP has a low affinity for β-lactam antibiotics, thus conferring resistance to this large class of antibiotics (Katayama and Hiramatsu, 2000).

Following decades of increased MRSA prevalence, the glycopeptide vancomycin became a preferred antibiotic for treatment of MRSA infections. Like β-lactams, vancomycin also targets the bacterial cell wall (Levine, 2006). The glycopeptide disrupts peptidoglycan assembly by high affinity binding to penultimate D-ala-D-ala residues in the cell wall, preventing further elongation and cross-linking of peptide chains during cell wall biosynthesis (Barna and Williams, 1984). Since widespread use of vancomycin began, both vancomycin resistant (VRSA) and intermediately resistant (VISA) *S. aureus* strains have been isolated. VRSA cases are rare as they are associated with horizontal gene transfer events in which enterococci transfer the *vanA* operon to *S. aureus* during co-infection (Weigel et al., 2003). The *vanA* operon allows *S. aureus* to hydrolyse D-ala-D-ala within the cell wall and replace them with D-ala-D-lactate precursors, which are recalcitrant to vancomycin binding (Arthur, Reynolds and Courvalin, 1996). Additional obstacles contributing to the rarity of VRSA include the incompatibility of methicillin resistance with the VRSA cell wall. This is due to PBP2a being unable to cross-link with the D-ala-D-lactate precursors found in the cell wall of *vanA* expressing strains (Gardete and Tomasz, 2014).

VISA strains are far more prevalent than VRSA, and are generated through the acquisition of multiple mutations that can present as a variety of phenotypes including increased cell wall thickness, reduced autolysis, changes to cell surface charge, increased peptidoglycan synthesis, and less cross-linking (Hiramatsu et al., 2014; McGuiness, Malachowa and

DeLeo, 2017). The degree of resistance differs widely among different VISA strains, with even marginal decreases in vancomycin susceptibility contributing to vancomycin treatment failure (Vestergaard, Frees and Ingmer, 2018). Mutations of VISA are often attributed to either the cell wall regulon (including the two-component systems (TCS) *vraSR*, *walRK*, *graRS*) which stimulate expression of *mprF* or the *dlt* operon which reduce negative cell surface charge leading to less vancomycin binding (Hiramatsu et al., 2014; McGuiness, Malachowa and DeLeo, 2017; Vestergaard, Frees and Ingmer, 2018).

The acquisition of stable antibiotic resistance genes or mutations typically result in resistance being conferred to all cells within the population. However, heteroresistance is observed when populations are not homogenously susceptible to antibiotic treatment, despite sharing the same susceptibilities. Instead, unstable resistance genes are amplified heterogeneously across the population, and subpopulations with a higher resistance gene 'dosage' are better able to survive antibiotic treatment (Band and Weiss, 2019). Vancomycin heteroresistance has been observed in *S. aureus* (Hiramatsu et al., 1997; Khatib et al., 2011), with resistant subpopulations causing treatment failure *in vivo* (Moore, Perdreau-Remington and Chambers, 2003). β-lactam resistance genes also appear to be expressed heterogeneously across *S. aureus* populations, in which there is a highly resistant subpopulation amongst a majority expressing resistance at low levels. The discrepancy in resistance gene expression between these subpopulations has been attributed to mutations in stress responses such as the stringent response (Kim et al., 2013). This demonstrates that the degree of antibiotic resistance is not simply dictated by resistance gene or mutation acquisition, but that wider *S. aureus* physiology also plays a role (Kim et al., 2013; Vestergaard, Frees and Ingmer, 2018).

Other mechanisms known to complicate antibiotic chemotherapy include persistence and tolerance (Balaban et al., 2019; Band and Weiss, 2019). Although both resiliencies result in increased antibiotic survival, they can be differentiated by their action at a population level. In the case of

persistence, a small subpopulation undergo a temporary period of dormancy or reduced growth. This quiescent subpopulation is able to endure antibiotic treatment due to inactivity of bactericidal antibiotic targets (Brauner et al., 2016; Balaban et al., 2019). This in turn diminishes the ability of bactericidal antibiotics to corrupt the function of these antibiotic targets and initiate downstream lethality (Lewis, 2005; Balaban et al., 2019). Due to only a small proportion of the initial population becoming persisters, it is thought that persistence leads to infection relapse following treatment cessation, but cannot alone cause acute treatment failure (Band and Weiss, 2019). Tolerance, which will be discussed further in chapter 3, is distinct from persistence in that the entire bacterial population is transiently capable of withstanding antibiotic treatment. Antibiotic tolerance can protect a susceptible bacterial population even against very high concentrations of antibiotics (Brauner et al., 2016; Balaban et al; 2019).

Both persistence and tolerance result in an antibiotic tolerant phenotype, and this phenotype can evolve stochastically (Zalis et al., 2019), be attributed to genetic traits (as heteroresistance often is) (Band and Weiss, 2019), or be triggered due to changes in the environment (Brauner et al., 2016; Balaban et al; 2019). Environmental factors linked with the induction of these phenotypes include oxygen concentration (Pabst et al., 2016), pH (Lamp et al., 1992), and lack of adequate nutrition (Gutierrez et al., 2017). Increased population densities are also associated with the development of an antibiotic tolerant phenotype due to starvation, accumulations of metabolic waste or signalling molecules (Fux et al., 2005). *S. aureus* can also recruit host tissue components to promote cell aggregation and aid in tolerance. This is evidenced by the recruitment of fibrinogen and fibronectin during septic arthritis and clustering with platelets and fibrin during endocarditis (Dastgheyb et al., 2015). These aggregations can then progress into abscesses, with infecting *S. aureus* cells encased in a protective capsule of necrotic tissue (Cheng et al., 2011). Antibiotic treatment failure in *S. aureus* abscesses is attributed to decreased antibiotic penetration as well as tolerance induced by the low

oxygen concentration and acidic pH within (Wagner, Sauermann and Joukhadar, 2006; Vulin et al., 2018). Similar tolerance mechanisms manifest within *S. aureus* biofilms, with chemical gradients across the microenvironment leading to physiological and metabolic heterogeneity, and therefore differential survival among cells within the same biofilm (Rani et al., 2007). Tolerance within biofilms increases with cell density and age (Wolcott et al., 2010; Stewart, 2015). Often, this results in implanted devices colonised with mature biofilms needing to be surgically removed due to total recalcitrance to antibiotic therapy (Zimmerli, Trampuz and Ochsner, 2004; Barberan et al., 2006). An additional contribution to treatment failure is credited to the ability of *S. aureus* to survive intracellularly in phagocytes (Peyrusson et al., 2020). The intracellular phenotype of *S. aureus* is associated with small colony variants (SCVs), which are characterised by reduced metabolism, gene expression and virulence (Loffler et al., 2014). SCV formation is often dynamic as cells typically revert from the tolerant phenotype upon subculturing in rich growth medium, where isolates display normal metabolism and colony sizes (Tuchscherr et al., 2011; Tuchscherr et al., 2015).

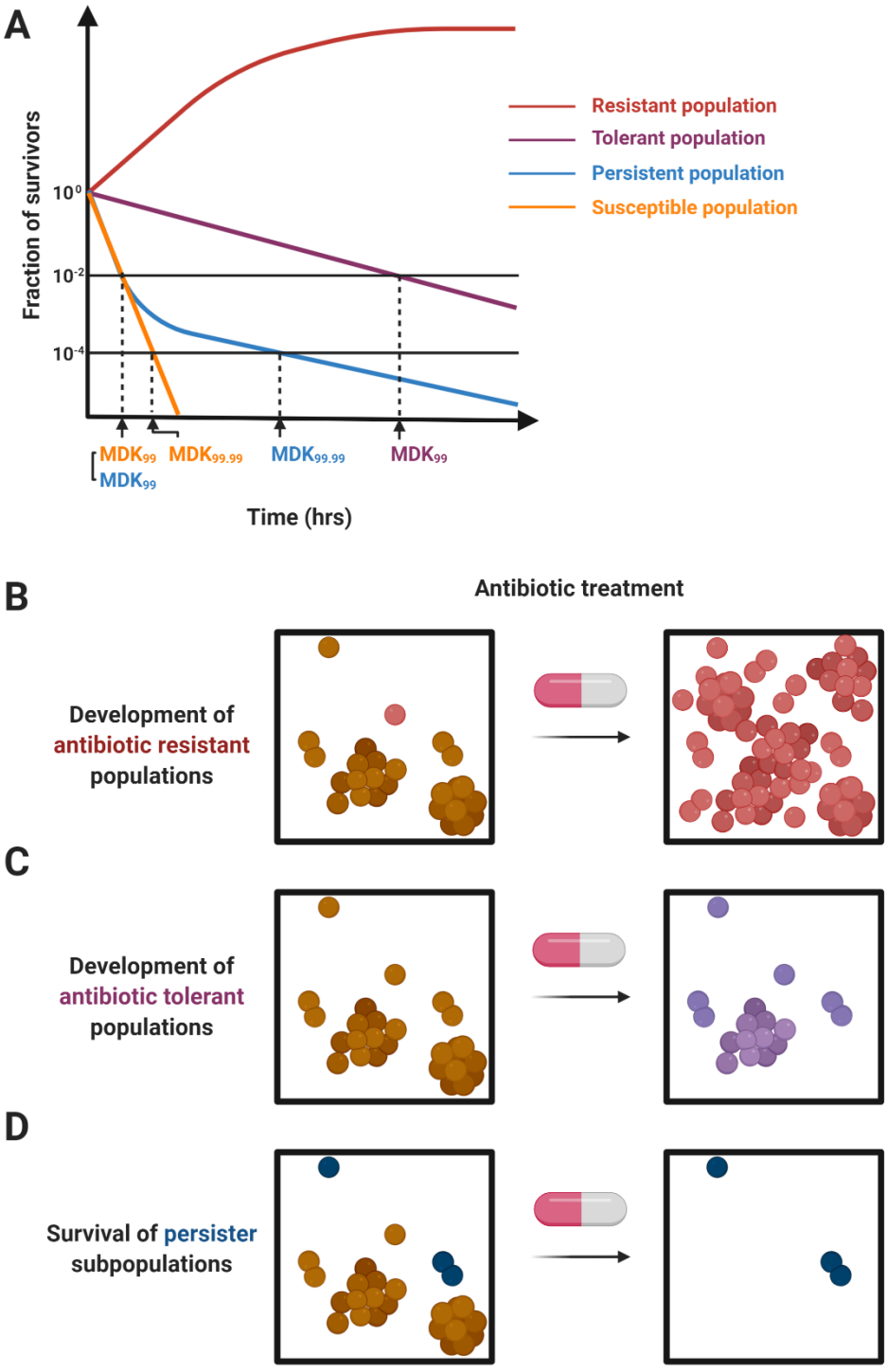



**Figure 1.3. Differentiating antibiotic resistance, tolerance, and persistence. A)** A graph showing survival of susceptible (orange), persister (blue), tolerant (purple), and resistant (red) populations during antibiotic treatment (Adapted from Brauner et al., 2016). Dotted lines highlights the minimum duration of killing (MDK) for various populations. $MDK_{99}$ shows the minimum duration for 99% of the population to be killed, whilst $MDK_{99.99}$ shows when 99.99% of the original bacterial population has been killed. $MDK_{99}$ and $MDK_{99.99}$ along the x-axis are colour coded to demonstrate which population has reached that MDK (susceptible: orange, persistent: blue, tolerant: purple).

Susceptible populations die rapidly after antibiotic treatment as $MDK_{99}$ and $MDK_{99.99}$ are reached in quick succession. Persister populations share the same $MDK_{99}$ as susceptible populations, but the presence of a persistent subpopulation means that it takes longer for killing of 99.99% of the population to be achieved. Unlike persistence, tolerance is typically population wide, and therefore it takes longer for a tolerant population to reach $MDK_{99}$ during antibiotic treatment compared to a persister or susceptible population. Bacteria that are resistant to the antibiotic treatment are able to continue multiplying, therefore MDK values are not observed in the timeframe of this graph. **B)** Antibiotic treatment kills susceptible bacteria (orange) whilst resistant cells (red) replicate, resulting in a resistant population. **C)** Once tolerance has been induced across a bacterial population; many tolerant bacteria (purple) may withstand antibiotic treatment but the population will not grow due to reduced activity. **D)** Susceptible bacteria (orange) within the population are killed by antibiotic treatment whilst a small persister subpopulation (blue) is able to endure.

To overcome the challenge of antibiotic treatment failure by tolerant *S. aureus*, alternative treatment strategies are being considered (Kuehl et al., 2020). These include using novel anti-tolerance compounds to inhibit targets that cause tolerance but are also not dependent on active growth or metabolism. Many of these compounds, such as retinoids and membrane-active small molecules, target the cell membrane (Kirstein et al., 2009; Conlon et al., 2013; Kim et al., 2018). Another prospect is the synthetic antibiotic ADEP4, which binds to the protease ClpP resulting in self-digestion and *S. aureus* cell death (Kirstein et al., 2009; Conlon et al., 2013). Unfortunately, many of these new agents are hampered clinically by obstacles including low bioavailability, rapid development of escape mutants, and unfavourable toxicity (Conlon et al., 2013; Defraine et al., 2018; Kuehl et al., 2020). Enhancing current treatment regimens may also aid in combatting tolerant *S. aureus*. Tolerant bacteria require a longer treatment duration to outlast the duration of tolerance, with 24 days of treatment being shown to completely eradicate tolerant *S. aureus* (Lechner, Lewis and Bertram, 2012). Fourteen days is typically prescribed, this short treatment course is likely a contributing factor in the relapse of even uncomplicated *S. aureus* infections (Chong et al., 2013). For decades, it has been suggested that antibiotics be prescribed intermittently to allow tolerant bacteria to ‘wake up’ between doses, therefore killing more bacteria with each successive round of treatment

(Bigger, 1944). Whilst this approach has provided promising results *in vitro*, there are still uncertainties as to how this will manifest clinically (Cogan et al., 2016). Lastly, resensitising tolerant *S. aureus* to antibiotics is being explored. This has mainly been investigated by adding metabolites to the environment in an effort to reinvigorate *S. aureus* metabolism (Kuehl et al., 2020). This approach has been shown to be effective in the case of fructose increasing aminoglycoside susceptibility (Allison, Brynildsen and Collins, 2011), whilst glucose increased killing by daptomycin, rifampicin and vancomycin (Prax et al., 2016). Due to the multitude of tolerance mechanisms, resensitisation is highly dependent on the antimicrobial and metabolite use, making it unlikely a single supplement could render tolerant *S. aureus* vulnerable to all antimicrobials (Allison, Brynildsen and Collins, 2011). Whilst there is progress in the treatment of tolerant *S. aureus* that may prevent antibiotic treatment failure, current strategies are still inundated with questions and drawbacks.

## 1.5 Widely used biocides

Biocides are chemical agents used to prevent, inhibit or eliminate the growth of both pathogenic and non-pathogenic microorganisms on surfaces. Unlike antibiotics, which target specific pathways or cellular targets, biocides work in a non-specific manner against multiple targets (Bridier et al., 2011). This wide-spectrum of activity makes biocides ideal for extensive use in domestic and industrial settings to control biofouling and destroy hygienically relevant microorganisms, as well as being used in healthcare environments to prevent the spread of pathogenic bacteria and fungi (Bridier et al., 2011).

The synthetic biocide triclosan demonstrates antimicrobial activity through inhibition of type II fatty acid synthesis (FASII) at the enoyl-acyl carrier protein reductase (FabI) step (Heath et al., 1999, Sadowski et al., 2014). FASII is the pathway responsible for the *de novo* synthesis of phospholipid precursors, and FabI is essential for catalysing the essential

elongation step of FASII (Fig 1.4A) (Morvan et al., 2017). In its apo form, FabI is a dimer consisting of two identical chains. However, when both triclosan and the FabI cofactor $NADP^+$ bind to FabI, the two dimers interact to form a tetramer (Fig 1.4B) (Scheibel et al., 2012). The strong inhibition exerted by triclosan upon FabI is attributed to triclosan binding a pocket composed of $NADP^+$ and hydrophobic residues (Fig 1.4C). The binding of the B-ring chlorine of triclosan with the carbonyl oxygen of Ala97 distinguishes triclosan from other FabI inhibitors, as this inhibition is particularly strong (Scheibel et al., 2012). At high concentrations, triclosan is capable of provoking membrane permeability and non-specific membrane damage (Morvan et al., 2017).

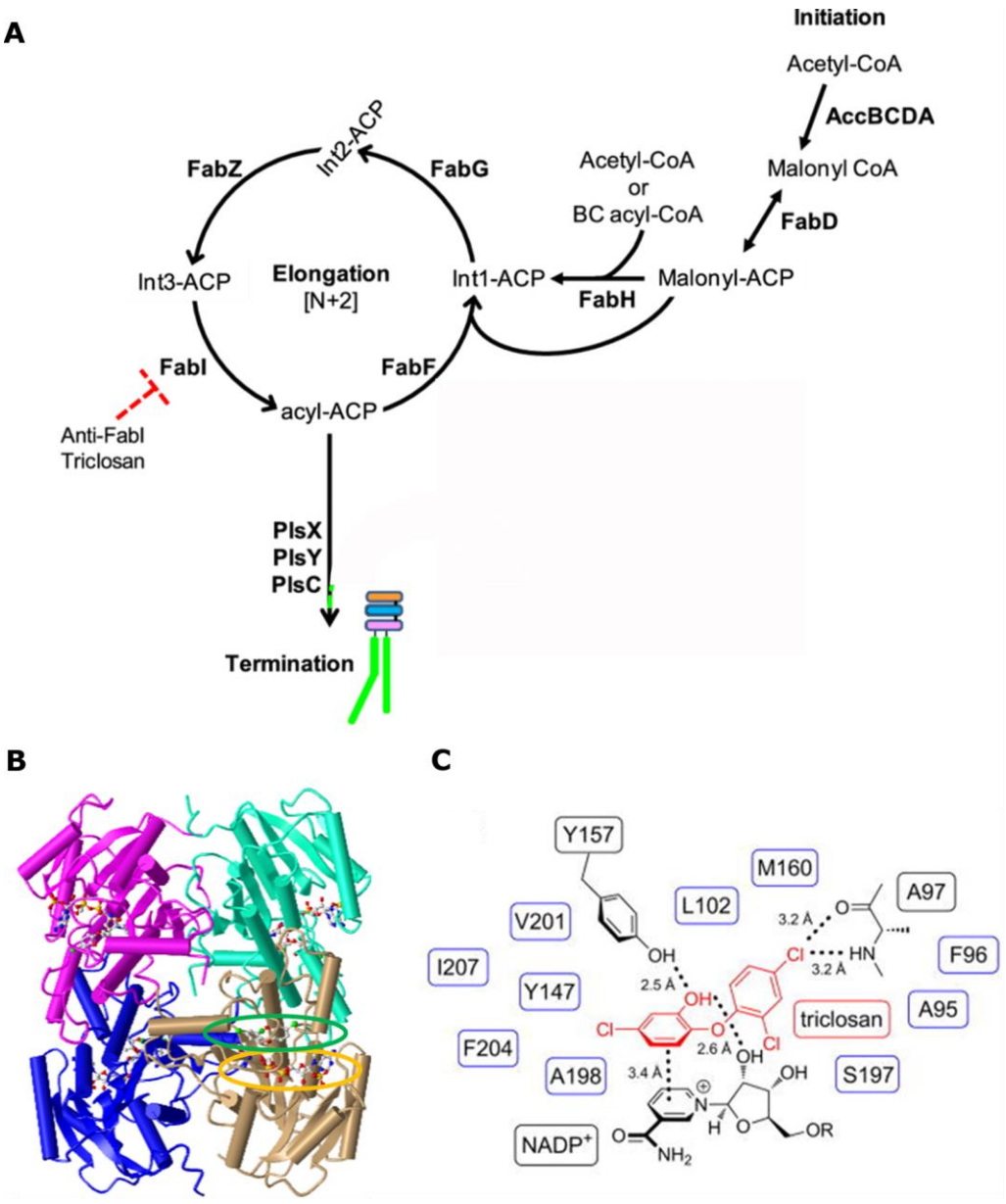


**Figure 1.4. The FASII pathway and the structure of FabI inhibition by triclosan in *S. aureus*. A)** The FASII pathway comprises 3 main steps: i) initiation, during which a priming molecule (short chain fatty acid) is synthesized; ii) elongation, during which 4 enzymes elongate the fatty acid chain by two carbons per iterative cycle; and iii) termination, in which a mature length acyl moiety is driven towards phospholipid synthesis enzymes. The enzymes involved in each stage of FASII in *S. aureus* are indicated; Int1-ACP to Int3-ACP represent reaction intermediates. The major fatty acids produced by *S. aureus* have branched chains (BC). The red dashed line indicates triclosan inhibition of FabI (Adapted from Morvan et al., 2017). **B)** Crystal structure of FabI tetramer in complex with $NADP^+$ and triclosan. Triclosan circled in green, $NADP^+$ circled in yellow (adapted from Priyadarshi, Kim and Hwang, 2010). **C)** Schematic representation of all residues interacting with triclosan (red). Directional interactions are depicted explicitly (black residues), amino acids creating the hydrophobic pocket are included in 1-letter code (residues in blue boxes). R = adenosine diphosphate (Scheibel et al., 2012).

In hospitals, triclosan is used as an MRSA decolonisation therapy (Brittain, 2004), antimicrobial hand wash (Brittain, 2004), antiseptic ointment (Gudapuri, 2017), and is impregnated into surgical sutures (Sewlikar et al., 2015) and urinary catheters (Singha et al., 2017). Triclosan is also widely used in domestic settings, with the biocide being found in many household products including soaps, toothpastes (MacIsaac et al., 2014), cosmetics and laundry detergents (Schweizer, 2001). This widespread use of triclosan has led to chronic exposure to the biocide in individuals that regularly use triclosan containing products, as well as the environments that these products inevitably contaminate. The biocide has been isolated in wastewater and aquatic ecosystems, soil, fish bile, human breast milk and urine (Adolfsson-Erici et al., 2002; McBain et al., 2003; Calafat et al., 2008; Lubarsky et al., 2012; Westfall et al., 2019). Concerns have been heightened further by findings suggesting triclosan is linked to skin cancer (Dinwiddie et al., 2014) and disruption of the endocrine system (Wang and Tian, 2015). Absorption of triclosan from triclosan containing toothpastes (TCT) is high, with triclosan blood concentration increasing from 0.81 ng/mL to 296 ng/mL after 14 days of TCT use (Allmyr et al., 2009), and urine concentrations averaging at 147 ng/mL (MacIsaac et al., 2014). The average urine

concentration of triclosan in patients exposed to the biocide during their hospital stay was 245 ng/mL, with concentrations reaching as high as 505 ng/mL (MacIsaac et al., 2014).

Triclosan usage has reduced, in part because the Food and Drug Administration in the USA banned triclosan in domestic hand soaps in 2016 because there was not significant benefit using triclosan-soap over existing antibacterial soap (Kampf, 2018). In addition to triclosan, other biocides are also used for disinfection, such as chlorhexidine gluconate (CHG) and benzalkonium chloride (BAC) (Russell, 2003). CHG is found in alcohol-based skin disinfectants (George et al., 2016). Chlorhexidine can adhere to skin, accumulating with recurrent applications and has antimicrobial activity up to 48 hours after exposure (Hibbard, 2005, Hennig et al., 2017). CHG has been found in the plasma of infants at concentrations ranging from 26-496 ng/mL (Johnsson et al., 1987), whilst Bonesvall (1977) reported that CHG remained in saliva for over 24 hours following mouthwash usage and subsequent rinsing. BAC is used in domestic and clinical settings, for example shampoo and ophthalmic solutions (Pereira and Tagkopoulus, 2019). BAC works by reducing the membrane integrity of bacteria and CHG works by destabilising bacterial cell walls, however neither of these mechanisms are as well characterised as that of triclosan (Meyer and Cookson, 2010).

## 1.6 Previous work and research aims

Recent work suggests that pretreatment with low levels of triclosan can induce antibiotic tolerance in both *Escherichia coli* and *S. aureus* (Westfall et al., 2019). In relation to the effect of biocides on biofilm formation, subinhibitory concentrations of triclosan stimulated production of the polysaccharide cellulose in established *Salmonella typhimirium* biofilms (Tabak et al., 2007). The biocide has also been shown to alter the biofilm development of environmental organisms in triclosan contaminated waterways (Lubarsky et al., 2012). Chlorhexidine meanwhile, was able to augment the biofilm inducing abilities of other

sub-lethal concentration antibiotics in *P. aeruginosa* (Aka and Haji, 2015). The biocides benzalkonium chloride and sodium hypochlorite have also been shown to increase biofilm formation in *Salmonella enterica* (Capita et al., 2019). As biocides are globally accessible and both biofilm formation and antibiotic tolerance have been associated with antibiotic treatment failure, augmentation or induction of these processes by biocide exposure could be a serious clinical concern.

This study sought to gain insight into the potential threat of biocide exposure on patient antimicrobial treatment. This would be achieved by evaluating the effects of biocide exposure, with an emphasis on triclosan, affecting the antibiotic tolerance, biofilm formation, and transcriptome of the pathogen *S. aureus*. This short introduction will be complemented by further introductory material that is pertinent to the later chapters of this thesis.

In chapter 3, this study will determine how triclosan exposure affects the antibiotic tolerance of both *S. aureus* single cells, planktonic cultures, and biofilms. This chapter will also seek to identify any underlying nutritional and molecular mechanisms associated with the biocide mediated adaption of *S. aureus*.

In chapter 4, this work seeks to investigate how biocide exposure can affect the development of *S. aureus* biofilms. This will be done by evaluating how triclosan exposure influences the chemical microenvironments and architecture of *S. aureus* biofilms. This will be further investigated by discerning whether triclosan exposure alters the matrix composition of *S. aureus* biofilms. Following characterisation of biocide exposed biofilms; identification of any underlying nutritional and molecular mechanisms will be carried out. The effect of triclosan on the polymicrobial biofilm formation of *S. aureus* and *Pseudomonas aeruginosa* will be assessed.

Lastly, in chapter 5 RNA-Sequencing will be used to elucidate the effects of triclosan exposure on the transcriptome of both *S. aureus* planktonic cultures and biofilms. This will be used to interrogate the effects of biocide

exposure on antibiotic tolerance and biofilm formation across both lifestyles, and how these changes are regulated.

# 2. Materials and Methods

## 2.1 Bacterial growth and culture media

*S. aureus* was grown at 37°C on brain heart infusion (BHI) agar (Oxoid™) plates for 16-20 hours. For growth in liquid media *S. aureus* was grown at 37°C in BHI broth (Oxoid™) with shaking at 200 rpm for aeration unless stated otherwise. For growth of *P. aeruginosa* Luria Bertani (LB) agar (Oxoid™) at 37°C or LB broth (Oxoid™) at 37°C with 200 rpm shaking was used depending on requirements. When required, antibiotics were added to growth medium as follows: tetracycline 10 µg/mL (*S. aureus*), chloramphenicol 10 µg/mL (*S. aureus*), tetracycline 125 µg/mL (*P. aeruginosa*).

## 2.2 Bacterial strains

**Table 2.1. Table of strains used in this study.**

| Strain | Description | Reference |
|---|---|---|
| | ***S. aureus*** | |
| SH1000 | Derivative of NCTC8325-4; *rsbU* repaired | (Horsburgh et al., 2002) |
| SH1000 Δ*agr* | SH1000 Δ*agr*::*tetM* | (Jordana-Lluch et al., 2020) |
| HG001 | Derivative of NCTC8325; *rsbU* repaired, *tcaR* defective, carries prophages Φ11, Φ12, and Φ13. | (Herbert et al., 2010) Kindly donated by the Wolz group (University of Tübingen) |
| HG001 (p)ppGpp$^0$ | HG001 rsh/relP/relQ triple mutant (Δ$rsh_{syn}$, Δ*relP*, Δ*relQ*) | (Geiger et al., 2014) Kindly donated by the Wolz group (University of Tübingen) |
| HG001 Δ*codY* | HG001 Δ*codY::tet* | (Pohl et al., 2009) Kindly donated by the Wolz group (University of Tübingen) |

| | | |
|---|---|---|
| HG001 Δ*codY*(p)ppGpp$^0$ | HG001 quadruple mutant (Δ*rsh*$_{syn}$, Δ*relP*, Δ*relQ,* Δ*codY::tet*) | Kindly donated by the Wolz group (University of Tübingen) |
| USA300 JE2 | CA-MRSA | (McDougal et al., 2003) |
| NCTC8325-4 | Derivative of NCTC8325; *rsbU* and *tcarR* defective, cured of prophages Φ11, Φ12, and Φ13. | (Novick, 1967) |
| NCTC8325-4 GFP | pS10-GFP; Cm$^R$ | (Doherty et al., 2006) |
| | ***P. aeruginosa*** | |
| PAO1-N (Nottingham) | Diverged laboratory PAO1 isolate | (Holloway et al., 1979) |
| PAO1-N Δ*pqsA* | *pqsA* in-frame deletion mutant; AQ-negative | (Diggle et al., 2007) |
| PAO1-N Δ*lasI* | *lasI* in-frame deletion mutant | This lab collection |
| PAO1-N Δ*rhlI* | *rhlI* in frame deletion mutant | This lab collection |
| PAO1-N Δ*lasI*Δ*rhlI* | *lasI rhlI* double deletion mutant | This lab collection |
| PAO1-N Δ*pqsA*Δ*lasI*Δ*rhlI* | *pqsA lasI rhlI* triple deletion mutant | This lab collection |
| PAO1-W (Washington) mCherry | pME6032 mCherry; Tc$^R$ | This lab collection |

## 2.3 Antibiotic susceptibility testing

### 2.3.1 Antibiotics tested

Antimicrobials used for these experiments were triclosan (Igrasan; Sigma-Aldrich), ciprofloxacin (Sigma-Aldrich), vancomycin (Sigma-Aldrich), rifampicin (Sigma-Aldrich), chlorhexidine digluconate (Alfa Aesar) and benzalkonium chloride (Sigma-Aldrich).

### 2.3.2 Minimum inhibitory concentration (MIC) determination

96 well microtitre plates (Greiner Bio-One) were inoculated with *S. aureus* strains at an optical density of 600 nm ($OD_{600}$) of 0.05 in Mueller-Hinton

broth (Oxoid™). Minimum inhibitory concentrations (MICs) were determined by the broth microdilution method in accordance with EUCAST guidelines ((ESCMID), 2003).

### 2.3.3 Minimum bactericidal concentration (MBC) determination

10 µL of culture from 2.3.2 was plated on Mueller-Hinton agar (Oxoid™) to determine the minimum bactericidal concentration (MBC). If no growth was visible after 24 hours at 37°C the lowest concentration at which no growth was observed was deemed the MBC.

### 2.3.4 Minimum biofilm eradication concentration (MBEC)

MBEC experiments were conducted by inoculating 96 well microtitre plates with *S. aureus* at an $OD_{600}$ of 0.05 in Mueller-Hinton broth and incubating for 24 hours at 37°C to allow biofilm formation. Following this, a 2-fold dilution series of antibiotics was added to wells and biofilms incubated again in Mueller-Hinton broth with antibiotics for a further 24 hours at 37°C. After incubation, biofilms were removed from wells by vigorous scraping with pipette tips and sonicating at 30 kHz for 1 minute in sonication bath (Fisherbrand™). Disrupted biofilms were then spotted out onto Mueller-Hinton agar plates and the MBEC defined as the minimum antibiotic concentration at which viable colonies are not detected.

## 2.4 Nanosensor synthesis

### 2.4.1 Nanosensor materials

Oregon Green® 488 carboxylic acid (OG), 5-(and-6)-carboxyfluorescein (FAM) and 5-(and-6)-carboxytetramethylrhodamine (TAMRA) were obtained from Invitrogen™, USA. Acrylamide (≥99%), N,N′-methylenebis(acrylamide) (bisacrylamide, 99%), dioctylsulfosuccinate sodium (AOT), ammonium persulphate (APS, ≥98%), 3-acrylamidopropyltrimethyl ammonium hydrochloride (ACTA, 75 wt. % in

$H_2O$), polyoxyethylene(4)lauryl ether (Brij L4®), sodium tetraborate decahydrate (≥99.5%) and N,N,N,N-tetramethyl-ethylenediamine (TEMED, 99%) were purchased from Sigma-Aldrich, US. N-(3-Aminopropyl) methacrylamide hydrochloride (APMA, >98%) was obtained from Polysciences Inc, Germany. Hexane, ethanol absolute (99.5%) and phosphate buffer saline (PBS) were obtained from Fisher Scientific, UK. Unless otherwise mentioned, all the chemicals used throughout were of analytical grade.

### 2.4.2 Conjugation of the OG, FAM and TAMRA fluorophores to APMA

A 50 mM (pH 9.5) sodium tetraborate decahydrate buffer in water was prepared and used to make a 0.002 mmol APMA solution. For each fluorophore, 1 mg was weighed out in separate vials and suspended in 200 µL of the APMA solution. The mixtures were sonicated for 5 min before being incubated on an oscillator and room temperature for 24 h in the dark. The dyes were stored at −20°C for further use.

### 2.4.3 Synthesis of polyacrylamide pH-sensitive fluorescent nanosensors

For the synthesis of the nanosensors, 1.59 g AOT and 3.08 g Brij L4 were weighed out, mixed in a 250 mL round bottom flask, and deoxygenated for 15-20 min using argon while being stirred. A 500 mL round-bottom flask was used to deoxygenate 100 mL hexane for 30 min using argon before 42 mL of the deoxygenated hexane was added to the AOT and Brij solution. The flask was sealed with a stopper and a balloon under an argon atmosphere with continuous stirring. For the synthesis of neutral polyacrylamide nanosensors, 540 mg acrylamide and 160 mg bisacrylamide were dissolved in 1.5 mL deionised water, whereas 513 mg acrylamide, 152 mg bisacrylamide and 119 µL ACTA were used the preparation of positively charged polyacrylamide nanosensors. The APMA-fluorophore conjugates were added to the acrylamide solution using 15 µL OG-APMA, 15 µL FAM-APMA and 60 µL TAMRA-APMA.

The mixture was deoxygenated and added to the flask containing the surfactants and hexane using a syringe. After 10 min, 30 µL of APS (10% w/v) and 15 µL TEMED were added. The flask was deoxygenated again, sealed, wrapped in aluminium foil, and incubated on the stirrer for 2 hours. After the incubation, the hexane was removed using a rotary evaporator at 30°C and 30 mL of ethanol (100%) was added. The mixture was transferred to a 50 mL falcon tube and spun down at 3800 x *g* for 3 min. The supernatant was discarded, and the pellet re-suspended in 30 mL of ethanol (90% in water). The mixture was spun down again at 3800 x *g* for 3 min and washed twice in 30 mL ethanol (100%) and then suspended in 10 mL of ethanol (100%). The mixture was transferred into a clean 250 mL flask and the ethanol was removed using the rotary evaporator at 30°C before the nanosensors were collected and stored at −20°C in the dark until further use.

## 2.5 Planktonic pH measurements of *S. aureus*

Polyacrylamide pH-sensitive nanosensors were suspended in BHI, filter sterilised using 0.22 µm PES filters (Merck), and added to 96 well microtitre plates. *S. aureus* was also added to wells at a normalised $OD_{600}$ of 0.05 alongside nanosensors at a final concentration of 1 mg/mL. As well as a BHI alone and *S. aureus* alone control, other conditions added to nanosensor *S. aureus* mixture included 500 ng/mL triclosan, 500 µM oleic acid (Sigma-Aldrich) solubilised in 0.1% Brij 58 (Sigma-Aldrich), and 0.1% Brij 58 alone. To ensure pH measurements could be taken, 12 wells containing 1 mg/mL nanosensors in different pH buffers (pH 2.5-8, increasing at 0.5 intervals) were added.

Microtitre plates were then read using a plate reader (TECAN Spark®) to detect bacterial growth (absorbance at 600 nm) and nanosensor fluorescence (OG/FAM Ex/Em 488/520; TAMRA Ex/Em 540/580). Temperature was maintained at 37°C and measurements were taken at 15 minute intervals for 10 hours with 10 seconds shaking before each

measurement. Measurement conditions were set using the SparkControl™ software.

## 2.6 Scanning electron microscopy (SEM)

Silicon wafers were sterilised by dipping into 70% v/v ethanol and passing through a flame. Wafers were then added to 12 well plates (Thermo Fisher Scientific). Wafers were then added to wells containing 3 mL of BHI inoculated with *S. aureus* SH1000 WT normalised to $OD_{600}$ 0.05. *S. aureus* was either untreated or treated with 500 ng/mL triclosan. Microtitre plates containing wafers were then incubated statically for 48 hours at 37°C to allow biofilm formation. Following incubation, wafers were removed from media, added to 10% formaldehyde, and left for 10 minutes to allow fixation of the biofilm. Following fixation, wafers were gently washed twice in PBS and left to dry. Following wafer preparation, all SEM was carried out by Marit Kjærvik, Surface Analysis and Interfacial Chemistry, Bundesanstalt für Materialforschung und -prüfung, Germany according to Kjærvik et al. (2018).

## 2.7 Time-kill curve assays

*S. aureus* strains at $OD_{600}$ 0.01 were inoculated into either untreated BHI broth or BHI broth supplemented with biocides. The biocides used throughout this study were triclosan (500 ng/mL; 0.25x MIC), chlorhexidine digluconate (0.0001%; 0.25x MIC), and benzalkonium chloride (0.0002%; 0.5x MIC). For conditions requiring fatty acid supplementation, 500 µM oleic acid and 0.1% v/v Brij 58 for solubilisation of oleic acid was also added. Cultures were then incubated at 37°C in shaking conditions (200 rpm) for a period of 30 minutes to allow for acclimatisation to biocide and/or fatty acid supplementation.

Following this, inhibitory concentrations of antibiotics were added to relevant conditions. Throughout this study the antibiotics ciprofloxacin (1

µg/mL), vancomycin (2 µg/mL), rifampicin (40 ng/mL) were used. This resulted in four conditions per strain being present in each experiment, consisting of untreated *S. aureus*, biocide exposed, antibiotic treated, biocide exposed + antibiotic treated. Cultures were then returned to the incubator and samples were then taken every hour for 6-10 hours depending on the experiment. From these samples, the $OD_{600}$ was taken to track bacterial growth. In addition, dilution series' were generated and 10 µL diluted sample was spotted plated onto BHI agar plates and incubated at 37°C for 24 hours to allow growth of colonies. Colony forming units (CFUs) were then calculated to assess bacterial viability.

## 2.8 Confocal laser scanning microscopy (CLSM) of biofilms

### 2.8.1 Growth of *S. aureus* biofilms with pH-sensitive fluorescent nanosensors

Overnight cultures of *S. aureus* were diluted in BHI to $OD_{600}$ 0.05 and loaded into µ-slide 8-well glass bottomed chambers (ibidi, glass bottom). To detect pH changes within biofilms, pH-sensitive fluorescent nanosensors were also added alongside inoculum prior to biofilm formation at a final concentration of 1 mg/mL. Triclosan was also added to relevant wells at varying concentrations (10 ng/mL, 100 ng/mL, 500 ng/mL). Chambers were protected from light and then placed in a 37°C incubator for 48 hours in static conditions. Following incubation, cells were stained for 15 minutes with the nucleic acid stain 4',6-diamidino-2-phenylindole (DAPI) (Invitrogen™), which was added at a final concentration of 10 µg/mL. After staining, growth medium was removed and biofilms were imaged using a Zeiss LSM 700 compact confocal laser scanning microscope. For imaging, the 40x objective and appropriate fluorescence settings were used (DAPI=405 nm laser, OG/FAM=488 nm laser, TAMRA=555 nm laser).

### 2.8.2 Live/dead staining of biofilms

Overnight cultures of *S. aureus* were diluted in BHI to $OD_{600}$ 0.05 and loaded into µ-slide 8-well glass bottomed chambers (ibidi, glass bottom). Either 500 ng/mL triclosan, 0.0001% v/v chlorhexidine digluconate, or 0.0002% v/v benzalkonium chloride were added to relevant wells, allowing biofilms to form in the presence of biocides. For conditions requiring fatty acid supplementation, 500 µM oleic acid and 0.1% Brij 58 was also added. Chambers were then placed in a 37°C incubator for 48 hours in static conditions. Following this incubation period, growth medium was removed from the biofilms and replaced with fresh BHI growth medium. To investigate antibiotic tolerance either 4096 µg/mL ciprofloxacin, 512 µg/mL vancomycin or 512 µg/mL rifampicin were added to wells for 3 hours. Next, live/dead staining was carried out using 6 µM syto 9 and 30 µM propidium iodide (BacLight, Molecular Probes). Following this, the biofilms were imaged using a Zeiss LSM 700 compact confocal laser scanning microscope using the 10x or 40x objective and appropriate fluorescence settings (syto 9=488 nm laser, propidium iodide=555 nm laser).

### 2.8.3 Staining of biofilm matrix components

Overnight cultures of *S. aureus* were diluted to $OD_{600}$ 0.05 in BHI and loaded into µ-slide 8-well glass bottomed chambers (ibidi, glass bottom). Either 500 ng/mL triclosan, 0.0001% chlorhexidine digluconate, or 0.0002% benzalkonium chloride were added to relevant wells, allowing biofilms to form in the presence of biocides. For conditions requiring fatty acid supplementation, 500 µM oleic acid and 0.1% Brij 58 was also added. Chambers were then placed in a 37°C incubator for 48 hours in static conditions. For timepoint experiments, triclosan was added 48 hours before imaging, 24 hours before imaging, or 3 hours before imaging. To examine biofilm structure, the nucleic acid stain 4',6-diamidino-2-phenylindole (DAPI) was added at a final concentration of 10 µg/mL and the polysaccharide stain fluorescein-conjugated wheat germ agglutinin (WGA) (Invitrogen™) was added at a final concentration

of 10 µg/mL. The eDNA stain YOYO-1 (Life Technologies) added at 40 nM, and the matrix protein stain SYPRO Ruby (Molecular Probes), of which 30 µL undiluted stain was added to each 300 µL well, were also used. Following this, the biofilms were imaged using a Zeiss LSM 700 compact confocal laser scanning microscope using the 10x or 40x objective and appropriate fluorescence settings (DAPI=405 nm laser, fluorescein/YOYO-1=488 nm laser, SYPRO ruby=555 nm laser).

### 2.8.4 Imaging polymicrobial biofilms

Overnight cultures of *S. aureus* NCTC8325-4 GFP were diluted to $OD_{600}$ 0.05 in RPMI growth medium and loaded into µ-slide 8-well glass bottomed chambers (ibidi, glass bottom). Triclosan was added at a final concentration of 500 ng/mL to relevant wells, allowing biofilms to form in the presence of the biocide. Chambers were then placed in a 37°C incubator for an initial incubation of 24 hours in static conditions. *S. aureus* biofilms were then taken from the incubator and media removed. *P. aeruginosa* PAO1-W mCherry was then added at $OD_{600}$ 0.005 in RPMI to *S. aureus* biofilms. Polymicrobial biofilms were then returned to the incubator for a further 24 hours of static incubation at 37°C before imaging. To examine polysaccharide distribution within the biofilm the polysaccharide stain Alexa Fluor 680-conjugated wheat germ agglutinin (WGA) (Invitrogen™) was added at a final concentration of 10 µg/mL. Following this, polymicrobial biofilms were imaged using a Zeiss LSM 700 compact confocal laser scanning microscope using the 40x objective and appropriate fluorescence settings (GFP=488 nm laser, mCherry=555 nm laser, Alexa Fluor 680=639 nm laser).

### 2.8.5 Image analysis using Comstat software

Biomass of live cells, dead cells, and stained matrix components was analysed using Comstat software. The analysis features of this software have been explained in detail previously (Heydorn et al., 2000).

## 2.9 Single cell imaging to determine changes in cell size

*S. aureus* HG001 WT and HG001 (p)ppGpp$^0$ were grown to $OD_{600}$ 0.1 in BHI. Following this 500 ng/mL triclosan was added to appropriate conditions and then all conditions were grown at 37°C at 200 rpm for 30 minutes to allow triclosan acclimatisation. Following this, 1 µg/mL of ciprofloxacin was added to relevant conditions and all conditions were then incubated for an additional hour. Cells were then stained with the membrane stain nile red (Invitrogen™) at a final concentration of 10 µg/mL and 2 µL of stained cells was mounted onto 1% agarose pads. Fluorescence microscopy was then carried out with a Nikon Eclipse 50i using a 100X oil lens fitted with Nikon intenselight C-HGFI for light illumination. Images were captured by using Nikon Digital Sight DS-U3 connected to Nikon NIS-Elements F4.00.06 software and image analysis was processed by Image J software. ImageJ software was used to apply regions of interest (ROI) around individual *S. aureus* cells within images and cell diameter was calculating through Feret's diameter of ROIs.

## 2.10 Quantification of total saccharide using phenol-sulfuric acid method

2.5 mL of BHI was added to 24 well plates (Greiner Bio-One) and inoculated with $OD_{600}$ 0.05 *S. aureus*. Relevant wells were then treated with either 500 ng/mL triclosan, 500 µM oleic acid solubilised in 0.1% Brij 58, or a combination of both triclosan and solubilised oleic acid. Biofilms were grown statically at 37°C for 48 hours. Extracellular matrix extraction and total saccharide quantification carried out as described previously (Chiba et al., 2015).

## 2.11 Crystal violet staining of biofilms

1 mL of BHI was added to 24 well plates and inoculated with $OD_{600}$ 0.05 *S. aureus*. Relevant wells were then treated with either 500 ng/mL

triclosan, 500 µM oleic acid solubilised in 0.1% Brij 58, or a combination of both triclosan and solubilised oleic acid. Biofilms were grown statically at 37°C for 24 hours. Following initial incubation the protocol was carried out as described previously (O'Toole, 2011).

## 2.12 Polymicrobial endpoint CFU experiments

To 24 well plates 1 mL of 20% BHI (diluted in $dH_2O$) is added and inoculated with $OD_{600}$ 0.05 *S. aureus* NCTC8325-4 WT. Relevant wells were also treated with 500 ng/mL of triclosan. 24 well plates were then placed in a 37°C incubator for an initial incubation of 24 hours in static conditions. *S. aureus* biofilms were then taken from the incubator and media removed. *P. aeruginosa* PAO1-N WT and mutants were then added at $OD_{600}$ 0.005 in 20% BHI to *S. aureus* biofilms. Polymicrobial biofilms were then returned to the incubator for a further 24 hours of static incubation at 37°C. Following incubation, medium was removed and 1 mL PBS was added. Biofilms were then sonicated at 30 kHz for 1 minute and wells were scraped vigorously with a pipette tip to remove all biofilm. Biofilm suspensions were then serially diluted and spot plated onto *Pseudomonas* isolation agar (Oxoid™) and mannitol salt agar (MSA) (Oxoid™) to specifically isolate *P. aeruginosa* and *S. aureus*, respectively. Colony forming units (CFUs) were then calculated to assess endpoint viability of each species within the polymicrobial biofilms.

## 2.13 Statistical analysis

Ordinary one-way ANOVA with Tukey's multiple comparisons test was carried out for statistical analysis of crystal violet assays, phenol-sulfuric acid assays, polymicrobial endpoint CFU experiments, and for determination of biofilm biovolume after Comstat analysis. 2way ANOVA with Tukey's multiple comparisons test was used to statistically analyse live/dead biofilms once live/dead biovolume had been determined by Comstat analysis. 2way ANOVA with Sidak's multiple comparisons test

was used for statistical analysis of differences in cell diameter during *S. aureus* cell sizing experiments. All statistical analysis was carried out using GraphPad Prism 8.4.3 for Windows, (GraphPad Software, San Diego, California, USA).

## 2.14 RNA-Sequencing

### 2.14.1 Preparation of samples and RNA extraction

For planktonic samples, *S. aureus* HG001 was inoculated into 5 mL BHI at $OD_{600}$ 0.01 and grown at 37°C with 200 rpm shaking to an $OD_{600}$ 0.8. Planktonic treated (PT) *S. aureus* was then treated with 500 ng/mL for 1 hour, whilst planktonic untreated (PU) was grown for an hour unsupplemented. Following 1 hour of triclosan exposure 5 mL was spun down at 10,000 x *g* for 10 minutes and pellet was resuspended in 500 µL of TE buffer (30 mM Tris-HCl, 1 mM EDTA, pH 8.0).

For biofilm samples, petri dishes (Thermo Fisher Scientific) were inoculated with *S. aureus* HG001 at $OD_{600}$ 0.05 in 25 Ml BHI. Treated biofilms (BFT) were treated with 500 ng/mL triclosan and incubated alongside untreated biofilms (BFU) for 12 hours statically at 37°C to allow biofilm formation. Following 12 hours, media was removed and biofilms were washed in 5 mL BHI, scraped vigorously using a pipette tip and sonicated at 30 kHz for 1 minute. Following removal of biofilms from petri dishes, biofilms were spun down at 10,000 x *g* for 10 minutes and pellet was resuspended in 500 µL of TE buffer.

Extraction of RNA from *S. aureus* planktonic cultures and biofilms was performed using RNeasy® Protect Bacteria Mini Kit (Qiagen) and carried out according to manufacturer's instructions, with minor alterations. For enzymatic lysis of bacteria, 0.1 mg/mL of lysostaphin (Sigma-Aldrich) was used alongside proteinase K (Qiagen) and was incubated at 37°C with 200 rpm shaking for 60 minutes. Following enzymatic and chemical lysis of bacteria, samples were added to 2 mL lysing matrix B tubes (MP Biomedicals). Physical disruption of samples was carried out via bead

beating using the FastPrep® 5G (MP Biomedicals), with 5 passes at 5.0 m/s for 40 s. Samples were cooled on ice for 60 s between each pass. Following completion of RNeasy® Protect Bacteria Mini Kit protocol, TURBO™ DNase (Invitrogen) treatment was carried out in accordance with manufacturer's instructions. RNA quantity and purity was determined using a NanoDrop™ 1000 spectrophotometer (Thermo Fisher Scientific) and RNA integrity was measured using the Agilent Bioanalyzer 2100 (Agilent).

### 2.14.2 Library preparation and transcriptome sequencing

Total RNA was used by Novogene (UK) Co., Ltd. (Cambridge, UK) to generate sequencing libraries using NEBNext® UltraTM RNA Library Prep Kit for Illumina® (NEB, USA) following manufacturers recommendations and index codes were added to attribute sequences to each sample. Briefly, mRNA was purified from total RNA using poly-T oligo-attached magnetic beads. Fragmentation was carried out using divalent cations under elevated temperature in NEBNext First Strand Synthesis Reaction Buffer (5X). First strand cDNA was synthesized using random hexamer primer and M-MuLV Reverse Transcriptase (RNase H-). Second strand cDNA synthesis was subsequently performed using DNA Polymerase I and RNase H. Remaining overhangs were converted into blunt ends via exonuclease/polymerase activities. After adenylation of 3' ends of DNA fragments, NEBNext Adaptor with hairpin loop structure ligated to prepare for hybridization. In order to select cDNA fragments of preferentially 150~200 bp in length, the library fragments were purified with AMPure XP system (Beckman Coulter, Beverly, USA). Then 3 µl USER Enzyme (NEB, USA) was used with size-selected, adaptor ligated cDNA at 37 °C for 15 min followed by 5 min at 95 °C before PCR. Then PCR was performed with Phusion High-Fidelity DNA polymerase, Universal PCR primers and Index (X) Primer. Lastly, PCR products were purified (AMPure XP system) and library quality was assessed on the Agilent Bioanalyzer 2100 system. The clustering of the index-coded samples was performed on a cBot Cluster Generation

System using PE Cluster Kit cBot-HS (Illumina) according to the manufacturer's instructions. After cluster generation, the library preparations were sequenced on an Illumina platform and paired-end reads were generated.

## 2.15 Data analysis of RNA-Seq data carried out by Novogene (UK) Co., Ltd

### 2.15.1 Quality control

All data analysis was carried out by Novogene (UK) Co., Ltd. (Cambridge, UK). Raw data (raw reads) of FASTQ format were firstly processed through fastp. In this step, clean data (clean reads) were obtained by trimming reads containing adapter and removing poly-N sequences and reads with low quality from raw data. At the same time, Q20, Q30 and GC content of the clean data were calculated. All the downstream analyses were based on the clean data with high quality.

### 2.15.2 Reads mapping to *S. aureus* NCTC8325 reference genome

NCTC8325 reference genome and gene model annotation files were downloaded from National Centre for Biotechnology Information (NCBI) website directly. Both building index of reference genome and aligning clean reads to reference genome were used Bowtie2. (Langmead and Salzberg, 2012)

### 2.15.3 Novel gene and gene structure analysing

Rockhopper was used to identify novel genes, operon and transcription start sites. It can be used for efficient and accurate analysis of bacterial RNA-seq data, and that it can aid with elucidation of bacterial transcriptomes (McClure et al., 2013). Then, we extract upstream 700bp sequence of Transcription Start Site for predicting promoter using TDNN (Time-Delay Neural Network).

### 2.15.4 Quantification of gene expression level

FeatureCounts was used to count the read numbers mapped to each gene. Then FPKM of each gene was calculated based on the length of the gene and read count mapped to this gene. FPKM, expected number of Fragments Per Kilobase of transcript sequence per Millions base pairs sequenced, considers the effect of sequencing depth and gene length for the reads count at the same time, and is currently the most commonly used method for estimating gene expression levels (Trapnell et al., 2010).

### 2.15.5 Differential expression analysis of biological replicates

Differential expression analysis of two conditions/groups (two biological replicates per condition) was performed using the DESeq2 R package. DESeq2 provide statistical routines for determining differential expression in digital gene expression data using a model based on the negative binomial distribution. The resulting P-values were adjusted using the Benjamini and Hochberg's approach for controlling the false discovery rate. Genes with an adjusted P-value <0.05 found by DESeq were assigned as differentially expressed.

### 2.15.6 KEGG enrichment analysis of differentially expressed genes

KEGG (Kyoto Encyclopaedia of Genes and Genomes) is a database resource for understanding high-level functions and utilities of the biological system, such as the cell, the organism and the ecosystem, from molecular level information, especially large-scale molecular datasets generated by genome sequencing and other high-through put experimental technologies. ClusterProfiler R package was used to test the statistical enrichment of differential expression genes in KEGG pathways.

# 3. Biocides can induce antibiotic tolerance in *Staphylococcus aureus* via multiple regulatory mechanisms

## 3.1 Introduction

### 3.1.1 Antibiotic tolerance

As described earlier in section 1.3, antibiotic tolerance is distinct from both antibiotic resistance and persistence. The definition provided by Kester and Fortune (2014), that tolerance enables bacterial cells to survive a transient exposure to antibiotics that would otherwise be lethal, will be employed throughout this chapter to describe antibiotic tolerance. Antibiotic tolerance can be conferred through either genetic mutation or induced by environmental changes, and is facilitated by the slowing or halting of bacterial growth (Brauner et al., 2016; Balaban et al., 2019). Slowly growing bacteria are more able to survive transient exposures to bactericidal antibiotics due to the reduced activity of antibiotic target machinery and processes (Stewart, 2015). Dormancy is often synonymous with tolerance due to the inertia of cellular processes within dormant bacteria (McDermott, 1958; Brauner et al., 2016). Unlike resistant bacteria which may need higher concentrations of an antimicrobial to achieve bacterial killing, tolerant bacteria require a longer exposure time to an antimicrobial to provide the same level of killing achieved against susceptible bacteria (Brauner et al., 2016). Resistant bacteria are typically protected against a single antibiotic or a small group of closely related antibiotics, whilst tolerant bacteria can typically better withstand a broad array of antimicrobials (Brauner et al., 2016; Balaban et al., 2019). Furthermore, whilst resistance can be developed against any antibiotic, tolerance only protects against bactericidal antibiotics. This is because bacteriostatic drugs only stall bacterial growth and are therefore non-lethal, as tolerance also functions to reduce bacterial

activity; any observed differences are minor if detected at all (Kester and Fortune, 2014). The presence of tolerant bacterial populations in clinical settings has resulted in the widespread misclassification of these bacteria as resistant (Brauner et al., 2016), leading to flawed antimicrobial treatments and risking recurrent infection in patients (Hoiby et al., 2010, Stewart, 2015).

Biofilms are communities of bacteria and reservoirs of antibiotic tolerance (Chua et al., 2016). There are numerous mechanisms by which biofilms withstand antimicrobial treatment including reduced penetration of antimicrobials into the biofilm matrix (Limoli et al., 2015), the transfer and expression of resistance genes (Hoiby et al., 2010) as well as a generally slow growth rate (Lebeaux et al., 2014). This reduced rate of growth serves to protect bacteria by diminishing the efficacy of the majority of antimicrobials. For instance, nongrowing cells are impervious to the effects of penicillin based antibiotics, since their activity is reliant on cell growth during which the target enzymes are active as peptidoglycan crosslinking is required to construct the expanding cell envelope (Lewis, 2001). Other antimicrobials, such as DNA-gyrase inhibitor ciprofloxacin, are capable of killing nongrowing cells, but their antibacterial activity is greatly diminished in biofilms (Lewis, 2001). Cells located in the deeper regions of the biofilm are among the most resilient within the matrix enclosed community. This is because these cells have less access to nutrients resulting in slow growth rates (Nguyen et al., 2011), in addition to the increased diffusion distance required for antimicrobials to traverse to reach them (Lebeaux et al., 2014). The enduring resilience of biofilms has made them a severe clinical concern, particular with regards to chronic infections caused by biofilm forming bacteria such as *S. aureus* (Lister and Horswill, 2014).

Antibiotic tolerance in *S. aureus* is becoming increasingly relevant clinically. This is exemplified by the finding that between 6%-43% of *S. aureus* clinical strains were vancomycin tolerant (Appleman and Citron., 2010). It has been suggested that tolerance to vancomycin in *S. aureus* could be used as general marker for antibiotic tolerance of *S. aureus*

isolates (Britt et al., 2017). Furthermore, increased vancomycin tolerance has been found to correlate with increased mortality of patients with MRSA bacteraemia (Miyazaki et al., 2011). To add to this, Pasticci et al. (2011) found that a high proportion of *S. aureus* isolates (63%) taken from bacteraemic endocarditis patients being tolerant to oxacillin. In terms of patient outcomes, antibiotic tolerant *S. aureus* infections can present no clinical difference when compared to susceptible isolates (Pasticci et al., 2011). Alternatively, drug tolerant *S. aureus* can cause prolonged fevers and extended bacteraemia duration, increased treatment failures and even increased mortality rates (Britt et al., 2017). The clinical relevance of antibiotic tolerant *S. aureus* appears to be dependent on the site of infection, with poorer outcomes only being observed in endocarditis patients but not in patients without endocarditis (Rajashekaraiah et al., 1980).

### 3.1.2 Mechanisms underlying antibiotic tolerance in *S. aureus*

Growth phase is a potent influence on the degree of antibiotic tolerance exhibited by *S. aureus,* with stationary phase bacteria being considerably more tolerant than those in the exponential phase of growth are (Brauner et al., 2016; Balaban et al., 2019). In addition to the stationary phase, the lag phase of bacterial growth is also associated with antibiotic tolerance (Brauner et al., 2016). This typically occurs when starved bacteria are being transferred to a fresh, rich culture. The lag phase is metabolically distinct from stationary phase, as lag phase bacteria must adapt to a nutritionally rich environment after surviving in an environment exhausted of nutrients (Madar et al., 2013). Antibiotic tolerance is observed in this adaption phase and is therefore short-lived as tolerance dissipates once bacteria begin exponential growth (Joers, Kaldalu and Tenson, 2010). Periods of metabolic inactivity are often accompanied by reduced levels of intracellular ATP (Shan et al., 2017). Without ATP to drive active processes within the cell, the efficacy of bactericidal antibiotics can be markedly decreased. However, it should be noted that antibiotic

tolerance can occur irrespective of intracellular ATP concentrations, indicating that low levels of ATP are not an essential determinate for antibiotic tolerance in *S. aureus* (Wang et al., 2018).

There is a broad range of molecular strategies employed by *S. aureus* to facilitate antibiotic tolerance (Kuehl et al., 2020). The stringent response is one such strategy and is conserved among most bacterial species as a means to combat nutritional deficiencies (Irving and Corrigan, 2018). During the stringent response the alarmones ppGpp and pppGpp (collectively known as (p)ppGpp) are synthesised from ATP and GTP (pppGpp) or GDP (ppGpp). In *S. aureus,* alarmone synthesis is driven by three alarmone synthetases. These are the two small alarmone synthetases RelP and RelQ, as well as a larger protein RSH. RSH is bifunctional and equipped with a synthetase domain for alarmone synthesis and a hydrolase domain for the purpose of alarmone degradation. Hydrolysis of these alarmones in *S. aureus* has been shown to be essential for survival, as accumulation of (p)ppGpp results in cell death (Geiger et al., 2010; Gratani et al, 2018). RSH, RelP, and RelQ are triggered by different inducing stresses, including various antibiotics. Numerous studies have used the antibiotic mupirocin, an antibiotic that induces amino acid starvation, to induce RSH activity (Geiger et al., 2010; Geiger et al., 2014; Corrigan et al., 2016). RSH has been shown to be the only (p)ppGpp synthetase that is sensitive to amino acid starvation, with both RelP and RelQ instead being stimulated by cell envelope stress (Geiger et al., 2014). RelP and RelQ expression has been triggered by exposure to the cell wall targeting antibiotics ampicillin, oxacillin, and vancomycin (Geiger et al., 2014; Peyrusson et al., 2020). RelP expression is also considered to be pH dependent, with increased transcription in both low-pH (Weinrick et al., 2004) and alkaline conditions being observed (Anderson et al., 2010; Geiger et al., 2014).

Once the stringent response has been triggered, (p)ppGpp orchestrates global changes in gene expression, with steep downregulations of genes associated with proliferative functions, such as protein synthesis and DNA replication (Wolz, Geiger and Georke, 2010). Examples of

(p)ppGpp targets include DNA primase, which alarmones directly bind to slow replication elongation (Rymer et al., 2012; Liu, Bittner and Wang, 2015). Other genes associated with replication that are repressed by the stringent response include those encoding DNA helicases and genes of the recombination/repair system (Geiger et al., 2012). Translational machinery is also drastically downregulated by the stringent response, with targets including ribosomal proteins, translation initiation factor and translation elongation factor (Geiger et al., 2010; Geiger et al., 2012). Corrigan et al. (2016) found that the stringent response strongly inhibited both GTP synthesis proteins and GTPases. This is significant as unlike in *Proteobacteria*; the stringent response of *Firmicutes* such as *S. aureus* does not directly interact with RNA polymerases, instead modulating intracellular GTP levels to control transcription (Wolz, Geiger and Georke, 2010; Irving and Corrigan, 2018). Reductions in GTP synthesis, combined with the usage of GTP for (p)ppGpp synthesis, leads to inhibition of transcription of rRNA genes as the initiating nucleotide GTP is unavailable. Furthermore, the lack of GTPase activity impedes ribosome maturation, therefore halting protein production and slowing growth (Corrigan et al., 2016). As bactericidal antibiotics rely on the corruption of the function of active targets, the metabolic shutdown and quiescence induced by the stringent response renders these drugs largely ineffectual (Hobbs and Boraston, 2019).

GTP is a ligand for the transcriptional repressor CodY. The rapid reduction in intracellular GTP required for the synthesis of (p)ppGpp alarmones during the stringent response leads to the derepression of CodY target genes (Wolz, Geiger and Georke, 2010; Geiger and Wolz, 2013; Irving and Corrigan, 2018). CodY is seen as the regulatory switch between exponential and stationary phase, with derepression facilitating the expression of genes associated with survival in hostile environments (Geiger and Wolz, 2014). Most of the genes repressed by CodY are associated with the synthesis and transport of amino acids (Pohl et al., 2009; Geiger and Wolz., 2014), enabling CodY to aid in alleviating nutritional stresses, such as amino acid starvation, that induced the

stringent response. In addition, CodY derepression is also associated with increased virulence gene expression, some of which aid in biofilm formation (Pohl et al., 2009). Although CodY can interact with some of these virulence factors directly (Pohl et al., 2009), virulence modulation by CodY is mainly through activation of the *agr* quorum sensing system (Majerczyk et al., 2008; Pohl et al., 2009), which is itself weakly repressed by CodY, and expression of *agr*-controlled genes (Geiger et al., 2010). Notably, early expression of *agr* has been indicated in persistent MRSA infection and antibiotic treatment failure (Abdelhady et al., 2015). However, numerous studies have also found that *agr* dysfunction may also increase antibiotic tolerance, likely due to increased biofilm formation through a decrease in *agr*-mediated dispersal (Paulander et al., 2013; George et al., 2019).

## 3.2 Chapter aims

The work in this chapter describes how the biocide triclosan influences the antibiotic tolerance of the human pathogen *S. aureus.* Since antibiotic tolerance is a process associated with many regulatory pathways, multiple molecular mechanisms will be scrutinised. This includes the hypothesis posed by Westfall (2019) that triclosan-induced antimicrobial tolerance is a result of fatty acid starvation triggering the stringent response (Sadowski et al., 2014, Westfall et al., 2019). The role of potential regulatory cascades after stringent response activation, such as CodY derepression and activation of *agr* quorum sensing will also be considered. Following this, the scale of biocide induced antibiotic tolerance will be explored, both in terms of how broad the protection provided against antimicrobials is, and whether triclosan is the only biocide capable of inducing such protection. The previous work by Westfall et al. (2019) observed triclosan-induced antibiotic tolerance in planktonic culture, but not in biofilms, which is the most predominant and clinically problematic lifestyle of bacteria. Whilst studies investigating antimicrobial induced antibiotic tolerance in biofilms remains scarce, recently Salzer et al. (2020) found that vancomycin could induce antibiotic tolerance in *S. aureus* biofilms following treatment with subinhibitory concentrations with vancomycin. This chapter will seek to complement the findings of both Westfall et al. (2019) and Salzer and colleagues (2020), to determine if physiologically relevant levels of triclosan can induce antibiotic tolerance in *S. aureus* planktonic cultures and biofilms.

## 3.3 Results

### 3.3.1 Susceptibility profiles among *S. aureus* strains across different antibiotics and biocides

In order to observe changes in the antibiotic tolerance of *S. aureus* it was vital to determine the antibiotic susceptibility profile of all strains used throughout this study. The minimum inhibitory concentrations (MIC) and minimum bactericidal concentrations (MBC) of numerous antibiotics and biocides were evaluated. The MIC is the minimum concentration required to inhibit visible growth, whilst the MBC is the minimum concentration required to prevent growth even after subculture to antibiotic free media. Both the MIC and MBC values apply only to planktonic cultures. The minimum biofilm eradication concentration (MBEC), the minimum concentration required to prevent subculture of a biofilm, was also determined to ensure appropriate antibiotic concentrations were used for future biofilm experiments. SH1000, HG001, and USA300 strains were investigated as all three strains are utilised in subsequent experiments.

**Table 3.1. Average minimum inhibitory concentration, minimum bactericidal concentration and minimum biofilm eradication concentration of *S. aureus* strains against a panel of antibiotics and biocides.**

| Strain | Antimicrobial | Average MIC (µg/mL) (n=3) | Average MBC (µg/mL) (n=3) | Average MBEC (µg/mL) (n=3) |
|---|---|---|---|---|
| ***S. aureus* SH1000** | Triclosan | 2 | 8 | 64 |
| | Ciprofloxacin | 1 | 16 | 2048 |
| | Vancomycin | 2 | 16 | 256 |
| | Rifampicin | 0.02 | 4 | 256 |
| ***S. aureus* HG001** | Triclosan | 2 | 8 | 64 |
| | Ciprofloxacin | 1 | 16 | 2048 |
| | Vancomycin | 2 | 16 | 256 |
| | Rifampicin | 0.02 | 4 | 256 |
| | Chlorhexidine digluconate | 0.0004% | 0.0008% | |
| | Benzalkonium Chloride | 0.0004% | 0.0016% | |
| ***S. aureus* USA300 JE2** | Triclosan | 2 | 8 | 64 |
| | Vancomycin | 2 | 16 | 256 |
| | Rifampicin | 0.02 | 4 | 256 |

The three strains tested exhibited comparable MICs, MBCs and MBECs (Table 3.1). As expected, substantially higher concentrations of antibiotics were required to eradicate *S. aureus* biofilms compared to planktonic cultures. These results were used to inform the antibiotic concentrations used future antibiotic tolerance experiments, particularly the MICs of antibiotics for planktonic antibiotic tolerance experiments (section 3.3.4) and the MBECs for biofilm antibiotic tolerance experiments (section 3.3.5).

### 3.3.2 Sub-MIC and physiologically relevant levels of triclosan inhibit growth and metabolism of *S. aureus*

The effect of a physiologically relevant, sub-MIC level of triclosan on growth and metabolism of *S. aureus* SH1000 WT was investigated. For insight into any alterations in metabolism that may occur due to biocide treatment, the pH of the extracellular environment was assessed using pH-sensitive fluorescent nanosensors. In parallel, optical density at 600 nm was measured to assess bacterial growth. Alongside triclosan, the effects of oleic acid were investigated to determine whether the presence of exogenous fatty acids could potentially overcome any inhibitory effects upon fatty acid synthesis caused by triclosan exposure.

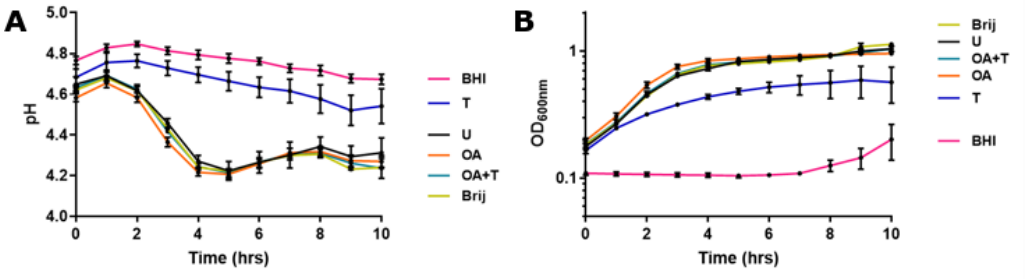



**Figure 3.1. Growth inhibition by triclosan corresponds with reduced environmental acidification. A)** Extracellular pH was measured using 1 mg/mL pH-sensitive fluorescent nanosensors. **B)** Optical density ($OD_{600}$) was also measured. Measurements were taken every 15 minutes with error bars (±SEM) shown every hour, n=3. Conditions include media alone (BHI), untreated *S. aureus* SH1000 (U) and cells

supplemented with either 0.1% Brij 58 (Brij), 500 ng/mL triclosan (T), 500 μM oleic acid solubilised in 0.1% Brij 58 (OA) or 500 μM oleic acid solubilised in 0.1% Brij 58 and 500 ng/mL triclosan (OA+T).

Treatment with sub-MIC, physiologically relevant levels of triclosan (500 ng/mL, 0.25x MIC) inhibited the growth of *S. aureus* (Fig 3.1B). This inhibition in growth was mirrored by changes in extracellular pH (Fig 3.1A), with pH decreasing at a far lower rate compared to untreated (U) conditions. An inverse relationship between growth and pH can be observed, with conditions displaying higher optical densities producing more acidic environments. Oleic acid and brij 58, which is used to solubilise oleic acid, caused no changes in pH or optical density compared to untreated samples. Notably, the combination of oleic acid and triclosan produced pH and optical densities nearly identical to untreated cells, indicating fatty acid supplementation can completely counteract the activity of this dosage of triclosan. It should be noted that the starting pH values for all conditions is lower than expected, for instance BHI typically has a pH of 7.4. This suggests the pH calibration for these experiments was inaccurate and shifted the pH of all conditions downward.

### 3.3.3. Inhibition in *S. aureus* cell division by physiological levels of triclosan can be observed at a single cell level

To further elucidate the effects of physiological levels of triclosan on *S. aureus* growth, *S. aureus* biofilms were imaged using SEM (Fig 3.2). *S. aureus* SH1000 biofilms were either untreated or exposed to triclosan upon initial inoculation and grown for 48 hours.

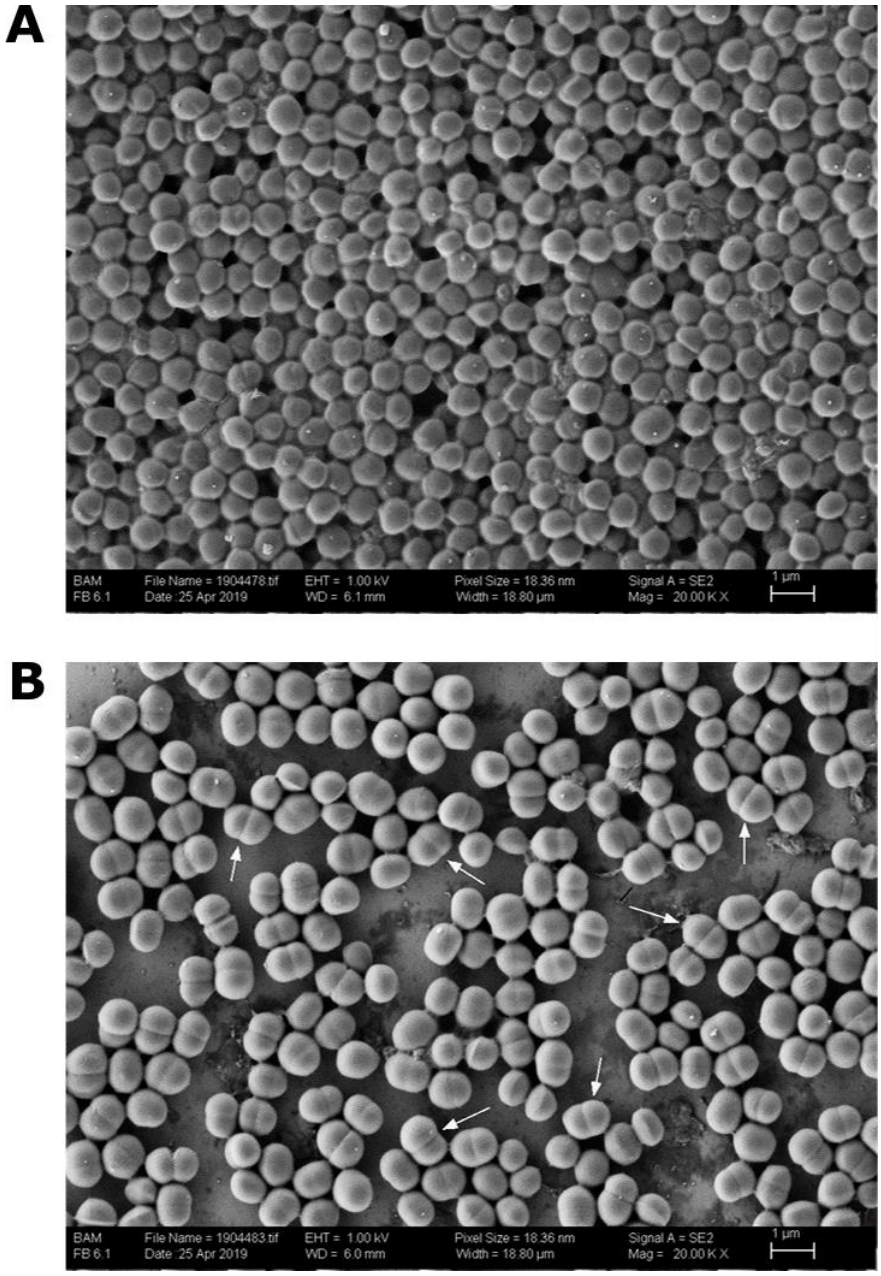



**Figure 3.2. Sub-MIC levels of triclosan impair cell division of *S. aureus*.** SEM images of *S. aureus* SH1000 untreated **(A)** and 500 ng/mL triclosan treated **(B)** 48 hr biofilms. Examples of prolonged septation are annotated using white arrows. Images were taken at 20000x magnification.

Untreated biofilms (Fig 3.2A) appear much more densely populated compared to triclosan exposed biofilms (Fig 3.2B). Triclosan treated biofilms also have a much higher proportion of bacteria in the septation stage of cell division. This, alongside the lower observable population of cells, suggests a delaying or halting of cell division in *S. aureus* after

triclosan exposure that persists throughout the entire 48 hrs of biofilm formation.

### 3.3.4 Pretreatment with physiologically relevant levels of triclosan induce antibiotic tolerance to ciprofloxacin in planktonic *S. aureus*

To determine if triclosan exposure was capable of inducing antibiotic tolerance in planktonic *S. aureus* cultures, triclosan was added to *S. aureus* SH1000 WT cultures 30 minutes prior to the addition of bactericidal concentrations of ciprofloxacin (1 µg/mL). Triclosan was added at the subinhibitory concentration of 500 ng/mL, corresponding to physiologically relevant concentrations of triclosan found in the urine of users of triclosan-containing products. Untreated, triclosan alone, and ciprofloxacin alone controls were included. Every hour, optical density measurements at 600 nm were taken to monitor growth whilst samples were spot plated to determine cell viability by colony forming units/mL (CFU/mL).

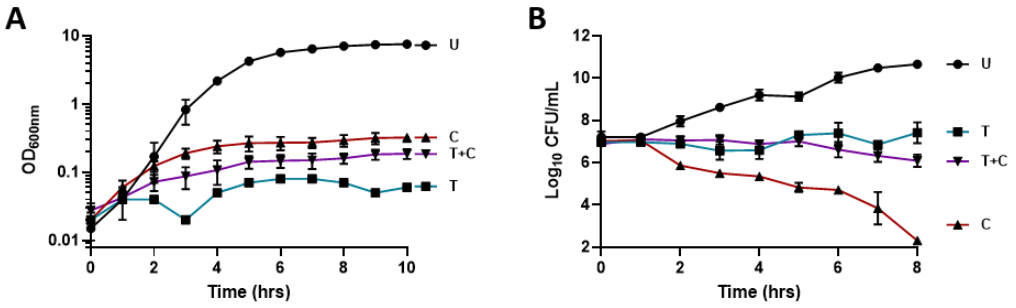
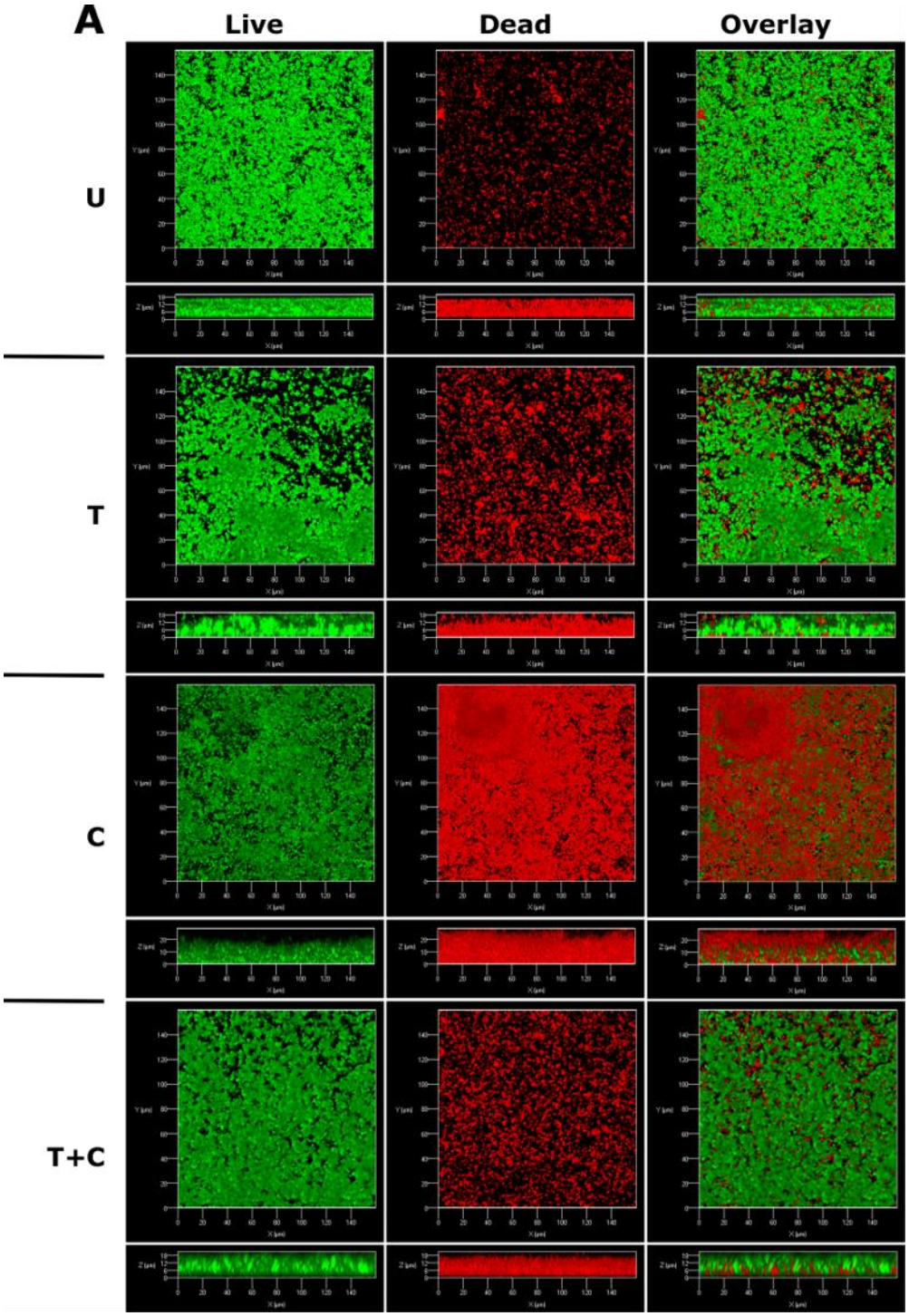



**Figure 3.3. Pretreatment with triclosan protects *S. aureus* from ciprofloxacin treatment.** *S. aureus* strain SH1000 was incubated in BHI in the presence or absence of triclosan for 30 mins at 37°C. Inhibitory concentrations of ciprofloxacin were added and incubation continued. Untreated (U), 500 ng/mL triclosan pretreated (T), 1 µg/mL ciprofloxacin treated (C), 500 ng/mL triclosan pretreated and 1 µg/mL ciprofloxacin treated (T+C) conditions are shown. **A)** Growth curve showing optical densities ($OD_{600}$) plotted against time. Error bars display ±SEM, n=3. **B)** Ciprofloxacin time-kill assays with $Log_{10}$ CFUs plotted against time. Error bars display ±SEM, n=3.

Triclosan pretreatment provided drastic protection from inhibitory concentrations of ciprofloxacin. Viable cell counts in all triclosan-exposed conditions remained relatively constant throughout the time-kill assays, whilst conditions treated with ciprofloxacin alone displayed a sharp decrease in cell viability over time. Triclosan-induced protection resulted in a 100-fold increase in cell survival in the presence of ciprofloxacin, a DNA gyrase inhibitor, by 3 hours of antibiotic exposure, and a 1000-fold difference by 5 hours (Fig 3.3A). The growth profiles in Fig 3.3B show that all treatments (T, C, T+C) lead to drastic inhibitions of growth, despite triclosan being administered at a sub-MIC dose. The mismatch between optical density and $\log_{10}$CFU/mL should be noted. Although the T, C, T+C conditions prevented detectable broth growth, biocide pretreated bacteria exhibited 2-3 log higher CFUs than ciprofloxacin only treated bacteria, illustrating the difference between growth and viability assays.

### 3.3.5 Exposure to subinhibitory concentrations throughout biofilm development can protect *S. aureus* biofilms from eradication by ciprofloxacin treatment

Following the demonstration that triclosan protects planktonic bacteria against ciprofloxacin, the ability of triclosan to induce tolerance *S. aureus* SH1000 WT biofilms was investigated. Triclosan was added alongside the initial inoculum of *S. aureus*, allowing the biocide to affect the bacteria throughout the full 48 hours of biofilm development. Following this, concentrations of ciprofloxacin above the minimum biofilm eradication concentration were added to biofilms and incubation continued for 3 hours. Biofilm viability was assessed by CLSM using the live/dead stains syto 9 and propidium iodide.


A
Live
Dead
Overlay
U
T
C
T+C

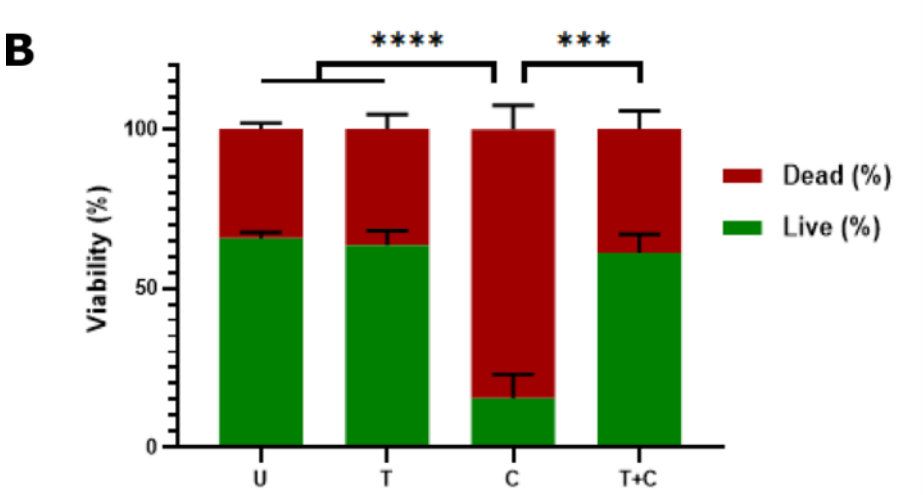



**Figure 3.4. Triclosan exposure increases biofilm tolerance to ciprofloxacin. A)** CLSM was used to assess the effect of triclosan on the antibiotic tolerance of *S. aureus* SH1000 WT. Syto 9 (green) was used to visualise live cells, whilst propidium iodide (red) was used to visualise cell death. Untreated (U), 500 ng/mL triclosan exposed (T), 4096 µg/mL ciprofloxacin treated (C) and 500 ng/mL triclosan exposed biofilms treated with 4096 µg/mL ciprofloxacin (T+C) are shown. For each condition, the top row shows the top surface of the *S. aureus* biofilms, with the biofilm thickness profile presented below. Horizontal lines on the left are used to segregate conditions. Images are representative of multiple experiments and were taken using the 40x objective (n = 3). **B)** Live/dead quantification was carried out using Comstat image analysis software. Error bars represent SEM, n=3. **** denotes P≤0.0001, *** denotes P≤0.001.

Treatment with high concentrations of ciprofloxacin (2x MBEC) resulted in a dramatic increase in cell death, however, ciprofloxacin treatment of triclosan pre-exposed biofilms resulted in significantly less cell death (Fig 3.4A-B). Triclosan pretreatment prior to ciprofloxacin treatment resulted in proportions of live cells comparable to those of untreated biofilms. Triclosan pretreatment alone also had minimal effect on biofilm viability.

### 3.3.6 Planktonic *S. aureus* can utilise exogenous fatty acids to prevent triclosan-induced antibiotic tolerance

Antibiotic tolerance is often associated with nutritional starvation. As triclosan is a fatty acid synthesis inhibitor, it was investigated whether oleic acid supplementation could counter fatty acid starvation caused by

triclosan, thereby preventing triclosan-induced antibiotic tolerance. A physiologically relevant concentration of oleic acid (500 μM), consistent with the levels of fatty acids found in human serum, was added alongside triclosan pretreatment. Following pretreatment, an inhibitory concentration of ciprofloxacin was added and optical densities and CFU/mL was measured every hour for 8 hours.

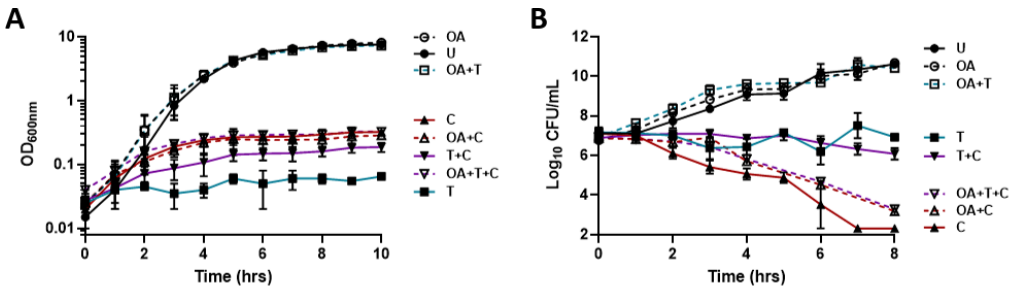
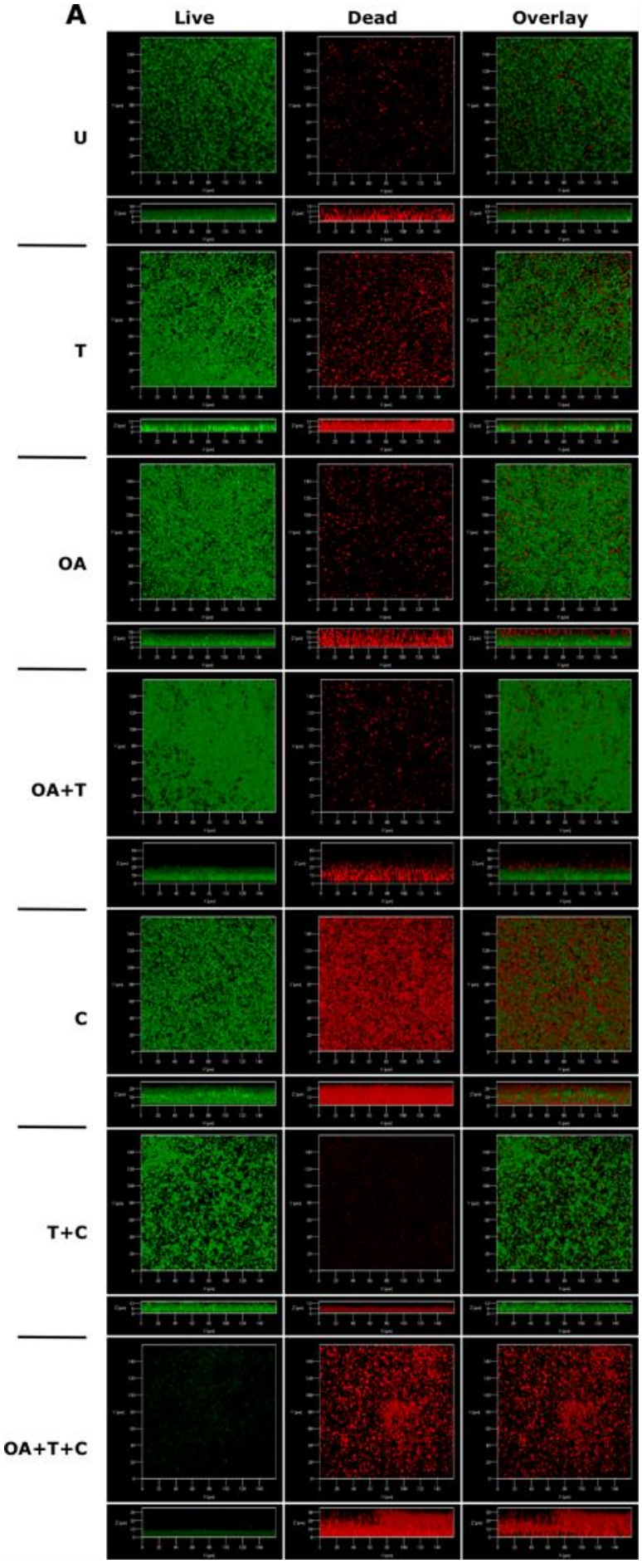



**Figure 3.5. Supplementation with exogenous fatty acids restores susceptibility to ciprofloxacin in triclosan exposed *S. aureus*.** *S. aureus* strain SH1000 was incubated in BHI in the presence or absence of triclosan, with or without 500 μM oleic acid solubilised in 0.1% Brij 58, for 30 mins at 37°C. Inhibitory concentrations of ciprofloxacin were added and incubation continued. Untreated (U, OA), 500 ng/mL triclosan pretreated (T, OA+T), 1 μg/mL ciprofloxacin treated (C, OA+C), 500 ng/mL triclosan treated and 1 μg/mL ciprofloxacin treated (T+C, OA+T+C) conditions are shown. **A)** Growth curve showing optical densities ($OD_{600}$) plotted against time. Error bars display ±SEM, n=3. **B)** Ciprofloxacin time-kill assays with $Log_{10}$ CFUs plotted against time. Error bars display ±SEM, n=3.

The data presented in Fig 3.5A suggest that fatty acid starvation caused by triclosan plays a role in protecting the bacteria against ciprofloxacin since oleic acid supplementation, caused triclosan pretreated cultures to be just as susceptible to ciprofloxacin (OA+T+C) as cultures that received no triclosan pretreatment (OA+C). Oleic acid had no effect on the growth or viability of untreated or ciprofloxacin alone conditions (OA, OA+C) (Fig 3.5B). OA+T conditions demonstrated growth and viability similar to an untreated sample, demonstrating that the presence of fatty acids negates the activity of subinhibitory concentrations of triclosan.

### 3.3.7 Oleic acid supplementation also restores susceptibility to ciprofloxacin in triclosan-exposed biofilms

Since oleic acid could alleviate triclosan-induced ciprofloxacin tolerance in planktonic culture, it was explored whether fatty acid supplementation could influence triclosan-induced antibiotic tolerance in *S. aureus* biofilms. Oleic acid was added alongside subinhibitory concentrations of triclosan during initial biofilm inoculation, and left for 48 hours prior to antibiotic treatment and imaging.


A
Live
Dead
Overlay
U
T
OA
OA+T
C
T+C
OA+T+C

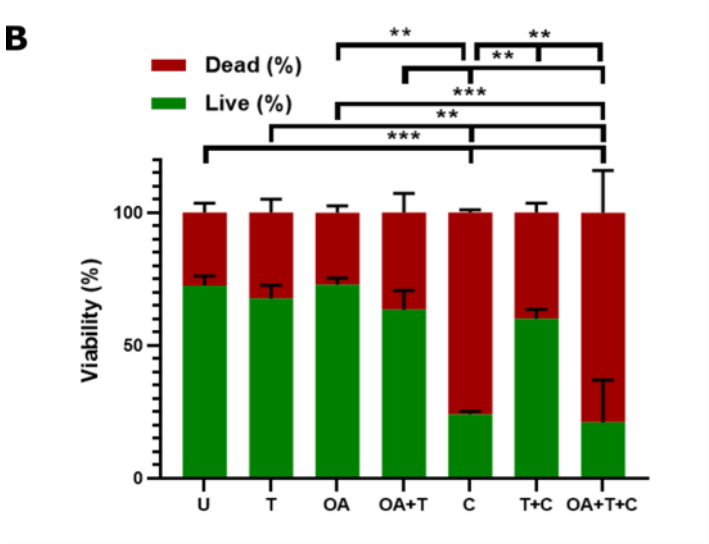



**Figure 3.6. Triclosan exposure increases biofilm tolerance to ciprofloxacin, but susceptibility can be restored with oleic acid supplementation. A)** CLSM was used to assess the effect of triclosan on the antibiotic tolerance of *S. aureus* SH1000 WT. Syto 9 (green) was used to visualise live cells, whilst propidium iodide (red) was used to visualise cell death. In the presence or absence of 500 µM oleic acid, untreated (U, OA), 500 ng/mL triclosan exposed (T, OA+T), 1 µg/mL ciprofloxacin treated (C) and 500 ng/mL triclosan exposed biofilms treated with 1 µg/mL ciprofloxacin (T+C, OA+T+C) are shown. For each condition, the top row shows the top surface of the *S. aureus* biofilms, whilst the second row of each condition shows the biofilm thickness profile. Horizontal lines on the left are used to segregate conditions. Images are representative of multiple experiments and were taken using the 40x objective (n = 3). **B)** Live/dead quantification was carried out using Comstat image analysis software. Error bars represent SEM, n=3. *** denotes P≤0.001, ** denotes P≤0.01.

The near identical appearance of live/dead biofilm images for untreated, triclosan treated and their oleic acid supplemented counterparts demonstrate that neither the fatty acid, biocide, nor the combination greatly alter biofilm viability (Fig 3.6A). Cell death in the OA+T+C treatment paralleled that of the ciprofloxacin only treatment and was significantly higher (~80%) compared to T+C biofilms (~40%) (Fig 3.6B). This finding demonstrates that oleic acid supplementation during biofilm formation can completely protect against triclosan-induced changes in ciprofloxacin susceptibility.

### 3.3.8 The *agr* quorum sensing system plays a role in triclosan-induced antibiotic tolerance in planktonic *S. aureus*

Past experiments have identified triclosan-induced antibiotic tolerance in *S. aureus* and ascertained that it is linked to fatty acid starvation caused by the biocide. However, a molecular mechanism for this has not been explored. As a first step towards characterising the mechanism behind triclosan-induced antibiotic tolerance in planktonic culture, an SH1000 strain with a defective *agr* quorum sensing system was compared to SH1000 WT since Agr influences a number of virulence and biofilm related phenotypes.

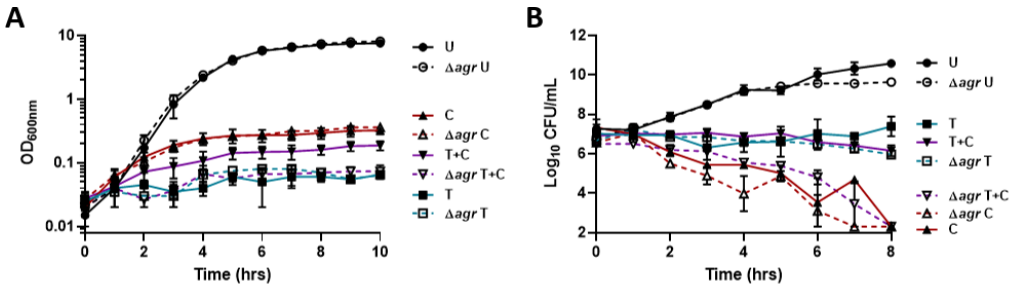


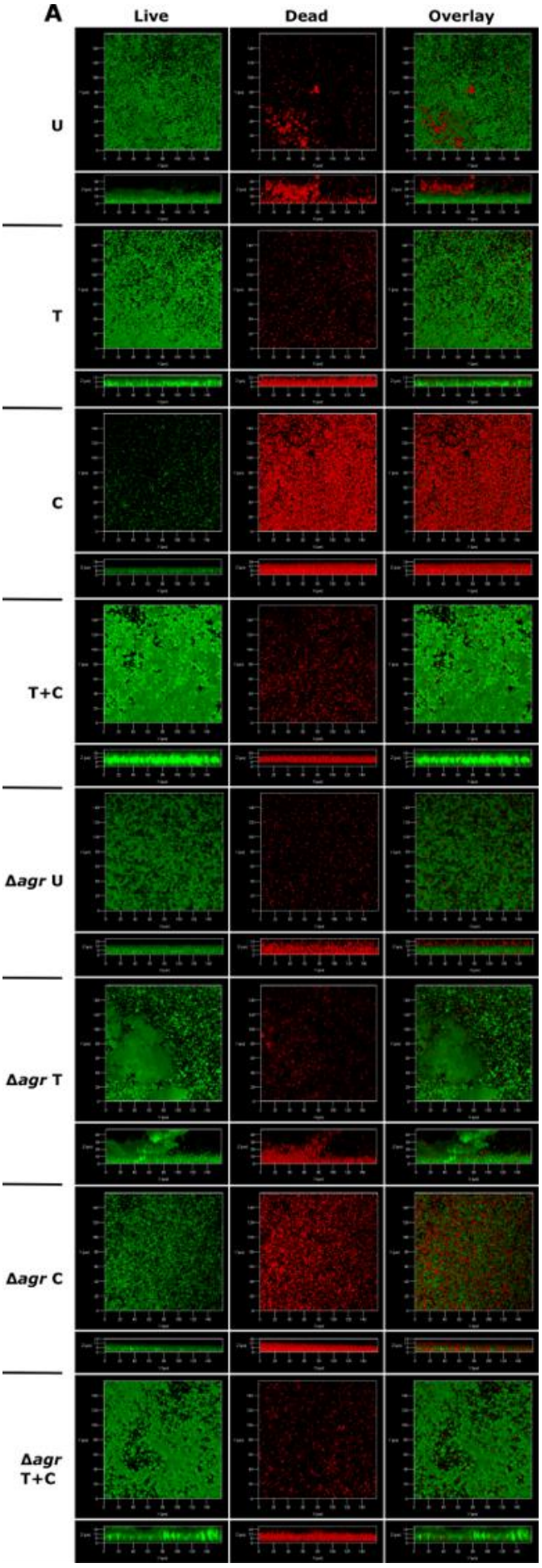

**Figure 3.7. Agr quorum sensing deficient mutants are not protected against ciprofloxacin by triclosan-induced tolerance.** *S. aureus* strains SH1000 WT and SH1000 Δ*agr* were incubated in BHI in the presence or absence of triclosan for 30 mins at 37°C. Inhibitory concentrations of ciprofloxacin were added and incubation continued. For both strains, untreated (U, Δ*agr* U), 500 ng/mL triclosan pretreated (T, Δ*agr* T), 1 µg/mL ciprofloxacin treated (C, Δ*agr* C), 500 ng/mL triclosan treated and 1 µg/mL ciprofloxacin treated (T+C, Δ*agr* T+C) conditions are shown. **A)** Growth curve showing optical densities ($OD_{600}$) plotted against time. Error bars display ±SEM, n=3. **B)** Ciprofloxacin time-kill assays with $Log_{10}$ CFUs plotted against time. Error bars display ±SEM, n=3.

Comparing $log_{10}$CFU/mL found that whilst notable differences in viability were detected between the C and T+C conditions in the WT, C and T+C in the Δ*agr* mutant displayed negligible differences (Fig 3.7A). The T+C conditions saw a 2-log reduction in survival at 5 hours and a 5-log reduction by 8 hours in the Δ*agr* mutant compared to the WT. These differences are despite the WT and Δ*agr* mutant displaying very similar viabilities for both the U and T conditions. Both strains also displayed

similar growth profiles to those seen in prior experiments, with T, C and T+C conditions showing arrested growth compared to the untreated condition. These results indicate the involvement of the *agr* quorum sensing system in triclosan-induced ciprofloxacin tolerance in *S. aureus*.

### 3.3.8 Triclosan-induced antibiotic tolerance in biofilms is unaffected by the *agr* quorum sensing system

After the promising results in planktonic culture showing that the *agr* quorum sensing system was necessary for biocide induced ciprofloxacin tolerance, the role of the *agr* system was assessed in *S. aureus* biofilms.


A
Live
Dead
Overlay
U
T
C
T+C
Δagr U
Δagr T
Δagr C
Δagr T+C

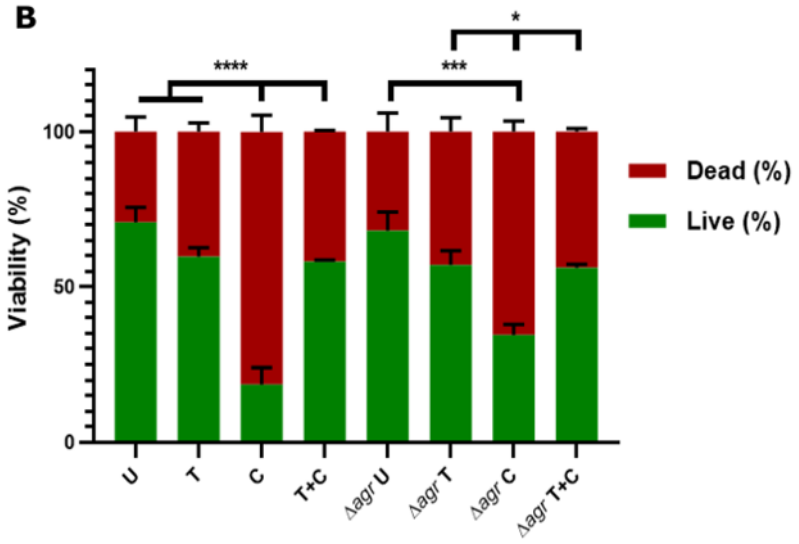



**Figure 3.8. The *agr* quorum sensing system does not prevent triclosan-induced ciprofloxacin tolerance in *S. aureus* biofilms. A)** CLSM was used to assess the effect of triclosan on the antibiotic tolerance of *S. aureus* SH1000 WT and *S. aureus* SH1000 Δ*agr*. Syto 9 (green) was used to visualise live cells, whilst propidium iodide (red) was used to visualise cell death. For both strains, untreated (U, Δ*agr* U), 500 ng/mL triclosan pretreated (T, Δ*agr* T), 4096 µg/mL ciprofloxacin treated (C, Δ*agr* C), 500 ng/mL triclosan pretreated and 4096 µg/mL ciprofloxacin treated (T+C, Δ*agr* T+C) biofilms are shown. For each condition, the top row shows the top surface of the *S. aureus* biofilms, whilst the second row of each condition shows the biofilm thickness profile. Horizontal lines on the left are used to segregate conditions. Images are representative of multiple experiments and were taken using the 40x objective (n = 3). **B)** Live/dead quantification was carried out using Comstat image analysis software. Error bars represent SEM, n=3. **** denotes P≤0.0001, *** denotes P≤0.001, * denotes P≤0.05.

Fig 3.8A shows little difference in the live/dead fluorescence between WT and Δ*agr* biofilms. Quantification of live/dead biomass during image analysis confirmed that conditions showed little notable variation between WT and mutant (Fig 3.8A). Δ*agr* showed modestly heightened survival against ciprofloxacin compared to the WT, but this was not statistically significant. Contrary to results seen in earlier planktonic experiments, the *agr* quorum sensing system does not appear to mediate biocide induced tolerance to ciprofloxacin in biofilms.

### 3.3.9 The global repressor CodY shows no involvement in biocide induced tolerance in planktonic culture

As the *agr* quorum sensing system did not demonstrate total responsibility for triclosan-induced tolerance in both planktonic and biofilm culture, other regulators were investigated. To determine whether the CodY global repressor was involved drug tolerance following biocide exposure, a Δ*codY* mutant was compared against the parental strain (HG001 WT) in a ciprofloxacin time-kill assay. CodY was selected due to its negative regulation of *agr*. Results in 3.3.8 suggested that *agr* may play a role in triclosan-induced antibiotic tolerance of planktonic *S. aureus* cultures. Using a Δ*codY* mutant, in which *agr* may have less negative regulation exerted upon it, may further inform on these previous results.

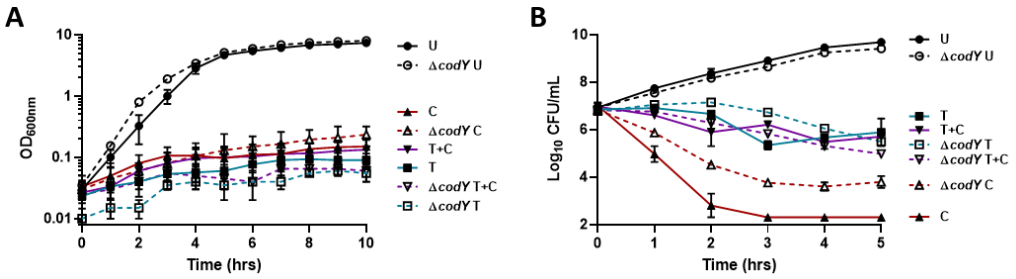



**Figure 3.9. The CodY repressor has no effect on triclosan-induced antibiotic tolerance in planktonic culture.** *S. aureus* strains HG001 WT and HG001 Δ*codY* were incubated in BHI in the presence or absence of triclosan for 30 mins at 37°C. Inhibitory concentrations of ciprofloxacin were added and incubation continued. For both strains, untreated (U, Δ*codY* U), 500 ng/mL triclosan pretreated (T, Δ*codY* T), 1 µg/mL ciprofloxacin treated (C, Δ*codY* C), 500 ng/mL triclosan treated and 1 µg/mL ciprofloxacin treated (T+C, Δ*codY* T+C) conditions are shown. **A)** Growth curve showing optical densities ($OD_{600}$) plotted against time. Error bars display ±SEM, n=2. **B)** Ciprofloxacin time-kill assays with $Log_{10}$ CFUs plotted against time. Error bars display ±SEM, n=2.

HG001 Δ*codY* displayed no obvious differences in viability when compared to HG001 WT across any of the conditions (Fig 3.9A). Likewise, no alterations in the growth profiles between the strains were detected by optical density (Fig 3.9B). From this data it appears that the

CodY repressor plays no role in planktonic biocide induced antibiotic tolerance.

### 3.3.10 The stringent response is essential for triclosan-induced antibiotic tolerance against multiple, mechanistically different antibiotics in planktonic culture

Previous literature has demonstrated that the stringent response can be associated with triclosan-induced antibiotic tolerance in planktonic *Escherichia coli* experiments. This study sought to determine whether this was also the case in *S. aureus* planktonic cultures and *S. aureus* biofilms. To assess this, an *S. aureus* stringent response mutant (HG001 (p)ppGpp$^0$; Δ*rsh* Δ*relP* Δ*relQ*) was subjected to planktonic time-kill assays, to determine if the stringent response is the molecular mechanism underlying triclosan-induced antibiotic tolerance in *S. aureus*.

Additionally, this experiment set out to determine the breadth of triclosan-induced tolerance by treating with inhibitory concentrations of other antibiotics alongside ciprofloxacin. These antibiotics were vancomycin (2 µg/mL, 1x MIC), an inhibitor of cell wall biosynthesis, and the protein synthesis inhibitor rifampicin (40 ng/mL, 2x MIC).

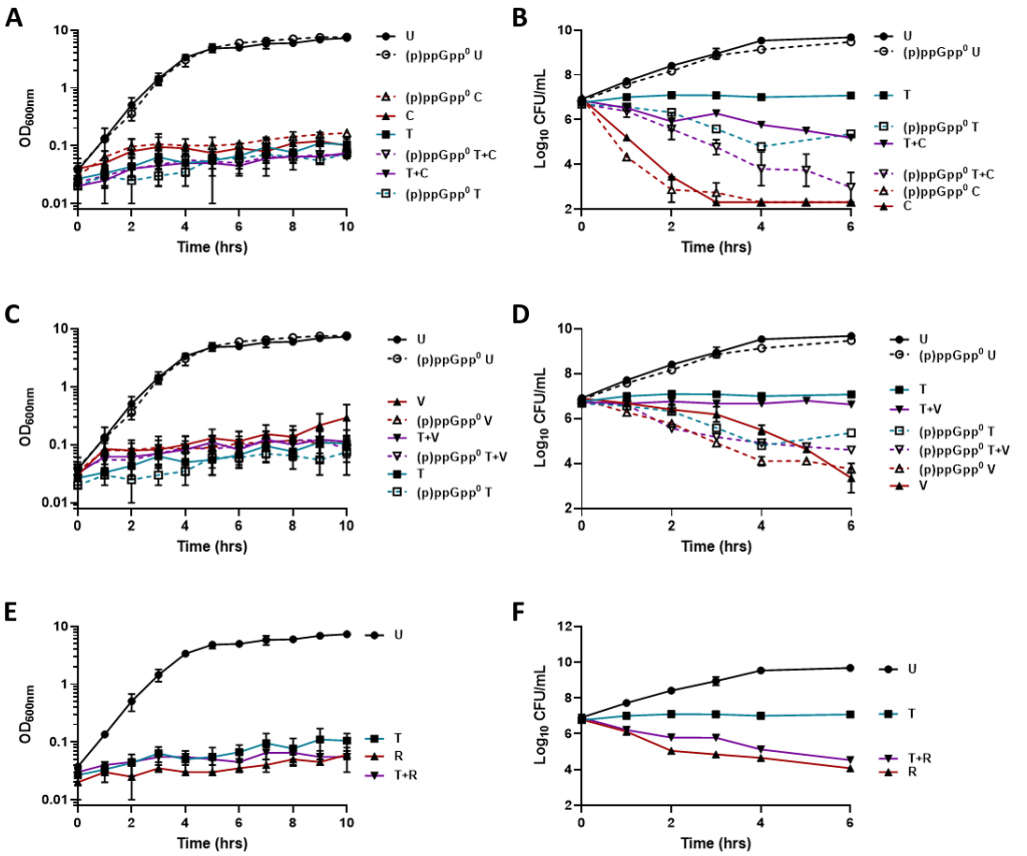


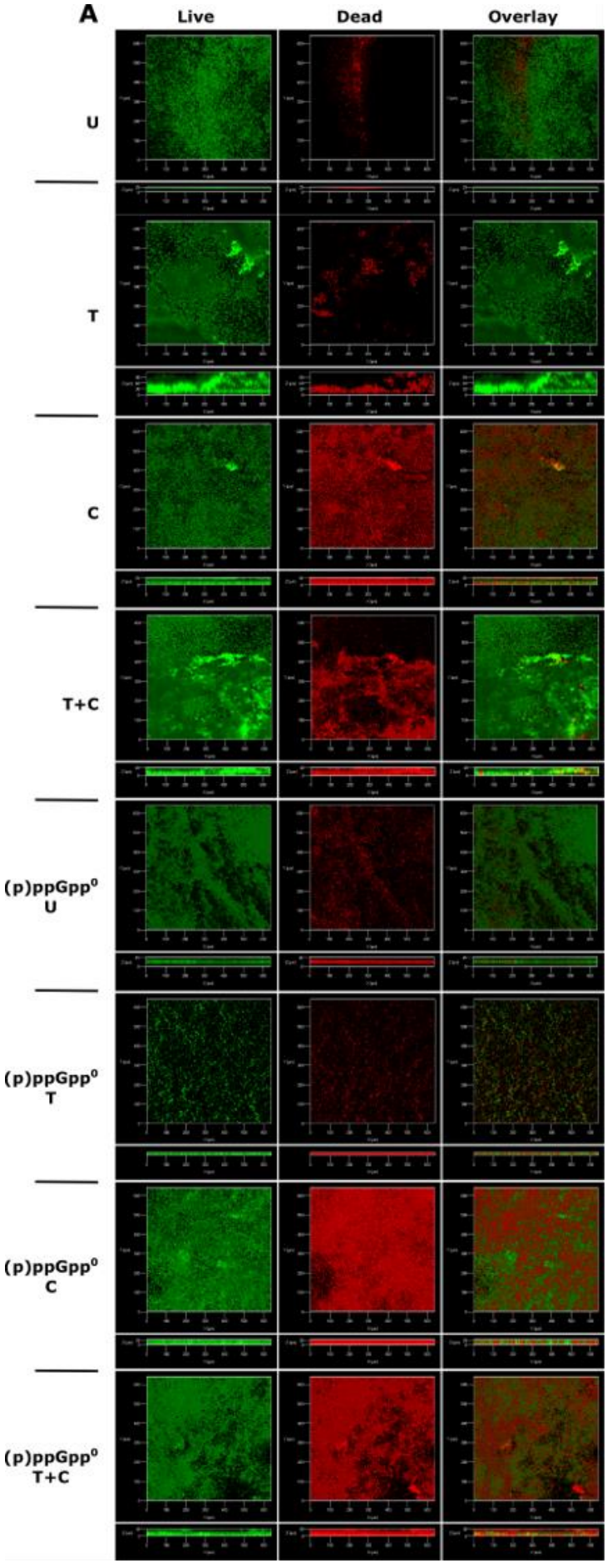

**Figure 3.10. The stringent response plays a role in triclosan-induced antibiotic tolerance against multiple antibiotics.** *S. aureus* strains HG001 WT and HG001 (p)ppGpp$^0$ were incubated in BHI in the presence or absence of triclosan for 30 mins at 37°C. Inhibitory concentrations of antibiotic were added and incubation continued. For both strains, untreated (U, (p)ppGpp$^0$ U), 500 ng/mL triclosan pretreated (T, (p)ppGpp$^0$ T), 1 µg/mL ciprofloxacin/2 µg/mL vancomycin/40 ng/mL rifampicin treated (respectively: C, V, R, (p)ppGpp$^0$ C, (p)ppGpp$^0$ V), 500 ng/mL triclosan treated and 1 µg/mL ciprofloxacin/2 µg/mL vancomycin/40 ng/mL rifampicin treated (T+C, T+V, T+R, (p)ppGpp$^0$ T+C, (p)ppGpp$^0$ T+V) conditions are shown. **A)** Growth curve showing optical densities ($OD_{600}$) plotted against time. Error bars display ±SEM, n=2. **B)** Ciprofloxacin, vancomycin or rifampicin time-kill assays with $Log_{10}$ CFUs plotted against time. Error bars display ±SEM, n=3 (ciprofloxacin, vancomycin), n=2 (rifampicin).

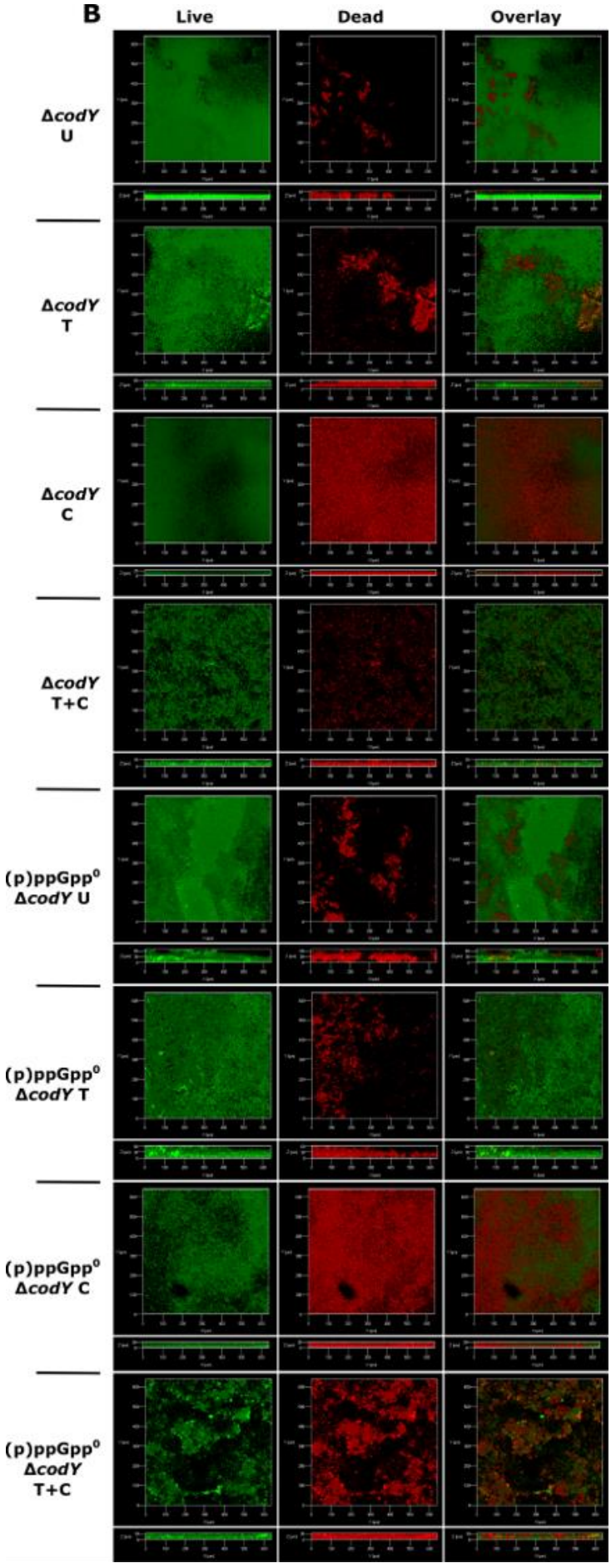
Optical densities displayed the same trends observed in previous experiments, with triclosan pretreatment, antibiotic treatments and triclosan antibiotic combination treatments halting growth (Figs 3.10B, 3.10D, 3.10F). No notable deviations in growth were observed between HG001 WT and HG001 (p)ppGpp$^0$ (Figs 3.10A, Figs 3.10C) nor in viable cell recovery in untreated conditions (Figs 3.10B, Figs 3.10D).

In the WT, triclosan protected *S. aureus* against both bactericidal antibiotics assessed (C and V). However, the mutant exhibited 2 log reductions in viability when exposed to C and V, irrespective of T pretreatment. This suggests a role for the stringent response in developing antibiotic tolerance following triclosan exposure. In contrast, triclosan pretreatment was unable to elicit a protective response against the bacteriostatic antibiotic rifampicin (Fig 3.10F), since minimal differences in viability between the R and T+R conditions were observed. These results show that triclosan can induce tolerance against vancomycin and that this tolerance may be mediated by the stringent response, but that triclosan cannot protect against the bacteriostatic antibiotic rifampicin.

### 3.3.11 The stringent response is essential for triclosan-induced antibiotic tolerance in biofilms, whilst the CodY repressor is not

Biofilm viability experiments were carried out to extend the interrogation of the molecular mechanisms underpinning triclosan-induced tolerance. The role of the stringent response was investigated using the HG001 (p)ppGpp$^0$ mutant, as triclosan pretreatment did not protect this strain from inhibitory concentrations of ciprofloxacin or vancomycin in planktonic time-kill assays. The HG001 Δ*codY* mutant was also explored despite showing no involvement in planktonic time-kill assays. This was because previous experiments using the SH1000 Δ*agr* mutant demonstrated the possibility of a regulatory system being involved in facilitating tolerance in one lifestyle, but not another. Finally, a Δ*codY*(p)ppGpp$^0$ mutant was used to determine if the loss of both the CodY repressor and the stringent response altered how triclosan-induced antibiotic tolerance was manifested.


A
Live
Dead
Overlay
U
T
C
T+C
(p)ppGpp0
U
(p)ppGpp0
T
(p)ppGpp0
C
(p)ppGpp0
T+C


B
Live
Dead
Overlay
ΔcodY U
ΔcodY T
ΔcodY C
ΔcodY T+C
(p)ppGpp0 ΔcodY U
(p)ppGpp0 ΔcodY T
(p)ppGpp0 ΔcodY C
(p)ppGpp0 ΔcodY T+C

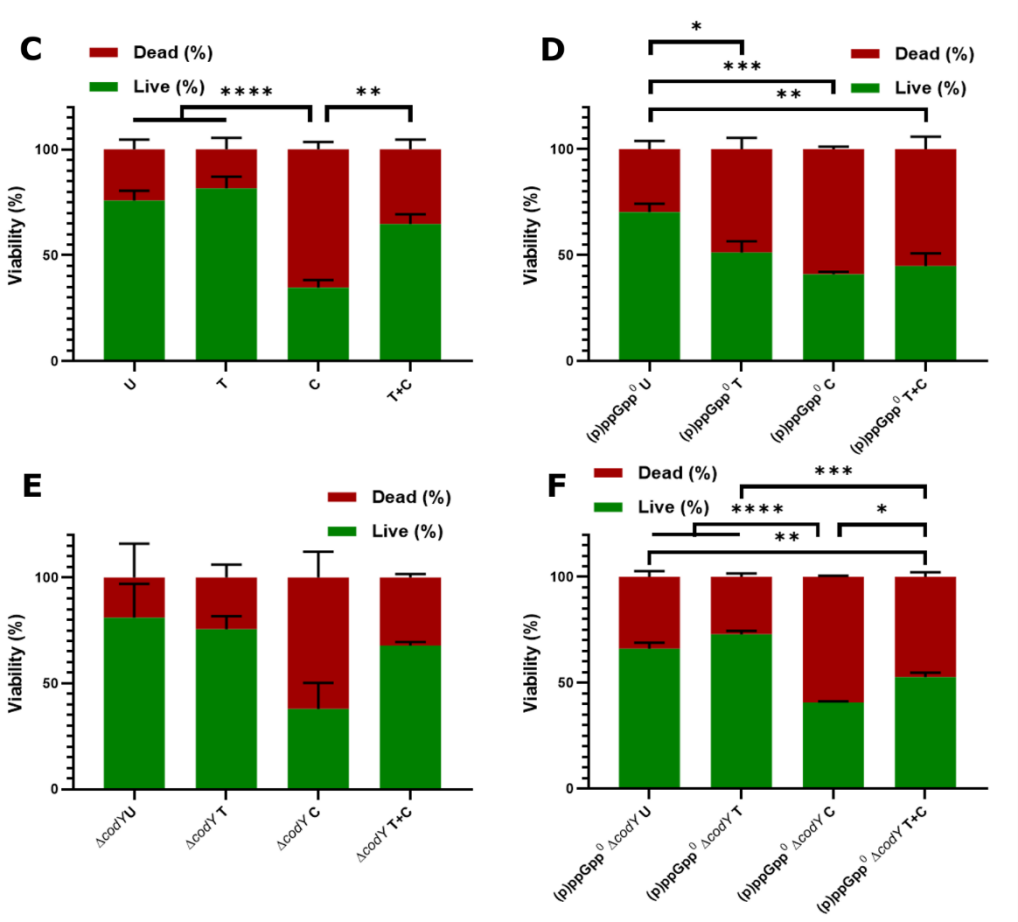
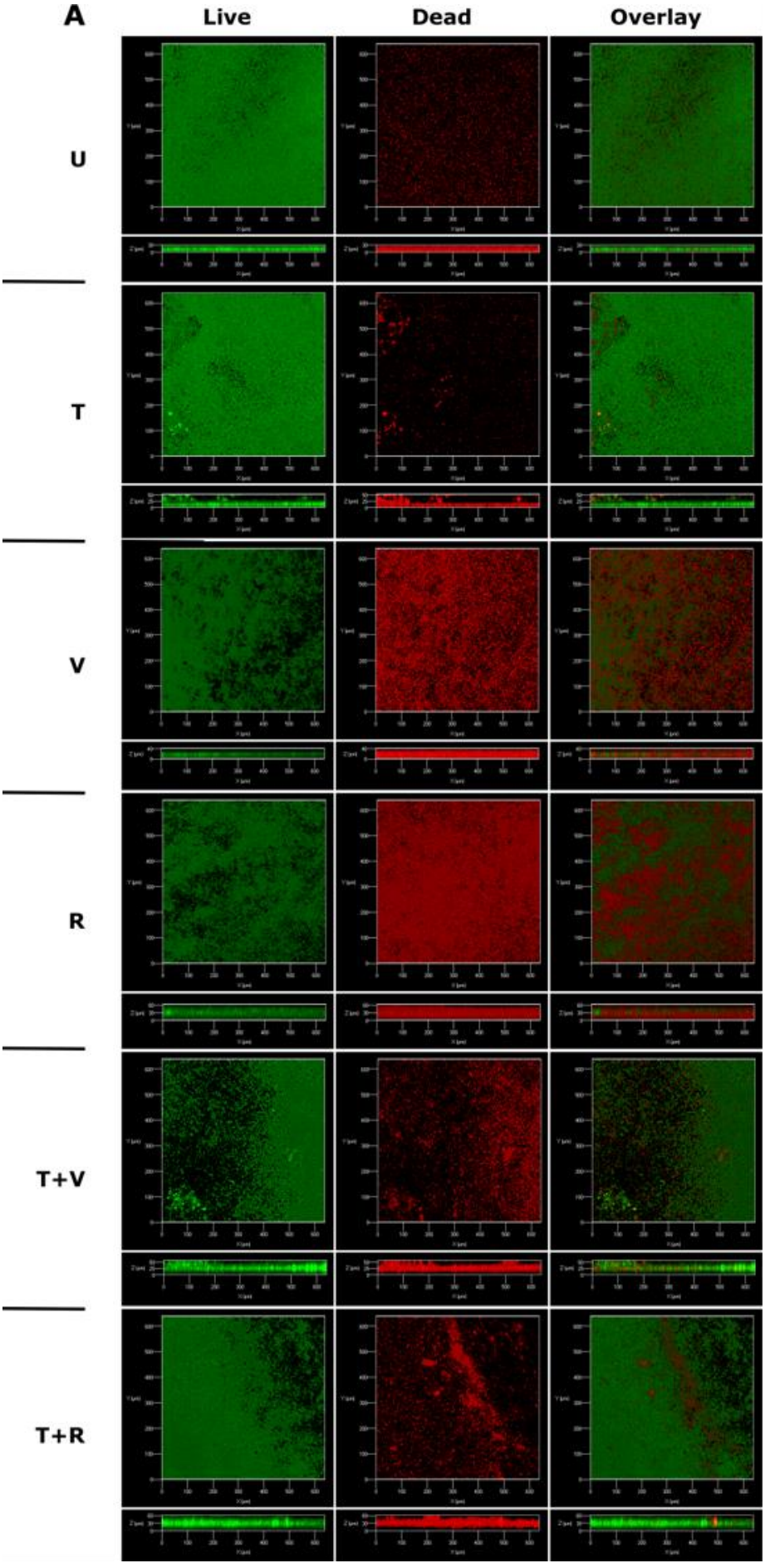


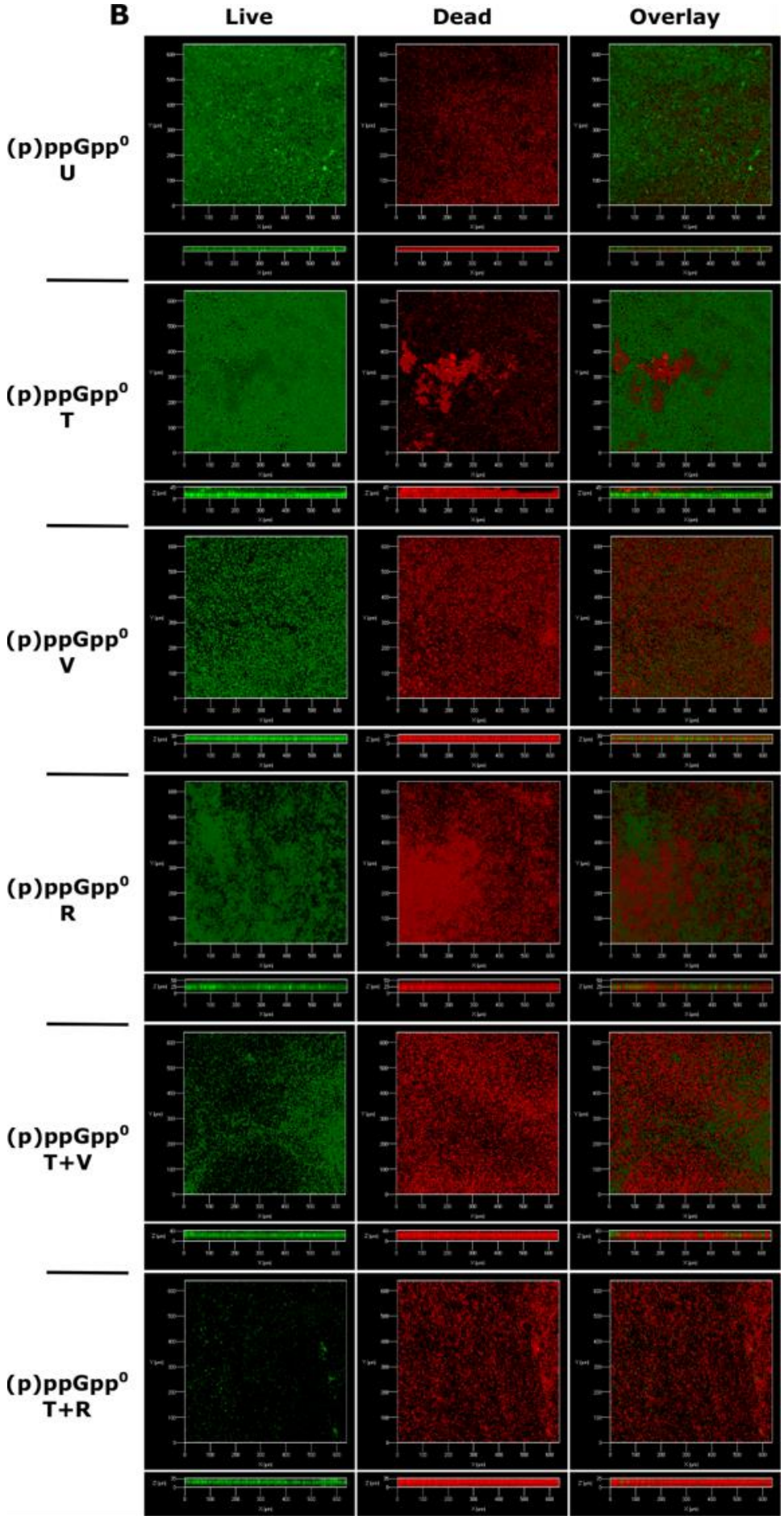

**Figure 3.11. The stringent response plays a role in triclosan-induced ciprofloxacin tolerance in *S. aureus* biofilms. However, the CodY repressor does not.** CLSM was used to assess the effect of triclosan on the antibiotic tolerance of *S. aureus* HG001 WT, HG001 (p)ppGpp$^0$ **(A)**, HG001 Δ*codY*, HG001 Δ*codY*(p)ppGpp$^0$ **(B)**. Syto 9 (green) was used to visualise live cells, whilst propidium iodide (red) was used to visualise cell death. For all strains, untreated (U, (p)ppGpp$^0$ U, Δ*codY* U, Δ*codY* (p)ppGpp$^0$ U), 500 ng/mL triclosan pretreated (T, (p)ppGpp$^0$ T, Δ*codY* T, Δ*codY* (p)ppGpp$^0$ T), 4096 µg/mL ciprofloxacin treated (C, (p)ppGpp$^0$ C, Δ*codY* C, Δ*codY* (p)ppGpp$^0$ C), 500 ng/mL triclosan pretreated and 4096 µg/mL ciprofloxacin treated (T+C, (p)ppGpp$^0$ T+C, Δ*codY* T+C, Δ*codY* (p)ppGpp$^0$ T+C) biofilms are shown. For each condition, the top row shows the top surface of the *S. aureus* biofilms, whilst the second row of each condition shows the biofilm thickness profile. Horizontal lines on the left are used to segregate conditions. Images are representative of multiple experiments and were taken using the 10x objective (Δ*codY* n=3, (p)ppGpp$^0$ n=3, Δ*codY* (p)ppGpp$^0$ n=2). **C-F)** Live/dead quantification was carried out using Comstat image analysis software. Error bars represent SEM, Δ*codY* n=3, (p)ppGpp$^0$ n=3, Δ*codY* (p)ppGpp$^0$ n=2. **** denotes P≤0.0001, *** denotes P≤0.001, ** denotes P≤0.01, * denotes P≤0.05.

Biofilm imaging in Fig 3.11A shows the (p)ppGpp$^0$ strain failing to withstand ciprofloxacin treatment despite triclosan exposure throughout biofilm maturation. This is mirrored in the quantification in which HG001 WT triclosan significantly protects HG001 WT against ciprofloxacin (Figs 3.11C), whilst the T+C condition of the (p)ppGpp$^0$ mutant demonstrates levels of viability comparative to C. Moreover, the inability of the (p)ppGpp$^0$ biofilm to handle stress is highlighted by the significant increase in cell death between the untreated and triclosan treated condition, two conditions that usually echo one another. The Δ*codY* mutant displays trends similar to that of the WT, though not significant (Fig 3.11E) whilst the Δ*codY* (p)ppGpp$^0$ quadruple mutant displays patterns in susceptibility very close to that of the (p)ppGpp$^0$ biofilm. One discernible difference between the (p)ppGpp$^0$ biofilms and the Δ*codY* (p)ppGpp$^0$ biofilms is that (p)ppGpp$^0$ has a reduced sensitivity to triclosan. To summarise, stringent response seems to play a key role in triclosan-induced antibiotic tolerance in *S. aureus* biofilms.

### 3.3.12 The stringent response facilitates triclosan-induced protection against differing classes of antibiotics in *S. aureus* biofilms

After establishing that triclosan-induced antibiotic tolerance occurred in *S. aureus* biofilms, and that it was enabled by the stringent response, the breadth of biocide induced tolerance in biofilms was examined. To expand on ciprofloxacin used in previous biofilm experiments, both vancomycin and rifampicin were added to biofilms at high concentrations (512 µg/mL, 2x MIC).


A
Live
Dead
Overlay
U
T
V
R
T+V
T+R


B
Live
Dead
Overlay
(p)ppGpp0
U
(p)ppGpp0
T
(p)ppGpp0
V
(p)ppGpp0
R
(p)ppGpp0
T+V
(p)ppGpp0
T+R

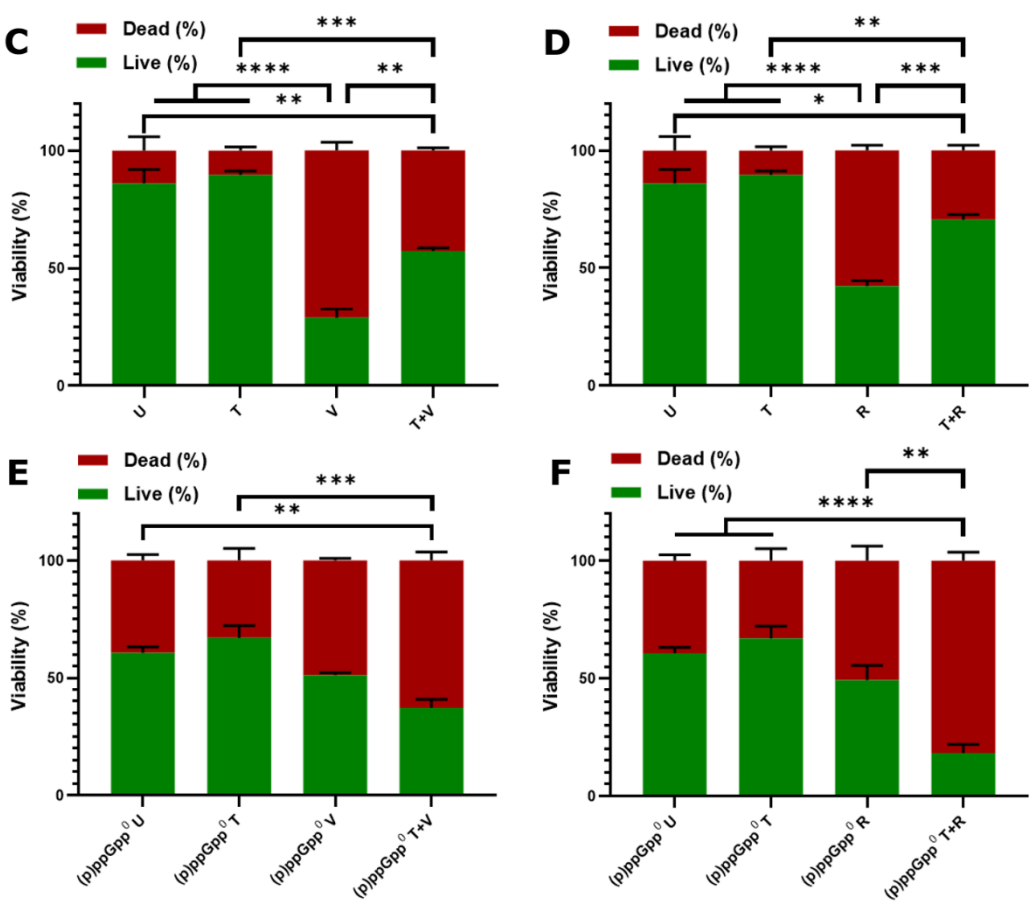



**Figure 3.12. The stringent response is also responsible for triclosan-induced antibiotic tolerance against vancomycin and rifampicin in *S. aureus* biofilms.** CLSM was used to assess the effect of triclosan on the antibiotic tolerance of *S. aureus* HG001 WT **(A)**, and HG001 (p)ppGpp$^0$ **(B)**. Syto 9 (green) was used to visualise live cells, whilst propidium iodide (red) was used to visualise cell death. For all strains, untreated (U, (p)ppGpp$^0$ U), 500 ng/mL triclosan pretreated (T, (p)ppGpp$^0$ T), 512 µg/mL vancomycin treated (V, (p)ppGpp$^0$ V), 512 µg/mL rifampicin treated (R, (p)ppGpp$^0$ R), 500 ng/mL triclosan pretreated and 512 µg/mL vancomycin treated (T+V, (p)ppGpp$^0$ T+V) and 500 ng/mL triclosan pretreated and 512 µg/mL rifampicin treated (T+R, (p)ppGpp$^0$ T+R) biofilms are shown. For each condition, the top row shows the top surface of the *S. aureus* biofilms, whilst the second row of each condition shows the biofilm thickness profile. Horizontal lines on the left are used to segregate conditions. Images are representative of multiple experiments and were taken using the 10x objective (n = 2). **C-F)** Live/dead quantification was carried out using Comstat image analysis software. Error bars represent SEM, n=2. **** denotes P≤0.0001, *** denotes P≤0.001, ** denotes P≤0.01, * denotes P≤0.05.

Live/dead confocal images in Fig 3.12A show visibly increased cell death (red fluorescence) in the V and R treatments compared to T+V and T+R

for the WT. These observations have been quantified in Figs 3.12C and 3.12D, from which it can be seen that triclosan pretreatment significantly protected against both vancomycin and rifampicin compared to antibiotic treatments alone. It should be noted that live cell percentages of the T+V and T+R conditions are significantly lower than untreated conditions, implying that whilst triclosan protection does significantly protect against antibiotic treatment, it does not provide complete protection. In contrast, Fig 3.12B shows visibly higher cell death relative to live cells in the V, R, T+V and T+R conditions in the (p)ppGpp$^0$ strain. Figs 3.12E and 3.12F show that not only does triclosan not protect against vancomycin and rifampicin, but that it acts additively with these antibiotics to increase cell death, in the case of rifampicin this is a statistically significant change.

### 3.3.13 Triclosan-induced antibiotic tolerance can be visualised at a single-cell level

The analysis presented so far has focused on the effects of triclosan exposure at both a population and biofilm community level, but did not interrogate the effects of antibiotic tolerance at a single-cell level. To focus on individual bacteria, fluorescence microscopy was used to visualise *S. aureus* cell clusters of both HG001 WT and HG001 (p)ppGpp0 strains after various treatments (Fig 3.13A). Quantitative analysis of images using the ImageJ analysis software revealed significant differences in cell diameter between different treatments.

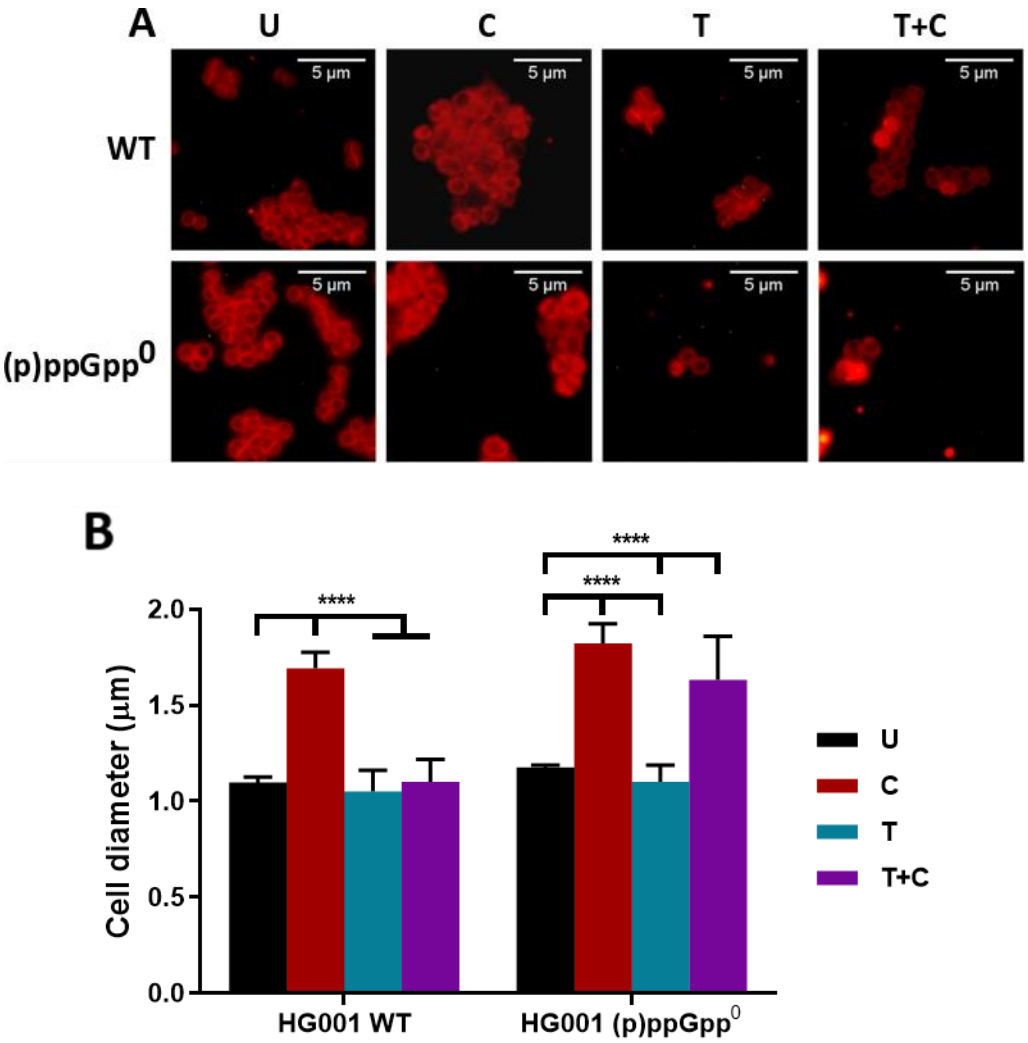


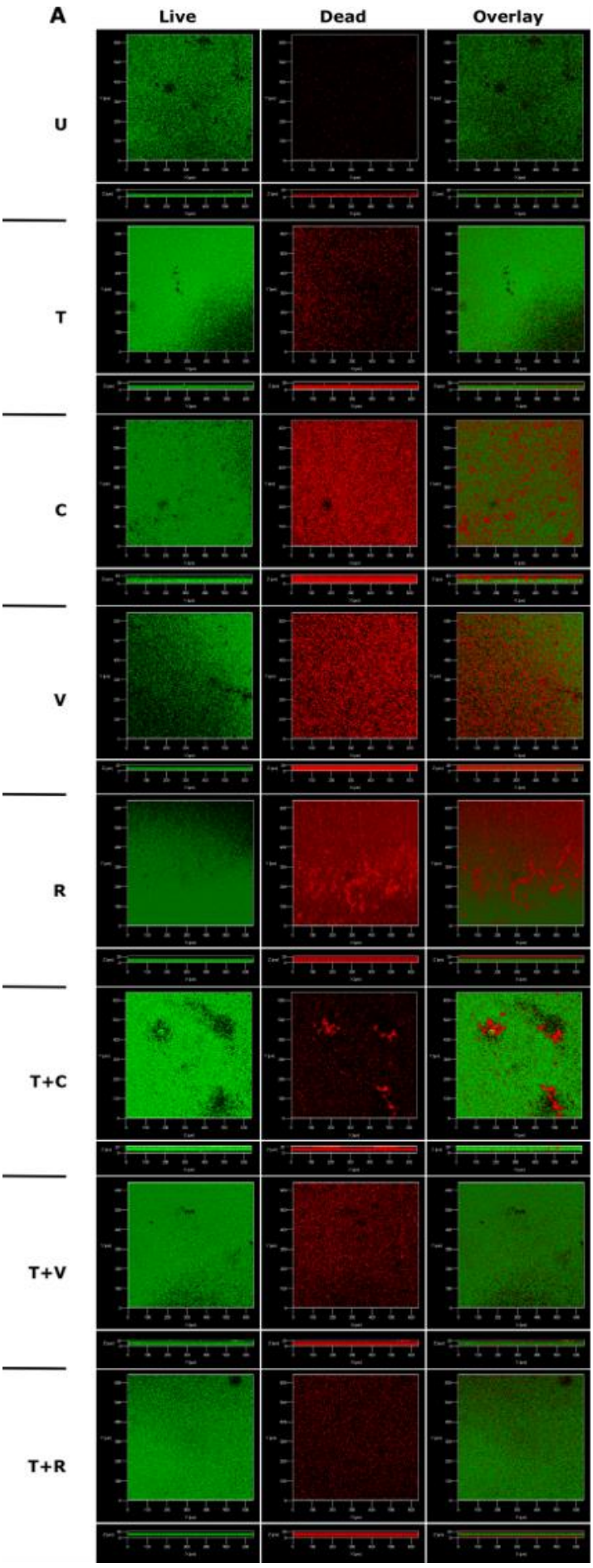

**Figure 3.13. Triclosan-induced antibiotic tolerance, and the influence of the stringent response on this phenotype, can be visualised at a single cell level. A)** Fluorescence microscopy images showing *S. aureus* clusters of HG001-WT and HG001 (p)ppGpp$^0$. Conditions include untreated (U), 1 hour 1 µg/mL ciprofloxacin treated (C), 30 min 500 ng/mL triclosan pretreated (T) and 30 min 500 ng/mL pretreated followed by 1 hour 1 µg/mL ciprofloxacin treatment (T+C). Cells were stained with the membrane stain Nile Red. Images are representative of multiple repeats, scale bar = 5 µm, n=3 (HG001-WT conditions), n=2 (HG001 (p)ppGpp$^0$ conditions). **B)** Quantitative analysis of cell diameter was carried out using masks generated in ImageJ analysis software. Error bars represent ±SEM, n=10. **** denotes P≤0.0001.

In the wild type strain, treating with ciprofloxacin for 1 hour led to a significant increase in cell diameter (50-80%) (Fig 4B). Pretreating with triclosan prior to ciprofloxacin exposure did not cause this same increase in diameter, with cell size remaining comparable to the untreated and triclosan alone conditions. This same increase in cell diameter was seen

in the (p)ppGpp$^0$ strain after ciprofloxacin treatment, however triclosan pretreatment did not prevent ciprofloxacin-induced increases in cell diameter in these cells.

### 3.3.14 Triclosan is able to induce antibiotic tolerance against multiple antibiotics in MRSA

After the interrogation of the underlying mechanisms behind triclosan-induced antibiotic tolerance in previous experiments, the effects of biocide triggered tolerance on a more clinically relevant strain were investigated. 48 hour biofilms formed by the community-associated MRSA (CA-MRSA) strain USA300 JE2 was treated high concentrations (2x MBEC) of ciprofloxacin, vancomycin and rifampicin, with or without sub-MIC triclosan pretreatment. Visualisation using live/dead imaging to assessed cell viability.


A
Live
Dead
Overlay
U
T
C
V
R
T+C
T+V
T+R

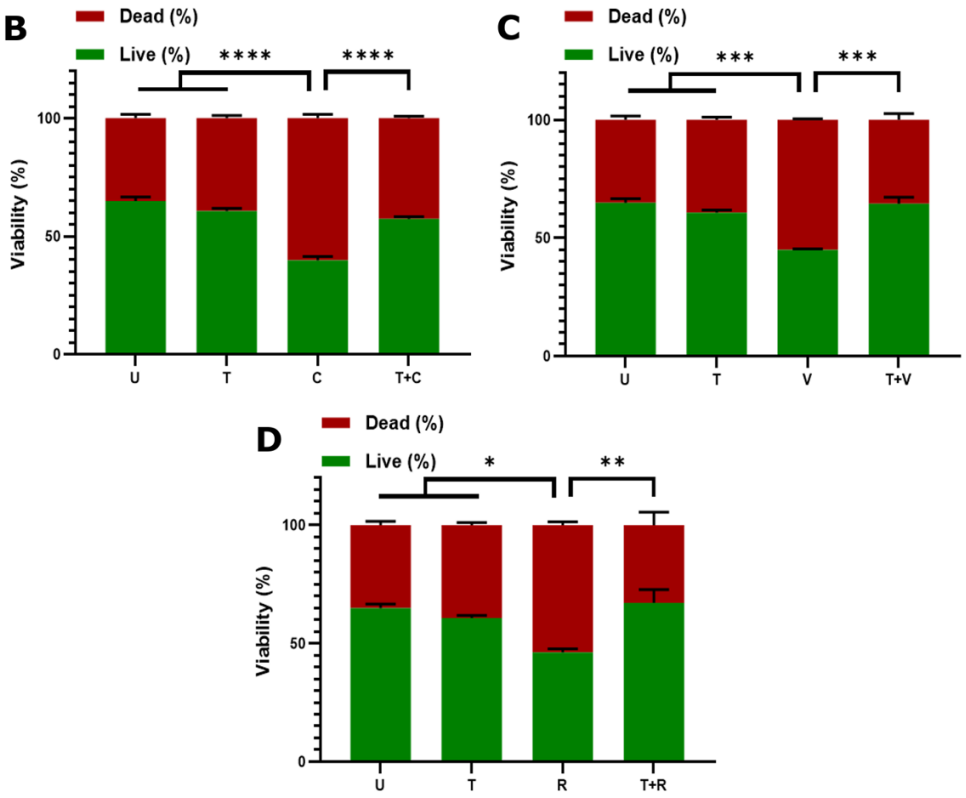



**Figure 3.14. Exposure to physiologically relevant levels of triclosan protects MRSA biofilms against multiple, mechanistically distinct antibiotics. A)** CLSM was used to assess the effect of triclosan on the antibiotic tolerance of *S. aureus* USA300 JE2 WT. Syto 9 (green) was used to visualise live cells, whilst propidium iodide (red) was used to visualise cell death. Untreated (U), 500 ng/mL triclosan pretreated (T), 4096 µg/mL ciprofloxacin treated (C), 512 µg/mL vancomycin treated (V), 512 µg/mL rifampicin treated (R), 500 ng/mL triclosan pretreated and 4096 µg/mL ciprofloxacin treated (T+C), 500 ng/mL triclosan pretreated and 512 µg/mL vancomycin treated (T+V) and 500 ng/mL triclosan pretreated and 512 µg/mL rifampicin treated (T+R) biofilms are shown. For each condition, the top row shows the top surface of the *S. aureus* biofilms, whilst the second row of each condition shows the biofilm thickness profile. Horizontal lines on the left are used to segregate conditions. Images are representative of multiple experiments and were taken using the 10x objective (n=2). **B-D)** Live/dead quantification was carried out using Comstat image analysis software. Error bars represent SEM, n=2. **** denotes P≤0.0001, *** denotes P≤0.001, ** denotes P≤0.01, * denotes P≤0.05.

Quantified imaging of USA300 biofilms showed significant increases in cell death when treated with ciprofloxacin, vancomycin or rifampicin compared to untreated or triclosan only treatment conditions (Fig 3.14A). As observed with laboratory strains, triclosan pretreatment followed by

antibiotic treatment led to significantly higher cell viability compared to antibiotic treatment alone.

### 3.3.15 The widely used biocides chlorhexidine digluconate and benzalkonium chloride can induce antibiotic tolerance in planktonic *S. aureus*, independent of the stringent response

Previous experiments in this chapter have focused on the induction of antibiotic tolerance by the biocide triclosan. Further experiments were carried out to assess whether chlorhexidine digluconate or benzalkonium chloride could also induce antibiotic tolerance in *S. aureus*. Since earlier experiments implicated the stringent response in triclosan-induced antibiotic tolerance, strains HG001 WT and HG001 (p)ppGpp$^0$ were included. As with triclosan pretreatment, bacteria were pretreated with subinhibitory concentrations of chlorhexidine digluconate (0.0001%, 0.25x MIC) or benzalkonium chloride (0.0002%, 0.5x MIC) for 30 minutes prior to treatment with an inhibitory dose of ciprofloxacin (1 µg/mL).

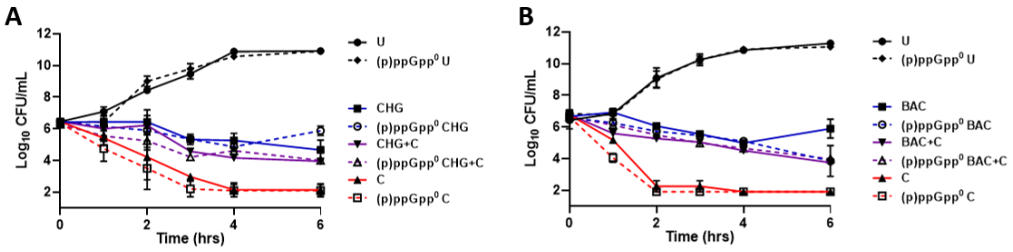



**Figure 3.15. Both chlorhexidine digluconate and benzalkonium chloride are capable of inducing antibiotic tolerance in planktonic *S. aureus*.** *S. aureus* strains HG001 WT and HG001 (p)ppGpp$^0$ were incubated in BHI in the presence or absence of either 0.0001% chlorhexidine digluconate or 0.0002% benzalkonium chloride for 30 mins at 37°C. Inhibitory concentrations of ciprofloxacin were added and incubation continued. **A)** Time-kill assays showing untreated (U, (p)ppGpp$^0$ U), chlorhexidine digluconate pretreated (CHG, (p)ppGpp$^0$ CHG), 1 µg/mL ciprofloxacin treated (C, (p)ppGpp$^0$ C), chlorhexidine digluconate pretreated and 1 µg/mL ciprofloxacin treated (CHG+C, (p)ppGpp$^0$ CHG+C). **B)** Time-kill assays showing untreated (U, (p)ppGpp$^0$ U), benzalkonium chloride pretreated (BAC, (p)ppGpp$^0$ BAC), 1 µg/mL ciprofloxacin treated (C, (p)ppGpp$^0$ C), benzalkonium chloride pretreated and 1 µg/mL ciprofloxacin treated

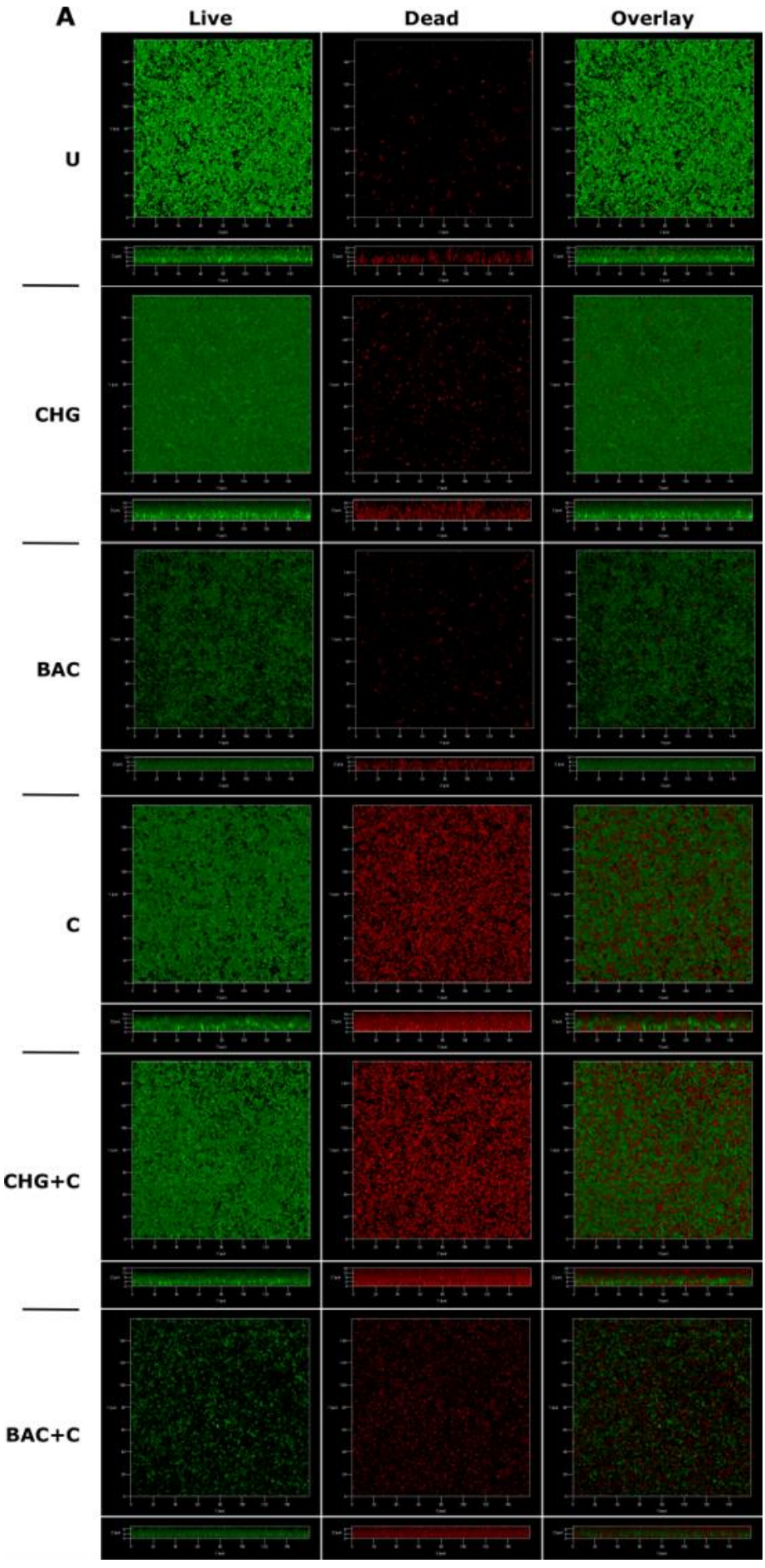
(BAC+C, (p)ppGpp$^0$ BAC+C). For both experiments, $Log_{10}$ CFUs are plotted against time. Error bars display ±SEM, n=3.

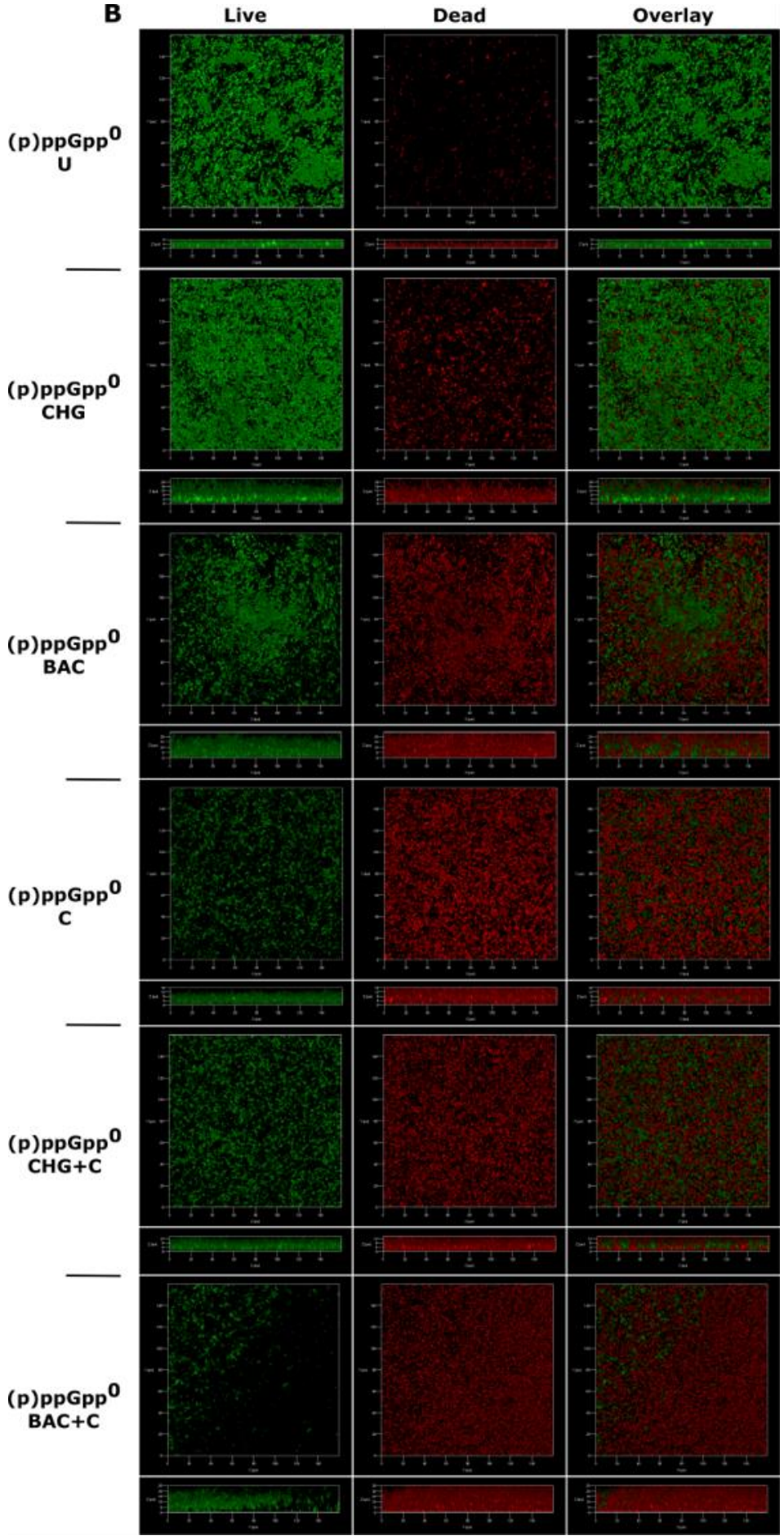
Exposure to either chlorhexidine digluconate (Fig 3.15A) or benzalkonium digluconate (Fig 3.15B) stalled increases in bacterial viability over time, but were not bactericidal in the doses used in this experiment. Both biocides were able to induce tolerance to ciprofloxacin. CHG+C provided a consistent 100-fold increase in viability when compared to ciprofloxacin only treatment. BAC+C produced a 1000-fold increase in bacterial viability over ciprofloxacin treatment for the first 4 hours, this reduced to 100-fold difference in viability by 6 hours. Concerning biocide induced tolerance, these biocides elicit an antibiotic tolerant phenotype similar to those observed after triclosan pretreatment. However, unlike with triclosan, antibiotic tolerance induced by these biocides occurs independently of the stringent response. This is demonstrated by comparing (p)ppGpp$^0$ biocide and antibiotic combination conditions which exhibited similar viabilities throughout the experiment, indicating another molecular mechanism is responsible to CHG and BAC induced antibiotic tolerance in *S. aureus*.

### 3.3.16 Exposure to sub-MIC doses of chlorhexidine digluconate or benzalkonium chloride are unable to induce antibiotic tolerance in *S. aureus* biofilms

Since both CHG and BAC had been shown to induce ciprofloxacin tolerance in *S. aureus* planktonic cultures, the effect of biocide exposure on antibiotic tolerance was investigated in biofilms. Sub-MIC concentrations of CHG (0.25x MIC) and BAC (0.5x MIC) were added alongside initial inoculation of *S. aureus,* and biofilms were grown for 48 hours. Following this, biofilms were treated ciprofloxacin (2x MBEC) for 3 hours before CLSM imaging. Both HG001 WT and HG001 (p)ppGpp$^0$ were investigated. Even though the stringent response was not implicated CHG and BAC experiments in planktonic culture, this chapter has shown that molecular mechanisms behind antibiotic tolerance may

only manifest in one lifestyle (the *agr* quorum sensing system in planktonic culture).


A
Live
Dead
Overlay
U
CHG
BAC
C
CHG+C
BAC+C


B
Live
Dead
Overlay
(p)ppGpp0 U
(p)ppGpp0 CHG
(p)ppGpp0 BAC
(p)ppGpp0 C
(p)ppGpp0 CHG+C
(p)ppGpp0 BAC+C

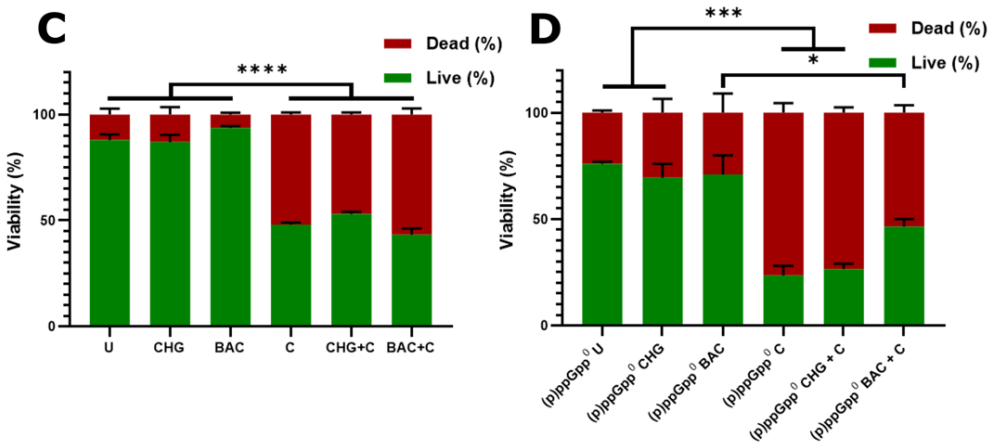



**Figure 3.16. Neither chlorhexidine digluconate nor benzalkonium chloride were able to induce antibiotic tolerance in *S. aureus* biofilms.** CLSM was used to assess the effect of triclosan on the antibiotic tolerance of *S. aureus* HG001 WT **(A)**, HG001 (p)ppGpp$^0$ **(B)**. Syto 9 (green) was used to visualise live cells, whilst propidium iodide (red) was used to visualise cell death. For all strains, untreated (U, (p)ppGpp$^0$ U), 0.0001% chlorhexidine digluconate pretreated (CHG, (p)ppGpp$^0$ T), 0.0002% benzalkonium chloride pretreated (BAC, (p)ppGpp$^0$ BAC), 4096 µg/mL ciprofloxacin treated (C, (p)ppGpp$^0$ C), 0.0001% chlorhexidine digluconate pretreated and 4096 µg/mL ciprofloxacin treated (CHG+C, (p)ppGpp$^0$ CHG+C) and 0.0002% benzalkonium chloride pretreated and 4096 µg/mL ciprofloxacin treated (BAC+C, (p)ppGpp$^0$ BAC+C) biofilms are shown. For each condition, the top row shows the top surface of the *S. aureus* biofilms, whilst the second row of each condition shows the biofilm thickness profile. Horizontal lines on the left are used to segregate conditions. Images are representative of multiple experiments and were taken using the 40x objective (n = 3). **C-D)** Live/dead quantification was carried out using Comstat image analysis software. Error bars represent SEM, n=3. **** denotes P≤0.0001, *** denotes P≤0.001, * denotes P≤0.05.

Live/dead imaging revealed that biocide pretreated biofilms were just as susceptible to ciprofloxacin as untreated biofilms (Fig 13.6A); with significant differences in cell death between ciprofloxacin treated and untreated conditions (Fig 13.6C). As expected, stringent response biofilms (Fig 13.6B) were more susceptible to ciprofloxacin as well as CHG and ciprofloxacin in combination. This increased susceptibility was not observed in the BAC and ciprofloxacin combination, but was not significantly different to other ciprofloxacin treated conditions (Fig 13.6D). Taken together, these results show that despite CHG and BAC inducing

tolerance in planktonic culture, this tolerance is not observable in 48 hour biofilms.

## 3.4 Discussion

Previously it was shown that triclosan pretreatment protected planktonic *E. coli* cultures against ampicillin, kanamycin, streptomycin and ciprofloxacin. However, whether this phenomenon offered broader resilience against antibiotics with differing mechanisms in the case of *S. aureus* was not reported. This study has found that the biocide triclosan can induce antibiotic tolerance in *S. aureus* to inhibitory concentrations of vancomycin, as reported by Westfall et al. (2019), but also against ciprofloxacin. This suggests that triclosan-induced antibiotic tolerance in *S. aureus* may be as pleiotropic as observed in *E. coli*. These results also demonstrate that triclosan can induce antibiotic tolerance at concentrations found in the human body (Allmyr et al., 2009; MacIsaac et al., 2014), against clinically relevant serum concentrations of ciprofloxacin (D'Espine et al., 1989). The data gathered in this chapter supports previous literature emphasising the importance of growth arrest on antibiotic tolerance. A common trend identified in experiments is that sub-MIC levels of triclosan could halt growth whilst having little effect on viability (Balaban et al. 2019). The use of pH-sensitive fluorescent nanosensors in this chapter also added a metabolic perspective to triclosan-induced growth inhibition, with reduced environmental acidification being observed in triclosan exposed *S. aureus* (Fig 3.1A). This is likely due to decreased metabolism of glucose in the medium resulting in a reduction in acidic products such as acetic acid (Rice et al., 2005).

Westfall et al. (2019) found that triclosan-induced tolerance was mediated by the stringent response, a process of physiological reprogramming in cells in response to nutrient limiting conditions. The stringent response results in cells halting active growth, and entering a state that promotes survival (Corrigan et al., 2016). Whilst in this state, bacteria are much more tolerant to treatment with multiple antibiotics ( Christensen et al., 2011; Ji et al., 2013; Chinag et al., 2016), and this has even been demonstrated previously with *S. aureus* tolerating ciprofloxacin treatment (Corrigan et al., 2016). Using an *S. aureus*

(p)ppGpp$^0$ strain (Geiger et al., 2014) in this study, it was shown that cells incapable of initiating a stringent response were not protected by triclosan against antibiotics (Fig 3.10A-F). Combining these findings with those of Westfall et al. (2019) show that physiological levels of triclosan induce the stringent response in both clinically relevant Gram-positive and Gram-negative bacteria, making them recalcitrant to treatment with multiple antibiotics of differing modes of action. In addition to the involvement of the stringent response, planktonic time-kill assays also implicated the *agr* quorum sensing system in biocide induced antibiotic tolerance when an *agr* deficient mutant was used (Fig 3.8A). The involvement of the *agr* system in drug tolerance is unexpected and perhaps surprising. Whilst early induction of the quorum sensing system has been hypothesised as an indicator for persistent MRSA infection against vancomycin (Abdelhady et al., 2015), other literature has demonstrated that the *agr* system negatively regulates the induction of tolerance (Bojer et al., 2018). It has even been demonstrated that *agr* deficient *S. aureus* clinical isolates are less susceptible to antibiotics, due to the fitness cost associated with expressing *agr* during antibiotic treatment (Paulander et al., 2012). These results may demonstrate that the role of *agr* in antibiotic tolerance is more complex than previously thought.

It is estimated that approximately 99% of all bacteria are associated within biofilms, and that 80% of all antibiotic-tolerant infections are derived from biofilms (Donne, 2015; Skogman et al., 2016). The prevalence of antibiotic inactivity is widely thought to be due to growth-arrest in biofilm-associated cells, typically induced by starvation (Nguyen et al., 2011). Whilst starvation inevitably halts growth and the activity of antibiotic targets, physiological processes such as the stringent response are required to harness starvation in a way that maximises bacterial survival (Nguyen et al., 2011). Here, we find that physiological levels of triclosan exposure during biofilm formation are able to increase levels of antibiotic tolerance in *S. aureus* biofilms via the induction of the stringent response (Fig 3.11A). Stringent-controlled gene expression protected

against ciprofloxacin, vancomycin and rifampicin (Fig 3.12B). Although triclosan did not protect against rifampicin in planktonic experiments (Fig 3.10E), this is likely due to the transition of rifampicin activity from bacteriostatic to bactericidal at high concentrations (Douthit et al., 2020). Due to antibiotic tolerance and treatment with bacteriostatic antibiotics both resulting in bacterial quiescence, the activity of bacteriostatic antibiotics is rarely influenced by tolerance mechanisms (Balaban et al., 2019). Contrastingly, despite involvement in planktonic tolerance, the *agr* system appeared to contribute nothing to triclosan-induced antibiotic protection in biofilms (Fig 3.8). This is unsurprising, as low levels of Staphylococcal quorum sensing is observed in biofilms, instead being associated with early stages of growth and infection and biofilm dispersal (Kong, Vuong and Otto, 2006). This is consistent with our observation that the *agr* system played a significant role in biocide induced drug tolerance in exponentially growing planktonic cultures, whilst demonstrating a negligible role in established biofilms. Likewise, the CodY repressor did not appear to provide any benefit to the initiation or maintenance of triclosan-induced tolerance (Fig 3.11B), despite being linked to multiple gene targets required for the induction of biofilm formation (Pohl et al., 2009). Alarmingly, this recalcitrance to antibiotics is able to persist at least 48 hours after initial exposure to subinhibitory triclosan concentrations.

This investigation not only visualised changes in *S. aureus* viability at a community level, but also at a single cell level. Cell morphology is a useful indicator in the dynamics of cellular processes, with antibiotic-induced changes to cell morphology being detected in multiple clinically relevant pathogens (Schilcher et al., 2016; Skogman et al., 2016; Zahir et al., 2019). The bacteriostatic effects of sub-MIC levels of triclosan were observed using SEM, showing fewer bacteria and a higher prevalence of cells in the septation stage of division (Fig 3.2B). This is likely due to the induction of the stringent response halting division and preventing the synthesis of peripheral peptidoglycan between new cells (Monteiro et al, 2015; Do et al., 2020). Fluorescence microscopy revealed that treatment

with ciprofloxacin significantly increased cell diameter (Fig 3.13). Triclosan-induced tolerance was evidenced at a single cell level, with triclosan pretreatment preventing ciprofloxacin-induced changes in cell size. However, when (p)ppGpp$^0$ cells were imaged (Fig 3.13A), it was apparent that triclosan pretreatment was unable to protect against morphological changes caused by ciprofloxacin treatment. In *E. coli*, the stringent response acts on SeqA, a protein implicated in strand initiation and chromosome segregation during DNA replication. Stringent control of *seqA* interferes with the activity of DNA topoisomerase IV (Ferullo and Lovett, 2008). As DNA topoisomerase IV is the primary target of ciprofloxacin in *S. aureus* (Rajendram et al., 2014), a mechanism homologous with that observed in *E. coli* may be at work in *S. aureus*.

Fatty acid starvation is one of the numerous nutritional deficiencies capable of instigating the stringent response. Oleic acid supplementation was used in this study to determine whether triclosan-induced tolerance manifested as a result of the fatty acid starving action of triclosan. Whilst oleic acid supplementation was unable to immediately prevent triclosan-induced tolerance, after approximately 5 hours of incubation with exogenous oleic acid, there was evidence that tolerance was overcome in planktonic cultures (Fig 3.5). This is striking, as there has been contentious debate as to whether exogenous fatty acids can overcome the effects of fatty acid synthesis inhibitors (Altenbern, 1977; Brinster et al., 2009; Parsons and Rock, 2011; Yao and Rock, 2015). Some organisms such as *Streptococci* can be completely saved from treatment with fatty acid synthesis inhibitors through exogenous fatty acid uptake alone (Marrakchi et al., 2003; Parsons et al., 2011). However, *S. aureus* is capable of meeting only 50% of its fatty acid requirements through exogenous fatty acids (Parsons et al., 2011), prompting confusion as to whether this is sufficient to rescue this pathogen from triclosan treatment (Altenbern, 1977; Parsons and Rock, 2011; Yao and Rock, 2015). Here, oleic acid supplementation prevented triclosan-induced tolerance, supporting the hypothesis that triclosan-induced tolerance could result from fatty acid starvation triggering the stringent response. Since the

concentration of triclosan used in this experiment was sub-inhibitory (500 ng/mL), it cannot be concluded whether fatty acid supplementation is sufficient to save *S. aureus* from inhibitory concentrations of triclosan. However, the data does suggest serum concentrations of oleic acid (Abdelmagid et al., 2015) would be sufficient to overcome tolerance induced by concentrations of triclosan that have accumulated in the human body ( Allmyr et al., 2009; MacIsaac et al., 2014).

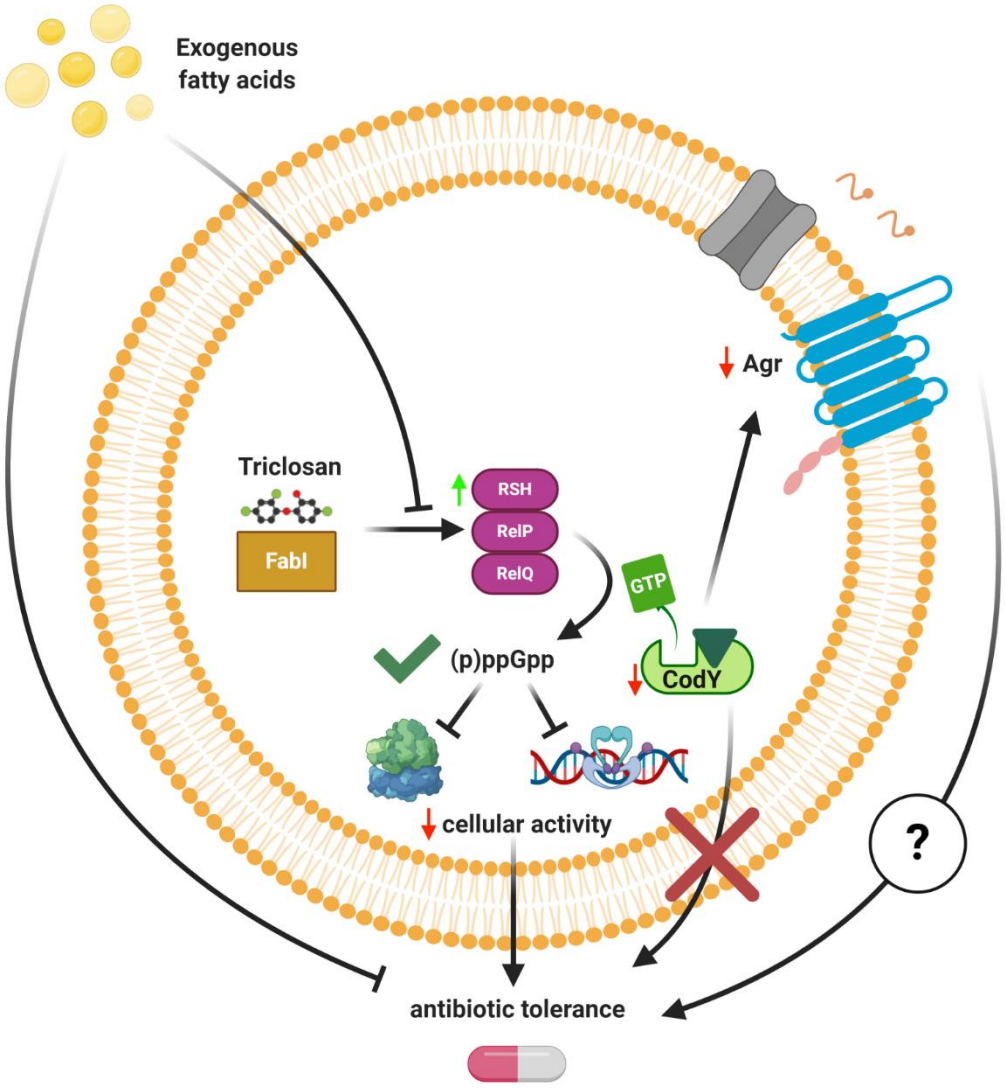



**Figure 3.17. Schematic diagram of potential mechanisms underlying triclosan-induced antibiotic tolerance.** Triclosan pretreatment induces antibiotic tolerance in *S. aureus*. The stringent response, which is triggered in response to triclosan exposure, was found to play an essential role in triclosan-induced antibiotic tolerance in both planktonic culture and biofilms. CodY is closely linked to the stringent response, as GTP

is essential for CodY to repress its target genes. Synthesis of stringent response alarmones uses intracellular GTP, therefore stringent response induction reduces the ability of CodY to repress less of the GTP cofactor is available. Another target of CodY repression, the *agr* system, may play a role in planktonic antibiotic tolerance. However, this study found *agr* plays no role in triclosan-induced antibiotic tolerance in biofilms. Exogenous fatty acids inhibit fatty acid starvation by triclosan and therefore prevent triclosan-induced antibiotic tolerance in both *S. aureus* planktonic cultures and biofilms. Green arrows indicate increased activity/production. Red arrows indicate reduced activity.

As seen with triclosan, pretreatment with sub-MIC CHG or BAC induced a tolerant phenotype in *S. aureus* planktonic cultures ciprofloxacin (Fig 3.15). Tolerance to bactericidal antibiotics after pretreatment of triclosan has been well characterised and furthermore it has been shown that BAC can promote tolerance to a range of antibiotics after several passages, but this is the first time it has been shown in BAC in a shorter time frame (Gadea et al., 2017). The mechanism of tolerance in this study is independent of the stringent response because (p)ppGpp$^0$ also managed to survive better when pretreated with biocides before ciprofloxacin exposure. This differs from triclosan where the stringent response protects the bacteria from bactericidal antibiotics (Westfall et al., 2019). Potentially, the *agr* quorum sensing system may be involved in CHG/BAC planktonic antibiotic tolerance, as this chapter has shown the contribution of *agr* in triclosan-induced ciprofloxacin. However, the insensitivity of CHG/BAC induced tolerance to the stringent response make this unlikely. The use of the (p)ppGpp$^0$ mutant has likely had indirect effects on *agr* function due to reduced CodY deprepression by reduction of intracellular GTP (Pohl et al., 2009). The difference in tolerance mechanism is likely due to the different mechanisms of action utilised by each biocide. Whilst triclosan can lead to fatty acid starvation, a distinct nutritional deficiency and known trigger of the stringent response (My et al., 2013), CHG and BAC respectively disrupt cell wall and membrane integrity (Meyer and Cookson, 2010). Therefore, any starvations induced by such mechanisms would be via cell leakage. Factoring in the low biocide doses

used, it is unlikely any deficiencies by leakage would be specific or acute enough to induce the stringent response.

Unlike the results seen with triclosan exposure, sub-MIC CHG or BAC exposure throughout biofilm maturation was unable to stimulate a protective response against high concentrations of ciprofloxacin (Fig 3.16). Biofilm triclosan exposure experiments also determined the essentiality of the stringent response for this tolerance. As planktonic experiments established that these biocides do not stimulate stringent response-dependent tolerance, it seems likely that this alternate mechanism of tolerance is unable to persist into the biofilm lifestyle, or at least not for a duration of 48 hours after initial induction. Triclosan has been shown to be highly stable within the environment (Weatherly and Gosse, 2017), potentially facilitating prolonged tolerance induction over time. However, evidence suggests that both biocides can persist in environments (Pereira and Tagkopoulus, 2019) and accumulate in biofilms (Lawrence at al., 2008; Forbes et al., 2019).

Although great strides have been made in recent years in banning triclosan from household soaps (Weatherly and Gosse, 2017), this ban is not worldwide, and biocides remain ubiquitous in many different domestic and healthcare products across the globe. The findings of this study show that triclosan exposure can make *S. aureus* biofilms, communities that are already extremely difficult to eradicate, even more recalcitrant to antibiotic treatment. These effects were even seen in the CA-MRSA strain USA300 (Fig 3.14), indicating that these effects also manifest in more clinically relevant *S. aureus* strains. This work was able to attribute the stringent response to triclosan-induced antibiotic tolerance in both planktonic cultures and biofilms. However, additional regulatory systems, such as the *agr* quorum sensing system, may be involved depending on bacterial lifestyle. Furthermore, antibiotic tolerance induced by BAC and CHG was induced independently of the stringent response. This expands not only on the scale of biocide-induced antibiotic tolerance, but also on its complexity. Demonstrating that multiple biocides can induce tolerance and that the mechanism of induction is biocide dependent. This chapter

proposes that triclosan exposure triggers multiple global regulatory systems, some of which remain unknown, to facilitate cell survival (Fig 3.17). The role of antibiotic tolerance and the stringent response is crucial in not only chronic and relapsing infection, but also in the acceleration of the emergence of antibiotic resistance (Strugeon et al., 2016; Windels et al., 2019). Tolerance has been acknowledged to precede resistance (Levin-Reisman et al., 2017), and previous studies have implicated the stringent response in both increased mutability of bacteria (Foster, 2007) and improved acquisition of resistance cassettes through increased integrase expression (Strugeon et al., 2016). This may be of significant impact considering biocides studied in this chapter are abundant in healthcare settings (Maillard, 2005; Sewlikar et al., 2015; Gudapuri, 2017; Singha et al., 2017). Considering this, understanding the mechanisms behind antibiotic tolerance, particularly those triggered by compounds in household products, is of significant importance. The effects of biocide exposure on *S. aureus* physiology will be further explored in chapter 4, in which biocide induced biofilm formation will be investigated. Chapter 5 will evaluate the transcriptome following triclosan exposure, which may potentially confirm the mechanisms proposed in this chapter.

# 4. Triclosan exposure alters *Staphylococcus aureus* biofilm formation and composition

## 4.1 Introduction

### 4.1.1 Stress-induced changes to biofilm formation

Whilst antibiotics are prescribed with the intent of eradicating bacteria and their biofilms, insufficiently dosed treatments can instead bolster these communities (Kaplan, 2011). For Staphylococci, there are descriptions of increased biofilm formation caused by sub-MIC levels of aminocoumarin (Kaplan, Jabbouri and Sadovskaya, 2011), β-lactam (Kaplan et al., 2012), cephalosporin (Haddadin et al., 2010; Subrt, Mesak and Davies, 2011), fluoroquinolone (Frank et al, 2007; Ahmed, Peterson and Scheie, 2009), glycylcyline (Kaplan, Jabbouri and Sadovskaya, 2011), glycopeptide (Kaplan, Jabbouri and Sadovskaya, 2011; Mirani and Jamil, 2011), lipopeptide (Frank et al., 2007), macrolide (Wang, Sun and Liu, 2010), oxazolidone (Frank et al., 2007), rifamycin (Schadow, Simpson and Christensen, 1988), streptogramin (Rachid et al., 2000), sulphonamide (Frank et al., 2007) and tetracycline (Ahmed, Peterson and Scheie, 2009) antibiotics. Unsurprisingly, the different mechanisms of action of these inducer antibiotics leads to antibiotic-induced biofilm formation manifesting in different ways. In *S. epidermidis*, erythromycin and tetracycline induce increased biofilm formation through increased *ica* expression, leading to higher exopolysaccharide production (Rachid et al., 2000). In *S. epidermidis*, antibiotic-induced biofilm formation can also be *ica* independent, with *ica* negative strains still exhibiting increased biofilm formation in the presence of 0.25x MIC macrolides (Wang, Sun and Liu, 2010). Vancomycin exposure induces increased eDNA release in *S. epidermidis*, whilst ¼ MIC tigecycline increased cell growth and increased production of both matrix eDNA and matrix exopolysaccharide (Kaplan et al., 2012). In *S. aureus*, the CA-MRSA strain USA300 has

been shown to grow thicker biofilms in the presence of sub-MIC mupirocin (Jin et al., 2020), clindamycin (Schilcher et al., 2016), and β-lactams (Kaplan et al., 2012) due to increased eDNA release. The rise in eDNA within the biofilm matrix was mediated by *cidA* and *atlA* autolysin activity. Vancomycin exposure caused increased biofilm formation due to elevated levels of both PIA and eDNA in the biofilm matrix. Interestingly, vancomycin-induced PIA production was intrinsically linked with eDNA release. Strains that were *cidA* deficient did not produce more PIA in the presence of vancomycin, despite maintaining a functional *ica* operon (Hsu et al., 2011). Currently, no examples of antibiotic-induced biofilm formation relying solely on PIA have been discovered in *S. aureus*.

Whether an antibiotic induces biofilm formation depends on a combination of specific factors. Whilst an antibiotic may induce biofilm formation in certain species, this is not universal across all bacteria. For instance, Frank et al (2007) found that *Staphylococcus lugdunensis* grows thicker biofilms in the presence of sub-inhibitory levels of ciprofloxacin, whilst sub-MIC ciprofloxacin inhibited the growth of *P. aeruginosa* biofilms (Aka and Haji, 2015). Moreover, strain to strain variation plays a role in whether additional biofilm formation occurs, as evidenced by differential polysaccharide production by different *S. epidermidis* strains in response to macrolides due to variance in *ica* expression (Wang, Sun and Liu, 2010). Differences in an antibiotics ability can even be observed among the same family of antibiotic. The effect of macrolides on *P. aeruginosa* illustrates this, with clarithromycin inducing biofilm formation (Garey et al., 2009) whilst low-levels of azithromycin maintain partial antibiotic activity against the pathogen (Ichimiya et al., 1996; Wagner et al., 2005). Lastly, the most enigmatic factor of antimicrobial induced biofilm formation appears to be drug concentration. For instance, studies investigating the effect of ½ MIC vancomycin on *S. epidermidis* found little change in biofilm formation (Wang, Sun and Liu, 2010); yet dramatic changes were observed upon ¾ MIC exposure (Kaplan, Jabbouri and Sadovskaya, 2011). The consensus is that ¼-½ MIC ranges stimulate antibiotic induced biofilm

formation (Kaplan, 2011), yet there are examples of biofilm alterations occurring at much lower concentrations (Rachid et al., 2000).

Antibiotics are not the only stress that can alter biofilm formation, with environmental factors also promoting a response. These include oxygen concentration and pH, with anaerobiosis stimulating PIA production in *S. epidermidis* (Crampton et al., 2001) and initial attachment being inhibited above pH 8.5 in *S. aureus* (Jones, Cochrane and Percival, 2015). Salicylic acid, the active component of aspirin, also mediates PIA-dependent biofilm formation in *S. aureus*. This process occurs by reduced *codY* transcription releasing the *ica* operon from CodY repression (Dotto et al., 2017). Biocides such as triclosan and chlorhexidine have been shown to promote biofilm formation. In established *Salmonella typhimirium* biofilms, triclosan stimulated production of the polysaccharide cellulose (Tabak et al., 2007). Chlorhexidine meanwhile, was able to augment the biofilm inducing abilities of other sub-lethal concentration antibiotics in *P. aeruginosa* (Aka and Haji, 2015).

### 4.1.2 Polymicrobial biofilms

Although literature is dominated by single species biofilm studies, polymicrobial biofilms are overwhelmingly more prevalent than monospecies biofilms in nature (Peters et al., 2012; Sanchez-Vizuete et al., 2015). The proximity of multiple microorganisms can facilitate mutualism or synergism to facilitate co-habitation and increase communal survival. Skin commensals demonstrate this; with *S. epidermidis* being shown to protect *Micrococcus luteus* from *S. aureus* mediated killing (Jordana-Lluch et al., 2020). Alternatively, polymicrobial interactions can result in antagonism. *P. aeruginosa* produces stapholytic enzymes such as LasA protease (Kessler et al., 1993) and pyocyanin to eradicate *S. aureus* (Dietrich et al., 2006). Mechanisms underlying polymicrobial interactions typically involve a combination of contact-dependent signalling, quorum sensing cross-talk, immunomodulation,

enhanced colonisation or amplified virulence (Peleg, Hogan and Mylonakis, 2010; Peters et al., 2012). Clinically, polymicrobial interactions can influence the virulence, persistence and antibiotic tolerance of the constituent species. In *S. aureus* and *Candida albicans* dual species biofilms, multi-drug tolerance was induced in *S. aureus* due to energy depletion because of competing for available nutrients (Nabb et al., 2019). Conversely, *C. albicans* mycofilms have been shown to facilitate *S. aureus* biofilm formation through binding to hyphal elements whilst also simultaneously decreasing the *C. albicans* susceptibility to miconazole (Kean et al., 2017). In an artificial wound model, it was found that the combined biofilm matrix components of *S. aureus* and *P. aeruginosa* co-cultured biofilms increased the gentamicin tolerance of both species (DeLeon et al., 2014).

Polymicrobial interactions can also alter how component species respond to biocides. There is evidence that individual species are better able to tolerate biocides when inhabiting multispecies biofilms compared to living in monoculture (Sanchez-Vizuete, 2015). This is often observed with commensal bacteria protecting pathogens from disinfection, such as *Lactobacillus plantarum* protecting *Listeria monocytogenes* against benzalkonium chloride (van der Veen and Abee, 2011). Biocide tolerance in polymicrobial biofilms manifests through similar mechanisms as antibiotic tolerance. *Veillonella parvula* and *Streptococcus mutans* coaggregate in oral biofilms producing a thick matrix, facilitating tolerance to the biocide chlorhexidine (Kara, Luppens and Cate, 2006). Currently, it appears there has been little research on how biocides mediate susceptibility of one species to another in a multispecies environment.

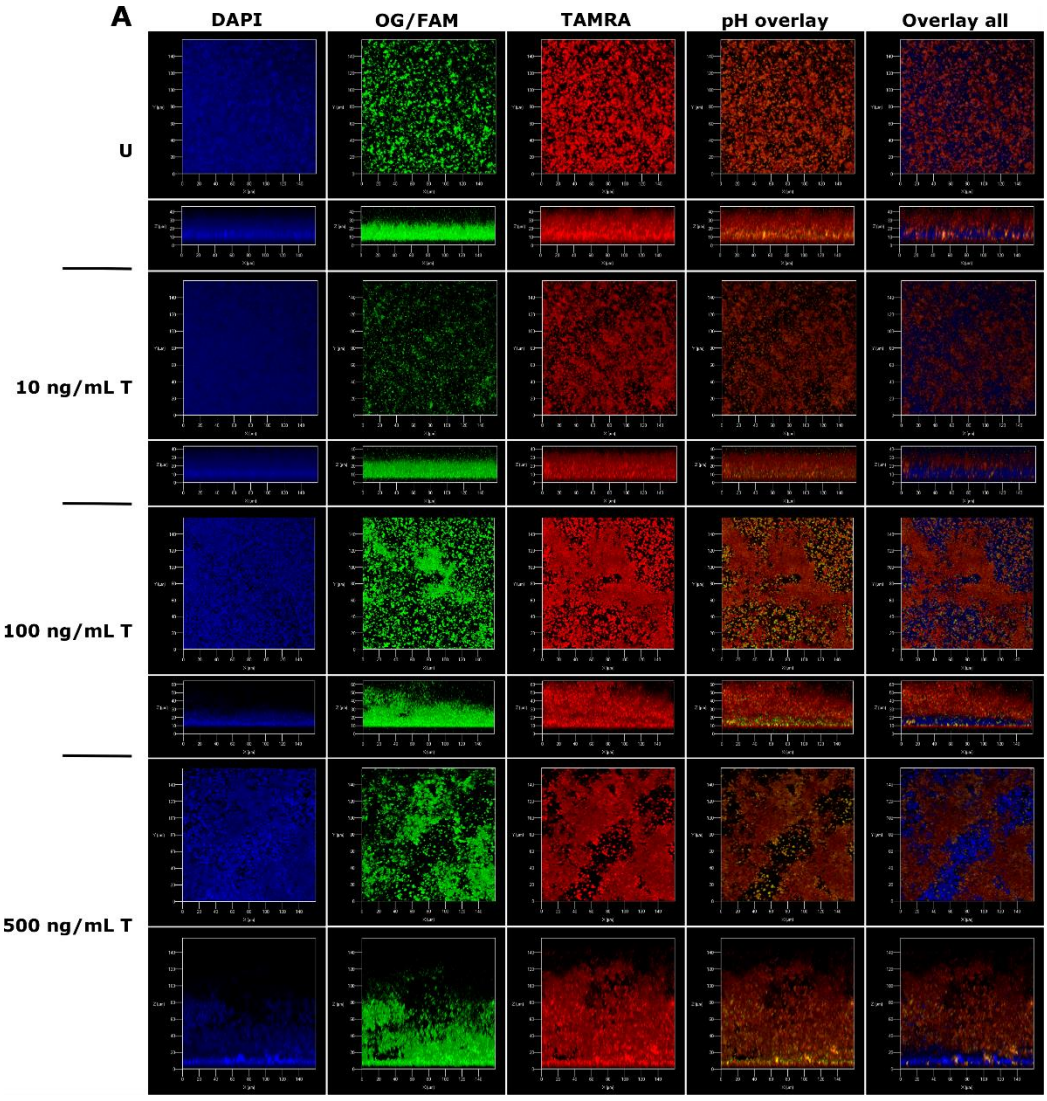
## 4.2 Chapter aims

This chapter investigates how biocide exposure affects the biofilm formation of *S. aureus,* with the aim of revealing the mechanisms underlying any observed changes. Biofilms were treated with physiological levels of triclosan and the resulting biofilm phenotypes characterised. Regulatory systems that were previously introduced in chapter 3, such as the stringent response, *agr* quorum sensing, and the CodY repressor were scrutinised. In addition to triclosan, the effects of other biocides were studied, namely chlorhexidine digluconate and benzalkonium chloride. To conclude this chapter, the effect of triclosan exposure on the formation and structure of polymicrobial biofilms was assessed. This was done by growing *S. aureus* with *P. aeruginosa*, a pathogen that frequently co-colonises alongside *S. aureus* (Fazli et al., 2009). Viability of each species was evaluated to discern if low concentrations of triclosan could alter interspecies competition.

## 4.3 Results

### 4.3.1 Triclosan does not greatly alter biofilm pH microenvironments, but does change biofilm structure in a concentration dependent manner

The effect of sub-MIC levels of triclosan on the pH microenvironment in *S. aureus* SH1000 WT biofilms was investigated. Biofilms were grown in the presence of pH-sensitive fluorescent nanosensors and exposed to a range of concentrations of triclosan (10 ng/mL, 100 ng/mL, 500 ng/mL). The nanosensors distributed throughout the entirety of the biofilm, allowing for ratiometric pH measurement across the total biofilm depth.



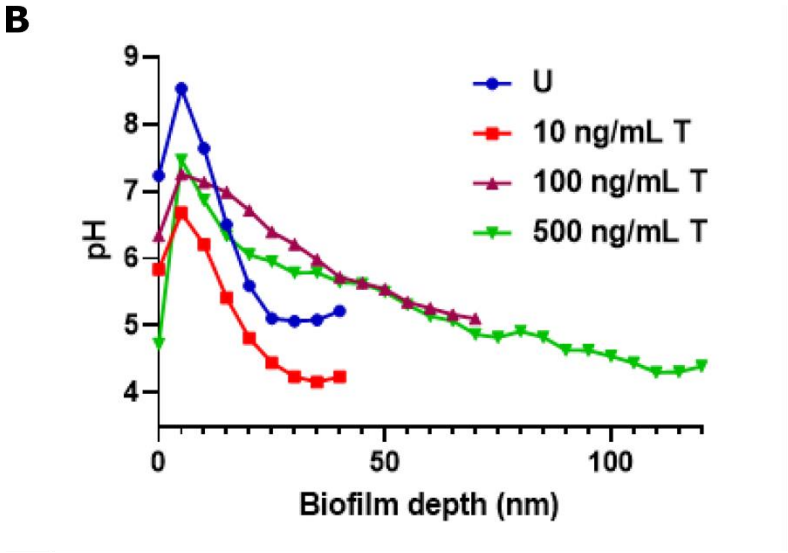



**Figure 4.1. Triclosan alters biofilm thickness in a concentration dependent manner, as revealed by fluorescent nanoparticles. A)** CLSM was used to assess the effect of triclosan on the pH microenvironments of *S. aureus* SH1000 WT biofilms. A range of triclosan concentrations were applied, including an untreated control (U), 10 ng/mL triclosan (10 ng/mL T), 100 ng/mL triclosan (100 ng/mL T), 500 ng/mL triclosan (500 ng/mL T). All conditions included 1 mg/mL pH-sensitive nanosensors to determine changes in pH. DAPI (blue) was used to visualise cells, OG/FAM (green) and TAMRA (red) are fluorophores encapsulated in the nanosensors. OG/FAM provide pH-sensitive fluorescence whilst TAMRA is pH-insensitive. For each condition, the top row of the panel shows the top surface of the *S. aureus* biofilms, with the biofilm thickness profile presented below. Horizontal lines on the left are used to segregate conditions. Images are representative of multiple experiments and were taken using the 40x objective (n=2). **B)** pH measurements of each condition acquired using positively charged pH sensitive fluorescent nanosensors across the depth of the biofilm at 5 nm intervals. Each condition has a different number of points due to differences in biofilm depth (n=1).

Across all conditions, the same pattern in pH change was observed. From the bottom of the biofilm to the top, there was an initial pH increase across the first few nanometres followed by a decline in pH until the top surface of the biofilm is reached (Fig 4.1B). Unexpectedly, increases in biofilm thickness were observed in a concentration dependent manner. Biofilms exposed to 10 ng/mL triclosan did not demonstrate increased thickness compared to untreated controls and stayed at approximately 40 nm, whilst 100 ng/mL triclosan exposed biofilms were 70 nm thick and 500 ng/mL triclosan biofilms were thicker still, measuring 120 nm. The thicker the biofilm, the more gradual the acidification across the biofilm

depth. Fig 4.1A illustrates that this extra thickness is not due to increased growth, as DAPI stained cells are not detected in the top regions of biofilms exposed to 100 ng/mL or 500 ng/mL triclosan. In regions of the biofilm with DAPI fluorescence, indicative of cells, nanosensor fluorescence is distributed evenly through the biofilm (U, 10 ng/mL T). However, where cells are sparse, nanosensors appear to be arranged into distinct aggregates on the top surface (100 ng/mL T, 500 ng/mL T). The presence of TAMRA fluorescence but reduced fluorescence from the pH-sensitive fluorophores OG/FAM signals that the structures the nanosensors are adhering to are acidic in nature.

### 4.3.2 Triclosan-induced changes to biofilm structure are caused by excess polysaccharide production

Having observed that triclosan exposure can alter biofilm thickness, the underlying structural changes were interrogated further. As the structures that nanosensors were associating with did not stain with DAPI, it was hypothesised that the nanosensors were interacting with an overproduced component of the biofilm matrix. Fluorescein conjugated WGA was used to stain the polysaccharide PIA, the predominant polysaccharide in the *S. aureus* biofilm matrix. To avoid cross-talk between WGA and OG/FAM fluorophores, single dye nanosensors were used. These nanosensors contain only the pH-insensitive fluorophore TAMRA, meaning that nanosensors will be able to be visualised due to their constant TAMRA fluorescence, but be unable to detect pH. These nanoparticles still use the same positively charged polyacrylamide shell as pH-sensitive nanosensors, meaning that they should behave exactly as observed in the previous experiment (4.3.1).

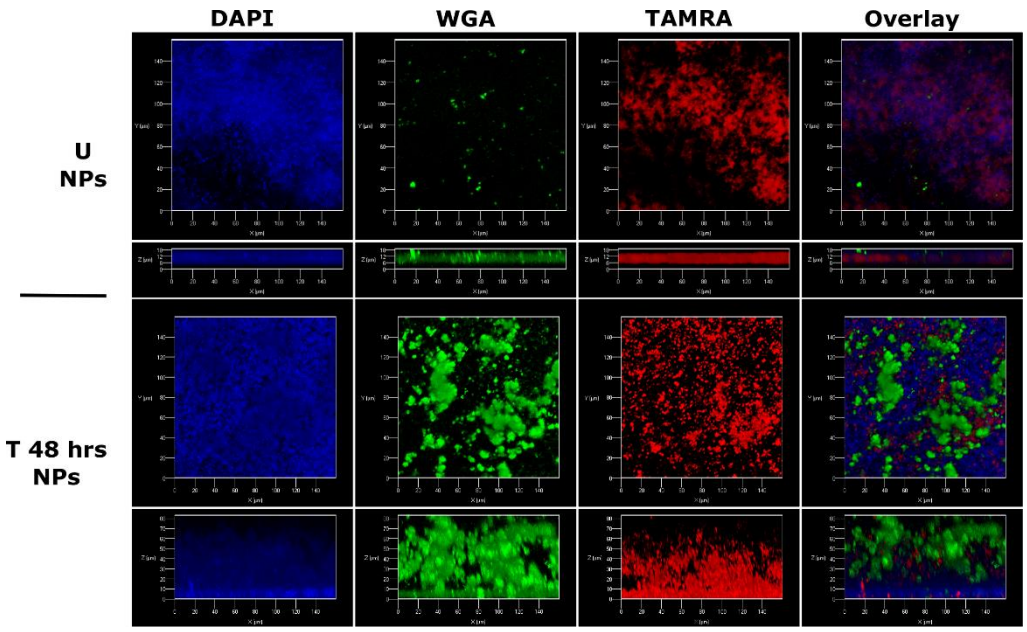


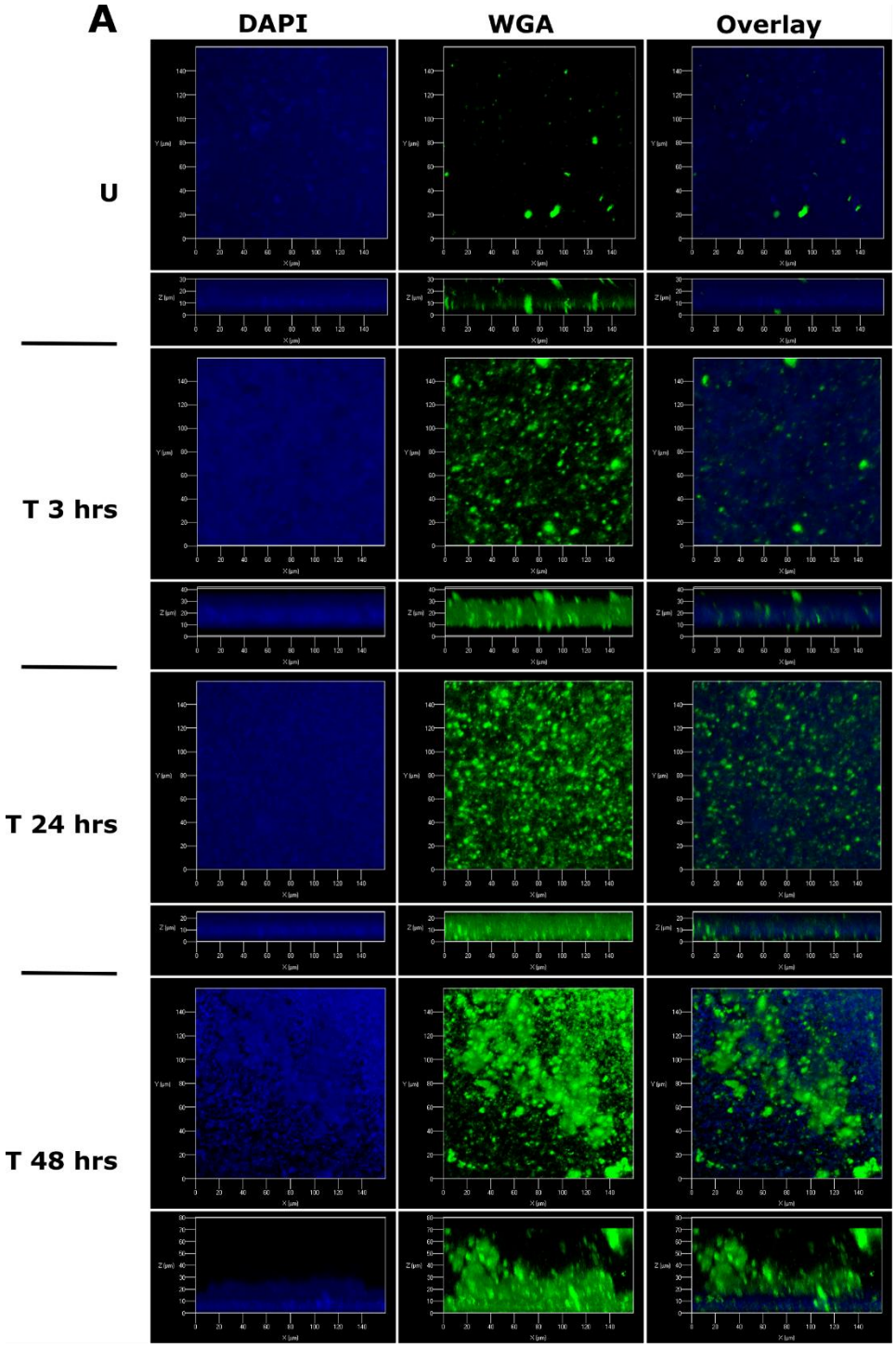

**Figure 4.2. Single dye fluorescent nanoparticles reveal that triclosan exposure increases the presence of biofilm polysaccharide.** CLSM was used to identify if polysaccharide was responsible for altering the biofilm formation of triclosan exposed *S. aureus* SH1000 WT biofilms. Untreated biofilms (U) and biofilms exposed to 500 ng/mL triclosan (500 ng/mL T) were compared. Both conditions included 1 mg/mL TAMRA only nanosensors to visualise nanosensor binding. DAPI (blue) was used to visualise cells, fluorescein-conjugated WGA (green) was used to visualise PNAG residues of polysaccharide. TAMRA (red) is encapsulated in the nanosensors and produces pH-insensitive signal. For both conditions, the top row of the panel shows the top surface of the *S. aureus* biofilms, with the biofilm thickness profile presented below. Horizontal lines on the left are used to segregate conditions. Images are representative of multiple experiments and were taken using the 40x objective (n = 2).

Confocal imaging revealed that, just as previously seen, biofilms grown in the presence of 500 ng/mL triclosan exhibited obvious differences in structure compared to untreated controls (Fig 4.2). Triclosan exposed biofilms were much thicker than control biofilms, with treated and untreated biofilms measuring 80 nm and 18 nm respectively. Single dye nanosensors were distributed across all depths of the biofilm. In treated biofilms, nanosensors were localised densely in the bottom layers and more diffusely arranged in the upper regions of the biofilm. WGA staining confirmed that triclosan-induced changes in biofilm structure were caused by excess levels of the polysaccharide PIA in the biofilm matrix. However, the nanosensors and polysaccharide do not perfectly colocalise, suggesting that the nanosensors may be trapped and

encased by the excess polysaccharide, as opposed to binding via electrostatic interactions.

### 4.3.3 Polysaccharide accumulation begins rapidly and continues for at least 48 hours after triclosan exposure

Continuing from the observation that triclosan exposure increased polysaccharide production in the biofilm matrix in 48 hour biofilms, it was investigated how triclosan-induced polysaccharide production manifests over time. This was examined by growing biofilms for a total of 48 hours, but exposing them to 500 ng/mL triclosan for different durations. Conditions selected were 48 hours (treated upon inoculation), 24 hours (treatment of one day old biofilms), and 3 hours (treatment of established biofilms, grown for 48 hours) before imaging. CLSM of biofilms was carried out, with DAPI staining to visualise cells and WGA staining to identify the distribution of exopolysaccharide. Untreated biofilms grown for 48 hours were used as a control.


A
DAPI
WGA
Overlay
U
T 3 hrs
T 24 hrs
T 48 hrs

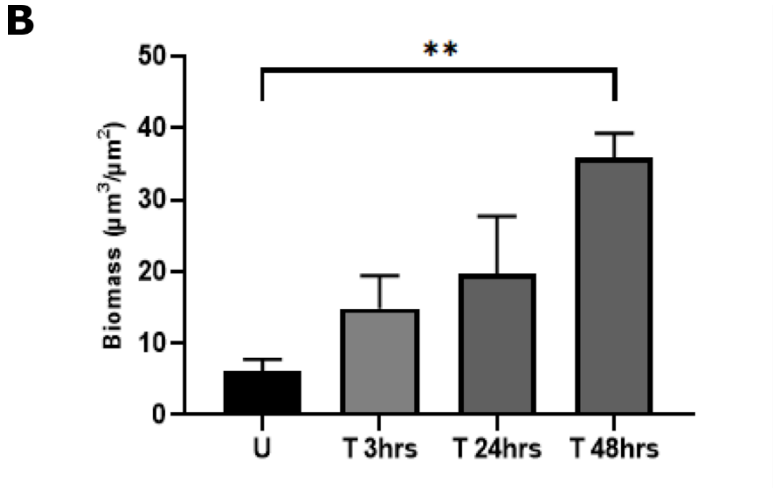
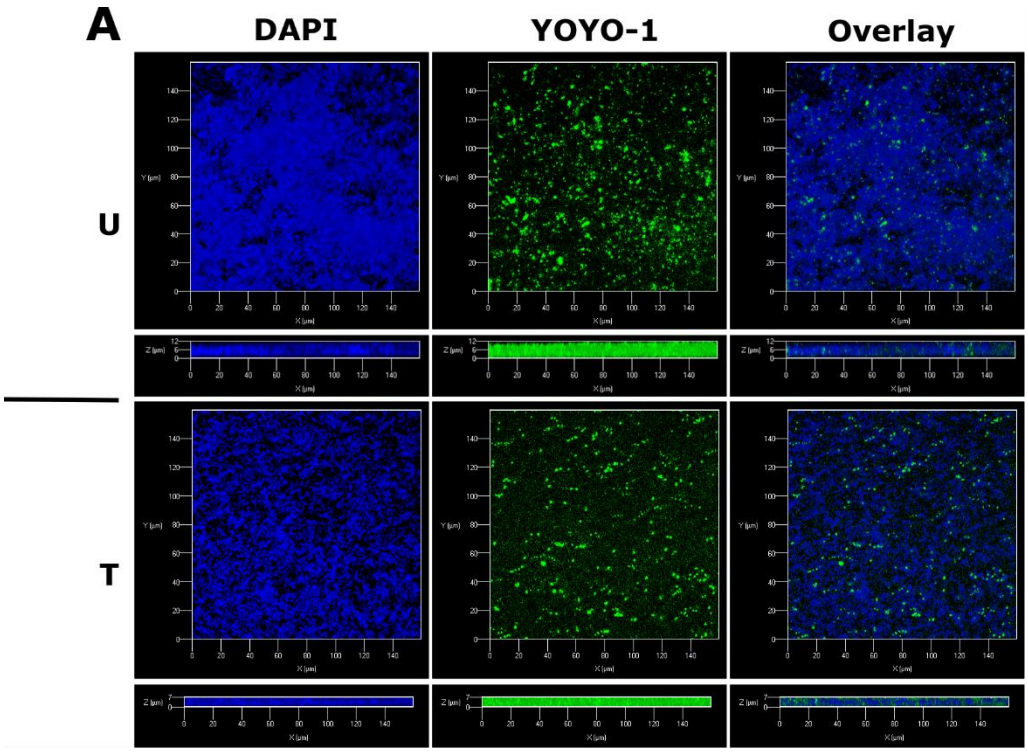



**Figure 4.3. Polysaccharide biomass increases over time. A)** CLSM was used to assess the effect of triclosan on the biofilm formation of *S. aureus* SH1000 WT over time. All biofilms were grown for 48 hours but triclosan was added at different timepoints before imaging. Biofilms were untreated (U) or exposed to 500 ng/mL triclosan 3 hours before imaging (T 3 hrs), 24 hours before imaging (T 24 hrs) or 48 hours before imaging (T 48 hrs). DAPI (blue) was used to visualise cells, fluorescein-conjugated WGA (green) was used to visualise PNAG residues of polysaccharide. For both conditions, the top row of the panel shows the top surface of the *S. aureus* biofilms, with the biofilm thickness profile presented below. Horizontal lines on the left are used to segregate conditions. Images are representative of multiple experiments and were taken using the 40x objective (n = 2). **B)** Quantification of polysaccharide biovolume was carried out using Comstat image analysis software. Error bars represent SEM, n=2. ** denotes P≤0.01.

Confocal imaging revealed that over time, polysaccharide was continually added into the biofilm matrix. Increases in polysaccharide production were seen after as little as 3 hours of triclosan treatment (Fig 4.3A). The highest polysaccharide concentrations were observed after 48 hours and intermediate levels after 24 hours of triclosan exposure. Comstat analysis quantified the increase in polysaccharide biovolume over time (Fig 4.3B). As no plateau is observed in these increases in biomass, it may be possible that polysaccharide levels would continue to increase past the 48 hour timepoint. By 48 hours of triclosan exposure, polysaccharide biovolume is significantly higher than untreated biofilms grown for the same duration.

### 4.3.4 Triclosan exposure does not alter the proportion of eDNA or protein in the biofilm matrix

As triclosan exposure could increase the proportion of polysaccharide within the *S. aureus* biofilm matrix, the next step was to determine if other matrix components were also altered. CLSM and targeted staining of 48 hour triclosan-exposed (500 ng/mL) and untreated SH1000 biofilms was carried out to determine if triclosan exposure stimulated an increase in matrix protein or eDNA production. Alongside DAPI staining to visualise cells, YOYO-1 was used to visualise eDNA whilst SYPRO Ruby matrix stain was used to reveal matrix proteins.



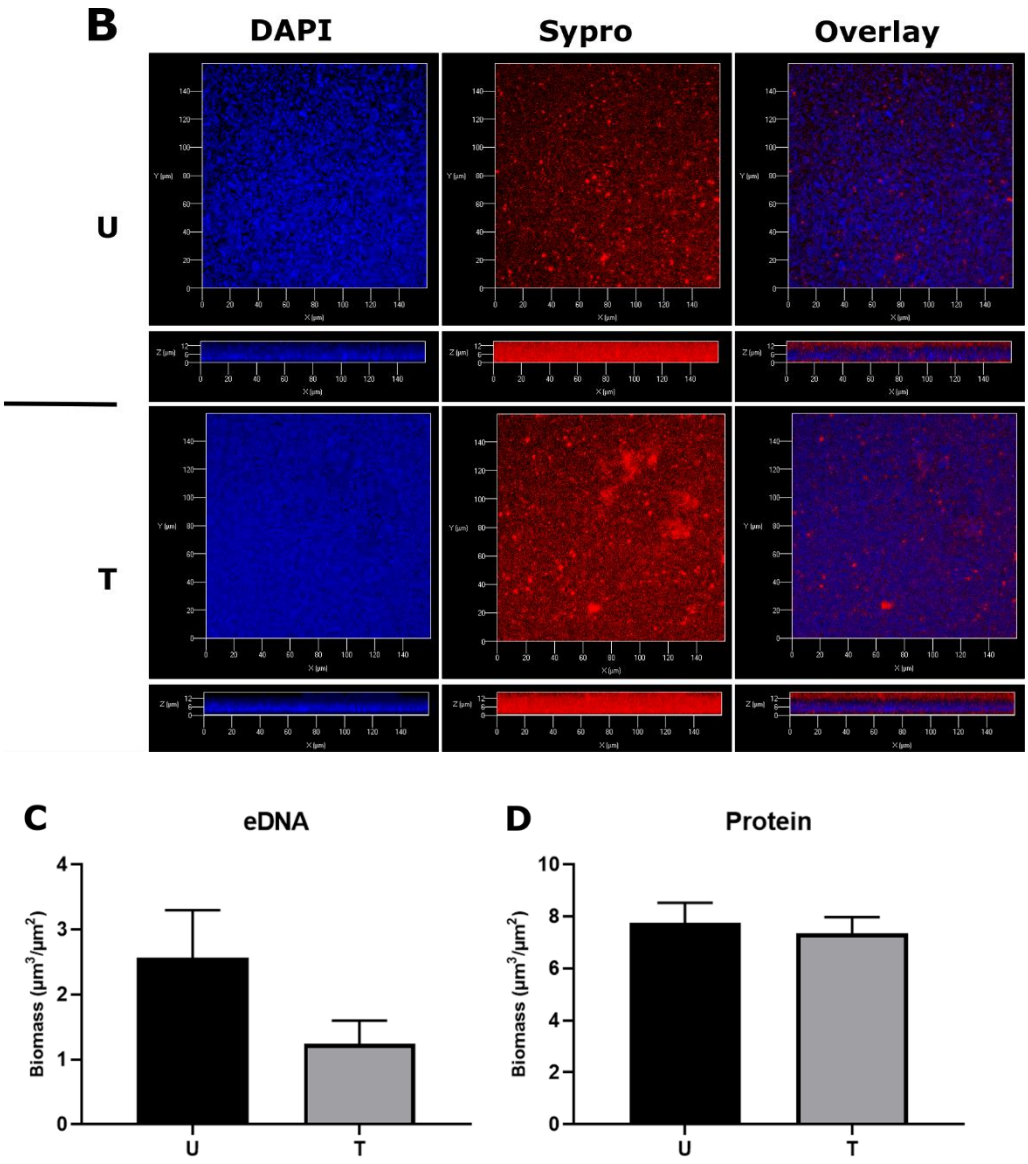
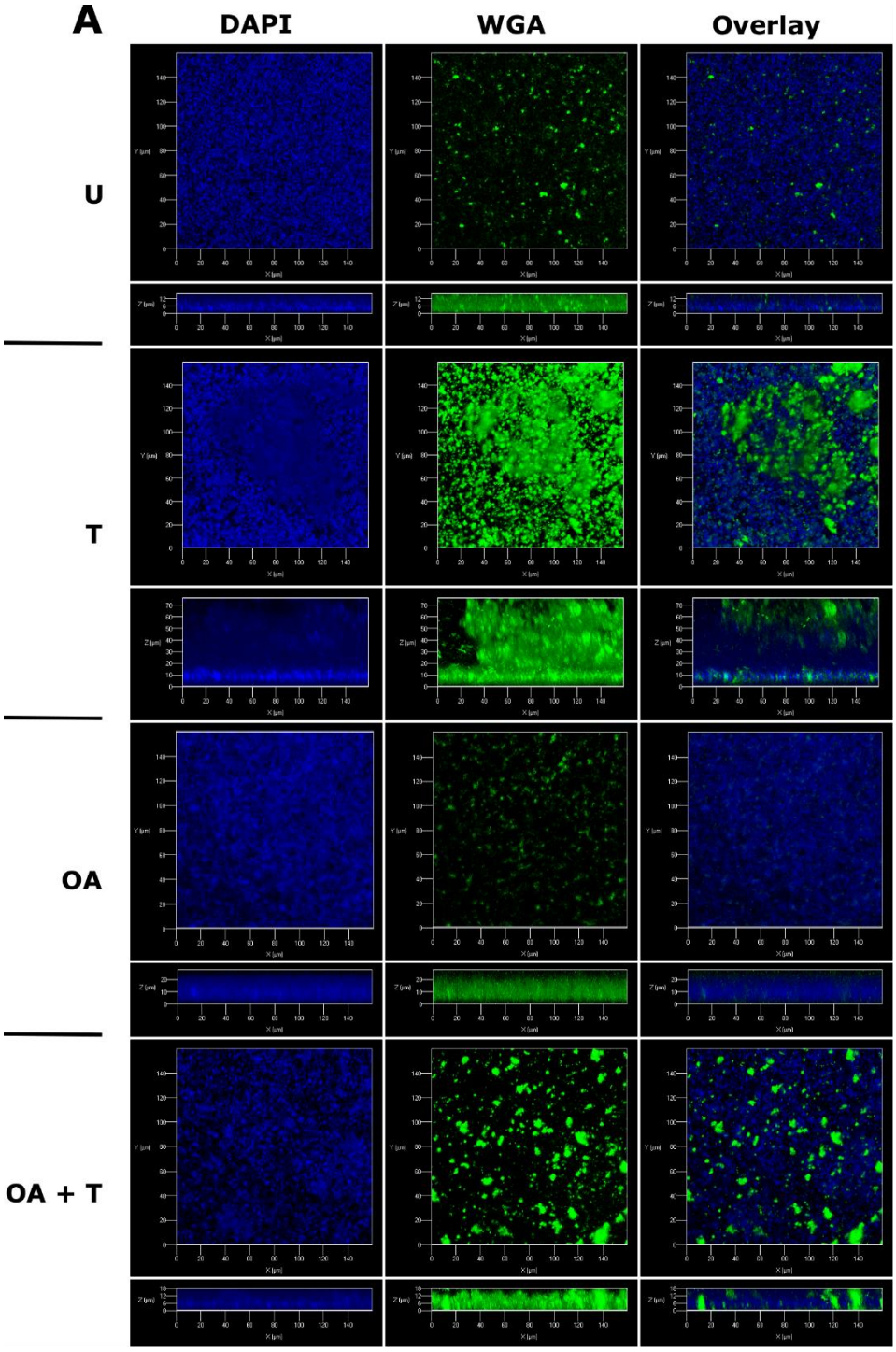



**Figure 4.4. Triclosan exposure does not significantly alter the proportion of eDNA and protein biofilm components in the SH1000 biofilm matrix.** CLSM was used to assess the effect of triclosan on the biofilm formation of *S. aureus* SH1000 biofilms. Biofilms were either untreated (U), or exposed to 500 ng/mL triclosan (T). **A)** DAPI (blue) was used to visualise cells, YOYO-1 (green) was used to visualise eDNA in the biofilm matrix. **B)** DAPI (blue) was used to visualise cells, SYPRO Ruby matrix stain (red) was used to visualise matrix proteins. For all conditions, the top row of the panel shows the top surface of the *S. aureus* biofilms, with the biofilm thickness profile presented below. Horizontal lines on the left are used to segregate conditions. Images staining for eDNA and protein are representative of multiple experiments and were taken using the 40x objective (n = 3). Quantification of eDNA biovolume **(C)**, and matrix protein biomass **(D)** was carried out using Comstat image analysis software. Error bars represent SEM, n=3.

Confocal imaging revealed that eDNA was distributed uniformly across the entire biofilm matrix, regardless of condition (Fig 4.4A). This same even distribution across conditions was also found with biofilm matrix proteins (Fig 4.4B). Subsequent Comstat analysis of protein biomass supported the observations that there is little difference in matrix protein between untreated and triclosan treated biofilms (Fig 4.4D). Contrastingly, Comstat analysis of eDNA biovolume indicated that triclosan exposure resulted in less eDNA being found in the biofilm matrix, however, this decrease was not significant. In light of these results, it is possible that triclosan exposure only increases production of matrix polysaccharide, but not other biofilm matrix components.

### 4.3.5 Triclosan-induced polysaccharide production is prevented in the presence of oleic acid

Since triclosan had been shown to alter biofilm formation, it was investigated whether oleic acid supplementation could overcome the biofilm-altering effects of the fatty acid synthesis inhibitor. Biofilms were exposed to oleic acid and sub-MIC levels of triclosan starting from initial inoculation. The physiologically relevant concentration of oleic acid (500 μM) was added to growth media. Imaging using CLSM took place after 48 hours of growth with DAPI used to image cells and WGA used to detect polysaccharide.


A
DAPI
WGA
Overlay
U
T
OA
OA + T

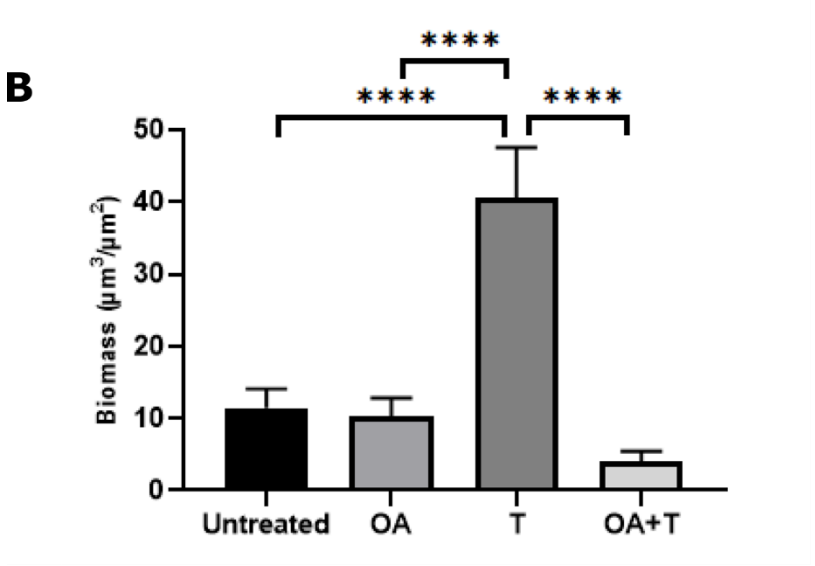


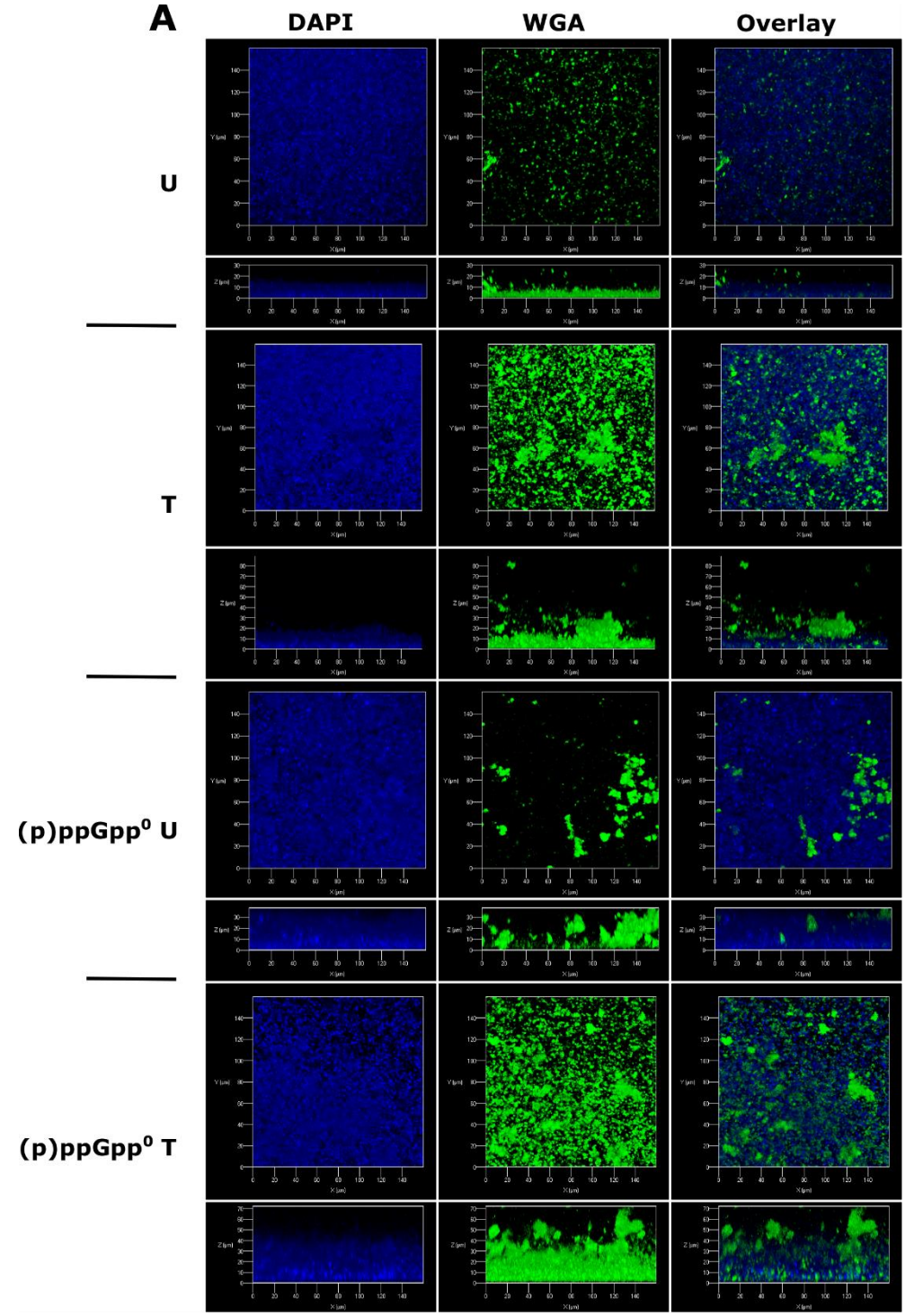

**Figure 4.5. Oleic acid supplementation significantly decreases polysaccharide biomass in triclosan exposed biofilms. A)** CLSM was used to assess the effect of triclosan and oleic acid supplementation on the biofilm formation of *S. aureus* SH1000 WT biofilms. Conditions include untreated biofilms (U), biofilms supplemented with 500 μM oleic acid (OA), exposed to 500 ng/mL triclosan (T), supplemented with 500 μM oleic acid and exposed to 500 ng/mL triclosan (OA+T). DAPI (blue) was used to visualise cells, fluorescein-conjugated WGA (green) was used to visualise PNAG residues of polysaccharide. For all conditions, the top row of the panel shows the top surface of the *S. aureus* biofilms, with the biofilm thickness profile presented below. Horizontal lines on the left are used to segregate conditions. Images are representative of multiple experiments and were taken using the 40x objective (n=3). **B)** Quantification of polysaccharide biomass was carried out using Comstat image analysis software. Error bars represent SEM, n=3 **** denotes P≤0.0001.

Microscopy confirmed the same biofilm appearance seen previously (Fig 4.2) in both untreated and triclosan exposed biofilms with regards to polysaccharide biovolume (Fig 4.5A). Oleic acid supplementation did not alter biofilm structure and when added in conjunction with triclosan (OA+T) produced significantly less polysaccharide compared to triclosan treated biofilms (Fig 4.5B). Oleic acid supplementation not only diminished excess polysaccharide production, but also prevented biofilm thickening. OA+T biofilms displayed thicknesses similar to OA and untreated biofilms, rather than the increased thickness presented by triclosan exposed biofilms. Although there was no notable increase in overall polysaccharide when oleic acid was present, polysaccharide did

seem to aggregate in these biofilms. The OA+T biofilm images in Fig 4.5A are a good example of this.

### 4.3.6 Despite a significant role in triclosan-induced antibiotic tolerance, the stringent response is not involved in triclosan-induced changes in biofilm structure

As the stringent response was implicated in other aspects of triclosan-induced changes to *S. aureus* physiology (3.3.10, 3.3.11), it was investigated whether this response also altered biofilm formation. The biofilm formation of the strain HG001 (p)ppGpp$^0$, a stringent response deletion mutant, was compared to HG001 WT to determine how interactions between triclosan and the stringent response affect biofilm structure and composition.


A
DAPI
WGA
Overlay
U
T
(p)ppGpp0 U
(p)ppGpp0 T

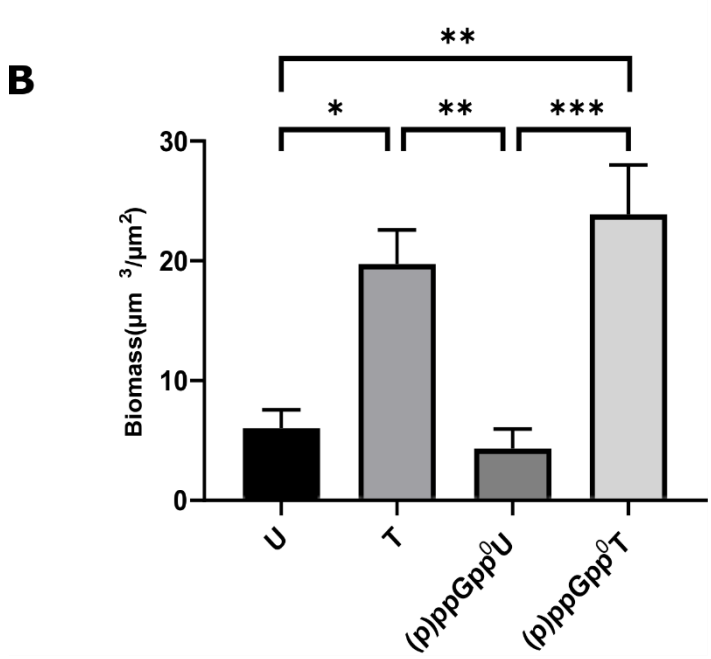
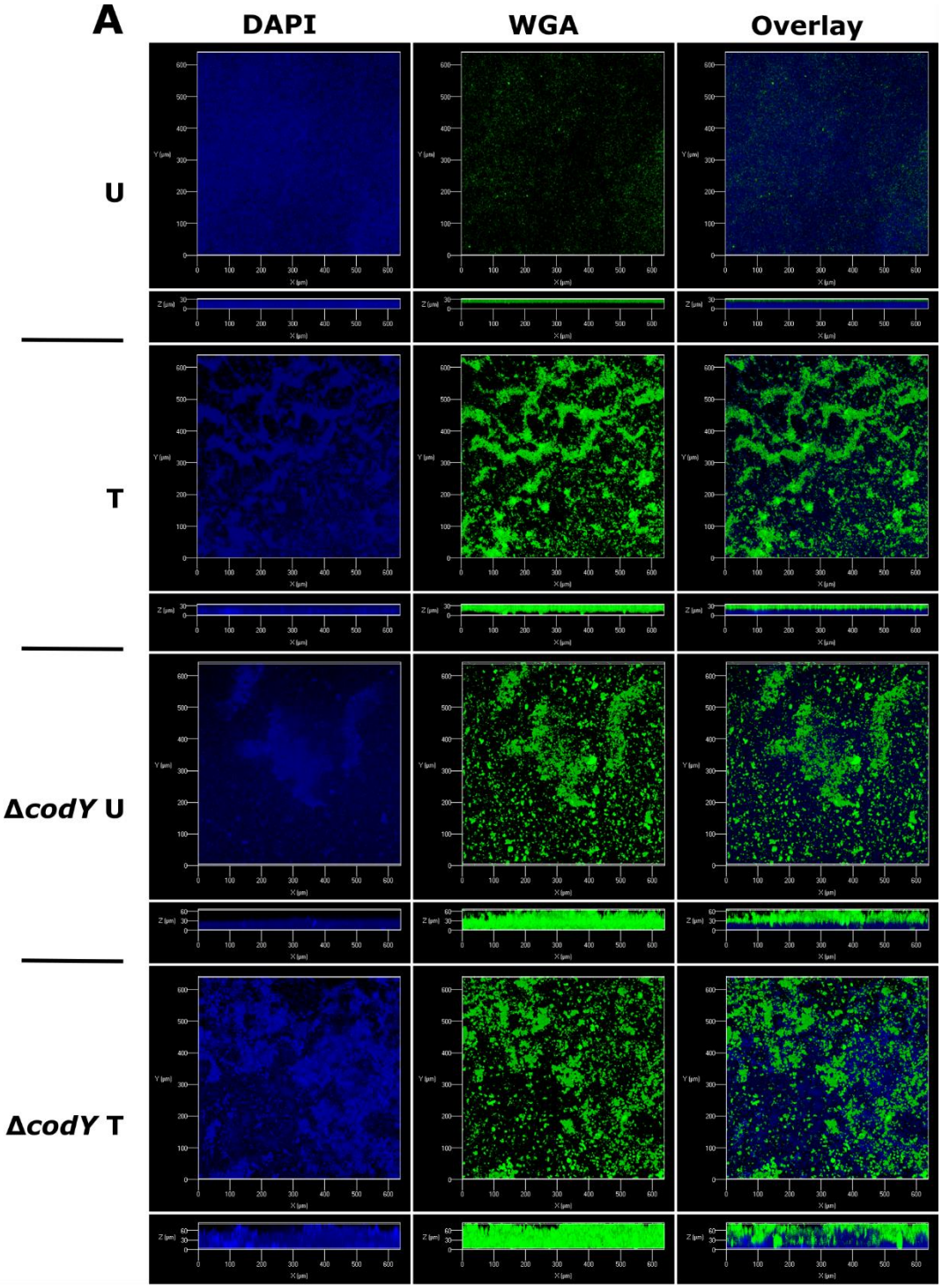



**Figure 4.6. The stringent response has no effect on triclosan-induced polysaccharide production. A)** CLSM was used to assess the effect of triclosan on the biofilm formation of *S. aureus* HG001 WT and HG001 (p)ppGpp$^0$ biofilms. For both strains, biofilms were either untreated (U, (p)ppGpp$^0$ U), or exposed to 500 ng/mL triclosan (T, (p)ppGpp$^0$ T). DAPI (blue) was used to visualise cells, fluorescein-conjugated WGA (green) was used to visualise PNAG residues of polysaccharide. For all conditions, the top row of the panel shows the top surface of the *S. aureus* biofilms, with the biofilm thickness profile presented below. Horizontal lines on the left are used to segregate conditions. Images are representative of multiple experiments and were taken using the 40x objective (n=3). **B)** Quantification of polysaccharide biomass was carried out using Comstat image analysis software. Error bars represent SEM, n=3. *** denotes P≤0.001, ** denotes P≤0.01, * denotes P≤0.05.

Staining with DAPI and WGA uncovered that the stringent response mutant displayed a similar biofilm composition compared to the wild type (Fig 4.6A). Triclosan exposed biofilms are thicker and rich in polysaccharide, with distinct structures extending above the top layers of cells. Fig 4.6B quantifies these observations, showing that triclosan treatment in both strains leads to significantly higher polysaccharide biomass in both strains. The lack of differences between HG001 WT and HG001 (p)ppGpp$^0$ suggest that the stringent response does not contribute to this altered biofilm structure.

### 4.3.7 The CodY repressor contributes to the regulation of polysaccharide production in *S. aureus* biofilms. However, this is in addition to, rather than the cause of triclosan-induced biofilm alterations

As the biosynthetic genes of PIA are repressed by CodY, it was hypothesised that the repressor played an essential role in triclosan-induced polysaccharide production. To investigate this a *codY* deletion mutant was used, in which polysaccharide production would not be repressed. If triclosan exposed biofilms exhibited the same quantities of polysaccharide as untreated *S. aureus* HG001 Δ*codY* biofilms, this would suggest that triclosan-induced changes in biofilm composition were due to derepression of CodY target genes.


A
DAPI
WGA
Overlay
U
T
ΔcodY U
ΔcodY T

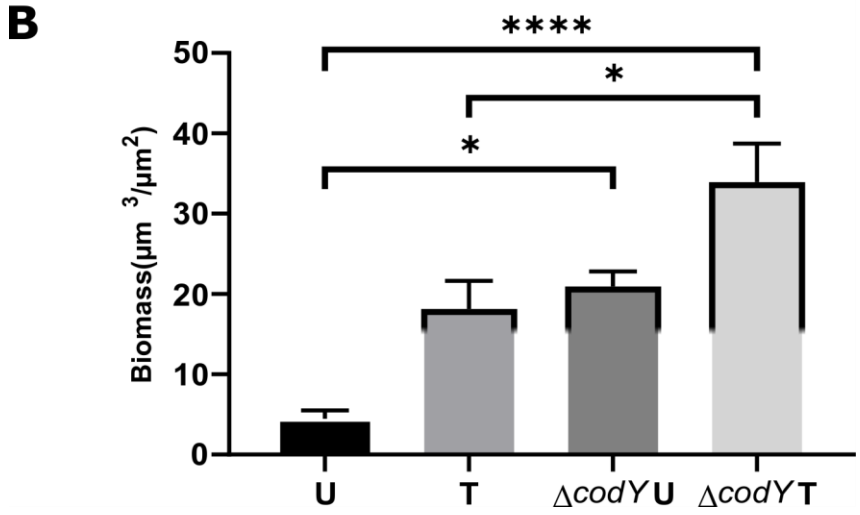


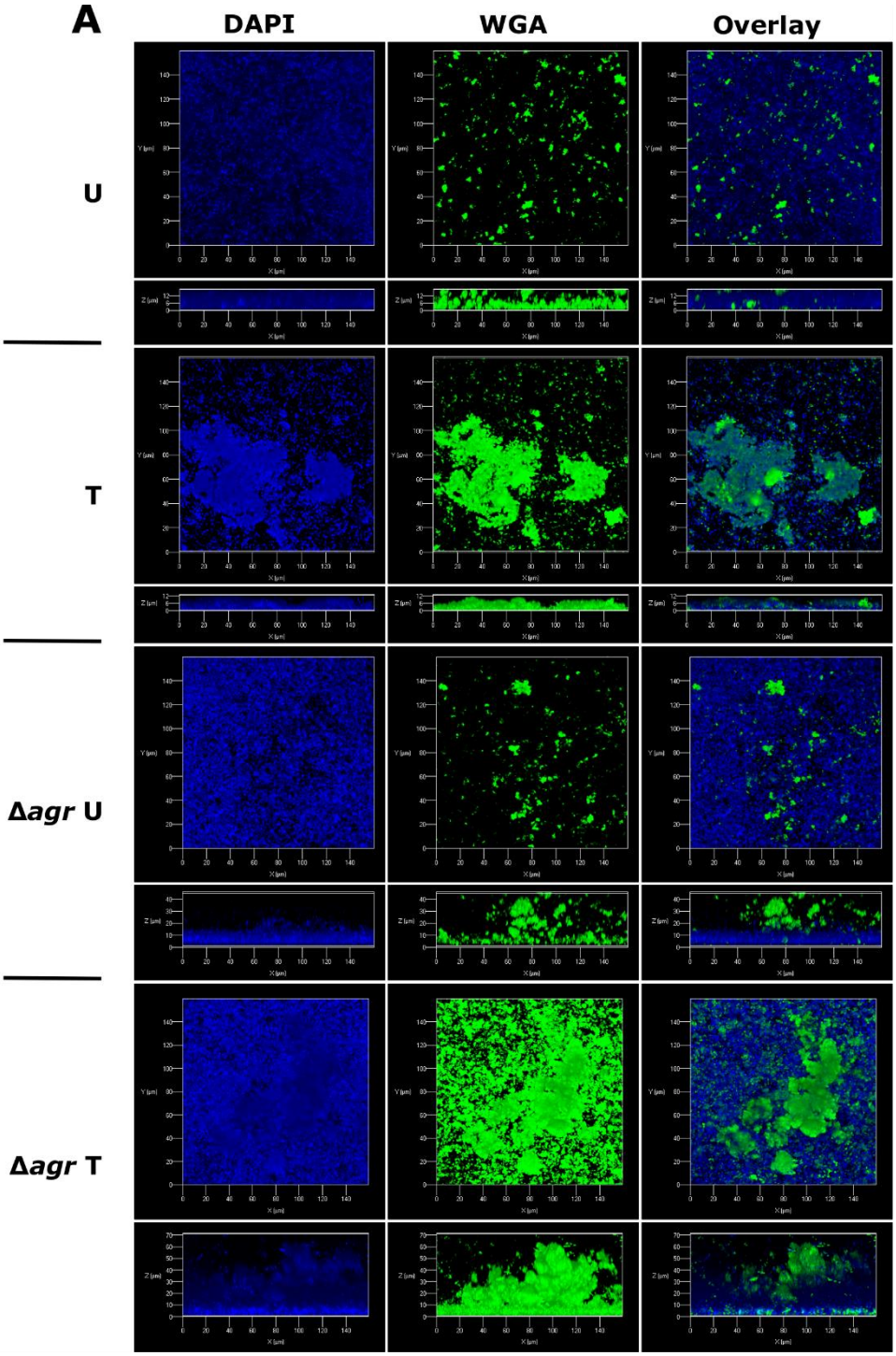

**Figure 4.7. Deletion of codY increases polysaccharide production. A)** CLSM was used to assess the effect of triclosan on the biofilm formation of *S. aureus* HG001 WT and HG001 Δ*codY* biofilms. For both strains, biofilms were either untreated (U, Δ*codY* U), or exposed to 500 ng/mL triclosan (T, Δ*codY* T). DAPI (blue) was used to visualise cells, fluorescein-conjugated WGA (green) was used to visualise PNAG residues of polysaccharide. For all conditions, the top row of the panel shows the top surface of the *S. aureus* biofilms, with the biofilm thickness profile presented below. Horizontal lines on the left are used to segregate conditions. Images are representative of multiple experiments and were taken using the 10x objective (n=3). **B)** Quantification of polysaccharide biomass was carried out using Comstat image analysis software. Error bars represent SEM, n=3. **** denotes P≤0.0001, * denotes P≤0.05.

CLSM revealed that CodY does indeed contribute to excess polysaccharide accumulating in biofilms, with more WGA fluorescence observed in T, Δ*codY* U and Δ*codY* T biofilms. Whilst this shared biofilm composition among triclosan treated WT and Δ*codY* biofilms initially seemed to indicate CodY was responsible for triclosan-induced polysaccharide production, further inspection showed otherwise. Comstat analysis of biofilms demonstrated that whilst there was no significant difference in the amount of polysaccharide between triclosan treated WT biofilms and untreated Δ*codY* biofilms, there was a significant difference between triclosan treated biofilms of both strains (T, Δ*codY* T Fig 4.7B). This significant increase in the Δ*codY* T condition appears to be a combination of both the lack of CodY repression upon polysaccharide biosynthetic genes and the effects induced by triclosan. This result would imply that although triclosan exposure and CodY

derepression both result in the same changes biofilm composition, they are not linked and display an additive, rather than causal effect in these conditions.

### 4.3.8 Biofilms of strains with deficient *agr* quorum sensing systems produce excess polysaccharide in the presence of triclosan

The *agr* quorum sensing system is associated with biofilm dispersal. An SH1000 Δ*agr* strain was used to determine whether triclosan-induced changes in biofilm structure were a result of shutting off the *agr* quorum sensing system. If this were the case, it would be expected that untreated and treated SH1000 Δ*agr* biofilms would exhibit the same biofilm changes observed when untreated SH1000 WT is exposed to triclosan throughout biofilm formation.


A
DAPI
WGA
Overlay
U
T
Δagr U
Δagr T

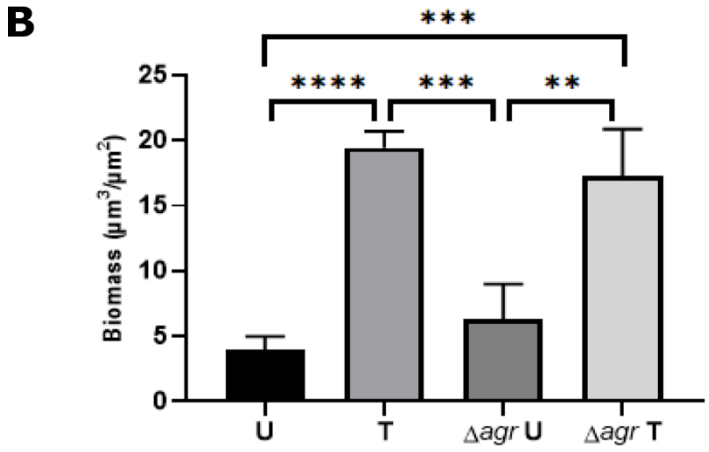
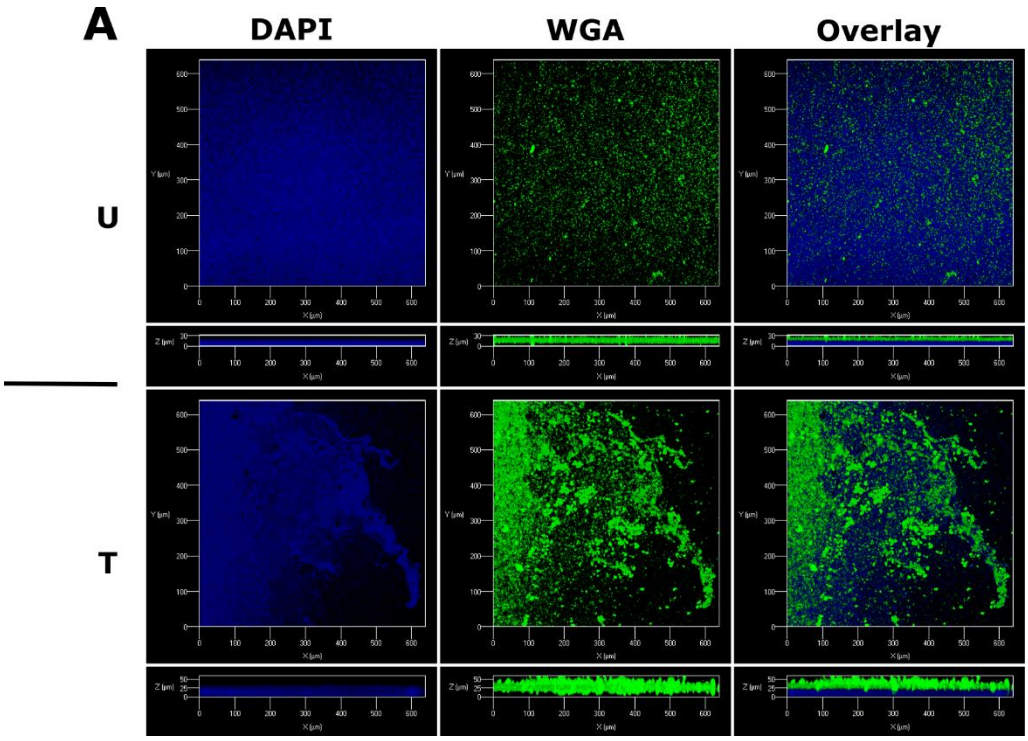


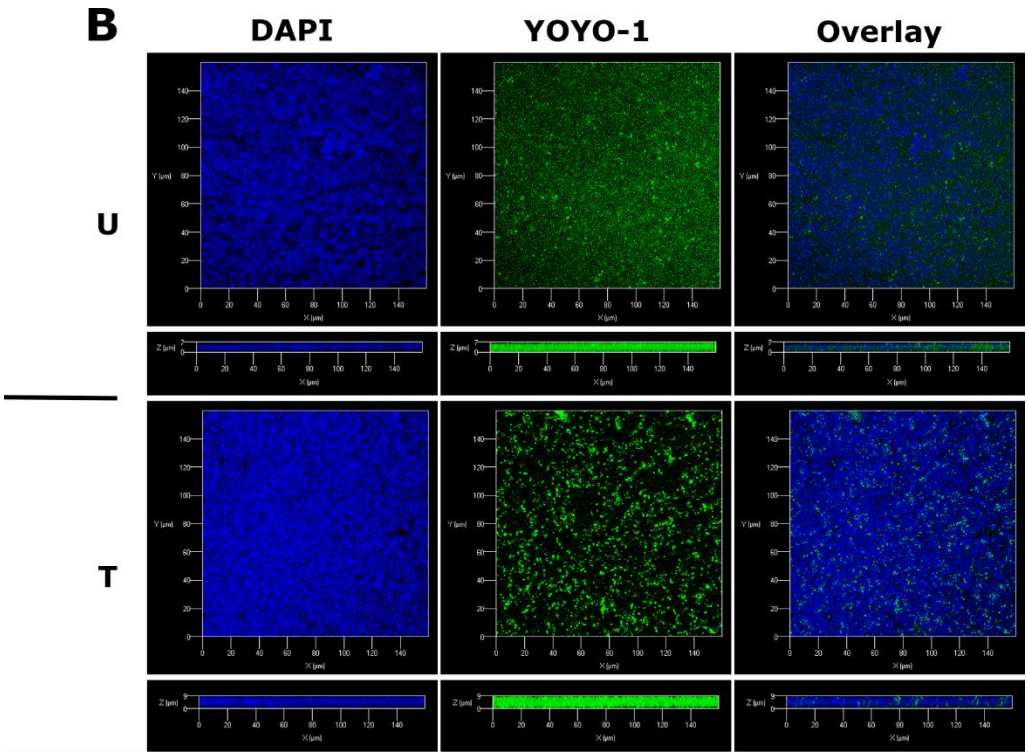

**Figure 4.8. Deletion of *agr* has no effect on triclosan-induced polysaccharide production. A)** CLSM was used to assess the effect of triclosan on the biofilm formation of *S. aureus* SH1000 WT and SH1000 Δ*agr* biofilms. For both strains, biofilms were either untreated (U, Δ*agr* U), or exposed to 500 ng/mL triclosan (T, Δ*agr* T). DAPI (blue) was used to visualise cells, fluorescein-conjugated WGA (green) was used to visualise PNAG residues of polysaccharide. For all conditions, the top row of the panel shows the top surface of the *S. aureus* biofilms, with the biofilm thickness profile presented below. Horizontal lines on the left are used to segregate conditions. Images are representative of multiple experiments and were taken using the 40x objective (n=3). **B)** Quantification of polysaccharide biomass was carried out using Comstat image analysis software. Error bars represent SEM, n=3. **** denotes P≤0.0001, *** denotes P≤0.001, ** denotes P≤0.01.

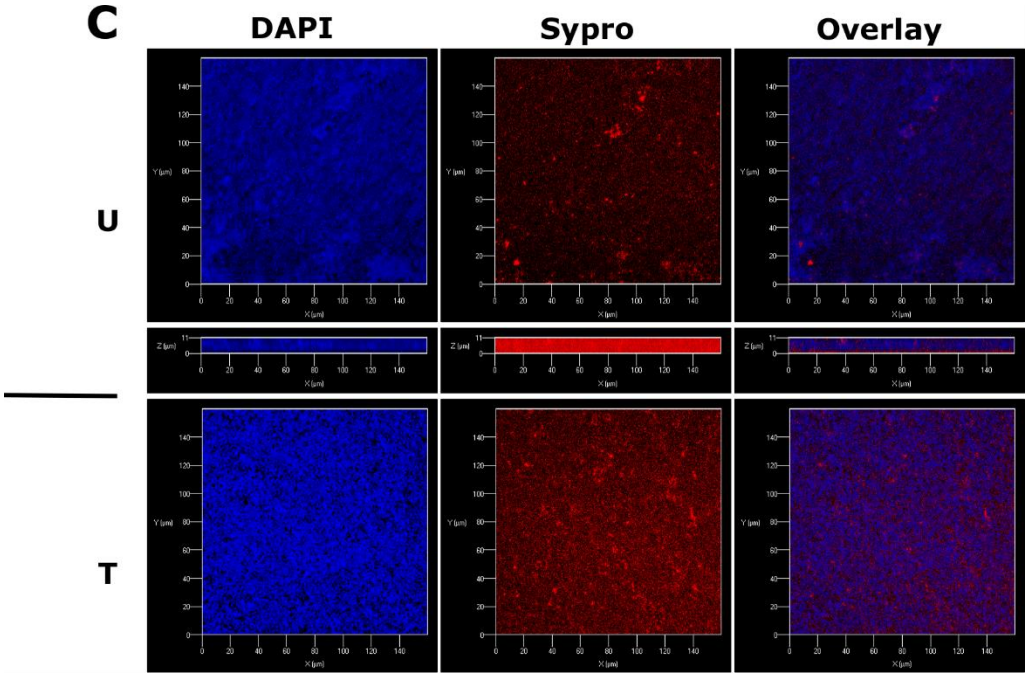
Fig 4.8A shows that triclosan exposure in both strains results in excess polysaccharide production. Quantification in Fig 4.8B shows that there is a significant increase in polysaccharide biomass for both strains. No significant differences were observed between the untreated SH1000 WT and SH1000 Δ*agr,* suggesting that *agr* function has a negligible effect on the formation of 48 hour biofilms in *S. aureus*. Due to the similarity of both strains, it is possible that even in the WT the *agr* system is either not expressed or expressed at very low levels during biofilm formation in the presence of triclosan. Taken together, these findings indicate that triclosan-induced changes to biofilm formation are mediated by mechanisms distinct from the control of the *agr* quorum sensing system.

### 4.3.9 Triclosan can alter the biofilm formation of the clinically relevant CA-MRSA strain USA300

Previous experiments attempted to discern the mechanism of triclosan-induced biofilm formation in wild type and mutant lab strains. This experiment, using the CA-MRSA strain USA300 JE2 was carried out to determine whether triclosan exposure could alter the biofilm formation of clinically relevant *S. aureus* strains. USA300 was grown and exposed to 500 ng/mL triclosan for 48 hours and imaged using CLSM in conjunction with DAPI, WGA, YOYO-1, and SYPRO Ruby staining.




B
DAPI
YOYO-1
Overlay
U
T


C
DAPI
Sypro
Overlay
U
T

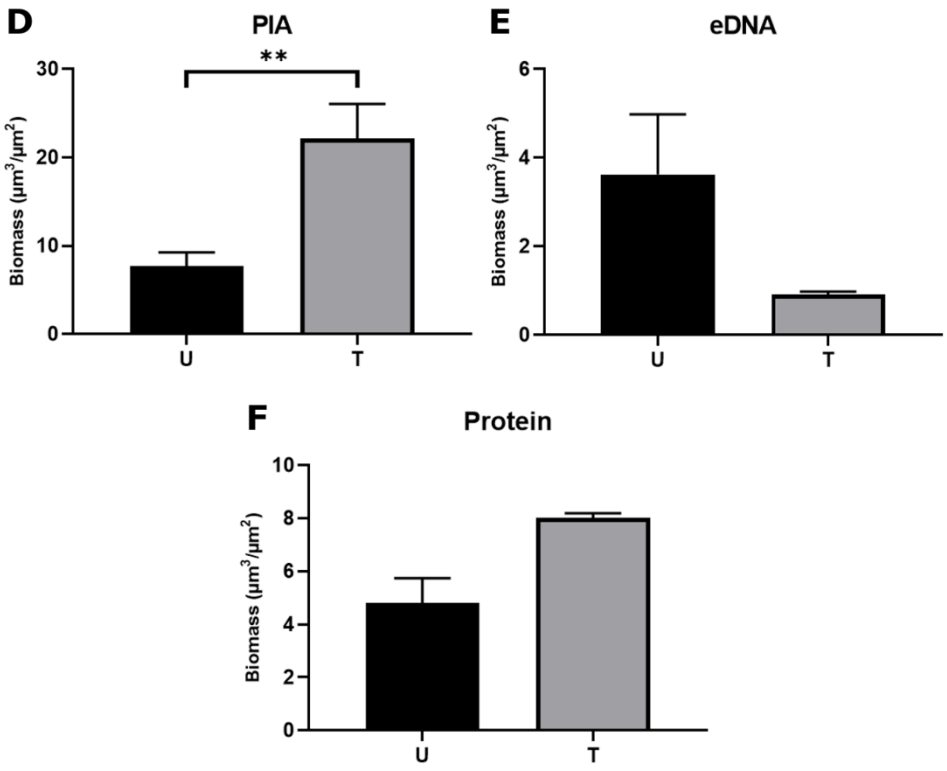



**Figure 4.9. Physiologically relevant levels of triclosan also alter the biofilm formation of MRSA.** CLSM was used to assess the effect of triclosan on the biofilm formation of *S. aureus* USA300 biofilms. Biofilms were either untreated (U), or exposed to 500 ng/mL triclosan (T). **A)** DAPI (blue) was used to visualise cells, fluorescein-conjugated WGA (green) was used to visualise PNAG residues of PIA polysaccharide. Images are representative of multiple experiments and were taken using the 10x objective (n=3). **B)** DAPI (blue) was used to visualise cells, YOYO-1 (green) was used to visualise eDNA in the biofilm matrix. **C)** DAPI (blue) was used to visualise cells, SYPRO Ruby matrix stain (red) was used to visualise matrix proteins. For all conditions, the top row of the panel shows the top surface of the *S. aureus* biofilms, with the biofilm thickness profile presented below. Horizontal lines on the left are used to segregate conditions. Images staining for eDNA and protein are representative of multiple experiments and were taken using the 40x objective (n=3). Quantification of polysaccharide biomass **(D)**, eDNA biomass **(E)**, and matrix protein biomass **(F)** was carried out using Comstat image analysis software. Error bars represent SEM, n=3. ** denotes P≤0.01.

Confocal imaging found that triclosan exposure did lead to increased polysaccharide biomass in USA300 biofilms (Fig 4.9A). This increase in biomass was statistically significant (Fig 4.9D), and matched the results found previously in the lab strains SH1000 and HG001. These results demonstrate that triclosan-induced changes in biofilm structure can be

observed in clinically relevant strains as well as lab strains. Triclosan exposure also appeared to result in less eDNA (Fig 4.9B) and more protein in the biofilm matrix (Fig 4.9C). However, the variance across samples for these findings meant that these trends were not statistically significant (Fig 4.9E, Fig 4.9F).

### 4.3.10 The phenol-sulfuric acid method confirms that triclosan exposure induces excess polysaccharide production

Previous experiments have shown that triclosan treated *S. aureus* biofilms accumulated significantly more exopolysaccharide within the biofilm matrix compared to untreated biofilms. However, this was only detected and analysed by microscopy and image analysis software, respectively. To confirm these findings with an alternate method, matrix polysaccharide was extracted using NaCl, followed by colorimetric quantification using the phenol sulfuric acid method. CFUs of HG001 WT biofilms were also measured in parallel, to enumerate the viable bacteria in each condition.

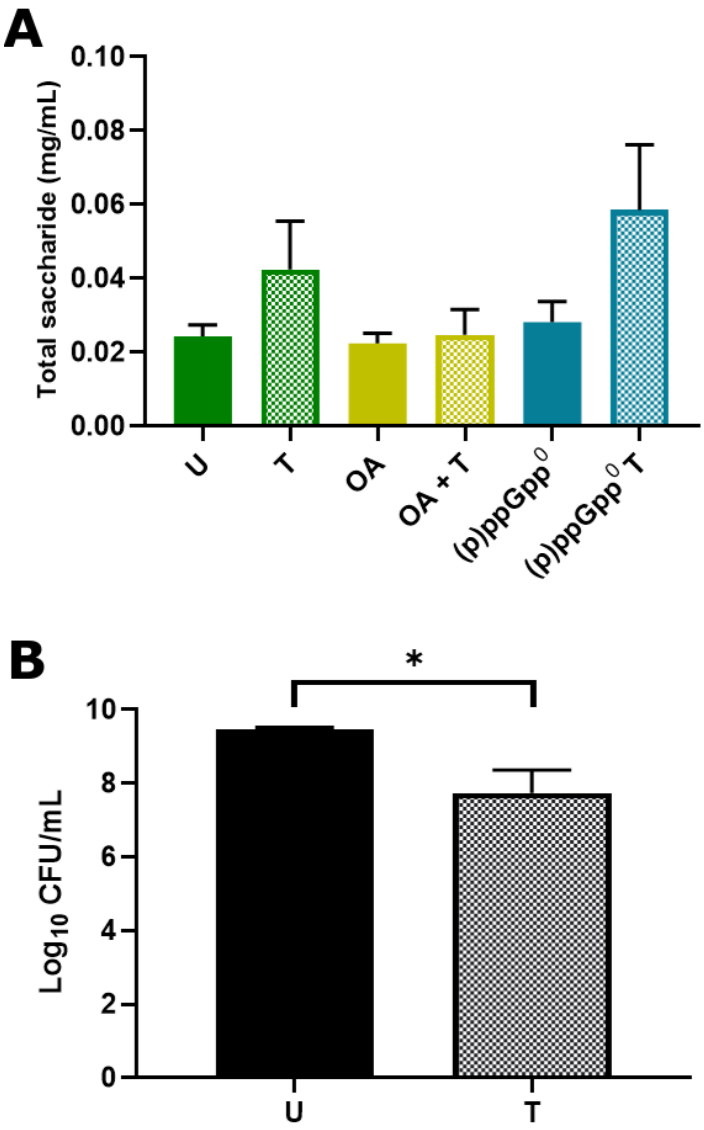



**Figure 4.10. Although triclosan exposed biofilms produce more polysaccharide, they consist of significantly fewer cells. A)** The phenol-sulfuric acid method was carried out to quantify total saccharide extracted from the biofilms of HG001 WT and HG001 (p)ppGpp$^0$. Both strains were untreated (U, (p)ppGpp$^0$) or exposed to 500 ng/mL triclosan (T, (p)ppGpp$^0$ T). HG001 WT was also supplemented with 500 µM oleic acid (OA) or supplemented with 500 µM oleic acid and exposed to 500 ng/mL triclosan (OA+T). Error bars represent SEM, n=3. **B)** Endpoint CFUs of untreated (U) or 500 ng/mL triclosan exposed (T) HG001 WT biofilms. Error bars represent SEM, n=3. * denotes P≤0.05.

All conditions followed the same trends in polysaccharide concentration as previously observed by CLSM imaging. Triclosan treated biofilms of both the HG001 WT and HG001 (p)ppGpp$^0$ strains produced approximately double the total saccharide of untreated biofilms (Fig 4.10A). Oleic acid supplemented biofilms did not produce excess

polysaccharide when exposed to triclosan, with approximately 0.025 mg/mL total saccharide being detected in both OA and OA+T biofilms. CFU enumeration of biofilms showed that triclosan exposed biofilms were populated by significantly less bacteria than untreated biofilms. Taken together, these results show that triclosan exposed *S. aureus* biofilms can produce approximately double the concentration of polysaccharide, despite consisting of significantly less cells.

### 4.3.11 Even though triclosan exposure increases matrix polysaccharide, overall biomass is reduced in triclosan treated biofilms

Experiment 4.3.10 highlighted the disparities in polysaccharide production and the number of cells in triclosan treated biofilms. To investigate how these factors contributed to overall biofilm biomass, crystal violet assays were carried out. HG001 WT, SH1000 WT, and USA300 WT biofilms were grown both with and without triclosan. Oleic acid supplementation was also included, as this had been previously shown to overcome the growth inhibitory effects of physiological levels of triclosan. Biofilms of the HG001 Δ*codY* strain were studied as these biofilms produce excess polysaccharide without triclosan exposure. Other mutant strains used in previous experiments HG001 (p)ppGpp$^0$ and SH1000 Δ*agr* were also investigated.

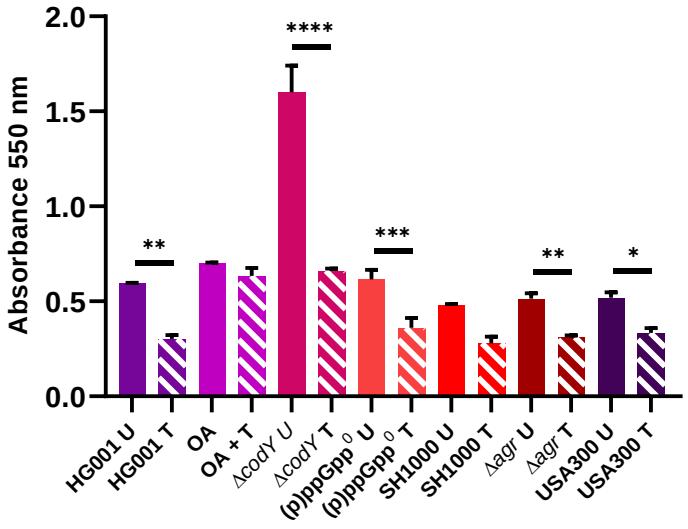



**Figure 4.11. Triclosan exposure significantly decreases biofilm biomass.** Crystal violet assays were carried out to assess the biomass of HG001 WT, HG001 Δ*codY*, HG001 (p)ppGpp$^0$, SH1000 WT, SH1000 Δ*agr*, and USA300 WT strains. All strains were untreated (U) or exposed to 500 ng/mL triclosan (T). HG001 WT was also supplemented with 500 µM oleic acid (OA) or supplemented with 500 µM oleic acid and exposed to 500 ng/mL triclosan (OA+T). Error bars represent SEM, n=3. **** denotes P≤0.0001, *** denotes P≤0.001, ** denotes P≤0.01, * denotes P≤0.05.

Crystal violet assays showed that biomass was significantly reduced in all strains when exposed to triclosan compared to untreated biofilms. This decrease is not significant for SH1000 WT biofilms, though biomass is still markedly reduced following growth in the presence of triclosan. However, this was not seen when triclosan exposed biofilms were also supplemented with oleic acid. Oleic acid only supplemented biofilms did not have increased growth compared to the untreated control, suggesting that the oleic acid in the OA+T biofilms prevented inhibition by triclosan, as opposed to overcompensating for triclosan-induced biomass decreases. The Δ*codY* untreated biofilms had significantly higher biomass compared to all other conditions, but triclosan exposure significantly reduced this. Despite triclosan-induced reduction of biomass in Δ*codY* biofilms, overall biomass of Δ*codY* biofilms was still higher than triclosan exposed HG001 WT biofilms. Taken together, these results indicate that regardless of the biomass forming potential of a strain,

triclosan exposure reduces this unless countered with fatty acid supplementation.

### 4.3.12 Neither chlorhexidine digluconate nor benzalkonium chloride significantly alter the concentration of biofilm matrix components

As shown previously, triclosan exposure during biofilm formation induced increased polysaccharide production in *S. aureus* biofilms. To determine whether other widely used biocides could induce changes to biofilm formation, biofilms were grown in the presence of sub-MIC concentrations of BAC (0.0002%) and (0.0001%) CHG. Alongside DAPI and WGA staining, YOYO-1 staining was used to visualise the distribution of eDNA in the biofilm matrix. In the previous chapter, it was shown that the stringent response was necessary for inducing antibiotic tolerance in *S. aureus* following exposure to CHG and BAC. To determine whether the stringent response facilitates any biocide induced changes in matrix composition, the HG001 (p)ppGpp$^0$ strain was investigated alongside the HG001 WT.

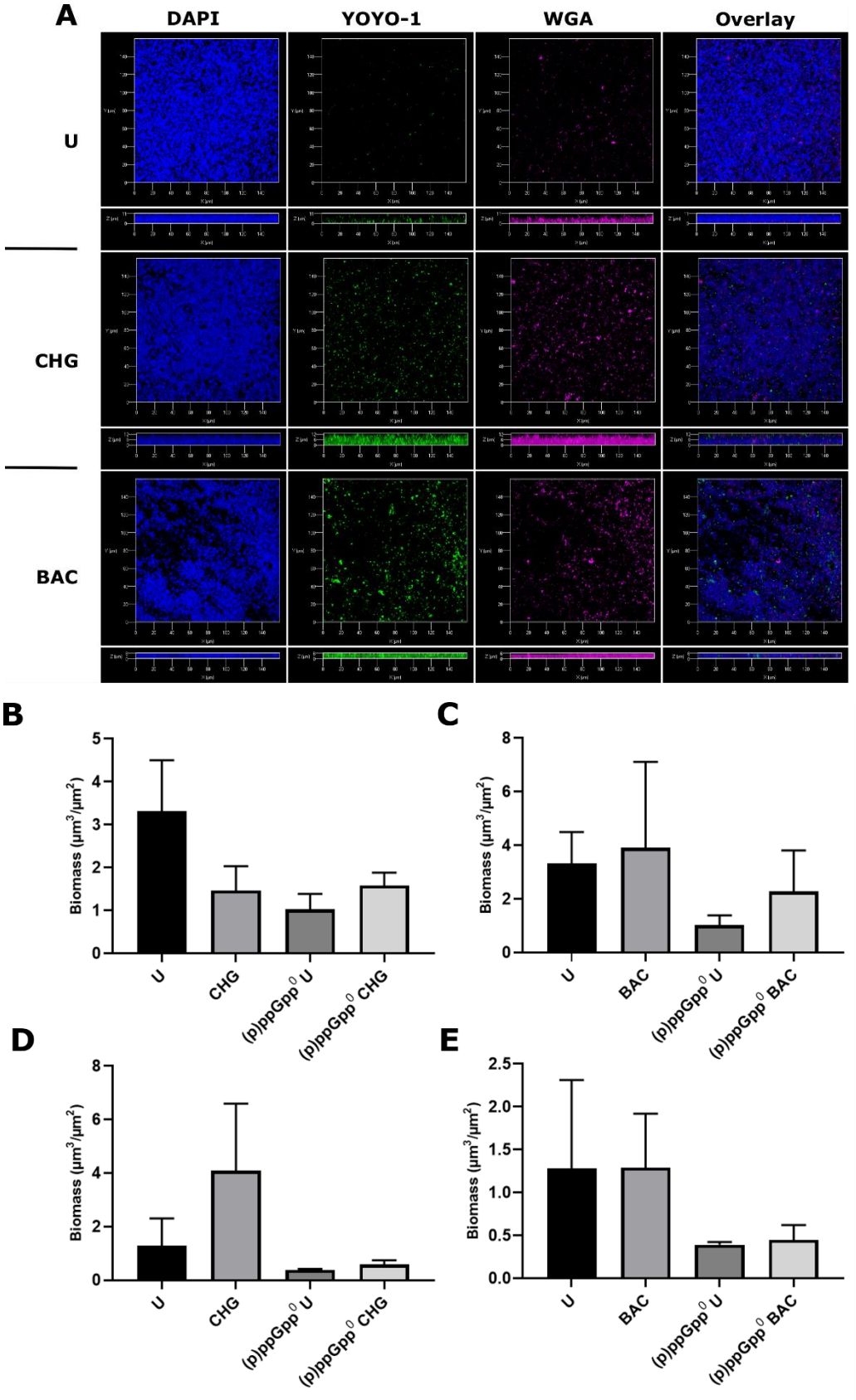



**Figure 4.12. Neither CHG or BAC exposure induced changes in biofilm structure.** **A)** CLSM was used to assess the effect of CHG or BAC on the biofilm formation of *S. aureus* HG001 WT biofilms. For both WT and (p)ppGpp$^0$ strains, biofilms were either

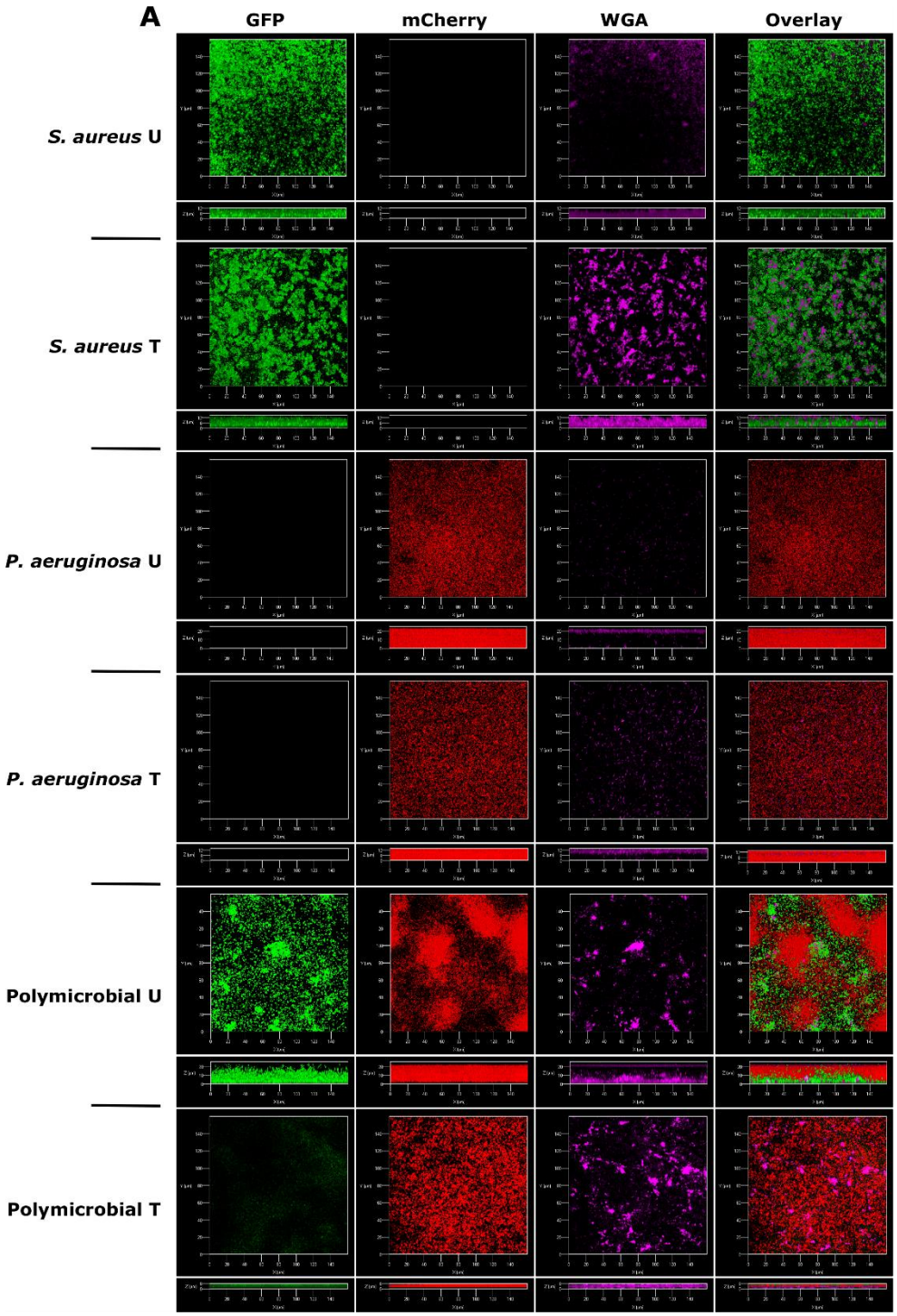
untreated (U, (p)ppGpp$^0$ U), exposed to 0.0001% CHG (CHG, (p)ppGpp$^0$ CHG), or exposed to 0.0002% BAC (BAC, (p)ppGpp$^0$ BAC). DAPI (blue) was used to visualise cells, YOYO-1 stains eDNA (green) and Alexa fluor 647-conjugated WGA (magenta) was used to visualise PNAG residues of polysaccharide. For all conditions, the top row of the panel shows the top surface of the *S. aureus* biofilms, with the biofilm thickness profile presented below. Horizontal lines on the left are used to segregate conditions. Images are representative of multiple experiments and were taken using the 40x objective (n=3). Quantification of polysaccharide biomass **(B, C)** and eDNA biomass **(D, E)** was carried out using Comstat image analysis software (n=3).

Images in Fig 4.12A show that biofilms exposed to either biocide exhibit a similar appearance to the untreated control in both strains ((p)ppGpp$^0$ biofilm images not shown). Any differences in the distribution of PIA (magenta) and eDNA (green) across conditions was minor. From the graphs, it appears BAC increases polysaccharide production (Fig 4.12C) and CHG increases eDNA in the biofilm (Fig 4.12D). However, neither of these results are significant and biomass measurements were highly variable between samples. Interestingly, the (p)ppGpp$^0$ strain exhibited both lower eDNA and polysaccharide biomass than the HG001 WT. Once again, these results were not statistically significant. Ultimately, it seems that neither CHG nor BAC exposure alters the composition of *S. aureus* biofilms.

### 4.3.13 Untreated *S. aureus* produces more polysaccharide in the presence of *P. aeruginosa*. However, triclosan-exposed *S. aureus* is less able to survive in a polymicrobial biofilm

Previous experiments have shown that triclosan exposure can induce both antibiotic tolerance and alter biofilm formation. This experiment was designed to see whether these biocide-induced phenotypic changes could increase the survival of *S. aureus* in the presence of *P. aeruginosa*, and whether the increased polysaccharide concentration altered polymicrobial biofilm formation. To assess this, GFP tagged *S. aureus* and mCherry tagged *P. aeruginosa* was used, alongside WGA to detect polysaccharide. *S. aureus* was grown in the presence of 500 ng/mL

triclosan for 48 hours, with *P. aeruginosa* being added 24 hours after initial *S. aureus* inoculation to prevent premature killing by *P. aeruginosa*.



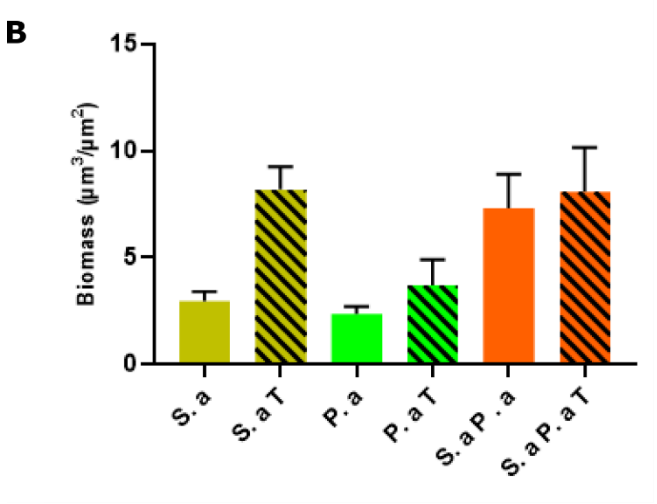



**Figure 4.13. Triclosan-induced polysaccharide production can be detected in polymicrobial biofilms even though *S. aureus* has been eradicated or rendered nonviable. A)** CLSM was used to assess the effect of triclosan on the formation of polymicrobial biofilms. GFP 8325-4 *S. aureus* was added at 0 hours and mCherry PAO1-W *P. aeruginosa* added at 24 hours in a 48 hour total incubation. Biofilms were either untreated monospecies (S. a, P. a), untreated polymicrobial (S. a P. a) or exposed to 500 ng/mL triclosan as monospecies (S. a T, P. a T) or polymicrobial (S. a P. a T) biofilms. GFP shows *S. aureus* in green, mCherry shows *P. aeruginosa* in red, Alexa fluor 647-conjugated WGA (magenta) visualises PNAG residues of polysaccharide. For all conditions, the top row of the panel shows the top surface of the biofilms, with the biofilm thickness profile presented below. Horizontal lines on the left are used to segregate conditions. Images are representative of multiple experiments and were taken using the 40x objective (n=2). **B)** Quantification of polysaccharide biomass was carried out using Comstat image analysis software (n=2).

Confocal imaging (Fig 4.13A) shows the distribution of *S. aureus*, *P. aeruginosa*, and polysaccharide in both monospecies and polymicrobial biofilms. Accumulation of polysaccharide can be seen in triclosan treated *S. aureus* biofilms, but not in triclosan treated *P. aeruginosa* biofilms. In untreated polymicrobial biofilms, GFP and mCherry fluorescence indicated that there were viable populations of both species present. Polysaccharide structures were observed in untreated polymicrobial biofilms, which was unexpected due to triclosan exposure usually being required for polysaccharide accumulation. In triclosan treated polymicrobial biofilms very little GFP fluorescence was detected, indicating far less viable *S. aureus* was present in these biofilms compared to untreated polymicrobial biofilms. However, in these biofilms

polysaccharide structures were still detected despite the absence of viable *S. aureus*, implying triclosan-exposed *S. aureus* produced polysaccharide before the addition of *P. aeruginosa* and that these structures persisted after the eradication of *S. aureus*. Comstat analysis quantifying polysaccharide biomass confirmed that more polysaccharide was produced by *S. aureus* in triclosan exposed monospecies and polymicrobial biofilms. Polysaccharide biomass is very similar in untreated polymicrobial biofilms compared to triclosan treated polymicrobial biofilms, implying the presence of *P. aeruginosa* may also induce polysaccharide production in *S. aureus* biofilms.

### 4.3.14 Triclosan exposure reduces *S. aureus* survival in polymicrobial biofilms, but *P. aeruginosa* is unaffected

Endpoint CFUs of monospecies and polymicrobial biofilms with or without triclosan treatment were counted to enumerate viable bacteria within these conditions. Selective solid media was used to count *S. aureus* and *P. aeruginosa* colonies separately.

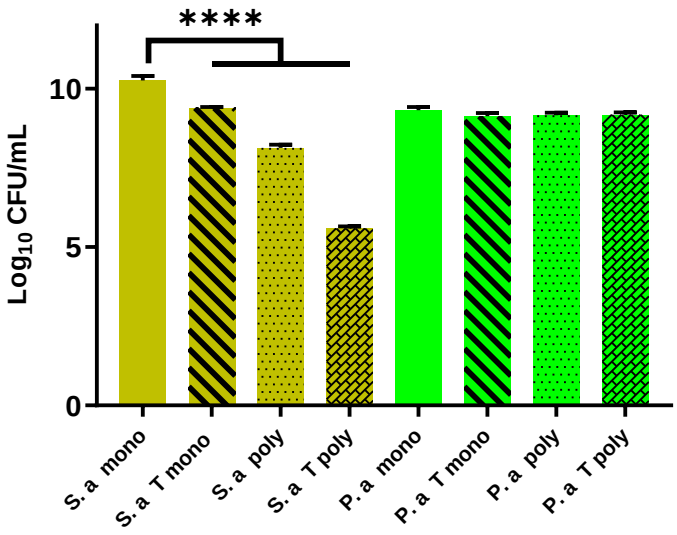



**Figure 4.14. Triclosan exposure makes *S. aureus* more susceptible to killing by *P. aeruginosa*.** Endpoint of $\log_{10}$ CFUs of *S. aureus* 8325-4 and *P. aeruginosa* PAO1-W monospecies (S. a mono, S. a T mono, P. a mono, P. a T mono) and polymicrobial

biofilms (S. a poly, S. a T poly, P. a poly, P. a T poly). Error bars represent SEM, n=3. **** denotes P≤0.0001.

Endpoint CFUs (Fig 4.14) showed that triclosan exposure during biofilm formation resulted in approximately 1 log reduction in the isolation of viable *S. aureus*, confirming observations in 4.3.10. Co-colonisation of biofilms with both *S. aureus* and *P. aeruginosa* resulted in significant reduction in viable *S. aureus* compared to untreated monospecies *S. aureus* biofilms. In agreement with confocal imaging seen in Fig 4.13A, *S. aureus* exposed to both *P. aeruginosa* and triclosan were significantly less culturable. In contrast, *P. aeruginosa* viability was unaffected by the presence of *S. aureus* or triclosan.

### 4.3.15 Triclosan exposed *S. aureus* is more susceptible to killing by *P. aeruginosa*, even when mutations in quorum sensing have reduced virulence

Previous polymicrobial experiments showed that triclosan exposure did not protect *S. aureus* against killing by *P. aeruginosa*, with susceptibility actually increasing. To investigate the mechanism of killing utilised by *P. aeruginosa* against *S. aureus*, multiple *P. aeruginosa* quorum sensing mutants were utilised. Strains deficient in quorum sensing exhibit reduced virulence and may therefore no longer produce factors responsible for killing *S. aureus*. *P. aeruginosa* mutants Δ*pqsA*, Δ*lasI*, Δ*rhlI*, Δ*lasI*Δ*rhlI*, Δ*pqsA*Δ*lasI*Δ*rhlI* were compared to the PAO1-N WT. All strains were untreated or exposed to triclosan, and grown in monospecies biofilms or polymicrobial biofilms alongside *S. aureus* NCTC8325-4 WT. Endpoint CFUs of biofilms were used to determine viability.

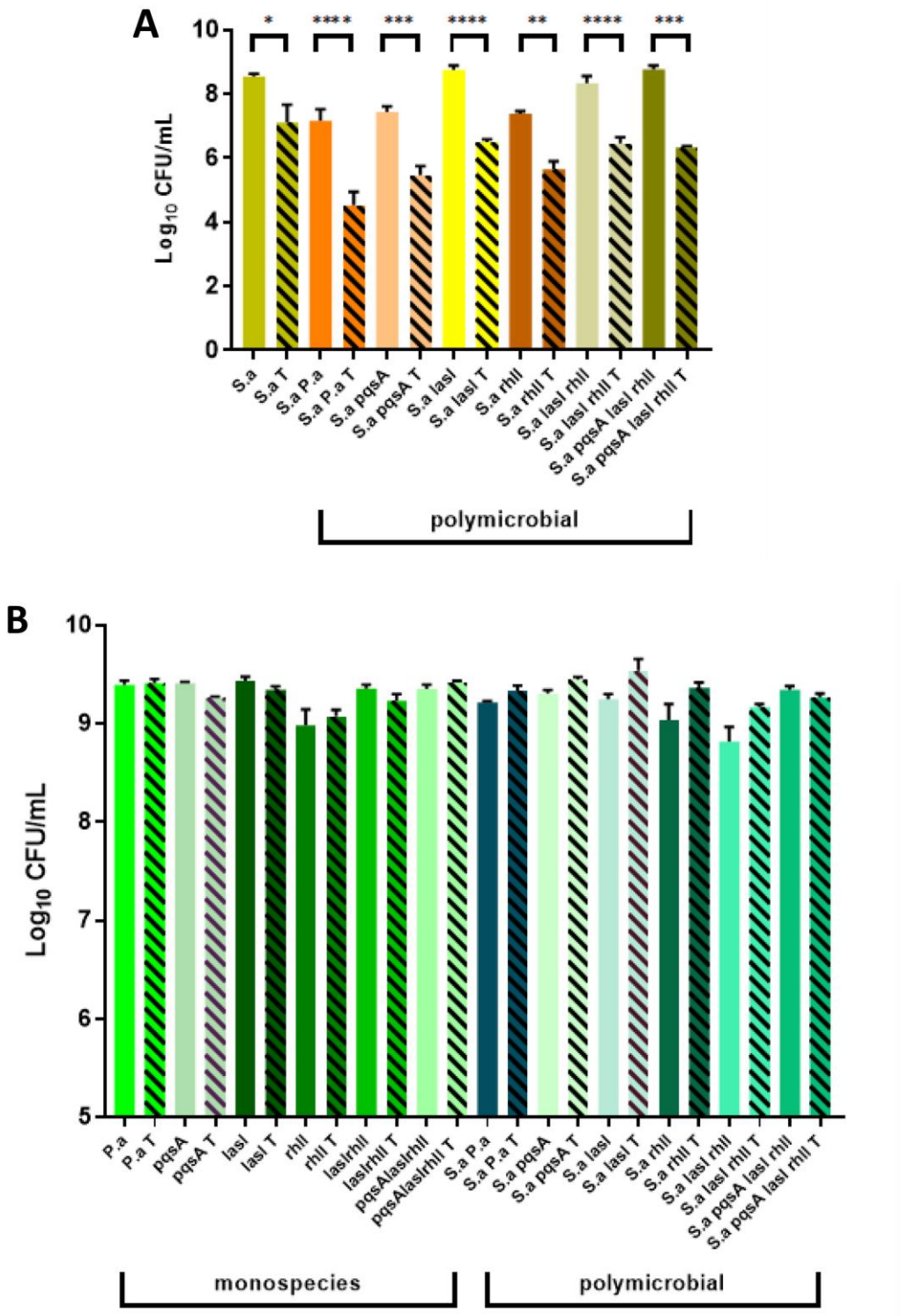



**Figure 4.15. Triclosan exposed *S. aureus* is more susceptible to killing by *P. aeruginosa* quorum sensing mutants, but the survival of *P. aeruginosa* remains unaffected.** Endpoint of $\log_{10}$ CFUs of *S. aureus* NCTC8325-4 WT and *P. aeruginosa* PAO1-N WT, Δ*pqsA*, Δ*lasI*, Δ*rhlI*, Δ*lasI*Δ*rhlI*, Δ*pqsA*Δ*lasI*Δ*rhlI* monospecies and polymicrobial biofilms. Treatment with 500 ng/mL indicated by T after the strain. **A)** Endpoint of CFUs of *S. aureus*. **B)** Endpoint CFUs of *P. aeruginosa*. Brackets beneath

conditions indicate whether a condition is polymicrobial. Error bars represent SEM, n=3. **** denotes P≤0.0001, *** denotes P≤0.001, ** denotes P≤0.01, * denotes P≤0.05.

Fig 4.15A suggests that *P. aeruginosa* requires *lasI* to reduce *S. aureus* populations in untreated polymicrobial biofilms, as reflected by the negligible reductions in viable *S. aureus* populations in all polymicrobial biofilms with a *lasI* deficient *P. aeruginosa* strain. Triclosan exposure significantly reduced the viability of all *S. aureus* conditions compared to their respective untreated controls. As expected, the lowest reductions are observed in the S. a P. a T condition; in which *S. aureus* was exposed to both triclosan and a fully virulent *P. aeruginosa* WT. Lower *S. aureus* reductions are observed in polymicrobial biofilms consisting of mutants with deletions of the quorum sensing components *lasI, rhlI*, and *pqsA*. *P. aeruginosa* was relatively unaffected by the presence of *S. aureus* (Fig 4.15B).

## 4.4 Discussion

Previous literature has demonstrated that antimicrobials can induce changes in the biofilm development of *S. aureus* (Kaplan, 2011). This study has found that changes to biofilm structure can also be induced by the biocide triclosan. Although previous studies have investigated whether low levels of triclosan can alter biofilm composition (Tabak et al., 2007), this is, to the author's knowledge, the first recorded instance of triclosan-induced biofilm alteration in *S. aureus*. This change in biofilm composition was found to primarily involve production of the polysaccharide PIA (Fig 4.2). Previous literature found that the predominant mechanism of antimicrobial induced biofilm formation in *S. aureus* involved eDNA release via autolysin activity (Hsu et al., 2011; Kaplan et al., 2012; Schilcher et al., 2016). Hsu (2011) describes an example of excess PIA production after *S. aureus* was exposed to vancomycin. However, this was in conjunction with eDNA release, with the authors hypothesising that exogenous and even xenogeneic DNA sources mediated increased biofilm formation (Hsu et al., 2011). Here, we describe observations of antimicrobial-induced biofilm formation in *S. aureus* that is dependent on PIA. This drastic shift in PIA production seen in this study is significant, as biofilm formation in staphylococci is often segregated into *ica*-dependent and *ica*-independent biofilm formation (O'Gara, 2007). Lab strain *S. aureus* SH1000 has been demonstrated to undergo *ica*-dependent biofilm formation (Fitzpatrick, Humphreys and O'Gara, 2005); whilst the lab strain HG001 and CA-MRSA strain were previously described as *ica*-independent biofilm formers (Lauderdale et al., 2009; Foulston et al., 2014). Foulston (2014) showed that the matrix of HG001 biofilms is largely proteinaceous due to the moonlighting of cytoplasmic proteins as extracellular matrix components. Conversely, USA300 produces strains favouring both protein and eDNA components in the biofilm matrix (Lauderdale et al., 2009). Unlike MSSA strains such as SH1000, MRSA strains such as USA300 typically shift away from *ica*-dependent biofilm formation. This has been evidenced by PIA-producing MSSA strains reducing transcription of *icaADBC* following introduction of

the *mecA* antibiotic resistance gene (Pozzi et al., 2012). This study shows that triclosan exposure can induce PIA production in not only the *ica*-dependent strain SH1000 (Fig 4.2), but also *ica*-independent strains HG001 (Fig 4.6A) and USA300 (Fig 4.9A). Results shown in both Fig 4.4 and Fig 4.9 suggest that triclosan exposure may further exaggerate strain to strain differences in biofilm formation. As demonstrated by USA300, a strain that typically produces a proteinaceous biofilm matrix (Lauderdale et al., 2009), increasing matrix proteins following triclosan exposure (Fig 4.9F). Conversely, triclosan exposure appears to reduce eDNA release into the biofilm matrix of both SH1000 and USA300 (Fig 4.4 and Fig 4.9), though not significantly. It could be speculated that this component is less vital due to increased polysaccharide within the matrix following incubation with triclosan. This illustrates not only that triclosan-induced polysaccharide production can occur in both MSSA and MRSA strains, but also it can radically shift the biofilm composition of strains that do not typically favour polysaccharide centric matrices. This apparent switching from *ica*-independent to *ica*-dependent biofilm formation further reinforces the views of Moormier and Bayles (2017), suggesting *S. aureus* biofilm formation is dynamic, rather than the biofilm formation of a given strain being reliant on a single matrix component. Furthermore, this shows that this dynamism can be stimulated by the extracellular environment, with biofilm composition being tailored by specific stresses.

Triclosan-induced changes to biofilm structure were initially detected using fluorescent nanosensors (Fig 4.1). Using these sensors it was found that there was a concentration dependent effect on how triclosan changed biofilm structure, with 10 ng/mL triclosan exposed biofilms looking similar to untreated biofilms, whilst biofilms exposed to 500 ng/mL triclosan had a thick layer on top of the biofilms in which the nanosensors had located in the apparent absence of bacteria. This demonstrates how effective a tool fluorescent nanoparticles can be in identifying changes to overall biofilm structure in ways that fluorescent strains and specific stains may miss. The dual function of these particles was also to discern the pH of the microenvironments within these biofilms. Determination of

pH is important as this can give insight into multiple processes, such as metabolism or modulatation of *agr* quorum sensing in *S. aureus* (Tan et al., 2018). Due to the high positive charge of PIA (Arciola et al., 2015) it is likely that any colocalisation of PIA and the positively charged nanosensors is a result of becoming encased by accumulating polysaccharide as opposed to an electrostatic interaction. In this study, pH was studied to determine whether biocide treatment altered biochemical gradients within biofilms. It was found that triclosan exposure did not greatly alter pH gradients in *S. aureus*, however thicker triclosan treated biofilms had a greater proportion of biofilm that exhibited an acidic pH. This acidification of the top region of the biofilm is likely due to the sequestration of the acidic products of glucose metabolism within the polysaccharide layer (Cerca et al., 2011). If this is the case, this may lead to more cell death in the upper layers of triclosan treated biofilms as accumulation of acidic waste from glucose metabolism has been shown to be harmful to *S. aureus* viability. It has also been shown that the greater the acidification of a biofilm, the less PNAG/PIA is produced in *S. aureus* (Cerca et al., 2011). The results posed here clearly oppose this, with the most acidified biofilms producing the most polysaccharide. The use of pH sensitive fluorescent nanosensors may be a very useful tool for investigating the biofilm formation of strains and species that are heavily reliant on protein matrix components. For instance, in the *S. aureus* HG001 strain it is found that dropping pH mediates the recruitment of cytoplasmic proteins to the biofilm matrix. By pH 4.5/5, the net charge of recruited cytoplasmic proteins is positive, facilitating binding to eDNA, which acts as an electrostatic web (Foulston et al., 2014). This is a potential explanation as to why USA300 biofilm matrices consisted of more protein. However, in SH1000, the strain in which acidification following triclosan exposure was found, matrix protein content did not increase. Likewise, the matrices of both strains exhibited reduced eDNA content, suggesting that triclosan exposure does not promote *S. aureus* to form an electrostatic web. Another example would be when *S. aureus* was exposed sialic acid, this prompted a change in

metabolism and a noticeable pH change, following be lowered transcription of CodY and increase PIA production (Dotto et al., 2017).

After polysaccharide production was observed, the manner in which it was induced was characterised. Firstly, it was found that triclosan-induced polysaccharide production is dependent on triclosan concentration (Fig 4.1A). Exposure to lower levels of triclosan elicited lower polysaccharide biovolume compared to higher concentrations such as 500 ng/mL. All of these concentrations can be considered physiologically relevant, with these levels of triclosan being isolated in human plasma and urine (MacIsaac et al., 2014). Concentration dependent antibiotic-induced biofilm formation has not previously been observed to occur gradually across a concentration gradient. Instead, there have been recorded instances of one antibiotic dilution (½ MIC) (Wang, Sun and Liu, 2010) inducing no change, unlike the next dilution (¾ MIC) (Kaplan, Jabbouri and Sadovskaya, 2011). It is possible no gradual change in biofilm structure was observed as the two concentrations were too distant from one another, as this study shows that even the difference in concentration between 100 ng/mL and 500 ng/mL triclosan (Fig 4.1) can lead to large divergences in biofilm architecture. Moreover, it is evident that biosynthetic pathways are mobilised quickly after triclosan exposure. Accumulation of polysaccharide amounting to approximately double the biomass of untreated biofilms were observed in as little as 3 hours after treatment, with further incremental increases in polysaccharide biovolume (Fig 4.3). Interestingly, when comparing CFUs to extracted polysaccharide, it seems that triclosan exposed biofilms produce twice the amount of polysaccharide despite containing tenfold fewer viable cells (Fig 4.10B). Additionally, crystal violet staining demonstrated that despite the higher polysaccharide production of triclosan exposed *S. aureus* biofilms, the growth inhibition by triclosan resulted in less overall biomass (Fig 4.11). This is exemplified by the Δ*codY* biofilms, in which untreated biofilms had a very high biomass due to cell dense biofilms overexpressing polysaccharide. However, once growth was inhibited by triclosan, there

was a significant drop in biomass, even though confocal image analysis showed that triclosan exposure is additive to the effects of CodY derepression on polysaccharide synthesis. Combined, these findings suggest that despite more biofilm matrix in triclosan treated biofilms, these biofilms have less biomass overall due to a greatly reduced viable population compared to untreated biofilms. The observation that more polysaccharide is produced by fewer cells is significant, as Kaplan (2011) demonstrated that more matrix was accompanied by more CFUs in multiple *Staphylococcus* species against many different classes of antibiotics. Perhaps this suggests an inversely proportional relationship between cells and matrix production may occur exclusively after exposure to fatty acid synthesis inhibitors such as triclosan.

The accumulation of exopolysaccharide after triclosan exposure could be of clinical concern as PIA greatly contributes to the immune evasion abilities of *S. aureus*. PIA surrounded *S. aureus* aggregates are better protected against both macrophages (Schommer et al., 2011) and neutrophils (Vuong et al., 2004) than their PIA deficient counterparts. Furthermore, *ica* expressing *S. epidermidis* strains were shown to elicit a reduced inflammatory response compared to *ica* negative strains, with lower levels of the pro-inflammatory cytokines IFN-γ, TNF-α, and IL-6 being detected. Contrary to the reduction in inflammatory cytokines, PIA still produced a pro-inflammatory affect via activation of complement (Fredheim et al., 2011). Paradoxically, PIA producing biofilms are better protected against complement despite activating it. This is due to PIA acting as a decoy, this mechanism similarly protects against opsonisation with exopolysaccharide acting as an antibody ‘sink’ (de Vor, Rooijakkers and van Strijp, 2020). Finally, the positively charged nature of PIA allows repulsion of cationic antimicrobial peptides (AMPs) and the sequestration of anionic AMPs (Vuong et al., 2004). In addition, a thicker biofilm matrix may have implications for antibiotic penetration, though current literature is unclear. There have been reports of polysaccharide significantly reducing antibiotic penetration of vancomycin and β-lactams through *S. epidermidis* biofilms (Souli and Giamarellou, 1998). Konig, Schwank and

Blaser (2001) confirm that vancomycin penetration is inhibited, but also contradict the findings that β-lactam penetration is impeded. It is difficult to say with certainty whether the results of either of these studies pertain directly to PIA, as both studies refer to the matrix as an exopolysaccharide slime, neglecting to quantify the presence of eDNA or proteins which may also interfere. Other studies have found that a thicker Staphylococcal biofilm matrix does nothing to retard the penetration of aminoglycosides or fluoroquinolones (Singh et al., 2010).

Multiple regulatory pathways were investigated to determine the mechanism of triclosan-induced polysaccharide production during biofilm formation. Just as in the previous chapter, oleic acid supplementation was able to significantly diminish polysaccharide production in the presence of triclosan compared to when exogenous fatty acids were absent (Fig 4.5). This suggested that the fatty acid starvation induced by triclosan was the initiator for excess polysaccharide production. As fatty acid starvation is a well known inducer of the stringent response, and was previously shown to be the mechanism behind triclosan-induced antibiotic tolerance, it was investigated whether the stringent response could induce polysaccharide production. There is no evidence from the literature to suggest that the stringent response itself directly acts upon the *ica* operon, however, the production of (p)ppGpp alarmones requires large quantities of intracellular GTP. GTP is a cofactor of CodY, a repressor of the *ica* operon (Geiger and Wolz, 2014). With reduced levels of GTP, *ica* expression, and subsequent PIA production, would be unimpeded. Derepression by CodY would also relieve the repression of its other targets, including the *agr* quorum sensing system (Geiger et al., 2010). This could be potentially significant due to the association between quorum sensing and biofilm dispersal (Boles and Horswill, 2008). The involvement of the *agr* system could account for the apparent reduced biovolume of triclosan-exposed biofilms. Although this is likely due to inhibited growth, this effect could be exacerbated by increased dispersal by the *agr* system, causing aggregates to disperse from the biofilm and be removed during the washing steps of experiments. In

summary, the stringent response would render CodY unable to repress its targets, which would then go on to cause increased matrix production via increased *ica* expression and increased dispersal by *agr* expression. This hypothesis was disproved however; as experiments concluded that neither the stringent response (Fig 4.6) nor the *agr* quorum sensing system (Fig 4.8) were involved in triclosan-induced altered biofilm formation. This was demonstrated by mutant strains exhibiting the same biofilm matrix composition as their respective wild types. The untreated Δ*codY* strain displayed a similar polysaccharide biovolume to triclosan exposed HG001 WT biofilms, which seemed to suggest that CodY derepression may be responsible for triclosan-induced alterations to biofilm composition (Fig 4.7). This hypothesis may seem contradictory considering that the stringent response has been shown to not be involved, and our previously hypothesis focused on CodY derepression by the stringent response consuming GTP required for CodY binding. However, CodY can be derepressed regardless of GTP concentrations due to branched chain amino acids (BCAAs) also being an essential cofactor, and the loss of these, regardless of GTP concentrations, would result in CodY derepression (Geiger and Wolz, 2014). This would mean that whilst the stringent response was not involved, triclosan exposure would somehow induce a starvation of branched chain amino acids that would lead to CodY derepression of the *ica* operon. However, further analysis of Δ*codY* biofilms found that triclosan exposure increased polysaccharide production further still. If CodY alone were responsible, triclosan exposure would not increase polysaccharide production in the Δ*codY* strain. Instead, another mechanism would be the cause of triclosan-induced biofilm formation, one that can cause an additive increase to polysaccharide production alongside CodY derepression.

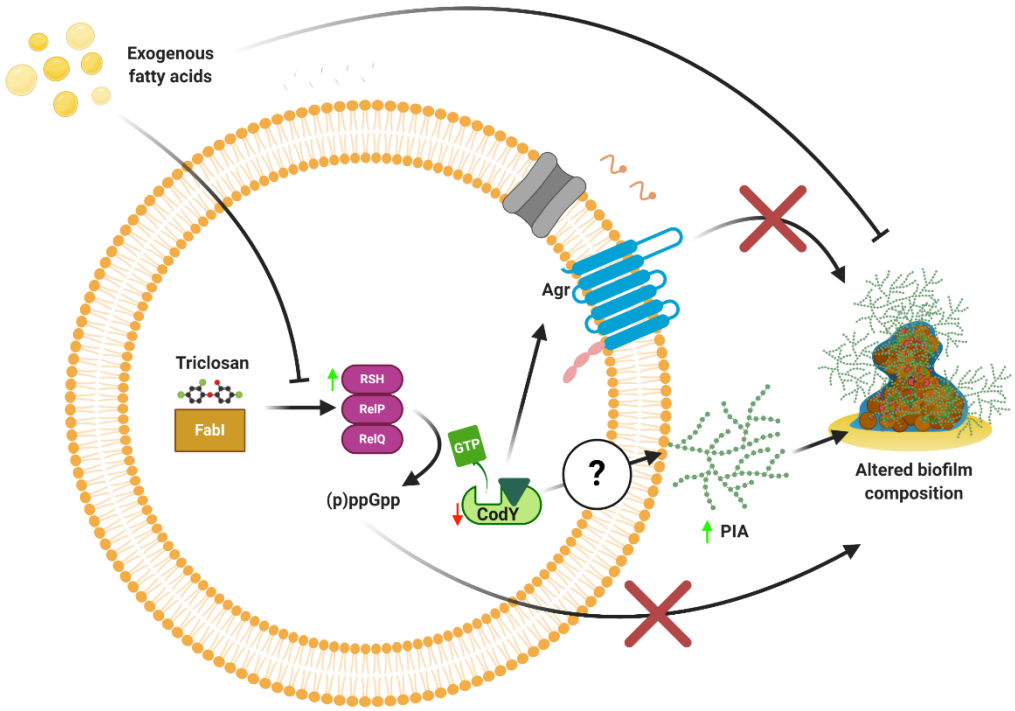



**Figure 4.16. Summary of triclosan-induced alterations to biofilm structure.** Triclosan activity alters biofilm formation through increased PIA production. The stringent response, which is triggered in response to triclosan exposure, did not play a role in triclosan-induced polysaccharide production. CodY, a repressor of the *ica* PIA biosynthesis genes may play a role. Triclosan pretreatment may lead to CodY derepression of *ica* due to depletion of GTP, as essential cofactor for CodY repression. This is due to triclosan exposure triggering the stringent response, which utilises GTP for alarmone ((p)ppGpp) synthesis, therefore depleting intracellular GTP. It is currently unclear if CodY is responsible for triclosan-induced PIA synthesis. Another target of CodY repression, the *agr* system (indicated by blue and grey proteins), may be upregulated in triclosan exposed biofilms due to reduced CodY activity. However, this study found *agr* plays no role in triclosan-induced alterations to biofilm structure. Exogenous fatty acids inhibit fatty acid starvation by triclosan and therefore prevent triclosan-induced changes to biofilm formation. Green arrows indicate increased activity/production. Red arrows indicate reduced activity.

*S. aureus* and *P. aeruginosa* have been shown to interact with one another in various ways. The production of 4-hydroxy-2-heptylquinoline-*N*- oxide (HQNO) by *P. aeruginosa* can stimulate *S. aureus* biofilm production and repress *agr* expression, preventing dispersal (Mitchell et al., 2010). The emergence of small colony variants (SCV) is also observed following HQNO exposure, facilitating vancomycin tolerance in *S. aureus* (Orazi and O'Toole, 2017). This study also sought to determine

how triclosan exposure influenced interspecies interactions. Triclosan did not confer additional protection against killing by *Pseudomonas*, in fact *S. aureus* susceptibility to *P. aeruginosa* increased. Although it may appear that *S. aureus* is eradicated in microscopy of polymicrobial biofilms (Fig 4.13A), one potential scenario is that due to triclosan-induced dormancy GFP may not be expressed. However, other studies have shown that antibiotic induced persister formation still translated GFP, albeit at a reduced rate (Peyrusson et al., 2020). Despite viable *S. aureus* not being detected by microscopy, triclosan-induced polysaccharide produced by *S. aureus* was still detectable (Fig 4.13). This is important, as PIA has been shown to significantly protect *P. aeruginosa* against gentamicin treatment (DeLeon et al., 2014). Therefore, triclosan-induced effects may contribute to persistent infections even after triclosan-exposed *S. aureus* has been eradicated. The decreased viability of *S. aureus* in the presence of both *P. aeruginosa* and triclosan may be due to HQNO. HQNO has previously been shown to increase the susceptibility of *S. aureus* to the membrane-targeting antiseptic chloroxylenol (Orazi, Ruoff and O'Toole, 2019). This is particularly relevant to triclosan as the biocide can also induce membrane destabilisation (Alfhili and Lee, 2019). During our investigation of *P. aeruginosa* QS mutants (Fig 4.15), it was found that the *las* system had the greatest effect on *S. aureus* survival, whilst the *pqs* system that produces HQNO, had little effect on *S. aureus* survival once both *lasI* and *rhlI* had been deleted. This agrees with the findings of Woods et al (2018) that the exoproducts produced by the *las* and *rhl* systems are essential for the removal of *S. aureus* from *P. aeruginosa* and *S. aureus* dual species biofilms.

*S. aureus* biofilms were also exposed to BAC and CHG during biofilm formation to discern whether they too could alter the formation of the biofilm matrix. Antibiotic-induced biofilm formation in Staphylococci is seen for all antibiotic classes (Kaplan, 2011), it is therefore logical that this phenomenon would be possible for different biocides as well. Indeed, chlorhexidine has been shown to alter the biofilm formation of *P.*

*aeruginosa* (Aka and Haji, 2015). In this study, it was found that neither BAC nor CHG altered the production of eDNA or polysaccharide in *S. aureus* biofilms (Fig 4.12). Despite these results, it is still possible that these biocides can alter the biofilm formation of *S. aureus*. As previously shown, antimicrobial-induced biofilm formation is highly concentration dependent (Wang, Sun and Liu, 2010; Kaplan, Jabbouri and Sadovskaya, 2011). It is therefore possible that other concentrations of BAC or CHG could alter the matrix composition of *S. aureus* biofilms.

As Kaplan (2011) has expertly reviewed, antibiotic-induced biofilm formation is not a rare occurrence. Yet despite this, biocide-induced biofilm formation has been widely ignored. A concerning oversight perhaps, considering that the use of biocides is both less regulated by the authorities, and more ubiquitous globally.

# 5. RNA-Sequencing reveals widespread transcriptomic changes in response to triclosan exposure in both planktonic and biofilm culture.

## 5.1 Introduction

### 5.1.1 Gene expression changes associated with survival

Multiple mechanisms are employed by *S. aureus* that allow the bacterium to survive stresses. Regarding antibiotic stresses, the stringent response plays an essential role through downregulation of genes encoding translation machinery such as *infA*, *tsf*, and *frr*. Turning off translation in turn induces antibiotic tolerance through the reduced activity of processes targeted by antibiotics, including DNA replication and cell wall biosynthesis (Reiss et al., 2012; Peyrussen et al., 2020). Furthermore, the stringent response can also induce the expression of genes to aid survival against antibiotic treatment. An example of this is stringent response induced upregulation of *fmtA*, which encodes a β-lactam resistant penicillin-binding protein (Komatsuzama et al., 1999; Fan et al., 2007; Peyrussen et al., 2020). The stringent response has been discussed in detail in chapter 3.1.2.

Alternative Sigma Factor B (SigB) plays a central role in cooridinating the *S. aureus* stress response. Sigma factors initiate transcription by bestowing promoter specificity to RNA polymerase holoenzyme (Paget and Helmann, 2003). Primary sigma factors are associated with essential cellular functions whilst alternative sigma factors respond to environmental changes, with SigB being strongly associated with stress response regulation (Jenul and Horswill, 2019). SigB is responsible protection against ROS, induction of acid tolerance (Chan et al., 1998), heat shock (Kullik et al., 1997), changes in growth phase (Kullik et al.,

1997), and alkaline shock (Kullik et al., 1998). In the context of antimicrobial tolerance, SigB has been linked to the induction of cell wall thickening to guard against β-lactam antibiotics (Morikawa et al., 2001). SigB can also protect *S. aureus* from stresses inflicted upon it by the host immune response. For instance, once within the phagosome of neutrophils, *S. aureus* is bombarded with cytotoxic products including cell wall hydrolases, antimicrobial peptides, reactive nitrogen (NO), and reactive oxygen species (ROS) (Spaan et al., 2013). To defend against these stresses, SigB can stimulate an upregulation of *crtM, sodA* and *sodM* genes (Kullik et al., 1998; Supa-Amornkul et al., 2019). The *crtM* encoded staphyloxanthin carotenoid pigment to protect against the hydroxyl radicals and hydrogen peroxide produced by neutrophils (Pelz et al., 2005). In addition, the SodA and SodM superoxide dimutases are utilised to defend against neutrophil superoxide production (Karavolos et al., 2003). SigB can also aid in biofilm formation through upregulation of the MSCRAMM genes *clfA* and *fnbA* (Speziale et al., 2014). Additionally, SigB represses expression of *icaR*, the repressor of the *ica* operon responsible for PIA biosynthesis. This repression of *icaR* therefore increases polysaccharide production due to increased *icaADBC* expression (Knobloch et al., 2004).

Lastly, SigB is also strongly connected to *S. aureus* virulence through SigB mediated silencing of both *agr* and *sarA*, preventing downstream expression of toxin genes such as *tsst-1* (Thoendel et al., 2011; Tuchscherr et al., 2015). Other literature however has indicated the SigB positively regulates *sarA* (Cheung, Nishina and Manna, 2008; Andrey et al., 2015).

### 5.1.2 RNA-Sequencing in *S. aureus*

Despite its relative infancy, RNA-Sequencing (RNA-Seq) has become an indispensable tool in understanding the complexities of bacterial genome function. Acquiring information on differentially expressed genes (DEGs) is often the primary objective of RNA-Seq, although other applications

such as investigating translation or RNA structure can be explored. A typical workflow for the attainment of DEG data consists of RNA extraction followed by ribosomal RNA depletion, cDNA synthesis and preparation of an adaptor ligated sequence library that is then sequenced. Following sequencing, the workflow is finalised with computational methods. These involve aligning sequencing reads to a transcriptome, quantifying reads that overlap transcripts, filtering and normalizing between samples, and statistical modelling of significant changes in the expression levels of individual genes and/or transcripts between sample groups (Stark, Grzelak and Hadfield, 2019).

Numerous RNA-Seq studies have been carried out in *S. aureus* to investigate various hypotheses. Peyrusson et al (2020) used RNA-Seq to investigate the transcriptome of *S. aureus* intracellular persisters vs controls. In this study, RNA-Seq revealed multiple genes associated with the cell wall stimulon, SOS response, stringent response, heat shock, energy metabolism, and translation that could mediate antibiotic tolerance to a plethora of antimicrobials. Additionally, it was observed that persistence prompted activation of many genes associated with the development of antibiotic resistance including increased efflux pump expression, elevated mutagenesis for mutational resistance, and amplified competence to facilitate acquisition of resistance genes by horizontal gene transfer. Ibberson and Whitely (2019) used RNA-Seq to determine how the *S. aureus* transcriptome varied in *in-vitro* cystic fibrosis (CF) models compared to clinical *S. aureus* samples from the CF lung. The findings of this study found that clinical samples had a distinct transcriptome fingerprint compared to *in-vitro* models, and that *S. aureus* CF isolates showed increased expression of the *hlgABC* (gamma-haemolysin), *lukG*, *ssl1-3, ssl5, ssl9-10, ssl12-14* (superantigen-like proteins), *fnbA,* and *icaABC* virulence factor genes. Upregulation of genes linked with iron acquisition and low oxygen conditions was also observed; demonstrating the differences in metabolic requirements for CF isolates compared to *S. aureus* in *in-vitro* CF models. Other studies have looked at how the addition of antimicrobials affect the transcriptome

of *S. aureus* biofilms. In 2018, Zhao and colleagues showed that the addition of tea tree oil resulted in a decrease in *sarA,* potentially decreasing virulence, whilst downregulation of *cidA* and upregulation of *icaADBC* indicated that the biofilm matrix consisted of less eDNA and more PIA respectively. Exposure of *S. aureus* biofilms to sub-MIC levels of ampicillin resulted in upregulation of genes associated with β-lactam tolerance, including genes encoding PBPs and the AbcA multidrug efflux pump. This was accompanied by upregulation of genes that may aid biofilm adhesion, including the MSCRAMM *clfB* and the capsular polysaccharide genes *capB* and *capC* (Liu et al., 2018). Currently, to the best of the authors knowledge, there have been no RNA-Seq studies comparing how a single antimicrobial agent affects the transcriptome of both planktonic and biofilm cultures. A study investigating this could give insight into how bacterial lifestyle and response to drug treatment intersect on a transcriptomic level.

## 5.2 Chapter Aims

This chapter will use RNA-Sequencing to investigate the differential gene expression of *S. aureus* in response to triclosan exposure in both planktonic and biofilm culture. The aim of this chapter is to confirm and/or determine the mechanisms behind antibiotic tolerance, as discussed in chapter 3, and alterations to biofilm structure found in chapter 4. This will be achieved by taking samples at 1 hour, as this is within the window of peak gene expression for stress response genes (Reiß et al., 2012, Peyrusson et al., 2020). In addition, samples will also be taken at 12 hours, as this is when peak expression of biofilm matrix components, including PIA, occurs (Zhao et al., 2018). Therefore, RNA-Sequencing will be carried out on 500 ng/mL triclosan treated planktonic cultures taken at 1 hour (PT) and biofilms exposed to 500 ng/mL triclosan for 12 hours (BFT). Furthermore, untreated controls of both the planktonic (PU) and biofilm (BFU) will be taken at 1 and 12 hours respectively to allow for differential expression analysis between treated and untreated conditions (PT vs PU, BFT vs BFU).

Regarding triclosan induced antibiotic tolerance, analysis of this transcriptomic data will focus on determining whether there is evidence of stringent response induction. This will be achieved by looking for differential expression of stringent response genes and genes whose expression is regulated via the stringent response following triclosan exposure. Additionally, expression efflux pump genes will be examined, as the upregulation of these genes can also contribute to antibiotic tolerance (Costa et al., 2013), with biocides previously being shown to induce expression (LaBreck et al., 2020).

To gain further clarity on the mechanisms behind triclosan induced PIA synthesis in *S. aureus* biofilms, the differential expression of the *ica* operon genes and their repressor *icaR* will be assessed. Furthermore, the expression of *sigB* will be investigated, as not only can SigB increase polysaccharide production through repression of *icaR* (Knobloch et al., 2004), but SigB can also contribute to antibiotic tolerance (Morikowa et

al., 2001). Differential expression of genes in the *sigB* regulon will be examined to gain further insight into whether *sigB* expression is altered by triclosan exposure. Genes of interest in the SigB regulon include *sarA*, due to repression of *icaR* by SarA (Valle et al., 2003), and the *agr* genes as the QS system is associated with biofilm dispersal (Yarwood et al., 2004; Periasamy et al., 2012).

## 5.3 Results

### 5.3.1 The transcriptome of *S. aureus* is extensively altered by both triclosan treatment and the transition from a planktonic to biofilm lifestyle

Planktonic *S. aureus* HG001 cultures were grown in BHI for one hour either untreated (PU) or treated with 500 ng/mL triclosan (PT). *S. aureus* HG001 biofilms were grown for 12 hours in BHI, with biofilm formation occurring either in the presence of 500 ng/mL triclosan (BFT) or without (BFU). The transcriptomic profile of these samples was evaluated using RNA-Sequencing and reads mapped to the *S. aureus* NCTC8325 reference genome. Expression of protein coding genes, small non-coding RNAs, and novel transcripts was recorded. Differential expression analysis of DEGs was carried out between PT and PU, to determine how triclosan exposure alters gene expression in planktonic *S. aureus* (PT vs PU). Similarly, gene expression of triclosan-exposed biofilms compared to untreated biofilms (BFT vs BFU) was also compared to determine the effect of triclosan on the *S. aureus* biofilm transcriptome. All significant changes in gene expression can be viewed in Table S2 (PT vs PU) and Table S3 (BFT vs BFU). Hierarchical clustering was also used to determine divergences between all four conditions.

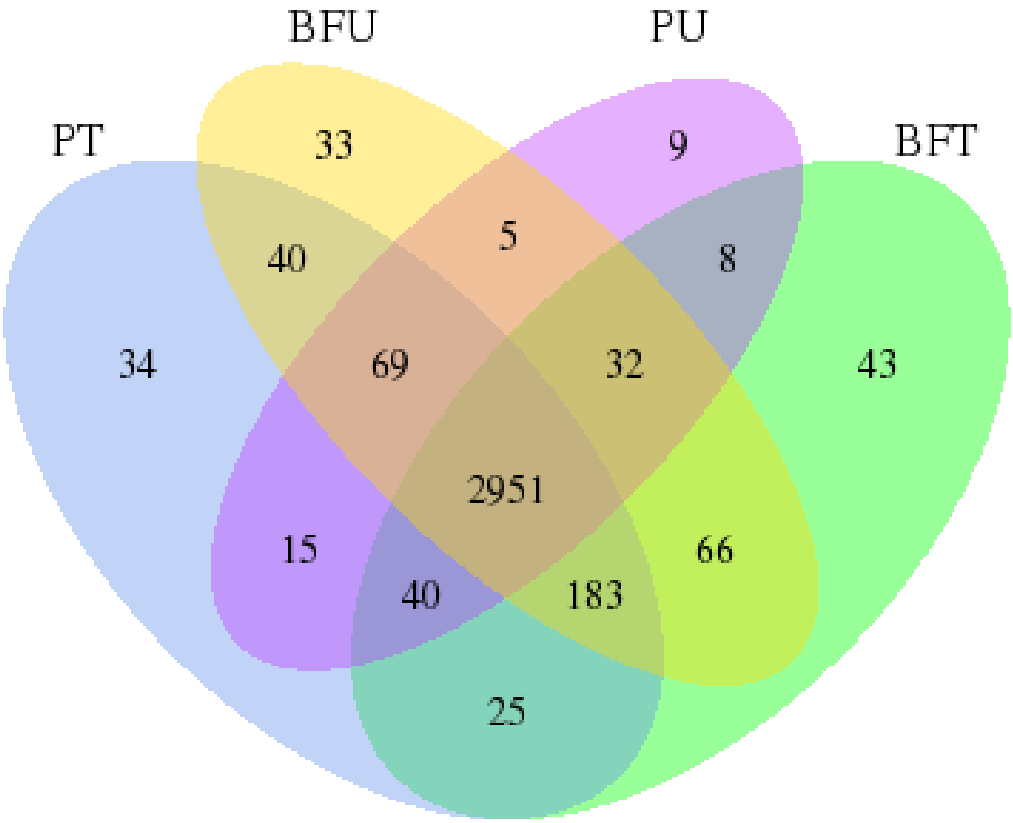



**Figure 5.1. The vast majority of *S. aureus* transcripts are co-expressed across multiple conditions.** A Venn diagram showing genes commonly and uniquely differentially expressed across planktonic treated (PT), biofilm untreated (BFU), planktonic untreated (PU), and biofilm treated (BFT) samples.

RNA-Seq detected 2742 protein-coding genes, 16 rRNA, 61 tRNA genes, 63 sRNAs and 671 novel transcripts. Co-expression analysis (Fig 5.1) shows that out of 3553 detected transcripts, over 83% (2951) are expressed in some capacity across all conditions. The number of transcripts uniquely expressed to a single condition was low. For instance, PU only expressed nine transcripts (0.25% of total transcripts) that were not detectable in any other condition; these were all protein-coding genes.

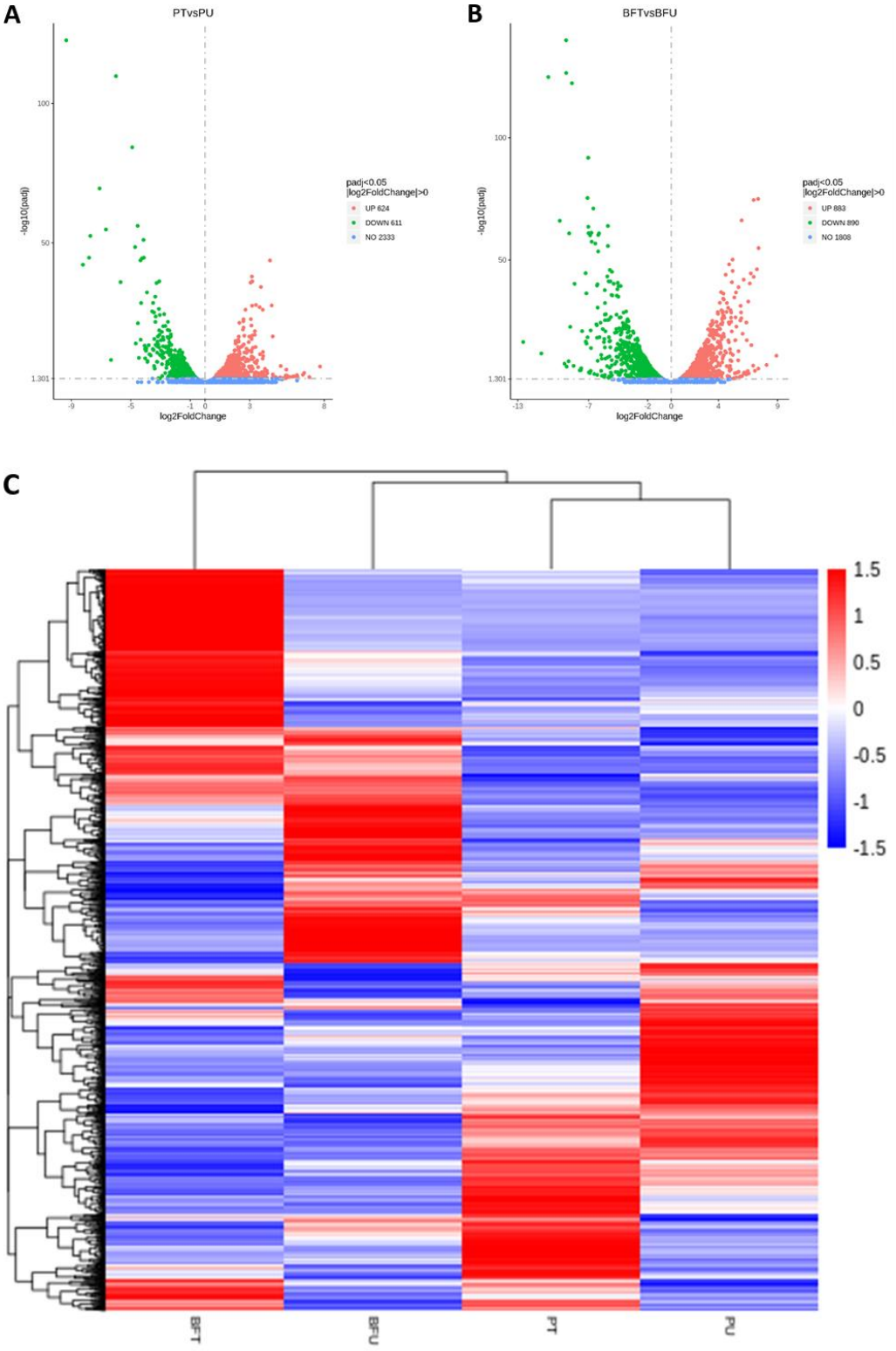



**Figure 5.2. Both triclosan exposure and bacterial lifestyle cause drastic changes in the transcriptome profile of *S. aureus*.** Patterns of gene expression values from RNA-Seq data for the planktonic treated vs planktonic untreated (PT vs PU) and biofilm treated vs biofilm untreated (BFT vs BFU) conditions are shown in volcano plots **A)** and **B)** respectively. Significantly upregulated genes are shown in pink and significantly downregulated genes are shown in green (False discovery rate-adjusted (FDR-

adjusted) P≤0.05). Grey broken lines illustrate the boundaries between up and down regulated genes (vertical) and statistical significance (horizontal). **C)** Heatmap showing hierarchical clustering of DEGs between biofilm treated (BFT), biofilm untreated (BFU), planktonic treated (PT) and planktonic untreated (PU). Dendrograms on the top x-axis and left y-axis illustrate how clusters were formed. Conditions (top x-axis) or genes (left y-axis) were paired with the most similar condition or gene. These pairs are then treated as a single condition or gene in subsequent steps until hierarchical clustering is completed. Colour coding determined using variance stabilising transformation.

Drastic differential gene expression is observed across all conditions, with DEGs comprising 34.6% in PT vs PU (Fig 5.2A) and 49.6% in BFT vs BFU (Fig 5.2B). The proportion of significantly upregulated vs significantly downregulated transcripts is almost identical for all conditions. PT vs PU is noticeably different in profile compared to BFT vs BFU. Differential expression in PT vs PU accounts for approximately a third of transcripts, whereas this proportion is closer to half in BFT vs BFU. This indicates that exposure of planktonic cultures to physiological levels of triclosan has a reduced effect on the transcriptome compared to biofilm formation in the presence of triclosan (BFT vs BFU). Hierarchical clustering found that all conditions were highly divergent from one another (Fig 5.2C).

### 5.3.2 KEGG enrichment shows significant upregulation and downregulation in response to triclosan exposure and changes in bacterial lifestyle

Kyoto Encyclopaedia of Genes and Genomes (KEGG) enrichment analysis is a statistical method for determining if sets of genes belonging to defined KEGG pathways are present more than would be expected to be by chance. For enrichment analysis, upregulated and downregulated DEGs of all comparisons were assigned to KEGG pathways. This provided an insight into which processes in *S. aureus* were affected by triclosan treatment and changes in bacterial lifestyle.

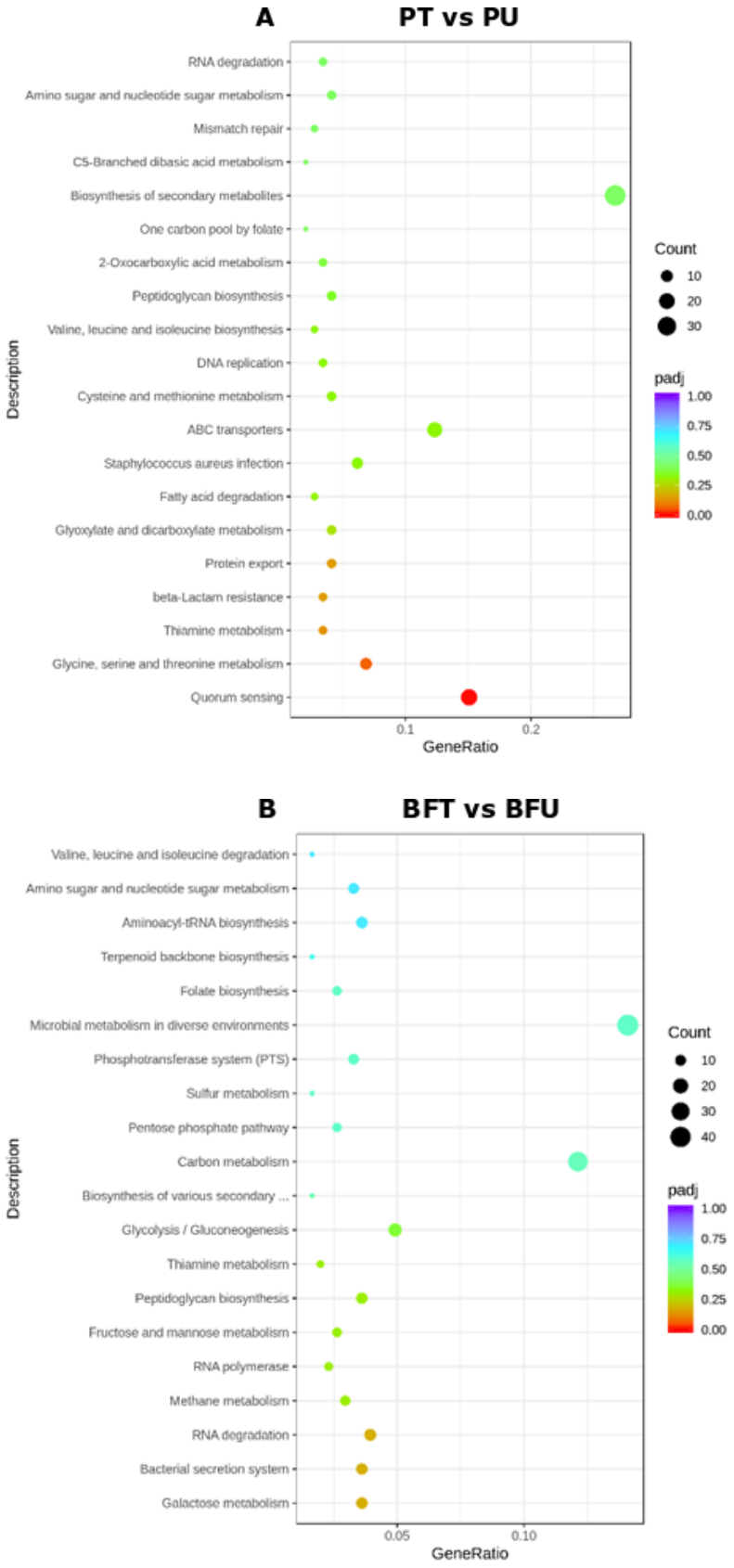
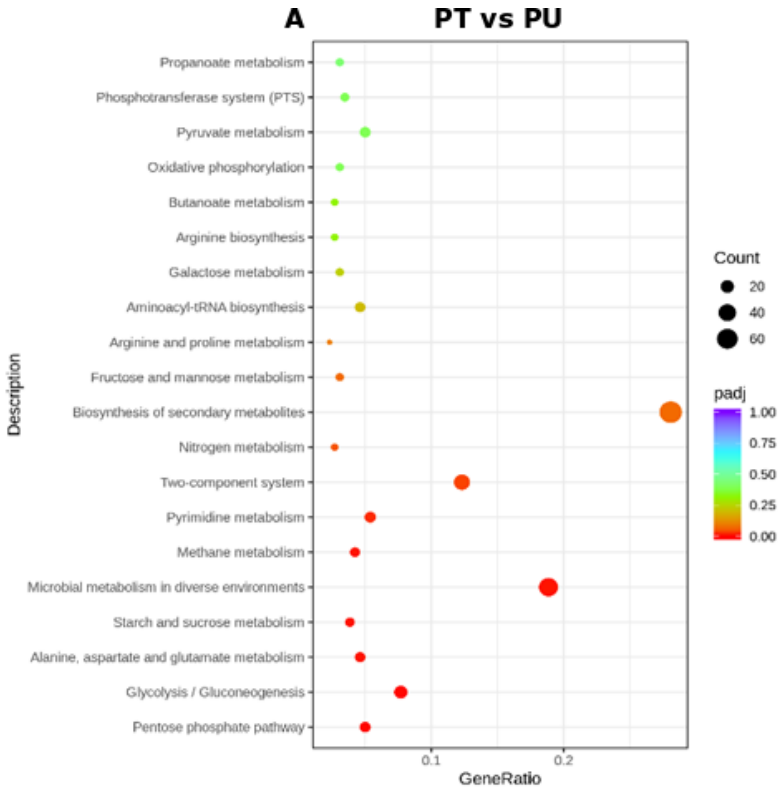



**Figure 5.3. KEGG enrichment analysis shows upregulation in diverse pathways in response to triclosan treatment and changes in bacterial lifestyle.** The top 20 upregulated KEGG pathways for planktonic treated vs planktonic untreated (PT vs PU)

and biofilm treated vs biofilm untreated (BFT vs BFU) conditions are shown in dot plots **A)** and **B),** respectively. The gene ratio corresponds to the number of DEGs in the pathway compared to the number of genes annotated in that pathway. The size of the dot corresponds to the number of DEGs and dot colour indicates FDR-adjusted statistical significance.

Upregulated genes were assigned to very different pathways across all four comparisons. The only significantly upregulated pathway for PT vs PU (Fig 5.3A) was quorum sensing, with 21 genes accounting for a gene ratio of 0.15. Biofilms displayed no significantly upregulated pathways when comparing treated to untreated conditions (Fig 5.3B).



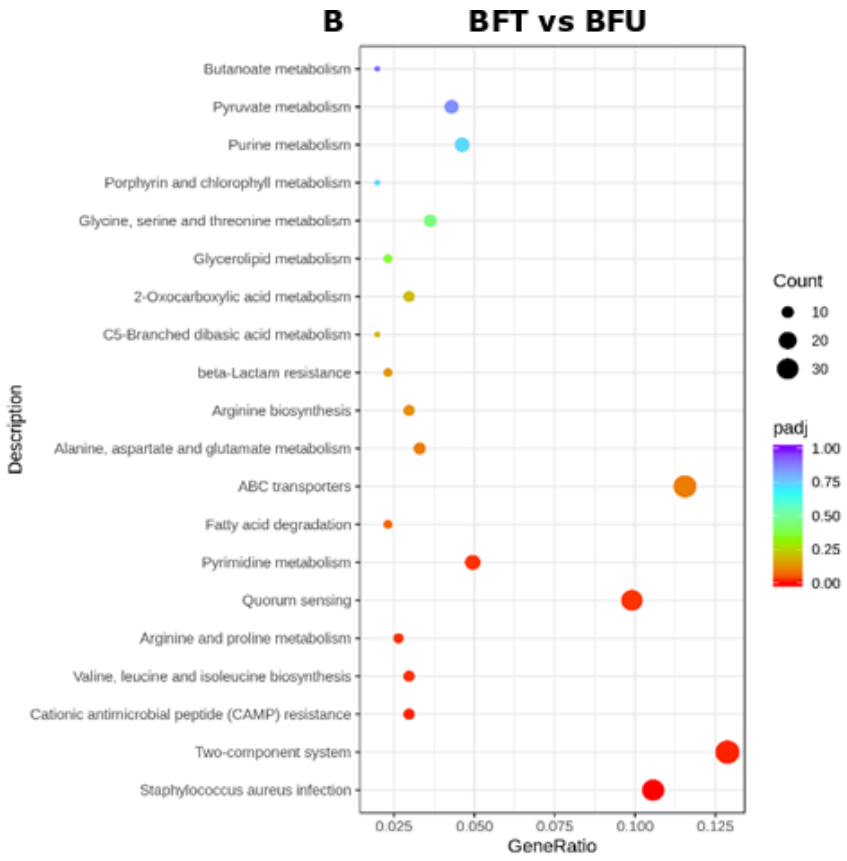



**Figure 5.4. KEGG enrichment analysis shows downregulation in diverse pathways in response to triclosan treatment and changes in bacterial lifestyle.** The top 20 downregulated KEGG pathways for planktonic treated vs planktonic untreated (PT vs PU) and biofilm treated vs biofilm untreated (BFT vs BFU) conditions are shown in dot plots **A)** and **B),** respectively. The gene ratio corresponds to the number of DEGs in the pathway compared to the number of genes annotated in that pathway. The size of the dot corresponds to the number of DEGs and dot colour indicates FDR-adjusted statistical significance.

Overall, triclosan exposure results in many more KEGG pathways being significantly downregulated (red dots in Fig 5.4) than significantly upregulated (red dots in Fig 5.3). In PT vs PU (Fig 5.4A) and BFT vs BFU (Fig 5.4B) there is significant downregulation of multiple metabolic and biosynthesis pathways. This suggests that triclosan exposure results in a less metabolically active phenotype in both planktonic *S. aureus* and *S. aureus* biofilms. BFT vs BFU also displays significant downregulations in quorum sensing, two component systems, and *S. aureus* infection, showing that exposure to triclosan throughout the 12 hours of biofilm

formation may impair *S. aureus* virulence. However, the opposite of this occurs in Fig 5.3A, in which quorum sensing is upregulated in PT vs PU.

### 5.3.3 Differential expression of stringent response associated genes provides evidence for triclosan mediated stringent response induction

To understand the induction of the stringent response upon triclosan exposure, the expression of *relP* and *relQ* genes (each encoding (p)ppGpp synthases) and *rsh* (encoding a bifunctional (p)ppGpp synthase/hydrolase) was evaluated. To acquire further evidence of whether the stringent response was induced, the gene expression of numerous stringent response target genes was assessed. These stringent response target genes included *fmtA*, which is associated with stringent response induced methicillin resistance, and genes associated with translation machinery (*infA*, *tsf*, and *frr*). The *codY* gene was also investigated, as stringent response induction typically impairs CodY activity.

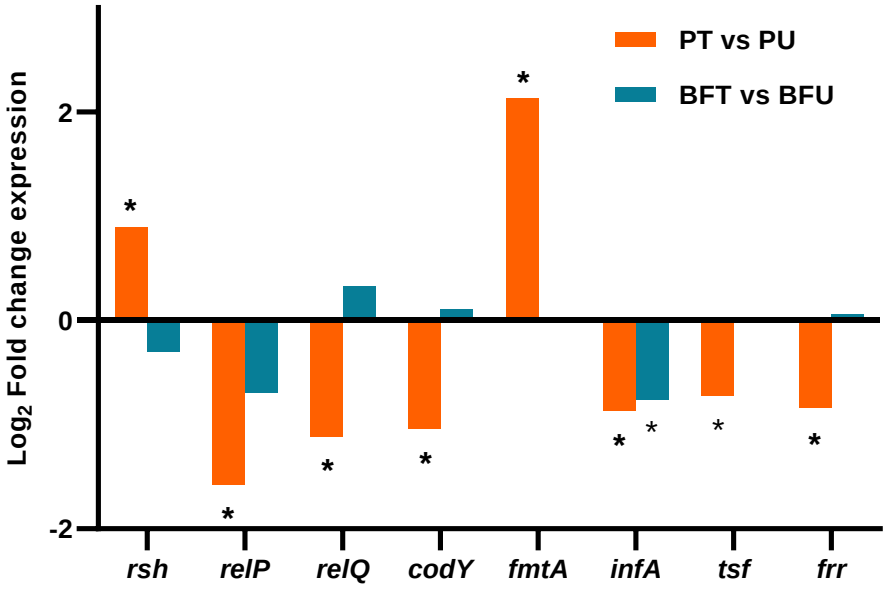


**Figure 5.5. Triclosan exposure induces patterns of gene expression indicative of stringent response induction.** Bar graph showing the mean $log_2$ fold change in gene expression of stringent response genes in PT vs PU (orange) and BFT vs BFU (blue). PU and BFT n=2, PT and BFU n=3. * denotes FDR-adjusted P≤0.05.

In PT vs PU (Fig 5.5), *rsh* is significantly upregulated whilst *relP* and *relQ* are downregulated. This could indicate either that *rsh* is the favoured (p)ppGpp synthase whilst *relP* and *relQ* are downregulated to modulate the response. Alternatively, due to RSH also functioning as a (p)ppGpp hydrolase, it is possible the stringent response was initiated earlier and *rsh* is still upregulated to hydrolyse excess alarmones. This is supported by *relP* and *relQ* downregulation to suppress alarmone production. The stringent response being induced in PT vs PU is supported by significant upregulation of *fmtA* and significant downregulation of translation associated genes *infA*, *tst* and *frr*, with this gene expression profile being typical of stringent response induction. Furthermore, stringent response induction reduces the capacity of CodY to repress its target genes, which can be further hampered by significant downregulation of *codY*. The BFT vs BFU condition did not display significant upregulation of *rsh, relP* or *relQ*. This, along with no significant changes in the expression of stringent response target genes (with the exception of *infA*), suggests the stringent response is no longer being triggered 12 hours after triclosan exposure (BFT vs BFU).

### 5.3.4 Triclosan exposure leads to significant upregulation of efflux pump genes, potentially further facilitating antibiotic tolerance

To determine if triclosan exposure could reduce antibiotic susceptibility via mechanisms independent to the stringent response, the expression of antibiotic efflux pump genes were investigated. These genes were *norA, norB, norC, mdeA, mepA, lmrS, tet38* and *abcA*, wich correspond to the majority of chromosomally encoded efflux pumps in the *S. aureus* genome.

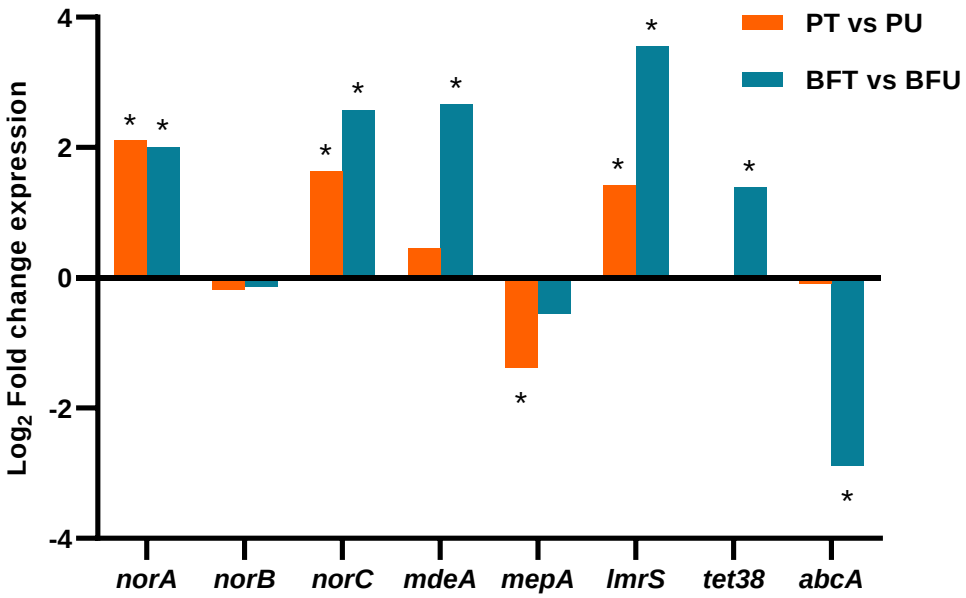



**Figure 5.6. Triclosan treatment prompts significant upregulation of genes encoding efflux pumps.** Bar graph showing the mean $log_2$ fold change in gene expression of stringent response genes in PT vs PU (orange) and BFT vs BFU (blue). PU and BFT n=2, PT and BFU n=3. * denotes FDR-adjusted P≤0.05.

PT vs PU shows a significant upregulation of *norA, norC* and *lmrS* efflux pump genes soon after triclosan exposure (Fig 5.6). BFT vs BFU comparisons indicate a further upregulation of efflux genes, with *mdeA* and *tet38* being significantly upregulated alongside efflux genes observed in PT vs PU. Notably, *norC, mdeA, lmrS* and *tet38* all exhibited higher gene expression in BFT vs BFU relative to the PT vs PU. This could potentially allude to increased efflux pump activity the longer *S. aureus* is exposed to triclosan. Whilst there are significant downregulations of the *mepA* gene (PT vs PU) and *abcA* gene (BFT vs BFU), and no changes in *norB* expression, overall it appears that triclosan exposure stimulates the expression of numerous multidrug efflux pump genes.

### 5.3.5 Triclosan exposed biofilms display significant downregulation of *icaR*, a repressor of PIA biosynthesis

To support experiments carried out in chapter 4, the expression of genes associated with the production of PIA was assessed. These genes were those of the *icaADBC* operon, which synthesise and export PIA, as well as *icaR*, the repressor of the *icaADBC* operon.

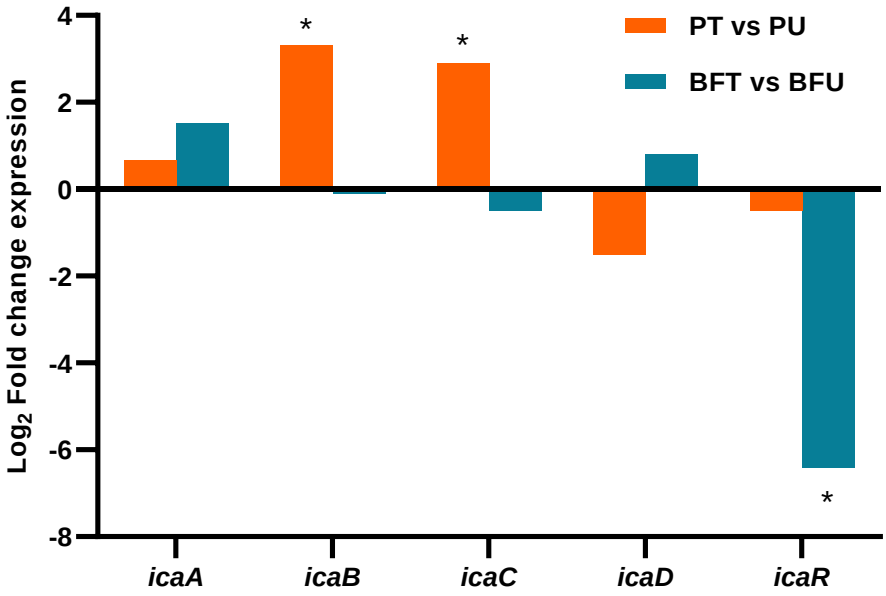



**Figure 5.7. Triclosan exposure in planktonic *S. aureus* increases expression of the PIA export genes *icaB* and *icaC*, whilst triclosan exposed biofilms downregulate the *icaR* repressor of PIA synthesis.** Bar graph showing the mean $log_2$ fold change in gene expression of stringent response genes in PT vs PU (orange) and BFT vs BFU (blue). PU and BFT n=2, PT and BFU n=3. * denotes FDR-adjusted P≤0.05.

PT vs PU (Fig 5.7) demonstrates that the *icaB* and *icaC* genes associated with PIA synthesis are significantly upregulated after triclosan exposure, indicating more PIA production even after 1 hour exposure to low levels of triclosan. Contrastingly, triclosan exposed biofilms (BFT vs BFU) do not exhibit increased expressed of any genes in the *icaADBC* operon. However, BFT vs BFU does display a highly significant decrease in *icaR* expression compared to untreated biofilms. This could facilitate PIA production through decreased repression of the *icaADBC* operon and increased expression of the operon in the near future.

### 5.3.6 SigB, an alternate sigma factor implicated in both antibiotic tolerance and altered biofilm formation, may be responsible for numerous triclosan induced changes

Following on from the results of section 5.3.5, in which it was found *icaR* was significantly reduced in BFT vs BFU, the expression of regulators known to repress *icaR* was assessed. For this, the expression of the *sigB* gene was investigated as SigB is known to repress *icaR* and upregulate *sarA*. SarA is also known to upregulation *ica* operon genes. To gain further evidence of *sigB* expression, other genes regulated by SigB were investigated alongside *sarA*, including *asp23, sodA* and *crtM*, which are upregulated by SigB. Additionally, the expression of the *agr* quorum sensing genes (*agrA, agrB, agrC* and *agrD*), which SigB represses, was evaluated.

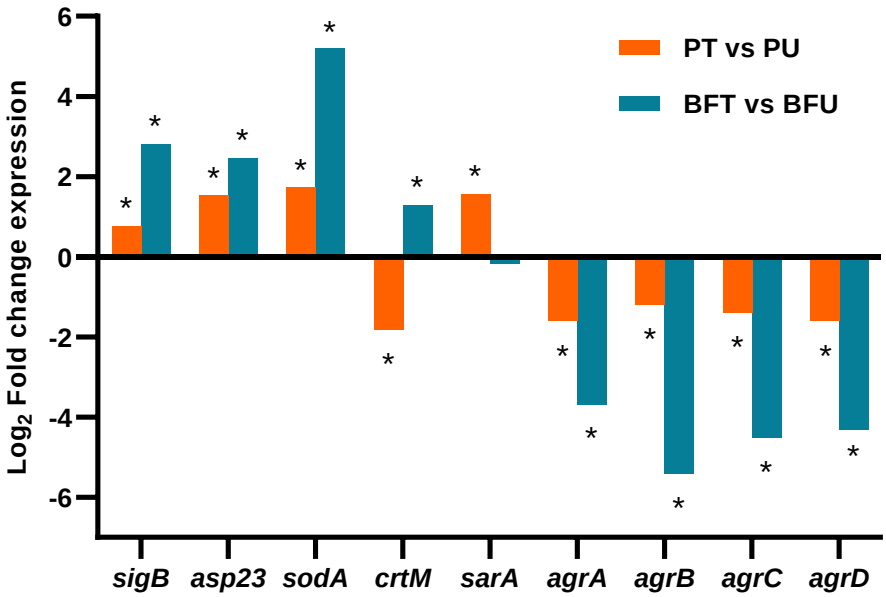



**Figure 5.8. Triclosan exposure results in increased *sigB* expression, upregulation of genes positively regulated by SigB, and downregulation of genes negatively controlled by SigB.** Bar graph showing the mean $log_2$ fold change in gene expression of stringent response genes in PT vs PU (orange) and BFT vs BFU (blue). PU and BFT n=2, PT and BFU n=3. * denotes FDR-adjusted P≤0.05.

Both PT vs PU and BFT vs BFU conditions displayed significant increases in *sigB* expression, with BFT vs BFU displaying the highest levels of differential *sigB* expression (Fig 5.8). Evidence of increased

SigB activity following triclosan exposure was also supported by significant upregulations of genes positively regulated by SigB, such as *asp23, sodA, crtM*, and *sarA.* Likewise, *agr* quorum sensing genes display downregulation that corresponds with upregulation of *sigB*.

## 5.4 Discussion

RNA-Seq was used to determine how low level triclosan exposure, consistent with concentrations shown to accumulate in the human body, altered the transcriptome of *S. aureus*. Both planktonic and biofilm cultures were interrogated to see how lifestyle influenced the response of transcriptomic *S. aureus* to triclosan. To link with previous chapters, the effects on genes associated with antibiotic tolerance and biofilm formation were examined. The PT vs PU and BFT vs BFU comparisons used in this chapter are able to directly determine how triclosan exposure influences the gene expression of either the planktonic or biofilm lifestyle.

This work clearly illustrates that exposure to the low levels of triclosan that accumulate in the human body can have significant and far-reaching effects on the *S. aureus* transcriptome (Fig 5.2). This has been demonstrated on both planktonic and biofilm cultures, and to the author's knowledge, is the first study to examine how antimicrobial stress can affect both lifestyles of *S. aureus*. RNA-Seq revealed 671 novel transcripts in the data set (Fig 5.1). Due to the large-scale changes to processes such as virulence, stress responses and quorum sensing, it is likely many of these novel transcripts are non-coding RNAs (ncRNA). Many ncRNAs bind to 5' untranslated region (UTR) to inhibit translation or mRNA degradation. Thus, ncRNAs play key roles in regulating physiology (Siezen, Wilson and Todt, 2010), and as this chapter shows, the *S. aureus* transcriptome, and potentially physiology, after triclosan exposure is drastically altered. This hypothesis is supported by the finding that some ncRNAs can be induced by niche switching (Yoder-Himes et al., 2009).

Fig 5.5 shows a significant increase in the expression of the RSH (p)ppGpp synthase gene *rsh*, suggesting rapid induction of the stringent response following triclosan exposure. Contrastingly, both *relP* and *relQ* which encode the RelP and RelQ (p)ppGpp synthases are significantly downregulated. Preferential expression of particular (p)ppGpp synthases has been shown previously, for example with RelP and RelQ

synthesising alarmones in response to cell wall stress (Geiger et al., 2014) whilst RSH is favoured following polymorphonuclear leukocyte internalisation (Geiger et al., 2012). Following this example, it could be suggested that RSH is the favoured (p)ppGpp synthase following fatty acid starvation induced by triclosan. RSH is the only (p)ppGpp synthase capable of hydrolysing (p)ppGpp alarmones, and this is essential as excess accumulation of alarmones has been shown to result in toxicity and cell death (Geiger et al., 2010; Gratani et al., 2018). In PT vs PU, upregulation of *rsh* may illustrate that RSH is degrading excess (p)ppGpp from a recently triggered stringent response. Downregulation of *relP* and *relQ* also contributes to this control by reducing alarmone synthesis by RelP and RelQ, therefore averting toxicity by excess (p)ppGpp (Geiger et al., 2014).

Differential expression of genes controlled by the stringent response are also observed in PT vs PU (Fig 5.5). Significant upregulation of *fmtA* and significant downregulation of *infA*, *tsf* and *frr* is indicative of stringent response induction. Significant changes in the expression of these genes not only support that the stringent response has been induced by triclosan, but provide insight into how the stringent response can protect *S. aureus* from antibiotics of different classes.

Upregulation of *fmtA* would lead to increased tolerance to β-lactam antibiotics due to increased utilisation of a β-lactam resistant penicillin-binding protein (Fan et al., 2007). Meanwhile, downregulation of *infA* (translation initiation factor IF-1), *tsf* (elongation factor Ts), and *frr* (ribosome-recyling factor) will lead to reduced initiation, elongation, and termination of translation, respectively. Decreased translation leads to bacterial quiescence and increases protection against all antibiotics that require active targets to induce bactericidal activity (Brauner et al., 2016; Balaban et al., 2019; Peyrussen et al., 2020; Huemer et al., 2021). The lack of significant changes in the expression of these genes in the BFT vs BFU conditions suggests the stringent response is not active in triclosan-exposed biofilms. This is logical due to the stringent response

being a stress response that needs to be triggered quickly after initial stress detection to ensure survival (Reiß et al., 2012).

CodY is closely related to the stringent response, and evidence of reduced repression by CodY would provide evidence for stringent response induction. The stringent response is initiated through the synthesis of (p)ppGpp alarmones which requires intracellular GTP, a cofactor of the repressor CodY. Intracellular GTP depletion means CodY can no longer repress its target genes, including genes associated with amino acid biosynthesis and transport (Geiger et al., 2014). Fig 5.5 suggests stringent response activation in PT vs PU by upregulation of *rsh* and downregulation of *codY*, therefore implying more (p)ppGpp synthesis and less CodY repression. KEGG mapping contributes further results that suggesting derepression of CodY targets. Genes associated with both amino acid metabolism and biosynthesis, and quorum sensing were upregulated in the PT vs PU (Fig 5.3A). Many CodY regulon genes are significantly upregulated in these KEGG pathways including amino acid biosynthesis genes *ilvB, gltB, thrC* and the amino acid transport genes of the *opp* operon (categorised as the quorum sensing KEGG pathway) (Table S1).

Efflux pump encoding genes were significantly upregulated following triclosan exposure (Fig 5.6). Between the upregulation of *norA, norC, mdeA, lmrS*, and *tet38*, triclosan exposed *S. aureus* can expel a battery of antimicrobials, potentially supplementing the antibiotic tolerance provided by the stringent response. Effluxed substrates include hydrophilic fluoroquinolones such as ciprofloxacin (effluxed by NorA, NorC, MdeA), hydrophobic fluoroquinolones such as moxifloxacin (NorC), quaternary ammonium compounds such as benzalkonium chloride (NorA, LmrS), fusidic acid (MdeA, LmrS) and dyes (NorA, NorC, MdeA, LmrS) (Kaatz, Seo and Ruble, 1993; Truong-Bolduc, Strahilevitz and Hooper, 2006; Yamada et al., 2006; Floyd et al., 2010). To supplement this already extensive antimicrobial coverage further, MdeA also effluxes virginiamycin, novobiocin, and mupirocin (Yamada et al., 2006), whilst LmrS ejects linezolid, chloramphenicol, trimethoprim,

erythromycin and kanamycin (Floyd et al., 2010). Lastly, Tet38 bestows protection to tetracycline and unsaturated fatty acids (Truong-Bolduc et al., 2015). Contrastingly, the *abcA* gene encoding the multidrug efflux pump AbcA is significantly downregulated in BFT vs BFU. Downregulation of *abcA* could be due to the additional role of AbcA in secretion of PSMs (Yoshikai et al., 2016). This would match the significant downregulation of *pmsα* in BFT vs BFU (Table S1) and is further supported by no differential expression of *abcA* being observed in PT vs PU, in which *pmsα* displays a slight upregulation.

Genes associated with the synthesis of PIA, an essential biofilm matrix component, display drastic changes in expression in both the planktonic and biofilm lifestyle (Fig 5.7). In planktonic cultures, triclosan stimulates a significant increase in the expression of both *icaB* and *icaC*, with the *icaADBC* repressor *icaR* also displaying a slight downregulation. IcaB and IcaC are both involved in PIA export, with IcaC translocating growing polysaccharide chains to the cell surface and IcaD deacetylising PNAG to allow cell surface attachment (O'Gara, 2007). Contrastingly, the established biofilms of the BFT vs BFU comparison show a massive decrease in *icaR* expression, decreasing repression of the *ica* operon and priming *ica* genes for overexpression. However, at the 12 hour timepoint at which these samples were taken this has not translated into significant upregulations in other *ica* genes, a trend of *ica* upregulation is emerging in BFT vs BFU. This is illustrated by the upregulation of *icaA* and *icaD*, the genes required for the first steps of PIA production. IcaA and IcaD work in tandem to form *N*-acetylglucosamine oligomers of up to 20 residues in length (O'Gara, 2007). Coexpression of *icaAD* and *icaC* is required for oligomers to grow larger (O'Gara, 2007), so after 12 hours of triclosan exposure it appears *S. aureus* biofilms begin to synthesise short polysaccharide chains because of a lack of IcaR repression on *icaAD*. From this data it once again appears physiological levels of triclosan drive early biofilm formation, with planktonic triclosan treated cultures exporting existing polysaccharide oligomers through IcaB and IcaC activity, whilst triclosan exposed biofilms synthesise new polysaccharide

chains through IcaR derepression of the *ica* operon. Taken together, *S. aureus* rapidly upregulates genes associated with initial attachment and biofilm formation after 1 hour of triclosan exposure during planktonic growth, with less emphasis on attachment and more focus on matrix component maintenance observed in established biofilms compared to untreated counterparts.

Following on from the findings *icaR* is significantly downregulated in triclosan-exposed biofilms, regulators that can repress *icaR* were investigated. SigB was of particular interest, as the alternative sigma factor is known to induce PIA synthesis (Knobloch et al., 2004) and coordinate stress responses (Tuchscherr et al., 2015), and triclosan exposure has been shown to induce both of these processes. The significant upregulation of *sigB* and significant downregulation of *icaR* in BFT vs BFU is a potential indication of SigB repressing *icaR* expression following triclosan exposure (Knobloch et al., 2004). SigB has also been known to induce PIA synthesis by acting directly upon the promoter of the *icaADBC* operon (Cerca, Brooks and Jefferson, 2008). The significant upregulation of *icaB* and *icaC* alongside the *sigB* upregulation in PT vs PU could suggest this in happening after 1 hour of triclosan exposure. Further findings suggesting that triclosan triggers *sigB* expression are observed when assessing the differential expression of stress response genes under SigB control.

SigB has been attributed with dynamically controlling the emergence of small-colony variants that facilitate persistence in diverse environments, including intracellularly (Tuchscherr et al., 2015) and within the CF lung (Moisan et al., 2006). The significance of SigB upregulation following triclosan exposure may result in the pathogen being capable of surviving many environmental stresses, including otherwise lethal changes in pH (Chan et al, 1998; Kullik et al, 1998) and temperature (Kullik et al, 1997). An example of this is observed in this Fig 5.8, in which *sigB* upregulation coincides with upregulation SigB controlled *asp23.* The *asp23* gene encodes alkaline shock protein, and upregulation could facilitate survival at increased pH (Chan et al, 1998; Kullik et al, 1998).

In addition, SigB controlled genes facilitate survival following exposure to ROS (Supa-Amornkul et al., 2019). SigB coordinates ROS tolerance through upregulation of genes *sodA* and *crtM* (Kullik et al., 1998; Supa-Amornkul et al., 2019). Respectively, these genes encode the SodA superoxide dimutase and the dehydrosqualene synthase required for staphyloxanthin pigment production (Song et al, 2009). SigB mediated ROS tolerance via SodA and staphyloxanthin can protect *S. aureus* against ROS produced by leukocytes (Beavers and Skaar, 2016). Furthermore, SigB ROS tolerance protects against ROS produced by competitors such as *Streptococcus pneumonia* and *P. aeruginosa* during interspecies competition (Margolis, 2009; Mitchell et al., 2010). Significant upregulations of both *crtM* (BFT vs BFU) and *sodA* (BFT vs BFU, PT vs PU) accompany significant increases in *sigB* expression in this data (Fig 5.8), further indicating SigB plays a role in coordinating the response of *S. aureus* to triclosan.

SigB drastically shifts virulence by downregulating the *agr* locus, consequently silencing the virulence factors under RNAIII control (Tuchscherr et al., 2015). A similar trend is observed in this data, in which *sigB* upregulations correspond with downregulation of *agr* locus genes (Fig 5.8) in PT vs PU and BFT vs BFU. Additionally, virulence genes under *agr* control, such as *hla*, *psmα*, and *lukGH*, are also significantly downregulated in triclosan exposed conditions (Table S1). SigB also regulates through control of *sarA*, though there is conflicting literature regarding how SigB regulates *sarA* expression. Some studies show SigB mediated silencing of *sarA* (Thoendel et al., 2011; Tuchscherr et al., 2015), whilst other studies demonstrate SigB mediated upregulation (Cheung, Nishina and Manna, 2008; Andrey et al., 2015). SarA typically increases toxin production through upregulation of *agr* RNAIII; however, this can be prevented by overriding SigB control of *agr* (Manna, Bayer and Cheung, 1998; Bischoff, Entenza and Giachino, 2001; Thoendel et al., 2011). SarA is of particular interest in this study not only because it is part of the SigB regulon, but because SarA is capable of upregulating *ica* operon expression (Valle et al., 2003; Cerca, Brooks and Jefferson,

2008) and hypothesised to repress *icaR* (Valle et al., 2003). From the data acquired in this study, significant upregulation of *sarA* is only seen in PT vs PU, whilst no significant change in gene expression is observed in BFT vs BFU (Fig 5.8). Whilst there is a consistent upregulation of *sigB* across both BFT vs BFU and PT vs PU, *sarA* does not display a similar, uniform response. This therefore makes it difficult to attribute changes in *sarA* expression to potential SigB activity, and reflects the current lack of consensus on how precisely SigB regulates *sarA* (Cheung, Nishina and Manna, 2008; Thoendel et al., 2011; Andrey et al., 2015; Tuchscherr et al., 2015). Upregulation of *sarA* did coincide with significant upregulations of *icaB* and *icaC*, and likewise, no significant changes in the expression of the *icaADBC* operon were observed when *sarA* was not significantly upregulated. This could potentially be illustrative of the role of SarA in direct upregulation of the *icaADBC* operon (Valle et al., 2003; Cerca, Brooks and Jefferson, 2008). However, the slight downregulation of *sarA* in BFT vs BFU alongside downregulation of *icaR* (Fig 5.7) suggests SigB is more likely to act of *icaR*.

The results found in this study are similar to others interrogating the *S. aureus* in response to stress. For instance, Riordan and colleagues (2011) found that *sigB* was upregulated in response to an anti-inflammatory drug. Peyrusson et al. (2020) found that treatment with oxacillin drastically reshape the *S. aureus* transcriptome into one adapted for intracellular persistence. After oxacillin exposure, RNA-Seq revealed the importance of CodY and the stringent response for survival, as well as upregulation of genes associated with the cell wall stress regulon and the SOS response. Overall, the work of Peyrusson et al (2020) bears striking resemblances to those uncovered in this study, suggesting that antibiotics of different classes can trigger a similar holistic survival response. Parallels between this work and a study investigating the effect on the *S. aureus* transcriptome after sub-MIC ethanol and chloramine T exposure can be drawn. Like this study, it was found that disinfectant exposure lead to the upregulation of *sigB* (Fig 5.8), *cap* and *clf* genes (Table S1) (Slany, Oppelt and Cincarova, 2017). Lastly, a study by Lui et

al. (2018) investigated the *S. aureus* transcriptome in response to low levels of ampicillin and found, as in this study, upregulation of PBP genes (Fig 5.5, *fmtA*). Contrastingly, they also detected upregulations of *abcA*. In the context of that study, this was likely due to the AbcA efflux pump using β-lactams, which in this instance induced stress, as a substrate. This illustrates how *S. aureus* can differentially express genes depending on the type of antimicrobial stress.

In summary, triclosan exposure radically alters the *S. aureus* transcriptome. Triclosan exposure prompts significant differential gene expression of genes associated with tolerance to antibiotic stresses. These genes include *rsh* of the stringent response, and genes that are regulated by the stringent response such as those associated with translation (*infA*, *tsf* and *frr*) and tolerance to β-lactams (*fmtA*). Furthermore, stringent response mediated antibiotic tolerance may be supplemented by multidrug efflux pumps, as significant upregulation of efflux pump genes is observed following triclosan exposure. This data also shows *sigB* upregulation, suggesting triclosan treatment stimulates SigB. Upregulation of *asp23* and *sodA* provide further evidence for a SigB coordinated stress response against multiple stresses such as increased pH and ROS. In addition, downregulations of *agr* alongside *sigB* upregulation are indicative of the silencing of *S. aureus* virulence that SigB mediates. This data also aids in the elucidation of triclosan induced PIA synthesis, with SigB potentially acting upon the *ica* operon in PT vs PU and repressing *icaR* in BFT vs BFU. SarA, which can act either independently or via SigB, may also be involved, as upregulation of *sarA* is observed alongside *icaBC* upregulation in PT vs PU.

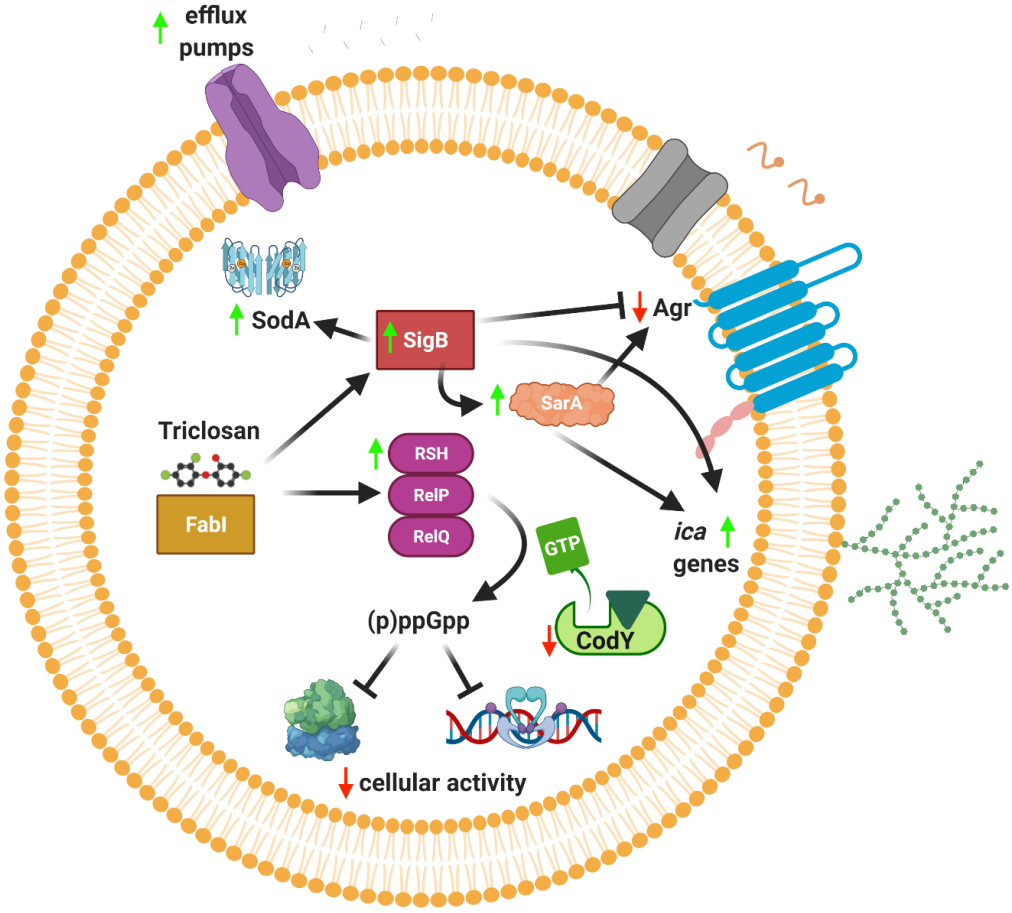



**Figure 5.9. Schematic of gene expression changes and proposed interactions following triclosan exposure.** Following 1 hour triclosan exposure, planktonic *S. aureus* initiates the stringent response by *rsh* upregulation leading to downregulation of cellular metabolism and activity. Increase in stringent response alarmone synthesis results in a decrease in CodY repression. Triclosan exposure also upregulates *sigB*, which indirectly upregulates PIA biosynthetic genes also. SigB also upregulates many other genes including *sodA* and *sarA*. Upregulation of *sarA* can also upregulate the PIA biosynthetic genes of the *ica* operon. SigB can also inhibit expression of *agr*. Downregulation of *agr* RNAIII leads to a reduction of many *agr* controlled virulence genes. Furthermore, numerous efflux pump genes are also upregulated. After 12 hours of triclosan exposure, *S. aureus* biofilms no longer exhibit significant changes in either *rsh* or *codY* expression, but decreased metabolism persists. Although trends of expression in many genes are not different compared to triclosan exposed planktonic cultures, these trends are more drastic in triclosan-exposed biofilms. For example, efflux pump are more upregulated whilst *agr* genes are further downregulated when compared to the differences seen in PT vs PU. Green arrows indicate significant upregulation of associated genes. Red arrows indicate significant downregulation of associated genes.

To conclude, this data provides evidence that triclosan stimulates both the stringent response and SigB, as illustrated by not only upregulations of *rsh* and *sigB,* but also significant changes to the respective regulons of both regulators. The triclosan-induced regulatory cascade caused by both the stringent response and SigB could induce tolerances to multiple different stresses.

# 6. Discussion

Biocides such as triclosan, chlorhexidine digluconate, and benzalkonium chloride have been used in a wealth of different applications across the globe for decades (Schweizer, 2001; Russell, 2003; Brittain, 2004; MacIsaac et al., 2014; Sewlikar et al., 2015; Gudapuri, 2017; Singha et al., 2017; Pereira and Tagkopoulus, 2019). The widespread use of these biocides enables an accumulation of the antimicrobial agents within the human body at low concentrations (Allmyr et al., 2009; MacIsaac et al., 2014). Currently, much is still unknown about the effects on bacterial pathogens following exposure to physiologically relevant levels of biocides that have accumulated within the host. In 2019, Westfall et al. revealed that exposure to physiologically relevant levels of triclosan could induce antibiotic tolerance in *E. coli* and *S. aureus*. In the case of *E. coli*, this was shown to be due to the stringent response (Westfall et al., 2019). These studies were only conducted on planktonic cultures, and the mechanisms underlying *S. aureus* antibiotic tolerance were not addressed. Many studies identifying antimicrobial-mediated antibiotic tolerance are largely carried out in planktonic culture. This neglects the biofilm lifestyle, which is arguably far more relevant clinically due to how ubiquitous biofilms are during infection and the extreme difficulties associated with their eradication (O'Toole, Kaplan and Kolter, 2000; Lewis, 2001; Nguyen et al., 2011; Lebeaux et al., 2014; Lister and Horswill, 2014; Flemming et al., 2016). Very recently, it was shown that sub-MIC exposure to vancomycin could induce further tolerance in *S. aureus* biofilms (Salzer et al., 2020); demonstrating this phenomenon can occur regardless of bacterial lifestyle. Furthermore, biofilm matrix modification has been attributed to exposure to sub-MIC biocides, in which different matrix components were present at increased proportions following treatment during biofilm formation (Tabak et al., 2007; Kaplan, Jabbouri and Sadovskaya, 2011; Kaplan, 2011).

In this study the effects of biocides on both the antibiotic tolerance and biofilm formation of *S. aureus* was evaluated. From this investigation, it

was found that not only did exposure to the biocide triclosan induce antibiotic tolerance in both planktonic and biofilm lifestyles, but that biofilm formation and composition was significantly altered. Whilst the stringent response was found to facilitate triclosan-induced antibiotic tolerance, the underlying mechanism behind triclosan-induced alterations in biofilm structure remained elusive. RNA-Seq was thus carried out to discern both the regulatory and effector genes involved in the establishment of a triclosan exposed phenotype.

The work shown here in both biofilms (Fig 3.11) and RNA-Seq data (Fig 5.5) complements that of Salzer and colleagues (2020). Salzer et al. found that sub-MIC levels of vancomycin enhanced the antibiotic tolerance of *S. aureus* HG001 biofilms by the stringent response. It was also found that both RelP and RelQ of the stringent response impacted biofilm formation of *S. aureus* when under the cell wall stress of vancomycin, and that this was independent of both CodY and *agr* (Salzer et al., 2020). Using deletion mutants, this work too found that neither CodY (Fig 4.6) nor *agr* (Fig 4.7) influenced biofilm formation under biocide-exposed conditions. Contrastingly, the stringent response had no impact on biofilm formation under triclosan exposure either. Both CV (Fig 4.10) and CLSM (Fig 4.5) experiments detected no differences in biofilm formation between the biofilms of (p)ppGpp$^0$ and WT strains. In this study, the only divergence in the biofilm phenotype of (p)ppGpp$^0$ and WT strains was the lack of triclosan-induced antibiotic tolerance in the stringent response mutant. This study also deviates from the findings of Salzer and colleagues by finding that triclosan exposure markedly alters biofilm composition. Whilst vancomycin exposed HG001 formed biofilms in an *ica*-independent manner and are composed mainly of eDNA and proteins, HG001 appears to form biofilms in an *ica*-dependent manner following triclosan exposure (Fig 4.2). Taken together, the findings of both this study and Salzer et al (2020) show that antibiotic tolerance in biofilms can be induced by multiple antimicrobials with very differing mechanisms of action. Likewise, it is shown that within the same strain biofilm

architecture can differ drastically depending on the nature of the inducing stress.

Despite the extensive changes to biofilm matrix architecture following triclosan exposure, this work found that increased matrix polysaccharide had negligible effect on the heightened antibiotic tolerance of triclosan exposed biofilms. Instead, through the use of a (p)ppGpp$^0$ strain, it was shown that the stringent response was entirely responsible for increased tolerance of triclosan exposed biofilms to ciprofloxacin, vancomycin, and rifampicin. The lack of antibiotic protection via excess polysaccharide production is evidenced by restored antibiotic susceptibility in the (p)ppGpp$^0$ strain (Fig 3.11) but excess polysaccharide still being detected (Fig 4.5). PIA is apparently advantageous to triclosan exposed *S. aureus* considering the substantial increase in synthesis of the matrix component, particularly as *S. aureus* has initiated a starvation response, implying resource scarcity. It can therefore be speculated that PIA production is prioritised for another purpose, perhaps for defence against opsonisation and phagocytosis (Cerca et al., 2006; de Vor, Rooijakkers and van Strijp, 2020), as well as driving biofilm formation (Fitzpatrick, Humphreys and O'Gara, 2005). Other genes regulated by both SigB and SarA that are associated with both biofilm formation and immune evasion, such as *fnbA* and *clfA* (Table S1), are also upregulated following triclosan exposure. This could suggest that triclosan exposure prompts earlier biofilm formation in *S. aureus* to better tolerate immune stresses.

Although it was hypothesised in chapter 4 that CodY may have been responsible for triclosan-induced polysaccharide production, no definitive evidence for this was apparent. Because the involvement of the stringent response in triclosan-induced tolerance had been observed, it seemed likely that CodY, which is closely associated with the stringent response and a repressor of the PIA biosynthetic *ica* genes (Pohl et al., 2009), would be involved in this biofilm phenotype. Transcriptomics did indeed find that in the PT vs PU comparison that *codY* was downregulated, which would suggest that CodY targets such as *ica* would no longer be repressed. However, experiments using the Δ*codY* strain revealed that a

lack of CodY repression of *ica* alongside triclosan further increased polysaccharide production (Fig 4.6). This suggests CodY is a supplementary mechanism of triclosan-induced PIA accumulation, rather than an essential mechanism.

RNA-Seq suggested that changes to biofilm composition were induced through SigB mediated repression of *icaR*. Reduced *icaR* repression of the *ica* operon could explain the increased PIA synthesis observed in triclosan exposed biofilms in chapter 4. SigB could contribute further to biofilm formation, as SigB can upregulate both *fnbA* and *clfA,* which are associated with the early stages of protein mediated biofilm formation (Speziale et al., 2014). Furthermore, SigB upregulates *sarA* and downregulates *agr*. This is significant as *sarA* is another positive regulator of *clfA* and *fnbA*, whilst *agr* is a negative regulator of these MSCRAMM genes (Speziale et al., 2014). The RNA-Seq data of this study did find significant upregulations of *clfA* and *fnbA* (Table S1), alongside significant upregulations of *sarA*, *sigB* and downregulations of *agr* genes (Fig 5.8) following triclosan exposure, potentially suggesting the biocide induced increased production of matrix proteins. However, staining for matrix protein did not find any significant differences in proportions of protein in the matrix of triclosan exposed biofilms (Fig 4.4D, Fig 4.9F).

The role of SigB may extend beyond biofilm formation, as SigB has also been associated with antibiotic tolerance (Morikowa et al., 2001; Cafiso et al., 2012). The SigB regulon has been associated with protection against cell wall active antimicrobials by inducing thickening of the peptidoglycan cell wall (Morikowa et al., 2001). Additionally, superoxide dismutases, such as those encoded by SigB controlled *sodA,* have been shown to induce vancomycin tolerance in *S. aureus* (Labjouzi et al., 2013).

Exposure to low concentrations of numerous antimicrobials, including triclosan and vancomycin, have been shown to induce antibiotic tolerance through the stringent response (Westfall et al., 2019; Salzer at

al., 2020). However, when pretreating *S. aureus* with sub-MIC concentrations of BAC or CHG it was found that despite inducing antibiotic tolerance against ciprofloxacin, this was independent of the stringent response (Fig 3.15). In addition, this antibiotic tolerance was only observed in planktonic culture and did not translate to *S. aureus* biofilms. Biofilms displayed no changes in antibiotic susceptibility following BAC or CHG exposure (Fig 3.16). Likewise, exposure to these biocides throughout biofilm formation did not stimulate changes to biofilm structure or composition (Fig 4.11). Both of these biocides must therefore stimulate different stress responses to enable survival against ciprofloxacin. SigB, which is also heavily involved in mediating *S. aureus* stress adaption is upregulated in response to triclosan and can protect from stresses independently of the stringent response (Moisan et al., 2006; Tuchscherr et al., 2015). However, it is unlikely these biocides stimulate *sigB* expression, as Supa-amornkul and colleagues (2019) found that biocides such as chlorhexidine and povidone-iodine were unable to stimulate SigB mediated protection. One alternative explanation is that, just as described in the transcriptomics experiments of triclosan exposed *S. aureus*, exposure to BAC and CHG at low concentrations stimulates upregulation of efflux pumps. The chromosome of *S. aureus* strain HG001 possesses genes encoding the efflux pumps NorA, NorB, and SepA, which are associated with tolerance to both CHG and BAC (Costa et al., 2013; Liu et al., 2015; LaBreck et al., 2020). Furthermore, chromosomally encoded efflux pumps MepA, MdeA, and LmrS can also efflux QACs such as BAC (Costa et al., 2013; Liu et al., 2015). It is therefore possible that biocide exposure upregulates efflux pump genes and causes cross-tolerance to ciprofloxacin. This is because many of these efflux pumps (MepA, MdeA, NorA, NorB, and NorC) can also extrude the hydrophilic fluoroquinolone as a substrate (Kaatz, Seo and Ruble, 1993; Truong-Bolduc, Strahilevitz and Hooper, 2006; Yamada et al., 2006; Floyd et al., 2010; Costa et al., 2013).

In this study, it was found that the *agr* system had no effect on triclosan-induced antibiotic tolerance in biofilms, nor did *agr* affect triclosan-

induced biofilm alterations. This was confirmed by RNA-Seq, in which all genes of the *agr* system were downregulated (Fig 5.8) and the *sigB* gene which encodes SigB, a known repressor of *agr*, was upregulated (Fig 5.8). However, the planktonic time-kill curve experiments discussed in section 3.3.8 show that *agr* null mutants are less protected by triclosan pretreatment against ciprofloxacin (Δ*agr* T+C; Fig 3.7B) compared to the WT strain (T+C Fig 3.7B). This reduced survival of the *agr* null mutant in the presence of triclosan would suggest that the *agr* system is required for triclosan to fully induce the antibiotic tolerant phenotype. This conflicts with previous literature which suggest that *agr* dysfunction would actually promote rather than inhibit persister formation (Xu et al., 2017). To support this further, it has been shown that ciprofloxacin treatment, which was also used in this experiment, actually drives selection of *agr* null mutants (Paulander et al., 2013; George et al., 2019). Triclosan too selects for *agr* deficiency in *S. aureus* to aid survival (Nielsen et al., 2013). Furthermore, the lack of a functioning *agr* system could prevent toxicity from PSM production, although it is possible PSMs are still produced by RSH of the stringent response (Geiger et al., 2012; Horvatek et al., 2020) after triclosan exposure. It should be noted that despite the selection of *agr* null mutants, *agr* function is still maintained by many strains (George et al., 2019). Maintaining low *agr* activity rather than abolishing the quorum sensing system gives *S. aureus* the flexibility to upregulate *agr* as required. Indeed, the *agr* system is dynamic in responding to environmental cues such as oxygen concentration (Kavanaugh and Horswill, 2016). For example, *agr* has been shown to be upregulated in hypoxic conditions, when the fitness burden of expressing the system is lower. This is due to PSMs generating less ROS under hypoxia compared to aerobic conditions (George et al., 2019). Therefore, although triclosan exposure downregulates the *agr* system, but low-level expression is still required to facilitate triclosan-induced tolerance. This hypothesis could be tested using reporters that monitor *agr* activity, for instance, Blower et al. (2020) describe a novel bioluminescent reporter linked to the P3 promotor of the *agr* system. However, future work should re-examine these results carefully in light of

the contradiction this result presents when compared to the consensus regarding *agr* and tolerance (Paulander et al., 2012; Nielsen et al., 2013; Xu et al., 2017; George et al., 2019).

Strains HG001, SH1000, and NCTC8325-4 have all been used in this study and are descended from the NCTC8325 *S. aureus* strain (Herbert et al., 2010). The NCTC8325 strain has defects in two regulatory genes: *rsbU* and *tcaR*. The *rsbU* gene is a positive activator of SigB, and is therefore closely entwined with coordination of the *S. aureus* stress response (Bischoff, Entenza and Giachino, 2001). Deficiency in the *tcaR* gene has not been shown to have profound effects on *S. aureus* (Herbert et al., 2010). In addition, NCTC8325 also harbours three prophages: Φ11, Φ12, and Φ13. Φ13 is particularly disruptive as it deprives *S. aureus* of β-toxin, but in return enables additional immunomodulatory functions due to its insertion (Coleman et al., 1991; Iandolo et al., 2002; van Wamel et al., 2006; Malachowa and DeLeo, 2011).

As mentioned, multiple strains used in this work are of the NCTC8325 lineage. HG001 has a repaired *rsbU* gene whilst NCTC8325-4 has gone through successive rounds of UV treatment to be cured of prophages Φ11, Φ12, and Φ13 (Novick, 1967). SH1000 is a direct descendent of NCTC8325-4 that has had the *rsbU* gene repaired (Horsburgh et al., 2002). The NCTC8325-4 GFP *S. aureus* strain used for confocal imaging (Fig 4.12) and NCTC8325-4 WT for endpoint biofilm CFU experiments (Fig 4.13) lack a functioning *rsbU* gene. RsbU is essential for SigB activation (Bischoff, Entenza and Giachino, 2001), and transcriptomics has found upregulation of *sigB* and concurrent changes in expression of SigB targets, including *sarA*, *agr*, and *icaR* following triclosan exposure. Since SigB has been shown to be associated with PIA biosynthesis (Knobloch et al., 2004), antibiotic tolerance (Morikoawa et al., 2001) and coordination of general stress responses (Jenul and Horswill, 2018), use of NCTC8325-4 limits investigation of the triclosan-induced phenotype of *S. aureus*. Despite the lack of both *rsbU*, NCTC8325-4 biofilms still consist of more PIA following triclosan exposure compared to untreated controls (Fig 4.12). This could be because of positive regulation of the *ica*

operon by SarA, which can promote PIA biosynthesis independently of SigB (Valle et al., 2003; Cerca, Brooks and Jefferson, 2008). It is difficult to directly compare NCTC8325-4 to HG001 or SH1000 biofilms without undertaking further analysis of NCTC8325-4 using the assays described in chapter 3. In the polymicrobial biofilms, it was necessary to alter growth conditions to allow for optimum recovery of both *S. aureus* and *P. aeruginosa* and this involved using RPMI-1640 (Jordana-Lluch et al., 2020), a medium that is not as rich as BHI, which was also used in *S. aureus* monospecies controls in this work. *P. aeruginosa* has a tendency to overwhelm *S. aureus* in richer medium, producing biofilms that are too mucoid to image without significant disruption during washing (Wijesinghe et al., 2019).

This study has shown that the global changes to *S. aureus* metabolism lead to subsequent changes to the pH gradients of the surrounding environment. This has been shown in both chapter 3, in which triclosan exposure limits both *S. aureus* growth and acidification of the extracellular environment (Fig 3.1A). Chapter 4 then showed that exposure to different concentrations of triclosan can alter biofilm thickness, and that different biofilm thicknesses displayed very different pH gradients (Fig 4.1B). pH is a very important environmental cue for *S. aureus* and being able to detect changes is the difference between survival and death (Tranchemontagne et al., 2015; Moldovan and Fraunholz, 2019). Weinrick et al (2004) showed that the transcript levels of approximately 400 genes were altered in response to pH decrease to 5.5 from 7.5. This is important as in Figure 4.1B it is shown that biofilms exposed to 500 ng/mL triclosan formed thicker biofilms with pH microenvironments spanning from 7.5 in the lower regions and 5.5 at the top layers. Triclosan exposed biofilms were not only more acidic than untreated biofilms, but maintained this acidic gradient over a greater proportion of biofilm depth. Therefore, triclosan-induced changes to biofilm thickness may result in more pronounced differential gene expression across biofilm layers. Top layers of the biofilm may even be more virulent, as acidic pH has been shown to induce the *agr* system,

which aids survival within the phagolysosome (Flannagan et al., 2018). Furthermore, the potential stimulation of SigB by triclosan exposure may allow *S. aureus* to tolerate extremes of pH (Chan et al., 1998; Kullik et al., 1998). An example of this is the upregulation of *asp23*, indicating alkaline shock induction. Additionally, genes associated with acid tolerance and detoxification are upregulated following triclosan exposure (Table S1), suggesting that triclosan-exposed *S. aureus* may be better able to cope with environmental stresses.

Future work for this project would mainly follow up on discoveries unearthed by RNA-Seq data. Firstly, RNA-Seq data would need to be validated by quantitative real-time PCR. This would also allow for a more systematic approach in the investigation of these genes at a much lower expense than RNA-Seq. Further exploration of how growth conditions and different time points affect the expression could also be undertaken. This would remedy the limitations of the BFU vs PU and BFT vs PT comparisons discussed in chapter 5, allowing gene expression to be monitored in cultures that have been grown in the same conditions at different time points. Quantitative real-time PCR could also monitor whether how gene expression changes after additional stresses, such as antibiotics, are added to triclosan exposed *S. aureus* biofilms or planktonic cultures. This could complement the antibiotic tolerance experiments described in chapter 3. Following this, more targeted investigations of genes that are differentially expressed in triclosan treated conditions would be needed. Transcriptomics has revealed additional mechanisms that compliment previously investigated processes such as triclosan-induced antibiotic tolerance and biofilm formation. Triclosan-induced antibiotic tolerance may be augmented by SigB mediated cell wall thickening or increased efflux pump expression. A multitude of experiments can be carried out to determine whether changes in gene expression found by RNA-Seq can translate into the triclosan-exposed phenotype. Ethidium bromide efflux assays can also be used to determine if efflux pumps have been upregulated following biocide exposure (Couto et al., 2008). Comparing strain NCTC8325-4

with HG001 or SH1000 would also be a convenient method for further understanding the role of SigB in the establishment of a triclosan exposed phenotype, due the NCTC8325-4 harbouring a defective *rsbU* gene, therefore inhibiting SigB activation.

Peyrusson et al (2020) found that oxacillin exposure prompted a general stress response that could protect against fluoroquinolones, macrolides and aminoglycosides. That is closely mirrored by the work shown here, in which triclosan protects *S. aureus* planktonic cultures (Fig 3.3; Fig 3.10C) and biofilms against ciprofloxacin and vancomycin (Fig 3.4; Fig 3.12A). Triclosan also protected biofilms against high doses of rifampicin (Fig 3.12A). Peyrusson and colleagues also concluded that multiple, redundant pathways were triggered to induce antibiotic tolerance in response to multiple stresses over a prolonged period, as indicated by stringent response expression only occurring transiently. This would appear to be the case in this work, in which *S. aureus* responds to triclosan exposure throughout planktonic growth or biofilm exposure. Additional stresses, such as antibiotic exposure in planktonic experiments, or environmental stresses such as nutrient limitation or pH change in biofilms, further compound the initial stress triggered by triclosan to produce a triclosan stressed phenotype. These stresses appear to be countered by a concerted effort primarily controlled by transient stringent response expression (Fig 5.5) and prolonged SigB upregulation (Fig 5.8). Whilst triclosan may not be the sole stress contributing to this endpoint physiology, it is certainly the initial catalyst. As demonstrated by remedying triclosan induced fatty acid starvation with exogenous oleic acid to prevent the manifestation of this phenotype (Fig 3.5; Fig 3.6). The notion proposed by Peyrusson et al (2020) that there is plasticity to persistence that depends on the degree of stress experienced is supported in this work. Proportionate responses to triclosan are observed when *S. aureus* biofilms are exposed to different doses but also to different time courses of triclosan exposure. Triclosan exposed biofilms exhibited far more nuanced changes to biofilm architecture after being treated with 10 ng/mL triclosan compared to of

500 ng/mL (Fig 4.1). Likewise, less polysaccharide was detected in established biofilms when they had been treated with 500 ng/mL triclosan for 3 hours compared to a full 48-hour exposure period (Fig 4.3).

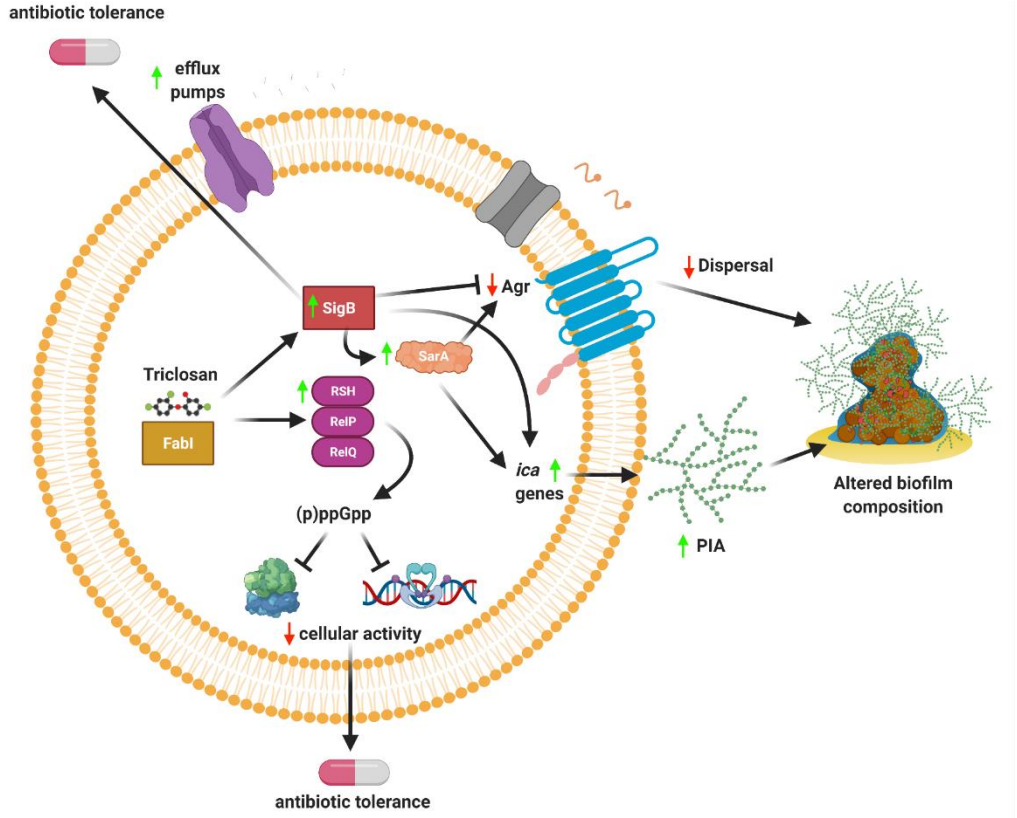



**Figure 6.1. Summary of the proposed mechanisms and responses to triclosan exposure.** Proposed mechanism of triclosan-induced antibiotic tolerance. Triclosan inhibits fatty acid synthesis through binding to FabI. Fatty acid starvation results in the induction of the stringent response and production of (p)ppGpp alarmones by the RSH. The stringent response reduces cellular activity, inducing antibiotic tolerance due to the reduced activity of many antibiotic targets. Triclosan also upregulates SigB, which can contribute to antibiotic tolerance by upregulation of *sodA* and genes associated with cell wall thickening. SigB can repress *agr,* and this study finding that *agr* was downregulated after triclosan exposure. Efflux pumps may be involved in antibiotic tolerance in triclosan exposed *S. aureus.* Proposed mechanism for triclosan-induced biofilm alterations. Triclosan-induced stress triggers upregulation of SigB. SigB can repress *agr*, reducing biofilm dispersal, and upregulate PIA production through downregulation of the *icaR* repressor. SarA, either through SigB or indenpendently, can increase PIA synthesis by positively regulating the *ica* operon.

To conclude, the findings presented in this work demonstrate that concentrations of triclosan, consistent with physiologically relevant accumulations in the human body (Allmyr et al., 2009; MacIsaac et al.,

2014), can markedly reshape the physiology of *S. aureus* (Fig 6.1). Phenotypically apparent markers of this change are evidenced by increased antibiotic tolerance to multiple different antimicrobial classes in both planktonic (Fig 3.10) and biofilm culture (Fig 3.4; Fig 3.12). This is complemented by obvious changes to biofilm structure and composition, with excess PIA being produced despite a reduced population of *S. aureus* (Fig 4.9). Lastly, the RNA-Seq carried out in this work illustrated that triclosan shifts the expression of many global regulators to facilitate these biocide induced alterations. Observed upregulations of the stringent response and SigB have been associated with antibiotic tolerance (Morikawa et al., 2001), whilst SigB can also act to stimulate PIA production (Knobloch et al., 2004), thus altering biofilm composition. One alarming finding of this study was that triclosan-induced antibiotic tolerance extends for at least 48 hours. This is of concern as this state of tolerance has been viewed as a crossroads which forks to either a reversion to a replicative state, at which acute infection may either continue, or to begin the process of making these changes permanent through mutation (Peyrusson et al., 2020). The switch from dynamic formation of a tolerant population to a population that is in a state of constant tolerance is troubling, due to these pathogens being able to establish or further entrench chronic infections, and live intracellularly within phagocytes almost indefinitely (Peyrusson et al., 2020; Tuchscherr, Loffler and Proctor, 2020). Intracellular persistence has even been suggested as a possible mechanism for disseminating *S. aureus* infection via haematogenous spread (Thwaites and Gant, 2011). Moreover, this biocide induced physiological change could accelerate antimicrobial resistance, due to tolerance being shown to precede resistance (Levin-Reisman et al., 2017). In light of these developments, it is essential to further understand the roles of biocides in the induction of tolerance and antibiotic treatment failure, and urgently review the global use of biocides in household products.

# 7. References


ESCMID 2003. Determination of minimum inhibitory concentrations (MICs) of antibacterial agents by broth dilution. *Clinical Microbiology and Infection,* 9**,** ix-xv.

Abdelhady, W., Chen, L., Bayer, A. S., Seidl, K., Yeaman, M. R., Kreiswirth, B. N. & Xiong, Y. Q. 2015. Early *agr* activation correlates with vancomycin treatment failure in multi-clonotype MRSA endovascular infections. *J Antimicrob Chemother,* 70**,** 1443-52.

Abdelmagid, S. A., Clarke, S. E., Nielsen, D. E., Badawi, A., El-Sohemy, A., Mutch, D. M. & Ma, D. W. 2015. Comprehensive profiling of plasma fatty acid concentrations in young healthy Canadian adults. *PLoS One,* 10**,** e0116195.

Adolfsson-Erici, M., Pettersson, M., Parkkonen, J. & Sturve, J. 2002. Triclosan, a commonly used bactericide found in human milk and in the aquatic environment in Sweden. *Chemosphere,* 46**,** 1485-9.

Ahmed, N. A., Petersen, F. C. & Scheie, A. A. 2008. Biofilm formation and autoinducer-2 signaling in *Streptococcus intermedius*: role of thermal and pH factors. *Oral Microbiol Immunol,* 23**,** 492-7.

Aka, S. T. & Haji, S. H. 2015. Sub-MIC of antibiotics induced biofilm formation of *Pseudomonas aeruginosa* in the presence of chlorhexidine. *Braz J Microbiol,* 46**,** 149-54.

Alfhili, M. A. & Lee, M. H. 2019. Triclosan: An Update on Biochemical and Molecular Mechanisms. *Oxid Med Cell Longev,* 2019**,** 1607304.

Allison, K. R., Brynildsen, M. P. & Collins, J. J. 2011. Metabolite-enabled eradication of bacterial persisters by aminoglycosides. *Nature,* 473**,** 216-20.

Allmyr, M., Panagiotidis, G., Sparve, E., Diczfalusy, U. & Sandborgh-Englund, G. 2009. Human Exposure to Triclosan via Toothpaste does not change CYP3A4 Activity or Plasma Concentrations of Thyroid Hormones. *Basic & Clinical Pharmacology & Toxicology,* 105**,** 339-344.

Altenbern, R. A. 1977. Cerulenin-Inhibited Cells of *Staphylococcus aureus* Resume Growth When Supplemented with Either a Saturated or an Unsaturated Fatty Acid. *Antimicrob Agents Chemother,* 11**,** 574-576.

Anderson, K. L., Roux, C. M., Olson, M. W., Luong, T. T., Lee, C. Y., Olson, R. & Dunman, P. M. 2010. Characterizing the effects of inorganic acid and alkaline shock on the *Staphylococcus aureus* transcriptome and messenger RNA turnover. *FEMS Immunol Med Microbiol,* 60**,** 208-50.

Andrey, D. O., Jousselin, A., Villanueva, M., Renzoni, A., Monod, A., Barras, C., Rodriguez, N. & Kelley, W. L. 2015. Impact of the Regulators SigB, Rot, SarA and *sarS* on the Toxic Shock Tst Promoter and TSST-1 Expression in *Staphylococcus aureus*. *PLoS One,* 10**,** e0135579.

Andrey, D. O., Renzoni, A., Monod, A., Lew, D. P., Cheung, A. L. & Kelley, W. L. 2010. Control of the *Staphylococcus aureus* toxic

shock *tst* promoter by the global regulator SarA. *J Bacteriol,* 192**,** 6077-85.

Appleman, M. D. & Citron, D. M. 2010. Efficacy of vancomycin and daptomycin against *Staphylococcus aureus* isolates collected over 29 years. *Diagn Microbiol Infect Dis,* 66**,** 441-4.

Arciola, C. R., Campoccia, D., Ravaioli, S. & Montanaro, L. 2015. Polysaccharide intercellular adhesin in biofilm: structural and regulatory aspects. *Front Cell Infect Microbiol,* 5**,** 7.

Arthur, M., Reynolds, P. & Courvalin, P. 1996. Glycopeptide resistance in *enterococci*. *Trends Microbiol,* 4**,** 401-7.

Ascione, T., Pagliano, P., Mariconda, M., Rotondo, R., Balato, G., Toro, A., Barletta, V., Conte, M. & Esposito, S. 2015. Factors related to outcome of early and delayed prosthetic joint infections. *J Infect,* 70**,** 30-6.

Balaban, N. Q., Helaine, S., Lewis, K., Ackermann, M., Aldridge, B., Andersson, D. I., Brynildsen, M. P., Bumann, D., Camilli, A., Collins, J. J., Dehio, C., Fortune, S., Ghigo, J. M., Hardt, W. D., Harms, A., Heinemann, M., Hung, D. T., Jenal, U., Levin, B. R., Michiels, J., Storz, G., Tan, M. W., Tenson, T., Van Melderen, L. & Zinkernagel, A. 2019. Definitions and guidelines for research on antibiotic persistence. *Nat Rev Microbiol,* 17**,** 441-448.

Band, V. I. & Weiss, D. S. 2019. Heteroresistance: A cause of unexplained antibiotic treatment failure? *PLoS Pathog,* 15**,** e1007726.

Barberan, J. 2006. Management of infections of osteoarticular prosthesis. *Clin Microbiol Infect,* 12 Suppl 3**,** 93-101.

Barna, J. C. & Williams, D. H. 1984. The structure and mode of action of glycopeptide antibiotics of the vancomycin group. *Annu Rev Microbiol,* 38**,** 339-57.

Bayer, A. S., Mishra, N. N., Chen, L., Kreiswirth, B. N., Rubio, A. & Yang, S. J. 2015. Frequency and Distribution of Single-Nucleotide Polymorphisms within *mprF* in Methicillin-Resistant *Staphylococcus aureus* Clinical Isolates and Their Role in Cross-Resistance to Daptomycin and Host Defense Antimicrobial Peptides. *Antimicrob Agents Chemother,* 59**,** 4930-7.

Beavers, W. N. & Skaar, E. P. 2016. Neutrophil-generated oxidative stress and protein damage in *Staphylococcus aureus*. *Pathog Dis,* 74.

Berg, T., Firth, N., Apisiridej, S., Hettiaratchi, A., Leelaporn, A. & Skurray, R. A. 1998. Complete nucleotide sequence of pSK41: evolution of staphylococcal conjugative multiresistance plasmids. *J Bacteriol,* 180**,** 4350-9.

Bigger, J. W. 1944. Treatment of staphylococcal infections with penicillin by intermittent sterilisation. *Lancet,* 244**,** 497-500.

Bischoff, M., Entenza, J. M. & Giachino, P. 2001. Influence of a functional *sigB* operon on the global regulators *sar* and *agr* in *Staphylococcus aureus*. *J Bacteriol,* 183**,** 5171-9.

Blower, I., Tong, C., Sun, X., Murray, E., Luckett, J., Chan, W., Williams, P. & Hill, P. 2020. Gaussia Luciferase as a reporter for Quorum Sensing in *Staphylococcus aureus*. *Sensors,* 20, 4305.

Bojer, M. S., Lindemose, S., Vestergaard, M. & Ingmer, H. 2018. Quorum Sensing-Regulated Phenol-Soluble Modulins Limit Persister Cell Populations in *Staphylococcus aureus*. *Front Microbiol,* 9**,** 255.

Boles, B. R. & Horswill, A. R. 2008. Agr-mediated dispersal of *Staphylococcus aureus* biofilms. *PLoS Pathog,* 4**,** e1000052.

Boles, B. R., Thoendel, M., Roth, A. J. & Horswill, A. R. 2010. Identification of genes involved in polysaccharide-independent *Staphylococcus aureus* biofilm formation. *PLoS One,* 5**,** e10146.

Bonesvoll, P. 1977. Oral pharmacology of chlorhexidine. *J Clin Periodontol,* 4**,** 49-65.

Boyle-Vavra, S. & Daum, R. S. 2016. *Molecular Strategies of Staphylococcus aureus for Resisting Antibiotics,* U.K., Caister Academic Press.

Brauner, A., Fridman, O., Gefen, O. & Balaban, N. Q. 2016. Distinguishing between resistance, tolerance and persistence to antibiotic treatment. *Nat Rev Microbiol,* 14**,** 320-30.

Bridier, A., Briandet, R., Thomas, V. & Dubois-Brissonnet, F. 2011. Resistance of bacterial biofilms to disinfectants: a review. *Biofouling,* 27**,** 1017-32.

Brinster, S., Lamberet, G., Staels, B., Trieu-Cuot, P., Gruss, A. & Poyart, C. 2009. Type II fatty acid synthesis is not a suitable antibiotic target for Gram-positive pathogens. *Nature,* 458**,** 83-6.

Britt, N. S., Patel, N., Shireman, T. I., El Atrouni, W. I., Horvat, R. T. & Steed, M. E. 2017. Relationship between vancomycin tolerance and clinical outcomes in *Staphylococcus aureus* bacteraemia. *J Antimicrob Chemother,* 72**,** 535-542.

Brittain, B. 2004. MRSA control: a simple approach using triclosan antiseptic wash. *Australian Infection Control,* 9**,** 70-72.

Brooks, J. L. & Jefferson, K. K. 2014. Phase variation of poly-N-acetylglucosamine expression in *Staphylococcus aureus*. *PLoS Pathog,* 10**,** e1004292.

Cafiso, V., Bertuccio, T., Spina, D., Purrello, S., Campanile, F., Di Pietro, C., Purrello, M. & Stefani, S. 2012. Modulating activity of vancomycin and daptomycin on the expression of autolysis cell-wall turnover and membrane charge genes in hVISA and VISA strains. *PLoS One,* 7**,** e29573.

Calafat, A. M., Ye, X., Wong, L. Y., Reidy, J. A. & Needham, L. L. 2008. Urinary concentrations of triclosan in the U.S. population: 2003-2004. *Environ Health Perspect,* 116**,** 303-7.

Capita, R., Fernandez-Perez, S., Buzon-Duran, L. & Alonso-Calleja, C. 2019. Effect of Sodium Hypochlorite and Benzalkonium Chloride on the Structural Parameters of the Biofilms Formed by Ten *Salmonella enterica* Serotypes. *Pathogens,* 8.

Cerca, N., Brooks, J. L. & Jefferson, K. K. 2008. Regulation of the Intercellular Adhesin Locus Regulator (*icaR*) by SarA, SigB, and IcaR in *Staphylococcus aureus. J Bacteriol,* 190, 6530-6533.

Cerca, N., Jefferson, K. K., Oliveira, R., Pier, G. B. & Azeredo, J. 2006. Comparative antibody-mediated phagocytosis of *Staphylococcus epidermidis* cells grown in a biofilm or in the planktonic state. *Infect Immun,* 74**,** 4849-55.

Chan, P. F., Foster, S. J., Ingham, E. & Clements, M. O. 1998. The *Staphylococcus aureus* alternative sigma factor sigmaB controls the environmental stress response but not starvation survival or pathogenicity in a mouse abscess model. *J Bacteriol,* 180**,** 6082-9.

Cheng, A. G., DeDent, A. C., Schneewind, O. & Missiakas, D. 2011. A play in four acts: *Staphylococcus aureus* abscess formation. *Trends Microbiol,* 19**,** 225-32.

Cheung, A. L., Nishina, K. & Manna, A. C. 2008. SarA of *Staphylococcus aureus* binds to the *sarA* promoter to regulate gene expression. *J Bacteriol,* 190**,** 2239-43.

Cheung, G. Y., Wang, R., Khan, B. A., Sturdevant, D. E. & Otto, M. 2011. Role of the accessory gene regulator *agr* in community-associated methicillin-resistant *Staphylococcus aureus* pathogenesis. *Infect Immun,* 79**,** 1927-35.

Chiba, A., Sugimoto, S., Sato, F., Hori, S. & Mizunoe, Y. 2015. A refined technique for extraction of extracellular matrices from bacterial biofilms and its applicability. *Microb Biotechnol,* 8**,** 392-403.

Chinag, Y., Huang, K. Y., Tong, S. & Xu, H. W. 2016. Stringent Response Triggered by Valine-Induced Amino Acid Starvation Does Not Increase Antibiotic Tolerance in *Escherichia coli* Cultures Grown at Low Cell Density. *J Exp Microbiol Immunol,* 20.

Chong, Y. P., Moon, S. M., Bang, K. M., Park, H. J., Park, S. Y., Kim, M. N., Park, K. H., Kim, S. H., Lee, S. O., Choi, S. H., Jeong, J. Y., Woo, J. H. & Kim, Y. S. 2013. Treatment duration for uncomplicated *Staphylococcus aureus* bacteremia to prevent relapse: analysis of a prospective observational cohort study. *Antimicrob Agents Chemother,* 57**,** 1150-6.

Christensen, E. G., Gram, L. & Kastbjerg, V. G. 2011. Sublethal triclosan exposure decreases susceptibility to gentamicin and other aminoglycosides in *Listeria monocytogenes*. *Antimicrob Agents Chemother,* 55**,** 4064-71.

Chua, S. L., Yam, J. K., Hao, P., Adav, S. S., Salido, M. M., Liu, Y., Givskov, M., Sze, S. K., Tolker-Nielsen, T. & Yang, L. 2016. Selective labelling and eradication of antibiotic-tolerant bacterial populations in *Pseudomonas aeruginosa* biofilms. *Nat Commun,* 7**,** 10750.

Cogan, N. G., Rath, H., Kommerein, N., Stumpp, S. N. & Stiesch, M. 2016. Theoretical and experimental evidence for eliminating persister bacteria by manipulating killing timing. *FEMS Microbiol Lett,* 363.

Coleman, D., Knights, J., Russell, R., Shanley, D., Birkbeck, T. H., Dougan, G. & Charles, I. 1991. Insertional inactivation of the *Staphylococcus aureus* beta-toxin by bacteriophage phi 13 occurs by site- and orientation-specific integration of the phi 13 genome. *Mol Microbiol,* 5**,** 933-9.

Conlon, B. P., Nakayasu, E. S., Fleck, L. E., LaFleur, M. D., Isabella, V. M., Coleman, K., Leonard, S. N., Smith, R. D., Adkins, J. N. & Lewis, K. 2013. Activated ClpP kills persisters and eradicates a chronic biofilm infection. *Nature,* 503**,** 365-70.

Corrigan, R. M., Bellows, L. E., Wood, A. & Grundling, A. 2016. ppGpp negatively impacts ribosome assembly affecting growth and antimicrobial tolerance in Gram-positive bacteria. *Proc Natl Acad Sci U S A,* 113**,** E1710-9.

Costa, S. S., Viveiros, M., Amaral, L. & Couto, I. 2013. Multidrug Efflux Pumps in *Staphylococcus aureus*: an Update. *Open Microbiol J,* 7**,** 59-71.

Couto, I., Costa, S. S., Viveiros, M., Martins, M. & Amaral, L. 2008. Efflux-mediated response of *Staphylococcus aureus* exposed to ethidium bromide. *J Antimicrob Chemother,* 62**,** 504-13.

Cui, L., Ma, X., Sato, K., Okuma, K., Tenover, F. C., Mamizuka, E. M., Gemmell, C. G., Kim, M. N., Ploy, M. C., El-Solh, N., Ferraz, V. & Hiramatsu, K. 2003. Cell wall thickening is a common feature of vancomycin resistance in *Staphylococcus aureus*. *J Clin Microbiol,* 41**,** 5-14.

Dastgheyb, S. S. & Otto, M. 2015. Staphylococcal adaptation to diverse physiologic niches: an overview of transcriptomic and phenotypic changes in different biological environments. *Future Microbiol,* 10**,** 1981-95.

Date, S. V., Modrusan, Z., Lawrence, M., Morisaki, J. H., Toy, K., Shah, I. M., Kim, J., Park, S., Xu, M., Basuino, L., Chan, L., Zeitschel, D., Chambers, H. F., Tan, M. W., Brown, E. J., Diep, B. A. & Hazenbos, W. L. 2014. Global gene expression of methicillin-resistant *Staphylococcus aureus* USA300 during human and mouse infection. *J Infect Dis,* 209**,** 1542-50.

de Vor, L., Rooijakkers, S. H. M. & van Strijp, J. A. G. 2020. Staphylococci evade the innate immune response by disarming neutrophils and forming biofilms. *FEBS Lett,* 594**,** 2556-2569.

Defraine, V., Fauvart, M. & Michiels, J. 2018. Fighting bacterial persistence: Current and emerging anti-persister strategies and therapeutics. *Drug Resist Updat,* 38**,** 12-26.

DeLeon, S., Clinton, A., Fowler, H., Everett, J., Horswill, A. R. & Rumbaugh, K. P. 2014. Synergistic interactions of *Pseudomonas aeruginosa* and *Staphylococcus aureus* in an *in vitro* wound model. *Infect Immun,* 82**,** 4718-28.

D'Espine, M., Bellido, F., Pechere, J. C., Auckenthaler, R., Rohner, P., Lew, D. & Hirschel, B. 1989. Serum Levels of Ciprofloxacin after Single Oral Doses in Patients with Septicemia *Eur J Clin Microbiol Infect Dis***,** 1019-1023

Dietrich, L. E., Price-Whelan, A., Petersen, A., Whiteley, M. & Newman, D. K. 2006. The phenazine pyocyanin is a terminal signalling factor in the quorum sensing network of *Pseudomonas aeruginosa*. *Mol Microbiol,* 61**,** 1308-21.

Diggle, S. P., Matthijs, S., Wright, V. J., Fletcher, M. P., Chhabra, S. R., Lamont, I. L., Kong, X., Hider, R. C., Cornelis, P., Camara, M. & Williams, P. 2007. The *Pseudomonas aeruginosa* 4-quinolone signal molecules HHQ and PQS play multifunctional roles in quorum sensing and iron entrapment. *Chem Biol,* 14**,** 87-96.

Dinwiddie, M. T., Terry, P. D. & Chen, J. 2014. Recent evidence regarding triclosan and cancer risk. *Int J Environ Res Public Health,* 11**,** 2209-17.

Do, T., Schaefer, K., Santiago, A. G., Coe, K. A., Fernandes, P. B., Kahne, D., Pinho, M. G. & Walker, S. 2020. *Staphylococcus aureus* cell growth and division are regulated by an amidase that trims peptides from uncrosslinked peptidoglycan. *Nat Microbiol,* 5**,** 291-303.

Doherty, N., Holden, M. T., Qazi, S. N., Williams, P. & Winzer, K. 2006. Functional analysis of *luxS* in *Staphylococcus aureus* reveals a role in metabolism but not quorum sensing. *J Bacteriol,* 188**,** 2885-97.

Donne, J. & Dewilde, S. 2015. The Challenging World of Biofilm Physiology. *Adv Microb Physiol,* 67**,** 235-92.

Dotto, C., Lombarte Serrat, A., Cattelan, N., Barbagelata, M. S., Yantorno, O. M., Sordelli, D. O., Ehling-Schulz, M., Grunert, T. & Buzzola, F. R. 2017. The Active Component of Aspirin, Salicylic Acid, Promotes *Staphylococcus aureus* Biofilm Formation in a PIA-dependent Manner. *Front Microbiol,* 8**,** 4.

Douthit, C., Gudenkauf, B., Hamood, A., Mudaliar, N., Caroom, C. & Jenkins, M. 2020. Effects of powdered rifampin and vancomycin solutions on biofilm production of *Staphylococcus aureus* on orthopedic implants. *J Clin Orthop Trauma,* 11**,** S113-S117.

Dunman, P. M., Murphy, E., Haney, S., Palacios, D., Tucker-Kellogg, G., Wu, S., Brown, E. L., Zagursky, R. J., Shlaes, D. & Projan, S. J. 2001. Transcription profiling-based identification of *Staphylococcus aureus* genes regulated by the *agr* and/or *sarA* loci. *J Bacteriol,* 183**,** 7341-53.

Etter, D., Corti, S., Spirig, S., Cernela, N., Stephan, R. & Johler, S. 2020. *Staphylococcus aureus* Population Structure and Genomic Profiles in Asymptomatic Carriers in Switzerland. *Front Microbiol,* 11**,** 1289.

Fan, X., Liu, Y., Smith, D., Konermann, L., Siu, K. W. M. & Golemi-Kotra, D. 2007. Diversity of penicillin-binding proteins. Resistance factor FmtA of *Staphylococcus aureus. J Biol Chem*, 282, 35143-52.

Farrell, D. J., Castanheira, M. & Chopra, I. 2011. Characterization of global patterns and the genetics of fusidic acid resistance. *Clin Infect Dis,* 52 Suppl 7**,** S487-92.

Fazli, M., Bjarnsholt, T., Kirketerp-Moller, K., Jorgensen, B., Andersen, A. S., Krogfelt, K. A., Givskov, M. & Tolker-Nielsen, T. 2009. Nonrandom distribution of *Pseudomonas aeruginosa* and *Staphylococcus aureus* in chronic wounds. *J Clin Microbiol,* 47**,** 4084-9.

Ferullo, D. J. & Lovett, S. T. 2008. The stringent response and cell cycle arrest in *Escherichia coli*. *PLoS Genet,* 4**,** e1000300.

Fitzpatrick, F., Humphreys, H. & O'Gara, J. P. 2005. The genetics of staphylococcal biofilm formation--will a greater understanding of pathogenesis lead to better management of device-related infection? *Clin Microbiol Infect,* 11**,** 967-73.

Flannagan, R. S., Kuiack, R. C., McGavin, M. J. & Heinrichs, D. E. 2018. *Staphylococcus aureus* Uses the GraXRS Regulatory System To Sense and Adapt to the Acidified Phagolysosome in Macrophages. *mBio,* 9.

Flemming, H. C., Wingender, J., Szewzyk, U., Steinberg, P., Rice, S. A. & Kjelleberg, S. 2016. Biofilms: an emergent form of bacterial life. *Nat Rev Microbiol,* 14**,** 563-75.

Floyd, J. L., Smith, K. P., Kumar, S. H., Floyd, J. T. & Varela, M. F. 2010. LmrS is a multidrug efflux pump of the major facilitator superfamily from *Staphylococcus aureus*. *Antimicrob Agents Chemother,* 54**,** 5406-12.

Forbes, S., Morgan, N., Humphreys, G. J., Amezquita, A., Mistry, H. & McBain, A. J. 2019. Loss of Function in *Escherichia coli* Exposed to Environmentally Relevant Concentrations of Benzalkonium Chloride. *Appl Environ Microbiol,* 85.

Foster, P. L. 2007. Stress-induced mutagenesis in bacteria. *Crit Rev Biochem Mol Biol,* 42**,** 373-97.

Foulston, L., Elsholz, A. K., DeFrancesco, A. S. & Losick, R. 2014. The extracellular matrix of *Staphylococcus aureus* biofilms comprises cytoplasmic proteins that associate with the cell surface in response to decreasing pH. *mBio,* 5**,** e01667-14.

Fowler, V. G., Jr., Olsen, M. K., Corey, G. R., Woods, C. W., Cabell, C. H., Reller, L. B., Cheng, A. C., Dudley, T. & Oddone, E. Z. 2003. Clinical identifiers of complicated *Staphylococcus aureus* bacteremia. *Arch Intern Med,* 163**,** 2066-72.

Frank, K. L., Reichert, E. J., Piper, K. E. & Patel, R. 2007. *In vitro* effects of antimicrobial agents on planktonic and biofilm forms of *Staphylococcus lugdunensis* clinical isolates. *Antimicrob Agents Chemother,* 51**,** 888-95.

Fredheim, E. G., Granslo, H. N., Flaegstad, T., Figenschau, Y., Rohde, H., Sadovskaya, I., Mollnes, T. E. & Klingenberg, C. 2011. *Staphylococcus epidermidis* polysaccharide intercellular adhesin activates complement. *FEMS Immunol Med Microbiol,* 63**,** 269-80.

Freidlin, J., Acharya, N., Lietman, T. M., Cevallos, V., Whitcher, J. P. & Margolis, T. P. 2007. Spectrum of eye disease caused by methicillin-resistant *Staphylococcus aureus*. *Am J Ophthalmol,* 144**,** 313-5.

Fu, Z., Liu, Y., Chen, C., Guo, Y., Ma, Y., Yang, Y., Hu, F., Xu, X. & Wang, M. 2016. Characterization of Fosfomycin Resistance Gene, *fosB*, in Methicillin-Resistant *Staphylococcus aureus* Isolates. *PLoS One,* 11**,** e0154829.

Fux, C. A., Costerton, J. W., Stewart, P. S. & Stoodley, P. 2005. Survival strategies of infectious biofilms. *Trends Microbiol,* 13**,** 34-40.

Gadea, R., Fernandez Fuentes, M. A., Perez Pulido, R., Galvez, A. & Ortega, E. 2017. Effects of exposure to quaternary-ammonium-based biocides on antimicrobial susceptibility and tolerance to physical stresses in bacteria from organic foods. *Food Microbiol,* 63**,** 58-71.

Gardete, S. & Tomasz, A. 2014. Mechanisms of vancomycin resistance in *Staphylococcus aureus*. *J Clin Invest,* 124**,** 2836-40.

Garey, K. W., Vo, Q. P., Lewis, R. E., Saengcharoen, W., LaRocco, M. T. & Tam, V. H. 2009. Increased bacterial adherence and biomass in *Pseudomonas aeruginosa* bacteria exposed to clarithromycin. *Diagn Microbiol Infect Dis,* 63**,** 81-6.

Garneau-Tsodikova, S. & Labby, K. J. 2016. Mechanisms of Resistance to Aminoglycoside Antibiotics: Overview and Perspectives. *Medchemcomm,* 7**,** 11-27.

Geiger, T., Francois, P., Liebeke, M., Fraunholz, M., Goerke, C., Krismer, B., Schrenzel, J., Lalk, M. & Wolz, C. 2012. The stringent response of *Staphylococcus aureus* and its impact on survival after phagocytosis through the induction of intracellular PSMs expression. *PLoS Pathog,* 8**,** e1003016.

Geiger, T., Goerke, C., Fritz, M., Schafer, T., Ohlsen, K., Liebeke, M., Lalk, M. & Wolz, C. 2010. Role of the (p)ppGpp synthase RSH, a RelA/SpoT homolog, in stringent response and virulence of *Staphylococcus aureus*. *Infect Immun,* 78**,** 1873-83.

Geiger, T., Kastle, B., Gratani, F. L., Goerke, C. & Wolz, C. 2014. Two small (p)ppGpp synthases in *Staphylococcus aureus* mediate tolerance against cell envelope stress conditions. *J Bacteriol,* 196**,** 894-902.

Geiger, T. & Wolz, C. 2014. Intersection of the stringent response and the CodY regulon in low GC Gram-positive bacteria. *Int J Med Microbiol,* 304**,** 150-5.

George, S., Leasure, A. R. & Horstmanshof, D. 2016. Effectiveness of Decolonization With Chlorhexidine and Mupirocin in Reducing Surgical Site Infections: A Systematic Review. *Dimens Crit Care Nurs,* 35**,** 204-22.

George, S. E., Hrubesch, J., Breuing, I., Vetter, N., Korn, N., Hennemann, K., Bleul, L., Willmann, M., Ebner, P., Gotz, F. & Wolz, C. 2019. Oxidative stress drives the selection of quorum sensing mutants in the *Staphylococcus aureus* population. *Proc Natl Acad Sci U S A,* 116**,** 19145-19154.

Gratani, F. L., Horvatek, P., Geiger, T., Borisova, M., Mayer, C., Grin, I., Wagner, S., Steinchen, W., Bange, G., Velic, A., Macek, B. & Wolz, C. 2018. Regulation of the opposing (p)ppGpp synthetase and hydrolase activities in a bifunctional RelA/SpoT homologue from *Staphylococcus aureus*. *PLoS Genet,* 14**,** e1007514.

Gross, M., Cramton, S. E., Gotz, F. & Peschel, A. 2001. Key role of teichoic acid net charge in *Staphylococcus aureus* colonization of artificial surfaces. *Infect Immun,* 69**,** 3423-6.

Gudapuri, L. 2017. Cross-Resistance between Antiseptic Agents and Antimicrobial Agents. *Journal of Epidemiology and Infectious Diseases,* 1.

Guo, Y., Song, G., Sun, M., Wang, J. & Wang, Y. 2020. Prevalence and Therapies of Antibiotic-Resistance in *Staphylococcus aureus*. *Front Cell Infect Microbiol,* 10**,** 107.

Gutierrez, A., Jain, S., Bhargava, P., Hamblin, M., Lobritz, M. A. & Collins, J. J. 2017. Understanding and Sensitizing Density-Dependent Persistence to Quinolone Antibiotics. *Mol Cell,* 68**,** 1147-1154 e3.

Haaber, J., Penades, J. R. & Ingmer, H. 2017. Transfer of Antibiotic Resistance in *Staphylococcus aureus*. *Trends Microbiol,* 25**,** 893-905.

Haddadin, R. N., Saleh, S., Al-Adham, I. S., Buultjens, T. E. & Collier, P. J. 2010. The effect of subminimal inhibitory concentrations of antibiotics on virulence factors expressed by *Staphylococcus aureus* biofilms. *J Appl Microbiol,* 108**,** 1281-91.

Hall-Stoodley, L., Costerton, J. W. & Stoodley, P. 2004. Bacterial biofilms: from the natural environment to infectious diseases. *Nat Rev Microbiol,* 2**,** 95-108.

Hampele, I. C., D'Arcy, A., Dale, G. E., Kostrewa, D., Nielsen, J., Oefner, C., Page, M. G., Schonfeld, H. J., Stuber, D. & Then, R. L. 1997. Structure and function of the dihydropteroate synthase from *Staphylococcus aureus*. *J Mol Biol,* 268**,** 21-30.

Heath, R. J., Rubin, J. R., Holland, D. R., Zhang, E., Snow, M. E. & Rock, C. O. 1999. Mechanism of Triclosan Inhibition of Bacterial Fatty Acid Synthesis. *Journal of Biological Chemistry,* 246**,** 11110-11114.

Hennig, T. J., Werner, S., Naujox, K. & Arndt, A. 2017. Chlorhexidine is not an essential component in alcohol-based surgical hand preparation: a comparative study of two handrubs based on a modified EN 12791 test protocol. *Antimicrob Resist Infect Control,* 6**,** 96.

Herbert, S., Ziebandt, A. K., Ohlsen, K., Schafer, T., Hecker, M., Albrecht, D., Novick, R. & Gotz, F. 2010. Repair of global regulators in *Staphylococcus aureus* 8325 and comparative analysis with other clinical isolates. *Infect Immun,* 78**,** 2877-89.

Heydorn, A., Nielsen, A. T., Hentzer, M., Sternberg, C., Givskov, M., Ersboll, B. K. & Molin, S. 2000. Quantification of biofilm structures by the novel computer program COMSTAT. *Microbiology,* 146 ( Pt 10)**,** 2395-407.

Hibbard, J. S. 2005. Analyses comparing the antimicrobial activity and safety of current antiseptic agents: a review. *J Infus Nurs,* 28**,** 194-207.

Hiramatsu, K., Hanaki, H., Ino, T., Yabuta, K., Oguri, T. & Tenover, F. C. 1997. Methicillin-resistant *Staphylococcus aureus* clinical strain with reduced vancomycin susceptibility. *J Antimicrob Chemother,* 40**,** 135-6.

Hiramatsu, K., Katayama, Y., Matsuo, M., Sasaki, T., Morimoto, Y., Sekiguchi, A. & Baba, T. 2014. Multi-drug-resistant *Staphylococcus aureus* and future chemotherapy. *J Infect Chemother,* 20**,** 593-601.

Hobbs, J. K. & Boraston, A. B. 2019. (p)ppGpp and the Stringent Response: An Emerging Threat to Antibiotic Therapy. *ACS Infect Dis,* 5**,** 1505-1517.

Hoiby, N., Bjarnsholt, T., Givskov, M., Molin, S. & Ciofu, O. 2010. Antibiotic resistance of bacterial biofilms. *Int J Antimicrob Agents,* 35**,** 322-32.

Holloway, B. W., Krishnapillai, V. & Morgan, A. F. 1979. Chromosomal genetics of *Pseudomonas*. *Microbiol Rev,* 43**,** 73-102.

Horsburgh, M. J., Aish, J. L., White, I. J., Shaw, L., Lithgow, J. K. & Foster, S. J. 2002. sigmaB modulates virulence determinant expression and stress resistance: characterization of a functional *rsbU* strain derived from *Staphylococcus aureus* 8325-4. *J Bacteriol,* 184**,** 5457-67.

Horvatek, P., Hanna, A. M. F., Gratani, F. L., Keinhörster, D., Korn, N. & Borisova, M. 2020. Inducible expression of (pp)pGpp synthetases in *Staphylococcus aureus* is associated with activation of stress response genes. *biorxiv*.

Hsu, C. Y., Lin, M. H., Chen, C. C., Chien, S. C., Cheng, Y. H., Su, I. N. & Shu, J. C. 2011. Vancomycin promotes the bacterial autolysis, release of extracellular DNA, and biofilm formation in vancomycin-non-susceptible *Staphylococcus aureus*. *FEMS Immunol Med Microbiol,* 63**,** 236-47.

Huemer, M., Mairpady, S. S., Bergada-Pijuan, J., Söderholm, S., Boumasmoud, M., Vulin, C., Gómez-Mejia, A., Antelo Varela, M., Tripathi, V., Götschi, S., Marques, M. E., Hasse, B., Brugger, S., Bumann, D., Schuepbach, R. & Zinkernagel, A. 2021. Molecular reprogramming and phenotype switching in *Staphylococcus aureus* lead to high antibiotic persistence and affect therapy success. *Proc Natl Acad Sci*, 118(7),

Humphreys, H. 2012. *Staphylococcus aureus*: the enduring pathogen in surgery. *Surgeon,* 10**,** 357-60.

Iandolo, J. J., Worrell, V., Groicher, K. H., Qian, Y., Tian, R., Kenton, S., Dorman, A., Ji, H., Lin, S., Loh, P., Qi, S., Zhu, H. & Roe, B. A. 2002. Comparative analysis of the genomes of the temperate bacteriophages phi 11, phi 12 and phi 13 of *Staphylococcus aureus* 8325. *Gene,* 289**,** 109-18.

Ibberson, C. B. & Whiteley, M. 2019. The *Staphylococcus aureus* Transcriptome during Cystic Fibrosis Lung Infection. *mBio,* 10.

Ichimiya, T., Takeoka, K., Hiramatsu, K., Hirai, K., Yamasaki, T. & Nasu, M. 1996. The influence of azithromycin on the biofilm formation of *Pseudomonas aeruginosa in vitro*. *Chemotherapy,* 42**,** 186-91.

Irving, S. E. & Corrigan, R. M. 2018. Triggering the stringent response: signals responsible for activating (p)ppGpp synthesis in bacteria. *Microbiology (Reading),* 164**,** 268-276.

Ito, H., Yoshida, H., Bogaki-Shonai, M., Niga, T., Hattori, H. & Nakamura, S. 1994. Quinolone resistance mutations in the DNA gyrase *gyrA* and *gyrB* genes of *Staphylococcus aureus*. *Antimicrob Agents Chemother,* 38**,** 2014-23.

Jenul, C. & Horswill, A. R. 2019. Regulation of *Staphylococcus aureus* Virulence. *Microbiol Spectr,* 7.

Ji, J., Kan, S., Lee, J. & Lysakowski, S. 2013. Antibiotic Tolerance in *Escherichia coli* Under Stringent

Response Correlates to Increased Catalase Activity. *J Exp Microbiol Immunol,* 17**,** 40-45.

Jin, Y., Guo, Y., Zhan, Q., Shang, Y., Qu, D. & Yu, F. 2020. Subinhibitory Concentrations of Mupirocin Stimulate *Staphylococcus aureus* Biofilm Formation by Upregulating cidA. *Antimicrob Agents Chemother,* 64.

Joers, A., Kaldalu, N. & Tenson, T. 2010. The frequency of persisters in *Escherichia coli* reflects the kinetics of awakening from dormancy. *J Bacteriol,* 192**,** 3379-84.

Johnsson, J., Seeberg, S. & Kjellmer, I. 1987. Blood concentrations of chlorhexidine in neonates undergoing routine cord care with 4% chlorhexidine gluconate solution. *Acta Paediatr Scand,* 76**,** 675-6.

Jones, E. M., Cochrane, C. A. & Percival, S. L. 2015. The Effect of pH on the Extracellular Matrix and Biofilms. *Adv Wound Care (New Rochelle),* 4**,** 431-439.

Jordana-Lluch, E., Garcia, V., Kingdon, A. D. H., Singh, N., Alexander, C., Williams, P. & Hardie, K. R. 2020. A Simple Polymicrobial Biofilm Keratinocyte Colonization Model for Exploring Interactions Between Commensals, Pathogens and Antimicrobials. *Front Microbiol,* 11**,** 291.

Kaatz, G. W., Seo, S. M. & Ruble, C. A. 1993. Efflux-mediated fluoroquinolone resistance in *Staphylococcus aureus*. *Antimicrob Agents Chemother,* 37**,** 1086-94.

Kampf, G. 2018. Biocidal Agents Used for Disinfection Can Enhance Antibiotic Resistance in Gram-Negative Species. *Antibiotics (Basel),* 7.

Kaplan, J. B. 2011. Antibiotic-induced biofilm formation. *Int J Artif Organs,* 34**,** 737-51.

Kaplan, J. B., Jabbouri, S. & Sadovskaya, I. 2011. Extracellular DNA-dependent biofilm formation by *Staphylococcus epidermidis* RP62A in response to subminimal inhibitory concentrations of antibiotics. *Res Microbiol,* 162**,** 535-41.

Kaplan, J. B., LoVetri, K., Cardona, S. T., Madhyastha, S., Sadovskaya, I., Jabbouri, S. & Izano, E. A. 2012. Recombinant human DNase I decreases biofilm and increases antimicrobial susceptibility in staphylococci. *J Antibiot (Tokyo),* 65**,** 73-7.

Kara, D., Luppens, S. B. & Cate, J. M. 2006. Differences between single- and dual-species biofilms of *Streptococcus mutans* and *Veillonella parvula* in growth, acidogenicity and susceptibility to chlorhexidine. *Eur J Oral Sci,* 114**,** 58-63.

Karavolos, M. H., Horsburgh, M. J., Ingham, E. & Foster, S. J. 2003. Role and regulation of the superoxide dismutases of *Staphylococcus aureus*. *Microbiology (Reading),* 149**,** 2749-2758.

Katayama, Y., Ito, T. & Hiramatsu, K. 2000. A new class of genetic element, staphylococcus cassette chromosome mec, encodes methicillin resistance in *Staphylococcus aureus*. *Antimicrob Agents Chemother,* 44**,** 1549-55.

Kato, F., Kadomoto, N., Iwamoto, Y., Bunai, K., Komatsuzawa, H. & Sugai, M. 2011. Regulatory mechanism for exfoliative toxin production in *Staphylococcus aureus*. *Infect Immun,* 79**,** 1660-70.

Kavanagh, N., Ryan, E. J., Widaa, A., Sexton, G., Fennell, J., O'Rourke, S., Cahill, K. C., Kearney, C. J., O'Brien, F. J. & Kerrigan, S. W. 2018. Staphylococcal Osteomyelitis: Disease Progression, Treatment Challenges, and Future Directions. *Clin Microbiol Rev,* 31.

Kavanaugh, J. S. & Horswill, A. R. 2016. Impact of Environmental Cues on Staphylococcal Quorum Sensing and Biofilm Development. *J Biol Chem,* 291**,** 12556-64.

Kean, R., Rajendran, R., Haggarty, J., Townsend, E. M., Short, B., Burgess, K. E., Lang, S., Millington, O., Mackay, W. G., Williams, C. & Ramage, G. 2017. *Candida albicans* Mycofilms Support *Staphylococcus aureus* Colonization and Enhances Miconazole Resistance in Dual-Species Interactions. *Front Microbiol,* 8**,** 258.

Kehrenberg, C., Schwarz, S., Jacobsen, L., Hansen, L. H. & Vester, B. 2005. A new mechanism for chloramphenicol, florfenicol and clindamycin resistance: methylation of 23S ribosomal RNA at A2503. *Mol Microbiol,* 57**,** 1064-73.

Kennedy, C. A. & O'Gara, J. P. 2004. Contribution of culture media and chemical properties of polystyrene tissue culture plates to biofilm development by *Staphylococcus aureus*. *J Med Microbiol,* 53**,** 1171-1173.

Kessler, E., Safrin, M., Olson, J. C. & Ohman, D. E. 1993. Secreted LasA of *Pseudomonas aeruginosa* is a staphylolytic protease. *J Biol Chem,* 268**,** 7503-8.

Kester, J. C. & Fortune, S. M. 2014. Persisters and beyond: mechanisms of phenotypic drug resistance and drug tolerance in bacteria. *Crit Rev Biochem Mol Biol,* 49**,** 91-101.

Khatib, R., Jose, J., Musta, A., Sharma, M., Fakih, M. G., Johnson, L. B., Riederer, K. & Shemes, S. 2011. Relevance of vancomycin-intermediate susceptibility and heteroresistance in methicillin-resistant *Staphylococcus aureus* bacteraemia. *J Antimicrob Chemother,* 66**,** 1594-9.

Kim, C., Mwangi, M., Chung, M., Milheirico, C., de Lencastre, H. & Tomasz, A. 2013. The mechanism of heterogeneous beta-lactam resistance in MRSA: key role of the stringent stress response. *PLoS One,* 8**,** e82814.

Kim, W., Zhu, W., Hendricks, G. L., Van Tyne, D., Steele, A. D., Keohane, C. E., Fricke, N., Conery, A. L., Shen, S., Pan, W., Lee, K., Rajamuthiah, R., Fuchs, B. B., Vlahovska, P. M., Wuest, W. M., Gilmore, M. S., Gao, H., Ausubel, F. M. & Mylonakis, E. 2018. A new class of synthetic retinoid antibiotics effective against bacterial persisters. *Nature,* 556**,** 103-107.

Kirby, W. M. 1944. Extraction of a Highly Potent Penicillin Inactivator from Penicillin Resistant Staphylococci. *Science,* 99**,** 452-3.

Kirstein, J., Hoffmann, A., Lilie, H., Schmidt, R., Rubsamen-Waigmann, H., Brotz-Oesterhelt, H., Mogk, A. & Turgay, K. 2009. The antibiotic ADEP reprogrammes ClpP, switching it from a regulated to an uncontrolled protease. *EMBO Mol Med,* 1**,** 37-49.

Kjærvik, M., Schwibbert, K., Dietrich, P., Thissen, A. & Unger, W. E. S. 2018. Surface characterisation of *Escherichia coli* under various conditions by near-ambient pressure XPS. *Surface Interface and Analysis***,** 1-5.

Kluytmans, J., van Belkum, A. & Verbrugh, H. 1997. Nasal carriage of *Staphylococcus aureus*: epidemiology, underlying mechanisms, and associated risks. *Clin Microbiol Rev,* 10**,** 505-20.

Knobloch, J. K., Jager, S., Horstkotte, M. A., Rohde, H. & Mack, D. 2004. RsbU-dependent regulation of *Staphylococcus epidermidis* biofilm formation is mediated via the alternative sigma factor sigmaB by repression of the negative regulator gene *icaR*. *Infect Immun,* 72**,** 3838-48.

Komatsuzawa, H., Ohta, K., Labischinski, H., Sugai, M. & Suginaka, H. 1999. Characterization of *fmtA*, a gene that modulates the expression of methicillin resistance in *Staphylococcus aureus*. *Antimicrob Agents Chemother,* 43**,** 2121-5.

Kong, K. F., Vuong, C. & Otto, M. 2006. *Staphylococcus* quorum sensing in biofilm formation and infection. *Int J Med Microbiol,* 296**,** 133-9.

Konig, C., Schwank, S. & Blaser, J. 2001. Factors compromising antibiotic activity against biofilms of *Staphylococcus epidermidis*. *Eur J Clin Microbiol Infect Dis,* 20**,** 20-6.

Kourtis, A. P., Hatfield, K., Baggs, J., Mu, Y., See, I., Epson, E., Nadle, J., Kainer, M. A., Dumyati, G., Petit, S., Ray, S. M., Emerging Infections Program, M. a. g., Ham, D., Capers, C., Ewing, H., Coffin, N., McDonald, L. C., Jernigan, J. & Cardo, D. 2019. Vital Signs: Epidemiology and Recent Trends in Methicillin-Resistant and in Methicillin-Susceptible *Staphylococcus aureus* Bloodstream Infections - United States. *MMWR Morb Mortal Wkly Rep,* 68**,** 214-219.

Kuehl, R., Morata, L., Meylan, S., Mensa, J. & Soriano, A. 2020. When antibiotics fail: a clinical and microbiological perspective on antibiotic tolerance and persistence of *Staphylococcus aureus*. *J Antimicrob Chemother,* 75**,** 1071-1086.

Kullik, I., Giachino, P. & Fuchs, T. 1998. Deletion of the alternative sigma factor sigmaB in *Staphylococcus aureus* reveals its function as a global regulator of virulence genes. *J Bacteriol,* 180**,** 4814-20.

Kullik, I. I. & Giachino, P. 1997. The alternative sigma factor sigmaB in *Staphylococcus aureus*: regulation of the *sigB* operon in response to growth phase and heat shock. *Arch Microbiol,* 167**,** 151-9.

LaBreck, P. T., Bochi-Layec, A. C., Stanbro, J., Dabbah-Krancher, G., Simons, M. P. & Merrell, D. S. 2020. Systematic Analysis of Efflux Pump-Mediated Antiseptic Resistance in *Staphylococcus aureus* Suggests a Need for Greater Antiseptic Stewardship. *mSphere,* 5.

Lamp, K. C., Rybak, M. J., Bailey, E. M. & Kaatz, G. W. 1992. *In vitro* pharmacodynamic effects of concentration, pH, and growth phase on serum bactericidal activities of daptomycin and vancomycin. *Antimicrob Agents Chemother,* 36**,** 2709-14.

Langmead, B. & Salzberg, S. L. 2012. Fast gapped-read alignment with Bowtie 2. *Nat Methods,* 9**,** 357-9.

Larsen, J., Clasen, J., Hansen, J. E., Paulander, W., Petersen, A., Larsen, A. R. & Frees, D. 2016. Copresence of *tet(K)* and *tet(M)* in Livestock-Associated Methicillin-Resistant *Staphylococcus aureus* Clonal Complex 398 Is Associated with Increased Fitness during Exposure to Sublethal Concentrations of Tetracycline. *Antimicrob Agents Chemother,* 60**,** 4401-3.

Lauderdale, K. J., Boles, B. R., Cheung, A. L. & Horswill, A. R. 2009. Interconnections between Sigma B, *agr*, and proteolytic activity in

*Staphylococcus aureus* biofilm maturation. *Infect Immun,* 77**,** 1623-35.

Lawrence, J. R., Zhu, B., Swerhone, G. D., Topp, E., Roy, J., Wassenaar, L. I., Rema, T. & Korber, D. R. 2008. Community-level assessment of the effects of the broad-spectrum antimicrobial chlorhexidine on the outcome of river microbial biofilm development. *Appl Environ Microbiol,* 74**,** 3541-50.

Lebeaux, D., Ghigo, J. M. & Beloin, C. 2014. Biofilm-related infections: bridging the gap between clinical management and fundamental aspects of recalcitrance toward antibiotics. *Microbiol Mol Biol Rev,* 78**,** 510-43.

Lechner, S., Lewis, K. & Bertram, R. 2012. *Staphylococcus aureus* persisters tolerant to bactericidal antibiotics. *J Mol Microbiol Biotechnol,* 22**,** 235-44.

Levine, D. P. 2006. Vancomycin: a history. *Clin Infect Dis,* 42 Suppl 1**,** S5-12.

Levin-Reisman, I., Ronin, I., Gefen, O., Braniss, I., Shoresh, N. & Balaban, N. Q. 2017. Antibiotic tolerance facilitates the evolution of resistance. *Science,* 355**,** 826-830.

Lewis, K. 2001. Riddle of biofilm resistance. *Antimicrob Agents Chemother,* 45**,** 999-1007.

Lewis, K. 2005. Persister cells and the riddle of biofilm survival. *Biochemistry (Mosc),* 70**,** 267-74.

Limoli, D. H., Jones, C. J. & Wozniak, D. J. 2015. Bacterial Extracellular Polysaccharides in Biofilm Formation and Function. *Microbiol Spectr,* 3.

Lister, J. L. & Horswill, A. R. 2014. *Staphylococcus aureus* biofilms: recent developments in biofilm dispersal. *Front Cell Infect Microbiol,* 4**,** 178.

Liu, J., Yang, L., Hou, Y., Soteyome, T., Zeng, B., Su, J., Li, L., Li, B., Chen, D., Li, Y., Wu, A., Shirtliff, M. E., Harro, J. M., Xu, Z. & Peters, B. M. 2018. Transcriptomics Study on *Staphylococcus aureus* Biofilm Under Low Concentration of Ampicillin. *Front Microbiol,* 9**,** 2413.

Liu, K., Bittner, A. N. & Wang, J. D. 2015. Diversity in (p)ppGpp metabolism and effectors. *Curr Opin Microbiol,* 24**,** 72-9.

Loffler, B., Tuchscherr, L., Niemann, S. & Peters, G. 2014. *Staphylococcus aureus* persistence in non-professional phagocytes. *Int J Med Microbiol,* 304**,** 170-6.

Lowy, F. D. 1998. *Staphylococcus aureus* infections. *N Engl J Med,* 339**,** 520-32.

Lubarsky, H. V., Gerbersdorf, S. U., Hubas, C., Behrens, S., Ricciardi, F. & Paterson, D. M. 2012. Impairment of the bacterial biofilm stability by triclosan. *PLoS One,* 7**,** e31183.

Maayan-Metzger, A., Strauss, T., Rubin, C., Jaber, H., Dulitzky, M., Reiss-Mandel, A., Leshem, E., Rahav, G. & Regev-Yochay, G. 2017. Clinical evaluation of early acquisition of *Staphylococcus aureus* carriage by newborns. *Int J Infect Dis,* 64**,** 9-14.

MacIsaac, J. K., Gerona, R. R., Blanc, P. D., Apatira, L., Friesen, M. W., Coppolino, M. & Janssen, S. 2014. Health care worker exposures

to the antibacterial agent triclosan. *J Occup Environ Med,* 56**,** 834-9.

Madar, D., Dekel, E., Bren, A., Zimmer, A., Porat, Z. & Alon, U. 2013. Promoter activity dynamics in the lag phase of *Escherichia coli*. *BMC Syst Biol,* 7**,** 136.

Maillard, J. Y. 2005. Antimicrobial biocides in the healthcare environment: efficacy, usage, policies, and perceived problems. *Ther Clin Risk Manag,* 1**,** 307-20.

Majerczyk, C. D., Sadykov, M. R., Luong T. T., Lee C., Somerville, G. A., Sonenshain, A. L. 2008. *Staphylococcus aureus* CodY Negatively Regulates Virulence Gene Expression. *J. Bacteriol.,* 190**,** 2257-2265.

Malachowa, N. & DeLeo, F. R. 2011. *Staphylococcus aureus* survival in human blood. *Virulence,* 2**,** 567-9.

Manna, A. C., Bayer, M. G. & Cheung, A. L. 1998. Transcriptional analysis of different promoters in the *sar* locus in *Staphylococcus aureus*. *J Bacteriol,* 180**,** 3828-36.

Margolis, E. 2009. Hydrogen peroxide-mediated interference competition by *Streptococcus pneumoniae* has no significant effect on *Staphylococcus aureus* nasal colonization of neonatal rats. *J Bacteriol,* 191**,** 571-5.

Marraffini, L. A., Dedent, A. C. & Schneewind, O. 2006. Sortases and the art of anchoring proteins to the envelopes of gram-positive bacteria. *Microbiol Mol Biol Rev,* 70**,** 192-221.

Marrakchi, H., DeWolf, W. E., Quinn, C., West, J., Polizzi, B. J., So, C. Y., Holmes, D. J., Reed, S. L., Heath, R. J., Payne, D. J., Rock, C. O. & Wallis, N. G. 2003. Characterization of *Streptococcus pneumoniae* enoyl-(acyl-carrier protein) reductase (FabK). *Biochem J,* 370**,** 1055-1062.

McBain, A. J., Bartolo, R. G., Catrenich, C. E., Charbonneau, D., Ledder, R. G., Price, B. B. & Gilbert, P. 2003. Exposure of sink drain microcosms to triclosan: population dynamics and antimicrobial susceptibility. *Appl Environ Microbiol,* 69**,** 5433-42.

McClure, R., Balasubramanian, D., Sun, Y., Bobrovskyy, M., Sumby, P., Genco, C. A., Vanderpool, C. K. & Tjaden, B. 2013. Computational analysis of bacterial RNA-Seq data. *Nucleic Acids Res,* 41**,** e140.

McDermott, W. 1958. Microbial persistence. *Yale J Biol Med,* 30**,** 257-91.

McDougal, L. K., Steward, C. D., Killgore, G. E., Chaitram, J. M., McAllister, S. K. & Tenover, F. C. 2003. Pulsed-field gel electrophoresis typing of oxacillin-resistant *Staphylococcus aureus* isolates from the United States: establishing a national database. *J Clin Microbiol,* 41**,** 5113-20.

McGuinness, W. A., Malachowa, N. & DeLeo, F. R. 2017. Vancomycin Resistance in *Staphylococcus aureus*. *Yale J Biol Med,* 90**,** 269-281.

Meyer, B. & Cookson, B. 2010. Does microbial resistance or adaptation to biocides create a hazard in infection prevention and control? *J Hosp Infect,* 76**,** 200-5.

Mirani, Z. A. & Jamil, N. 2011. Effect of sub-lethal doses of vancomycin and oxacillin on biofilm formation by vancomycin intermediate resistant *Staphylococcus aureus*. *J Basic Microbiol,* 51**,** 191-5.

Mitchell, G., Seguin, D. L., Asselin, A. E., Deziel, E., Cantin, A. M., Frost, E. H., Michaud, S. & Malouin, F. 2010. *Staphylococcus aureus* sigma B-dependent emergence of small-colony variants and biofilm production following exposure to *Pseudomonas aeruginosa* 4-hydroxy-2-heptylquinoline-N-oxide. *BMC Microbiol,* 10**,** 33.

Moisan, H., Brouillette, E., Jacob, C. L., Langlois-Begin, P., Michaud, S. & Malouin, F. 2006. Transcription of virulence factors in *Staphylococcus aureus* small-colony variants isolated from cystic fibrosis patients is influenced by SigB. *J Bacteriol,* 188**,** 64-76.

Moldovan, A. & Fraunholz, M. J. 2019. In or out: Phagosomal escape of *Staphylococcus aureus*. *Cell Microbiol,* 21**,** e12997.

Monteiro, R., Hebraud, M., Chafsey, I., Chambon, C., Viala, D., Torres, C., Poeta, P. & Igrejas, G. 2015. Surfaceome and exoproteome of a clinical sequence type 398 methicillin resistant *Staphylococcus aureus* strain. *Biochem Biophys Rep,* 3**,** 7-13.

Moore, M. R., Perdreau-Remington, F. & Chambers, H. F. 2003. Vancomycin treatment failure associated with heterogeneous vancomycin-intermediate *Staphylococcus aureus* in a patient with endocarditis and in the rabbit model of endocarditis. *Antimicrob Agents Chemother,* 47**,** 1262-6.

Moormeier, D. E. & Bayles, K. W. 2017. *Staphylococcus aureus* biofilm: a complex developmental organism. *Mol Microbiol,* 104**,** 365-376.

Moormeier, D. E., Bose, J. L., Horswill, A. R. & Bayles, K. W. 2014. Temporal and stochastic control of *Staphylococcus aureus* biofilm development. *mBio,* 5**,** e01341-14.

Morikawa, K., Maruyama, A., Inose, Y., Higashide, M., Hayashi, H. & Ohta, T. 2001. Overexpression of sigma factor, sigma(B), urges *Staphylococcus aureus* to thicken the cell wall and to resist beta-lactams. *Biochem Biophys Res Commun,* 288**,** 385-9.

Morvan, C., Kenanian, G., Pathania, A., Anba-Mondoloni, J., Lamberet, G., Gruss, A., & Gloux, K. 2017. The *Staphylococcus aureus* FASII bypass escape route from FASII inhibitors. *Biochimie*. 141, 40-46.

My, L., Rekoske, B., Lemke, J. J., Viala, J. P., Gourse, R. L. & Bouveret, E. 2013. Transcription of the *Escherichia coli* fatty acid synthesis operon *fabHDG* is directly activated by FadR and inhibited by ppGpp. *J Bacteriol,* 195**,** 3784-95.

Nabb, D. L., Song, S., Kluthe, K. E., Daubert, T. A., Luedtke, B. E. & Nuxoll, A. S. 2019. Polymicrobial Interactions Induce Multidrug Tolerance in *Staphylococcus aureus* Through Energy Depletion. *Front Microbiol,* 10**,** 2803.

Nguyen, D., Joshi-Datar, A., Lepine, F., Bauerle, E., Olakanmi, O., Beer, K., McKay, G., Siehnel, R., Schafhauser, J., Wang, Y., Britigan, B. E. & Singh, P. K. 2011. Active starvation responses mediate antibiotic tolerance in biofilms and nutrient-limited bacteria. *Science,* 334**,** 982-6.

Nielsen, L. N., Larsen, M. H., Skovgaard, S., Kastbjerg, V., Westh, H., Gram, L. & Ingmer, H. 2013. *Staphylococcus aureus* but not *Listeria monocytogenes* adapt to triclosan and adaptation correlates with increased *fabI* expression and *agr* deficiency. *BMC Microbiol,* 13**,** 177.

Nouwen, J., Schouten, J., Schneebergen, P., Snijders, S., Maaskant, J., Koolen, M., van Belkum, A. & Verbrugh, H. A. 2006. *Staphylococcus aureus* carriage patterns and the risk of infections associated with continuous peritoneal dialysis. *J Clin Microbiol,* 44**,** 2233-6.

Novick, R. 1967. Properties of a cryptic high-frequency transducing phage in *Staphylococcus aureus*. *Virology,* 33**,** 155-66.

Novick, R. P., Projan, S. J., Kornblum, J., Ross, H. F., Ji, G., Kreiswirth, B., Vandenesch, F. & Moghazeh, S. 1995. The *agr* P2 operon: an autocatalytic sensory transduction system in *Staphylococcus aureus*. *Mol Gen Genet,* 248**,** 446-58.

Novick, R. P., Ross, H. F., Projan, S. J., Kornblum, J., Kreiswirth, B. & Moghazeh, S. 1993. Synthesis of staphylococcal virulence factors is controlled by a regulatory RNA molecule. *EMBO J,* 12**,** 3967-75.

O'Gara, J. P. 2007. *ica* and beyond: biofilm mechanisms and regulation in *Staphylococcus epidermidis* and *Staphylococcus aureus*. *FEMS Microbiol Lett,* 270**,** 179-88.

Orazi, G. & O'Toole, G. A. 2017. *Pseudomonas aeruginosa* Alters *Staphylococcus aureus* Sensitivity to Vancomycin in a Biofilm Model of Cystic Fibrosis Infection. *mBio,* 8.

Orazi, G., Ruoff, K. L. & O'Toole, G. A. 2019. *Pseudomonas aeruginosa* Increases the Sensitivity of Biofilm-Grown *Staphylococcus aureus* to Membrane-Targeting Antiseptics and Antibiotics. *mBio,* 10.

O'Toole, G., Kaplan, H. B. & Kolter, R. 2000. Biofilm formation as microbial development. *Annu Rev Microbiol,* 54**,** 49-79.

O'Toole, G. A. 2011. Microtiter dish biofilm formation assay. *J Vis Exp*.

Pabst, B., Pitts, B., Lauchnor, E. & Stewart, P. S. 2016. Gel-Entrapped *Staphylococcus aureus* Bacteria as Models of Biofilm Infection Exhibit Growth in Dense Aggregates, Oxygen Limitation, Antibiotic Tolerance, and Heterogeneous Gene Expression. *Antimicrob Agents Chemother,* 60**,** 6294-301.

Paget, M. S. & Helmann, J. D. 2003. The sigma70 family of sigma factors. *Genome Biol,* 4**,** 203.

Palmqvist, N., Foster, T., Tarkowski, A. & Josefsson, E. 2002. Protein A is a virulence factor in *Staphylococcus aureus* arthritis and septic death. *Microb Pathog,* 33**,** 239-49.

Parsons, J. B. & Rock, C. O. 2011. Is bacterial fatty acid synthesis a valid target for antibacterial drug discovery? *Curr Opin Microbiol,* 14**,** 544-9.

Paulander, W., Nissen Varming, A., Baek, K. T., Haaber, J., Frees, D. & Ingmer, H. 2013. Antibiotic-mediated selection of quorum-sensing-negative *Staphylococcus aureus*. *mBio,* 3**,** e00459-12.

Peleg, A. Y., Hogan, D. A. & Mylonakis, E. 2010. Medically important bacterial-fungal interactions. *Nat Rev Microbiol,* 8**,** 340-9.

Peleg, A. Y., Miyakis, S., Ward, D. V., Earl, A. M., Rubio, A., Cameron, D. R., Pillai, S., Moellering, R. C., Jr. & Eliopoulos, G. M. 2012. Whole genome characterization of the mechanisms of daptomycin resistance in clinical and laboratory derived isolates of *Staphylococcus aureus*. *PLoS One,* 7**,** e28316.

Pelz, A., Wieland, K. P., Putzbach, K., Hentschel, P., Albert, K. & Gotz, F. 2005. Structure and biosynthesis of staphyloxanthin from *Staphylococcus aureus*. *J Biol Chem,* 280**,** 32493-8.

Peng, H. L., Novick, R. P., Kreiswirth, B., Kornblum, J. & Schlievert, P. 1988. Cloning, characterization, and sequencing of an accessory gene regulator (*agr*) in *Staphylococcus aureus*. *J Bacteriol,* 170**,** 4365-72.

Pereira, B. & Tagkopoulos, I. 2019. Benzalkonium Chlorides: Uses, Regulatory Status, and Microbial Resistance. *Appl Environ Microbiol,* 85.

Periasamy, S., Joo, H. S., Duong, A. C., Bach, T. H., Tan, V. Y., Chatterjee, S. S., Cheung, G. Y. & Otto, M. 2012. How *Staphylococcus aureus* biofilms develop their characteristic structure. *Proc Natl Acad Sci U S A,* 109**,** 1281-6.

Peters, B. M., Jabra-Rizk, M. A., O'May, G. A., Costerton, J. W. & Shirtliff, M. E. 2012. Polymicrobial interactions: impact on pathogenesis and human disease. *Clin Microbiol Rev,* 25**,** 193-213.

Peyrusson, F., Varet, H., Nguyen, T. K., Legendre, R., Sismeiro, O., Coppee, J. Y., Wolz, C., Tenson, T. & Van Bambeke, F. 2020. Intracellular *Staphylococcus aureus* persisters upon antibiotic exposure. *Nat Commun,* 11**,** 2200.

Piroth, L., Que, Y. A., Widmer, E., Panchaud, A., Piu, S., Entenza, J. M. & Moreillon, P. 2008. The fibrinogen- and fibronectin-binding domains of *Staphylococcus aureus* fibronectin-binding protein A synergistically promote endothelial invasion and experimental endocarditis. *Infect Immun,* 76**,** 3824-31.

Pohl, K., Francois, P., Stenz, L., Schlink, F., Geiger, T., Herbert, S., Goerke, C., Schrenzel, J. & Wolz, C. 2009. CodY in *Staphylococcus aureus*: a regulatory link between metabolism and virulence gene expression. *J Bacteriol,* 191**,** 2953-63.

Pozzi, C., Waters, E. M., Rudkin, J. K., Schaeffer, C. R., Lohan, A. J., Tong, P., Loftus, B. J., Pier, G. B., Fey, P. D., Massey, R. C. & O'Gara, J. P. 2012. Methicillin resistance alters the biofilm phenotype and attenuates virulence in *Staphylococcus aureus* device-associated infections. *PLoS Pathog,* 8**,** e1002626.

Prax, M., Mechler, L., Weidenmaier, C. & Bertram, R. 2016. Glucose Augments Killing Efficiency of Daptomycin Challenged *Staphylococcus aureus* Persisters. *PLoS One,* 11**,** e0150907.

Priyadarshi, A., Kim, E. E. & Hwang, K. Y. 2010. Structural insights into *Staphylococcus aureus* enoyl-ACP reductase (FabI), incomplex with NADP and triclosan. *Proteins,* 78, 480-486.

Rachid, S., Ohlsen, K., Witte, W., Hacker, J. & Ziebuhr, W. 2000. Effect of subinhibitory antibiotic concentrations on polysaccharide intercellular adhesin expression in biofilm-forming *Staphylococcus epidermidis*. *Antimicrob Agents Chemother,* 44**,** 3357-63.

Rajashekaraiah, K. R., Rice, T., Rao, V. S., Marsh, D., Ramakrishna, B. & Kallick, C. A. 1980. Clinical significance of tolerant strains of *Staphylococcus aureus* in patients with endocarditis. *Ann Intern Med,* 93**,** 796-801.

Rajendram, M., Hurley, K. A., Foss, M. H., Thornton, K. M., Moore, J. T., Shaw, J. T. & Weibel, D. B. 2014. Gyramides prevent bacterial growth by inhibiting DNA gyrase and altering chromosome topology. *ACS Chem Biol,* 9**,** 1312-9.

Rani, S. A., Pitts, B., Beyenal, H., Veluchamy, R. A., Lewandowski, Z., Davison, W. M., Buckingham-Meyer, K. & Stewart, P. S. 2007. Spatial patterns of DNA replication, protein synthesis, and oxygen concentration within bacterial biofilms reveal diverse physiological states. *J Bacteriol,* 189**,** 4223-33.

Reiss, S., Pane-Farre, J., Fuchs, S., Francois, P., Liebeke, M., Schrenzel, J., Lindequist, U., Lalk, M., Wolz, C., Hecker, M. & Engelmann, S. 2012. Global analysis of the *Staphylococcus aureus* response to mupirocin. *Antimicrob Agents Chemother,* 56**,** 787-804.

Reyes, D., Andrey, D. O., Monod, A., Kelley, W. L., Zhang, G. & Cheung, A. L. 2011. Coordinated regulation by AgrA, SarA, and SarR to control agr expression in *Staphylococcus aureus*. *J Bacteriol,* 193**,** 6020-31.

Rice, K. C., Nelson, J. B., Patton, T. G., Yang, S. J. & Bayles, K. W. 2005. Acetic acid induces expression of the *Staphylococcus aureus cidABC* and *lrgAB* murein hydrolase regulator operons. *J Bacteriol,* 187**,** 813-21.

Riordan, J. T., Dupre, J. M., Cantore-Matyi, S. A., Kumar-Singh, A., Song, Y., Zaman, S., Horan, S., Helal, N. S., Nagarajan, V., Elasri, M. O., Wilkinson, B. J. & Gustafson, J. E. 2011. Alterations in the transcriptome and antibiotic susceptibility of *Staphylococcus aureus* grown in the presence of diclofenac. *Ann Clin Microbiol Antimicrob,* 10**,** 30.

Roberts, M. C. 2008. Update on macrolide-lincosamide-streptogramin, ketolide, and oxazolidinone resistance genes. *FEMS Microbiol Lett,* 282**,** 147-59.

Rolo, J., Worning, P., Boye Nielsen, J., Sobral, R., Bowden, R., Bouchami, O., Damborg, P., Guardabassi, L., Perreten, V., Westh, H., Tomasz, A., de Lencastre, H. & Miragaia, M. 2017. Evidence for the evolutionary steps leading to *mecA*-mediated beta-lactam resistance in *Staphylococci*. *PLoS Genet,* 13**,** e1006674.

Russell, A. D. 2003. Biocide use and antibiotic resistance: the relevance of laboratory findings to clinical and environmental situations. *Lancet Infect Dis,* 3**,** 794-803.

Rymer, R. U., Solorio, F. A., Tehranchi, A. K., Chu, C., Corn, J. E., Keck, J. L., Wang, J. D. & Berger, J. M. 2012. Binding mechanism of metalNTP substrates and stringent-response alarmones to bacterial DnaG-type primases. *Structure,* 20**,** 1478-89.

Sadowski, M. C., Pouwer, H. R., Gunter, J. H., Lubik, A. A., Quinn, R. J. & Nelson, C. C. 2014. The fatty acid synthase inhibitor triclosan:

repurposing an antimicrobial agent for targeting prostate cancer. *Oncotraget,* 5**,** 9362-9381.

Sakr, A., Bregeon, F., Mege, J. L., Rolain, J. M. & Blin, O. 2018. *Staphylococcus aureus* Nasal Colonization: An Update on Mechanisms, Epidemiology, Risk Factors, and Subsequent Infections. *Front Microbiol,* 9**,** 2419.

Salzer, A., Keinhorster, D., Kastle, C., Kastle, B. & Wolz, C. 2020. Small Alarmone Synthetases RelP and RelQ of *Staphylococcus aureus* Are Involved in Biofilm Formation and Maintenance Under Cell Wall Stress Conditions. *Front Microbiol,* 11**,** 575882.

Sanchez-Vizuete, P., Orgaz, B., Aymerich, S., Le Coq, D. & Briandet, R. 2015. Pathogens protection against the action of disinfectants in multispecies biofilms. *Front Microbiol,* 6**,** 705.

Schadow, K. H., Simpson, W. A. & Christensen, G. D. 1988. Characteristics of adherence to plastic tissue culture plates of coagulase-negative staphylococci exposed to subinhibitory concentrations of antimicrobial agents. *J Infect Dis,* 157**,** 71-7.

Scheibel, J., Chang, A., Lu, H., Baxter, B. V., Tonge, P. J. & Kisker, C. 2012. *Staphylococcus aureus* FabI: Inhibition, Substrate Recognition and Potential Implications for *In Vivo* essentiality. *Structure*, 20, 802-813.

Schilcher, K., Andreoni, F., Dengler Haunreiter, V., Seidl, K., Hasse, B. & Zinkernagel, A. S. 2016. Modulation of *Staphylococcus aureus* Biofilm Matrix by Subinhibitory Concentrations of Clindamycin. *Antimicrob Agents Chemother,* 60**,** 5957-67.

Schommer, N. N., Christner, M., Hentschke, M., Ruckdeschel, K., Aepfelbacher, M. & Rohde, H. 2011. *Staphylococcus epidermidis* uses distinct mechanisms of biofilm formation to interfere with phagocytosis and activation of mouse macrophage-like cells 774A.1. *Infect Immun,* 79**,** 2267-76.

Schwarz, S., Kehrenberg, C., Doublet, B. & Cloeckaert, A. 2004. Molecular basis of bacterial resistance to chloramphenicol and florfenicol. *FEMS Microbiol Rev,* 28**,** 519-42.

Schweizer, H. P. 2001. Triclosan: a widely used biocide and its link to antibiotics. *FEMS Microbiol Lett,* 202**,** 1-7.

Sewlikar, S., Pillai, R., Mahajan, N. & Desai, A. 2015. Triclosan coated sutures: an overview of safety and efficacy in reducing risk of surgical site infection. *International Surgery Journal,* 2**,** 1.

Shan, Y., Brown Gandt, A., Rowe, S. E., Deisinger, J. P., Conlon, B. P. & Lewis, K. 2017. ATP-Dependent Persister Formation in *Escherichia coli*. *mBio,* 8.

Siezen, R. J., Wilson, G. & Todt, T. 2010. Prokaryotic whole-transcriptome analysis: deep sequencing and tiling arrays. *Microb Biotechnol,* 3**,** 125-30.

Singh, R., Ray, P., Das, A. & Sharma, M. 2010. Penetration of antibiotics through *Staphylococcus aureus* and *Staphylococcus epidermidis* biofilms. *J Antimicrob Chemother,* 65**,** 1955-8.

Singha, P., Locklin, J. & Handa, H. 2017. A review of the recent advances in antimicrobial coatings for urinary catheters. *Acta Biomater,* 50**,** 20-40.

Skogman, M. E., Vuorela, P. M. & Fallarero, A. 2016. A Platform of Anti-biofilm Assays Suited to the Exploration of Natural Compound Libraries. *J Vis Exp*.

Slany, M., Oppelt, J. & Cincarova, L. 2017. Formation of *Staphylococcus aureus* Biofilm in the Presence of Sublethal Concentrations of Disinfectants Studied via a Transcriptomic Analysis Using Transcriptome Sequencing (RNA-seq). *Appl Environ Microbiol,* 83.

Song, Y., Liu, C. I., Lin, F. Y., No, J. H., Hensler, M., Liu, Y. L., Jeng, W. Y., Low, J., Liu, G. Y., Nizet, V., Wang, A. H. & Oldfield, E. 2009. Inhibition of staphyloxanthin virulence factor biosynthesis in *Staphylococcus aureus: in vitro, in vivo*, and crystallographic results. *J Med Chem,* 52**,** 3869-80.

Souli, M. & Giamarellou, H. 1998. Effects of slime produced by clinical isolates of coagulase-negative *staphylococci* on activities of various antimicrobial agents. *Antimicrob Agents Chemother,* 42**,** 939-41.

Spaan, A. N., Surewaard, B. G., Nijland, R. & van Strijp, J. A. 2013. Neutrophils versus *Staphylococcus aureus*: a biological tug of war. *Annu Rev Microbiol,* 67**,** 629-50.

Speziale, P., Pietrocola, G., Foster, T. J. & Geoghegan, J. A. 2014. Protein-based biofilm matrices in *Staphylococci*. *Front Cell Infect Microbiol,* 4**,** 171.

Speziale, P., Pietrocola, G., Rindi, S., Provenzano, M., Provenza, G., Di Poto, A., Visai, L. & Arciola, C. R. 2009. Structural and functional role of *Staphylococcus aureus* surface components recognizing adhesive matrix molecules of the host. *Future Microbiol,* 4**,** 1337-52.

Stark, R., Grzelak, M. & Hadfield, J. 2019. RNA sequencing: the teenage years. *Nat Rev Genet,* 20**,** 631-656.

Stewart, P. S. 2015. Antimicrobial Tolerance in Biofilms. *Microbiol Spectr,* 3.

Strugeon, E., Tilloy, V., Ploy, M. C. & Da Re, S. 2016. The Stringent Response Promotes Antibiotic Resistance Dissemination by Regulating Integron Integrase Expression in Biofilms. *mBio,* 7.

Subrt, N., Mesak, L. R. & Davies, J. 2011. Modulation of virulence gene expression by cell wall active antibiotics in *Staphylococcus aureus*. *J Antimicrob Chemother,* 66**,** 979-84.

Supa-Amornkul, S., Mongkolsuk, P., Summpunn, P., Chaiyakunvat, P., Navaratdusit, W., Jiarpinitnun, C. & Chaturongakul, S. 2019. Alternative Sigma Factor B in Bovine Mastitis-Causing *Staphylococcus aureus*: Characterization of Its Role in Biofilm Formation, Resistance to Hydrogen Peroxide Stress, Regulon Members. *Front Microbiol,* 10**,** 2493.

Tabak, M., Scher, K., Hartog, E., Romling, U., Matthews, K. R., Chikindas, M. L. & Yaron, S. 2007. Effect of triclosan on *Salmonella typhimurium* at different growth stages and in biofilms. *FEMS Microbiol Lett,* 267**,** 200-6.

Tan, L., Li, S. R., Jiang, B., Hu, X. M. & Li, S. 2018. Therapeutic Targeting of the *Staphylococcus aureus* Accessory Gene Regulator (*agr*) System. *Front Microbiol,* 9**,** 55.

Tenover, F. C., McDougal, L. K., Goering, R. V., Killgore, G., Projan, S. J., Patel, J. B. & Dunman, P. M. 2006. Characterization of a strain of community-associated methicillin-resistant *Staphylococcus aureus* widely disseminated in the United States. *J Clin Microbiol,* 44**,** 108-18.

Thoendel, M. & Horswill, A. R. 2010. Biosynthesis of peptide signals in gram-positive bacteria. *Adv Appl Microbiol,* 71**,** 91-112.

Thoendel, M., Kavanaugh, J. S., Flack, C. E. & Horswill, A. R. 2011. Peptide signaling in the *Staphylococci. Chem Rev,* 111**,** 117-51.

Thomas, C. M., Hothersall, J., Willis, C. L. & Simpson, T. J. 2010. Resistance to and synthesis of the antibiotic mupirocin. *Nat Rev Microbiol,* 8**,** 281-9.

Thwaites, G. E. & Gant, V. 2011. Are bloodstream leukocytes Trojan Horses for the metastasis of *Staphylococcus aureus*? *Nat Rev Microbiol,* 9**,** 215-22.

Tong, S. Y., Davis, J. S., Eichenberger, E., Holland, T. L. & Fowler, V. G., Jr. 2015. *Staphylococcus aureus* infections: epidemiology, pathophysiology, clinical manifestations, and management. *Clin Microbiol Rev,* 28**,** 603-61.

Tranchemontagne, Z. R., Camire, R. B., O'Donnell, V. J., Baugh, J. & Burkholder, K. M. 2016. *Staphylococcus aureus* Strain USA300 Perturbs Acquisition of Lysosomal Enzymes and Requires Phagosomal Acidification for Survival inside Macrophages. *Infect Immun,* 84**,** 241-53.

Trapnell, C., Williams, B. A., Pertea, G., Mortazavi, A., Kwan, G., van Baren, M. J., Salzberg, S. L., Wold, B. J. & Pachter, L. 2010. Transcript assembly and quantification by RNA-Seq reveals unannotated transcripts and isoform switching during cell differentiation. *Nat Biotechnol,* 28**,** 511-5.

Truong-Bolduc, Q. C., Bolduc, G. R., Medeiros, H., Vyas, J. M., Wang, Y. & Hooper, D. C. 2015. Role of the Tet38 Efflux Pump in *Staphylococcus aureus* Internalization and Survival in Epithelial Cells. *Infect Immun,* 83**,** 4362-72.

Truong-Bolduc, Q. C., Strahilevitz, J. & Hooper, D. C. 2006. NorC, a new efflux pump regulated by MgrA of *Staphylococcus aureus*. *Antimicrob Agents Chemother,* 50**,** 1104-7.

Tuchscherr, L., Bischoff, M., Lattar, S. M., Noto Llana, M., Pfortner, H., Niemann, S., Geraci, J., Van de Vyver, H., Fraunholz, M. J., Cheung, A. L., Herrmann, M., Volker, U., Sordelli, D. O., Peters, G. & Loffler, B. 2015. Sigma Factor SigB Is Crucial to Mediate *Staphylococcus aureus* Adaptation during Chronic Infections. *PLoS Pathog,* 11**,** e1004870.

Tuchscherr, L., Loffler, B. & Proctor, R. A. 2020. Persistence of *Staphylococcus aureus*: Multiple Metabolic Pathways Impact the Expression of Virulence Factors in Small-Colony Variants (SCVs). *Front Microbiol,* 11**,** 1028.

Tuchscherr, L., Medina, E., Hussain, M., Volker, W., Heitmann, V., Niemann, S., Holzinger, D., Roth, J., Proctor, R. A., Becker, K., Peters, G. & Loffler, B. 2011. *Staphylococcus aureus* phenotype switching: an effective bacterial strategy to escape host immune response and establish a chronic infection. *EMBO Mol Med,* 3**,** 129-41.

van der Veen, S. & Abee, T. 2011. Mixed species biofilms of *Listeria monocytogenes* and *Lactobacillus plantarum* show enhanced resistance to benzalkonium chloride and peracetic acid. *Int J Food Microbiol,* 144**,** 421-31.

van Hal, S. J., Jensen, S. O., Vaska, V. L., Espedido, B. A., Paterson, D. L. & Gosbell, I. B. 2012. Predictors of mortality in *Staphylococcus aureus* Bacteremia. *Clin Microbiol Rev,* 25**,** 362-86.

van Wamel, W. J., Rooijakkers, S. H., Ruyken, M., van Kessel, K. P. & van Strijp, J. A. 2006. The innate immune modulators staphylococcal complement inhibitor and chemotaxis inhibitory protein of *Staphylococcus aureus* are located on beta-hemolysin-converting bacteriophages. *J Bacteriol,* 188**,** 1310-5.

Vazquez, V., Liang, X., Horndahl, J. K., Ganesh, V. K., Smeds, E., Foster, T. J. & Hook, M. 2011. Fibrinogen is a ligand for the *Staphylococcus aureus* microbial surface components recognizing adhesive matrix molecules (MSCRAMM) bone sialoprotein-binding protein (Bbp). *J Biol Chem,* 286**,** 29797-805.

Vestergaard, M., Frees, D. & Ingmer, H. 2019. Antibiotic Resistance and the MRSA Problem. *Microbiol Spectr,* 7.

Vulin, C., Leimer, N., Huemer, M., Ackermann, M. & Zinkernagel, A. S. 2018. Prolonged bacterial lag time results in small colony variants that represent a sub-population of persisters. *Nat Commun,* 9**,** 4074.

Vuong, C., Kocianova, S., Voyich, J. M., Yao, Y., Fischer, E. R., DeLeo, F. R. & Otto, M. 2004. A crucial role for exopolysaccharide modification in bacterial biofilm formation, immune evasion, and virulence. *J Biol Chem,* 279**,** 54881-6.

Wagner, C., Sauermann, R. & Joukhadar, C. 2006. Principles of antibiotic penetration into abscess fluid. *Pharmacology,* 78**,** 1-10.

Wagner, T., Soong, G., Sokol, S., Saiman, L. & Prince, A. 2005. Effects of azithromycin on clinical isolates of *Pseudomonas aeruginosa* from cystic fibrosis patients. *Chest,* 128**,** 912-9.

Wang, C. F. & Tian, Y. 2015. Reproductive endocrine-disrupting effects of triclosan: Population exposure, present evidence and potential mechanisms. *Environ Pollut,* 206**,** 195-201.

Wang, Q., Sun, F. J., Liu, Y., Xiong, L. R., Xie, L. L. & Xia, P. Y. 2010. Enhancement of biofilm formation by subinhibitory concentrations of macrolides in *icaADBC*-positive and -negative clinical isolates of *Staphylococcus epidermidis*. *Antimicrob Agents Chemother,* 54**,** 2707-11.

Wang, R., Braughton, K. R., Kretschmer, D., Bach, T. H., Queck, S. Y., Li, M., Kennedy, A. D., Dorward, D. W., Klebanoff, S. J., Peschel, A., DeLeo, F. R. & Otto, M. 2007. Identification of novel cytolytic

peptides as key virulence determinants for community-associated MRSA. *Nat Med,* 13**,** 1510-4.

Wang, Y., Bojer, M. S., George, S. E., Wang, Z., Jensen, P. R., Wolz, C. & Ingmer, H. 2018. Inactivation of TCA cycle enhances *Staphylococcus aureus* persister cell formation in stationary phase. *Sci Rep,* 8**,** 10849.

Wardenburg, J., Patel, R. J. & Schneewind, O. 2007. Surface proteins and exotoxins are required for the pathogenesis of *Staphylococcus aureus* pneumonia. *Infect Immun,* 75**,** 1040-4.

Weatherly, L. M. & Gosse, J. A. 2017. Triclosan exposure, transformation, and human health effects. *J Toxicol Environ Health B Crit Rev,* 20**,** 447-469.

Weigel, L. M., Clewell, D. B., Gill, S. R., Clark, N. C., McDougal, L. K., Flannagan, S. E., Kolonay, J. F., Shetty, J., Killgore, G. E. & Tenover, F. C. 2003. Genetic analysis of a high-level vancomycin-resistant isolate of *Staphylococcus aureus*. *Science,* 302**,** 1569-71.

Weinrick, B., Dunman, P. M., McAleese, F., Murphy, E., Projan, S. J., Fang, Y. & Novick, R. P. 2004. Effect of mild acid on gene expression in *Staphylococcus aureus*. *J Bacteriol,* 186**,** 8407-23.

Welsh, K. J., Skrobarcek, K. A., Abbott, A. N., Lewis, C. T., Kruzel, M. C., Lewis, E. M., Gardiner, J. M., Mohr, J. F., Armitige, L. Y. & Wanger, A. 2011. Predictors of relapse of methicillin-resistant *Staphylococcus aureus* bacteremia after treatment with vancomycin. *J Clin Microbiol,* 49**,** 3669-72.

Wertheim, H. F., Melles, D. C., Vos, M. C., van Leeuwen, W., van Belkum, A., Verbrugh, H. A. & Nouwen, J. L. 2005. The role of nasal carriage in *Staphylococcus aureus* infections. *Lancet Infect Dis,* 5**,** 751-62.

Westfall, C., Flores-Mireles, A. L., Robinson, J. I., Lynch, A. J. L., Hultgren, S., Henderson, J. P. & Levin, P. A. 2019. The Widely Used Antimicrobial Triclosan Induces High Levels of Antibiotic Tolerance *In Vitro* and Reduces Antibiotic Efficacy up to 100-Fold *In Vivo*. *Antimicrob Agents Chemother,* 63.

Wichelhaus, T. A., Boddinghaus, B., Besier, S., Schafer, V., Brade, V. & Ludwig, A. 2002. Biological cost of rifampin resistance from the perspective of *Staphylococcus aureus*. *Antimicrob Agents Chemother,* 46**,** 3381-5.

Wijesinghe, G., Dilhari, A., Gayani, B., Kottegoda, N., Samaranayake, L. & Weerasekera, M. 2019. Influence of Laboratory Culture Media on *in vitro* Growth, Adhesion, and Biofilm Formation of *Pseudomonas aeruginosa* and *Staphylococcus aureus*. *Med Princ Pract,* 28**,** 28-35.

Windels, E. M., Michiels, J. E., Van den Bergh, B., Fauvart, M. & Michiels, J. 2019. Antibiotics: Combatting Tolerance To Stop Resistance. *mBio,* 10.

Wolcott, R. D., Rhoads, D. D., Bennett, M. E., Wolcott, B. M., Gogokhia, L., Costerton, J. W. & Dowd, S. E. 2010. Chronic wounds and the medical biofilm paradigm. *J Wound Care,* 19**,** 45-6, 48-50, 52-3.

Wolz, C., Geiger, T. & Goerke, C. 2010. The synthesis and function of the alarmone (p)ppGpp in *Firmicutes*. *Int J Med Microbiol,* 300**,** 142-7.

Woods, P. W., Haynes, Z. M., Mina, E. G. & Marques, C. N. H. 2018. Maintenance of *S. aureus* in Co-culture With *P. aeruginosa* While Growing as Biofilms. *Front Microbiol,* 9**,** 3291.

Xu, T., Wang, X. Y., Cui, P., Zhang, Y. M., Zhang, W. H. & Zhang, Y. 2017. The Agr Quorum Sensing System Represses Persister Formation through Regulation of Phenol Soluble Modulins in *Staphylococcus aureus*. *Front Microbiol,* 8**,** 2189.

Yamada, Y., Hideka, K., Shiota, S., Kuroda, T. & Tsuchiya, T. 2006. Gene cloning and characterization of SdrM, a chromosomally-encoded multidrug efflux pump, from *Staphylococcus aureus*. *Biol Pharm Bull,* 29**,** 554-6.

Yao, J. & Rock, C. O. 2015. How bacterial pathogens eat host lipids: implications for the development of fatty acid synthesis therapeutics. *J Biol Chem,* 290**,** 5940-6.

Yarwood, J. M., Bartels, D. J., Volper, E. M. & Greenberg, E. P. 2004. Quorum sensing in *Staphylococcus aureus* biofilms. *J Bacteriol,* 186**,** 1838-50.

Yoder-Himes, D. R., Chain, P. S., Zhu, Y., Wurtzel, O., Rubin, E. M., Tiedje, J. M. & Sorek, R. 2009. Mapping the *Burkholderia cenocepacia* niche response via high-throughput sequencing. *Proc Natl Acad Sci U S A,* 106**,** 3976-81.

Yoshikai, H., Kizaki, H., Saito, Y., Omae, Y., Sekimizu, K. & Kaito, C. 2016. Multidrug-Resistance Transporter AbcA Secretes *Staphylococcus aureus* Cytolytic Toxins. *J Infect Dis,* 213**,** 295-304.

Zahir, T., Camacho, R., Vitale, R., Ruckebusch, C., Hofkens, J., Fauvart, M. & Michiels, J. 2019. High-throughput time-resolved morphology screening in bacteria reveals phenotypic responses to antibiotics. *Commun Biol,* 2**,** 269.

Zalis, E. A., Nuxoll, A. S., Manuse, S., Clair, G., Radlinski, L. C., Conlon, B. P., Adkins, J. & Lewis, K. 2019. Stochastic Variation in Expression of the Tricarboxylic Acid Cycle Produces Persister Cells. *mBio,* 10.

Zhao, X., Liu, Z., Liu, Z., Meng, R., Shi, C., Chen, X., Bu, X. & Guo, N. 2018. Phenotype and RNA-seq-Based transcriptome profiling of *Staphylococcus aureus* biofilms in response to tea tree oil. *Microb Pathog,* 123**,** 304-313.

Zimmerli, W., Trampuz, A. & Ochsner, P. E. 2004. Prosthetic-joint infections. *N Engl J Med,* 351**,** 1645-54.

# 8. Appendix

## 8.1 Supplementary data

**Supplementary table 1. Fold changes and hypothesised roles of additional selected genes from RNA-Seq data of triclosan treated *S. aureus*, ns = not significant.**

| Gene | Significant $log_2$ fold change in PT vs PU | Significant $log_2$ fold change in BFT vs BFU | Potential impact on triclosan exposed *S. aureus* |
|---|---|---|---|
| **Genes associated with stress tolerance** | | | |
| ***bstA*** | -1.34 | 3.34 | Acid tolerance. Salt tolerance. Detoxification of $H_2O_2$ and antimicrobials fosfomycin, rifamycin S, cerulenin (Perera et al., 2014). |
| ***lexA, recA*** | -0.77; ns | -1.41; ns | Induction of SOS response. Downregulation suggests reduced SOS response induction (Cirz et al., 2006) |
| ***vraR-vraS* TCS** | -0.46; -0.16 | -1.70; -1.07 | Control of cell wall stress stimulon and tolerance to β-lactams (Yin, Daum and Boyle-Vavra, 2006) |
| ***dnaK*** | 1.73 | 1.82 | Induction of heat shock (Anderson et al., 2006; Fleury et al., 2009) |
| ***groEL*** | 3.14 | 3.10 | |
| ***groES*** | 3.34 | 3.32 | |
| ***grpE*** | 2.30 | 1.26 | |
| ***clpB*** | 1.68 | ns | |
| **Cold shock protein *cspB*** | 3.17 | 2.24 | Induction of cold shock (Anderson et al., 2006) |
| **Urease** | | | Acid tolerance (Zhou et al., 2019) |
| ***ureA*** | 3.31 | 5.08 | |
| ***ureB*** | 2.22 | 6.65 | |
| ***ureC*** | 2.28 | 5.48 | |
| ***ureD*** | ns | 3.96 | |
| ***ureE*** | ns | 4.06 | |
| ***ureF*** | ns | 4.34 | |
| ***ureG*** | ns | 3.82 | |
| **GTPase *era*** | -0.94 | 1.15 | Less GTP results in less rRNA gene transcription (Corrigan et al., 2016) |

| | | | |
|---|---|---|---|
| **Genes associated with translation** | | | Stringent response mediated. Downregulation results in reduced translation (Geiger et al., 2010; Peyrusson et al., 2020) |
| ***pth*** | ns | -1.97 | |
| ***rplA*** | -0.94 | 1.22 | |
| ***rplM*** | ns | -0.71 | |
| ***rplGB*** | ns | -1.98 | |
| **Genes associated with amino acid biosynthesis** | | | Altered amino acid synthesis profile (Peyrusson et al., 2020), varies depending on amino acid. |
| ***ilvB*** | 1.68 | -1.17 | |
| ***gltB*** | 2.88 | ns | |
| ***thrC*** | 0.79 | -1.44 | |
| ***lysS*** | -0.69 | 0.72 | |
| ***serS*** | -2.67 | -4.48 | |
| ***leuS*** | ns | 2.02 | |
| ***lac* operon** | | | Increased lactose metabolism (Rosey, Oskouian and Stewart, 1991) in biofilms, reduced in planktonic culture. |
| ***lacA*** | ns | 4.06 | |
| ***lacB*** | -1.08 | 3.18 | |
| ***lacC*** | -1.1 | 4.12 | |
| ***lacD*** | -1.63 | 3.68 | |
| ***lacE*** | -1.69 | 3.88 | |
| ***lacF*** | -2.04 | 3.51 | |
| ***lacG*** | ns | 3.38 | |
| **Global regulator** | | | Upregulation leads to activation of *cap* genes, efflux pumps, and surface protein expression (Truong-Bolduc et al., 2005; Gupta et al., 2013; Crosby et al., 2016). |
| ***mgrA*** | -0.71 | ns | |
| **Genes associated with antibiotic targets** | | | |
| **DNA topoisomerase IV *parC*** | ns | 1.13 | Upregulation may increase tolerance to fluoroquinolones (Cirz et al., 2006). |
| ***fabI*** | -1.36 | ns | Involved in FASII. Drug target of triclosan (Fan et al., 2002). |
| ***fabF*** | ns | 1.99 | Involved in FASII. Targeted by platencin, platensimycin, thiolactomycin and cerulenin (Parsons et al., 2015). |
| **Genes associated with virulence** | | | |
| ***capA*** | 1.86 | ns | Capsular polysaccharide biosynthesis genes. Roles in Complement inactivation, |
| ***capB*** | 1.9 | 1.1 | |
| ***capC*** | 2.1 | 1.7 | |
| ***capD*** | 2 | 3 | |
| ***capE*** | 1.7 | 3.4 | |
| ***capF*** | 1.5 | 3.5 | |

| | | | |
|---|---|---|---|
| ***capG*** | 3 | 3.4 | opsonin cloaking (van Wamel et al., 2002). |
| ***capH*** | 2.1 | 3.4 | |
| ***capI*** | 1.8 | 3.4 | |
| ***capJ*** | 1.8 | 4 | |
| ***capK*** | 1.8 | 4 | |
| ***capL*** | 1.2 | 3.6 | |
| ***capM*** | 2.1 | 3.1 | |
| ***capN*** | 1.5 | 2.7 | |
| ***capO*** | 1.4 | 2.4 | |
| ***capP*** | ns | 1.7 | |
| ***saeR-saeS*** | -0.9, ns | -3.7, -3.57 | Virulence regulator controlling toxin and MSCRAMM genes (Voyich et al., 2009; Mainiero et al., 2010). |
| ***arlR-arlS*** | 1.24, ns | 1.35, 2.24 | Negatively regulates the *agr* system (Fournier, Klier, Rapoport, 2001), sugar uptake genes (Liang et al., 2005), and genes associated with autolysis (Fournier and Hooper, 2000). |
| **Clumping factor A *clfA*** | 0.81 | 1.24 | Platelet adhesion, complement inactivation, opsonin cloaking (Bischoff et al., 2004; Entenza et al., 2005). |
| **Fibronecting binding protein A *fnbA*** | 1.76 | 1.69 | Adhesins for fibrinogen, fibronectin and elastin (Bischoff et al., 2004; Entenza et al., 2005). |
| **Protein A *spa*** | -2.01 | -4.07 | Degradation of antibodies, complement inactivation (Sasso, Silverman and Mannik, 1989). |
| **Chemotaxis inhibitory protein *chp*** | 2.37 | -3.7 | Inhibit neutrophil chemotaxis (Thammavongsa et al., 2015). |
| **Extracellular adherence protein *eap*** | 0.75 | -4.29 | MHC-II analog protein; adhesion to *S. aureus* cells and host cells; involved in biofilm formation |

| | | | |
|---|---|---|---|
| | | | (Eisenbeis et al., 2018). |
| **Aureolysin *aur*** | ns | -1.58 | Metalloprotease; complement inactivation (Laarman et al., 2011). |
| **Staphylokinase *sak*** | -0.82 | -1.75 | Plasminogen activator, complement inactivation, degradation of antibodies (Malachowa and DeLeo, 2011). |
| **α-haemolysin *hla*** | ns | -7.19 | Cytolytic pore-forming toxin (Wardenburg and Schneewind, 2008; Wilke and Wardenburg, 2010). |
| **Exfoliative toxin A *eta*** | -2.06 | -5.28 | Exotoxin with superantigen activity (Fraser and Proft, 2008). |
| **Leukocidin G, leucocidin H *lukG, lukH*** | -0.74, ns | -4.69, -6.09 | Leukocidins; kill leukocytes (DuMont et al., 2013). |
| **Phenol soluble modulin *psmα*** | ns | -1.75 | Pore-forming toxins with detergent activity (Surewaard et al., 2013). |

**Supplementary table 2. All significant fold changes of genes in PT vs PU.** Genes with non-significant fold changes were not included. Padj is the adjusted P value (significance threshold P<0.05). Genes ordered by significance.

| Gene id | log2 Fold Change | padj | Gene description |
|---|---|---|---|
| SAOUHSC_02671 | -9.3 | 2.2E-123 | conserved hypothetical protein |
| SAOUHSC_00204 | -6.0 | 1.7E-110 | Globin domain protein |
| SAOUHSC_00229 | -4.9 | 5.5E-85 | ScdA protein%2C putative |
| SAOUHSC_00203 | -7.1 | 3.2E-70 | conserved hypothetical protein |
| SAOUHSC_02781 | -4.5 | 8.6E-57 | conserved hypothetical protein |
| SAOUHSC_02684 | -6.7 | 1.7E-55 | assimilatory nitrite reductase [NAD(P)H]%2C large subunit%2C putative |
| SAOUHSC_02681 | -7.7 | 3.5E-53 | nitrate reductase%2C alpha subunit |
| SAOUHSC_00233 | -4.1 | 9.4E-52 | holin-like protein LrgB%2C putative |
| SAOUHSC_00634 | -4.7 | 3.4E-49 | ABC transporter%2C substrate-binding protein%2C putative |
| SAOUHSC_02680 | -7.8 | 2.3E-45 | nitrate reductase%2C beta subunit |
| SAOUHSC_00188 | -4.1 | 2.3E-45 | pyruvate formate-lyase 1 activating enzyme%2C putative |
| SAOUHSC_00146 | -4.2 | 4.3E-45 | conserved hypothetical protein |
| SAOUHSC_02661 | -4.3 | 2.0E-44 | PTS system sucrose-specific IIBC component%2C putative |
| SAOUHSC_00544 | 4.4 | 2.2E-44 | sdrC protein%2C putative |
| SAOUHSC_02679 | -8.2 | 7.5E-43 | respiratory nitrate reductase%2C delta subunit%2C putative |
| SAOUHSC_02254 | 3.1 | 1.4E-38 | chaperonin%2C 60 kDa%2C GrpEL%2C putative |
| SAOUHSC_02676 | -3.1 | 6.7E-37 | conserved hypothetical protein |
| SAOUHSC_03045 | 3.2 | 6.7E-37 | cold shock protein%2C putative |
| SAOUHSC_02682 | -5.7 | 1.3E-36 | uroporphyrin-III C-methyltransferase%2C putative |
| SAOUHSC_00093 | 3.1 | 2.0E-36 | superoxide dismutase%2C putative |
| SAOUHSC_02648 | -3.3 | 2.8E-36 | L-lactate permease |
| SAOUHSC_00704 | 3.8 | 7.2E-35 | conserved hypothetical protein |
| SAOUHSC_00206 | -3.9 | 6.4E-33 | L-lactate dehydrogenase |
| SAOUHSC_00617 | -3.4 | 2.1E-31 | conserved hypothetical protein |
| SAOUHSC_00608 | -3.5 | 3.9E-29 | alcohol dehydrogenase I%2C putative |
| SAOUHSC_02872 | -4.3 | 4.2E-29 | conserved hypothetical protein |
| SAOUHSC_01504 | 3.4 | 2.1E-28 | ferredoxin%2C putative |
| SAOUHSC_00961 | 4.5 | 3.2E-28 | conserved hypothetical protein |
| SAOUHSC_02572 | 3.2 | 3.8E-28 | conserved hypothetical protein |
| SAOUHSC_02855 | 3.7 | 1.3E-27 | LysM domain protein |
| SAOUHSC_01884 | -3.1 | 5.3E-27 | conserved hypothetical protein |
| SAOUHSC_02704 | 2.7 | 1.1E-26 | conserved hypothetical protein |
| SAOUHSC_01979 | 3.9 | 1.1E-26 | conserved hypothetical protein |
| SAOUHSC_00636 | -3.6 | 4.0E-26 | iron (chelated) ABC transporter%2C permease protein%2C putative |
| SAOUHSC_00187 | -3.4 | 1.0E-25 | formate acetyltransferase |
| SAOUHSC_00232 | -2.8 | 4.2E-25 | conserved hypothetical protein |
| SAOUHSC_00637 | -3.1 | 7.8E-25 | conserved hypothetical protein |
| SAOUHSC_00514 | -3.3 | 2.9E-24 | conserved hypothetical protein |
| SAOUHSC_00661 | 3.1 | 2.5E-23 | conserved hypothetical protein |
| SAOUHSC_02812 | 2.6 | 2.7E-23 | conserved hypothetical protein |
| SAOUHSC_02389 | 2.6 | 1.4E-22 | cation efflux family protein%2C putative |
| SAOUHSC_02703 | -2.5 | 2.3E-22 | phosphoglycerate mutase%2C putative |
| SAOUHSC_02909 | -3.4 | 2.5E-22 | dihydroorotate dehydrogenase |
| SAOUHSC_01684 | 2.3 | 5.2E-22 | co-chaperone GrpE |
| SAOUHSC_00746 | -4.5 | 7.5E-22 | conserved hypothetical protein |
| SAOUHSC_01265 | 3.1 | 4.9E-21 | conserved hypothetical protein |
| SAOUHSC_00009 | -2.7 | 6.7E-21 | seryl-tRNA synthetase |
| SAOUHSC_01990 | -2.8 | 8.7E-21 | amino acid ABC transporter%2C ATP-binding protein%2C putative |
| SAOUHSC_02018 | 2.6 | 2.8E-20 | conserved hypothetical phage protein |
| SAOUHSC_01332 | 2.5 | 1.3E-19 | conserved hypothetical protein |
| SAOUHSC_00652 | -2.5 | 1.9E-19 | iron compound ABC transporter%2C ATP-binding protein |
| SAOUHSC_00749 | -3.1 | 2.6E-19 | conserved hypothetical protein |
| SAOUHSC_02753 | -2.4 | 3.1E-19 | membrane protein%2C putative |
| SAOUHSC_01682 | 3.3 | 5.2E-19 | DnaJ protein |
| SAOUHSC_02678 | -2.9 | 9.6E-19 | respiratory nitrate reductase%2C gamma subunit |
| SAOUHSC_02942 | -2.3 | 7.9E-18 | anaerobic ribonucleoside-triphosphate reductase%2C putative |
| SAOUHSC_02912 | -3.1 | 1.0E-17 | conserved hypothetical protein |
| SAOUHSC_02255 | 3.3 | 1.1E-17 | chaperonin%2C 10 kDa%2C GroES%2C putative |
| SAOUHSC_02814 | 3.2 | 1.8E-17 | conserved hypothetical protein |
| SAOUHSC_00662 | 2.6 | 2.2E-17 | conserved hypothetical protein |
| SAOUHSC_02331 | 4.5 | 3.8E-17 | conserved hypothetical protein |
| SAOUHSC_01887 | 3.0 | 4.5E-17 | riboflavin biosynthesis protein%2C putative |
| SAOUHSC_00865 | -2.3 | 4.5E-17 | conserved hypothetical protein |
| SAOUHSC_01685 | 2.3 | 4.5E-17 | heat-inducible transcription repressor HrcA |
| SAOUHSC_00898 | -3.2 | 4.7E-17 | argininosuccinate lyase |
| SAOUHSC_02568 | -2.5 | 6.1E-17 | conserved hypothetical protein |
| SAOUHSC_02941 | -2.8 | 7.0E-17 | conserved hypothetical protein |
| SAOUHSC_02335 | -2.4 | 2.2E-16 | conserved hypothetical protein |
| SAOUHSC_00130 | -3.4 | 3.4E-16 | conserved hypothetical protein |
| SAOUHSC_02622 | 3.1 | 3.5E-16 | sodium/glutamate symporter |
| SAOUHSC_01169 | -4.3 | 6.1E-16 | carbamoyl-phosphate synthase%2C small subunit |
| SAOUHSC_00511 | -2.8 | 6.8E-16 | cysteinyl-tRNA synthetase |
| SAOUHSC_02668 | 2.2 | 6.8E-16 | conserved hypothetical protein |
| SAOUHSC_02677 | -3.0 | 9.4E-16 | conserved hypothetical protein |
| SAOUHSC_01978 | 2.1 | 1.9E-15 | conserved hypothetical protein |
| SAOUHSC_03024 | 2.0 | 1.9E-15 | conserved hypothetical protein |
| SAOUHSC_01170 | -3.2 | 2.9E-15 | carbamoyl-phosphate synthase%2C large subunit |
| SAOUHSC_02660 | 2.3 | 2.9E-15 | conserved hypothetical protein |
| SAOUHSC_01022 | 2.9 | 4.6E-15 | conserved hypothetical protein |
| SAOUHSC_02610 | -2.4 | 4.9E-15 | formiminoglutamase |
| SAOUHSC_00711 | 2.1 | 1.1E-14 | conserved hypothetical protein |
| SAOUHSC_01166 | -4.7 | 1.4E-14 | aspartate carbamoyltransferase |
| SAOUHSC_01320 | 2.1 | 1.5E-14 | homoserine dehydrogenase%2C putative |
| SAOUHSC_01267 | 2.6 | 2.9E-14 | conserved hypothetical protein |
| SAOUHSC_02430 | -3.2 | 3.2E-14 | ABC transporter periplasmic binding protein%2C putative |
| SAOUHSC_00177 | -3.3 | 4.1E-14 | maltose ABC transporter%2C permease protein%2C putative |

| | | | |
|---|---|---|---|
| SAOUHSC_00891 | -2.3 | 4.1E-14 | peptidyl-prolyl cis-trans isomerase%2C cyclophilin-type%2C putative |
| SAOUHSC_02388 | 2.6 | 5.0E-14 | conserved hypothetical protein |
| SAOUHSC_01452 | -3.8 | 5.3E-14 | alanine dehydrogenase |
| SAOUHSC_01165 | -4.1 | 7.8E-14 | uracil permease%2C putative |
| SAOUHSC_02654 | -2.4 | 9.8E-14 | conserved hypothetical protein |
| SAOUHSC_02435 | -3.2 | 1.2E-13 | conserved hypothetical protein |
| SAOUHSC_00774 | 2.5 | 1.4E-13 | conserved hypothetical protein |
| SAOUHSC_00513 | -2.8 | 1.4E-13 | conserved hypothetical protein |
| SAOUHSC_02741 | 2.5 | 1.6E-13 | amino acid ABC transporter%2C permease protein%2C putative |
| SAOUHSC_02366 | -2.6 | 1.8E-13 | conserved hypothetical protein |
| SAOUHSC_00505 | 2.2 | 2.5E-13 | endopeptidase%2C putative |
| SAOUHSC_02419 | 3.4 | 2.5E-13 | conserved hypothetical protein |
| SAOUHSC_00991 | 2.4 | 3.2E-13 | conserved hypothetical protein |
| SAOUHSC_00795 | -3.1 | 3.2E-13 | glyceraldehyde-3-phosphate dehydrogenase%2C type I |
| SAOUHSC_01032 | -2.7 | 3.5E-13 | cytochrome d ubiquinol oxidase%2C subunit II%2C putative |
| SAOUHSC_02869 | -2.6 | 3.8E-13 | delta-1-pyrroline-5-carboxylate dehydrogenase%2C putative |
| SAOUHSC_01903 | 3.2 | 4.9E-13 | conserved hypothetical protein |
| SAOUHSC_00748 | -3.9 | 8.1E-13 | conserved hypothetical protein |
| SAOUHSC_01439 | 2.8 | 9.1E-13 | conserved hypothetical protein |
| SAOUHSC_02767 | -2.5 | 1.1E-12 | peptide ABC transporter%2C peptide-binding protein%2C putative |
| SAOUHSC_01172 | -3.5 | 1.3E-12 | orotate phosphoribosyltransferase |
| SAOUHSC_01690 | 2.2 | 2.0E-12 | conserved hypothetical protein |
| SAOUHSC_01143 | -1.7 | 3.0E-12 | S-adenosyl-methyltransferase MraW |
| SAOUHSC_01171 | -3.5 | 3.0E-12 | orotidine 5'-phosphate decarboxylase |
| SAOUHSC_01949 | -2.3 | 3.3E-12 | intracellular serine protease%2C putative |
| SAOUHSC_02867 | -2.0 | 3.7E-12 | conserved hypothetical protein |
| SAOUHSC_02675 | -2.4 | 3.8E-12 | conserved hypothetical protein |
| SAOUHSC_02338 | 3.1 | 3.8E-12 | conserved hypothetical protein |
| SAOUHSC_02587 | 2.0 | 3.8E-12 | conserved hypothetical protein |
| SAOUHSC_01438 | 2.0 | 3.8E-12 | conserved hypothetical protein |
| SAOUHSC_02662 | -3.0 | 4.3E-12 | PTS system sucrose-specific IIBC component |
| SAOUHSC_00703 | 2.0 | 4.6E-12 | quinolone resistance norA protein%2C putative |
| SAOUHSC_00435 | 2.9 | 4.7E-12 | glutamate synthase%2C large subunit%2C putative |
| SAOUHSC_01168 | -4.0 | 5.8E-12 | dihydroorotase |
| SAOUHSC_03030 | -2.9 | 1.0E-11 | sodium%2C sulfate symporter%2C putative |
| SAOUHSC_01233 | 2.3 | 1.4E-11 | conserved hypothetical protein |
| SAOUHSC_01649 | -1.8 | 1.4E-11 | rhomboid family protein |
| SAOUHSC_00537 | 3.9 | 1.5E-11 | conserved hypothetical protein |
| SAOUHSC_00580 | 3.1 | 1.5E-11 | conserved hypothetical protein |
| SAOUHSC_00094 | -2.6 | 1.5E-11 | conserved hypothetical protein |
| SAOUHSC_02975 | -2.4 | 1.6E-11 | PTS system%2C fructose-specific IIABC component%2C putative |
| SAOUHSC_01917 | 2.8 | 1.9E-11 | conserved hypothetical protein |
| SAOUHSC_01378 | 2.6 | 2.2E-11 | peptide ABC transporter%2C ATP-binding protein%2C putative |
| SAOUHSC_00561 | -2.5 | 2.2E-11 | conserved hypothetical protein |
| SAOUHSC_02441 | -1.5 | 2.4E-11 | conserved hypothetical protein |
| SAOUHSC_00899 | -3.2 | 2.7E-11 | argininosuccinate synthase |
| SAOUHSC_00881 | -2.3 | 2.7E-11 | conserved hypothetical protein |
| SAOUHSC_01991 | -2.8 | 2.7E-11 | ABC transporter%2C permease protein%2C putative |
| SAOUHSC_02799 | 2.8 | 3.0E-11 | staphylococcal accessory regulator T%2C putative |
| SAOUHSC_00306 | -2.8 | 6.3E-11 | conserved hypothetical protein |
| SAOUHSC_01220 | 2.3 | 7.7E-11 | conserved hypothetical protein |
| SAOUHSC_02330 | 3.7 | 9.6E-11 | phosphomethylpyrimidine kinase |
| SAOUHSC_01451 | -3.7 | 1.0E-10 | threonine dehydratase |
| SAOUHSC_00421 | 1.9 | 1.1E-10 | conserved hypothetical protein |
| SAOUHSC_01650 | -1.6 | 1.2E-10 | conserved hypothetical protein |
| SAOUHSC_02744 | 2.1 | 1.6E-10 | amino acid ABC transporter%2C ATP-binding protein%2C putative |
| SAOUHSC_00178 | -3.0 | 1.7E-10 | maltose ABC transporter%2C permease protein |
| SAOUHSC_02751 | -2.4 | 1.9E-10 | conserved hypothetical protein |
| SAOUHSC_02881 | -2.1 | 2.1E-10 | conserved hypothetical protein |
| SAOUHSC_01683 | 1.7 | 2.4E-10 | DNAk protein%2C putative |
| SAOUHSC_00562 | -1.9 | 2.5E-10 | phosphomethylpyrimidine kinase |
| SAOUHSC_00281 | -2.2 | 2.5E-10 | conserved hypothetical protein |
| SAOUHSC_02134 | -2.1 | 2.5E-10 | nitric oxide synthase%2C oxygenase domain%2C putative |
| SAOUHSC_00999 | -3.7 | 2.6E-10 | quinol oxidase%2C subunit IV%2C putative |
| SAOUHSC_00133 | -1.7 | 2.9E-10 | conserved hypothetical protein |
| SAOUHSC_01460 | 1.9 | 3.1E-10 | conserved hypothetical protein |
| SAOUHSC_02329 | 3.9 | 3.9E-10 | hydroxyethylthiazole kinase%2C putative |
| SAOUHSC_00556 | 2.2 | 3.9E-10 | proline/betaine transporter%2C putative |
| SAOUHSC_00158 | -2.2 | 4.5E-10 | PTS system component |
| SAOUHSC_01983 | -2.0 | 4.5E-10 | fumarate hydratase%2C class II |
| SAOUHSC_00362 | -1.5 | 4.8E-10 | conserved hypothetical protein |
| SAOUHSC_01024 | 3.1 | 5.8E-10 | hypothetical protein |
| SAOUHSC_00577 | 1.7 | 6.7E-10 | mevalonate kinase%2C putative |
| SAOUHSC_01632 | 2.0 | 7.2E-10 | glycine cleavage system P-protein subunit II%2C putative |
| SAOUHSC_01427 | 1.6 | 7.6E-10 | conserved hypothetical protein |
| SAOUHSC_00237 | -2.9 | 8.0E-10 | conserved hypothetical protein |
| SAOUHSC_02853 | -2.1 | 9.0E-10 | conserved hypothetical protein |
| SAOUHSC_01947 | -2.2 | 1.1E-09 | membrane protein%2C putative |
| SAOUHSC_01627 | 1.9 | 1.1E-09 | conserved hypothetical protein |
| SAOUHSC_00954 | 1.7 | 1.3E-09 | UDP-N-acetylmuramoylalanyl-D-glutamate--2%2C 6-diaminopimelate ligase |
| SAOUHSC_00069 | -2.0 | 1.3E-09 | protein A |
| SAOUHSC_01863 | 2.6 | 1.4E-09 | conserved hypothetical protein |
| SAOUHSC_00729 | 1.8 | 1.4E-09 | ABC transporter%2C ATP-binding protein |
| SAOUHSC_00369 | -1.4 | 1.6E-09 | conserved hypothetical protein |
| SAOUHSC_02467 | -2.8 | 1.6E-09 | alpha-acetolactate decarboxylase |
| SAOUHSC_02612 | -2.1 | 1.8E-09 | ribose 5-phosphate isomerase%2C putative |
| SAOUHSC_00775 | 3.3 | 1.8E-09 | conserved hypothetical protein |
| SAOUHSC_02727 | -1.7 | 1.8E-09 | conserved hypothetical protein |
| SAOUHSC_00521 | -2.8 | 1.9E-09 | ribosomal protein L7/L12 |
| SAOUHSC_02685 | -4.5 | 1.9E-09 | conserved hypothetical protein |
| SAOUHSC_01706 | 1.8 | 1.9E-09 | conserved hypothetical protein |
| SAOUHSC_00836 | -1.8 | 2.5E-09 | glycine cleavage system H protein |
| SAOUHSC_00202 | -4.0 | 2.9E-09 | conserved hypothetical protein |
| SAOUHSC_00555 | 2.4 | 2.9E-09 | hydrolase%2C haloacid dehalogenase-like |

| | | | |
|---|---|---|---|
| SAOUHSC_00663 | -1.4 | 3.0E-09 | conserved hypothetical protein |
| SAOUHSC_00712 | -1.6 | 3.2E-09 | conserved hypothetical protein |
| SAOUHSC_01021 | 2.5 | 3.3E-09 | conserved hypothetical protein |
| SAOUHSC_01192 | 1.7 | 3.6E-09 | conserved hypothetical protein |
| SAOUHSC_00434 | 3.9 | 3.7E-09 | transcriptional regulator%2C lysR family%2C putative |
| SAOUHSC_00998 | 2.1 | 3.7E-09 | fmt protein%2C putative |
| SAOUHSC_01065 | -1.5 | 4.9E-09 | heme A synthase%2C putative |
| SAOUHSC_02129 | 3.2 | 5.0E-09 | conserved hypothetical protein |
| SAOUHSC_00912 | 1.7 | 5.3E-09 | ATP-dependent Clp protease%2C ATP-binding subunit ClpB |
| SAOUHSC_02880 | -2.3 | 5.6E-09 | conserved hypothetical protein |
| SAOUHSC_00975 | 3.1 | 5.7E-09 | conserved hypothetical protein |
| SAOUHSC_01820 | -2.0 | 5.8E-09 | acetate kinase |
| SAOUHSC_00035 | 2.8 | 5.8E-09 | conserved hypothetical protein |
| SAOUHSC_02108 | 2.5 | 6.1E-09 | ferritin%2C putative |
| SAOUHSC_00041 | -2.3 | 7.0E-09 | conserved hypothetical protein |
| SAOUHSC_01714 | -2.0 | 7.4E-09 | transcription elongation factor GreA |
| SAOUHSC_02659 | 2.2 | 8.0E-09 | conserved hypothetical protein |
| SAOUHSC_01971 | 2.9 | 8.3E-09 | conserved hypothetical protein |
| SAOUHSC_01375 | 1.9 | 8.3E-09 | conserved hypothetical protein |
| SAOUHSC_01653 | 1.7 | 9.1E-09 | superoxide dismutase%2C Mn%2C putative |
| SAOUHSC_02866 | -1.9 | 9.6E-09 | conserved hypothetical protein |
| SAOUHSC_00788 | -1.6 | 1.0E-08 | conserved hypothetical protein |
| SAOUHSC_02972 | -1.7 | 1.0E-08 | conserved hypothetical protein |
| SAOUHSC_00728 | 1.5 | 1.1E-08 | conserved hypothetical protein |
| SAOUHSC_02683 | -6.3 | 1.1E-08 | assimilatory nitrite reductase [NAD(P)H]%2C small subunit%2C putative |
| SAOUHSC_02810 | -1.9 | 1.3E-08 | conserved hypothetical protein |
| SAOUHSC_00290 | 2.2 | 1.3E-08 | conserved hypothetical protein |
| SAOUHSC_01005 | -2.1 | 1.3E-08 | conserved hypothetical protein |
| SAOUHSC_02876 | -1.7 | 1.4E-08 | conserved hypothetical protein |
| SAOUHSC_02468 | -1.8 | 1.4E-08 | acetolactate synthase%2C putative |
| SAOUHSC_01379 | 2.3 | 1.4E-08 | oligopeptide transporter putative membrane permease domain |
| SAOUHSC_02813 | 2.0 | 1.4E-08 | conserved hypothetical protein |
| SAOUHSC_02164 | 3.5 | 1.8E-08 | conserved hypothetical phage protein |
| SAOUHSC_00371 | -1.9 | 1.8E-08 | conserved hypothetical protein |
| SAOUHSC_00863 | 2.9 | 2.2E-08 | conserved hypothetical protein |
| SAOUHSC_01380 | 2.3 | 2.2E-08 | oligopeptide transporter putative membrane permease domain |
| SAOUHSC_00895 | -1.8 | 2.2E-08 | glutamate dehydrogenase%2C NAD-specific%2C putative |
| SAOUHSC_02033 | -1.6 | 2.6E-08 | phage tape measure protein |
| SAOUHSC_00747 | -3.9 | 2.6E-08 | conserved hypothetical protein |
| SAOUHSC_00646 | 1.9 | 3.4E-08 | penicillin-binding protein 4%2C putative |
| SAOUHSC_02396 | -1.4 | 3.5E-08 | conserved hypothetical protein |
| SAOUHSC_02110 | 1.7 | 3.5E-08 | conserved hypothetical protein |
| SAOUHSC_00336 | -1.6 | 3.5E-08 | acetyl-CoA acetyltransferase%2C putative |
| SAOUHSC_00074 | -2.5 | 3.6E-08 | periplasmic binding protein%2C putative |
| SAOUHSC_02645 | 2.7 | 3.8E-08 | conserved hypothetical protein |
| SAOUHSC_00437 | -2.0 | 4.0E-08 | conserved hypothetical protein |
| SAOUHSC_00414 | -1.7 | 4.1E-08 | conserved hypothetical protein |
| SAOUHSC_01601 | -1.9 | 4.3E-08 | alpha-glucosidase%2C putative |
| SAOUHSC_00802 | 1.6 | 4.5E-08 | carboxylesterase precursor%2C putative |
| SAOUHSC_01831 | -1.4 | 4.6E-08 | conserved hypothetical protein |
| SAOUHSC_01819 | -2.6 | 4.7E-08 | conserved hypothetical protein |
| SAOUHSC_02864 | -3.2 | 4.7E-08 | ferrous iron transport protein B |
| SAOUHSC_02665 | -1.6 | 4.7E-08 | conserved hypothetical protein |
| SAOUHSC_00305 | -3.2 | 5.7E-08 | conserved hypothetical protein |
| SAOUHSC_00860 | -1.7 | 6.2E-08 | 5-nucleotidase family protein |
| SAOUHSC_00902 | 1.5 | 6.9E-08 | Signal peptidase IA%2C putative |
| SAOUHSC_00882 | -2.2 | 7.0E-08 | conserved hypothetical protein |
| SAOUHSC_00540 | 3.3 | 7.0E-08 | conserved hypothetical protein |
| SAOUHSC_01948 | -2.2 | 7.0E-08 | ABC transporter domain protein |
| SAOUHSC_01120 | -2.2 | 8.5E-08 | conserved hypothetical protein |
| SAOUHSC_02599 | 2.1 | 8.5E-08 | Hex regulon repressor%2C putative |
| SAOUHSC_02112 | 1.5 | 9.0E-08 | conserved hypothetical protein |
| SAOUHSC_02576 | 1.9 | 9.9E-08 | secretory antigen precursor SsaA%2C putative |
| SAOUHSC_02360 | 1.8 | 1.0E-07 | thymidine kinase%2C putative |
| SAOUHSC_00859 | -2.0 | 1.0E-07 | conserved hypothetical protein |
| SAOUHSC_02979 | -1.6 | 1.0E-07 | conserved hypothetical protein |
| SAOUHSC_00501 | -1.4 | 1.0E-07 | conserved hypothetical protein |
| SAOUHSC_01908 | 1.5 | 1.1E-07 | conserved hypothetical protein |
| SAOUHSC_02794 | 2.2 | 1.1E-07 | conserved hypothetical protein |
| SAOUHSC_00512 | -2.2 | 1.2E-07 | conserved hypothetical protein |
| SAOUHSC_00838 | -2.1 | 1.3E-07 | conserved hypothetical protein |
| SAOUHSC_00173 | 2.0 | 1.4E-07 | acyl carrier phosphodiesterase |
| SAOUHSC_02294 | 3.4 | 1.7E-07 | hypothetical protein |
| SAOUHSC_02334 | 1.9 | 1.9E-07 | bacteriophage L54a%2C single-stranded DNA binding protein |
| SAOUHSC_00503 | 1.8 | 1.9E-07 | UvrB/uvrC motif domain protein |
| SAOUHSC_01629 | -1.3 | 2.0E-07 | conserved hypothetical protein |
| SAOUHSC_01514 | 2.4 | 2.0E-07 | hypothetical phage protein |
| SAOUHSC_02883 | 2.2 | 2.0E-07 | LysM domain protein |
| SAOUHSC_02860 | -1.5 | 2.0E-07 | HMG-CoA synthase%2C putative |
| SAOUHSC_00164 | -1.7 | 2.0E-07 | conserved hypothetical protein |
| SAOUHSC_02140 | -1.8 | 2.1E-07 | conserved hypothetical protein |
| SAOUHSC_02043 | -1.7 | 2.3E-07 | phage head protein%2C putative |
| SAOUHSC_02729 | -2.0 | 2.5E-07 | amino acid ABC transporter-like protein%2C putative |
| SAOUHSC_00131 | -2.5 | 2.5E-07 | conserved hypothetical protein |
| SAOUHSC_02380 | -2.6 | 2.7E-07 | purine nucleoside phosphorylase |
| SAOUHSC_00466 | 1.8 | 2.7E-07 | 4-diphosphocytidyl-2C-methyl-D-erythritol kinase |
| SAOUHSC_00532 | -1.5 | 2.8E-07 | conserved hypothetical protein |
| SAOUHSC_00605 | 1.4 | 2.9E-07 | conserved hypothetical protein |
| SAOUHSC_00516 | 1.4 | 2.9E-07 | preprotein translocase SecE subunit |
| SAOUHSC_01413 | 1.8 | 3.2E-07 | conserved hypothetical protein |
| SAOUHSC_01497 | 1.8 | 3.4E-07 | L-asparaginase%2C putative |
| SAOUHSC_02863 | -2.9 | 3.6E-07 | conserved hypothetical protein |
| SAOUHSC_01322 | 1.9 | 3.6E-07 | homoserine kinase |
| SAOUHSC_01734 | -1.2 | 3.7E-07 | conserved hypothetical protein |

| | | | |
|---|---|---|---|
| SAOUHSC_00951 | -1.4 | 3.9E-07 | conserved hypothetical protein |
| SAOUHSC_02444 | 1.7 | 3.9E-07 | osmoprotectant transporter%2C BCCT family%2C opuD-like protein%2C putative |
| SAOUHSC_02385 | 1.5 | 3.9E-07 | mannose-6-phosphate isomerase%2C class I |
| SAOUHSC_00520 | -1.5 | 3.9E-07 | ribosomal protein L10 |
| SAOUHSC_00817 | -1.7 | 3.9E-07 | conserved hypothetical protein |
| SAOUHSC_02520 | -2.0 | 4.0E-07 | sugar transporter%2C putative |
| SAOUHSC_01761 | -1.6 | 4.0E-07 | conserved hypothetical protein |
| SAOUHSC_03026 | 1.6 | 4.1E-07 | conserved hypothetical protein |
| SAOUHSC_02801 | -1.4 | 4.2E-07 | UTP-glucose-1-phosphate uridylyltransferase |
| SAOUHSC_00350 | -2.6 | 5.2E-07 | ribosomal protein S18 |
| SAOUHSC_01319 | 2.1 | 5.2E-07 | aspartate kinase%2C putative |
| SAOUHSC_00713 | -1.6 | 5.6E-07 | conserved hypothetical protein |
| SAOUHSC_02038 | -1.9 | 5.7E-07 | phage protein%2C HK97 gp10 family |
| SAOUHSC_02418 | 1.4 | 6.4E-07 | conserved hypothetical protein |
| SAOUHSC_00660 | 1.8 | 6.5E-07 | conserved hypothetical protein |
| SAOUHSC_01037 | 2.6 | 7.1E-07 | hypothetical protein |
| SAOUHSC_00767 | -2.0 | 7.1E-07 | conserved hypothetical protein |
| SAOUHSC_00757 | -1.5 | 7.3E-07 | peptidase T%2C putative |
| SAOUHSC_02403 | -1.3 | 7.6E-07 | mannitol-1-phosphate 5-dehydrogenase%2C putative |
| SAOUHSC_00465 | 1.8 | 7.9E-07 | conserved hypothetical protein |
| SAOUHSC_02862 | -1.3 | 8.5E-07 | ATP-dependent Clp protease%2C ATP-binding subunit ClpC%2C putative |
| SAOUHSC_02926 | -2.1 | 8.9E-07 | fructose-bisphosphate aldolase class-I%2C putative |
| SAOUHSC_01450 | -2.0 | 9.4E-07 | conserved hypothetical protein |
| SAOUHSC_01431 | -1.2 | 9.5E-07 | methionine sulfoxide reductase%2C putative |
| SAOUHSC_02300 | 1.4 | 9.9E-07 | STAS domain%2C putative |
| SAOUHSC_02465 | -1.7 | 1.0E-06 | conserved hypothetical protein |
| SAOUHSC_02042 | -2.0 | 1.0E-06 | phi Mu50B-like protein |
| SAOUHSC_02600 | -1.7 | 1.0E-06 | conserved hypothetical protein |
| SAOUHSC_00504 | 1.8 | 1.1E-06 | ATP:guanido phosphotransferase%2C C-terminal catalytic domain protein |
| SAOUHSC_00200 | 2.6 | 1.1E-06 | membrane protein%2C putative |
| SAOUHSC_00114 | 1.9 | 1.2E-06 | capsular polysaccharide biosynthesis protein%2C putative |
| SAOUHSC_02118 | 1.6 | 1.2E-06 | glutamyl-tRNA(Gln) amidotransferase%2C C subunit |
| SAOUHSC_00554 | -1.2 | 1.3E-06 | SIS domain protein |
| SAOUHSC_00755 | 1.6 | 1.3E-06 | conserved hypothetical protein |
| SAOUHSC_01082 | -2.1 | 1.4E-06 | conserved hypothetical protein |
| SAOUHSC_02554 | -1.6 | 1.5E-06 | conserved hypothetical protein |
| SAOUHSC_00799 | -2.2 | 1.6E-06 | enolase |
| SAOUHSC_02163 | 2.6 | 1.6E-06 | conserved hypothetical phage protein |
| SAOUHSC_02332 | 5.1 | 1.6E-06 | conserved hypothetical protein |
| SAOUHSC_01456 | -3.4 | 1.6E-06 | conserved hypothetical protein |
| SAOUHSC_00284 | 1.9 | 1.8E-06 | 5'-nucleotidase%2C lipoprotein e(P4) family |
| SAOUHSC_02226 | -1.7 | 1.8E-06 | conserved hypothetical phage protein |
| SAOUHSC_02811 | -1.6 | 1.9E-06 | conserved hypothetical protein |
| SAOUHSC_00718 | 3.1 | 2.0E-06 | conserved hypothetical protein |
| SAOUHSC_02742 | 2.1 | 2.2E-06 | amino acid transporter%2C putative |
| SAOUHSC_01282 | -1.2 | 2.2E-06 | conserved hypothetical protein |
| SAOUHSC_00868 | 3.0 | 2.2E-06 | conserved hypothetical protein |
| SAOUHSC_00248 | 1.7 | 2.3E-06 | peptidoglycan hydrolase%2C putative |
| SAOUHSC_01067 | -1.7 | 2.3E-06 | conserved hypothetical protein |
| SAOUHSC_02458 | 1.8 | 2.4E-06 | conserved hypothetical protein |
| SAOUHSC_T00050 | 7.7 | 2.4E-06 | tRNA-Ser |
| SAOUHSC_00740 | 2.0 | 2.7E-06 | conserved hypothetical protein |
| SAOUHSC_01009 | -2.2 | 2.7E-06 | phosphoribosylaminoimidazole carboxylase%2C ATPase subunit |
| SAOUHSC_00754 | 1.4 | 2.7E-06 | conserved hypothetical protein |
| SAOUHSC_01635 | 2.3 | 2.7E-06 | shikimate kinase%2C putative |
| SAOUHSC_00973 | 1.7 | 2.7E-06 | conserved hypothetical protein |
| SAOUHSC_01072 | 1.8 | 2.7E-06 | conserved hypothetical protein |
| SAOUHSC_02017 | 2.2 | 2.7E-06 | conserved hypothetical phage protein |
| SAOUHSC_00120 | 3.0 | 3.0E-06 | UDP-N-acetylglucosamine 2-epimerase |
| SAOUHSC_00510 | -1.8 | 3.0E-06 | serine acetyltransferase%2C putative |
| SAOUHSC_00176 | -2.1 | 3.0E-06 | bacterial extracellular solute-binding protein%2C putative |
| SAOUHSC_02262 | -1.6 | 3.4E-06 | conserved hypothetical protein |
| SAOUHSC_00861 | -1.5 | 4.1E-06 | lipoic acid synthetase |
| SAOUHSC_02125 | -1.5 | 4.2E-06 | conserved hypothetical protein |
| SAOUHSC_T0003 | 3.6 | 4.2E-06 | tRNA-Ala |
| SAOUHSC_01429 | -1.4 | 4.2E-06 | conserved hypothetical protein |
| SAOUHSC_01292 | 2.2 | 4.2E-06 | conserved hypothetical protein |
| SAOUHSC_01405 | 1.5 | 4.3E-06 | conserved hypothetical protein |
| SAOUHSC_00643 | -1.5 | 4.5E-06 | tagB protein%2C putative |
| SAOUHSC_00673 | 1.4 | 4.5E-06 | conserved hypothetical protein |
| SAOUHSC_00552 | -1.7 | 4.9E-06 | conserved hypothetical protein |
| SAOUHSC_02626 | -1.3 | 5.4E-06 | conserved hypothetical protein |
| SAOUHSC_01899 | 1.8 | 5.5E-06 | conserved hypothetical protein |
| SAOUHSC_00199 | 2.5 | 5.7E-06 | conserved hypothetical protein |
| SAOUHSC_00436 | 2.1 | 5.7E-06 | NADH-glutamate synthase small subunit%2C putative |
| SAOUHSC_02265 | -1.6 | 5.8E-06 | accessory gene regulator protein A |
| SAOUHSC_01590 | 1.4 | 6.0E-06 | conserved hypothetical protein |
| SAOUHSC_02309 | 1.4 | 6.0E-06 | conserved hypothetical protein |
| SAOUHSC_00358 | -2.1 | 6.3E-06 | conserved hypothetical protein |
| SAOUHSC_00502 | 1.2 | 6.4E-06 | conserved hypothetical protein |
| SAOUHSC_02474 | -1.3 | 6.5E-06 | conserved hypothetical protein |
| SAOUHSC_02808 | -1.6 | 6.6E-06 | gluconate kinase |
| SAOUHSC_03023 | -1.8 | 7.9E-06 | Drp35 |
| SAOUHSC_02766 | -2.6 | 8.0E-06 | peptide ABC transporter%2C permease protein%2C putative |
| SAOUHSC_01019 | 2.5 | 8.6E-06 | conserved hypothetical protein |
| SAOUHSC_00469 | -1.4 | 8.6E-06 | conserved hypothetical protein |
| SAOUHSC_02630 | -1.3 | 8.7E-06 | conserved hypothetical protein |
| SAOUHSC_02247 | 1.9 | 8.9E-06 | cation transport protein%2C putative |
| SAOUHSC_00871 | 1.6 | 9.1E-06 | D-alanyl carrier protein |
| SAOUHSC_00181 | -1.5 | 9.4E-06 | conserved hypothetical protein |
| SAOUHSC_01666 | -1.4 | 9.6E-06 | glycyl-tRNA synthetase |
| SAOUHSC_02328 | 3.0 | 1.0E-05 | thiamine-phosphate pyrophosphorylase |
| SAOUHSC_01972 | -1.1 | 1.0E-05 | protein export protein PrsA%2C putative |

| | | | |
|---|---|---|---|
| SAOUHSC_00901 | 1.2 | 1.0E-05 | conserved hypothetical protein |
| SAOUHSC_00639 | -1.6 | 1.1E-05 | conserved hypothetical protein |
| SAOUHSC_02670 | 1.4 | 1.3E-05 | conserved hypothetical protein |
| SAOUHSC_00001 | -1.2 | 1.3E-05 | chromosomal replication initiator protein DnaA |
| SAOUHSC_02264 | -1.4 | 1.3E-05 | accessory gene regulator protein C |
| SAOUHSC_01208 | -1.6 | 1.3E-05 | ribosomal protein S16 |
| SAOUHSC_02041 | -1.8 | 1.3E-05 | phi Mu50B-like protein |
| SAOUHSC_02386 | 2.5 | 1.3E-05 | conserved hypothetical protein |
| SAOUHSC_02034 | -1.7 | 1.4E-05 | conserved hypothetical phage protein |
| SAOUHSC_02769 | -3.4 | 1.4E-05 | conserved hypothetical protein |
| SAOUHSC_01278 | -1.3 | 1.4E-05 | conserved hypothetical protein |
| SAOUHSC_03022 | -1.2 | 1.4E-05 | conserved hypothetical protein |
| SAOUHSC_02280 | 1.5 | 1.5E-05 | conserved hypothetical protein |
| SAOUHSC_01334 | 3.2 | 1.5E-05 | conserved hypothetical protein |
| SAOUHSC_02809 | -1.6 | 1.6E-05 | gluconate operon transcriptional repressor%2C putative |
| SAOUHSC_00313 | -2.2 | 1.6E-05 | conserved hypothetical protein |
| SAOUHSC_00866 | -1.2 | 1.7E-05 | D-isomer specific 2-hydroxyacid dehydrogenase%2C NAD binding domain protein |
| SAOUHSC_01798 | 1.3 | 1.7E-05 | conserved hypothetical protein |
| SAOUHSC_01180 | 1.4 | 1.7E-05 | conserved hypothetical protein |
| SAOUHSC_00272 | -1.7 | 1.9E-05 | conserved hypothetical protein |
| SAOUHSC_00800 | 2.0 | 2.0E-05 | conserved hypothetical protein |
| SAOUHSC_02819 | 2.4 | 2.0E-05 | conserved hypothetical protein |
| SAOUHSC_00972 | 2.4 | 2.2E-05 | conserved hypothetical protein |
| SAOUHSC_01468 | 1.5 | 2.2E-05 | conserved hypothetical protein |
| SAOUHSC_00831 | -1.2 | 2.3E-05 | conserved hypothetical protein |
| SAOUHSC_02135 | -1.4 | 2.3E-05 | conserved hypothetical protein |
| SAOUHSC_00900 | -1.4 | 2.4E-05 | glucose-6-phosphate isomerase |
| SAOUHSC_01628 | 2.1 | 2.4E-05 | conserved hypothetical protein |
| SAOUHSC_00198 | 3.1 | 2.4E-05 | conserved hypothetical protein |
| SAOUHSC_02571 | 1.7 | 2.5E-05 | secretory antigen precursor%2C putative |
| SAOUHSC_02861 | -1.7 | 2.5E-05 | methylated-DNA--protein-cysteine methyltransferase%2C putative |
| SAOUHSC_02886 | 2.1 | 2.7E-05 | conserved hypothetical protein |
| SAOUHSC_02629 | -1.6 | 2.7E-05 | drug resistance transporter%2C EmrB/QacA subfamily%2C putative |
| SAOUHSC_02656 | -1.4 | 2.7E-05 | conserved hypothetical protein |
| SAOUHSC_01264 | 1.8 | 2.9E-05 | conserved hypothetical protein |
| SAOUHSC_02937 | 1.7 | 2.9E-05 | choline transporter%2C putative |
| SAOUHSC_01108 | 1.3 | 2.9E-05 | conserved hypothetical protein |
| SAOUHSC_00957 | 1.5 | 3.0E-05 | conserved hypothetical protein |
| SAOUHSC_02299 | 1.2 | 3.0E-05 | anti-sigma B factor%2C putative |
| SAOUHSC_01737 | -1.6 | 3.0E-05 | aspartyl-tRNA synthetase |
| SAOUHSC_00943 | -1.2 | 3.1E-05 | ATP-NAD kinase%2C putative |
| SAOUHSC_00753 | 5.5 | 3.2E-05 | conserved hypothetical protein |
| SAOUHSC_01806 | -2.0 | 3.3E-05 | pyruvate kinase |
| SAOUHSC_02093 | 2.4 | 3.6E-05 | conserved hypothetical protein |
| SAOUHSC_02593 | -1.7 | 3.6E-05 | conserved hypothetical protein |
| SAOUHSC_00613 | 1.4 | 3.7E-05 | iron compound ABC transporter%2C substrate-binding protein%2C putative |
| SAOUHSC_01266 | 2.2 | 3.7E-05 | conserved hypothetical protein |
| SAOUHSC_01663 | 1.1 | 3.9E-05 | DNA primase%2C putative |
| SAOUHSC_00771 | 1.5 | 3.9E-05 | peptide chain release factor 2%2C putative |
| SAOUHSC_00170 | 1.7 | 3.9E-05 | conserved hypothetical protein |
| SAOUHSC_01718 | 2.0 | 3.9E-05 | conserved hypothetical protein |
| SAOUHSC_02036 | -1.4 | 4.1E-05 | phage structural protein%2C putative |
| SAOUHSC_00934 | -1.2 | 4.1E-05 | conserved hypothetical protein |
| SAOUHSC_00401 | 1.3 | 4.3E-05 | conserved hypothetical protein |
| SAOUHSC_01136 | -1.9 | 4.3E-05 | conserved hypothetical protein |
| SAOUHSC_01895 | 1.6 | 4.3E-05 | conserved hypothetical protein |
| SAOUHSC_00567 | -1.3 | 4.6E-05 | conserved hypothetical protein |
| SAOUHSC_00113 | -2.0 | 4.6E-05 | alcohol dehydrogenase%2C iron-containing%2C putative |
| SAOUHSC_02029 | -1.3 | 4.7E-05 | phi ETA orf 56-like protein |
| SAOUHSC_00826 | -1.5 | 4.7E-05 | conserved hypothetical protein |
| SAOUHSC_02372 | 1.3 | 4.7E-05 | conserved hypothetical protein |
| SAOUHSC_00404 | 1.7 | 4.8E-05 | conserved hypothetical protein |
| SAOUHSC_01675 | -1.0 | 5.0E-05 | conserved hypothetical protein |
| SAOUHSC_02973 | 2.4 | 5.0E-05 | conserved hypothetical protein |
| SAOUHSC_02333 | 1.3 | 5.0E-05 | sceD protein%2C putative |
| SAOUHSC_00408 | 1.1 | 5.0E-05 | conserved hypothetical protein |
| SAOUHSC_02306 | 1.5 | 5.0E-05 | holo-(acyl-carrier-protein) synthase |
| SAOUHSC_01119 | -1.9 | 5.1E-05 | conserved hypothetical protein |
| SAOUHSC_01889 | 1.7 | 5.3E-05 | riboflavin biosynthesis protein RibD |
| SAOUHSC_00830 | 1.3 | 5.3E-05 | conserved hypothetical protein |
| SAOUHSC_03034 | 1.5 | 5.3E-05 | conserved hypothetical protein |
| SAOUHSC_01634 | 1.8 | 5.3E-05 | glycine cleavage system T protein |
| SAOUHSC_01346 | 2.3 | 5.3E-05 | glycine betaine transporter%2C putative |
| SAOUHSC_00407 | 1.6 | 5.5E-05 | conserved hypothetical protein |
| SAOUHSC_00014 | 1.1 | 5.6E-05 | conserved hypothetical protein |
| SAOUHSC_02932 | 1.9 | 5.8E-05 | choline dehydrogenase |
| SAOUHSC_01351 | 1.3 | 6.1E-05 | DNA topoisomerase IV%2C B subunit |
| SAOUHSC_01902 | 2.7 | 6.2E-05 | conserved hypothetical protein |
| SAOUHSC_02649 | -1.1 | 6.3E-05 | conserved hypothetical protein |
| SAOUHSC_00307 | -2.2 | 6.4E-05 | conserved hypothetical protein |
| SAOUHSC_02367 | 1.4 | 6.4E-05 | conserved hypothetical protein |
| SAOUHSC_01191 | -1.5 | 6.5E-05 | ribosomal protein L28 |
| SAOUHSC_00268 | -1.1 | 6.9E-05 | conserved hypothetical protein |
| SAOUHSC_01592 | -1.3 | 6.9E-05 | transcriptional regulator%2C Fur%2C putative |
| SAOUHSC_02991 | -1.3 | 7.0E-05 | conserved hypothetical protein |
| SAOUHSC_01966 | 1.1 | 7.0E-05 | conserved hypothetical protein |
| SAOUHSC_01174 | -1.5 | 7.1E-05 | conserved hypothetical protein |
| SAOUHSC_01665 | -1.1 | 7.2E-05 | CBS domain protein |
| SAOUHSC_01226 | -1.4 | 7.3E-05 | heat shock protein HslVU%2C ATPase subunit HslU |
| SAOUHSC_02611 | 1.2 | 7.4E-05 | conserved hypothetical protein |
| SAOUHSC_00304 | -2.2 | 7.5E-05 | conserved hypothetical protein |
| SAOUHSC_01406 | 1.1 | 7.5E-05 | acylphosphatase |
| SAOUHSC_00960 | -1.0 | 7.6E-05 | conserved hypothetical protein |

| | | | |
|---|---|---|---|
| SAOUHSC_02040 | -1.9 | 7.8E-05 | conserved hypothetical phage protein |
| SAOUHSC_02743 | 2.4 | 7.8E-05 | amino acid ABC transporter%2C permease protein%2C putative |
| SAOUHSC_00440 | 4.1 | 7.8E-05 | conserved hypothetical protein |
| SAOUHSC_02035 | -1.5 | 7.8E-05 | conserved hypothetical phage protein |
| SAOUHSC_01289 | 4.2 | 8.5E-05 | conserved hypothetical protein |
| SAOUHSC_T00031 | 2.7 | 8.5E-05 | tRNA-Leu |
| SAOUHSC_00736 | -1.2 | 8.6E-05 | conserved hypothetical protein |
| SAOUHSC_00766 | 1.5 | 9.0E-05 | conserved hypothetical protein |
| SAOUHSC_02460 | -1.7 | 9.5E-05 | conserved hypothetical protein |
| SAOUHSC_01513 | 3.1 | 9.5E-05 | conserved hypothetical protein |
| SAOUHSC_01681 | 1.4 | 9.5E-05 | ribosomal protein L11 methyltransferase |
| SAOUHSC_01297 | 1.9 | 9.7E-05 | conserved hypothetical protein |
| SAOUHSC_00641 | -1.0 | 9.9E-05 | teichoic acid translocation ATP-binding protein%2C putative |
| SAOUHSC_01307 | 1.9 | 9.9E-05 | conserved hypothetical protein |
| SAOUHSC_01760 | -1.6 | 1.0E-04 | conserved hypothetical protein |
| SAOUHSC_00301 | -1.2 | 1.1E-04 | conserved hypothetical protein |
| SAOUHSC_01142 | -1.1 | 1.1E-04 | conserved hypothetical protein |
| SAOUHSC_01291 | 3.1 | 1.2E-04 | conserved hypothetical protein |
| SAOUHSC_01624 | 1.5 | 1.2E-04 | acetyl-CoA carboxylase%2C biotin carboxyl carrier protein |
| SAOUHSC_02088 | 1.3 | 1.2E-04 | excisionase-related protein |
| SAOUHSC_01474 | -1.4 | 1.2E-04 | conserved hypothetical protein |
| SAOUHSC_01420 | 1.2 | 1.3E-04 | DNA-binding response regulator%2C putative |
| SAOUHSC_01303 | 1.5 | 1.3E-04 | conserved hypothetical protein |
| SAOUHSC_01437 | 1.1 | 1.4E-04 | conserved hypothetical protein |
| SAOUHSC_02797 | 1.6 | 1.4E-04 | conserved hypothetical protein |
| SAOUHSC_02374 | 1.3 | 1.4E-04 | aminobenzoyl-glutamate utilization protein B%2C putative |
| SAOUHSC_00702 | -1.2 | 1.4E-04 | conserved hypothetical protein |
| SAOUHSC_01797 | -1.0 | 1.4E-04 | DNA polymerase I |
| SAOUHSC_00876 | 1.4 | 1.4E-04 | conserved hypothetical protein |
| SAOUHSC_02778 | -1.2 | 1.5E-04 | conserved hypothetical protein |
| SAOUHSC_02443 | -1.5 | 1.7E-04 | conserved hypothetical protein |
| SAOUHSC_00308 | -2.0 | 1.7E-04 | conserved hypothetical protein |
| SAOUHSC_00116 | 2.1 | 1.7E-04 | capsular polysaccharide synthesis enzyme Cap8C |
| SAOUHSC_00017 | -1.1 | 1.8E-04 | ribosomal protein L9 |
| SAOUHSC_01377 | 1.3 | 1.8E-04 | oligopeptide ABC transporter%2C ATP-binding protein%2C putative |
| SAOUHSC_01043 | -1.8 | 1.8E-04 | dihydrolipoamide dehydrogenase |
| SAOUHSC_00620 | 1.6 | 1.8E-04 | staphylococcal accessory regulator T%2C putative |
| SAOUHSC_01967 | 0.9 | 1.8E-04 | ABC transporter%2C ATP-binding protein%2C putative |
| SAOUHSC_02371 | -1.5 | 1.8E-04 | conserved hypothetical protein |
| SAOUHSC_00825 | 1.9 | 1.9E-04 | conserved hypothetical protein |
| SAOUHSC_00070 | -1.2 | 2.0E-04 | staphylococcal accessory regulator-like protein |
| SAOUHSC_00287 | -1.2 | 2.0E-04 | ABC transporter%2C ATP-binding protein%2C putative |
| SAOUHSC_01605 | -1.2 | 2.1E-04 | 6-phosphogluconate dehydrogenase%2C decarboxylating |
| SAOUHSC_00359 | -1.3 | 2.1E-04 | phosphoglycerate mutase family protein |
| SAOUHSC_02030 | -1.2 | 2.1E-04 | phi ETA orf 55-like protein |
| SAOUHSC_02352 | -1.4 | 2.2E-04 | UDP-N-acetylglucosamine 2-epimerase |
| SAOUHSC_01719 | -1.5 | 2.2E-04 | conserved hypothetical protein |
| SAOUHSC_00547 | -1.1 | 2.3E-04 | conserved hypothetical protein |
| SAOUHSC_01201 | -1.4 | 2.3E-04 | acyl carrier protein |
| SAOUHSC_01392 | -1.3 | 2.4E-04 | ABC transporter%2C ATP-binding protein%2C putative |
| SAOUHSC_00002 | -1.2 | 2.4E-04 | DNA polymerase III%2C beta subunit |
| SAOUHSC_01287 | -1.6 | 2.4E-04 | glutamine synthetase%2C type I |
| SAOUHSC_00925 | 1.7 | 2.5E-04 | conserved hypothetical protein |
| SAOUHSC_02445 | 1.1 | 2.5E-04 | conserved hypothetical protein |
| SAOUHSC_01023 | 3.8 | 2.5E-04 | hypothetical protein |
| SAOUHSC_01219 | 1.5 | 2.6E-04 | cell wall hydrolase%2C putative |
| SAOUHSC_02379 | -1.7 | 2.6E-04 | deoxyribose-phosphate aldolase |
| SAOUHSC_00927 | 1.4 | 2.7E-04 | oligopeptide ABC transporter%2C substrate-binding protein%2C putative |
| SAOUHSC_02594 | -1.2 | 2.7E-04 | conserved hypothetical protein |
| SAOUHSC_01150 | -1.4 | 2.7E-04 | cell division protein FtsZ |
| SAOUHSC_02003 | 1.4 | 2.8E-04 | ABC transporter%2C ATP-binding/permease protein%2C putative |
| SAOUHSC_00196 | 3.4 | 2.8E-04 | conserved hypothetical protein |
| SAOUHSC_02482 | -1.1 | 2.9E-04 | ABC transporter%2C ATP-binding protein%2C putative |
| SAOUHSC_01394 | -1.4 | 2.9E-04 | aspartokinase II%2C putative |
| SAOUHSC_01576 | -1.2 | 2.9E-04 | exonuclease family |
| SAOUHSC_00690 | -1.2 | 2.9E-04 | conserved hypothetical protein |
| SAOUHSC_00468 | -1.3 | 2.9E-04 | conserved hypothetical protein |
| SAOUHSC_02927 | -1.2 | 3.0E-04 | malate:quinone-oxidoreductase |
| SAOUHSC_00278 | 1.9 | 3.0E-04 | conserved hypothetical protein |
| SAOUHSC_00115 | 1.9 | 3.0E-04 | capsular polysaccharide synthesis enzyme Cap5B |
| SAOUHSC_00668 | 1.3 | 3.1E-04 | ABC transporter permease%2C putative |
| SAOUHSC_02575 | -1.4 | 3.3E-04 | conserved hypothetical protein |
| SAOUHSC_00282 | 1.6 | 3.3E-04 | branched-chain amino acid transport system II carrier protein |
| SAOUHSC_01000 | -2.0 | 3.4E-04 | cytochrome c oxidase subunit III%2C putative |
| SAOUHSC_00310 | -1.9 | 3.4E-04 | conserved hypothetical protein |
| SAOUHSC_01964 | -1.1 | 3.4E-04 | conserved hypothetical protein |
| SAOUHSC_00833 | -1.0 | 3.5E-04 | conserved hypothetical protein |
| SAOUHSC_01788 | -1.4 | 3.5E-04 | threonyl-tRNA synthetase |
| SAOUHSC_01156 | 1.1 | 3.6E-04 | conserved hypothetical protein |
| SAOUHSC_01131 | 1.2 | 3.6E-04 | conserved hypothetical protein |
| SAOUHSC_00947 | -1.4 | 3.7E-04 | enoyl-(acyl-carrier-protein) reductase |
| SAOUHSC_02791 | 1.3 | 3.7E-04 | pyrophosphohydrolase%2C putative |
| SAOUHSC_00738 | -1.5 | 3.9E-04 | conserved hypothetical protein |
| SAOUHSC_02433 | -1.3 | 3.9E-04 | conserved hypothetical protein |
| SAOUHSC_01855 | -1.6 | 3.9E-04 | conserved hypothetical protein |
| SAOUHSC_01432 | -1.0 | 3.9E-04 | peptide methionine sulfoxide reductase |
| SAOUHSC_00588 | 2.7 | 4.0E-04 | conserved hypothetical protein |
| SAOUHSC_02613 | -1.2 | 4.0E-04 | conserved hypothetical protein |
| SAOUHSC_02756 | 1.1 | 4.0E-04 | conserved hypothetical protein |
| SAOUHSC_01867 | -0.9 | 4.0E-04 | D-amino acid aminotransferase |
| SAOUHSC_02930 | -1.6 | 4.1E-04 | conserved hypothetical protein |
| SAOUHSC_00061 | -2.3 | 4.1E-04 | conserved hypothetical protein |
| SAOUHSC_01030 | 1.7 | 4.1E-04 | conserved hypothetical protein |
| SAOUHSC_01290 | 2.9 | 4.3E-04 | conserved hypothetical protein |

| | | | |
|---|---|---|---|
| SAOUHSC_01702 | 1.1 | 4.3E-04 | MTA/SAH nucleosidase |
| SAOUHSC_00964 | 1.2 | 4.3E-04 | conserved hypothetical protein |
| SAOUHSC_01063 | 1.1 | 4.4E-04 | conserved hypothetical protein |
| SAOUHSC_02132 | -1.3 | 4.4E-04 | NAD+ synthetase |
| SAOUHSC_01176 | 0.9 | 4.5E-04 | guanylate kinase |
| SAOUHSC_00940 | -1.8 | 4.5E-04 | conserved hypothetical protein |
| SAOUHSC_00480 | 1.1 | 4.5E-04 | conserved hypothetical protein |
| SAOUHSC_01827 | -0.9 | 4.5E-04 | conserved hypothetical protein |
| SAOUHSC_02787 | 1.9 | 4.5E-04 | conserved hypothetical protein |
| SAOUHSC_03005 | 2.9 | 4.5E-04 | intercellular adhesion protein C%2C putative |
| SAOUHSC_01661 | 1.6 | 4.6E-04 | conserved hypothetical protein |
| SAOUHSC_02361 | -1.9 | 4.6E-04 | ribosomal protein L31 |
| SAOUHSC_02148 | -1.2 | 4.6E-04 | conserved hypothetical protein |
| SAOUHSC_01694 | 1.1 | 4.6E-04 | conserved hypothetical protein |
| SAOUHSC_01705 | 1.7 | 4.8E-04 | enterotoxin family protein |
| SAOUHSC_01238 | 1.3 | 4.8E-04 | conserved hypothetical protein |
| SAOUHSC_02836 | -1.2 | 4.8E-04 | conserved hypothetical protein |
| SAOUHSC_00195 | 3.4 | 4.9E-04 | acetyl-CoA acetyltransferase%2C putative |
| SAOUHSC_00948 | -1.0 | 5.0E-04 | conserved hypothetical protein |
| SAOUHSC_00279 | 1.3 | 5.0E-04 | conserved hypothetical protein |
| SAOUHSC_00300 | 1.4 | 5.0E-04 | lipase precursor |
| SAOUHSC_01997 | -1.1 | 5.0E-04 | ferric uptake regulator-like protein%2C putative |
| SAOUHSC_01295 | 6.7 | 5.0E-04 | conserved hypothetical protein |
| SAOUHSC_02485 | -1.6 | 5.2E-04 | DNA-directed RNA polymerase alpha chain%2C putative |
| SAOUHSC_02845 | -1.4 | 5.2E-04 | conserved hypothetical protein |
| SAOUHSC_01414 | -1.4 | 5.4E-04 | conserved hypothetical protein |
| SAOUHSC_01011 | -2.7 | 5.4E-04 | phosphoribosylformylglycinamidine synthase%2C PurS protein |
| SAOUHSC_01223 | 1.5 | 5.5E-04 | gid protein |
| SAOUHSC_02747 | 1.0 | 5.6E-04 | conserved hypothetical protein |
| SAOUHSC_00117 | 2.0 | 5.7E-04 | capsular polysaccharide biosynthesis protein Cap5D%2C putative |
| SAOUHSC_01609 | -1.2 | 5.7E-04 | conserved hypothetical protein |
| SAOUHSC_00595 | 3.6 | 5.7E-04 | conserved hypothetical protein |
| SAOUHSC_00654 | -1.6 | 5.8E-04 | ferrichrome ABC transporter (permease)%2C putative |
| SAOUHSC_01430 | -1.6 | 5.9E-04 | phosphotransferase system enzyme IIA%2C putative |
| SAOUHSC_02641 | 1.2 | 5.9E-04 | permease%2C putative domain protein |
| SAOUHSC_00922 | 1.5 | 5.9E-04 | conserved hypothetical protein |
| SAOUHSC_02527 | -1.0 | 6.0E-04 | FmhB protein%2C putative |
| SAOUHSC_02561 | 2.3 | 6.0E-04 | urease%2C alpha subunit |
| SAOUHSC_02943 | 2.6 | 6.0E-04 | citrate transporter%2C putative |
| SAOUHSC_03004 | 3.3 | 6.1E-04 | icaB protein%2C putative |
| SAOUHSC_00309 | -1.0 | 6.2E-04 | conserved hypothetical protein |
| SAOUHSC_02308 | 1.2 | 6.4E-04 | conserved hypothetical protein |
| SAOUHSC_01221 | 4.2 | 6.5E-04 | conserved hypothetical protein |
| SAOUHSC_02450 | -1.7 | 6.5E-04 | pts system%2C lactose-specific IIBC component%2C putative |
| SAOUHSC_00036 | 2.2 | 6.5E-04 | conserved hypothetical protein |
| SAOUHSC_00723 | -1.2 | 6.6E-04 | conserved hypothetical protein |
| SAOUHSC_02470 | -1.6 | 6.8E-04 | conserved hypothetical protein |
| SAOUHSC_02037 | -1.4 | 6.8E-04 | conserved hypothetical phage protein |
| SAOUHSC_02321 | 1.1 | 7.2E-04 | conserved hypothetical protein |
| SAOUHSC_01672 | -0.9 | 7.3E-04 | conserved hypothetical protein |
| SAOUHSC_01896 | 1.1 | 7.4E-04 | conserved hypothetical protein |
| SAOUHSC_02994 | -1.5 | 7.5E-04 | conserved hypothetical protein |
| SAOUHSC_01870 | 1.0 | 7.5E-04 | ribosomal small subunit pseudouridine synthase A%2C putative |
| SAOUHSC_02921 | -1.1 | 7.6E-04 | alpha-acetolactate decarboxylase |
| SAOUHSC_02158 | -0.9 | 7.6E-04 | conserved hypothetical protein |
| SAOUHSC_00822 | 1.5 | 7.8E-04 | conserved hypothetical protein |
| SAOUHSC_00058 | 1.6 | 7.9E-04 | conserved hypothetical protein |
| SAOUHSC_02156 | 2.4 | 7.9E-04 | conserved hypothetical protein |
| SAOUHSC_01097 | 1.1 | 8.0E-04 | conserved hypothetical protein |
| SAOUHSC_01237 | 1.2 | 8.1E-04 | undecaprenyl diphosphate synthase |
| SAOUHSC_01055 | -1.0 | 8.2E-04 | inositol monophosphatase family protein%2C putative |
| SAOUHSC_01992 | -1.1 | 8.4E-04 | Phosphotransferase system%2C EIIC domain protein |
| SAOUHSC_00438 | -1.0 | 8.4E-04 | alpha amylase family protein%2C putative |
| SAOUHSC_01314 | 1.1 | 8.4E-04 | conserved hypothetical protein |
| SAOUHSC_02708 | -1.9 | 8.4E-04 | gamma-hemolysin h-gamma-ii subunit%2C putative |
| SAOUHSC_02273 | 1.3 | 8.4E-04 | conserved hypothetical protein |
| SAOUHSC_01010 | -2.0 | 8.5E-04 | phosphoribosylaminoimidazole-succinocarboxamide synthase |
| SAOUHSC_00280 | -1.2 | 8.5E-04 | conserved hypothetical protein |
| SAOUHSC_00433 | 1.5 | 8.6E-04 | conserved hypothetical protein |
| SAOUHSC_02806 | -1.7 | 8.7E-04 | gluconate permease%2C putative |
| SAOUHSC_02369 | 1.0 | 8.8E-04 | DNA-directed RNA polymerase%2C delta subunit%2C putative |
| SAOUHSC_00123 | 1.8 | 9.2E-04 | capsular polysaccharide biosynthesis protein Cap5J%2C putative |
| SAOUHSC_02317 | -0.9 | 9.2E-04 | UDP-N-acetylmuramoylalanyl-D-glutamyl-2%2C6-diaminopimelate--D-alanyl-D-alanyl ligase |
| SAOUHSC_02534 | 1.7 | 9.2E-04 | conserved hypothetical protein |
| SAOUHSC_00500 | -1.1 | 9.2E-04 | conserved hypothetical protein |
| SAOUHSC_01106 | 1.2 | 9.6E-04 | glutamate racemase |
| SAOUHSC_00796 | -1.9 | 1.0E-03 | phosphoglycerate kinase%2C putative |
| SAOUHSC_00855 | 1.8 | 1.1E-03 | conserved hypothetical protein |
| SAOUHSC_01816 | -0.8 | 1.1E-03 | conserved hypothetical protein |
| SAOUHSC_01742 | 0.9 | 1.1E-03 | GTP pyrophosphokinase |
| SAOUHSC_02016 | 1.4 | 1.1E-03 | conserved hypothetical phage protein |
| SAOUHSC_01625 | -1.5 | 1.1E-03 | translation elongation factor P |
| SAOUHSC_00971 | 1.7 | 1.1E-03 | conserved hypothetical protein |
| SAOUHSC_00995 | 2.0 | 1.1E-03 | conserved hypothetical protein |
| SAOUHSC_01463 | -1.0 | 1.1E-03 | conserved hypothetical protein |
| SAOUHSC_00431 | 1.0 | 1.1E-03 | conserved hypothetical protein |
| SAOUHSC_00254 | 2.8 | 1.2E-03 | conserved hypothetical protein |
| SAOUHSC_02779 | -1.1 | 1.2E-03 | conserved hypothetical protein |
| SAOUHSC_02589 | -1.0 | 1.2E-03 | conserved hypothetical protein |
| SAOUHSC_02362 | -1.1 | 1.2E-03 | transcription termination factor Rho |
| SAOUHSC_01337 | -0.9 | 1.2E-03 | transketolase |
| SAOUHSC_01835 | 0.9 | 1.2E-03 | conserved hypothetical protein |
| SAOUHSC_02570 | 1.3 | 1.3E-03 | conserved hypothetical protein |

| | | | |
|---|---|---|---|
| SAOUHSC_R00016 | 3.6 | 1.3E-03 | 5S Ribosomal RNA |
| SAOUHSC_00141 | 0.9 | 1.3E-03 | conserved hypothetical protein |
| SAOUHSC_02621 | -1.7 | 1.3E-03 | DNA-3-methyladenine glycosylase%2C putative |
| SAOUHSC_02757 | 1.7 | 1.3E-03 | conserved hypothetical protein |
| SAOUHSC_01365 | -0.8 | 1.4E-03 | conserved hypothetical protein |
| SAOUHSC_00450 | -1.1 | 1.4E-03 | Orn/Lys/Arg decarboxylase%2C putative |
| SAOUHSC_00695 | -0.9 | 1.4E-03 | conserved hypothetical protein |
| SAOUHSC_02275 | -1.8 | 1.4E-03 | hypothetical protein |
| SAOUHSC_02785 | 1.7 | 1.4E-03 | conserved hypothetical protein |
| SAOUHSC_00349 | -0.9 | 1.4E-03 | bacteriophage L54a%2C single-stranded DNA binding protein |
| SAOUHSC_01368 | -1.4 | 1.4E-03 | anthranilate phosphoribosyltransferase |
| SAOUHSC_00550 | 1.1 | 1.4E-03 | conserved hypothetical protein |
| SAOUHSC_02885 | 0.8 | 1.5E-03 | conserved hypothetical protein |
| SAOUHSC_00985 | -1.4 | 1.5E-03 | enoyl-CoA hydratase/isomerase family protein%2C putative |
| SAOUHSC_00625 | -1.2 | 1.5E-03 | conserved hypothetical protein |
| SAOUHSC_02096 | -1.3 | 1.5E-03 | conserved hypothetical protein |
| SAOUHSC_T00035 | 2.3 | 1.5E-03 | tRNA-Lys |
| SAOUHSC_00398 | 1.1 | 1.5E-03 | restriction modification system specificity subunit%2C putative |
| SAOUHSC_01222 | 1.2 | 1.5E-03 | DNA topoisomerase I |
| SAOUHSC_02322 | 1.0 | 1.5E-03 | conserved hypothetical protein |
| SAOUHSC_01318 | 0.9 | 1.5E-03 | conserved hypothetical protein |
| SAOUHSC_02955 | -1.0 | 1.6E-03 | sensor histidine kinase%2C putative |
| SAOUHSC_01310 | -1.0 | 1.6E-03 | cardiolipin synthetase%2C putative |
| SAOUHSC_00942 | -1.1 | 1.6E-03 | GTP pyrophosphokinase%2C putative |
| SAOUHSC_00916 | 2.5 | 1.6E-03 | conserved hypothetical protein |
| SAOUHSC_00484 | 1.0 | 1.6E-03 | conserved hypothetical protein |
| SAOUHSC_02929 | 0.8 | 1.6E-03 | acetyl-CoA synthetase%2C putative |
| SAOUHSC_01133 | -2.1 | 1.6E-03 | conserved hypothetical protein |
| SAOUHSC_01986 | -1.0 | 1.6E-03 | conserved hypothetical protein |
| SAOUHSC_00033 | 2.0 | 1.6E-03 | conserved hypothetical protein |
| SAOUHSC_01092 | -1.3 | 1.6E-03 | phenylalanyl-tRNA synthetase%2C alpha subunit |
| SAOUHSC_02111 | -1.2 | 1.6E-03 | ImpB/MucB/SamB family superfamily |
| SAOUHSC_01433 | -1.1 | 1.7E-03 | conserved hypothetical protein |
| SAOUHSC_00184 | -1.4 | 1.7E-03 | Response regulator receiver domain protein |
| SAOUHSC_00915 | 4.5 | 1.7E-03 | conserved hypothetical protein |
| SAOUHSC_01861 | -0.8 | 1.7E-03 | conserved hypothetical protein |
| SAOUHSC_01744 | 1.2 | 1.7E-03 | conserved hypothetical protein |
| SAOUHSC_00249 | -1.3 | 1.8E-03 | conserved hypothetical protein |
| SAOUHSC_00687 | 1.0 | 1.8E-03 | conserved hypothetical protein |
| SAOUHSC_01860 | -1.1 | 1.8E-03 | conserved hypothetical protein |
| SAOUHSC_02261 | -1.2 | 1.8E-03 | accessory gene regulator protein B |
| SAOUHSC_03046 | -2.0 | 1.8E-03 | Helix-turn-helix domain protein |
| SAOUHSC_00858 | -1.0 | 1.8E-03 | conserved hypothetical protein |
| SAOUHSC_02631 | 1.1 | 1.8E-03 | conserved hypothetical protein |
| SAOUHSC_00126 | 2.1 | 1.8E-03 | capsular polysaccharide biosynthesis protein Cap8M |
| SAOUHSC_02031 | -1.2 | 1.8E-03 | conserved hypothetical phage protein |
| SAOUHSC_00794 | -1.3 | 1.8E-03 | glycolytic operon regulator |
| SAOUHSC_02272 | 1.5 | 1.8E-03 | conserved hypothetical protein |
| SAOUHSC_02627 | -1.1 | 1.8E-03 | conserved hypothetical protein |
| SAOUHSC_02370 | 0.9 | 1.8E-03 | conserved hypothetical protein |
| SAOUHSC_02828 | 1.5 | 1.9E-03 | conserved hypothetical protein |
| SAOUHSC_02340 | -0.9 | 1.9E-03 | ATP synthase F1%2C epsilon subunit |
| SAOUHSC_02384 | 1.2 | 1.9E-03 | conserved hypothetical protein |
| SAOUHSC_02887 | 1.5 | 2.0E-03 | immunodominant antigen A%2C putative |
| SAOUHSC_01679 | 1.5 | 2.0E-03 | conserved hypothetical protein |
| SAOUHSC_02822 | -1.3 | 2.0E-03 | conserved hypothetical protein |
| SAOUHSC_02472 | -1.1 | 2.1E-03 | conserved hypothetical protein |
| SAOUHSC_03028 | -1.3 | 2.1E-03 | conserved hypothetical protein |
| SAOUHSC_01399 | -1.3 | 2.1E-03 | conserved hypothetical protein |
| SAOUHSC_02859 | -0.8 | 2.1E-03 | hydroxymethylglutaryl-CoA reductase%2C degradative |
| SAOUHSC_00676 | -1.2 | 2.2E-03 | conserved hypothetical protein |
| SAOUHSC_01664 | -0.8 | 2.2E-03 | conserved hypothetical protein |
| SAOUHSC_00615 | -1.2 | 2.2E-03 | haloacid dehalogenase-like hydrolase%2C putative |
| SAOUHSC_01923 | 2.2 | 2.3E-03 | conserved hypothetical protein |
| SAOUHSC_01145 | -1.0 | 2.3E-03 | penicillin-binding protein 1 |
| SAOUHSC_03016 | 1.4 | 2.3E-03 | conserved hypothetical protein |
| SAOUHSC_02286 | 1.9 | 2.4E-03 | 3-isopropylmalate dehydrogenase |
| SAOUHSC_02650 | -1.1 | 2.4E-03 | lipoprotein%2C putative |
| SAOUHSC_02143 | -0.8 | 2.4E-03 | conserved hypothetical protein |
| SAOUHSC_00792 | -1.0 | 2.4E-03 | conserved hypothetical protein |
| SAOUHSC_01113 | 2.4 | 2.4E-03 | conserved hypothetical protein |
| SAOUHSC_01594 | -0.9 | 2.4E-03 | conserved hypothetical protein |
| SAOUHSC_02910 | -1.7 | 2.4E-03 | conserved hypothetical protein |
| SAOUHSC_00128 | 1.4 | 2.5E-03 | cap5O protein/UDP-N-acetyl-D-mannosaminuronic acid dehydrogenase |
| SAOUHSC_02028 | -1.1 | 2.5E-03 | phiETA ORF57-like protein |
| SAOUHSC_01977 | -1.4 | 2.6E-03 | conserved hypothetical protein |
| SAOUHSC_00172 | -1.0 | 2.6E-03 | conserved hypothetical protein |
| SAOUHSC_02048 | -1.1 | 2.6E-03 | phage portal protein%2C SPP1 family |
| SAOUHSC_02827 | -1.6 | 2.6E-03 | conserved hypothetical protein |
| SAOUHSC_T00027 | 1.9 | 2.7E-03 | tRNA-His |
| SAOUHSC_01829 | -1.4 | 2.7E-03 | ribosomal protein S4 |
| SAOUHSC_00843 | 1.3 | 2.7E-03 | conserved hypothetical protein |
| SAOUHSC_01316 | 1.1 | 2.7E-03 | conserved hypothetical protein |
| SAOUHSC_00659 | 1.0 | 2.7E-03 | conserved hypothetical protein |
| SAOUHSC_02597 | -1.3 | 2.7E-03 | PTS system component%2C putative |
| SAOUHSC_00894 | -1.0 | 2.7E-03 | ornithine aminotransferase%2C putative |
| SAOUHSC_00551 | 1.4 | 2.7E-03 | conserved hypothetical protein |
| SAOUHSC_02004 | 0.9 | 2.8E-03 | conserved hypothetical protein |
| SAOUHSC_02104 | 1.4 | 2.8E-03 | conserved hypothetical protein |
| SAOUHSC_02879 | -1.8 | 2.8E-03 | squalene desaturase%2C putative |
| SAOUHSC_01199 | -0.9 | 2.8E-03 | 3-oxoacyl-(acyl-carrier-protein) reductase%2C putative |
| SAOUHSC_00535 | -0.9 | 2.8E-03 | conserved hypothetical protein |
| SAOUHSC_01440 | 1.4 | 2.8E-03 | conserved hypothetical protein |
| SAOUHSC_00574 | -1.1 | 2.9E-03 | phosphate acetyltransferase |

| | | | |
|---|---|---|---|
| SAOUHSC_01015 | -1.7 | 2.9E-03 | phosphoribosylformylglycinamidine cyclo-ligase |
| SAOUHSC_00032 | 6.2 | 2.9E-03 | conserved hypothetical protein |
| SAOUHSC_T00051 | 1.7 | 2.9E-03 | tRNA-Ser |
| SAOUHSC_00481 | 0.9 | 3.0E-03 | conserved hypothetical protein |
| SAOUHSC_01772 | -1.4 | 3.0E-03 | porphobilinogen synthase |
| SAOUHSC_01930 | 2.7 | 3.0E-03 | conserved hypothetical protein |
| SAOUHSC_02776 | 1.2 | 3.1E-03 | conserved hypothetical protein |
| SAOUHSC_02667 | 0.7 | 3.1E-03 | conserved hypothetical protein |
| SAOUHSC_02012 | -1.1 | 3.1E-03 | Transglycosylase domain protein |
| SAOUHSC_02798 | -1.1 | 3.2E-03 | conserved hypothetical protein |
| SAOUHSC_00827 | 1.9 | 3.2E-03 | conserved hypothetical protein |
| SAOUHSC_02298 | 0.8 | 3.2E-03 | sigma factor B%2C putative |
| SAOUHSC_00624 | 0.8 | 3.3E-03 | integrase/recombinase%2C putative |
| SAOUHSC_00589 | 2.5 | 3.3E-03 | hypothetical protein |
| SAOUHSC_00122 | 1.8 | 3.4E-03 | capsular polysaccharide biosynthesis protein Cap5I%2C putative |
| SAOUHSC_00970 | 1.4 | 3.4E-03 | ABC transporter%2C ATP-binding protein%2C putative |
| SAOUHSC_01250 | -1.1 | 3.4E-03 | ribosomal protein S15 |
| SAOUHSC_00797 | -1.6 | 3.5E-03 | triosephosphate isomerase |
| SAOUHSC_02475 | -1.4 | 3.5E-03 | conserved hypothetical protein |
| SAOUHSC_02364 | 0.8 | 3.6E-03 | conserved hypothetical protein |
| SAOUHSC_02795 | 1.8 | 3.6E-03 | conserved hypothetical protein |
| SAOUHSC_00769 | 0.9 | 3.6E-03 | preprotein translocase%2C SecA subunit |
| SAOUHSC_01680 | 1.0 | 3.6E-03 | conserved hypothetical protein |
| SAOUHSC_02541 | 1.4 | 3.6E-03 | molybdopterin-guanine dinucleotide biosynthesis protein MobB |
| SAOUHSC_02336 | -1.4 | 3.7E-03 | beta-hydroxyacyl-ACP dehydratase%2C putative |
| SAOUHSC_00518 | 1.0 | 3.7E-03 | ribosomal protein L11 |
| SAOUHSC_00142 | 1.9 | 3.8E-03 | formate dehydrogenase%2C NAD-dependent%2C putative |
| SAOUHSC_00315 | -1.4 | 3.8E-03 | conserved hypothetical protein |
| SAOUHSC_02451 | -2.0 | 3.8E-03 | PTS system lactose-specific IIA component%2C putative |
| SAOUHSC_02454 | -1.1 | 3.9E-03 | galactose-6-phosphate isomerase%2C LacB subunit |
| SAOUHSC_00271 | 1.1 | 3.9E-03 | conserved hypothetical protein |
| SAOUHSC_01313 | 0.9 | 3.9E-03 | Histidine kinase-%2C DNA gyrase B-%2C and HSP90-like ATPase domain protein |
| SAOUHSC_01969 | -0.8 | 3.9E-03 | conserved hypothetical protein |
| SAOUHSC_01715 | -0.8 | 4.0E-03 | uridine kinase |
| SAOUHSC_A02254 | 5.4 | 4.0E-03 | hypothetical protein |
| SAOUHSC_00684 | 1.2 | 4.3E-03 | conserved hypothetical protein |
| SAOUHSC_01651 | 1.4 | 4.3E-03 | ribosomal protein L33 |
| SAOUHSC_01407 | 1.1 | 4.3E-03 | conserved hypothetical protein |
| SAOUHSC_T00025 | 5.5 | 4.3E-03 | tRNA-Gly |
| SAOUHSC_02913 | -1.3 | 4.4E-03 | conserved hypothetical protein |
| SAOUHSC_00644 | -1.0 | 4.4E-03 | tagX protein%2C putative |
| SAOUHSC_00810 | 1.8 | 4.6E-03 | conserved hypothetical protein |
| SAOUHSC_02044 | -1.2 | 4.6E-03 | conserved hypothetical phage protein |
| SAOUHSC_01907 | -0.8 | 4.8E-03 | conserved hypothetical protein |
| SAOUHSC_02789 | 1.1 | 4.8E-03 | conserved hypothetical protein |
| SAOUHSC_00118 | 1.7 | 4.9E-03 | capsular polysaccharide biosynthesis protein Cap5E%2C putative |
| SAOUHSC_02976 | -1.8 | 4.9E-03 | mannose-6-phosphate isomerase%2C class I |
| SAOUHSC_02250 | 1.8 | 5.0E-03 | phage terminase%2C small subunit%2C putative |
| SAOUHSC_01838 | -0.9 | 5.0E-03 | conserved hypothetical protein |
| SAOUHSC_02569 | 1.2 | 5.1E-03 | conserved hypothetical protein |
| SAOUHSC_01034 | -0.9 | 5.1E-03 | conserved hypothetical protein |
| SAOUHSC_00497 | 1.5 | 5.1E-03 | conserved hypothetical protein |
| SAOUHSC_01721 | -1.1 | 5.2E-03 | conserved hypothetical protein |
| SAOUHSC_00918 | 1.0 | 5.2E-03 | truncated MHC class II analog protein |
| SAOUHSC_02014 | -1.3 | 5.3E-03 | conserved hypothetical protein |
| SAOUHSC_01583 | 1.2 | 5.4E-03 | conserved hypothetical phage protein |
| SAOUHSC_02726 | 1.1 | 5.4E-03 | positive transcriptional activator%2C putative |
| SAOUHSC_02145 | 0.9 | 5.5E-03 | conserved hypothetical protein |
| SAOUHSC_00355 | 1.5 | 5.6E-03 | conserved hypothetical protein |
| SAOUHSC_01305 | 2.9 | 5.6E-03 | conserved hypothetical protein |
| SAOUHSC_02427 | -1.7 | 5.7E-03 | conserved hypothetical protein |
| SAOUHSC_00840 | -0.8 | 5.7E-03 | conserved hypothetical protein |
| SAOUHSC_02284 | 1.7 | 5.8E-03 | ketol-acid reductoisomerase |
| SAOUHSC_02442 | -1.1 | 6.1E-03 | conserved hypothetical protein |
| SAOUHSC_01927 | -2.5 | 6.1E-03 | transposase%2C IS3 family%2C truncation-related protein%2C putative |
| SAOUHSC_02488 | -0.8 | 6.1E-03 | ribosomal protein L36 |
| SAOUHSC_02793 | -0.9 | 6.2E-03 | conserved hypothetical protein |
| SAOUHSC_02459 | 1.4 | 6.2E-03 | conserved hypothetical protein |
| SAOUHSC_01922 | -1.2 | 6.2E-03 | conserved hypothetical protein |
| SAOUHSC_02532 | 1.0 | 6.4E-03 | conserved hypothetical protein |
| SAOUHSC_00616 | -0.8 | 6.4E-03 | conserved hypothetical protein |
| SAOUHSC_02969 | -2.9 | 6.5E-03 | arginine deiminase |
| SAOUHSC_00134 | -0.9 | 6.5E-03 | conserved hypothetical protein |
| SAOUHSC_00685 | 1.1 | 6.5E-03 | conserved hypothetical protein |
| SAOUHSC_00545 | 0.8 | 6.7E-03 | sdrD protein%2C putative |
| SAOUHSC_02303 | 0.9 | 6.7E-03 | conserved hypothetical protein |
| SAOUHSC_01886 | 1.1 | 6.7E-03 | riboflavin synthase%2C beta subunit |
| SAOUHSC_00363 | -1.0 | 6.8E-03 | conserved hypothetical protein |
| SAOUHSC_01974 | -0.7 | 6.8E-03 | conserved hypothetical protein |
| SAOUHSC_00593 | 2.0 | 6.8E-03 | conserved hypothetical protein |
| SAOUHSC_02011 | -0.8 | 6.8E-03 | conserved hypothetical protein |
| SAOUHSC_00612 | 1.1 | 6.9E-03 | endonuclease III%2C putative |
| SAOUHSC_01228 | -1.0 | 6.9E-03 | conserved hypothetical protein |
| SAOUHSC_00018 | 1.1 | 7.1E-03 | replicative DNA helicase |
| SAOUHSC_02113 | -1.1 | 7.2E-03 | RNA methyltransferase%2C TrmA family%2C putative |
| SAOUHSC_00880 | -1.7 | 7.4E-03 | conserved hypothetical protein |
| SAOUHSC_01604 | -0.8 | 7.4E-03 | conserved hypothetical protein |
| SAOUHSC_01637 | 3.3 | 7.4E-03 | conserved hypothetical protein |
| SAOUHSC_02481 | -1.0 | 7.5E-03 | cobalt transport protein%2C putative |
| SAOUHSC_01839 | -0.9 | 7.5E-03 | tyrosyl-tRNA synthetase |
| SAOUHSC_00422 | 1.0 | 7.5E-03 | trans-sulfuration enzyme family protein%2C putative |
| SAOUHSC_02287 | 1.6 | 7.7E-03 | 3-isopropylmalate dehydratase%2C large subunit |
| SAOUHSC_01341 | 1.1 | 7.8E-03 | conserved hypothetical protein |

| | | | |
|---|---|---|---|
| SAOUHSC_01349 | 0.8 | 7.8E-03 | conserved hypothetical protein |
| SAOUHSC_02647 | -0.9 | 7.8E-03 | malate:quinone-oxidoreductase |
| SAOUHSC_00486 | 0.8 | 7.8E-03 | conserved hypothetical protein |
| SAOUHSC_00715 | -0.9 | 7.9E-03 | response regulator%2C putative |
| SAOUHSC_02640 | 0.9 | 7.9E-03 | conserved hypothetical protein |
| SAOUHSC_00402 | 1.8 | 8.0E-03 | conserved hypothetical protein |
| SAOUHSC_01078 | -1.0 | 8.0E-03 | ribosomal protein L32 |
| SAOUHSC_02406 | 0.9 | 8.0E-03 | conserved hypothetical protein |
| SAOUHSC_T00015 | 2.0 | 8.2E-03 | tRNA-Cys |
| SAOUHSC_01928 | -1.5 | 8.3E-03 | transposase family protein%2C putative |
| SAOUHSC_01864 | -0.9 | 8.5E-03 | conserved hypothetical protein |
| SAOUHSC_00364 | 1.4 | 8.5E-03 | alkyl hydroperoxide reductase%2C subunit F%2C putative |
| SAOUHSC_02154 | -1.1 | 8.6E-03 | ABC transporter%2C ATP-binding protein%2C putative |
| SAOUHSC_01610 | -0.8 | 8.6E-03 | conserved hypothetical protein |
| SAOUHSC_00412 | -1.4 | 8.7E-03 | NADH dehydrogenase subunit 5%2C putative |
| SAOUHSC_02922 | -0.8 | 8.7E-03 | L-lactate dehydrogenase |
| SAOUHSC_00924 | 1.2 | 8.7E-03 | conserved hypothetical protein |
| SAOUHSC_00997 | 1.0 | 8.7E-03 | conserved hypothetical protein |
| SAOUHSC_00373 | 1.3 | 8.7E-03 | xanthine permease%2C putative |
| SAOUHSC_01904 | 1.1 | 8.9E-03 | conserved hypothetical protein |
| SAOUHSC_01638 | 2.9 | 9.0E-03 | conserved hypothetical protein |
| SAOUHSC_01232 | 0.9 | 9.2E-03 | ribosomal protein S2 |
| SAOUHSC_00977 | 1.4 | 9.2E-03 | conserved hypothetical protein |
| SAOUHSC_T00026 | 3.6 | 9.3E-03 | tRNA-His |
| SAOUHSC_00416 | 0.9 | 9.3E-03 | conserved hypothetical protein |
| SAOUHSC_02557 | 0.9 | 9.3E-03 | urea transporter%2C putative |
| SAOUHSC_01888 | 1.5 | 9.4E-03 | riboflavin synthase%2C alpha subunit |
| SAOUHSC_00814 | 2.5 | 9.6E-03 | truncated secreted von Willebrand factor-binding protein (coagulase) VWbp%2C putative |
| SAOUHSC_00926 | 1.1 | 9.7E-03 | oligopeptide ABC transporter%2C ATP-binding protein%2C putative |
| SAOUHSC_01840 | 0.9 | 9.8E-03 | transglycosylase domain protein |
| SAOUHSC_01766 | -0.9 | 1.0E-02 | folylpolyglutamate synthase/dihydrofolate synthase%2C putative |
| SAOUHSC_02983 | -1.0 | 1.0E-02 | conserved hypothetical protein |
| SAOUHSC_01060 | -1.0 | 1.0E-02 | conserved hypothetical protein |
| SAOUHSC_00168 | 1.9 | 1.0E-02 | conserved hypothetical protein |
| SAOUHSC_00812 | 0.8 | 1.0E-02 | clumping factor |
| SAOUHSC_01768 | -0.9 | 1.0E-02 | conserved hypothetical protein |
| SAOUHSC_02516 | -1.2 | 1.0E-02 | conserved hypothetical protein |
| SAOUHSC_00423 | 1.2 | 1.0E-02 | conserved hypothetical protein |
| SAOUHSC_00832 | -0.7 | 1.0E-02 | 3-dehydroquinate dehydratase%2C type I |
| SAOUHSC_02536 | -0.7 | 1.0E-02 | molybdopterin cofactor biosynthesis protein A%2C putative |
| SAOUHSC_01743 | 1.1 | 1.0E-02 | adenine phosphoribosyltransferase |
| SAOUHSC_01039 | 0.9 | 1.0E-02 | conserved hypothetical protein |
| SAOUHSC_02365 | 0.8 | 1.0E-02 | UDP-N-acetylglucosamine 1-carboxyvinyltransferase |
| SAOUHSC_02515 | 1.0 | 1.1E-02 | conserved hypothetical protein |
| SAOUHSC_01403 | -1.0 | 1.1E-02 | cold shock protein%2C putative |
| SAOUHSC_01814 | -0.9 | 1.1E-02 | conserved hypothetical protein |
| SAOUHSC_00955 | 1.0 | 1.1E-02 | conserved hypothetical protein |
| SAOUHSC_00506 | 5.9 | 1.1E-02 | hypothetical protein |
| SAOUHSC_00390 | -1.2 | 1.1E-02 | conserved hypothetical protein |
| SAOUHSC_01755 | -0.7 | 1.1E-02 | ribosomal protein L27 |
| SAOUHSC_01758 | 1.0 | 1.1E-02 | conserved hypothetical protein |
| SAOUHSC_01181 | -1.3 | 1.1E-02 | conserved hypothetical protein |
| SAOUHSC_01914 | -1.5 | 1.1E-02 | conserved hypothetical protein |
| SAOUHSC_00492 | 1.2 | 1.1E-02 | conserved hypothetical protein |
| SAOUHSC_01818 | -1.1 | 1.1E-02 | alanine dehydrogenase |
| SAOUHSC_02558 | 3.3 | 1.1E-02 | urease%2C gamma subunit |
| SAOUHSC_01274 | -0.9 | 1.1E-02 | glycerol uptake operon antiterminator regulatory protein%2C putative |
| SAOUHSC_01580 | 1.9 | 1.1E-02 | phi PVL ORF 30-like protein |
| SAOUHSC_00966 | -1.0 | 1.1E-02 | conserved hypothetical protein |
| SAOUHSC_02307 | 0.7 | 1.2E-02 | conserved hypothetical protein |
| SAOUHSC_00787 | -1.0 | 1.2E-02 | conserved hypothetical protein |
| SAOUHSC_00119 | 1.5 | 1.2E-02 | capsular polysaccharide synthesis enzyme Cap8F |
| SAOUHSC_00153 | 0.9 | 1.2E-02 | indolepyruvate decarboxylase%2C putative |
| SAOUHSC_01336 | 0.8 | 1.2E-02 | conserved hypothetical protein |
| SAOUHSC_00121 | 2.0 | 1.2E-02 | capsular polysaccharide synthesis enzyme O-acetyl transferase Cap5H%2C putative |
| SAOUHSC_02434 | -1.1 | 1.2E-02 | conserved hypothetical protein |
| SAOUHSC_00700 | -1.3 | 1.2E-02 | conserved hypothetical protein |
| SAOUHSC_00405 | 1.0 | 1.2E-02 | conserved hypothetical protein |
| SAOUHSC_00681 | 0.9 | 1.3E-02 | major facilitator superfamily protein superfamily |
| SAOUHSC_01418 | -1.1 | 1.3E-02 | 2-oxoglutarate dehydrogenase%2C E1 component |
| SAOUHSC_00523 | -0.8 | 1.3E-02 | conserved hypothetical protein |
| SAOUHSC_00231 | 1.1 | 1.3E-02 | two-component response regulator%2C putative |
| SAOUHSC_02935 | 0.9 | 1.3E-02 | conserved hypothetical protein |
| SAOUHSC_02022 | -0.8 | 1.3E-02 | phage tail fiber protein%2C putative |
| SAOUHSC_00683 | 1.3 | 1.3E-02 | conserved hypothetical protein |
| SAOUHSC_02282 | 1.7 | 1.3E-02 | acetolactate synthase%2C large subunit%2C biosynthetic type |
| SAOUHSC_01615 | -0.7 | 1.3E-02 | DNA repair protein RecN |
| SAOUHSC_00339 | 2.1 | 1.3E-02 | conserved hypothetical protein |
| SAOUHSC_00698 | 1.0 | 1.3E-02 | conserved hypothetical protein |
| SAOUHSC_01626 | 0.8 | 1.3E-02 | proline dipeptidase%2C putative |
| SAOUHSC_01424 | -0.9 | 1.4E-02 | UDP-N-acetylglucosamine--N-acetylmuramyl-(pentapeptide) pyrophosphoryl-undecaprenol N-acetylglucosamine transferase |
| SAOUHSC_02982 | -0.7 | 1.4E-02 | conserved hypothetical protein |
| SAOUHSC_01915 | -1.0 | 1.4E-02 | conserved hypothetical protein |
| SAOUHSC_02740 | 1.2 | 1.4E-02 | drug transporter%2C putative |
| SAOUHSC_T00022 | 2.5 | 1.4E-02 | tRNA-Gly |
| SAOUHSC_00839 | -1.7 | 1.4E-02 | conserved hypothetical protein |
| SAOUHSC_01053 | 1.1 | 1.4E-02 | conserved hypothetical protein |
| SAOUHSC_01727 | 0.8 | 1.4E-02 | conserved hypothetical protein |
| SAOUHSC_00994 | 1.0 | 1.4E-02 | bifunctional autolysin precursor%2C putative |
| SAOUHSC_02377 | -1.0 | 1.4E-02 | pyrimidine nucleoside phosphorylase%2C putative |
| SAOUHSC_00485 | 1.0 | 1.4E-02 | hypoxanthine phosphoribosyltransferase |

| | | | |
|---|---|---|---|
| SAOUHSC_00793 | 0.9 | 1.4E-02 | conserved hypothetical protein |
| SAOUHSC_02770 | -2.5 | 1.4E-02 | conserved hypothetical protein |
| SAOUHSC_T00048 | 1.9 | 1.4E-02 | tRNA-Ser |
| SAOUHSC_01868 | 0.8 | 1.4E-02 | conserved hypothetical protein |
| SAOUHSC_00247 | -1.2 | 1.4E-02 | conserved hypothetical protein |
| SAOUHSC_01639 | 2.1 | 1.4E-02 | conserved hypothetical protein |
| SAOUHSC_01749 | 1.1 | 1.4E-02 | S-adenosylmethionine:tRNA ribosyltransferase-isomerase |
| SAOUHSC_02461 | -1.1 | 1.4E-02 | transcriptional regulator%2C merR family%2C putative |
| SAOUHSC_00085 | 1.5 | 1.5E-02 | conserved hypothetical protein |
| SAOUHSC_02157 | -2.1 | 1.5E-02 | conserved hypothetical protein |
| SAOUHSC_00783 | -1.0 | 1.5E-02 | conserved hypothetical protein |
| SAOUHSC_02102 | -0.8 | 1.5E-02 | methionine aminopeptidase%2C type I |
| SAOUHSC_00581 | 1.0 | 1.5E-02 | conserved hypothetical protein |
| SAOUHSC_01828 | -1.1 | 1.5E-02 | GAF domain protein |
| SAOUHSC_00376 | 1.3 | 1.5E-02 | conserved hypothetical protein |
| SAOUHSC_01159 | -1.0 | 1.5E-02 | isoleucyl-tRNA synthetase |
| SAOUHSC_00584 | -1.2 | 1.5E-02 | conserved hypothetical protein |
| SAOUHSC_01421 | 5.7 | 1.5E-02 | hypothetical protein |
| SAOUHSC_01236 | -0.8 | 1.5E-02 | ribosome recycling factor |
| SAOUHSC_02256 | 0.8 | 1.5E-02 | abortive infection protein |
| SAOUHSC_01472 | -0.8 | 1.5E-02 | DnaQ family exonuclease/DinG family helicase%2C putative |
| SAOUHSC_00244 | 1.2 | 1.5E-02 | conserved hypothetical protein |
| SAOUHSC_01784 | -1.2 | 1.5E-02 | ribosomal protein L20 |
| SAOUHSC_01311 | 2.6 | 1.5E-02 | ABC transporter%2C ATP-binding protein%2C putative |
| SAOUHSC_02259 | -0.8 | 1.6E-02 | conserved hypothetical protein |
| SAOUHSC_02877 | -1.1 | 1.6E-02 | squalene synthase%2C putative |
| SAOUHSC_02452 | -1.6 | 1.6E-02 | tagatose 1%2C6-diphosphate aldolase |
| SAOUHSC_02409 | -1.2 | 1.6E-02 | arginase |
| SAOUHSC_02893 | 1.3 | 1.7E-02 | conserved hypothetical protein |
| SAOUHSC_02023 | -0.8 | 1.7E-02 | bifunctional autolysin precursor |
| SAOUHSC_00027 | -1.0 | 1.7E-02 | conserved hypothetical protein |
| SAOUHSC_T00038 | 4.7 | 1.7E-02 | tRNA-Met |
| SAOUHSC_00167 | 1.0 | 1.7E-02 | peptide ABC transporter%2C ATP-binding protein%2C putative |
| SAOUHSC_02103 | -1.2 | 1.7E-02 | conserved hypothetical protein |
| SAOUHSC_00890 | -0.8 | 1.8E-02 | conserved hypothetical protein |
| SAOUHSC_01185 | -0.9 | 1.8E-02 | radical SAM enzyme%2C Cfr family |
| SAOUHSC_00928 | 1.9 | 1.8E-02 | oligopeptide ABC transporter%2C substrate-binding protein%2C putative |
| SAOUHSC_01268 | 1.2 | 1.8E-02 | conserved hypothetical protein |
| SAOUHSC_01789 | 2.9 | 1.8E-02 | conserved hypothetical protein |
| SAOUHSC_00127 | 1.5 | 1.8E-02 | cap5N protein/UDP-glucose 4-epimerase%2C putative |
| SAOUHSC_00585 | 2.1 | 1.8E-02 | conserved hypothetical protein |
| SAOUHSC_02803 | 1.8 | 1.8E-02 | fibronectin-binding protein precursor%2C putative |
| SAOUHSC_02669 | -0.9 | 1.8E-02 | conserved hypothetical protein |
| SAOUHSC_01822 | -0.7 | 1.8E-02 | conserved hypothetical protein |
| SAOUHSC_02171 | -0.8 | 1.8E-02 | staphylokinase precursor%2C putative |
| SAOUHSC_02302 | 0.9 | 1.8E-02 | sigmaB regulation protein RsbU%2C putative |
| SAOUHSC_01787 | -1.2 | 1.8E-02 | conserved hypothetical protein |
| SAOUHSC_02540 | 1.0 | 1.8E-02 | molybdopterin converting factor moa%2C putative |
| SAOUHSC_01738 | -1.0 | 1.8E-02 | histidyl-tRNA synthetase |
| SAOUHSC_00607 | 0.8 | 1.8E-02 | conserved hypothetical protein |
| SAOUHSC_01670 | -1.1 | 1.9E-02 | cytidine deaminase |
| SAOUHSC_02456 | -0.9 | 1.9E-02 | lactose phosphotransferase system repressor%2C putative |
| SAOUHSC_02153 | 1.4 | 1.9E-02 | conserved hypothetical protein |
| SAOUHSC_02961 | -0.8 | 1.9E-02 | conserved hypothetical protein |
| SAOUHSC_00183 | -1.9 | 1.9E-02 | membrane protein%2C putative |
| SAOUHSC_01596 | 0.9 | 1.9E-02 | conserved hypothetical protein |
| SAOUHSC_02552 | 1.9 | 1.9E-02 | conserved hypothetical protein |
| SAOUHSC_02882 | -0.9 | 1.9E-02 | conserved hypothetical protein |
| SAOUHSC_02416 | 4.8 | 1.9E-02 | hypothetical protein |
| SAOUHSC_00699 | -0.7 | 1.9E-02 | deoxyribodipyrimidine photolyase%2C putative |
| SAOUHSC_01655 | 1.4 | 1.9E-02 | conserved hypothetical protein |
| SAOUHSC_02047 | -0.9 | 2.0E-02 | phage putative head morphogenesis protein%2C SPP1 gp7 family domain protein |
| SAOUHSC_02911 | 1.1 | 2.0E-02 | conserved hypothetical protein |
| SAOUHSC_02899 | 1.2 | 2.0E-02 | conserved hypothetical protein |
| SAOUHSC_01478 | 1.4 | 2.0E-02 | conserved hypothetical protein |
| SAOUHSC_01508 | 1.6 | 2.0E-02 | conserved hypothetical protein |
| SAOUHSC_02020 | -1.0 | 2.0E-02 | holin |
| SAOUHSC_01435 | 0.6 | 2.0E-02 | thymidylate synthase%2C putative |
| SAOUHSC_02504 | -1.3 | 2.1E-02 | ribosomal protein L29 |
| SAOUHSC_00693 | -0.8 | 2.1E-02 | conserved hypothetical protein |
| SAOUHSC_00297 | -0.9 | 2.1E-02 | conserved hypothetical protein |
| SAOUHSC_01360 | -1.0 | 2.1E-02 | peptide methionine sulfoxide reductase |
| SAOUHSC_01373 | 0.8 | 2.1E-02 | methicillin resistance factor%2C FemA%2C putative |
| SAOUHSC_01877 | 1.3 | 2.1E-02 | conserved hypothetical protein |
| SAOUHSC_00439 | -0.9 | 2.2E-02 | conserved hypothetical protein |
| SAOUHSC_01471 | -0.6 | 2.2E-02 | asparaginyl-tRNA synthetase%2Cputative |
| SAOUHSC_00575 | -1.0 | 2.2E-02 | conserved hypothetical protein |
| SAOUHSC_00345 | 1.2 | 2.3E-02 | conserved hypothetical protein |
| SAOUHSC_00665 | -0.9 | 2.3E-02 | conserved hypothetical protein |
| SAOUHSC_02832 | 1.6 | 2.3E-02 | conserved hypothetical protein |
| SAOUHSC_00097 | 1.6 | 2.3E-02 | purine nucleoside phosphorylase |
| SAOUHSC_00911 | 0.9 | 2.3E-02 | conserved hypothetical protein |
| SAOUHSC_00798 | -1.4 | 2.4E-02 | phosphoglycerate mutase%2C 2%2C3-bisphosphoglycerate-independent |
| SAOUHSC_02531 | 1.7 | 2.4E-02 | conserved hypothetical protein |
| SAOUHSC_00162 | -0.7 | 2.4E-02 | type I site-specific deoxyribonuclease%2C HsdR family%2C putative |
| SAOUHSC_00138 | 1.3 | 2.4E-02 | conserved hypothetical protein |
| SAOUHSC_00169 | 1.5 | 2.4E-02 | peptide ABC transporter%2C permease protein%2C putative |
| SAOUHSC_00887 | -1.2 | 2.4E-02 | Na+/H+ antiporter subunit%2C putative |
| SAOUHSC_02324 | -1.2 | 2.4E-02 | conserved hypothetical protein |
| SAOUHSC_02457 | -1.1 | 2.4E-02 | transcriptional regulator%2C Sir2 family%2C putative |
| SAOUHSC_01720 | -0.7 | 2.4E-02 | conserved hypothetical protein |
| SAOUHSC_00821 | -0.7 | 2.4E-02 | conserved hypothetical protein |
| SAOUHSC_01535 | -1.0 | 2.4E-02 | conserved hypothetical phage protein |

| | | | |
|---|---|---|---|
| SAOUHSC_01001 | -1.3 | 2.4E-02 | quinol oxidase%2C subunit I |
| SAOUHSC_01799 | -0.7 | 2.5E-02 | Histidine kinase-%2C DNA gyrase B-%2C and HSP90-like ATPase domain protein |
| SAOUHSC_02733 | 1.0 | 2.5E-02 | membrane protein%2C putative |
| SAOUHSC_01162 | 0.8 | 2.5E-02 | lipoprotein signal peptidase |
| SAOUHSC_01919 | -1.1 | 2.5E-02 | conserved hypothetical protein |
| SAOUHSC_02784 | 1.2 | 2.5E-02 | conserved hypothetical protein |
| SAOUHSC_01975 | -0.6 | 2.5E-02 | conserved hypothetical protein |
| SAOUHSC_00903 | 0.8 | 2.5E-02 | Signal peptidase IB%2C putative |
| SAOUHSC_01973 | -0.6 | 2.6E-02 | conserved hypothetical protein |
| SAOUHSC_01285 | -0.9 | 2.6E-02 | conserved hypothetical protein |
| SAOUHSC_00161 | 1.6 | 2.6E-02 | conserved hypothetical protein |
| SAOUHSC_02473 | -2.3 | 2.6E-02 | hypothetical protein |
| SAOUHSC_00124 | 1.8 | 2.6E-02 | capsular polysaccharide biosynthesis protein Cap5K%2C putative |
| SAOUHSC_01372 | 0.9 | 2.7E-02 | tryptophan synthase%2C alpha subunit |
| SAOUHSC_02126 | -0.7 | 2.7E-02 | adenylosuccinate lyase |
| SAOUHSC_01038 | 0.7 | 2.7E-02 | polypeptide deformylase |
| SAOUHSC_02547 | -0.8 | 2.7E-02 | molybdenum ABC transporter%2C permease protein%2C putative |
| SAOUHSC_00406 | 0.7 | 2.7E-02 | conserved hypothetical protein |
| SAOUHSC_01962 | 0.7 | 2.7E-02 | uroporphyrinogen decarboxylase |
| SAOUHSC_00427 | 0.9 | 2.8E-02 | autolysin precursor%2C putative |
| SAOUHSC_02900 | 0.7 | 2.8E-02 | conserved hypothetical protein |
| SAOUHSC_01473 | -0.6 | 2.8E-02 | BirA bifunctional protein%2C putative |
| SAOUHSC_01691 | 1.1 | 2.8E-02 | DNA internalization-related competence protein ComEC/Rec2 |
| SAOUHSC_02119 | 0.8 | 2.8E-02 | proline uptake protein |
| SAOUHSC_01695 | 0.7 | 2.8E-02 | conserved hypothetical protein |
| SAOUHSC_01369 | -1.4 | 2.8E-02 | indole-3-glycerol phosphate synthase%2C putative |
| SAOUHSC_03035 | -0.7 | 2.8E-02 | conserved hypothetical protein |
| SAOUHSC_01771 | 0.7 | 2.9E-02 | glutamate-1-semialdehyde-2%2C1-aminomutase |
| SAOUHSC_01047 | -1.2 | 2.9E-02 | spermidine/putrescine ABC transporter%2C permease protein%2C putative |
| SAOUHSC_02161 | 0.7 | 2.9E-02 | MHC class II analog protein |
| SAOUHSC_00694 | -0.7 | 2.9E-02 | conserved hypothetical protein |
| SAOUHSC_00953 | 0.6 | 2.9E-02 | conserved hypothetical protein |
| SAOUHSC_01813 | -0.6 | 3.0E-02 | conserved hypothetical protein |
| SAOUHSC_00870 | 0.8 | 3.0E-02 | dltB protein%2C putative |
| SAOUHSC_02522 | 0.9 | 3.0E-02 | conserved hypothetical protein |
| SAOUHSC_01598 | 0.7 | 3.0E-02 | AtsA/ElaC family protein |
| SAOUHSC_01044 | -1.0 | 3.0E-02 | conserved hypothetical protein |
| SAOUHSC_02176 | -1.3 | 3.0E-02 | conserved hypothetical phage protein |
| SAOUHSC_02908 | -0.8 | 3.0E-02 | conserved hypothetical protein |
| SAOUHSC_02375 | -1.0 | 3.0E-02 | autoinducer-2 production protein LuxS%2C putative |
| SAOUHSC_01258 | 0.7 | 3.0E-02 | conserved hypothetical protein |
| SAOUHSC_01647 | 1.1 | 3.0E-02 | conserved hypothetical protein |
| SAOUHSC_00096 | -1.1 | 3.0E-02 | transcriptional regulator%2C GntR family%2C putative |
| SAOUHSC_00143 | 0.8 | 3.0E-02 | conserved hypothetical protein |
| SAOUHSC_00354 | 0.8 | 3.1E-02 | conserved hypothetical protein |
| SAOUHSC_00559 | 5.1 | 3.1E-02 | conserved hypothetical protein |
| SAOUHSC_02376 | -0.9 | 3.2E-02 | conserved hypothetical protein |
| SAOUHSC_01999 | 0.8 | 3.2E-02 | conserved hypothetical protein |
| SAOUHSC_00163 | -0.6 | 3.2E-02 | conserved hypothetical protein |
| SAOUHSC_01879 | -0.9 | 3.2E-02 | virulence factor regulator protein |
| SAOUHSC_02150 | -0.7 | 3.2E-02 | conserved hypothetical protein |
| SAOUHSC_01593 | -0.7 | 3.2E-02 | NUDIX domain protein |
| SAOUHSC_00428 | -0.9 | 3.2E-02 | conserved hypothetical protein |
| SAOUHSC_02974 | -0.9 | 3.2E-02 | conserved hypothetical protein |
| SAOUHSC_02984 | -0.8 | 3.3E-02 | conserved hypothetical protein |
| SAOUHSC_00877 | -1.0 | 3.3E-02 | conserved hypothetical protein |
| SAOUHSC_T0004 | 3.5 | 3.3E-02 | tRNA-Arg |
| SAOUHSC_02353 | -1.0 | 3.3E-02 | uracil phosphoribosyltransferase |
| SAOUHSC_01173 | 2.6 | 3.3E-02 | conserved hypothetical protein |
| SAOUHSC_00473 | 2.5 | 3.4E-02 | hypothetical protein |
| SAOUHSC_02895 | -0.6 | 3.4E-02 | conserved hypothetical protein |
| SAOUHSC_02249 | 0.8 | 3.4E-02 | conserved hypothetical protein |
| SAOUHSC_01306 | 3.1 | 3.4E-02 | conserved hypothetical protein |
| SAOUHSC_01932 | 0.7 | 3.4E-02 | type I restriction-modification enzyme%2C S subunit%2C EcoA family%2C putative |
| SAOUHSC_01668 | -0.9 | 3.5E-02 | GTP-binding protein Era |
| SAOUHSC_00923 | 0.8 | 3.5E-02 | conserved hypothetical protein |
| SAOUHSC_03047 | -2.4 | 3.5E-02 | conserved hypothetical protein |
| SAOUHSC_01261 | 0.8 | 3.5E-02 | competence-damage inducible protein cinA |
| SAOUHSC_01918 | -0.8 | 3.5E-02 | conserved hypothetical protein |
| SAOUHSC_01240 | -1.0 | 3.6E-02 | prolyl-tRNA synthetase |
| SAOUHSC_00034 | 2.4 | 3.6E-02 | conserved hypothetical protein |
| SAOUHSC_02248 | 0.8 | 3.6E-02 | conserved hypothetical protein |
| SAOUHSC_02758 | 1.9 | 3.6E-02 | conserved hypothetical protein |
| SAOUHSC_00941 | -0.8 | 3.6E-02 | conserved hypothetical protein |
| SAOUHSC_00779 | -0.7 | 3.6E-02 | excinuclease ABC subunit B%2C putative |
| SAOUHSC_02980 | -0.6 | 3.7E-02 | conserved hypothetical protein |
| SAOUHSC_01327 | 0.6 | 3.7E-02 | catalase |
| SAOUHSC_01401 | -0.8 | 3.7E-02 | diaminopimelate decarboxylase |
| SAOUHSC_00030 | 0.7 | 3.7E-02 | conserved hypothetical protein |
| SAOUHSC_00125 | 1.2 | 3.7E-02 | cap5L protein/glycosyltransferase%2C putative |
| SAOUHSC_00332 | 1.0 | 3.8E-02 | conserved hypothetical protein |
| SAOUHSC_01982 | -0.6 | 3.8E-02 | ribosomal large subunit pseudouridine synthase%2C RluD subfamily%2C putative |
| SAOUHSC_02107 | -0.7 | 3.8E-02 | UDP-N-acetylmuramyl tripeptide synthetase%2C putative |
| SAOUHSC_01807 | -0.8 | 3.8E-02 | 6-phosphofructokinase%2C putative |
| SAOUHSC_00056 | -0.6 | 3.9E-02 | conserved hypothetical protein |
| SAOUHSC_01123 | -1.1 | 3.9E-02 | conserved hypothetical protein |
| SAOUHSC_00773 | 1.2 | 4.0E-02 | LysM domain protein |
| SAOUHSC_02368 | -0.6 | 4.0E-02 | CTP synthase |
| SAOUHSC_02046 | -2.0 | 4.0E-02 | conserved hypothetical phage protein |
| SAOUHSC_02535 | 1.6 | 4.0E-02 | conserved hypothetical protein |
| SAOUHSC_00197 | 2.4 | 4.0E-02 | conserved hypothetical protein |

| | | | |
|---|---|---|---|
| SAOUHSC_02486 | -1.4 | 4.0E-02 | ribosomal protein S11%2C putative |
| SAOUHSC_00493 | -0.7 | 4.1E-02 | lysyl-tRNA synthetase |
| SAOUHSC_01301 | 4.8 | 4.1E-02 | conserved hypothetical protein |
| SAOUHSC_00846 | 1.3 | 4.1E-02 | conserved hypothetical protein |
| SAOUHSC_02166 | 1.5 | 4.1E-02 | hypothetical phage protein |
| SAOUHSC_01859 | -0.8 | 4.2E-02 | conserved hypothetical protein |
| SAOUHSC_00864 | -0.9 | 4.2E-02 | conserved hypothetical protein |
| SAOUHSC_01234 | -0.7 | 4.2E-02 | translation elongation factor Ts |
| SAOUHSC_00152 | 1.0 | 4.2E-02 | conserved hypothetical protein |
| SAOUHSC_00606 | 0.6 | 4.2E-02 | conserved hypothetical protein |
| SAOUHSC_00226 | -0.7 | 4.2E-02 | conserved hypothetical protein |
| SAOUHSC_01255 | 0.8 | 4.2E-02 | conserved hypothetical protein |
| SAOUHSC_02581 | -0.8 | 4.3E-02 | conserved hypothetical protein |
| SAOUHSC_A01436 | 1.7 | 4.3E-02 | hypothetical protein |
| SAOUHSC_02271 | 1.2 | 4.3E-02 | conserved hypothetical protein |
| SAOUHSC_02169 | 2.4 | 4.3E-02 | conserved hypothetical phage protein |
| SAOUHSC_02992 | 2.0 | 4.3E-02 | conserved hypothetical protein |
| SAOUHSC_02956 | -0.9 | 4.4E-02 | DNA-binding response regulator%2C putative |
| SAOUHSC_01633 | 1.0 | 4.4E-02 | glycine cleavage system P-protein subunit I%2C putative |
| SAOUHSC_01304 | 1.0 | 4.4E-02 | conserved hypothetical protein |
| SAOUHSC_02087 | -0.7 | 4.5E-02 | conserved hypothetical phage protein |
| SAOUHSC_03019 | 0.9 | 4.5E-02 | ABC transporter%2C ATP-binding protein%2C putative |
| SAOUHSC_00065 | -0.7 | 4.5E-02 | conserved hypothetical protein |
| SAOUHSC_02690 | -0.6 | 4.5E-02 | conserved hypothetical protein |
| SAOUHSC_00380 | 2.8 | 4.5E-02 | hypothetical protein |
| SAOUHSC_00889 | 0.8 | 4.5E-02 | Na+/H+ antiporter subunit%2C putative |
| SAOUHSC_01333 | -0.8 | 4.6E-02 | LexA repressor |
| SAOUHSC_02089 | 1.0 | 4.6E-02 | integrase%2C phage family%2C putative |
| SAOUHSC_01762 | -0.9 | 4.6E-02 | conserved hypothetical protein |
| SAOUHSC_00844 | -0.6 | 4.6E-02 | conserved hypothetical protein |
| SAOUHSC_01893 | 1.0 | 4.7E-02 | arsenical pump membrane protein subfamily |
| SAOUHSC_00651 | 0.7 | 4.7E-02 | conserved hypothetical protein |
| SAOUHSC_00326 | 2.9 | 4.7E-02 | conserved hypothetical protein |
| SAOUHSC_02694 | -0.9 | 4.7E-02 | conserved hypothetical protein |
| SAOUHSC_02241 | -0.7 | 4.7E-02 | conserved hypothetical protein |
| SAOUHSC_03006 | -1.1 | 4.7E-02 | lipase |
| SAOUHSC_02721 | -1.0 | 4.7E-02 | conserved hypothetical protein |
| SAOUHSC_02633 | -0.7 | 4.7E-02 | conserved hypothetical protein |
| SAOUHSC_02718 | 0.9 | 4.8E-02 | conserved hypothetical protein |
| SAOUHSC_T00040 | 1.5 | 4.8E-02 | tRNA-Met |
| SAOUHSC_01891 | 1.1 | 4.8E-02 | arsenate operon regulator |
| SAOUHSC_02390 | 0.7 | 4.8E-02 | lytic regulatory protein%2C putative |
| SAOUHSC_01676 | -0.7 | 4.8E-02 | conserved hypothetical protein |
| SAOUHSC_01189 | -0.8 | 4.9E-02 | ribulose-phosphate 3-epimerase |
| SAOUHSC_01312 | 1.6 | 4.9E-02 | conserved hypothetical protein |
| SAOUHSC_01434 | -0.7 | 4.9E-02 | dihydrofolate reductase |
| SAOUHSC_01729 | 0.9 | 4.9E-02 | conserved hypothetical protein |
| SAOUHSC_02476 | -0.8 | 4.9E-02 | conserved hypothetical protein |
| SAOUHSC_01704 | 2.3 | 5.0E-02 | conserved hypothetical protein |
| SAOUHSC_02106 | -0.6 | 5.0E-02 | conserved hypothetical protein |
| SAOUHSC_00445 | -0.8 | 5.0E-02 | recombination protein RecR |

**Supplementary table 3. All significant fold changes of genes in BFT vs BFU.** Genes with non-significant fold changes were not included. Padj is the adjusted P value (significance threshold P<0.05). Genes ordered by significance.

| Gene id | log2 Fold Change | padj | Gene description |
|---|---|---|---|
| SAOUHSC_00898 | -8.9 | 1.3E-140 | argininosuccinate lyase |
| SAOUHSC_00899 | -8.9 | 3.3E-127 | argininosuccinate synthase |
| SAOUHSC_01135 | -10.4 | 1.4E-125 | conserved hypothetical protein |
| SAOUHSC_02260 | -8.4 | 4.8E-123 | delta-hemolysin precursor |
| SAOUHSC_01919 | -7.0 | 1.5E-92 | conserved hypothetical protein |
| SAOUHSC_01166 | -7.1 | 4.5E-76 | aspartate carbamoyltransferase |
| SAOUHSC_02333 | 7.4 | 1.1E-75 | sceD protein%2C putative |
| SAOUHSC_02646 | 7.0 | 2.9E-75 | conserved hypothetical protein |
| SAOUHSC_01168 | -6.6 | 8.9E-72 | dihydroorotase |
| SAOUHSC_00533 | 6.0 | 6.7E-67 | conserved hypothetical protein |
| SAOUHSC_01110 | -9.4 | 9.0E-67 | fibrinogen-binding protein-related |
| SAOUHSC_01170 | -5.4 | 1.3E-64 | carbamoyl-phosphate synthase%2C large subunit |
| SAOUHSC_00808 | -7.0 | 2.6E-64 | conserved hypothetical protein |
| SAOUHSC_01165 | -6.8 | 7.9E-62 | uracil permease%2C putative |
| SAOUHSC_01164 | -7.0 | 1.2E-61 | PyrR bifunctional protein |
| SAOUHSC_02767 | -6.1 | 1.4E-61 | peptide ABC transporter%2C peptide-binding protein%2C putative |
| SAOUHSC_01918 | -8.6 | 1.4E-61 | conserved hypothetical protein |
| SAOUHSC_01169 | -6.2 | 5.9E-61 | carbamoyl-phosphate synthase%2C small subunit |
| SAOUHSC_00717 | -6.9 | 8.8E-61 | conserved hypothetical protein |
| SAOUHSC_00608 | -6.7 | 3.5E-58 | alcohol dehydrogenase I%2C putative |
| SAOUHSC_03001 | -6.4 | 1.9E-57 | ica operon transcriptional regulator IcaR%2C putative |
| SAOUHSC_02261 | -5.4 | 1.9E-56 | accessory gene regulator protein B |
| SAOUHSC_02866 | 7.4 | 1.5E-55 | conserved hypothetical protein |
| SAOUHSC_00257 | -6.2 | 3.2E-54 | conserved hypothetical protein |
| SAOUHSC_00569 | 5.2 | 7.3E-51 | conserved hypothetical protein |
| SAOUHSC_02402 | 4.9 | 6.8E-49 | PTS system%2C mannitol-specific IIa component%2C putative |
| SAOUHSC_01879 | -5.2 | 1.3E-46 | virulence factor regulator protein |
| SAOUHSC_01653 | 5.2 | 3.1E-46 | superoxide dismutase%2C Mn%2C putative |
| SAOUHSC_01171 | -5.0 | 7.4E-46 | orotidine 5'-phosphate decarboxylase |
| SAOUHSC_01120 | -7.3 | 2.6E-45 | conserved hypothetical protein |
| SAOUHSC_02403 | 4.6 | 1.1E-44 | mannitol-1-phosphate 5-dehydrogenase%2C putative |
| SAOUHSC_00830 | -5.4 | 5.5E-44 | conserved hypothetical protein |
| SAOUHSC_00831 | 7.0 | 8.5E-44 | conserved hypothetical protein |
| SAOUHSC_00634 | -5.2 | 5.6E-42 | ABC transporter%2C substrate-binding protein%2C putative |
| SAOUHSC_01180 | -5.3 | 5.9E-42 | conserved hypothetical protein |
| SAOUHSC_02264 | -4.5 | 2.4E-41 | accessory gene regulator protein C |
| SAOUHSC_02559 | 6.6 | 4.1E-41 | urease%2C beta subunit%2C putative |
| SAOUHSC_01096 | -4.9 | 5.2E-41 | conserved hypothetical protein |
| SAOUHSC_02163 | -8.2 | 5.7E-41 | conserved hypothetical phage protein |
| SAOUHSC_00716 | -6.3 | 9.3E-41 | conserved hypothetical protein |
| SAOUHSC_00637 | -6.3 | 2.9E-40 | conserved hypothetical protein |
| SAOUHSC_02589 | -4.3 | 4.7E-40 | conserved hypothetical protein |
| SAOUHSC_02909 | -4.5 | 5.0E-40 | dihydroorotate dehydrogenase |
| SAOUHSC_02641 | 5.7 | 1.4E-39 | permease%2C putative domain protein |
| SAOUHSC_01997 | -4.6 | 9.5E-39 | ferric uptake regulator-like protein%2C putative |
| SAOUHSC_00636 | -5.6 | 2.4E-38 | iron (chelated) ABC transporter%2C permease protein%2C putative |
| SAOUHSC_02900 | 4.2 | 1.6E-37 | conserved hypothetical protein |
| SAOUHSC_02561 | 5.5 | 1.9E-37 | urease%2C alpha subunit |
| SAOUHSC_02709 | -7.2 | 4.6E-37 | leukocidin s subunit precursor%2C putative |
| SAOUHSC_02013 | 4.4 | 5.8E-37 | conserved hypothetical protein |
| SAOUHSC_01788 | -5.1 | 2.1E-36 | threonyl-tRNA synthetase |
| SAOUHSC_02566 | -5.0 | 3.1E-36 | conserved hypothetical protein |
| SAOUHSC_01131 | -4.6 | 3.9E-36 | conserved hypothetical protein |
| SAOUHSC_00009 | -4.5 | 1.1E-35 | seryl-tRNA synthetase |
| SAOUHSC_02604 | 5.3 | 2.2E-35 | conserved hypothetical protein |
| SAOUHSC_02363 | 4.4 | 7.4E-35 | aldehyde dehydrogenase%2C putative |
| SAOUHSC_00554 | 4.4 | 1.5E-34 | SIS domain protein |
| SAOUHSC_00036 | 6.5 | 1.0E-33 | conserved hypothetical protein |
| SAOUHSC_00553 | 4.1 | 3.4E-33 | conserved hypothetical protein |
| SAOUHSC_00882 | -5.6 | 4.3E-33 | conserved hypothetical protein |
| SAOUHSC_02772 | 4.7 | 4.3E-33 | conserved hypothetical protein |
| SAOUHSC_02645 | 5.9 | 6.0E-32 | conserved hypothetical protein |
| SAOUHSC_02974 | -6.2 | 3.1E-31 | conserved hypothetical protein |
| SAOUHSC_00798 | 4.8 | 4.1E-31 | phosphoglycerate mutase%2C 2%2C3-bisphosphoglycerate-independent |
| SAOUHSC_00061 | 4.3 | 3.8E-30 | conserved hypothetical protein |
| SAOUHSC_02744 | -3.8 | 1.2E-29 | amino acid ABC transporter%2C ATP-binding protein%2C putative |
| SAOUHSC_00796 | 4.7 | 1.8E-29 | phosphoglycerate kinase%2C putative |
| SAOUHSC_00123 | 3.9 | 1.9E-29 | capsular polysaccharide biosynthesis protein Cap5J%2C putative |
| SAOUHSC_00421 | 5.9 | 3.0E-29 | conserved hypothetical protein |
| SAOUHSC_00001 | -4.0 | 3.3E-29 | chromosomal replication initiator protein DnaA |
| SAOUHSC_00135 | 4.3 | 3.4E-29 | conserved hypothetical protein |
| SAOUHSC_02565 | 4.0 | 1.1E-28 | urease accessory protein UreD%2C putative |
| SAOUHSC_02708 | -5.5 | 1.6E-28 | gamma-hemolysin h-gamma-ii subunit%2C putative |
| SAOUHSC_02905 | -5.6 | 2.2E-28 | conserved hypothetical protein |
| SAOUHSC_01318 | -4.6 | 2.5E-28 | conserved hypothetical protein |
| SAOUHSC_00422 | 4.5 | 6.0E-28 | trans-sulfuration enzyme family protein%2C putative |
| SAOUHSC_00855 | 4.4 | 7.5E-28 | conserved hypothetical protein |
| SAOUHSC_00253 | -5.1 | 2.4E-27 | conserved hypothetical protein |
| SAOUHSC_01566 | 5.4 | 3.0E-27 | phi APSE P51-like protein |
| SAOUHSC_00992 | -4.3 | 3.1E-27 | transcriptional regulator%2C MarR family%2C putative |
| SAOUHSC_00617 | -4.4 | 3.8E-27 | conserved hypothetical protein |
| SAOUHSC_02640 | 5.1 | 3.9E-27 | conserved hypothetical protein |
| SAOUHSC_00797 | 4.5 | 4.9E-27 | triosephosphate isomerase |
| SAOUHSC_02563 | 4.3 | 7.0E-27 | urease accessory protein UreF%2C putative |
| SAOUHSC_02936 | 4.3 | 1.6E-26 | conserved hypothetical protein |

| | | | |
|---|---|---|---|
| SAOUHSC_00715 | -3.7 | 1.8E-26 | response regulator%2C putative |
| SAOUHSC_01133 | -5.3 | 2.5E-26 | conserved hypothetical protein |
| SAOUHSC_00199 | -5.4 | 3.7E-26 | conserved hypothetical protein |
| SAOUHSC_00195 | -5.6 | 4.7E-26 | acetyl-CoA acetyltransferase%2C putative |
| SAOUHSC_00035 | 5.9 | 5.6E-26 | conserved hypothetical protein |
| SAOUHSC_01027 | 3.5 | 8.3E-26 | conserved hypothetical protein |
| SAOUHSC_00163 | -3.6 | 1.1E-25 | conserved hypothetical protein |
| SAOUHSC_00767 | -3.8 | 1.4E-25 | conserved hypothetical protein |
| SAOUHSC_02558 | 5.1 | 1.8E-25 | urease%2C gamma subunit |
| SAOUHSC_02564 | 3.8 | 2.1E-25 | urease accessory protein UreG |
| SAOUHSC_02387 | 4.9 | 3.3E-25 | conserved hypothetical protein |
| SAOUHSC_00795 | 4.3 | 3.5E-25 | glyceraldehyde-3-phosphate dehydrogenase%2C type I |
| SAOUHSC_01565 | 6.4 | 4.0E-25 | phage-related protein |
| SAOUHSC_00196 | -6.0 | 5.0E-25 | conserved hypothetical protein |
| SAOUHSC_01319 | -4.1 | 5.9E-25 | aspartate kinase%2C putative |
| SAOUHSC_00119 | 3.5 | 7.5E-25 | capsular polysaccharide synthesis enzyme Cap8F |
| SAOUHSC_02665 | 4.9 | 1.5E-24 | conserved hypothetical protein |
| SAOUHSC_02899 | 4.2 | 1.9E-24 | conserved hypothetical protein |
| SAOUHSC_00272 | -6.3 | 2.0E-24 | conserved hypothetical protein |
| SAOUHSC_02401 | 4.3 | 2.1E-24 | conserved hypothetical protein |
| SAOUHSC_02849 | 3.3 | 2.7E-24 | pyruvate oxidase%2C putative |
| SAOUHSC_00544 | -3.9 | 2.8E-24 | sdrC protein%2C putative |
| SAOUHSC_00854 | 3.5 | 3.0E-24 | conserved hypothetical protein |
| SAOUHSC_01991 | -3.9 | 3.7E-24 | ABC transporter%2C permease protein%2C putative |
| SAOUHSC_02953 | -4.0 | 6.7E-24 | permease%2C putative domain protein |
| SAOUHSC_00923 | -3.8 | 6.8E-24 | conserved hypothetical protein |
| SAOUHSC_02669 | -3.7 | 8.0E-24 | conserved hypothetical protein |
| SAOUHSC_01815 | 3.9 | 9.4E-24 | conserved hypothetical protein |
| SAOUHSC_00287 | 3.4 | 1.0E-23 | ABC transporter%2C ATP-binding protein%2C putative |
| SAOUHSC_00300 | -3.6 | 2.2E-23 | lipase precursor |
| SAOUHSC_00069 | -4.1 | 2.4E-23 | protein A |
| SAOUHSC_00280 | -3.6 | 4.8E-23 | conserved hypothetical protein |
| SAOUHSC_00279 | -4.1 | 6.6E-23 | conserved hypothetical protein |
| SAOUHSC_02858 | -4.4 | 9.2E-23 | conserved hypothetical protein |
| SAOUHSC_02152 | -4.0 | 9.6E-23 | ABC transporter%2C ATP-binding protein%2C putative |
| SAOUHSC_01172 | -4.1 | 9.6E-23 | orotate phosphoribosyltransferase |
| SAOUHSC_02994 | 4.1 | 9.6E-23 | conserved hypothetical protein |
| SAOUHSC_02695 | -3.8 | 1.2E-22 | conserved hypothetical protein |
| SAOUHSC_00258 | -4.7 | 1.8E-22 | conserved hypothetical protein |
| SAOUHSC_00198 | -5.8 | 1.9E-22 | conserved hypothetical protein |
| SAOUHSC_02444 | 4.1 | 2.0E-22 | osmoprotectant transporter%2C BCCT family%2C opuD-like protein%2C putative |
| SAOUHSC_02244 | 3.2 | 3.5E-22 | conserved hypothetical protein |
| SAOUHSC_02036 | 3.5 | 4.0E-22 | phage structural protein%2C putative |
| SAOUHSC_01281 | -4.2 | 4.1E-22 | host factor 1 protein%2C putative |
| SAOUHSC_00120 | 3.4 | 5.3E-22 | UDP-N-acetylglucosamine 2-epimerase |
| SAOUHSC_02906 | -6.8 | 7.1E-22 | conserved hypothetical protein |
| SAOUHSC_02932 | -4.3 | 7.3E-22 | choline dehydrogenase |
| SAOUHSC_02995 | 3.8 | 7.5E-22 | conserved hypothetical protein |
| SAOUHSC_00281 | -3.6 | 1.4E-21 | conserved hypothetical protein |
| SAOUHSC_02907 | -7.6 | 1.4E-21 | conserved hypothetical protein |
| SAOUHSC_02167 | -5.6 | 1.6E-21 | conserved hypothetical phage protein |
| SAOUHSC_01661 | 3.8 | 1.7E-21 | conserved hypothetical protein |
| SAOUHSC_00669 | -3.2 | 1.7E-21 | conserved hypothetical protein |
| SAOUHSC_00118 | 3.4 | 2.1E-21 | capsular polysaccharide biosynthesis protein Cap5E%2C putative |
| SAOUHSC_00125 | 3.6 | 2.9E-21 | cap5L protein/glycosyltransferase%2C putative |
| SAOUHSC_00206 | -3.6 | 3.1E-21 | L-lactate dehydrogenase |
| SAOUHSC_02865 | -4.6 | 3.2E-21 | conserved hypothetical protein |
| SAOUHSC_02043 | 3.3 | 3.3E-21 | phage head protein%2C putative |
| SAOUHSC_00094 | -4.2 | 5.1E-21 | conserved hypothetical protein |
| SAOUHSC_02265 | -3.7 | 5.3E-21 | accessory gene regulator protein A |
| SAOUHSC_02710 | -4.8 | 6.0E-21 | leukocidin f subunit precursor |
| SAOUHSC_01650 | -3.2 | 7.7E-21 | conserved hypothetical protein |
| SAOUHSC_00122 | 3.4 | 1.4E-20 | capsular polysaccharide biosynthesis protein Cap5I%2C putative |
| SAOUHSC_02051 | 4.4 | 1.7E-20 | int gene activator RinA |
| SAOUHSC_02418 | 3.6 | 2.0E-20 | conserved hypothetical protein |
| SAOUHSC_00794 | 3.8 | 4.9E-20 | glycolytic operon regulator |
| SAOUHSC_00121 | 3.4 | 5.5E-20 | capsular polysaccharide synthesis enzyme O-acetyl transferase Cap5H%2C putative |
| SAOUHSC_00124 | 4.0 | 5.6E-20 | capsular polysaccharide biosynthesis protein Cap5K%2C putative |
| SAOUHSC_02862 | 3.2 | 6.2E-20 | ATP-dependent Clp protease%2C ATP-binding subunit ClpC%2C putative |
| SAOUHSC_02028 | 3.5 | 7.5E-20 | phiETA ORF57-like protein |
| SAOUHSC_00545 | -3.5 | 1.0E-19 | sdrD protein%2C putative |
| SAOUHSC_00136 | 4.2 | 1.7E-19 | conserved hypothetical protein |
| SAOUHSC_02933 | -3.7 | 3.9E-19 | betaine aldehyde dehydrogenase |
| SAOUHSC_02243 | -6.1 | 4.2E-19 | conserved hypothetical protein |
| SAOUHSC_00256 | -5.3 | 4.3E-19 | conserved hypothetical protein |
| SAOUHSC_01860 | 3.5 | 4.7E-19 | conserved hypothetical protein |
| SAOUHSC_00406 | -3.5 | 5.6E-19 | conserved hypothetical protein |
| SAOUHSC_01303 | -6.3 | 6.5E-19 | conserved hypothetical protein |
| SAOUHSC_00647 | -2.9 | 1.5E-18 | conserved hypothetical protein |
| SAOUHSC_02400 | 3.6 | 1.7E-18 | PTS system%2C mannitol-specific component%2C putative |
| SAOUHSC_00197 | -5.7 | 2.0E-18 | conserved hypothetical protein |
| SAOUHSC_00788 | 3.1 | 3.7E-18 | conserved hypothetical protein |
| SAOUHSC_00230 | -3.0 | 4.6E-18 | two-component sensor histidine kinase%2C putative |
| SAOUHSC_01574 | 5.4 | 6.1E-18 | Helix-turn-helix domain protein |
| SAOUHSC_02161 | -4.3 | 6.7E-18 | MHC class II analog protein |
| SAOUHSC_01464 | -2.8 | 6.9E-18 | conserved hypothetical protein |
| SAOUHSC_01571 | 5.4 | 7.9E-18 | SLT orf 71-like protein-related protein |
| SAOUHSC_01563 | 4.8 | 7.9E-18 | phage encoded DNA polymerase I |
| SAOUHSC_02029 | 3.2 | 1.1E-17 | phi ETA orf 56-like protein |
| SAOUHSC_00922 | -5.2 | 1.3E-17 | conserved hypothetical protein |
| SAOUHSC_02850 | 2.9 | 1.9E-17 | conserved hypothetical protein |
| SAOUHSC_00113 | -5.2 | 2.3E-17 | alcohol dehydrogenase%2C iron-containing%2C putative |
| SAOUHSC_00974 | -7.2 | 2.7E-17 | glycosyl transferase%2C group 1 |

| | | | |
|---|---|---|---|
| SAOUHSC_00806 | -4.0 | 2.8E-17 | conserved hypothetical protein |
| SAOUHSC_03035 | 4.1 | 3.4E-17 | conserved hypothetical protein |
| SAOUHSC_01114 | -12.5 | 3.7E-17 | fibrinogen-binding protein |
| SAOUHSC_02737 | 3.9 | 4.0E-17 | epimerase/dehydratase%2C putative |
| SAOUHSC_00488 | 3.1 | 4.1E-17 | conserved hypothetical protein |
| SAOUHSC_01387 | 4.9 | 4.6E-17 | conserved hypothetical protein |
| SAOUHSC_02151 | -3.9 | 5.2E-17 | conserved hypothetical protein |
| SAOUHSC_02532 | -4.1 | 5.4E-17 | conserved hypothetical protein |
| SAOUHSC_00160 | -3.8 | 7.5E-17 | conserved hypothetical protein |
| SAOUHSC_00714 | -3.6 | 8.1E-17 | sensor histidine kinase SaeS%2C putative |
| SAOUHSC_02455 | 4.1 | 8.4E-17 | galactose-6-phosphate isomerase%2C LacA subunit |
| SAOUHSC_01990 | -3.6 | 1.2E-16 | amino acid ABC transporter%2C ATP-binding protein%2C putative |
| SAOUHSC_02298 | 2.8 | 1.7E-16 | sigma factor B%2C putative |
| SAOUHSC_01121 | -7.2 | 1.7E-16 | alpha-hemolysin precursor |
| SAOUHSC_01143 | -2.9 | 2.0E-16 | S-adenosyl-methyltransferase MraW |
| SAOUHSC_00299 | -4.5 | 2.1E-16 | conserved hypothetical protein |
| SAOUHSC_02299 | 2.8 | 3.0E-16 | anti-sigma B factor%2C putative |
| SAOUHSC_00046 | -3.3 | 4.2E-16 | conserved hypothetical protein |
| SAOUHSC_00037 | 4.2 | 4.4E-16 | conserved hypothetical protein |
| SAOUHSC_02134 | -3.1 | 5.8E-16 | nitric oxide synthase%2C oxygenase domain%2C putative |
| SAOUHSC_02262 | -4.3 | 5.9E-16 | conserved hypothetical protein |
| SAOUHSC_02769 | -4.0 | 6.3E-16 | conserved hypothetical protein |
| SAOUHSC_02694 | -3.1 | 6.8E-16 | conserved hypothetical protein |
| SAOUHSC_01570 | 6.8 | 7.2E-16 | PVL orf 37-like protein |
| SAOUHSC_02047 | 3.4 | 7.6E-16 | phage putative head morphogenesis protein%2C SPP1 gp7 family domain protein |
| SAOUHSC_02648 | -3.0 | 8.8E-16 | L-lactate permease |
| SAOUHSC_02449 | 3.4 | 9.3E-16 | 6-phospho-beta-galactosidase |
| SAOUHSC_00330 | 3.0 | 1.1E-15 | conserved hypothetical protein |
| SAOUHSC_01971 | -3.7 | 1.1E-15 | conserved hypothetical protein |
| SAOUHSC_02383 | -2.8 | 1.1E-15 | conserved hypothetical protein |
| SAOUHSC_02562 | 4.1 | 1.4E-15 | urease accessory protein UreE%2C putative |
| SAOUHSC_02033 | 2.9 | 1.4E-15 | phage tape measure protein |
| SAOUHSC_01386 | 4.2 | 1.5E-15 | phosphate ABC transporter%2C permease protein%2C putative |
| SAOUHSC_01280 | -3.0 | 1.5E-15 | tRNA delta(2)-isopentenylpyrophosphate transferase |
| SAOUHSC_02973 | -4.4 | 1.8E-15 | conserved hypothetical protein |
| SAOUHSC_00162 | -2.7 | 1.9E-15 | type I site-specific deoxyribonuclease%2C HsdR family%2C putative |
| SAOUHSC_00137 | 3.5 | 2.3E-15 | conserved hypothetical protein |
| SAOUHSC_02095 | 3.2 | 2.4E-15 | conserved hypothetical protein |
| SAOUHSC_02985 | 3.1 | 3.3E-15 | preprotein translocase%2C SecA subunit%2C putative |
| SAOUHSC_00892 | -3.4 | 3.8E-15 | conserved hypothetical protein |
| SAOUHSC_01112 | -3.9 | 4.1E-15 | conserved hypothetical protein |
| SAOUHSC_02041 | 3.4 | 5.1E-15 | phi Mu50B-like protein |
| SAOUHSC_00975 | -5.2 | 5.7E-15 | conserved hypothetical protein |
| SAOUHSC_00948 | -2.8 | 5.7E-15 | conserved hypothetical protein |
| SAOUHSC_01920 | -5.6 | 5.9E-15 | conserved hypothetical protein |
| SAOUHSC_02154 | -3.3 | 6.0E-15 | ABC transporter%2C ATP-binding protein%2C putative |
| SAOUHSC_00309 | 2.9 | 7.3E-15 | conserved hypothetical protein |
| SAOUHSC_02450 | 3.9 | 7.7E-15 | pts system%2C lactose-specific IIBC component%2C putative |
| SAOUHSC_00407 | -4.3 | 8.1E-15 | conserved hypothetical protein |
| SAOUHSC_02399 | 2.8 | 8.4E-15 | glucosamine--fructose-6-phosphate aminotransferase%2C isomerizing |
| SAOUHSC_02034 | 3.5 | 9.8E-15 | conserved hypothetical phage protein |
| SAOUHSC_00927 | -2.8 | 1.0E-14 | oligopeptide ABC transporter%2C substrate-binding protein%2C putative |
| SAOUHSC_02963 | -2.7 | 1.1E-14 | clumping factor B%2C putative |
| SAOUHSC_02766 | -6.8 | 1.1E-14 | peptide ABC transporter%2C permease protein%2C putative |
| SAOUHSC_00469 | 3.4 | 1.1E-14 | conserved hypothetical protein |
| SAOUHSC_02016 | 4.2 | 1.2E-14 | conserved hypothetical phage protein |
| SAOUHSC_00139 | 3.2 | 1.3E-14 | conserved hypothetical protein |
| SAOUHSC_00426 | 3.5 | 1.5E-14 | ABC transporter%2C substrate-binding protein%2C putative |
| SAOUHSC_02770 | -4.6 | 1.8E-14 | conserved hypothetical protein |
| SAOUHSC_00316 | -3.3 | 1.8E-14 | conserved hypothetical protein |
| SAOUHSC_01081 | -4.1 | 1.9E-14 | conserved hypothetical protein |
| SAOUHSC_01119 | -4.5 | 2.2E-14 | conserved hypothetical protein |
| SAOUHSC_02254 | 3.1 | 2.4E-14 | chaperonin%2C 60 kDa%2C GrpEL%2C putative |
| SAOUHSC_01266 | 2.5 | 2.4E-14 | conserved hypothetical protein |
| SAOUHSC_00424 | 3.8 | 2.5E-14 | ABC transporter%2C permease protein%2C putative |
| SAOUHSC_02031 | 3.2 | 2.5E-14 | conserved hypothetical phage protein |
| SAOUHSC_00531 | 2.9 | 2.9E-14 | conserved hypothetical protein |
| SAOUHSC_00465 | -3.1 | 3.2E-14 | conserved hypothetical protein |
| SAOUHSC_02771 | 5.0 | 3.2E-14 | conserved hypothetical protein |
| SAOUHSC_00127 | 2.7 | 3.9E-14 | cap5N protein/UDP-glucose 4-epimerase%2C putative |
| SAOUHSC_02888 | -3.3 | 4.5E-14 | conserved hypothetical protein |
| SAOUHSC_02452 | 3.7 | 4.5E-14 | tagatose 1%2C6-diphosphate aldolase |
| SAOUHSC_02241 | -4.7 | 7.6E-14 | conserved hypothetical protein |
| SAOUHSC_01662 | 2.7 | 7.9E-14 | RNA polymerase sigma factor%2C putative |
| SAOUHSC_00924 | -2.7 | 8.3E-14 | conserved hypothetical protein |
| SAOUHSC_01130 | 3.0 | 9.6E-14 | conserved hypothetical protein |
| SAOUHSC_01627 | -3.0 | 9.8E-14 | conserved hypothetical protein |
| SAOUHSC_00807 | -3.7 | 1.1E-13 | conserved hypothetical protein |
| SAOUHSC_02874 | -3.5 | 1.1E-13 | cation-transporting ATPase%2C E1-E2 family%2C putative |
| SAOUHSC_00070 | -4.2 | 1.2E-13 | staphylococcal accessory regulator-like protein |
| SAOUHSC_01144 | -2.6 | 1.4E-13 | conserved hypothetical protein |
| SAOUHSC_02135 | -2.8 | 1.4E-13 | conserved hypothetical protein |
| SAOUHSC_00408 | -2.8 | 1.5E-13 | conserved hypothetical protein |
| SAOUHSC_00819 | -4.1 | 1.5E-13 | conserved hypothetical protein |
| SAOUHSC_02255 | 3.3 | 1.5E-13 | chaperonin%2C 10 kDa%2C GroES%2C putative |
| SAOUHSC_00876 | 2.7 | 1.9E-13 | conserved hypothetical protein |
| SAOUHSC_01567 | 5.7 | 2.0E-13 | conserved hypothetical phage protein |
| SAOUHSC_02077 | 4.6 | 2.1E-13 | phi PV83 orf 12-like protein-related protein |
| SAOUHSC_00736 | 2.6 | 2.2E-13 | conserved hypothetical protein |
| SAOUHSC_01002 | -2.8 | 2.3E-13 | quinol oxidase AA3%2C subunit II%2C putative |
| SAOUHSC_02044 | 3.0 | 2.7E-13 | conserved hypothetical phage protein |
| SAOUHSC_02754 | 3.3 | 2.7E-13 | ABC transporter%2C ATP-binding protein%2C putative |
| SAOUHSC_01219 | -3.1 | 2.9E-13 | cell wall hydrolase%2C putative |

| | | | |
|---|---|---|---|
| SAOUHSC_02812 | 2.4 | 2.9E-13 | conserved hypothetical protein |
| SAOUHSC_00126 | 3.0 | 3.6E-13 | capsular polysaccharide biosynthesis protein Cap8M |
| SAOUHSC_00811 | 2.8 | 4.1E-13 | conserved hypothetical protein |
| SAOUHSC_01634 | 2.6 | 4.6E-13 | glycine cleavage system T protein |
| SAOUHSC_01223 | 2.9 | 4.7E-13 | gid protein |
| SAOUHSC_02700 | 2.7 | 5.0E-13 | conserved hypothetical protein |
| SAOUHSC_02042 | 3.4 | 5.2E-13 | phi Mu50B-like protein |
| SAOUHSC_01747 | -3.6 | 5.7E-13 | preprotein translocase%2C YajC subunit |
| SAOUHSC_00925 | -2.7 | 6.1E-13 | conserved hypothetical protein |
| SAOUHSC_02448 | 2.5 | 6.2E-13 | conserved hypothetical protein |
| SAOUHSC_00362 | -2.6 | 7.4E-13 | conserved hypothetical protein |
| SAOUHSC_01389 | 4.2 | 8.1E-13 | phosphate ABC transporter%2C periplasmic phosphate-binding protein%2C putative |
| SAOUHSC_02925 | 4.6 | 8.5E-13 | conserved hypothetical protein |
| SAOUHSC_00789 | 2.6 | 8.9E-13 | conserved hypothetical protein |
| SAOUHSC_02697 | 2.9 | 8.9E-13 | amino acid ABC transporter%2C ATP-binding protein%2C putative |
| SAOUHSC_02610 | 2.8 | 9.8E-13 | formiminoglutamase |
| SAOUHSC_02119 | -3.1 | 1.2E-12 | proline uptake protein |
| SAOUHSC_01767 | 2.5 | 1.2E-12 | valyl-tRNA synthetase |
| SAOUHSC_00117 | 3.0 | 1.3E-12 | capsular polysaccharide biosynthesis protein Cap5D%2C putative |
| SAOUHSC_00907 | 3.6 | 1.4E-12 | conserved hypothetical protein |
| SAOUHSC_02908 | 3.1 | 1.5E-12 | conserved hypothetical protein |
| SAOUHSC_02149 | -2.8 | 1.5E-12 | conserved hypothetical protein |
| SAOUHSC_03028 | 3.3 | 1.6E-12 | conserved hypothetical protein |
| SAOUHSC_01738 | 2.6 | 1.7E-12 | histidyl-tRNA synthetase |
| SAOUHSC_00802 | 2.4 | 1.8E-12 | carboxylesterase precursor%2C putative |
| SAOUHSC_02453 | 4.1 | 1.8E-12 | tagatose-6-phosphate kinase |
| SAOUHSC_01115 | -11.0 | 1.8E-12 | conserved hypothetical protein |
| SAOUHSC_02336 | 3.0 | 2.0E-12 | beta-hydroxyacyl-ACP dehydratase%2C putative |
| SAOUHSC_01222 | 2.7 | 2.0E-12 | DNA topoisomerase I |
| SAOUHSC_02475 | -3.0 | 2.3E-12 | conserved hypothetical protein |
| SAOUHSC_02038 | 3.1 | 2.9E-12 | phage protein%2C HK97 gp10 family |
| SAOUHSC_01497 | 2.8 | 3.0E-12 | L-asparaginase%2C putative |
| SAOUHSC_00689 | 3.1 | 3.1E-12 | conserved hypothetical protein |
| SAOUHSC_02137 | -2.5 | 3.1E-12 | sodium-dependent transporter (huNaDC-1)%2C putative |
| SAOUHSC_00926 | -2.7 | 3.5E-12 | oligopeptide ABC transporter%2C ATP-binding protein%2C putative |
| SAOUHSC_02073 | 3.6 | 3.6E-12 | conserved hypothetical phage protein |
| SAOUHSC_00284 | -3.1 | 4.8E-12 | 5'-nucleotidase%2C lipoprotein e(P4) family |
| SAOUHSC_03024 | 3.2 | 5.2E-12 | conserved hypothetical protein |
| SAOUHSC_01975 | -2.5 | 5.3E-12 | conserved hypothetical protein |
| SAOUHSC_00363 | -3.0 | 6.2E-12 | conserved hypothetical protein |
| SAOUHSC_01082 | -5.9 | 6.6E-12 | conserved hypothetical protein |
| SAOUHSC_02314 | -2.9 | 6.7E-12 | sensor protein KdpD%2C putative |
| SAOUHSC_02057 | 5.2 | 6.8E-12 | dUTP pyrophosphatase |
| SAOUHSC_02019 | 2.6 | 7.6E-12 | autolysin |
| SAOUHSC_00128 | 2.4 | 7.6E-12 | cap5O protein/UDP-N-acetyl-D-mannosaminuronic acid dehydrogenase |
| SAOUHSC_00803 | 2.2 | 8.0E-12 | ribonuclease R%2C putative |
| SAOUHSC_02274 | -2.4 | 8.1E-12 | ABC transporter%2C ATP-binding protein%2C putative |
| SAOUHSC_02048 | 2.6 | 8.4E-12 | phage portal protein%2C SPP1 family |
| SAOUHSC_00156 | -3.6 | 9.2E-12 | conserved hypothetical protein |
| SAOUHSC_00405 | -3.0 | 1.0E-11 | conserved hypothetical protein |
| SAOUHSC_02247 | -3.0 | 1.0E-11 | cation transport protein%2C putative |
| SAOUHSC_00034 | 4.4 | 1.1E-11 | conserved hypothetical protein |
| SAOUHSC_02050 | 3.0 | 1.1E-11 | terminase small subunit%2C putative |
| SAOUHSC_02030 | 2.8 | 1.1E-11 | phi ETA orf 55-like protein |
| SAOUHSC_00187 | -3.2 | 1.1E-11 | formate acetyltransferase |
| SAOUHSC_01694 | 2.7 | 1.2E-11 | conserved hypothetical protein |
| SAOUHSC_02040 | 3.1 | 1.3E-11 | conserved hypothetical phage protein |
| SAOUHSC_00961 | -3.5 | 1.3E-11 | conserved hypothetical protein |
| SAOUHSC_01823 | 2.9 | 1.4E-11 | conserved hypothetical protein |
| SAOUHSC_02954 | -3.5 | 1.4E-11 | ABC transporter%2C ATP-binding protein%2C putative |
| SAOUHSC_01573 | 8.9 | 1.6E-11 | conserved hypothetical phage protein |
| SAOUHSC_02607 | -3.1 | 1.6E-11 | urocanate hydratase |
| SAOUHSC_02160 | -3.9 | 1.9E-11 | conserved hypothetical protein |
| SAOUHSC_00138 | 3.5 | 2.0E-11 | conserved hypothetical protein |
| SAOUHSC_02035 | 3.4 | 2.2E-11 | conserved hypothetical phage protein |
| SAOUHSC_02910 | -2.8 | 2.2E-11 | conserved hypothetical protein |
| SAOUHSC_02049 | 2.7 | 2.2E-11 | phage terminase%2C large subunit%2C PBSX family |
| SAOUHSC_00810 | 2.7 | 2.5E-11 | conserved hypothetical protein |
| SAOUHSC_00738 | -2.6 | 2.6E-11 | conserved hypothetical protein |
| SAOUHSC_01568 | 4.4 | 2.6E-11 | conserved hypothetical phage protein |
| SAOUHSC_01660 | 2.5 | 2.7E-11 | conserved hypothetical protein |
| SAOUHSC_00202 | -2.9 | 2.7E-11 | conserved hypothetical protein |
| SAOUHSC_00027 | -2.5 | 3.3E-11 | conserved hypothetical protein |
| SAOUHSC_01378 | 2.8 | 3.6E-11 | peptide ABC transporter%2C ATP-binding protein%2C putative |
| SAOUHSC_03026 | 4.4 | 4.3E-11 | conserved hypothetical protein |
| SAOUHSC_01729 | 3.9 | 4.4E-11 | conserved hypothetical protein |
| SAOUHSC_02935 | -2.2 | 4.7E-11 | conserved hypothetical protein |
| SAOUHSC_01847 | -3.0 | 4.8E-11 | conserved hypothetical protein |
| SAOUHSC_02759 | -3.4 | 5.0E-11 | conserved hypothetical protein |
| SAOUHSC_01984 | -3.5 | 5.2E-11 | conserved hypothetical protein |
| SAOUHSC_02023 | 2.6 | 5.5E-11 | bifunctional autolysin precursor |
| SAOUHSC_02305 | 2.6 | 5.7E-11 | alanine racemase |
| SAOUHSC_00713 | 2.3 | 5.8E-11 | conserved hypothetical protein |
| SAOUHSC_00040 | -3.9 | 6.1E-11 | conserved hypothetical protein |
| SAOUHSC_02832 | -4.5 | 6.1E-11 | conserved hypothetical protein |
| SAOUHSC_01297 | -5.4 | 6.8E-11 | conserved hypothetical protein |
| SAOUHSC_01137 | 2.2 | 7.3E-11 | conserved hypothetical protein |
| SAOUHSC_02306 | 2.4 | 8.6E-11 | holo-(acyl-carrier-protein) synthase |
| SAOUHSC_01884 | -3.6 | 9.3E-11 | conserved hypothetical protein |
| SAOUHSC_01952 | -4.1 | 1.0E-10 | lantibiotic epidermin biosynthesis protein EpiB%2C putative |
| SAOUHSC_00220 | -2.3 | 1.0E-10 | conserved hypothetical protein |
| SAOUHSC_02303 | -2.2 | 1.1E-10 | conserved hypothetical protein |
| SAOUHSC_01586 | -2.3 | 1.2E-10 | DNA-binding response regulator%2C putative |

| | | | |
|---|---|---|---|
| SAOUHSC_02668 | -2.7 | 1.4E-10 | conserved hypothetical protein |
| SAOUHSC_00584 | -2.5 | 1.4E-10 | conserved hypothetical protein |
| SAOUHSC_02470 | 3.4 | 1.8E-10 | conserved hypothetical protein |
| SAOUHSC_00613 | -2.7 | 1.8E-10 | iron compound ABC transporter%2C substrate-binding protein%2C putative |
| SAOUHSC_02706 | -3.9 | 1.9E-10 | immunoglobulin G-binding protein Sbi%2C putative |
| SAOUHSC_00746 | -3.7 | 2.1E-10 | conserved hypothetical protein |
| SAOUHSC_01123 | -5.6 | 2.2E-10 | conserved hypothetical protein |
| SAOUHSC_01852 | -2.1 | 2.3E-10 | conserved hypothetical protein |
| SAOUHSC_02010 | -2.3 | 2.3E-10 | conserved hypothetical protein |
| SAOUHSC_02474 | -2.9 | 2.6E-10 | conserved hypothetical protein |
| SAOUHSC_02972 | -2.3 | 2.6E-10 | conserved hypothetical protein |
| SAOUHSC_00973 | -5.9 | 2.6E-10 | conserved hypothetical protein |
| SAOUHSC_00626 | 3.6 | 2.8E-10 | conserved hypothetical protein |
| SAOUHSC_01696 | 2.4 | 2.9E-10 | conserved hypothetical protein |
| SAOUHSC_02582 | 2.1 | 3.3E-10 | formate dehydrogenase%2C alpha subunit%2C putative |
| SAOUHSC_00248 | 2.5 | 3.3E-10 | peptidoglycan hydrolase%2C putative |
| SAOUHSC_02842 | 2.9 | 3.5E-10 | conserved hypothetical protein |
| SAOUHSC_00834 | 2.8 | 3.8E-10 | thioredoxin%2C putative |
| SAOUHSC_02062 | 3.8 | 4.4E-10 | helix-turn-helix DNA binding protein |
| SAOUHSC_01766 | 2.2 | 4.5E-10 | folylpolyglutamate synthase/dihydrofolate synthase%2C putative |
| SAOUHSC_00950 | -2.6 | 4.5E-10 | conserved hypothetical protein |
| SAOUHSC_02377 | -2.2 | 4.8E-10 | pyrimidine nucleoside phosphorylase%2C putative |
| SAOUHSC_02433 | 2.3 | 5.2E-10 | conserved hypothetical protein |
| SAOUHSC_01001 | -2.3 | 5.5E-10 | quinol oxidase%2C subunit I |
| SAOUHSC_00934 | -2.4 | 5.9E-10 | conserved hypothetical protein |
| SAOUHSC_02864 | -2.7 | 6.0E-10 | ferrous iron transport protein B |
| SAOUHSC_01452 | -3.4 | 6.3E-10 | alanine dehydrogenase |
| SAOUHSC_00864 | -2.6 | 7.7E-10 | conserved hypothetical protein |
| SAOUHSC_00194 | -4.2 | 8.7E-10 | hypothetical protein |
| SAOUHSC_00423 | 2.6 | 9.7E-10 | conserved hypothetical protein |
| SAOUHSC_01382 | -2.5 | 9.8E-10 | conserved hypothetical protein |
| SAOUHSC_01944 | -5.0 | 9.9E-10 | conserved hypothetical protein |
| SAOUHSC_01261 | 2.3 | 1.0E-09 | competence-damage inducible protein cinA |
| SAOUHSC_02441 | 2.5 | 1.0E-09 | conserved hypothetical protein |
| SAOUHSC_01949 | 2.3 | 1.0E-09 | intracellular serine protease%2C putative |
| SAOUHSC_02271 | 5.0 | 1.0E-09 | conserved hypothetical protein |
| SAOUHSC_01787 | 3.6 | 1.1E-09 | conserved hypothetical protein |
| SAOUHSC_02052 | 5.7 | 1.1E-09 | hypothetical phage protein |
| SAOUHSC_02020 | 3.8 | 1.2E-09 | holin |
| SAOUHSC_00044 | -2.5 | 1.3E-09 | conserved hypothetical protein |
| SAOUHSC_00920 | 2.6 | 1.4E-09 | conserved hypothetical protein |
| SAOUHSC_02699 | 2.5 | 1.4E-09 | conserved hypothetical protein |
| SAOUHSC_00804 | 2.5 | 1.4E-09 | SsrA-binding protein |
| SAOUHSC_01657 | -2.8 | 1.6E-09 | ABC transporter%2C putative |
| SAOUHSC_02753 | 2.4 | 1.6E-09 | membrane protein%2C putative |
| SAOUHSC_00221 | -2.2 | 1.8E-09 | alcohol dehydrogenase%2C zinc-containing |
| SAOUHSC_00683 | -2.1 | 1.8E-09 | conserved hypothetical protein |
| SAOUHSC_01122 | -6.2 | 1.8E-09 | conserved hypothetical protein |
| SAOUHSC_00151 | -2.3 | 2.0E-09 | branched-chain amino acid transport system II carrier protein |
| SAOUHSC_02101 | -3.4 | 2.1E-09 | conserved hypothetical protein |
| SAOUHSC_01874 | 2.5 | 2.4E-09 | conserved hypothetical protein |
| SAOUHSC_01385 | 3.0 | 2.5E-09 | phosphate ABC transporter ATP-binding protein%2C putative |
| SAOUHSC_02025 | 5.1 | 2.5E-09 | phi SLT orf 99-like protein |
| SAOUHSC_02071 | 2.8 | 2.6E-09 | single-strand DNA-binding protein%2C putative |
| SAOUHSC_00696 | -2.0 | 2.8E-09 | conserved hypothetical protein |
| SAOUHSC_01136 | -8.7 | 2.9E-09 | conserved hypothetical protein |
| SAOUHSC_01488 | -2.2 | 3.2E-09 | conserved hypothetical protein |
| SAOUHSC_02451 | 3.5 | 3.3E-09 | PTS system lactose-specific IIA component%2C putative |
| SAOUHSC_00662 | -2.4 | 3.6E-09 | conserved hypothetical protein |
| SAOUHSC_00415 | -2.8 | 4.1E-09 | conserved hypothetical protein |
| SAOUHSC_02067 | 2.9 | 4.1E-09 | bacteriophage L54a%2C DnaB-like helicase family protein |
| SAOUHSC_02275 | -4.6 | 4.1E-09 | hypothetical protein |
| SAOUHSC_02606 | -2.7 | 4.2E-09 | imidazolonepropionase |
| SAOUHSC_01947 | 2.6 | 4.2E-09 | membrane protein%2C putative |
| SAOUHSC_01419 | 2.2 | 4.4E-09 | conserved hypothetical protein |
| SAOUHSC_01877 | 2.2 | 4.5E-09 | conserved hypothetical protein |
| SAOUHSC_02682 | 2.9 | 4.8E-09 | uroporphyrin-III C-methyltransferase%2C putative |
| SAOUHSC_02307 | 2.3 | 5.1E-09 | conserved hypothetical protein |
| SAOUHSC_02367 | -2.2 | 5.4E-09 | conserved hypothetical protein |
| SAOUHSC_01285 | -2.3 | 5.5E-09 | conserved hypothetical protein |
| SAOUHSC_02337 | 2.1 | 5.8E-09 | UDP-N-acetylglucosamine 1-carboxyvinyltransferase |
| SAOUHSC_02678 | -2.0 | 6.1E-09 | respiratory nitrate reductase%2C gamma subunit |
| SAOUHSC_02404 | -2.3 | 6.2E-09 | conserved hypothetical protein |
| SAOUHSC_00033 | 3.4 | 6.4E-09 | conserved hypothetical protein |
| SAOUHSC_02323 | -2.0 | 6.4E-09 | cardiolipin synthetase%2C putative |
| SAOUHSC_00541 | -2.7 | 6.7E-09 | conserved hypothetical protein |
| SAOUHSC_00237 | -3.0 | 7.4E-09 | conserved hypothetical protein |
| SAOUHSC_01403 | -3.2 | 7.5E-09 | cold shock protein%2C putative |
| SAOUHSC_02046 | 4.3 | 8.2E-09 | conserved hypothetical phage protein |
| SAOUHSC_01676 | -2.1 | 9.3E-09 | conserved hypothetical protein |
| SAOUHSC_00131 | -2.8 | 1.0E-08 | conserved hypothetical protein |
| SAOUHSC_00619 | 1.9 | 1.0E-08 | conserved hypothetical protein |
| SAOUHSC_02600 | -2.6 | 1.0E-08 | conserved hypothetical protein |
| SAOUHSC_01279 | -2.1 | 1.1E-08 | hydrolase%2C alpha/beta fold family domain protein |
| SAOUHSC_01128 | -3.9 | 1.1E-08 | ornithine carbamoyltransferase |
| SAOUHSC_02068 | 2.9 | 1.1E-08 | conserved hypothetical phage protein |
| SAOUHSC_02876 | -2.0 | 1.2E-08 | conserved hypothetical protein |
| SAOUHSC_00633 | -2.1 | 1.4E-08 | conserved hypothetical protein |
| SAOUHSC_00501 | -2.1 | 1.4E-08 | conserved hypothetical protein |
| SAOUHSC_00402 | -4.1 | 1.4E-08 | conserved hypothetical protein |
| SAOUHSC_01854 | 2.3 | 1.4E-08 | conserved hypothetical protein |
| SAOUHSC_00691 | 2.4 | 1.5E-08 | undecaprenol kinase%2C putative |
| SAOUHSC_00614 | -2.4 | 1.5E-08 | conserved hypothetical protein |
| SAOUHSC_02300 | 2.4 | 1.5E-08 | STAS domain%2C putative |

| | | | |
|---|---|---|---|
| SAOUHSC_01682 | 2.2 | 1.5E-08 | DnaJ protein |
| SAOUHSC_00450 | -2.4 | 1.6E-08 | Orn/Lys/Arg decarboxylase%2C putative |
| SAOUHSC_02848 | 3.3 | 1.6E-08 | PTS system glucose-specific IIABC component |
| SAOUHSC_00616 | -2.1 | 1.7E-08 | conserved hypothetical protein |
| SAOUHSC_02058 | 4.0 | 1.7E-08 | conserved hypothetical phage protein |
| SAOUHSC_01045 | -2.5 | 1.7E-08 | conserved hypothetical protein |
| SAOUHSC_00909 | -2.2 | 1.7E-08 | conserved hypothetical protein |
| SAOUHSC_00164 | -2.3 | 1.7E-08 | conserved hypothetical protein |
| SAOUHSC_00732 | 1.9 | 1.9E-08 | amino acid ABC transporter%2C permease protein%2C putative |
| SAOUHSC_02466 | 2.6 | 2.2E-08 | truncated MHC class II analog protein |
| SAOUHSC_00174 | 2.4 | 2.2E-08 | M23/M37 peptidase domain protein |
| SAOUHSC_02674 | -2.9 | 2.3E-08 | conserved hypothetical protein |
| SAOUHSC_02066 | 3.3 | 2.3E-08 | conserved hypothetical phage protein |
| SAOUHSC_01737 | 2.0 | 2.4E-08 | aspartyl-tRNA synthetase |
| SAOUHSC_01547 | 2.2 | 2.5E-08 | conserved hypothetical phage protein |
| SAOUHSC_01706 | -2.4 | 2.7E-08 | conserved hypothetical protein |
| SAOUHSC_01304 | -2.3 | 2.7E-08 | conserved hypothetical protein |
| SAOUHSC_00204 | -2.1 | 2.8E-08 | Globin domain protein |
| SAOUHSC_00972 | -9.0 | 2.9E-08 | conserved hypothetical protein |
| SAOUHSC_00625 | 2.7 | 3.4E-08 | conserved hypothetical protein |
| SAOUHSC_01290 | -4.8 | 3.8E-08 | conserved hypothetical protein |
| SAOUHSC_00547 | -2.0 | 3.8E-08 | conserved hypothetical protein |
| SAOUHSC_02037 | 2.9 | 3.9E-08 | conserved hypothetical phage protein |
| SAOUHSC_02926 | 1.8 | 4.0E-08 | fructose-bisphosphate aldolase class-I%2C putative |
| SAOUHSC_00893 | 2.1 | 4.3E-08 | FMN oxidoreductase%2C putative |
| SAOUHSC_00688 | 2.8 | 4.5E-08 | conserved hypothetical protein |
| SAOUHSC_00624 | 2.4 | 4.6E-08 | integrase/recombinase%2C putative |
| SAOUHSC_00610 | -2.1 | 4.6E-08 | conserved hypothetical protein |
| SAOUHSC_00439 | 2.5 | 4.7E-08 | conserved hypothetical protein |
| SAOUHSC_02472 | -2.5 | 5.0E-08 | conserved hypothetical protein |
| SAOUHSC_00853 | -4.2 | 5.0E-08 | conserved hypothetical protein |
| SAOUHSC_02436 | -2.0 | 5.1E-08 | conserved hypothetical protein |
| SAOUHSC_03027 | 3.3 | 5.5E-08 | conserved hypothetical protein |
| SAOUHSC_02983 | 2.1 | 5.7E-08 | conserved hypothetical protein |
| SAOUHSC_00787 | -1.9 | 5.7E-08 | conserved hypothetical protein |
| SAOUHSC_00188 | -2.6 | 6.0E-08 | pyruvate formate-lyase 1 activating enzyme%2C putative |
| SAOUHSC_02768 | -3.7 | 6.5E-08 | conserved hypothetical protein |
| SAOUHSC_01322 | -2.4 | 6.7E-08 | homoserine kinase |
| SAOUHSC_02620 | -2.5 | 6.7E-08 | conserved hypothetical protein |
| SAOUHSC_00233 | -2.5 | 7.1E-08 | holin-like protein LrgB%2C putative |
| SAOUHSC_01435 | 1.9 | 7.5E-08 | thymidylate synthase%2C putative |
| SAOUHSC_02434 | 1.9 | 7.7E-08 | conserved hypothetical protein |
| SAOUHSC_00049 | -2.2 | 7.8E-08 | conserved hypothetical protein |
| SAOUHSC_02017 | 2.3 | 8.7E-08 | conserved hypothetical phage protein |
| SAOUHSC_02393 | -2.4 | 8.8E-08 | conserved hypothetical protein |
| SAOUHSC_02379 | -2.3 | 8.9E-08 | deoxyribose-phosphate aldolase |
| SAOUHSC_02443 | 1.9 | 9.0E-08 | conserved hypothetical protein |
| SAOUHSC_02026 | 8.1 | 9.3E-08 | phi ETA orf 58-like protein-related protein |
| SAOUHSC_02576 | 1.9 | 9.4E-08 | secretory antigen precursor SsaA%2C putative |
| SAOUHSC_01267 | 1.8 | 9.7E-08 | conserved hypothetical protein |
| SAOUHSC_02424 | -1.9 | 1.0E-07 | conserved hypothetical protein |
| SAOUHSC_02069 | 2.7 | 1.1E-07 | phi PV83 orf 20-like protein |
| SAOUHSC_01837 | -2.3 | 1.1E-07 | 1-acyl-sn-glycerol-3-phosphate acyltransferases domain protein |
| SAOUHSC_00850 | 2.0 | 1.1E-07 | conserved hypothetical protein |
| SAOUHSC_01076 | -2.1 | 1.2E-07 | conserved hypothetical protein |
| SAOUHSC_01945 | 2.5 | 1.2E-07 | membrane protein%2C putative |
| SAOUHSC_03006 | -3.2 | 1.2E-07 | lipase |
| SAOUHSC_00500 | -2.2 | 1.3E-07 | conserved hypothetical protein |
| SAOUHSC_02915 | 2.1 | 1.4E-07 | conserved hypothetical protein |
| SAOUHSC_02740 | 2.3 | 1.4E-07 | drug transporter%2C putative |
| SAOUHSC_01922 | -2.5 | 1.4E-07 | conserved hypothetical protein |
| SAOUHSC_00020 | -1.8 | 1.5E-07 | two-component response regulator%2C putative |
| SAOUHSC_00605 | -2.0 | 1.5E-07 | conserved hypothetical protein |
| SAOUHSC_02581 | 2.2 | 1.6E-07 | conserved hypothetical protein |
| SAOUHSC_01675 | -2.2 | 1.6E-07 | conserved hypothetical protein |
| SAOUHSC_01380 | 2.3 | 1.6E-07 | oligopeptide transporter putative membrane permease domain |
| SAOUHSC_02599 | -2.5 | 1.7E-07 | Hex regulon repressor%2C putative |
| SAOUHSC_01320 | -2.3 | 1.7E-07 | homoserine dehydrogenase%2C putative |
| SAOUHSC_02072 | 6.9 | 1.7E-07 | conserved hypothetical phage protein |
| SAOUHSC_00615 | -2.2 | 1.8E-07 | haloacid dehalogenase-like hydrolase%2C putative |
| SAOUHSC_00475 | -2.0 | 1.9E-07 | peptidyl-tRNA hydrolase |
| SAOUHSC_02272 | 3.0 | 1.9E-07 | conserved hypothetical protein |
| SAOUHSC_01049 | 1.9 | 2.1E-07 | spermidine/putrescine ABC transporter%2C spermidine/putrescine-binding protein%2C putative |
| SAOUHSC_00499 | -2.3 | 2.2E-07 | pyridoxine biosynthesis protein |
| SAOUHSC_01292 | -8.3 | 2.2E-07 | conserved hypothetical protein |
| SAOUHSC_02335 | -2.3 | 2.2E-07 | conserved hypothetical protein |
| SAOUHSC_00664 | -1.8 | 2.6E-07 | conserved hypothetical protein |
| SAOUHSC_02661 | -3.0 | 2.7E-07 | PTS system sucrose-specific IIBC component%2C putative |
| SAOUHSC_00058 | 2.6 | 2.8E-07 | conserved hypothetical protein |
| SAOUHSC_00051 | -3.1 | 2.9E-07 | 1-phosphatidylinositol phosphodiesterase precursor%2C putative |
| SAOUHSC_00712 | 1.9 | 2.9E-07 | conserved hypothetical protein |
| SAOUHSC_02979 | -2.7 | 2.9E-07 | conserved hypothetical protein |
| SAOUHSC_01556 | 4.7 | 2.9E-07 | PVL orf 52-like protein |
| SAOUHSC_00208 | -5.4 | 2.9E-07 | hypothetical protein |
| SAOUHSC_02962 | -2.0 | 3.0E-07 | tributyrin esterase%2C putative |
| SAOUHSC_02454 | 3.2 | 3.0E-07 | galactose-6-phosphate isomerase%2C LacB subunit |
| SAOUHSC_00977 | -2.5 | 3.1E-07 | conserved hypothetical protein |
| SAOUHSC_02683 | 3.3 | 3.1E-07 | assimilatory nitrite reductase [NAD(P)H]%2C small subunit%2C putative |
| SAOUHSC_02087 | -1.9 | 3.1E-07 | conserved hypothetical phage protein |
| SAOUHSC_01681 | 2.4 | 3.1E-07 | ribosomal protein L11 methyltransferase |
| SAOUHSC_02950 | -3.4 | 3.2E-07 | hypothetical protein |
| SAOUHSC_02573 | 2.5 | 3.2E-07 | Na+/H+ antiporter NhaC |
| SAOUHSC_01274 | 1.9 | 3.3E-07 | glycerol uptake operon antiterminator regulatory protein%2C putative |

| | | | |
|---|---|---|---|
| SAOUHSC_00381 | 2.4 | 3.5E-07 | conserved hypothetical protein |
| SAOUHSC_01421 | 3.8 | 3.5E-07 | hypothetical protein |
| SAOUHSC_00383 | 2.1 | 3.6E-07 | conserved hypothetical protein |
| SAOUHSC_02984 | 2.2 | 3.6E-07 | conserved hypothetical protein |
| SAOUHSC_02374 | 1.8 | 3.7E-07 | aminobenzoyl-glutamate utilization protein B%2C putative |
| SAOUHSC_00355 | 3.3 | 3.7E-07 | conserved hypothetical protein |
| SAOUHSC_02388 | -3.6 | 3.8E-07 | conserved hypothetical protein |
| SAOUHSC_00314 | -2.2 | 3.8E-07 | conserved hypothetical protein |
| SAOUHSC_02557 | 2.5 | 3.8E-07 | urea transporter%2C putative |
| SAOUHSC_01789 | -2.0 | 4.0E-07 | conserved hypothetical protein |
| SAOUHSC_01379 | 2.6 | 4.3E-07 | oligopeptide transporter putative membrane permease domain |
| SAOUHSC_01896 | -2.0 | 4.3E-07 | conserved hypothetical protein |
| SAOUHSC_02074 | 3.0 | 4.4E-07 | phi PVL orf 39-like protein |
| SAOUHSC_00967 | -3.0 | 4.4E-07 | hypothetical protein |
| SAOUHSC_01875 | 2.0 | 4.5E-07 | leucyl-tRNA synthetase |
| SAOUHSC_00158 | -2.8 | 4.5E-07 | PTS system component |
| SAOUHSC_02916 | 2.2 | 4.5E-07 | aspartate 1-decarboxylase |
| SAOUHSC_02781 | -2.3 | 4.5E-07 | conserved hypothetical protein |
| SAOUHSC_02856 | -2.8 | 4.5E-07 | hypothetical protein |
| SAOUHSC_02633 | -2.1 | 4.8E-07 | conserved hypothetical protein |
| SAOUHSC_03023 | -2.3 | 5.1E-07 | Drp35 |
| SAOUHSC_02892 | -2.0 | 5.3E-07 | conserved hypothetical protein |
| SAOUHSC_00641 | -1.9 | 5.7E-07 | teichoic acid translocation ATP-binding protein%2C putative |
| SAOUHSC_03047 | -2.5 | 5.9E-07 | conserved hypothetical protein |
| SAOUHSC_01412 | 1.9 | 6.0E-07 | conserved hypothetical protein |
| SAOUHSC_00849 | 2.0 | 6.3E-07 | aminotransferase%2C class V superfamily%2C putative |
| SAOUHSC_01849 | -3.1 | 6.5E-07 | conserved hypothetical protein |
| SAOUHSC_01645 | 2.1 | 7.1E-07 | conserved hypothetical protein |
| SAOUHSC_00695 | -2.2 | 7.8E-07 | conserved hypothetical protein |
| SAOUHSC_00157 | -3.1 | 7.9E-07 | conserved hypothetical protein |
| SAOUHSC_01051 | -1.9 | 8.3E-07 | conserved hypothetical protein |
| SAOUHSC_00703 | 2.0 | 8.6E-07 | quinolone resistance norA protein%2C putative |
| SAOUHSC_01677 | -2.0 | 8.6E-07 | conserved hypothetical protein |
| SAOUHSC_00921 | 2.0 | 8.7E-07 | 3-oxoacyl- synthase%2C putative |
| SAOUHSC_01084 | -3.3 | 9.5E-07 | conserved hypothetical protein |
| SAOUHSC_02185 | 2.2 | 9.8E-07 | phi PVL orf 13-like protein |
| SAOUHSC_01931 | -3.0 | 1.0E-06 | conserved hypothetical protein |
| SAOUHSC_02097 | 1.7 | 1.1E-06 | conserved hypothetical protein |
| SAOUHSC_01858 | 1.8 | 1.2E-06 | conserved hypothetical protein |
| SAOUHSC_00329 | 2.3 | 1.3E-06 | mttA/Hcf106 family protein-related protein |
| SAOUHSC_01392 | 1.9 | 1.3E-06 | ABC transporter%2C ATP-binding protein%2C putative |
| SAOUHSC_00222 | -1.9 | 1.4E-06 | tagB protein%2C putative |
| SAOUHSC_00285 | 1.6 | 1.5E-06 | conserved hypothetical protein |
| SAOUHSC_01543 | 2.7 | 1.5E-06 | phi related protein |
| SAOUHSC_00356 | 2.2 | 1.6E-06 | conserved hypothetical protein |
| SAOUHSC_01142 | -2.2 | 1.6E-06 | conserved hypothetical protein |
| SAOUHSC_02704 | 2.5 | 1.6E-06 | conserved hypothetical protein |
| SAOUHSC_01824 | 2.0 | 1.8E-06 | thiamine biosynthesis protein ThiI |
| SAOUHSC_02098 | -1.7 | 1.8E-06 | DNA-binding response regulator VraR%2C putative |
| SAOUHSC_02698 | 1.9 | 1.8E-06 | amino acid ABC transproter%2C permease protein%2C putative |
| SAOUHSC_00008 | -2.1 | 1.9E-06 | histidine ammonia-lyase |
| SAOUHSC_00754 | -2.2 | 1.9E-06 | conserved hypothetical protein |
| SAOUHSC_00801 | 2.8 | 1.9E-06 | preprotein translocase%2C SecG subunit |
| SAOUHSC_01899 | -2.0 | 2.0E-06 | conserved hypothetical protein |
| SAOUHSC_00134 | 2.1 | 2.0E-06 | conserved hypothetical protein |
| SAOUHSC_00953 | -1.8 | 2.3E-06 | conserved hypothetical protein |
| SAOUHSC_03034 | 2.1 | 2.4E-06 | conserved hypothetical protein |
| SAOUHSC_02799 | -3.6 | 2.4E-06 | staphylococcal accessory regulator T%2C putative |
| SAOUHSC_00203 | -2.4 | 2.4E-06 | conserved hypothetical protein |
| SAOUHSC_00454 | -1.8 | 2.5E-06 | DNA polymerase III%2C delta prime subunit%2C putative |
| SAOUHSC_03045 | 2.2 | 2.5E-06 | cold shock protein%2C putative |
| SAOUHSC_01557 | 4.9 | 2.6E-06 | conserved hypothetical phage protein |
| SAOUHSC_00962 | -2.3 | 2.6E-06 | conserved hypothetical protein |
| SAOUHSC_01822 | 2.2 | 2.8E-06 | conserved hypothetical protein |
| SAOUHSC_01633 | 1.9 | 2.9E-06 | glycine cleavage system P-protein subunit I%2C putative |
| SAOUHSC_01554 | 7.4 | 3.0E-06 | PV83 orf 27-like protein |
| SAOUHSC_01689 | -1.8 | 3.1E-06 | ribosomal protein S20 |
| SAOUHSC_00024 | -1.9 | 3.3E-06 | conserved hypothetical protein |
| SAOUHSC_00799 | 2.2 | 3.3E-06 | enolase |
| SAOUHSC_00223 | 1.7 | 3.4E-06 | teichoic acid biosynthesis protein F%2C putative |
| SAOUHSC_02153 | -2.9 | 3.7E-06 | conserved hypothetical protein |
| SAOUHSC_02022 | 2.1 | 3.7E-06 | phage tail fiber protein%2C putative |
| SAOUHSC_01798 | -2.0 | 3.8E-06 | conserved hypothetical protein |
| SAOUHSC_00665 | -1.9 | 4.0E-06 | conserved hypothetical protein |
| SAOUHSC_01964 | -1.7 | 4.0E-06 | conserved hypothetical protein |
| SAOUHSC_01542 | 2.1 | 4.0E-06 | SNF2 family N-terminal domain protein |
| SAOUHSC_01972 | -1.8 | 4.2E-06 | protein export protein PrsA%2C putative |
| SAOUHSC_00437 | 2.5 | 4.2E-06 | conserved hypothetical protein |
| SAOUHSC_02463 | -2.1 | 4.2E-06 | hyaluronate lyase |
| SAOUHSC_01146 | 1.9 | 4.2E-06 | phospho-N-acetylmuramoyl-pentapeptide-transferase |
| SAOUHSC_00071 | 2.2 | 4.5E-06 | lipoprotein%2C SirC%2C putative |
| SAOUHSC_00166 | -2.1 | 4.5E-06 | conserved hypothetical protein |
| SAOUHSC_01978 | 1.9 | 4.6E-06 | conserved hypothetical protein |
| SAOUHSC_00628 | 2.6 | 4.6E-06 | conserved hypothetical protein |
| SAOUHSC_01009 | -2.1 | 4.7E-06 | phosphoribosylaminoimidazole carboxylase%2C ATPase subunit |
| SAOUHSC_01476 | -1.8 | 4.8E-06 | conserved hypothetical protein |
| SAOUHSC_02619 | -2.2 | 4.8E-06 | conserved hypothetical protein |
| SAOUHSC_00740 | 2.1 | 4.8E-06 | conserved hypothetical protein |
| SAOUHSC_00890 | -1.8 | 5.0E-06 | conserved hypothetical protein |
| SAOUHSC_00144 | -1.8 | 5.2E-06 | conserved hypothetical protein |
| SAOUHSC_00129 | 1.7 | 5.3E-06 | UDP-N-acetylglucosamine 2-epimerase |
| SAOUHSC_00611 | -1.6 | 5.3E-06 | arginyl-tRNA synthetase |
| SAOUHSC_02992 | -2.9 | 5.3E-06 | conserved hypothetical protein |
| SAOUHSC_01220 | -2.7 | 5.3E-06 | conserved hypothetical protein |

| | | | |
|---|---|---|---|
| SAOUHSC_02308 | 1.7 | 5.5E-06 | conserved hypothetical protein |
| SAOUHSC_01388 | 5.0 | 5.5E-06 | hypothetical protein |
| SAOUHSC_02001 | -1.6 | 5.8E-06 | conserved hypothetical protein |
| SAOUHSC_02621 | -2.5 | 5.8E-06 | DNA-3-methyladenine glycosylase%2C putative |
| SAOUHSC_02912 | -2.3 | 5.9E-06 | conserved hypothetical protein |
| SAOUHSC_01615 | -1.7 | 6.0E-06 | DNA repair protein RecN |
| SAOUHSC_02114 | -1.6 | 6.1E-06 | conserved hypothetical protein |
| SAOUHSC_02523 | -2.0 | 6.1E-06 | conserved hypothetical protein |
| SAOUHSC_00173 | 2.1 | 6.5E-06 | acyl carrier phosphodiesterase |
| SAOUHSC_00690 | 2.1 | 6.6E-06 | conserved hypothetical protein |
| SAOUHSC_01757 | 2.0 | 6.8E-06 | ribosomal protein L21 |
| SAOUHSC_02929 | 1.6 | 6.8E-06 | acetyl-CoA synthetase%2C putative |
| SAOUHSC_02012 | -1.9 | 6.8E-06 | Transglycosylase domain protein |
| SAOUHSC_01253 | 1.8 | 6.9E-06 | conserved hypothetical protein |
| SAOUHSC_01433 | 1.6 | 7.2E-06 | conserved hypothetical protein |
| SAOUHSC_00653 | 2.3 | 7.3E-06 | ferrichrome transport permease fhuB%2C putative |
| SAOUHSC_02078 | 2.1 | 7.5E-06 | phi PV83 orf 10-like protein |
| SAOUHSC_00999 | -2.3 | 7.8E-06 | quinol oxidase%2C subunit IV%2C putative |
| SAOUHSC_01240 | 1.6 | 8.0E-06 | prolyl-tRNA synthetase |
| SAOUHSC_02310 | 2.3 | 8.5E-06 | potassium-transporting ATPase%2C C subunit |
| SAOUHSC_00526 | -1.9 | 9.4E-06 | conserved hypothetical protein |
| SAOUHSC_02123 | 1.6 | 9.7E-06 | ATP-dependent DNA helicase PcrA |
| SAOUHSC_01503 | -2.0 | 1.0E-05 | conserved hypothetical protein |
| SAOUHSC_00431 | 2.3 | 1.0E-05 | conserved hypothetical protein |
| SAOUHSC_01589 | -1.6 | 1.0E-05 | conserved hypothetical protein |
| SAOUHSC_00143 | -2.0 | 1.0E-05 | conserved hypothetical protein |
| SAOUHSC_01948 | 2.0 | 1.0E-05 | ABC transporter domain protein |
| SAOUHSC_02389 | -2.3 | 1.1E-05 | cation efflux family protein%2C putative |
| SAOUHSC_02877 | 2.0 | 1.1E-05 | squalene synthase%2C putative |
| SAOUHSC_00851 | 2.0 | 1.1E-05 | conserved hypothetical protein |
| SAOUHSC_02018 | 2.0 | 1.1E-05 | conserved hypothetical phage protein |
| SAOUHSC_02079 | 2.4 | 1.1E-05 | conserved hypothetical phage protein |
| SAOUHSC_01499 | 1.7 | 1.2E-05 | conserved hypothetical protein |
| SAOUHSC_02725 | -1.6 | 1.2E-05 | conserved hypothetical protein |
| SAOUHSC_00971 | -3.2 | 1.3E-05 | conserved hypothetical protein |
| SAOUHSC_00640 | -1.6 | 1.3E-05 | conserved hypothetical protein |
| SAOUHSC_00410 | -2.4 | 1.3E-05 | conserved hypothetical protein |
| SAOUHSC_02381 | 2.0 | 1.4E-05 | conserved hypothetical protein |
| SAOUHSC_01233 | 1.9 | 1.4E-05 | conserved hypothetical protein |
| SAOUHSC_02465 | -1.9 | 1.4E-05 | conserved hypothetical protein |
| SAOUHSC_02362 | 1.7 | 1.4E-05 | transcription termination factor Rho |
| SAOUHSC_00067 | 1.9 | 1.5E-05 | L-lactate permease |
| SAOUHSC_01724 | -1.9 | 1.5E-05 | conserved hypothetical protein |
| SAOUHSC_00201 | -1.8 | 1.5E-05 | conserved hypothetical protein |
| SAOUHSC_01102 | 1.6 | 1.5E-05 | excinuclease ABC%2C C subunit |
| SAOUHSC_02934 | -7.8 | 1.6E-05 | conserved hypothetical protein |
| SAOUHSC_02727 | -1.5 | 1.7E-05 | conserved hypothetical protein |
| SAOUHSC_02779 | 1.6 | 1.7E-05 | conserved hypothetical protein |
| SAOUHSC_00846 | 1.9 | 1.8E-05 | conserved hypothetical protein |
| SAOUHSC_02320 | 1.8 | 1.9E-05 | conserved hypothetical protein |
| SAOUHSC_01541 | 2.3 | 1.9E-05 | conserved hypothetical phage protein |
| SAOUHSC_02126 | -1.6 | 1.9E-05 | adenylosuccinate lyase |
| SAOUHSC_01693 | 2.1 | 2.0E-05 | conserved hypothetical protein |
| SAOUHSC_02666 | -1.5 | 2.0E-05 | conserved hypothetical protein |
| SAOUHSC_02360 | -1.5 | 2.1E-05 | thymidine kinase%2C putative |
| SAOUHSC_00840 | 2.0 | 2.1E-05 | conserved hypothetical protein |
| SAOUHSC_02857 | -3.9 | 2.1E-05 | conserved hypothetical protein |
| SAOUHSC_02369 | 1.7 | 2.2E-05 | DNA-directed RNA polymerase%2C delta subunit%2C putative |
| SAOUHSC_02736 | -1.6 | 2.2E-05 | conserved hypothetical protein |
| SAOUHSC_01569 | 7.1 | 2.2E-05 | conserved hypothetical phage protein |
| SAOUHSC_03032 | 1.7 | 2.3E-05 | conserved hypothetical protein |
| SAOUHSC_00484 | -1.6 | 2.3E-05 | conserved hypothetical protein |
| SAOUHSC_00440 | 4.0 | 2.3E-05 | conserved hypothetical protein |
| SAOUHSC_03054 | -2.0 | 2.3E-05 | ribonuclease P protein component |
| SAOUHSC_01359 | -1.9 | 2.3E-05 | conserved hypothetical protein |
| SAOUHSC_01375 | -1.5 | 2.4E-05 | conserved hypothetical protein |
| SAOUHSC_03016 | -1.9 | 2.4E-05 | conserved hypothetical protein |
| SAOUHSC_02886 | -2.5 | 2.4E-05 | conserved hypothetical protein |
| SAOUHSC_00916 | -6.8 | 2.6E-05 | conserved hypothetical protein |
| SAOUHSC_01000 | -1.8 | 2.6E-05 | cytochrome c oxidase subunit III%2C putative |
| SAOUHSC_01291 | -4.2 | 2.6E-05 | conserved hypothetical protein |
| SAOUHSC_01210 | 1.7 | 2.7E-05 | tRNA (guanine-N1)-methyltransferase |
| SAOUHSC_00639 | -2.1 | 2.7E-05 | conserved hypothetical protein |
| SAOUHSC_01264 | 2.2 | 2.7E-05 | conserved hypothetical protein |
| SAOUHSC_02138 | 1.7 | 2.7E-05 | conserved hypothetical protein |
| SAOUHSC_02258 | -1.5 | 2.8E-05 | conserved hypothetical protein |
| SAOUHSC_02990 | -1.6 | 2.8E-05 | conserved hypothetical protein |
| SAOUHSC_02680 | 2.9 | 2.8E-05 | nitrate reductase%2C beta subunit |
| SAOUHSC_00030 | -1.7 | 2.8E-05 | conserved hypothetical protein |
| SAOUHSC_00792 | 1.7 | 2.8E-05 | conserved hypothetical protein |
| SAOUHSC_01153 | -1.6 | 2.9E-05 | conserved hypothetical protein |
| SAOUHSC_00632 | 2.3 | 3.0E-05 | conserved hypothetical protein |
| SAOUHSC_00088 | -3.3 | 3.1E-05 | conserved hypothetical protein |
| SAOUHSC_01794 | -2.0 | 3.1E-05 | glyceraldehyde-3-phosphate dehydrogenase%2C type I |
| SAOUHSC_02467 | 1.9 | 3.3E-05 | alpha-acetolactate decarboxylase |
| SAOUHSC_02837 | -1.9 | 3.3E-05 | conserved hypothetical protein |
| SAOUHSC_00697 | -2.8 | 3.4E-05 | conserved hypothetical protein |
| SAOUHSC_00862 | -1.6 | 3.4E-05 | conserved hypothetical protein |
| SAOUHSC_00704 | -1.8 | 3.4E-05 | conserved hypothetical protein |
| SAOUHSC_00627 | 2.4 | 3.4E-05 | conserved hypothetical protein |
| SAOUHSC_01329 | -1.9 | 3.4E-05 | ribosomal protein S14p/S29e |
| SAOUHSC_01865 | -1.6 | 3.4E-05 | conserved hypothetical protein |
| SAOUHSC_00539 | -1.8 | 3.6E-05 | conserved hypothetical protein |
| SAOUHSC_01593 | -1.6 | 3.6E-05 | NUDIX domain protein |

| | | | |
|---|---|---|---|
| SAOUHSC_00729 | -1.6 | 3.6E-05 | ABC transporter%2C ATP-binding protein |
| SAOUHSC_02302 | -1.5 | 3.6E-05 | sigmaB regulation protein RsbU%2C putative |
| SAOUHSC_01138 | -2.0 | 3.7E-05 | conserved hypothetical protein |
| SAOUHSC_01902 | -2.5 | 3.8E-05 | conserved hypothetical protein |
| SAOUHSC_01649 | -2.0 | 4.0E-05 | rhomboid family protein |
| SAOUHSC_02702 | -2.4 | 4.3E-05 | conserved hypothetical protein |
| SAOUHSC_00002 | -1.6 | 4.7E-05 | DNA polymerase III%2C beta subunit |
| SAOUHSC_02287 | -1.6 | 4.7E-05 | 3-isopropylmalate dehydratase%2C large subunit |
| SAOUHSC_00660 | 1.8 | 4.7E-05 | conserved hypothetical protein |
| SAOUHSC_01066 | -1.4 | 4.7E-05 | protoheme IX farnesyltransferase |
| SAOUHSC_00956 | 1.4 | 4.8E-05 | peptide chain release factor 3 |
| SAOUHSC_01209 | 1.9 | 4.8E-05 | conserved hypothetical protein |
| SAOUHSC_01688 | -1.6 | 4.8E-05 | conserved hypothetical protein |
| SAOUHSC_02471 | -2.0 | 4.9E-05 | conserved hypothetical protein |
| SAOUHSC_01683 | 1.8 | 5.0E-05 | DNAk protein%2C putative |
| SAOUHSC_02608 | -2.0 | 5.1E-05 | conserved hypothetical protein |
| SAOUHSC_02625 | 1.5 | 5.2E-05 | conserved hypothetical protein |
| SAOUHSC_01251 | -1.4 | 5.3E-05 | polyribonucleotide nucleotidyltransferase%2C putative |
| SAOUHSC_02447 | 1.7 | 5.3E-05 | conserved hypothetical protein |
| SAOUHSC_02276 | -2.1 | 5.4E-05 | MutS domain V protein |
| SAOUHSC_02601 | 1.8 | 5.4E-05 | Na+/H+ antiporter%2C putative |
| SAOUHSC_01036 | -2.4 | 5.5E-05 | conserved hypothetical protein |
| SAOUHSC_02428 | 2.6 | 5.8E-05 | conserved hypothetical protein |
| SAOUHSC_00958 | -1.5 | 5.8E-05 | serine protease HtrA%2C putative |
| SAOUHSC_00485 | -1.5 | 5.9E-05 | hypoxanthine phosphoribosyltransferase |
| SAOUHSC_02742 | -1.8 | 6.1E-05 | amino acid transporter%2C putative |
| SAOUHSC_00739 | 2.0 | 6.2E-05 | conserved hypothetical protein |
| SAOUHSC_00743 | -1.7 | 6.4E-05 | ribonucleotide-disphosphate reductase beta chain%2C putative |
| SAOUHSC_02234 | 2.7 | 6.4E-05 | repressor-like protein-related protein |
| SAOUHSC_01377 | 1.8 | 6.7E-05 | oligopeptide ABC transporter%2C ATP-binding protein%2C putative |
| SAOUHSC_00908 | -1.6 | 6.8E-05 | coenzyme A disulfide reductase%2C putative |
| SAOUHSC_02650 | -1.9 | 6.9E-05 | lipoprotein%2C putative |
| SAOUHSC_01873 | -1.6 | 6.9E-05 | conserved hypothetical protein |
| SAOUHSC_00848 | 1.3 | 7.1E-05 | conserved hypothetical protein |
| SAOUHSC_02011 | -1.7 | 7.2E-05 | conserved hypothetical protein |
| SAOUHSC_01548 | 2.9 | 7.2E-05 | conserved hypothetical phage protein |
| SAOUHSC_01317 | -1.7 | 7.5E-05 | conserved hypothetical protein |
| SAOUHSC_02301 | -1.5 | 7.6E-05 | sigmaB regulation protein RsbU%2C putative |
| SAOUHSC_01592 | -2.0 | 7.8E-05 | transcriptional regulator%2C Fur%2C putative |
| SAOUHSC_02705 | -4.5 | 7.8E-05 | conserved hypothetical protein |
| SAOUHSC_01957 | -2.0 | 7.8E-05 | conserved hypothetical protein |
| SAOUHSC_01690 | -1.8 | 8.1E-05 | conserved hypothetical protein |
| SAOUHSC_00951 | -1.8 | 8.4E-05 | conserved hypothetical protein |
| SAOUHSC_00629 | 2.5 | 8.8E-05 | conserved hypothetical protein |
| SAOUHSC_02171 | -1.8 | 9.1E-05 | staphylokinase precursor%2C putative |
| SAOUHSC_01878 | 1.6 | 9.4E-05 | conserved hypothetical protein |
| SAOUHSC_02373 | 1.5 | 9.4E-05 | conserved hypothetical protein |
| SAOUHSC_00096 | -1.5 | 1.0E-04 | transcriptional regulator%2C GntR family%2C putative |
| SAOUHSC_01864 | -1.9 | 1.0E-04 | conserved hypothetical protein |
| SAOUHSC_01194 | -1.4 | 1.0E-04 | ATP-dependent DNA helicase RecG |
| SAOUHSC_02911 | -2.2 | 1.0E-04 | conserved hypothetical protein |
| SAOUHSC_00438 | 1.9 | 1.1E-04 | alpha amylase family protein%2C putative |
| SAOUHSC_A02450 | 6.2 | 1.1E-04 | conserved hypothetical protein |
| SAOUHSC_00753 | -2.5 | 1.1E-04 | conserved hypothetical protein |
| SAOUHSC_00945 | 1.4 | 1.1E-04 | magnesium transporter |
| SAOUHSC_00401 | -1.8 | 1.1E-04 | conserved hypothetical protein |
| SAOUHSC_01374 | 1.4 | 1.2E-04 | methicillin resistance factor%2C putative |
| SAOUHSC_01552 | 5.6 | 1.2E-04 | bacteriophage L54a%2C deoxyuridine 5-triphosphate nucleotidohydrolase |
| SAOUHSC_02937 | -1.9 | 1.2E-04 | choline transporter%2C putative |
| SAOUHSC_01413 | 1.6 | 1.2E-04 | conserved hypothetical protein |
| SAOUHSC_02930 | 1.5 | 1.2E-04 | conserved hypothetical protein |
| SAOUHSC_00781 | -1.3 | 1.2E-04 | HPr(Ser) kinase/phosphatase |
| SAOUHSC_01667 | 2.1 | 1.2E-04 | conserved hypothetical protein |
| SAOUHSC_00686 | 1.6 | 1.2E-04 | conserved hypothetical protein |
| SAOUHSC_00057 | 1.6 | 1.2E-04 | conserved hypothetical protein |
| SAOUHSC_02855 | 1.7 | 1.3E-04 | LysM domain protein |
| SAOUHSC_01907 | 1.4 | 1.3E-04 | conserved hypothetical protein |
| SAOUHSC_02605 | -1.5 | 1.3E-04 | conserved hypothetical protein |
| SAOUHSC_02056 | 3.4 | 1.3E-04 | conserved hypothetical phage protein |
| SAOUHSC_01942 | -6.9 | 1.4E-04 | serine protease SplA |
| SAOUHSC_02689 | -1.9 | 1.4E-04 | conserved hypothetical protein |
| SAOUHSC_01591 | -1.6 | 1.4E-04 | integrase/recombinase XerD |
| SAOUHSC_02289 | -1.5 | 1.4E-04 | thereonine dehydratase%2C putative |
| SAOUHSC_00780 | 1.4 | 1.4E-04 | excinuclease ABC%2C A subunit |
| SAOUHSC_00989 | -1.7 | 1.5E-04 | conserved hypothetical protein |
| SAOUHSC_00901 | -1.5 | 1.5E-04 | conserved hypothetical protein |
| SAOUHSC_01406 | 1.6 | 1.5E-04 | acylphosphatase |
| SAOUHSC_00902 | -1.4 | 1.6E-04 | Signal peptidase IA%2C putative |
| SAOUHSC_01313 | -1.7 | 1.6E-04 | Histidine kinase-%2C DNA gyrase B-%2C and HSP90-like ATPase domain protein |
| SAOUHSC_00296 | -2.2 | 1.7E-04 | ROK family protein |
| SAOUHSC_02806 | 2.5 | 1.7E-04 | gluconate permease%2C putative |
| SAOUHSC_02332 | 3.0 | 1.7E-04 | conserved hypothetical protein |
| SAOUHSC_02009 | -1.3 | 1.7E-04 | conserved hypothetical protein |
| SAOUHSC_01983 | -1.4 | 1.7E-04 | fumarate hydratase%2C class II |
| SAOUHSC_00742 | -1.3 | 1.7E-04 | ribonucleotide-diphosphate reductase alpha chain%2C putative |
| SAOUHSC_00741 | -1.3 | 1.8E-04 | ribonucleoside-diphosphate reductase 2%2C putative |
| SAOUHSC_02800 | -6.9 | 1.8E-04 | conserved hypothetical protein |
| SAOUHSC_01232 | 1.6 | 1.9E-04 | ribosomal protein S2 |
| SAOUHSC_00025 | -1.9 | 1.9E-04 | conserved hypothetical protein |
| SAOUHSC_00946 | 1.4 | 1.9E-04 | conserved hypothetical protein |
| SAOUHSC_01039 | -1.7 | 1.9E-04 | conserved hypothetical protein |
| SAOUHSC_02269 | -1.4 | 2.0E-04 | sucrose operon repressor%2C putative |
| SAOUHSC_01755 | 1.6 | 2.1E-04 | ribosomal protein L27 |

| | | | |
|---|---|---|---|
| SAOUHSC_02080 | 2.1 | 2.1E-04 | bacteriophage L54a%2C antirepressor%2C putative |
| SAOUHSC_01432 | 1.5 | 2.1E-04 | peptide methionine sulfoxide reductase |
| SAOUHSC_01989 | 1.5 | 2.1E-04 | conserved hypothetical protein |
| SAOUHSC_01350 | -1.9 | 2.1E-04 | conserved hypothetical protein |
| SAOUHSC_00659 | -1.5 | 2.1E-04 | conserved hypothetical protein |
| SAOUHSC_00724 | -1.6 | 2.2E-04 | chorismate binding enzyme%2C putative |
| SAOUHSC_00818 | -3.2 | 2.2E-04 | thermonuclease precursor |
| SAOUHSC_03053 | -1.4 | 2.2E-04 | tRNA modification GTPase TrmE |
| SAOUHSC_01986 | 1.6 | 2.2E-04 | conserved hypothetical protein |
| SAOUHSC_01529 | 1.9 | 2.2E-04 | major tail protein |
| SAOUHSC_00911 | -1.9 | 2.3E-04 | conserved hypothetical protein |
| SAOUHSC_02860 | 1.6 | 2.3E-04 | HMG-CoA synthase%2C putative |
| SAOUHSC_01443 | -2.0 | 2.4E-04 | conserved hypothetical protein |
| SAOUHSC_00404 | -2.1 | 2.4E-04 | conserved hypothetical protein |
| SAOUHSC_01106 | 1.3 | 2.4E-04 | glutamate racemase |
| SAOUHSC_02027 | 2.9 | 2.4E-04 | SLT orf 129-like protein |
| SAOUHSC_01328 | -1.5 | 2.5E-04 | ribosomal protein L33 |
| SAOUHSC_02743 | -1.9 | 2.5E-04 | amino acid ABC transporter%2C permease protein%2C putative |
| SAOUHSC_00084 | -2.3 | 2.6E-04 | conserved hypothetical protein |
| SAOUHSC_00776 | -1.4 | 2.7E-04 | excinuclease ABC%2C B subunit |
| SAOUHSC_01559 | 6.6 | 2.7E-04 | conserved hypothetical phage protein |
| SAOUHSC_02286 | -1.3 | 2.7E-04 | 3-isopropylmalate dehydrogenase |
| SAOUHSC_00503 | 1.7 | 2.7E-04 | UvrB/uvrC motif domain protein |
| SAOUHSC_00116 | 1.7 | 2.8E-04 | capsular polysaccharide synthesis enzyme Cap8C |
| SAOUHSC_02296 | 1.4 | 2.9E-04 | conserved hypothetical protein |
| SAOUHSC_01010 | -2.4 | 2.9E-04 | phosphoribosylaminoimidazole-succinocarboxamide synthase |
| SAOUHSC_02922 | -1.3 | 3.0E-04 | L-lactate dehydrogenase |
| SAOUHSC_02322 | -1.5 | 3.0E-04 | conserved hypothetical protein |
| SAOUHSC_00731 | 1.3 | 3.1E-04 | ABC transporter domain protein |
| SAOUHSC_02288 | -1.4 | 3.1E-04 | 3-isopropylmalate dehydratase%2C small subunit |
| SAOUHSC_01646 | 1.4 | 3.2E-04 | glucokinase%2C putative |
| SAOUHSC_01447 | -1.4 | 3.2E-04 | conserved hypothetical protein |
| SAOUHSC_00666 | -1.3 | 3.2E-04 | conserved hypothetical protein |
| SAOUHSC_01514 | -2.1 | 3.2E-04 | hypothetical phage protein |
| SAOUHSC_01429 | 1.6 | 3.3E-04 | conserved hypothetical protein |
| SAOUHSC_00983 | 1.4 | 3.3E-04 | 2-succinyl-6-hydroxy-2%2C4-cyclohexadiene-1-carboxylic acid synthase/2-oxoglutarate decarboxylase |
| SAOUHSC_01723 | -1.3 | 3.3E-04 | conserved hypothetical protein |
| SAOUHSC_01663 | -1.3 | 3.3E-04 | DNA primase%2C putative |
| SAOUHSC_01728 | 1.6 | 3.4E-04 | conserved hypothetical protein |
| SAOUHSC_02798 | -1.7 | 3.5E-04 | conserved hypothetical protein |
| SAOUHSC_00433 | -1.4 | 3.6E-04 | conserved hypothetical protein |
| SAOUHSC_01632 | 1.6 | 3.7E-04 | glycine cleavage system P-protein subunit ll%2C putative |
| SAOUHSC_00894 | -1.4 | 3.7E-04 | ornithine aminotransferase%2C putative |
| SAOUHSC_00865 | -1.3 | 3.7E-04 | conserved hypothetical protein |
| SAOUHSC_00603 | 1.3 | 4.0E-04 | conserved hypothetical protein |
| SAOUHSC_01600 | -1.3 | 4.0E-04 | conserved hypothetical protein |
| SAOUHSC_02146 | -1.4 | 4.1E-04 | conserved hypothetical protein |
| SAOUHSC_01028 | 1.7 | 4.2E-04 | phosphocarrier protein hpr%2C putative |
| SAOUHSC_00654 | 1.7 | 4.2E-04 | ferrichrome ABC transporter (permease)%2C putative |
| SAOUHSC_02971 | -1.6 | 4.2E-04 | aureolysin%2C putative |
| SAOUHSC_01760 | 1.6 | 4.3E-04 | conserved hypothetical protein |
| SAOUHSC_00074 | -1.7 | 4.4E-04 | periplasmic binding protein%2C putative |
| SAOUHSC_00347 | 2.7 | 4.4E-04 | conserved hypothetical protein |
| SAOUHSC_00651 | -1.4 | 4.5E-04 | conserved hypothetical protein |
| SAOUHSC_02426 | -1.6 | 4.7E-04 | membrane protein%2C putative |
| SAOUHSC_02423 | -1.2 | 4.7E-04 | UDP-N-acetylglucosamine pyrophosphorylase%2C putative |
| SAOUHSC_01024 | 2.3 | 4.8E-04 | hypothetical protein |
| SAOUHSC_01437 | 1.3 | 4.8E-04 | conserved hypothetical protein |
| SAOUHSC_00041 | -2.0 | 4.8E-04 | conserved hypothetical protein |
| SAOUHSC_02527 | 1.3 | 4.9E-04 | FmhB protein%2C putative |
| SAOUHSC_01394 | 1.3 | 5.0E-04 | aspartokinase II%2C putative |
| SAOUHSC_01065 | -1.5 | 5.0E-04 | heme A synthase%2C putative |
| SAOUHSC_00963 | -1.7 | 5.1E-04 | lipoyltransferase and lipoate-protein ligase%2C putative |
| SAOUHSC_01525 | 1.6 | 5.1E-04 | phage tail tape meausure protein%2C TP901 family%2C core region domain protein |
| SAOUHSC_01174 | -1.7 | 5.2E-04 | conserved hypothetical protein |
| SAOUHSC_01205 | 1.5 | 5.2E-04 | signal recognition particle-docking protein FtsY |
| SAOUHSC_00938 | -1.3 | 5.2E-04 | conserved hypothetical protein |
| SAOUHSC_01893 | 1.5 | 5.4E-04 | arsenical pump membrane protein subfamily |
| SAOUHSC_02970 | -2.5 | 5.4E-04 | conserved hypothetical protein |
| SAOUHSC_00242 | 1.4 | 5.5E-04 | conserved hypothetical protein |
| SAOUHSC_01356 | -1.8 | 5.5E-04 | transcriptional antiterminator |
| SAOUHSC_01843 | -1.6 | 5.5E-04 | conserved hypothetical protein |
| SAOUHSC_01795 | 1.4 | 5.6E-04 | dephospho-CoA kinase |
| SAOUHSC_00812 | 1.2 | 5.6E-04 | clumping factor |
| SAOUHSC_01846 | -2.0 | 5.7E-04 | acetyl-CoA synthetase%2C putative |
| SAOUHSC_00393 | -1.9 | 5.7E-04 | conserved hypothetical protein |
| SAOUHSC_01901 | -1.3 | 5.8E-04 | conserved hypothetical protein |
| SAOUHSC_01295 | -4.4 | 5.8E-04 | conserved hypothetical protein |
| SAOUHSC_01599 | -1.2 | 5.8E-04 | glucose-6-phosphate 1-dehydrogenase |
| SAOUHSC_02958 | 2.2 | 5.9E-04 | alkaline phosphatase III precursor%2C putative |
| SAOUHSC_02427 | 1.7 | 6.0E-04 | conserved hypothetical protein |
| SAOUHSC_01605 | 1.3 | 6.0E-04 | 6-phosphogluconate dehydrogenase%2C decarboxylating |
| SAOUHSC_02696 | -1.8 | 6.2E-04 | fmhA protein%2C putative |
| SAOUHSC_01825 | 1.5 | 6.2E-04 | conserved hypothetical protein |
| SAOUHSC_02125 | -1.8 | 6.2E-04 | conserved hypothetical protein |
| SAOUHSC_01420 | 1.3 | 6.2E-04 | DNA-binding response regulator%2C putative |
| SAOUHSC_01042 | 1.5 | 6.5E-04 | dihydrolipoamide S-acetyltransferase component of pyruvate dehydrogenase complex E2%2C putative |
| SAOUHSC_00879 | -1.3 | 6.5E-04 | probable cytosol aminopeptidase |
| SAOUHSC_01866 | -1.3 | 6.6E-04 | conserved hypothetical protein |
| SAOUHSC_00847 | 1.2 | 6.7E-04 | ABC transporter%2C ATP-binding protein%2C putative |
| SAOUHSC_02093 | 1.6 | 6.7E-04 | conserved hypothetical protein |

| | | | |
|---|---|---|---|
| SAOUHSC_00845 | 1.4 | 6.9E-04 | conserved hypothetical protein |
| SAOUHSC_01863 | -2.2 | 7.0E-04 | conserved hypothetical protein |
| SAOUHSC_02803 | 1.7 | 7.0E-04 | fibronectin-binding protein precursor%2C putative |
| SAOUHSC_01853 | 6.4 | 7.1E-04 | hypothetical protein |
| SAOUHSC_01127 | -2.6 | 7.3E-04 | conserved hypothetical protein |
| SAOUHSC_01814 | -1.4 | 7.3E-04 | conserved hypothetical protein |
| SAOUHSC_00191 | -1.8 | 7.3E-04 | conserved hypothetical protein |
| SAOUHSC_01736 | -2.5 | 7.6E-04 | conserved hypothetical protein |
| SAOUHSC_02070 | 3.3 | 7.6E-04 | phi PV83 orf 19-like protein |
| SAOUHSC_02840 | -2.1 | 7.7E-04 | L-serine dehydratase%2C iron-sulfur-dependent%2C beta subunit |
| SAOUHSC_00302 | -1.5 | 7.9E-04 | conserved hypothetical protein |
| SAOUHSC_02316 | 1.4 | 8.0E-04 | ATP-dependent RNA helicase%2C DEAD box family%2C putative |
| SAOUHSC_00940 | -1.3 | 8.0E-04 | conserved hypothetical protein |
| SAOUHSC_01213 | -1.5 | 8.0E-04 | conserved hypothetical protein |
| SAOUHSC_03033 | 1.6 | 8.2E-04 | high affinity nickel transporter%2C putative |
| SAOUHSC_00518 | 1.6 | 8.2E-04 | ribosomal protein L11 |
| SAOUHSC_01072 | -1.6 | 8.4E-04 | conserved hypothetical protein |
| SAOUHSC_00428 | 1.8 | 8.5E-04 | conserved hypothetical protein |
| SAOUHSC_02918 | 1.3 | 8.6E-04 | pantoate--beta-alanine ligase |
| SAOUHSC_00455 | 1.3 | 8.7E-04 | conserved hypothetical protein |
| SAOUHSC_01930 | -4.5 | 8.7E-04 | conserved hypothetical protein |
| SAOUHSC_00399 | -2.9 | 8.8E-04 | conserved hypothetical protein |
| SAOUHSC_02103 | -1.9 | 8.8E-04 | conserved hypothetical protein |
| SAOUHSC_00357 | -1.8 | 8.9E-04 | conserved hypothetical protein |
| SAOUHSC_02538 | 1.6 | 8.9E-04 | molybdopterin converting factor%2C subunit 1 |
| SAOUHSC_00382 | 1.4 | 8.9E-04 | conserved hypothetical protein |
| SAOUHSC_02747 | 1.3 | 9.0E-04 | conserved hypothetical protein |
| SAOUHSC_02522 | 1.6 | 9.0E-04 | conserved hypothetical protein |
| SAOUHSC_01785 | 1.7 | 9.4E-04 | ribosomal protein L35 |
| SAOUHSC_01784 | 2.1 | 9.4E-04 | ribosomal protein L20 |
| SAOUHSC_01431 | 1.5 | 9.4E-04 | methionine sulfoxide reductase%2C putative |
| SAOUHSC_01118 | -3.9 | 9.4E-04 | conserved hypothetical protein |
| SAOUHSC_00412 | 1.4 | 9.4E-04 | NADH dehydrogenase subunit 5%2C putative |
| SAOUHSC_01054 | -1.4 | 9.5E-04 | conserved hypothetical protein |
| SAOUHSC_02330 | 1.7 | 9.5E-04 | phosphomethylpyrimidine kinase |
| SAOUHSC_01714 | 1.6 | 9.5E-04 | transcription elongation factor GreA |
| SAOUHSC_02764 | -2.8 | 9.6E-04 | peptide ABC transporter%2C ATP-binding protein%2C putative |
| SAOUHSC_01730 | 1.9 | 9.6E-04 | conserved hypothetical protein |
| SAOUHSC_01179 | 1.2 | 1.0E-03 | primosomal protein N |
| SAOUHSC_02202 | 4.0 | 1.0E-03 | conserved hypothetical phage protein |
| SAOUHSC_00722 | -3.0 | 1.0E-03 | para-aminobenzoate synthase%2C glutamine amidotransferase%2C component II%2C putative |
| SAOUHSC_01561 | 4.3 | 1.0E-03 | PVL orf 50-like protein |
| SAOUHSC_01162 | -1.3 | 1.1E-03 | lipoprotein signal peptidase |
| SAOUHSC_00146 | -1.4 | 1.1E-03 | conserved hypothetical protein |
| SAOUHSC_02629 | 1.5 | 1.1E-03 | drug resistance transporter%2C EmrB/QacA subfamily%2C putative |
| SAOUHSC_A01081 | -6.3 | 1.1E-03 | conserved hypothetical protein |
| SAOUHSC_01451 | -1.8 | 1.1E-03 | threonine dehydratase |
| SAOUHSC_01321 | -1.4 | 1.1E-03 | threonine synthase |
| SAOUHSC_01361 | -1.3 | 1.1E-03 | transcriptional regulator%2C putative |
| SAOUHSC_00980 | 1.4 | 1.1E-03 | conserved hypothetical protein |
| SAOUHSC_01882 | -1.4 | 1.1E-03 | conserved hypothetical protein |
| SAOUHSC_00093 | 1.5 | 1.1E-03 | superoxide dismutase%2C putative |
| SAOUHSC_02575 | -1.7 | 1.1E-03 | conserved hypothetical protein |
| SAOUHSC_00181 | 1.6 | 1.2E-03 | conserved hypothetical protein |
| SAOUHSC_00012 | -1.5 | 1.2E-03 | conserved hypothetical protein |
| SAOUHSC_02841 | -1.5 | 1.2E-03 | conserved hypothetical protein |
| SAOUHSC_00409 | -1.5 | 1.2E-03 | conserved hypothetical protein |
| SAOUHSC_01923 | -2.0 | 1.2E-03 | conserved hypothetical protein |
| SAOUHSC_00673 | -1.5 | 1.2E-03 | conserved hypothetical protein |
| SAOUHSC_00843 | 1.3 | 1.2E-03 | conserved hypothetical protein |
| SAOUHSC_01652 | -1.1 | 1.2E-03 | penicillin-binding protein 3 |
| SAOUHSC_00913 | -5.6 | 1.2E-03 | conserved hypothetical protein |
| SAOUHSC_02315 | -1.6 | 1.3E-03 | DNA-binding response regulator%2C putative |
| SAOUHSC_00099 | 1.4 | 1.3E-03 | conserved hypothetical protein |
| SAOUHSC_01362 | 1.5 | 1.3E-03 | 4-oxalocrotonate tautomerase%2C putative |
| SAOUHSC_02148 | -1.5 | 1.3E-03 | conserved hypothetical protein |
| SAOUHSC_00874 | 1.4 | 1.3E-03 | conserved hypothetical protein |
| SAOUHSC_02921 | -1.3 | 1.3E-03 | alpha-acetolactate decarboxylase |
| SAOUHSC_00186 | -1.5 | 1.3E-03 | lipoprotein%2C putative |
| SAOUHSC_01773 | 1.9 | 1.3E-03 | uroporphyrinogen-III synthase%2C putative |
| SAOUHSC_00193 | -4.4 | 1.3E-03 | hypothetical protein |
| SAOUHSC_01890 | 1.4 | 1.4E-03 | conserved hypothetical protein |
| SAOUHSC_00556 | 1.3 | 1.4E-03 | proline/betaine transporter%2C putative |
| SAOUHSC_00793 | 1.8 | 1.4E-03 | conserved hypothetical protein |
| SAOUHSC_00270 | -1.8 | 1.4E-03 | conserved hypothetical protein |
| SAOUHSC_02324 | -1.4 | 1.5E-03 | conserved hypothetical protein |
| SAOUHSC_00295 | -2.2 | 1.5E-03 | N-acetylneuraminate lyase subunit%2C putative |
| SAOUHSC_02459 | -1.7 | 1.5E-03 | conserved hypothetical protein |
| SAOUHSC_00392 | -1.5 | 1.5E-03 | conserved hypothetical protein |
| SAOUHSC_02836 | -1.2 | 1.5E-03 | conserved hypothetical protein |
| SAOUHSC_01778 | 1.4 | 1.5E-03 | ATP-dependent Clp protease%2C ATP-binding subunit ClpX |
| SAOUHSC_00817 | -2.4 | 1.6E-03 | conserved hypothetical protein |
| SAOUHSC_00915 | -3.7 | 1.6E-03 | conserved hypothetical protein |
| SAOUHSC_02476 | -1.4 | 1.6E-03 | conserved hypothetical protein |
| SAOUHSC_02593 | -1.4 | 1.7E-03 | conserved hypothetical protein |
| SAOUHSC_01224 | -1.1 | 1.7E-03 | site-specific recombinase%2C putative |
| SAOUHSC_01113 | -5.0 | 1.7E-03 | conserved hypothetical protein |
| SAOUHSC_00021 | -1.1 | 1.7E-03 | sensory box histidine kinase VicK%2C putative |
| SAOUHSC_00077 | 1.9 | 1.7E-03 | conserved hypothetical protein |
| SAOUHSC_02828 | 1.2 | 1.7E-03 | conserved hypothetical protein |
| SAOUHSC_01276 | 1.2 | 1.7E-03 | glycerol kinase |
| SAOUHSC_01242 | -1.2 | 1.8E-03 | conserved hypothetical protein |
| SAOUHSC_00250 | -2.1 | 1.8E-03 | conserved hypothetical protein |

| | | | |
|---|---|---|---|
| SAOUHSC_00320 | 1.5 | 1.8E-03 | NADPH-dependent FMN reductase%2C putative |
| SAOUHSC_02231 | 2.3 | 1.8E-03 | anti repressor |
| SAOUHSC_02245 | -2.3 | 1.8E-03 | conserved hypothetical protein |
| SAOUHSC_02409 | -1.4 | 1.8E-03 | arginase |
| SAOUHSC_01338 | 1.6 | 1.8E-03 | conserved hypothetical protein |
| SAOUHSC_01821 | 1.3 | 1.8E-03 | conserved hypothetical protein |
| SAOUHSC_00988 | -1.6 | 1.9E-03 | glutamyl endopeptidase precursor%2C putative |
| SAOUHSC_01487 | -1.2 | 2.0E-03 | menaquinone biosynthesis methyltransferase%2C putative |
| SAOUHSC_02947 | -1.1 | 2.0E-03 | sulfite reductase (NADPH) flavoprotein alpha-component%2C putative |
| SAOUHSC_00254 | -5.7 | 2.0E-03 | conserved hypothetical protein |
| SAOUHSC_02100 | -1.3 | 2.0E-03 | conserved hypothetical protein |
| SAOUHSC_01588 | -1.4 | 2.0E-03 | conserved hypothetical protein |
| SAOUHSC_01333 | -1.4 | 2.1E-03 | LexA repressor |
| SAOUHSC_00785 | 1.1 | 2.2E-03 | thioredoxin reductase |
| SAOUHSC_00052 | -3.6 | 2.2E-03 | conserved hypothetical protein |
| SAOUHSC_00708 | 1.7 | 2.3E-03 | fructose specific permease%2C putative |
| SAOUHSC_02942 | -1.1 | 2.3E-03 | anaerobic ribonucleoside-triphosphate reductase%2C putative |
| SAOUHSC_00244 | -1.9 | 2.3E-03 | conserved hypothetical protein |
| SAOUHSC_02099 | -1.1 | 2.3E-03 | histidine kinase%2C putative |
| SAOUHSC_02338 | 1.7 | 2.3E-03 | conserved hypothetical protein |
| SAOUHSC_01425 | 1.3 | 2.3E-03 | conserved hypothetical protein |
| SAOUHSC_01685 | 1.6 | 2.4E-03 | heat-inducible transcription repressor HrcA |
| SAOUHSC_01803 | -1.2 | 2.4E-03 | conserved hypothetical protein |
| SAOUHSC_02750 | -1.1 | 2.4E-03 | conserved hypothetical protein |
| SAOUHSC_02956 | -1.2 | 2.4E-03 | DNA-binding response regulator%2C putative |
| SAOUHSC_02816 | -1.3 | 2.5E-03 | conserved hypothetical protein |
| SAOUHSC_02778 | -1.1 | 2.5E-03 | conserved hypothetical protein |
| SAOUHSC_00758 | 1.7 | 2.5E-03 | conserved hypothetical protein |
| SAOUHSC_02944 | 2.3 | 2.5E-03 | conserved hypothetical protein |
| SAOUHSC_00964 | 1.2 | 2.5E-03 | conserved hypothetical protein |
| SAOUHSC_01241 | 1.0 | 2.5E-03 | DNA polymerase III%2C alpha subunit%2C Gram-positive type |
| SAOUHSC_02543 | 1.4 | 2.5E-03 | molybdenum cofactor biosynthesis protein C |
| SAOUHSC_00822 | -1.8 | 2.5E-03 | conserved hypothetical protein |
| SAOUHSC_00968 | -2.4 | 2.5E-03 | conserved hypothetical protein |
| SAOUHSC_01577 | -3.6 | 2.6E-03 | conserved hypothetical phage protein |
| SAOUHSC_02003 | 1.4 | 2.6E-03 | ABC transporter%2C ATP-binding/permease protein%2C putative |
| SAOUHSC_02739 | 1.4 | 2.6E-03 | 2-dehydropantoate 2-reductase |
| SAOUHSC_02913 | -1.3 | 2.6E-03 | conserved hypothetical protein |
| SAOUHSC_01477 | 1.6 | 2.6E-03 | conserved hypothetical protein |
| SAOUHSC_02686 | 1.3 | 2.6E-03 | conserved hypothetical protein |
| SAOUHSC_03015 | -2.5 | 2.6E-03 | conserved hypothetical protein |
| SAOUHSC_00130 | -2.2 | 2.8E-03 | conserved hypothetical protein |
| SAOUHSC_02519 | -1.1 | 2.8E-03 | conserved hypothetical protein |
| SAOUHSC_02392 | -1.7 | 2.8E-03 | truncated resolvase |
| SAOUHSC_00249 | -1.8 | 2.9E-03 | conserved hypothetical protein |
| SAOUHSC_02721 | 2.0 | 2.9E-03 | conserved hypothetical protein |
| SAOUHSC_01594 | 1.1 | 2.9E-03 | conserved hypothetical protein |
| SAOUHSC_01208 | 1.8 | 3.0E-03 | ribosomal protein S16 |
| SAOUHSC_02553 | -1.4 | 3.0E-03 | conserved hypothetical protein |
| SAOUHSC_01851 | -2.2 | 3.1E-03 | hypothetical protein |
| SAOUHSC_00832 | 1.2 | 3.1E-03 | 3-dehydroquinate dehydratase%2C type I |
| SAOUHSC_00007 | -1.4 | 3.1E-03 | conserved hypothetical protein |
| SAOUHSC_02777 | -1.3 | 3.1E-03 | conserved hypothetical protein |
| SAOUHSC_00524 | 1.3 | 3.1E-03 | RNA polymerase beta chain%2C putative |
| SAOUHSC_00255 | -1.9 | 3.2E-03 | conserved hypothetical protein |
| SAOUHSC_02729 | -1.7 | 3.2E-03 | amino acid ABC transporter-like protein%2C putative |
| SAOUHSC_01046 | -1.4 | 3.2E-03 | ABC transporter domain protein |
| SAOUHSC_02061 | 4.8 | 3.2E-03 | phi PVL orf 50-like protein |
| SAOUHSC_02726 | 1.6 | 3.2E-03 | positive transcriptional activator%2C putative |
| SAOUHSC_02457 | -1.2 | 3.3E-03 | transcriptional regulator%2C Sir2 family%2C putative |
| SAOUHSC_01987 | 1.1 | 3.3E-03 | conserved hypothetical protein |
| SAOUHSC_00949 | -1.3 | 3.3E-03 | conserved hypothetical protein |
| SAOUHSC_00014 | -1.1 | 3.3E-03 | conserved hypothetical protein |
| SAOUHSC_00766 | 1.5 | 3.3E-03 | conserved hypothetical protein |
| SAOUHSC_03009 | 2.3 | 3.3E-03 | phosphoribosylformimino-5-aminoimidazole carboxamide ribotide isomerase%2C putative |
| SAOUHSC_01726 | 1.2 | 3.3E-03 | (5-methylaminomethyl-2-thiouridylate)-methyltransferase |
| SAOUHSC_01463 | 1.2 | 3.4E-03 | conserved hypothetical protein |
| SAOUHSC_02618 | -1.2 | 3.4E-03 | conserved hypothetical protein |
| SAOUHSC_01597 | -1.0 | 3.4E-03 | pyrroline-5-carboxylate reductase |
| SAOUHSC_00317 | -1.7 | 3.4E-03 | glycerol-3-phosphate transporter |
| SAOUHSC_01974 | -1.1 | 3.4E-03 | conserved hypothetical protein |
| SAOUHSC_01601 | 1.1 | 3.4E-03 | alpha-glucosidase%2C putative |
| SAOUHSC_01029 | 1.1 | 3.5E-03 | phosphoenolpyruvate-protein phosphotransferase |
| SAOUHSC_01011 | -2.3 | 3.6E-03 | phosphoribosylformylglycinamidine synthase%2C PurS protein |
| SAOUHSC_00085 | -1.5 | 3.6E-03 | conserved hypothetical protein |
| SAOUHSC_03048 | -2.0 | 3.6E-03 | conserved hypothetical protein |
| SAOUHSC_01423 | 1.2 | 3.7E-03 | conserved hypothetical protein |
| SAOUHSC_00578 | 1.2 | 3.7E-03 | diphosphomevalonate decarboxylase |
| SAOUHSC_00473 | 2.9 | 3.7E-03 | hypothetical protein |
| SAOUHSC_02993 | -2.4 | 3.7E-03 | conserved hypothetical protein |
| SAOUHSC_00047 | -1.6 | 3.7E-03 | conserved hypothetical protein |
| SAOUHSC_01582 | -2.2 | 3.7E-03 | bacteriophage integrase |
| SAOUHSC_02096 | 1.4 | 3.8E-03 | conserved hypothetical protein |
| SAOUHSC_01492 | -1.0 | 3.8E-03 | conserved hypothetical protein |
| SAOUHSC_00291 | -2.1 | 3.8E-03 | pfkB family carbohydrate kinase family%2C putative |
| SAOUHSC_01326 | -1.1 | 3.9E-03 | conserved hypothetical protein |
| SAOUHSC_01628 | -1.6 | 4.0E-03 | conserved hypothetical protein |
| SAOUHSC_00427 | -1.0 | 4.0E-03 | autolysin precursor%2C putative |
| SAOUHSC_01324 | -1.4 | 4.0E-03 | conserved hypothetical protein |
| SAOUHSC_02733 | -1.5 | 4.0E-03 | membrane protein%2C putative |
| SAOUHSC_00790 | 1.5 | 4.0E-03 | ATP-dependent Clp protease%2C proteolytic subunit ClpP |
| SAOUHSC_00987 | -1.4 | 4.0E-03 | cysteine protease precursor%2C putative |
| SAOUHSC_02623 | 1.1 | 4.0E-03 | conserved hypothetical protein |

| | | | |
|---|---|---|---|
| SAOUHSC_01612 | 1.1 | 4.0E-03 | 2-oxoisovalerate dehydrogenase%2C E1 component%2C beta subunit%2C putative |
| SAOUHSC_00548 | -1.1 | 4.1E-03 | conserved hypothetical protein |
| SAOUHSC_02282 | -1.2 | 4.2E-03 | acetolactate synthase%2C large subunit%2C biosynthetic type |
| SAOUHSC_02217 | 2.2 | 4.2E-03 | phi ETA orf 22-like protein |
| SAOUHSC_00259 | -5.3 | 4.2E-03 | conserved hypothetical protein |
| SAOUHSC_02891 | -1.3 | 4.2E-03 | conserved hypothetical protein |
| SAOUHSC_02801 | -1.2 | 4.3E-03 | UTP-glucose-1-phosphate uridylyltransferase |
| SAOUHSC_02283 | -1.5 | 4.3E-03 | conserved hypothetical protein |
| SAOUHSC_01808 | 1.2 | 4.3E-03 | acetyl-CoA carboxylase%2C carboxyl transferase%2C alpha subunit |
| SAOUHSC_01025 | -1.1 | 4.3E-03 | conserved hypothetical protein |
| SAOUHSC_01287 | -1.0 | 4.3E-03 | glutamine synthetase%2C type I |
| SAOUHSC_01352 | 1.1 | 4.4E-03 | DNA topoisomerase IV%2C A subunit |
| SAOUHSC_02331 | 1.5 | 4.4E-03 | conserved hypothetical protein |
| SAOUHSC_01100 | 1.4 | 4.6E-03 | thioredoxin |
| SAOUHSC_01818 | -1.2 | 4.7E-03 | alanine dehydrogenase |
| SAOUHSC_00841 | 1.4 | 4.7E-03 | conserved hypothetical protein |
| SAOUHSC_01485 | -1.7 | 4.7E-03 | nucleoside diphosphate kinase%2C putative |
| SAOUHSC_01148 | 1.1 | 4.7E-03 | cell division protein%2C putative |
| SAOUHSC_02131 | 1.2 | 4.8E-03 | conserved hypothetical protein |
| SAOUHSC_01813 | -1.1 | 4.8E-03 | conserved hypothetical protein |
| SAOUHSC_00373 | 1.2 | 4.8E-03 | xanthine permease%2C putative |
| SAOUHSC_01969 | 1.0 | 4.8E-03 | conserved hypothetical protein |
| SAOUHSC_01486 | -1.1 | 4.8E-03 | heptaprenyl diphosphate syntase component II%2C putative |
| SAOUHSC_02852 | -1.1 | 4.9E-03 | conserved hypothetical protein |
| SAOUHSC_02004 | -1.3 | 4.9E-03 | conserved hypothetical protein |
| SAOUHSC_01867 | -1.1 | 4.9E-03 | D-amino acid aminotransferase |
| SAOUHSC_00586 | -1.6 | 4.9E-03 | conserved hypothetical protein |
| SAOUHSC_01307 | -1.3 | 4.9E-03 | conserved hypothetical protein |
| SAOUHSC_01467 | 1.2 | 5.0E-03 | penicillin-binding protein 2 |
| SAOUHSC_02790 | -1.0 | 5.0E-03 | conserved hypothetical protein |
| SAOUHSC_00667 | -1.1 | 5.0E-03 | ABC transporter ATP-binding protein%2C putative |
| SAOUHSC_00944 | 1.0 | 5.0E-03 | conserved hypothetical protein |
| SAOUHSC_02021 | 1.4 | 5.0E-03 | phi ETA orf 63-like protein |
| SAOUHSC_02785 | -1.5 | 5.1E-03 | conserved hypothetical protein |
| SAOUHSC_01796 | 1.0 | 5.1E-03 | formamidopyrimidine-DNA glycosylase |
| SAOUHSC_01869 | 1.2 | 5.1E-03 | conserved hypothetical protein |
| SAOUHSC_00863 | 1.6 | 5.2E-03 | conserved hypothetical protein |
| SAOUHSC_02961 | -1.0 | 5.2E-03 | conserved hypothetical protein |
| SAOUHSC_00367 | -1.4 | 5.3E-03 | conserved hypothetical protein |
| SAOUHSC_00350 | 1.8 | 5.4E-03 | ribosomal protein S18 |
| SAOUHSC_01603 | 5.8 | 5.5E-03 | hypothetical protein |
| SAOUHSC_00857 | 3.2 | 5.5E-03 | conserved hypothetical protein |
| SAOUHSC_00133 | 1.2 | 5.5E-03 | conserved hypothetical protein |
| SAOUHSC_01201 | 1.5 | 5.6E-03 | acyl carrier protein |
| SAOUHSC_01456 | -1.5 | 5.6E-03 | conserved hypothetical protein |
| SAOUHSC_01914 | 1.3 | 5.6E-03 | conserved hypothetical protein |
| SAOUHSC_02053 | 4.9 | 5.6E-03 | transcriptional activator rinb-related protein |
| SAOUHSC_02319 | -1.3 | 5.8E-03 | conserved hypothetical protein |
| SAOUHSC_00351 | -1.8 | 5.9E-03 | conserved hypothetical protein |
| SAOUHSC_01859 | 1.3 | 5.9E-03 | conserved hypothetical protein |
| SAOUHSC_01545 | 2.0 | 5.9E-03 | conserved hypothetical phage protein |
| SAOUHSC_00319 | 1.0 | 6.0E-03 | conserved hypothetical protein |
| SAOUHSC_00474 | 1.3 | 6.0E-03 | ribosomal 5S rRNA E-loop binding protein Ctc/L25/TL5 |
| SAOUHSC_00318 | 1.0 | 6.1E-03 | conserved hypothetical protein |
| SAOUHSC_00182 | -5.7 | 6.2E-03 | conserved hypothetical protein |
| SAOUHSC_02722 | 1.6 | 6.2E-03 | conserved hypothetical protein |
| SAOUHSC_01400 | -1.1 | 6.3E-03 | alanine racemase%2C putative |
| SAOUHSC_00607 | -1.3 | 6.4E-03 | conserved hypothetical protein |
| SAOUHSC_01247 | -1.2 | 6.5E-03 | ribosome-binding factor A |
| SAOUHSC_00682 | 1.8 | 6.6E-03 | conserved hypothetical protein |
| SAOUHSC_00763 | -1.2 | 6.6E-03 | conserved hypothetical protein |
| SAOUHSC_00701 | 1.5 | 6.8E-03 | conserved hypothetical protein |
| SAOUHSC_01305 | -2.0 | 6.9E-03 | conserved hypothetical protein |
| SAOUHSC_02483 | -1.0 | 6.9E-03 | ABC transporter%2C ATP-binding protein%2C putative |
| SAOUHSC_00684 | 1.3 | 6.9E-03 | conserved hypothetical protein |
| SAOUHSC_01988 | 1.1 | 7.0E-03 | conserved hypothetical protein |
| SAOUHSC_00192 | -1.4 | 7.0E-03 | coagulase |
| SAOUHSC_02405 | 1.2 | 7.1E-03 | phosphoglucosamine mutase |
| SAOUHSC_01857 | 1.0 | 7.1E-03 | conserved hypothetical protein |
| SAOUHSC_00572 | -1.2 | 7.2E-03 | conserved hypothetical protein |
| SAOUHSC_02145 | 1.1 | 7.2E-03 | conserved hypothetical protein |
| SAOUHSC_01239 | 1.0 | 7.2E-03 | conserved hypothetical protein |
| SAOUHSC_01926 | 1.3 | 7.3E-03 | conserved hypothetical protein |
| SAOUHSC_00589 | -3.4 | 7.3E-03 | hypothetical protein |
| SAOUHSC_00976 | -1.5 | 7.3E-03 | conserved hypothetical protein |
| SAOUHSC_02969 | -1.3 | 7.5E-03 | arginine deiminase |
| SAOUHSC_01061 | 1.1 | 7.8E-03 | conserved hypothetical protein |
| SAOUHSC_02684 | 1.5 | 7.8E-03 | assimilatory nitrite reductase [NAD(P)H]%2C large subunit%2C putative |
| SAOUHSC_01769 | -1.0 | 7.8E-03 | conserved hypothetical protein |
| SAOUHSC_01850 | -1.0 | 7.9E-03 | catabolite control protein A |
| SAOUHSC_01062 | -1.5 | 7.9E-03 | conserved hypothetical protein |
| SAOUHSC_00878 | 1.2 | 7.9E-03 | conserved hypothetical protein |
| SAOUHSC_00212 | -5.7 | 8.2E-03 | conserved hypothetical protein |
| SAOUHSC_02355 | 1.2 | 8.2E-03 | conserved hypothetical protein |
| SAOUHSC_00824 | -1.7 | 8.3E-03 | conserved hypothetical protein |
| SAOUHSC_01891 | 1.3 | 8.3E-03 | arsenate operon regulator |
| SAOUHSC_02859 | -1.0 | 8.4E-03 | hydroxymethylglutaryl-CoA reductase%2C degradative |
| SAOUHSC_02357 | -1.3 | 8.7E-03 | conserved hypothetical protein |
| SAOUHSC_02545 | -1.0 | 8.7E-03 | conserved hypothetical protein |
| SAOUHSC_00200 | -1.7 | 8.7E-03 | membrane protein%2C putative |
| SAOUHSC_01436 | 1.2 | 8.7E-03 | conserved hypothetical protein |
| SAOUHSC_01337 | 1.0 | 8.7E-03 | transketolase |
| SAOUHSC_00344 | 1.2 | 8.7E-03 | conserved hypothetical protein |

| | | | |
|---|---|---|---|
| SAOUHSC_01091 | -1.0 | 8.8E-03 | conserved hypothetical protein |
| SAOUHSC_01762 | 1.6 | 8.8E-03 | conserved hypothetical protein |
| SAOUHSC_00470 | 2.5 | 8.9E-03 | conserved hypothetical protein |
| SAOUHSC_00555 | 1.6 | 8.9E-03 | hydrolase%2C haloacid dehalogenase-like |
| SAOUHSC_01668 | 1.1 | 9.3E-03 | GTP-binding protein Era |
| SAOUHSC_02703 | 1.1 | 9.3E-03 | phosphoglycerate mutase%2C putative |
| SAOUHSC_01490 | 1.0 | 9.3E-03 | DNA-binding protein HU%2C putative |
| SAOUHSC_02869 | -1.4 | 9.4E-03 | delta-1-pyrroline-5-carboxylate dehydrogenase%2C putative |
| SAOUHSC_00342 | -1.2 | 9.4E-03 | chromosome partioning protein%2C ParB family%2C putative |
| SAOUHSC_01097 | -1.0 | 9.5E-03 | conserved hypothetical protein |
| SAOUHSC_00149 | -2.0 | 9.5E-03 | N-acetylglutamate gamma-semialdehyde dehydrogenase%2C putative |
| SAOUHSC_02652 | 1.1 | 9.6E-03 | conserved hypothetical protein |
| SAOUHSC_T00023 | -2.8 | 9.7E-03 | tRNA-Gly |
| SAOUHSC_02277 | 1.3 | 9.8E-03 | O-sialoglycoprotein endopeptidase%2C putative |
| SAOUHSC_01075 | -1.0 | 1.0E-02 | pantetheine-phosphate adenylyltransferase |
| SAOUHSC_00844 | 1.1 | 1.0E-02 | conserved hypothetical protein |
| SAOUHSC_01956 | 1.4 | 1.0E-02 | conserved hypothetical protein |
| SAOUHSC_02647 | -1.2 | 1.0E-02 | malate:quinone-oxidoreductase |
| SAOUHSC_00663 | -1.1 | 1.0E-02 | conserved hypothetical protein |
| SAOUHSC_00889 | -1.0 | 1.0E-02 | Na+/H+ antiporter subunit%2C putative |
| SAOUHSC_01921 | -2.5 | 1.0E-02 | conserved hypothetical protein |
| SAOUHSC_00502 | 1.3 | 1.0E-02 | conserved hypothetical protein |
| SAOUHSC_00372 | -1.4 | 1.1E-02 | xanthine phosphoribosyltransferase |
| SAOUHSC_02676 | -1.0 | 1.1E-02 | conserved hypothetical protein |
| SAOUHSC_00234 | -1.1 | 1.1E-02 | conserved hypothetical protein |
| SAOUHSC_01376 | -1.2 | 1.1E-02 | conserved hypothetical protein |
| SAOUHSC_00828 | -1.3 | 1.1E-02 | conserved hypothetical protein |
| SAOUHSC_03030 | -1.4 | 1.1E-02 | sodium%2C sulfate symporter%2C putative |
| SAOUHSC_01360 | 1.0 | 1.1E-02 | peptide methionine sulfoxide reductase |
| SAOUHSC_02158 | -0.9 | 1.1E-02 | conserved hypothetical protein |
| SAOUHSC_01700 | 1.0 | 1.1E-02 | conserved hypothetical protein |
| SAOUHSC_01358 | -1.2 | 1.1E-02 | conserved hypothetical protein |
| SAOUHSC_01511 | -1.9 | 1.1E-02 | conserved hypothetical protein |
| SAOUHSC_00507 | 1.0 | 1.1E-02 | DNA repair protein RadA |
| SAOUHSC_02761 | -1.1 | 1.2E-02 | conserved hypothetical protein |
| SAOUHSC_02246 | -2.0 | 1.2E-02 | conserved hypothetical protein |
| SAOUHSC_01872 | -1.0 | 1.2E-02 | conserved hypothetical protein |
| SAOUHSC_02211 | 4.9 | 1.2E-02 | phi PVL orf 50-like protein |
| SAOUHSC_00872 | -1.0 | 1.2E-02 | extramembranal protein |
| SAOUHSC_00720 | 1.4 | 1.2E-02 | 6-pyruvoyl tetrahydropterin synthase superfamily%2C putative |
| SAOUHSC_02555 | 1.5 | 1.2E-02 | conserved hypothetical protein |
| SAOUHSC_00519 | 1.2 | 1.2E-02 | ribosomal protein L1 |
| SAOUHSC_01992 | 1.0 | 1.2E-02 | Phosphotransferase system%2C EIIC domain protein |
| SAOUHSC_02464 | -1.2 | 1.2E-02 | conserved hypothetical protein |
| SAOUHSC_01399 | -1.1 | 1.2E-02 | conserved hypothetical protein |
| SAOUHSC_01272 | 1.0 | 1.2E-02 | DNA mismatch repair protein MutS |
| SAOUHSC_00505 | 1.3 | 1.2E-02 | endopeptidase%2C putative |
| SAOUHSC_02556 | 1.1 | 1.2E-02 | conserved hypothetical protein |
| SAOUHSC_02537 | 1.1 | 1.2E-02 | molybdopterin-guanine dinucleotide biosynthesis mobA%2C putative |
| SAOUHSC_01786 | 1.2 | 1.2E-02 | translation initiation factor IF-3 |
| SAOUHSC_01686 | -1.3 | 1.2E-02 | conserved hypothetical protein |
| SAOUHSC_00417 | 1.3 | 1.2E-02 | conserved hypothetical protein |
| SAOUHSC_02628 | -1.2 | 1.3E-02 | conserved hypothetical protein |
| SAOUHSC_02482 | -1.0 | 1.3E-02 | ABC transporter%2C ATP-binding protein%2C putative |
| SAOUHSC_00414 | -0.9 | 1.3E-02 | conserved hypothetical protein |
| SAOUHSC_00231 | -1.4 | 1.3E-02 | two-component response regulator%2C putative |
| SAOUHSC_00301 | -1.0 | 1.3E-02 | conserved hypothetical protein |
| SAOUHSC_01064 | -0.9 | 1.3E-02 | pyruvate carboxylase |
| SAOUHSC_00297 | -1.0 | 1.4E-02 | conserved hypothetical protein |
| SAOUHSC_00652 | 1.0 | 1.4E-02 | iron compound ABC transporter%2C ATP-binding protein |
| SAOUHSC_01715 | 1.0 | 1.4E-02 | uridine kinase |
| SAOUHSC_01034 | 0.9 | 1.4E-02 | conserved hypothetical protein |
| SAOUHSC_01560 | 4.3 | 1.4E-02 | conserved hypothetical phage protein |
| SAOUHSC_00685 | -1.5 | 1.4E-02 | conserved hypothetical protein |
| SAOUHSC_02813 | -0.9 | 1.4E-02 | conserved hypothetical protein |
| SAOUHSC_00888 | -1.0 | 1.4E-02 | monovalent cation:proton antiporter subfamily%2C putative |
| SAOUHSC_00891 | 1.0 | 1.4E-02 | peptidyl-prolyl cis-trans isomerase%2C cyclophilin-type%2C putative |
| SAOUHSC_02635 | -0.9 | 1.4E-02 | conserved hypothetical protein |
| SAOUHSC_01282 | 0.9 | 1.4E-02 | conserved hypothetical protein |
| SAOUHSC_00109 | -3.5 | 1.5E-02 | replication initiation protein%2C putative |
| SAOUHSC_02901 | -1.5 | 1.5E-02 | conserved hypothetical protein |
| SAOUHSC_00328 | 1.3 | 1.5E-02 | conserved hypothetical protein |
| SAOUHSC_02130 | 1.7 | 1.5E-02 | conserved hypothetical protein |
| SAOUHSC_01684 | 1.3 | 1.5E-02 | co-chaperone GrpE |
| SAOUHSC_01861 | 1.0 | 1.5E-02 | conserved hypothetical protein |
| SAOUHSC_00251 | -1.6 | 1.5E-02 | conserved hypothetical protein |
| SAOUHSC_00984 | 1.1 | 1.5E-02 | conserved hypothetical protein |
| SAOUHSC_00661 | 1.1 | 1.5E-02 | conserved hypothetical protein |
| SAOUHSC_00031 | 5.5 | 1.5E-02 | conserved hypothetical protein |
| SAOUHSC_02649 | -0.9 | 1.5E-02 | conserved hypothetical protein |
| SAOUHSC_01735 | -0.9 | 1.5E-02 | conserved hypothetical protein |
| SAOUHSC_01129 | -1.3 | 1.5E-02 | carbamate kinase |
| SAOUHSC_00504 | 1.1 | 1.6E-02 | ATP:guanido phosphotransferase%2C C-terminal catalytic domain protein |
| SAOUHSC_02092 | 1.0 | 1.6E-02 | aminopeptidase PepS%2C putative |
| SAOUHSC_02536 | 0.9 | 1.6E-02 | molybdopterin cofactor biosynthesis protein A%2C putative |
| SAOUHSC_00866 | -0.9 | 1.6E-02 | D-isomer specific 2-hydroxyacid dehydrogenase%2C NAD binding domain protein |
| SAOUHSC_01187 | 0.9 | 1.6E-02 | conserved hypothetical protein |
| SAOUHSC_00642 | -0.9 | 1.6E-02 | teichoic acid biosynthesis protein%2C putative |
| SAOUHSC_01540 | 5.5 | 1.6E-02 | bacteriophage L54a%2C HNH endonuclease family protein |
| SAOUHSC_A02273 | -5.3 | 1.7E-02 | hypothetical protein |
| SAOUHSC_01455 | -0.9 | 1.7E-02 | conserved hypothetical protein |
| SAOUHSC_00082 | 1.6 | 1.7E-02 | conserved hypothetical protein |
| SAOUHSC_01344 | 1.9 | 1.7E-02 | conserved hypothetical protein |

| | | | |
|---|---|---|---|
| SAOUHSC_03052 | -1.1 | 1.7E-02 | glucose inhibited division protein A%2C putative |
| SAOUHSC_01424 | 1.0 | 1.7E-02 | UDP-N-acetylglucosamine--N-acetylmuramyl-(pentapeptide) pyrophosphoryl-undecaprenol N-acetylglucosamine transferase |
| SAOUHSC_02233 | 2.0 | 1.7E-02 | phi PVL orf 32-like protein |
| SAOUHSC_02751 | -1.0 | 1.8E-02 | conserved hypothetical protein |
| SAOUHSC_01383 | -1.1 | 1.8E-02 | conserved hypothetical protein |
| SAOUHSC_01502 | 1.0 | 1.8E-02 | ATP-dependent DNA helicase RecQ%2C putative |
| SAOUHSC_01526 | 5.4 | 1.8E-02 | conserved hypothetical phage protein |
| SAOUHSC_A02254 | -2.5 | 1.8E-02 | hypothetical protein |
| SAOUHSC_00573 | -1.1 | 1.8E-02 | conserved hypothetical protein |
| SAOUHSC_00153 | -1.2 | 1.8E-02 | indolepyruvate decarboxylase%2C putative |
| SAOUHSC_00092 | -1.2 | 1.8E-02 | conserved hypothetical protein |
| SAOUHSC_00043 | -1.6 | 1.8E-02 | conserved hypothetical protein |
| SAOUHSC_01284 | 0.9 | 1.8E-02 | conserved hypothetical protein |
| SAOUHSC_02982 | 0.9 | 1.8E-02 | conserved hypothetical protein |
| SAOUHSC_00080 | 1.5 | 1.8E-02 | conserved hypothetical protein |
| SAOUHSC_02366 | 1.2 | 1.9E-02 | conserved hypothetical protein |
| SAOUHSC_00644 | -1.0 | 1.9E-02 | tagX protein%2C putative |
| SAOUHSC_02304 | -1.0 | 1.9E-02 | conserved hypothetical protein |
| SAOUHSC_01909 | -1.0 | 1.9E-02 | S-adenosylmethionine synthetase |
| SAOUHSC_02169 | -3.7 | 1.9E-02 | conserved hypothetical phage protein |
| SAOUHSC_02660 | 1.0 | 1.9E-02 | conserved hypothetical protein |
| SAOUHSC_00755 | 1.0 | 1.9E-02 | conserved hypothetical protein |
| SAOUHSC_00870 | -0.9 | 2.0E-02 | dltB protein%2C putative |
| SAOUHSC_02902 | -2.7 | 2.0E-02 | conserved hypothetical protein |
| SAOUHSC_01721 | 1.0 | 2.0E-02 | conserved hypothetical protein |
| SAOUHSC_01651 | 1.5 | 2.0E-02 | ribosomal protein L33 |
| SAOUHSC_01549 | 4.8 | 2.0E-02 | transcriptional activator rinB-related protein |
| SAOUHSC_01630 | 1.2 | 2.0E-02 | conserved hypothetical protein |
| SAOUHSC_02285 | -0.9 | 2.1E-02 | 2-isopropylmalate synthase |
| SAOUHSC_00294 | -1.4 | 2.1E-02 | conserved hypothetical protein |
| SAOUHSC_02256 | -1.1 | 2.1E-02 | abortive infection protein |
| SAOUHSC_01716 | 1.0 | 2.1E-02 | conserved hypothetical protein |
| SAOUHSC_02216 | 2.1 | 2.1E-02 | phage DnaC-like protein |
| SAOUHSC_01576 | -1.4 | 2.1E-02 | exonuclease family |
| SAOUHSC_00525 | 1.0 | 2.1E-02 | DNA directed RNA polymerase beta-prime chain%2C putative |
| SAOUHSC_01840 | -1.2 | 2.1E-02 | transglycosylase domain protein |
| SAOUHSC_01296 | -3.8 | 2.2E-02 | conserved hypothetical protein |
| SAOUHSC_02200 | 1.3 | 2.2E-02 | conserved hypothetical phage protein |
| SAOUHSC_02879 | 1.3 | 2.2E-02 | squalene desaturase%2C putative |
| SAOUHSC_02825 | 1.3 | 2.2E-02 | conserved hypothetical protein |
| SAOUHSC_02370 | 1.0 | 2.3E-02 | conserved hypothetical protein |
| SAOUHSC_02611 | 0.9 | 2.3E-02 | conserved hypothetical protein |
| SAOUHSC_02129 | -1.4 | 2.3E-02 | conserved hypothetical protein |
| SAOUHSC_00468 | 1.3 | 2.3E-02 | conserved hypothetical protein |
| SAOUHSC_00022 | -0.9 | 2.3E-02 | conserved hypothetical protein |
| SAOUHSC_00723 | -1.2 | 2.3E-02 | conserved hypothetical protein |
| SAOUHSC_00816 | -2.5 | 2.3E-02 | extracellular matrix and plasma binding protein%2C putative |
| SAOUHSC_00860 | 0.9 | 2.3E-02 | 5-nucleotidase family protein |
| SAOUHSC_02425 | 1.3 | 2.4E-02 | conserved hypothetical protein |
| SAOUHSC_01587 | -0.9 | 2.4E-02 | ribosomal large subunit pseudouridine synthase B%2C putative |
| SAOUHSC_01140 | 2.7 | 2.4E-02 | hypothetical protein |
| SAOUHSC_A02635 | -2.3 | 2.4E-02 | hypothetical protein |
| SAOUHSC_02978 | -0.8 | 2.4E-02 | phage infection protein%2C putative |
| SAOUHSC_00719 | 1.0 | 2.4E-02 | conserved hypothetical protein |
| SAOUHSC_01466 | 0.9 | 2.4E-02 | conserved hypothetical protein |
| SAOUHSC_00115 | 1.1 | 2.4E-02 | capsular polysaccharide synthesis enzyme Cap5B |
| SAOUHSC_01149 | -0.8 | 2.4E-02 | cell division protein%2C putative |
| SAOUHSC_00508 | 1.0 | 2.4E-02 | conserved hypothetical protein |
| SAOUHSC_00939 | -0.9 | 2.4E-02 | conserved hypothetical protein |
| SAOUHSC_00457 | -1.1 | 2.5E-02 | conserved hypothetical protein |
| SAOUHSC_02880 | 1.3 | 2.5E-02 | conserved hypothetical protein |
| SAOUHSC_02802 | -1.4 | 2.5E-02 | fibronectin binding protein B%2C putative |
| SAOUHSC_01981 | -1.0 | 2.5E-02 | sensor histidine kinase%2C putative |
| SAOUHSC_00567 | 1.2 | 2.5E-02 | conserved hypothetical protein |
| SAOUHSC_02765 | -3.4 | 2.5E-02 | nickel ABC transporter%2C permease protein%2C putative |
| SAOUHSC_02297 | 0.9 | 2.5E-02 | S1 RNA binding domain protein |
| SAOUHSC_02585 | -0.9 | 2.5E-02 | conserved hypothetical protein |
| SAOUHSC_01722 | 0.9 | 2.6E-02 | alanyl-tRNA synthetase |
| SAOUHSC_02819 | -2.0 | 2.6E-02 | conserved hypothetical protein |
| SAOUHSC_02385 | -0.9 | 2.6E-02 | mannose-6-phosphate isomerase%2C class I |
| SAOUHSC_01743 | 0.9 | 2.6E-02 | adenine phosphoribosyltransferase |
| SAOUHSC_01026 | -0.9 | 2.6E-02 | conserved hypothetical protein |
| SAOUHSC_T00025 | -2.6 | 2.6E-02 | tRNA-Gly |
| SAOUHSC_01725 | 0.8 | 2.6E-02 | tRNA methyl transferase%2C putative |
| SAOUHSC_00612 | -1.2 | 2.6E-02 | endonuclease III%2C putative |
| SAOUHSC_02076 | 1.8 | 2.6E-02 | phi PVL orf 38-like protein-related protein |
| SAOUHSC_02112 | -1.0 | 2.6E-02 | conserved hypothetical protein |
| SAOUHSC_01635 | 0.9 | 2.6E-02 | shikimate kinase%2C putative |
| SAOUHSC_02875 | -0.9 | 2.6E-02 | D-lactate dehydrogenase%2C putative |
| SAOUHSC_00764 | -1.1 | 2.7E-02 | conserved hypothetical protein |
| SAOUHSC_02512 | 1.0 | 2.7E-02 | ribosomal protein L3%2C putative |
| SAOUHSC_01181 | 0.9 | 2.7E-02 | conserved hypothetical protein |
| SAOUHSC_01774 | 0.9 | 2.7E-02 | porphobilinogen deaminase |
| SAOUHSC_00991 | -1.3 | 2.7E-02 | conserved hypothetical protein |
| SAOUHSC_03008 | 1.2 | 2.7E-02 | imidazole glycerol phosphate synthase subunit hisF%2C putative |
| SAOUHSC_01504 | 1.1 | 2.7E-02 | ferredoxin%2C putative |
| SAOUHSC_01192 | -0.9 | 2.7E-02 | conserved hypothetical protein |
| SAOUHSC_00145 | -0.8 | 2.8E-02 | conserved hypothetical protein |
| SAOUHSC_02059 | 5.5 | 2.8E-02 | phi PVL orf 52-like protein |
| SAOUHSC_01598 | -0.9 | 2.8E-02 | AtsA/ElaC family protein |
| SAOUHSC_01951 | -1.5 | 2.8E-02 | epidermin biosynthesis protein EpiC%2C authentic point mutation |
| SAOUHSC_01391 | -0.8 | 2.8E-02 | conserved hypothetical protein |
| SAOUHSC_02810 | -0.8 | 2.8E-02 | conserved hypothetical protein |

| | | | |
|---|---|---|---|
| SAOUHSC_00442 | 0.9 | 2.8E-02 | DNA polymerase III%2C gamma and tau subunits%2C putative |
| SAOUHSC_00081 | 1.7 | 2.9E-02 | conserved hypothetical protein |
| SAOUHSC_01032 | 0.9 | 2.9E-02 | cytochrome d ubiquinol oxidase%2C subunit II%2C putative |
| SAOUHSC_01092 | 1.2 | 2.9E-02 | phenylalanyl-tRNA synthetase%2C alpha subunit |
| SAOUHSC_02226 | -1.0 | 2.9E-02 | conserved hypothetical phage protein |
| SAOUHSC_00914 | -2.7 | 2.9E-02 | 2-isopropylmalate synthase%2C putative |
| SAOUHSC_01528 | 1.2 | 2.9E-02 | bacteriophage L54a%2C bacterial Ig-like domain group 2 family protein |
| SAOUHSC_03014 | -2.8 | 2.9E-02 | ATP phosphoribosyltransferase%2C putative |
| SAOUHSC_00676 | 1.0 | 2.9E-02 | conserved hypothetical protein |
| SAOUHSC_01134 | -1.8 | 2.9E-02 | conserved hypothetical protein |
| SAOUHSC_00441 | -0.9 | 3.0E-02 | conserved hypothetical protein |
| SAOUHSC_01259 | -0.8 | 3.0E-02 | conserved hypothetical protein |
| SAOUHSC_00707 | 1.2 | 3.0E-02 | fructose 1-phosphate kinase%2C putative |
| SAOUHSC_01147 | 0.9 | 3.0E-02 | UDP-N-acetylmuramoylalanine--D-glutamate ligase |
| SAOUHSC_02630 | 1.1 | 3.0E-02 | conserved hypothetical protein |
| SAOUHSC_00345 | 1.1 | 3.0E-02 | conserved hypothetical protein |
| SAOUHSC_00970 | 1.5 | 3.1E-02 | ABC transporter%2C ATP-binding protein%2C putative |
| SAOUHSC_02775 | -1.2 | 3.1E-02 | conserved hypothetical protein |
| SAOUHSC_01468 | -1.0 | 3.1E-02 | conserved hypothetical protein |
| SAOUHSC_00558 | 1.2 | 3.1E-02 | acetyl-CoA acetyltransferase%2C putative |
| SAOUHSC_02000 | 0.8 | 3.1E-02 | glutamate-1-semialdehyde-2%2C1-aminomutase%2C putative |
| SAOUHSC_02364 | -0.8 | 3.1E-02 | conserved hypothetical protein |
| SAOUHSC_01093 | 0.8 | 3.1E-02 | phenylalanyl-tRNA synthetase%2C beta subunit |
| SAOUHSC_01583 | -0.9 | 3.1E-02 | conserved hypothetical phage protein |
| SAOUHSC_01817 | -1.4 | 3.2E-02 | conserved hypothetical protein |
| SAOUHSC_01868 | -0.8 | 3.2E-02 | conserved hypothetical protein |
| SAOUHSC_00678 | -0.9 | 3.2E-02 | conserved hypothetical protein |
| SAOUHSC_02208 | 3.2 | 3.2E-02 | PV83 orf 27-like protein |
| SAOUHSC_02309 | 1.0 | 3.2E-02 | conserved hypothetical protein |
| SAOUHSC_00298 | -1.3 | 3.2E-02 | conserved hypothetical protein |
| SAOUHSC_02220 | 2.5 | 3.3E-02 | phi ETA orf 18-like protein |
| SAOUHSC_01941 | -3.6 | 3.3E-02 | serine protease SplB |
| SAOUHSC_01962 | -0.8 | 3.3E-02 | uroporphyrinogen decarboxylase |
| SAOUHSC_01531 | 2.8 | 3.3E-02 | SLT orf 123-like protein |
| SAOUHSC_02391 | 1.1 | 3.3E-02 | conserved hypothetical protein |
| SAOUHSC_00029 | -2.7 | 3.4E-02 | conserved hypothetical protein |
| SAOUHSC_00268 | -0.8 | 3.4E-02 | conserved hypothetical protein |
| SAOUHSC_02232 | -0.9 | 3.4E-02 | phi PVL orf 33-like protein |
| SAOUHSC_00026 | -2.3 | 3.4E-02 | conserved hypothetical protein |
| SAOUHSC_00205 | -3.6 | 3.5E-02 | hypothetical protein |
| SAOUHSC_00827 | 1.3 | 3.5E-02 | conserved hypothetical protein |
| SAOUHSC_01704 | -2.3 | 3.5E-02 | conserved hypothetical protein |
| SAOUHSC_01776 | -0.8 | 3.5E-02 | glutamyl-tRNA reductase |
| SAOUHSC_02317 | 0.8 | 3.5E-02 | UDP-N-acetylmuramoylalanyl-D-glutamyl-2%2C6-diaminopimelate--D-alanyl-D-alanyl ligase |
| SAOUHSC_00954 | 0.8 | 3.5E-02 | UDP-N-acetylmuramoylalanyl-D-glutamate--2%2C 6-diaminopimelate ligase |
| SAOUHSC_00189 | -2.3 | 3.5E-02 | conserved hypothetical protein |
| SAOUHSC_00183 | -1.4 | 3.5E-02 | membrane protein%2C putative |
| SAOUHSC_01718 | -0.9 | 3.6E-02 | conserved hypothetical protein |
| SAOUHSC_02774 | 1.1 | 3.7E-02 | conserved hypothetical protein |
| SAOUHSC_01610 | -1.0 | 3.7E-02 | conserved hypothetical protein |
| SAOUHSC_00579 | 0.9 | 3.7E-02 | phosphomevalonate kinase |
| SAOUHSC_00430 | 0.9 | 3.7E-02 | conserved hypothetical protein |
| SAOUHSC_00877 | 1.5 | 3.7E-02 | conserved hypothetical protein |
| SAOUHSC_02110 | -1.0 | 3.8E-02 | conserved hypothetical protein |
| SAOUHSC_02594 | -0.8 | 3.8E-02 | conserved hypothetical protein |
| SAOUHSC_00100 | 2.1 | 3.8E-02 | deoxyribose-phosphate aldolase |
| SAOUHSC_02808 | 1.6 | 3.9E-02 | gluconate kinase |
| SAOUHSC_01007 | -0.8 | 3.9E-02 | FolD bifunctional protein%2C putative |
| SAOUHSC_00561 | 0.9 | 3.9E-02 | conserved hypothetical protein |
| SAOUHSC_02442 | 1.1 | 3.9E-02 | conserved hypothetical protein |
| SAOUHSC_00905 | 0.7 | 3.9E-02 | ATP-dependent nuclease subunit A%2C putative |
| SAOUHSC_00353 | -2.2 | 3.9E-02 | conserved hypothetical protein |
| SAOUHSC_02084 | -1.0 | 4.0E-02 | phage repressor protein%2C putative |
| SAOUHSC_02791 | -1.1 | 4.0E-02 | pyrophosphohydrolase%2C putative |
| SAOUHSC_02809 | 1.3 | 4.1E-02 | gluconate operon transcriptional repressor%2C putative |
| SAOUHSC_03046 | -1.2 | 4.1E-02 | Helix-turn-helix domain protein |
| SAOUHSC_01501 | -0.8 | 4.1E-02 | elastin binding protein |
| SAOUHSC_00462 | 1.0 | 4.1E-02 | conserved hypothetical protein |
| SAOUHSC_02830 | -1.1 | 4.1E-02 | D-lactate dehydrogenase%2C putative |
| SAOUHSC_02142 | -0.8 | 4.2E-02 | aldehyde dehydrogenase%2C putative |
| SAOUHSC_00180 | 1.3 | 4.2E-02 | conserved hypothetical protein |
| SAOUHSC_00445 | -1.1 | 4.2E-02 | recombination protein RecR |
| SAOUHSC_01471 | 0.8 | 4.2E-02 | asparaginyl-tRNA synthetase%2Cputative |
| SAOUHSC_02687 | -1.0 | 4.2E-02 | formate/nitrite transporter%2C putative |
| SAOUHSC_01665 | 0.9 | 4.2E-02 | CBS domain protein |
| SAOUHSC_00978 | -1.0 | 4.2E-02 | conserved hypothetical protein |
| SAOUHSC_02756 | -1.1 | 4.3E-02 | conserved hypothetical protein |
| SAOUHSC_00672 | -1.0 | 4.3E-02 | conserved hypothetical protein |
| SAOUHSC_01756 | 0.8 | 4.3E-02 | conserved hypothetical protein |
| SAOUHSC_02091 | 0.9 | 4.3E-02 | conserved hypothetical protein |
| SAOUHSC_01047 | -1.3 | 4.4E-02 | spermidine/putrescine ABC transporter%2C permease protein%2C putative |
| SAOUHSC_02677 | -0.8 | 4.4E-02 | conserved hypothetical protein |
| SAOUHSC_02824 | 1.2 | 4.5E-02 | conserved hypothetical protein |
| SAOUHSC_02675 | -0.9 | 4.5E-02 | conserved hypothetical protein |
| SAOUHSC_00588 | -1.8 | 4.5E-02 | conserved hypothetical protein |
| SAOUHSC_02822 | -1.1 | 4.5E-02 | conserved hypothetical protein |
| SAOUHSC_01263 | -0.8 | 4.5E-02 | conserved hypothetical protein |
| SAOUHSC_02763 | -1.9 | 4.5E-02 | peptide ABC transporter%2C ATP-binding protein%2C putative |
| SAOUHSC_01966 | 0.8 | 4.6E-02 | conserved hypothetical protein |
| SAOUHSC_02964 | 1.0 | 4.6E-02 | conserved hypothetical protein |
| SAOUHSC_01977 | -1.0 | 4.6E-02 | conserved hypothetical protein |
| SAOUHSC_02667 | -0.8 | 4.6E-02 | conserved hypothetical protein |
| SAOUHSC_00060 | 0.7 | 4.6E-02 | conserved hypothetical protein |

| | | | |
|---|---|---|---|
| SAOUHSC_01613 | 0.8 | 4.6E-02 | 2-oxoisovalerate dehydrogenase%2C E1 component%2C alpha subunit%2C putative |
| SAOUHSC_02991 | -1.0 | 4.6E-02 | conserved hypothetical protein |
| SAOUHSC_03031 | -0.9 | 4.6E-02 | conserved hypothetical protein |
| SAOUHSC_01800 | 0.8 | 4.6E-02 | two-component response regulator%2C putative |
| SAOUHSC_01717 | 0.8 | 4.6E-02 | conserved hypothetical protein |
| SAOUHSC_02509 | 0.9 | 4.6E-02 | ribosomal protein L2 |
| SAOUHSC_00668 | -0.8 | 4.6E-02 | ABC transporter permease%2C putative |
| SAOUHSC_00493 | 0.7 | 4.7E-02 | lysyl-tRNA synthetase |
| SAOUHSC_01404 | -1.6 | 4.7E-02 | hypothetical protein |
| SAOUHSC_02329 | 1.0 | 4.7E-02 | hydroxyethylthiazole kinase%2C putative |
| SAOUHSC_00532 | -0.8 | 4.7E-02 | conserved hypothetical protein |
| SAOUHSC_01314 | -0.8 | 4.8E-02 | conserved hypothetical protein |
| SAOUHSC_02312 | -1.6 | 4.8E-02 | potassium-transporting ATPase%2C A subunit |
| SAOUHSC_A02013 | -1.4 | 4.8E-02 | conserved hypothetical protein |
| SAOUHSC_02663 | -1.0 | 4.8E-02 | conserved hypothetical protein |
| SAOUHSC_00038 | -2.4 | 4.9E-02 | conserved hypothetical protein |
| SAOUHSC_01707 | 1.0 | 4.9E-02 | conserved hypothetical protein |
| SAOUHSC_01698 | -1.1 | 5.0E-02 | conserved hypothetical protein |
| SAOUHSC_02521 | 3.5 | 5.0E-02 | conserved hypothetical protein |
| SAOUHSC_01816 | 0.8 | 5.0E-02 | conserved hypothetical protein |

## 8.2 Supplementary references


Anderson, K. L., Roberts, C., Disz, T., Vonstein, V., Hwang, K., Overbeek, R., Olson, P. D., Projan, S. J. & Dunman, P. M. 2006. Characterization of the *Staphylococcus aureus* heat shock, cold shock, stringent, and SOS responses and their effects on log-phase mRNA turnover. *J Bacteriol,* 188**,** 6739-56.

Anderson, K. L., Roux, C. M., Olson, M. W., Luong, T. T., Lee, C. Y., Olson, R. & Dunman, P. M. 2010. Characterizing the effects of inorganic acid and alkaline shock on the *Staphylococcus aureus* transcriptome and messenger RNA turnover. *FEMS Immunol Med Microbiol,* 60**,** 208-50.

Bischoff, M., Dunman, P., Kormanec, J., Macapagal, D., Murphy, E., Mounts, W., Berger-Bachi, B. & Projan, S. 2004. Microarray-based analysis of the *Staphylococcus aureus* sigmaB regulon. *J Bacteriol,* 186**,** 4085-99.

Cirz, R. T., Jones, M. B., Gingles, N. A., Minogue, T. D., Jarrahi, B., Peterson, S. N. & Romesberg, F. E. 2007. Complete and SOS-mediated response of *Staphylococcus aureus* to the antibiotic ciprofloxacin. *J Bacteriol,* 189**,** 531-9.

Corrigan, R. M., Bellows, L. E., Wood, A. & Grundling, A. 2016. ppGpp negatively impacts ribosome assembly affecting growth and antimicrobial tolerance in Gram-positive bacteria. *Proc Natl Acad Sci U S A,* 113**,** E1710-9.

Crosby, H. A., Schlievert, P. M., Merriman, J. A., King, J. M., Salgado-Pabon, W. & Horswill, A. R. 2016. The *Staphylococcus aureus* Global Regulator MgrA Modulates Clumping and Virulence by Controlling Surface Protein Expression. *PLoS Pathog,* 12**,** e1005604.

DuMont, A. L., Yoong, P., Surewaard, B. G., Benson, M. A., Nijland, R., van Strijp, J. A. & Torres, V. J. 2013. *Staphylococcus aureus* elaborates leukocidin AB to mediate escape from within human neutrophils. *Infect Immun,* 81**,** 1830-41.

Eisenbeis, J., Saffarzadeh, M., Peisker, H., Jung, P., Thewes, N., Preissner, K. T., Herrmann, M., Molle, V., Geisbrecht, B. V., Jacobs, K. & Bischoff, M. 2018. The *Staphylococcus aureus* Extracellular Adherence Protein Eap Is a DNA Binding Protein Capable of Blocking Neutrophil Extracellular Trap Formation. *Front Cell Infect Microbiol,* 8**,** 235.

Entenza, J. M., Moreillon, P., Senn, M. M., Kormanec, J., Dunman, P. M., Berger-Bachi, B., Projan, S. & Bischoff, M. 2005. Role of sigmaB in the expression of *Staphylococcus aureus* cell wall adhesins ClfA and FnbA and contribution to infectivity in a rat model of experimental endocarditis. *Infect Immun,* 73**,** 990-8.

Fan, F., Yan, K., Wallis, N. G., Reed, S., Moore, T. D., Rittenhouse, S. F., DeWolf, W. E., Jr., Huang, J., McDevitt, D., Miller, W. H., Seefeld, M. A., Newlander, K. A., Jakas, D. R., Head, M. S. & Payne, D. J. 2002. Defining and combating the mechanisms of triclosan resistance in clinical isolates of *Staphylococcus aureus*. *Antimicrob Agents Chemother,* 46**,** 3343-7.

Fleury, B., Kelley, W. L., Lew, D., Gotz, F., Proctor, R. A. & Vaudaux, P. 2009. Transcriptomic and metabolic responses of *Staphylococcus aureus* exposed to supra-physiological temperatures. *BMC Microbiol,* 9**,** 76.

Fournier, B. & Hooper, D. C. 2000. A new two-component regulatory system involved in adhesion, autolysis, and extracellular proteolytic activity of *Staphylococcus aureus*. *J Bacteriol,* 182**,** 3955-64.

Fournier, B., Klier, A. & Rapoport, G. 2001. The two-component system ArlS-ArlR is a regulator of virulence gene expression in *Staphylococcus aureus*. *Mol Microbiol,* 41**,** 247-61.

Fraser, J. D. & Proft, T. 2008. The bacterial superantigen and superantigen-like proteins. *Immunol Rev,* 225**,** 226-43.

Geiger, T., Goerke, C., Fritz, M., Schafer, T., Ohlsen, K., Liebeke, M., Lalk, M. & Wolz, C. 2010. Role of the (p)ppGpp synthase RSH, a RelA/SpoT homolog, in stringent response and virulence of *Staphylococcus aureus*. *Infect Immun,* 78**,** 1873-83.

Gupta, R. K., Alba, J., Xiong, Y. Q., Bayer, A. S. & Lee, C. Y. 2013. MgrA activates expression of capsule genes, but not the alpha-toxin gene in experimental *Staphylococcus aureus* endocarditis. *J Infect Dis,* 208**,** 1841-8.

Laarman, A. J., Ruyken, M., Malone, C. L., van Strijp, J. A., Horswill, A. R. & Rooijakkers, S. H. 2011. *Staphylococcus aureus* metalloprotease aureolysin cleaves complement C3 to mediate immune evasion. *J Immunol,* 186**,** 6445-53.

Liang, X., Zheng, L., Landwehr, C., Lunsford, D., Holmes, D. & Ji, Y. 2005. Global regulation of gene expression by ArlRS, a two-component signal transduction regulatory system of *Staphylococcus aureus*. *J Bacteriol,* 187**,** 5486-92.

Mainiero, M., Goerke, C., Geiger, T., Gonser, C., Herbert, S. & Wolz, C. 2010. Differential target gene activation by the *Staphylococcus aureus* two-component system *saeRS*. *J Bacteriol,* 192**,** 613-23.

Malachowa, N. & DeLeo, F. R. 2011. *Staphylococcus aureus* survival in human blood. *Virulence,* 2**,** 567-9.

Parsons, J. B., Yao, J., Frank, M. W. & Rock, C. O. 2015. FabH mutations confer resistance to FabF-directed antibiotics in *Staphylococcus aureus*. *Antimicrob Agents Chemother,* 59**,** 849-58.

Perera, V. R., Newton, G. L., Parnell, J. M., Komives, E. A. & Pogliano, K. 2014. Purification and characterization of the *Staphylococcus aureus* bacillithiol transferase BstA. *Biochim Biophys Acta,* 1840**,** 2851-61.

Peyrusson, F., Varet, H., Nguyen, T. K., Legendre, R., Sismeiro, O., Coppee, J. Y., Wolz, C., Tenson, T. & Van Bambeke, F. 2020. Intracellular *Staphylococcus aureus* persisters upon antibiotic exposure. *Nat Commun,* 11**,** 2200.

Rosey, E. L., Oskouian, B. & Stewart, G. C. 1991. Lactose metabolism by *Staphylococcus aureus*: characterization of *lacABCD*, the structural genes of the tagatose 6-phosphate pathway. *J Bacteriol,* 173**,** 5992-8.

Sasso, E. H., Silverman, G. J. & Mannik, M. 1989. Human IgM molecules that bind staphylococcal protein A contain VHIII H chains. *J Immunol,* 142**,** 2778-83.

Surewaard, B. G., de Haas, C. J., Vervoort, F., Rigby, K. M., DeLeo, F. R., Otto, M., van Strijp, J. A. & Nijland, R. 2013. Staphylococcal alpha-phenol soluble modulins contribute to neutrophil lysis after phagocytosis. *Cell Microbiol,* 15**,** 1427-37.

Thammavongsa, V., Kim, H. K., Missiakas, D. & Schneewind, O. 2015. Staphylococcal manipulation of host immune responses. *Nat Rev Microbiol,* 13**,** 529-43.

Truong-Bolduc, Q. C., Dunman, P. M., Strahilevitz, J., Projan, S. J. & Hooper, D. C. 2005. MgrA is a multiple regulator of two new efflux pumps in *Staphylococcus aureus*. *J Bacteriol,* 187**,** 2395-405.

van Wamel, W., Xiong, Y. Q., Bayer, A. S., Yeaman, M. R., Nast, C. C. & Cheung, A. L. 2002. Regulation of *Staphylococcus aureus* type 5 capsular polysaccharides by *agr* and *sarA in vitro* and in an experimental endocarditis model. *Microb Pathog,* 33**,** 73-9.

Voyich, J. M., Vuong, C., DeWald, M., Nygaard, T. K., Kocianova, S., Griffith, S., Jones, J., Iverson, C., Sturdevant, D. E., Braughton, K. R., Whitney, A. R., Otto, M. & DeLeo, F. R. 2009. The SaeR/S gene regulatory system is essential for innate immune evasion by *Staphylococcus aureus*. *J Infect Dis,* 199**,** 1698-706.

Wardenburg, J. & Schneewind, O. 2008. Vaccine protection against *Staphylococcus aureus* pneumonia. *J Exp Med,* 205**,** 287-94.

Wilke, G. A. & Wardenburg, J. 2010. Role of a disintegrin and metalloprotease 10 in *Staphylococcus aureus* alpha-hemolysin-mediated cellular injury. *Proc Natl Acad Sci U S A,* 107**,** 13473-8.

Yin, S., Daum, R. S. & Boyle-Vavra, S. 2006. VraSR two-component regulatory system and its role in induction of *pbp2* and *vraSR* expression by cell wall antimicrobials in *Staphylococcus aureus*. *Antimicrob Agents Chemother,* 50**,** 336-43.

Zhou, C., Bhinderwala, F., Lehman, M. K., Thomas, V. C., Chaudhari, S. S., Yamada, K. J., Foster, K. W., Powers, R., Kielian, T. & Fey, P. D. 2019. Urease is an essential component of the acid response network of *Staphylococcus aureus* and is required for a persistent murine kidney infection. *PLoS Pathog,* 15**,** e1007538.

## 8.3 Profession Internship for PhD students

**Institution:** Department of Respiratory Sciences, University of Leicester

**Details of placement:**

From the end of February to the end of May 2019, I worked in the lab of Professor Michael Barer at the University of Leicester. The work involved refinement of a novel mask-based diagnostic for the diagnosis of *Mycobacterium tuberculosis*, the causative organism of TB. My work complemented an ongoing clinical trial in South Africa, which was investigating the efficacy of this diagnostic. The filters within these masks were designed to capture *M. tuberculosis* in the exhaled respiratory droplets of the wearer. These filters could then be removed and nucleic acids extracted to allow for detection of the pathogen by qRT-PCR. My work centred upon determining whether these mask filters were compatible with Mycobacterium Growth Indicator Tubes (MGIT), a system that is essential for *M. tuberculosis* diagnoses in developing countries in which TB is endemic. My work concluded that the mask diagnostic was indeed compatible with the MGIT system. As both the mask-based diagnostic and MGIT system are inexpensive in terms of cost and diagnostic infrastructure compared to currently used molecular methods for TB diagnosis, this diagnostic workflow will be much more accessible to the nations that need TB diagnostics the most.